The effect of mineralogical variation in the UG2 chromitite on recovery of platinum-group elements

by

Catharina Johanna Penberthy

Submitted in partial fulfillment of the requirements for the degree PhD Geology in the Faculty of Natural & Agricultural Sciences

University of Pretoria

Pretoria

December 2001

The effect of mineralogical variation in the UG2 chromitite on recovery of platinum-group elements

by

Catharina Johanna Penberthy

Supervisor: Prof. S.A. de Waal Co-Supervisor: Prof. R.K.W. Merkle

Degree: PhD

Department: Earth Sciences

Platinum-group elements (PGEs) are recovered from UG2 chromitite by milling and flotation. The mechanisms involved during beneficiation of this type of ore are still poorly understood, partly because of its complex nature. Image-analysis techniques were used to characterise the mineralogy of UG2 chromitite from diverse geological environments, as well as the milling and flotation products derived from each of these ores.

Postmagmatic alteration of UG2 chromitite has a profound effect on the mineralogy, chemistry and recovery characteristics of the UG2 chromitite. Relatively unaltered UG2 chromitite consists predominantly of chromite and primary silicates, mostly bronzite and plagioclase with minor phlogopite, and small amounts of secondary silicates such as talc and chlorite. Trace quantities of base-metal sulphides, predominantly pentlandite, pyrrhotite and chalcopyrite ± pyrite, generally occur at chromite-silicate grain boundaries. PGEs are present both as discrete PGE minerals, and, to a lesser extent, sub-microscopically in other phases, mostly palladium and rhodium in pentlandite.

The PGE mineral assemblage is characterised by sulphide minerals, mostly braggite, cooperite, nickeloan malanite and laurite, and is closely associated with the base-metal sulphides. Recovery of PGE minerals is strongly dependent on the degree of liberation, with liberated PGE minerals and PGE minerals associated with liberated

base-metal sulphides, the fastest-floating particles. PGE minerals report to flotation tailings predominantly as fine-grained inclusions in coarse silicate particles.

In places, the footwall rocks have been replaced by iron-rich ultrabasic pegmatoid. As a result of interaction with Fe- and Ti-rich fluids, the chromite grains in the UG2 chromitite have been enlarged due to sintering, and the PGE mineral assemblage replaced by one consisting predominantly of laurite, Pt-Fe alloy and other non-sulphide PGE minerals. The non-sulphide PGE mineral grains appear to be slower-floating than sulphide PGE minerals.

Low temperature hydrothermal alteration appears to have caused relatively widespread alteration of the UG2 chromitite in some areas, resulting in corrosion and redistribution of sulphide minerals, as well as the replacement of primary magmatic silicates by secondary silicates such as pumpellyite, epidote, prehnite, albite, talc, chlorite and quartz. Ore from such areas are characterised by a base-metal sulphide assemblage consisting predominantly of millerite, chalcopyrite, and pyrite. Base-metal sulphide and PGE minerals occur in fine-grained intergrowths with silicates, resulting in poor liberation. In the samples investigated, composite particles were often faster-floating than expected, at least partly due to the presence of naturally floatable talc.

The effect of faulting on the mineralogy of the UG2 chromitite probably depends on distance from the fault zone, and possibly also timing of faulting, and can cause cataclasis of the ore. Where cataclasis occurred, broken mineral grains are cemented by secondary, hydrous silicates. Liberation of base-metal sulphides and PGE minerals are poor, and recoveries consequently very low.

It was demonstrated that reasonable estimates of total PGE+Au recovery can be made from the mineralogical characteristics of UG2 chromitite ore. Based on the mineralogy of ore from a specific area, provision can be made for appropriate adjustments to metallurgical flowsheets.

Die effek van mineralogiese variasie in die UG2 chromitiet op herwinning van platinum-groep elemente

deur

Catharina Johanna Penberthy

Toesighouer: Prof. S.A. de Waal Medetoesighouer: Prof. R.K.W. Merkle

Graad: PhD

Departement: Aardwetenskappe

Platinum-group elemente (PGE) word herwin uit die UG2 chromitiet deur middel van maling en flottasie. Die meganismes betrokke tydens opgradering van hierdie tipe erts word nog nie goed verstaan nie, deels as gevolg van die komplekse aard van die erts. Beeldanalise-tegnieke is ingespan om UG2 chromitiet vanaf verskillende geologiese omgewings te karakteriseer, asook die maal- en flottasieprodukte afkomstig uit elkeen van hierdie ertse.

Na-magmatiese verandering het dikwels 'n ingrypende effek op die chemie, mineralogie en herwinningseienskappe van die UG2 chromitiet. Relatief onveranderde UG2 chromitiet bestaan hoofsaaklik uit chromiet en primêre silikate, hoofsaaklik bronsiet en plagioklaas, met min flogopiet, en klein hoeveelhede sekondêre silikate soos talk en chloriet. Spoorhoeveelhede onedelmetaal-sulfiede, hoofsaaklik pentlandiet, pirrotiet en chalkopiriet ±piriet, kom oor die algemeen gewoonlik voor langs chromiet-silikaat korrelgrense. PGE is teenwoordig beide as diskrete PGE mineraalkorrels, en, tot 'n mindere mate, submikroskopies, hoofsaaklik palladium en rhodium in pentlandiet.

Die PGE mineraal versameling bestaan sulfiedminerale, hoofsaaklik braggiet, cooperiet, nikkeldraende malaniet, en lauriet, en kom nou geassosïeer met die onedelmetaal-sulfiede voor. Herwinning van PGE minerale hang grotendeels af van graad van bevryding, met bevryde PGE mineraalkorrels, en PGE minerale geassosieer met bevryde onedelmetaal-sulfiede die mees vinnigsfloterende partikels. PGE

minerale in die flottasie uitskotte kom hoofsaaklik voor as fynkorrelrige insluitsels in groot silikaatpartikels.

In sekere areas, is die vloergesteentes vervang deur ysterryke ultrabasiese pegmatoïed. As gevolg van die interaksie met Fe- en Ti-ryke vloeistowwe, is die chromietkorrels in die UG2 chromitiet vergroot deur 'n sinteringsproses, en die PGE mineraalversameling vervang deur een wat grootliks bestaan uit lauriet, Pt-Fe allooi, en ander nie-sulfied PGE minerale. Dit wil voorkom asof die nie-sulfied PGE minerale stadiger flotteer as PGE sulfiedminerale.

Lae temperatuur hidrotermale verandering het in sekere gebiede relatief wydverspreide verandering van die UG2 chromitiet veroorsaak. Die resultaat is korrosie en herverspreiding van sulfiedminerale, asook die vervanging van primêre magmatiese silikaatminerale deur sekondêre silikaatminerale soos pumpelliet, epidoot, prehniet, talk, chloriet, kwarts en albiet. Hierdie monsters work gekenmerk deur onedelmetaal-sulfiedversamelings wat bestaan hoofsaaklik uit milleriet, chalkopiriet en piriet. Onedelmetaal-sulfiede en PGE minerale kom fynvergroeid met silikate voor. Dit lei tot swak bevryding. In die monsters wat ondersoek is, is egter gevind dat saamgestelde partikels in hierdie monsters beter flotteer as wat verwag is, deels as gevolg van die teenwoordigheid van natuurlik flotterende talk.

Die uitwerking van verskuiwings op die mineralogie van die UG2 chromitiet, hang waarskynlik af van die afstand vanaf die verskuiwingsssone, en moontlik ook die stadium waarop die verskuiwing plaasgevind het, en kan kataklastiese teksture in die erts veroorsaak. Waar dit voorkom, is gebreekte mineraalpartikels deur sekondêre silikate gesementeer. Bevryding van onedelmetaal sulfiede en PGE minerale is gevolglik swak, en herwinning laag.

Totale PGE+Au herwinning kan redelik goed voorspel word uit die mineralogiese eienskappe van die UG2 chromitiet. Op grond van die mineralogie van erts afkomstig vanaf 'n spesifieke area, kan voorsiening gemaak word vir geskikte aanpassings aan metallurgiese vloeikaarte.

ACKNOWLEDGEMENTS

I am indebted to the Council for Mineral Technology (Mintek) for allowing me to undertake the investigation, and to use the results for this thesis.

Lonrho's Platinum Division is gratefully acknowledged for supplying the samples and permission to publish the results.

To my husband Cecil and my son Martin, I wish to express my sincerest appreciation for their unfailing support and encouragement, and for having tolerated the intrusion of my studies into our lives for so long.

A special thanks to the following people and institutions:

Mr. Jan van der Merwe and his team of Geologists at Lonrho's Platinum Division for collecting the samples.

Drs. J. P.R. de Villiers, E.J. Oosthuyzen, J. Nell and Mr. E.A. Viljoen from Mintek for their continued guidance and support.

Profs. S.A. de Waal and R.K.W. Merkle from the University of Pretoria for their constructive criticism and encouragement.

Mr. M. Hay (previously at Lonrho) and Messrs. P. Marais and M. Valenta (both at Mintek during the initial stages of the research) for taking the time to teach me about the milling and flotation aspects of the study.

Staff at the Analytical Services Division at Mintek for chemical analyses.

Staff at the Minerals Engineering Division at Mintek for milling and flotation tests.

Messrs. V.H.M. Duarte and B. Moeketsi for the preparation of polished sections.

Mr. E.A. Viljoen and the other members of the Microbeam Analysis Group at Mintek, for assistance with the electron-microprobe analyses.

And last, but not least, all the many other colleagues at Mintek who helped and supported me in so many ways over the past few years.

CONTENTS

LIST OF ILLUSTRATIONS

LIST OF TABLES

LIST OF ABBREVIATIONS

SEM – scanning-electron microscopy

EDS – energy-dispersive X-ray spectroscopy

IA – image analysis

XRD – X-ray diffraction

PGE – platinum-group element

PGEM – platinum-group mineral. This abbreviation was used rather than the more commonly accepted PGM to avoid confusion, as PGM is also used to indicate platinum-group metal.

BMS – base-metal sulphide

ECD – equivalent circle diameter

GB – grain boundary

Mintek – Council for Mineral Technology

1. INTRODUCTION

1.1 Historical background

The Merensky, UG2 and Plat Reefs of the Bushveld Complex contain about 75% and 50%, respectively, of the world's reserves of platinum and palladium (Cawthorn, 1999). However, for many years the UG2 layer remained unexploited, mainly due to seemingly insurmountable problems associated with its beneficiation. The gravity separation processes, used to upgrade the Merensky ore, proved to be unsuitable for the UG2 ore with its smaller PGE mineral grain sizes. Later, when flotation processes were considered, the need to maintain chromite recovery below the critical level determined by the smelting process, and yet maximise PGE recoveries, presented a new set of problems (Corrans *et al.*, 1982; Overbeek *et al.*, 1985; Hiemstra, 1988b; Hossy, 1991).

Since exploitation of the UG2 ore would have more than doubled resources, the incentive for development of a suitable process was high. In addition, the higher rhodium content of the UG2 ore, the production of chromite as a potentially valuable by-product, the higher PGE+Au content at some localities, and the fact that it could be mined using existing facilities, were further advantages (Brugman, 1985; Overbeek *et al.*, 1985; *Anon.*, 1987; Hossy, 1991).

After extensive research and testwork at Mintek and Western Platinum Mine, the metallurgical extraction problems were largely overcome (Corrans *et al.*, 1982; Overbeek *et al.*, 1985; Liddell *et al.*, 1986; *Anon.*, 1988; Hossy, 1991). The first plant to treat UG2 ore on its own was commissioned at Western Platinum Mine in 1984 (Brugman, 1985).

Typically, concentrate containing ~300 to 400 g/t PGE+Au and ~3% Cr_2O_3 (Vermaak, 1995) is produced from UG2 ore by means of multistage size reduction and froth flotation. This concentrate is subjected to matte smelting, followed by a converting step. The next step is the separation of the base metals from the precious metals by hydrometallurgical treatment of the matte, or by magnetic separation of PGE-rich Cu-Ni±Fe alloy after slow cooling. The final phase is the refining step, which involves the separation and purification of the six PGEs, gold and silver.

1.2 Reasons for undertaking this study

Mineralogical analysis provides information that can be used to predict and explain the behaviour of ores, minerals, and metallurgical products in metallurgical processes. The mineralogical characterisation of a suite of samples, consisting of unbroken ore, as well as samples generated during comminution and concentration, leads to a better understanding of the mineralogical factors affecting the behaviour of an ore during extraction. Additional improvements in recovery can be attained if the questions of where and why losses occur can be answered with some degree of confidence.

Flotation processes are being fine-tuned to allow for the beneficiation of more and more complex ores. Flow sheets are becoming more complicated with flotation conditions geared towards very specific types of particles (Koniggsman, 1985; Wesely, 1985; Kallioinen & Heiskanen, 1993). This is only possible with the aid of reliable mineralogical information.

Total PGE+Au recoveries to the flotation concentrates of UG2 ore are generally between 80 and 90 per cent, which means that significant amounts of valuable metals are lost to the flotation tailings. Much of these losses can be attributed to mineralogical factors. Large lateral variations exist in the characteristics of the UG2 layer. These differences pertain to the thickness of the layer (McLaren, 1980; McLaren & DeVilliers, 1982; Gain, 1985; 1986; Mossom, 1986; Von Gruenewaldt *et al.*, 1990; Davey, 1992; Maier & Eales, 1994; Lea, 1996; Maier & Bowen, 1996), chromite composition (McLaren, 1980; McLaren & DeVilliers, 1982), the vertical distribution of the PGEs (McLaren, 1980; McLaren & DeVilliers, 1982; Gain, 1985; Hiemstra, 1985, 1986; Mossom, 1986; Viljoen *et al.*, 1986a, b; Von Gruenewaldt *et al.*, 1990; Grimbeek, 1995), the grade and relative proportions of PGEs (McLaren & DeVilliers, 1982; Gain, 1985; Edwards, 1988; Viljoen & Schürmann, 1998) and the mineralogy, particularly of the base-metal sulphides and PGE minerals (McLaren, 1980; McLaren & DeVilliers, 1982; Kinloch, 1982; Peyerl, 1982; Von Gruenewaldt *et al.*, 1990; Winkels-Herding *et al.*, 1991; Hofmeyr & Adair, 1993; Grimbeek, 1995). However, the effect of variations in mineralogical parameters on the behaviour of UG2 ore during processing is still poorly understood.

There are several reasons for this:

- The major players in the platinum industry in South Africa (Anglo Platinum and Impala Platinum) have traditionally concentrated more on exploitation of the Merensky Reef. This situation has been changing over the past few years (Vermaak, 1995).

- In addition, the atmosphere of secrecy prevailing in the platinum industry means that even where research is being done on this subject, the results are generally not published.

- The mineralogy of UG2 ore and metallurgical product samples is difficult to characterise. PGE grades are low - ±5 g/t and <1 g/t for flotation feed and tailings samples respectively. In addition, the PGEs in the UG2 chromitite occur both as discrete, microscopically visible, PGE mineral grains (McLaren & de Villiers, 1982; Peyerl, 1982; Hofmeyr & Adair, 1993; Winkels-Herding *et al.*, 1991; Grimbeek, 1995), and, to a lesser extent, sub-microscopically* in other phases, predominantly the base-metal sulphides (Paktunc *et al.*, 1990), and possibly also oxide and silicate minerals (Peyerl, 1983; Hofmeyr, 1998).

- For many years the electron microprobe (EMP) was the only technique available to quantitatively determine the distribution of trace quantities of PGEs occurring sub-microscopically in other minerals, in particular the base-metal sulphides. The minimum detection limits achievable using EMP are relatively high (a few hundred ppm) (Cabri, 1991) making it impossible to calculate satisfactory PGE mineralogical mass balances for this type of deposit. Over the past twenty years major advances have been made in this field. Recently, detection limits as low as 10 ppm have been reported using improved electron-microprobe techniques (Johanson & Kojonen, 1995; Weiser *et al.*, 1998). Detection limits of a few ppm

---

* Cabri (1992) defines sub-microscopic PGE as PGE occurring as finely divided 'invisible' mineral grains less than 0.1μm in diameter, colloidal-size particulates, clusters of less than ~ 100 atoms, or true solid solution.

can be achieved with the proton microprobe using PIXE (Particle Induced X-Ray Emission) (Cabri *et al.*, 1984, Paktunc *et al.*, 1990; Cabri, 1992, Czamanske *et al.*, 1992), and down to the ppb range using SIMS (Secondary Ion Mass Spectrometry) (Ripley & Chryssoulis, 1994; Cabri & McMahon, 1995; 1996; Oberthür *et al.*, 1997).

Despite these developments only one set of measurements of PGEs in the base-metal sulphides of the UG2 chromitite has been published (Paktunc *et al.*, 1990). There are several reasons for this – for one thing, such instruments are not readily available, nor are suitable calibration standards. For another, in the UG2 chromitite, the base-metal sulphides themselves occur in trace amounts and as small grains.

- Very little attention has been given to techniques to characterise the mineralogy of the microscopically visible PGE minerals. In addition to being present in trace amounts, the PGE minerals are usually so fine-grained, and so difficult to identify, that traditional mineralogical techniques such as ore microscopy and X-ray diffraction provide insufficient information (Hiemstra, 1988a).

SEM-based image analysis techniques have been successfully applied in a variety of mineral processing related problems (Miller *et al.*, 1982; Petruk, 1983; 1988b; Dilks & Graham, 1985; Petruk & Smith, 1989; Gottlieb *et al.*, 1993; Van den Heever, 1995; Lastra *et al.*, 1999, to name but a few). Automated image analysis allows for the collection of statistically valid data in a reasonable time. In many cases, the image analyser makes it possible to carry out measurements on a scale which was out of the question using manual means, even though it was theoretically possible. However, the use of such techniques for the characterisation of PGE-bearing ores, remains a largely untested option. This aspect formed the focus of the present study.

1.3 Previous work

McLaren (1980) and McLaren and de Villiers (1982) reported on a mineralogical study of UG2 ore from different localities. Data on more than 6000 individual PGE mineral grains were collected manually, providing the first quantitative evaluation of

the PGE mineralogy of the UG2 chromitite layer. McLaren concluded that the mineralogy of UG2 chromitite varies from one location to the next, giving rise to different PGE+Au recoveries. Data collected by other researchers (Kinloch, 1982; Peyerl, 1982; Winkels-Herding *et al.*, 1991; Hofmeyr & Adair, 1993; Grimbeek, 1995) also indicated variations in the mineralogical characteristics of UG2 chromitite, often related to geological disturbances such as pothole structures or ultrabasic pipes. Although most of these researchers did not dwell on the metallurgical implications of these variations, Hofmeyr and Adair (1993), investigating the changes in the mineralogy of the Merensky and UG2 reefs in areas affected by iron-rich ultrabasic pegmatoid replacement, reported lower than expected PGE+Au recoveries from such localities.

Peyerl (1983, 1992) found a definite relationship between the mode of occurrence of PGE minerals and PGE recovery. As the percentage of PGE minerals entirely enclosed in silicate and chromite increases, the PGE recovery decreases.

The work performed by these investigators highlights the need for reliable mineralogical techniques for the characterisation of the PGE mineralogy of the UG2 ore. The advent of increasingly faster and powerful image analysis systems now provides the opportunity to launch such studies.

1.5 Objectives

The objectives of this study were:

- To develop and explore the use of automated image analysis to characterise the mineralogy of UG2 chromitite ore and mineral processing products
- To determine how differences in the geological environment affect the mineralogy of the UG2 chromitite
- To determine whether variations in the mineralogy of the UG2 chromitite can be related to differences in flotation behaviour
- To identify the factors affecting the recovery of PGE mineral-bearing particles from UG2 chromitite.

2. GEOLOGY AND REGIONAL SETTING

2.1 General

The Bushveld Complex is one of the world's greatest geological phenomena. It is not only the largest known intrusion of its kind in the world, but also contains vast reserves of PGEs, chromium and vanadium, nickel, cobalt, copper, tin, iron, fluorspar, andalusite, magnesite and chrysotile asbestos (Willemse, 1964; Coetzee, 1976; Vermaak & Von Gruenewaldt, 1986).

Situated in the northern half of the Kaapvaal craton, the Bushveld Complex covers an area of approximately 65 000 km^2 (SACS, 1980) (Figure 1). The magmatic events resulting in the formation of the Bushveld Complex (2.05 to 2.06 Ga), commenced with the extrusion of the basic and acid volcanics of the Rooiberg Group along a regional unconformity, marking the top of the Transvaal sedimentary succession. Contemporaneous with the Rooiberg volcanism, the Rashoop Suite granophyre was emplaced. This was followed by the emplacement of the layered ultrabasic to basic intrusives of the Rustenburg Layered Suite, and subsequently the intrusion of the Bushveld Granites (Lebowa Granite Suite) (Cheney & Twist, 1988; Walraven *et al.*, 1990; Walraven & Hattingh, 1993; Schweitzer *et al.*,1995; Schweitzer & Hatton,1995a; 1995b; Walraven, 1997).

2.2 The Rustenburg Layered Suite

The Rustenburg Layered Suite comprises a 7000-9000 m thick pile of basic and ultrabasic rocks which is informally subdivided into five zones, namely the Upper, Main, Critical, Lower and Marginal Zones (Figure 2) (SACS, 1980; Walraven, 1986; Von Gruenewaldt *et al.*, 1985). The UG2 chromitite forms part of a series of chromitite layers, traditionally divided into the Lower Group, Middle Group and Upper Group chromitites, present in the Critical Zone (Cousins & Feringa, 1964; Von Gruenewaldt *et al.*, 1986; Vermaak, 1995).

The Lower Group chromitites (numbered LG1 to LG7 from the bottom upwards) occur within the pyroxenites of the lower part of the Critical zone. The Middlle Group chromitites (MG1 to MG4) straddle the boundary between the pyroxenitic lower and plagioclase-rich upper part of the Critical Zone. The Upper Group

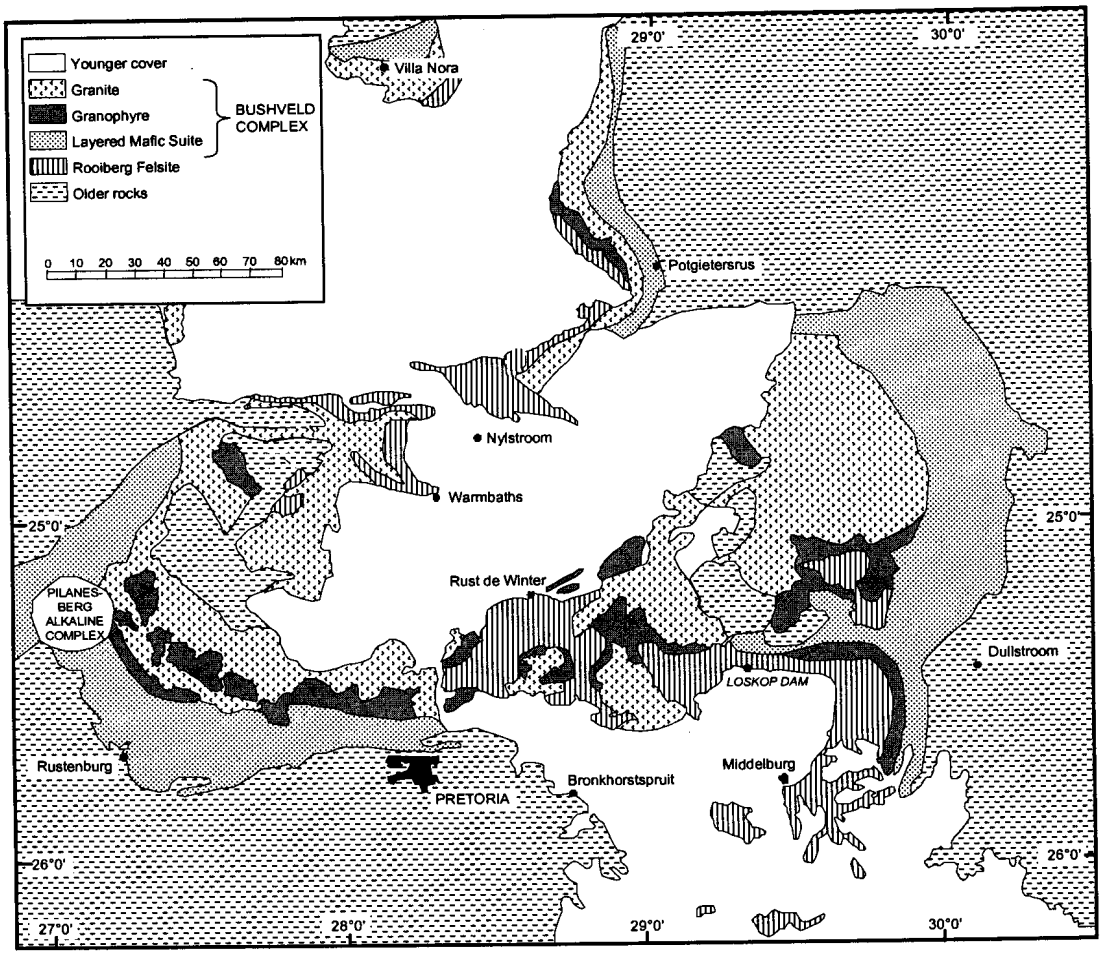

Figure 1 *Geological sketchmap showing the distribution of the rocks of the Bushveld Complex. (Courtesy of Department of Earth Sciences, University of Pretoria)*

chromitites, UG1 and UG2 (indicated in Figure 2), are found near the top of the Critical Zone. The Upper Critical subzone also hosts the platiniferous Merensky Reef.

2.3 The UG2 chromitite layer

The UG2 layer is located near the base of a 5 to 12 m thick felspathic pyroxenite layer, situated in the succession between the UG1 chromitite layer below, and the Merensky Reef above (Figure 2). Except for a few local interruptions, it can be followed continuously along strike in both the eastern and western portions of the Bushveld Complex (McLaren & de Villiers, 1982; Davey, 1992; Maier & Eales, 1994; Maier & Bowen, 1996).

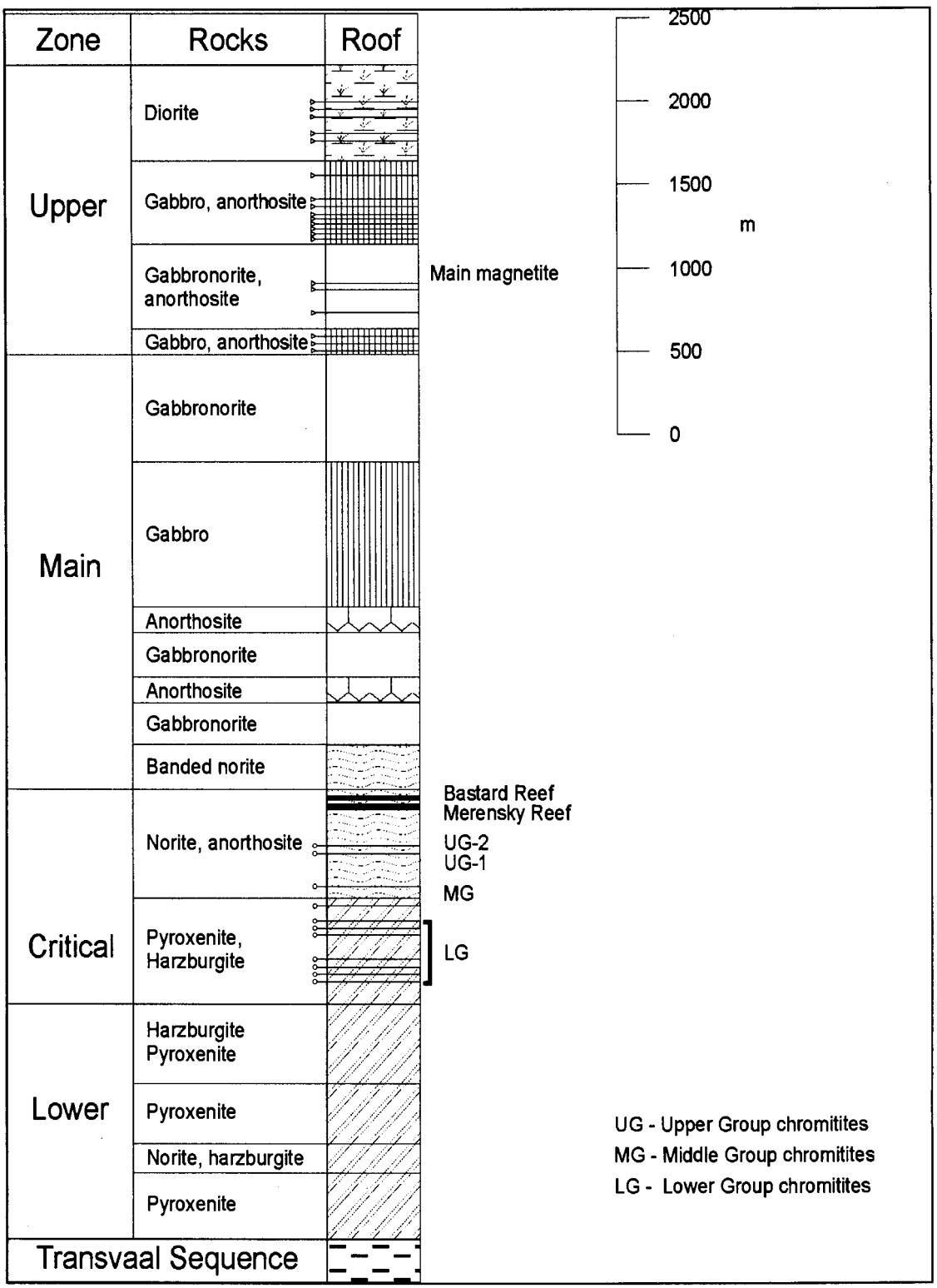

Figure 2 *Stratigraphic succession of the Rustenburg Layered Suite (after Vermaak, 1995). Chromitite and magnetite layers are indicated by o— and >— respectively.*

The thickness of the UG2 chromitite layer is usually about 1 m. A variable number of thin leaders (10-15 cm) may be present within the overlying UG2 pyroxenite, up to 3 m above the main layer (McLaren, 1980; McLaren & de Villiers, 1982; Gain,1985; 1986; Mossom, 1986; Davey, 1992; Maier & Eales, 1994; Lea, 1996; Maier & Bowen, 1996).

The UG2 layer has in many places been disrupted by late- to postmagmatic structures such as faults, potholes and iron-rich ultrabasic replacement pegmatoids. As will be discussed below, much of the reported mineralogical variation in the UG2 chromitite can be related to such disturbances. The following 'types' of UG2 chromitite have been described:

2.3.1 Undisturbed or normal UG2

In many areas the UG2 chromitite appears to be relatively undisturbed with few signs of replacement, cataclasis, recrystallisation, or talcification, with a footwall of either norite or anorthosite (Farquhar, 1986; Hiemstra, 1986; Davey,1992; Maier & Bowen, 1996; Van der Merwe *et al.*, 1998). Normal UG2 chromitite consists predominantly of chromite (60-90 volume per cent) with interstitial orthopyroxene and plagioclase. Chalcopyrite, pyrrhotite, pyrite and pentlandite are the major base-metal sulphide minerals, usually present in trace amounts at chromite-silicate grain boundaries. The PGE minerals are predominantly sulphides, mostly laurite, cooperite, an unnamed Pt-Rh-Cu-Ir-sulphide, braggite, an unnamed Pt-Pb-Cu-sulphide, and rarely, vysotskite. These minerals tend to be strongly associated with base-metal sulphide minerals, exhibiting a preference to occur at grain boundaries of base-metal sulphides with chromite and/or silicate (McLaren, 1980; McLaren & de Villiers, 1982; Viljoen & Hieber, 1986; Viljoen *et al.*, 1986a; Hiemstra, 1988b; Grimbeek, 1995).

2.3.2 UG2 with pegmatoid footwall

The UG2 chromitite is in many places underlain by a coarse-grained felspathic pegmatoid (Viljoen *et al.*, 1986b; Hiemstra, 1988a; Cawthorn & Barry, 1992; Davey, 1992; Van der Merwe *et al.*, 1998). Cawthorn and Barry (1992) reported that this pegmatoid has essentially the same mineralogy and texture as underlying pyroxenites, only the grain size is coarser. These authors postulated that the introduction of hot

primitive magma caused recrystallisation of pyroxenite, producing the coarse grain size.

During recrystallisation of the footwall, some changes also occurred in the UG2 chromitite layer itself (Hiemstra, 1985). In places the chromitite foundered and slumped into the underlying pegmatoid. Hiemstra (1985) estimated that the UG2 layer could have lost a few centimetres in this manner. Sintering (annealing or densification) of chromite, a process during which the chromite grains are enlarged until they border against each other, eliminating interstitial silicates, may be linked to this type of recrystallisation (Hiemstra, 1985; Hiemstra, 1988a, b). Redistribution of copper and nickel, and to a lesser extent the PGEs, can occur (Hiemstra, 1985). Hiemstra (1988a) speculated that changes in the grain size of base-metal sulphides and PGE minerals may occur.

2.3.3 Iron-rich ultrabasic replacement pegmatoid

Iron-rich ultrabasic pegmatoid replaced the UG2 chromitite and its associated rocks in some places (Viljoen & Scoon, 1985; Gain, 1985; Leeb-du-Toit, 1986; Viljoen *et al.*, 1986a, b; Viljoen & Hieber, 1986; Farquhar, 1986; Hofmeyr & Adair, 1993; Grimbeek, 1995). These pegmatoids are often transgressive, and their chemical effects on the surrounding lithologies are extensive. The introduction of iron, titanium, vanadium and calcium (Viljoen *et al.*, 1986b; Grimbeek, 1995) causes the formation of phases such as titaniferous magnetite and ilmenite (Viljoen & Scoon, 1985; Hiemstra, 1988b; McLaren & De Villiers, 1982; Grimbeek, 1995).

An increase in the grain sizes of chromite, sulphides, and possibly the PGE minerals, have been reported (Hiemstra, 1988b; McLaren & de Villiers, 1982; Grimbeek, 1995). Alteration of orthopyroxene and plagioclase results in the formation of low temperature hydrous silicates such as amphibole, chlorite, talc, serpentine and clay minerals (Grimbeek, 1995). The magmatic sulphides may be replaced by low temperature sulphides such as millerite, violarite, heazlewoodite, chalcocite, covellite and bornite (Hiemstra, 1988b; Grimbeek, 1995). In other places, the appearance of coarse sulphide blebs (up to 2 mm in diameter), rich in pyrrhotite, was noted (Hiemstra, 1988a; Hiemstra, 1988b; Grimbeek, 1995). Hiemstra (1988b) also reported the replacement of pyrrhotite by magnetite in some samples.

The PGE mineral assemblage is dominated by non-sulphide minerals such as alloys of Pt, Pd and Rh with Cu and Fe, PGE sulpharsenides, and Pt and Pd compounds with Sb, Bi, Te, Hg and Pb (Hiemstra, 1988b; Hofmeyr & Adair, 1993; Grimbeek, 1995).

2.3.4 UG2 associated with pothole structures

In plan, potholes are roughly circular structures, disturbing the UG2 and its surrounding lithology, causing the UG2 chromitite to occur below its normal stratigraphic elevation. They may be up to several hundred metres wide, and range from a few metres to several tens of metres deep, varying from gentle slump structures, in which the UG2 is continuous but transgresses the footwall units (Figure 3), to carrot-shaped structures in which the UG2 is broken up. Pothole structures have been reported from all over the Bushveld Complex (Leeb-Du Toit, 1986; Viljoen *et al.*, 1986a, b; Viljoen & Hieber, 1986; Farquhar, 1986; Mossom, 1986; Gain, 1986; Cawthorn & Barry, 1992; Hahn & Ovendale, 1994; Lea, 1996; Van der Merwe *et al.*, 1998; Lomberg *et al.*, 1999).

In the case of the Merensky Reef, pothole formation is associated with changes in mineralogy and mineral chemistry in the vicinity of these structures. Pegmatoidal textures, increased replacement of magmatic silicates by low temperature hydrous phyllosilicates, the presence of graphite, changes in chromite composition, and the appearance of Pt-Fe alloys as a major component of the PGE mineral assemblage have been reported (Buntin *et al.*, 1985; Ballhaus, 1988; Kinloch & Peyerl, 1990; Reid *et al.*, 1993).

Theories concerning the origin of these features abound. These theories include mechanical scouring (Schmidt, 1952), thermochemical erosion (Campbell, 1986), and the upward movement of residual magmatic liquids and/or hydrothermal fluids (Buntin, *et al.*, 1985; Ballhaus, 1988; Cawthorn & Poulton, 1988; Boudreau, 1992; Reid *et al.*, 1993). The possibility of a genetic relationship between Fe-rich replacement pegmatoid and potholes has been suggested by several investigators (Viljoen & Hieber, 1986; Farquhar, 1986; Kinloch & Peyerl, 1990).

While the involvement of a fluid phase would explain the observed changes in mineralogy, isotopic evidence presented by Carr *et al.* (1999), indicated that there was no interaction between footwall material and the overlying magma during, or after, the

formation of Merensky Reef potholes. These authors postulated that potholes represent structural features formed during depocenter subsidence (Carr *et al.*, 1994a, b), with laterally migrating Merensky magma providing the fill-in material (Carr *et al.*, 1999), offering no explanation for the reported changes in mineralogy.

No published information is available on the mineralogy of the UG2 layer in the vicinity of pothole structures. Cawthorn and Poulton (1988), during a study of pegmatoid underlying the UG2 chromitite, found no evidence of the involvement of a fluid phase during the formation of UG2 potholes.

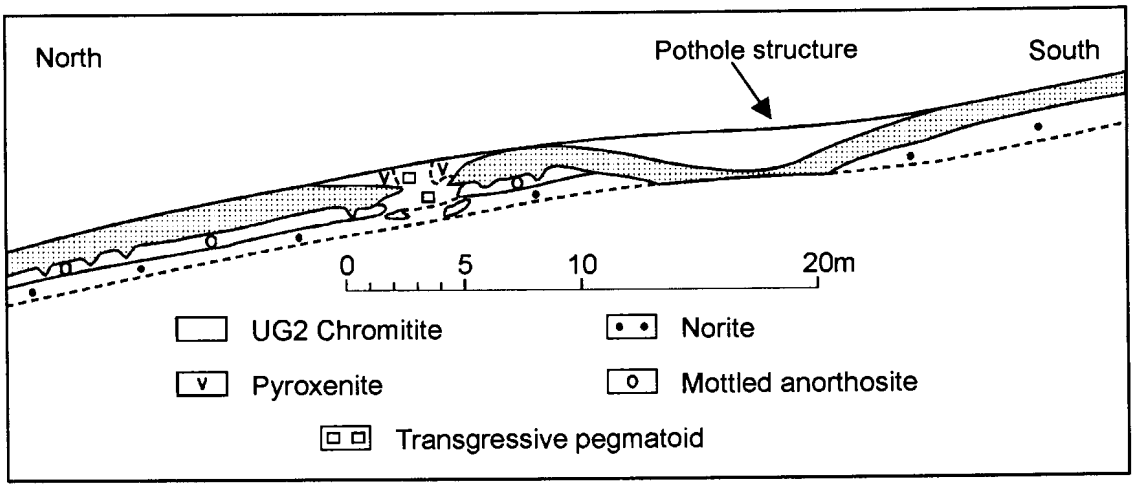

Figure 3 *Cross section through a pothole structure in the UG2 ore (Farquhar, 1986).*

2.3.5 Faulted and fractured UG2 chromitite

The rocks of the Bushveld Complex have commonly been disrupted by faulting and fracturing (Gain, 1986; Viljoen & Hieber, 1986; Viljoen *et al.*, 1986a, b). Cataclastic textures, as well as an increase in the concentration of hydrous phyllosilicate phases, can be observed in the UG2 chromitite in faulted areas (Hiemstra, 1988a).

The formation of massive chromitite from faulted areas have been reported by Kupferbürger *et al.* (1937). Worst (1986) contends that the formation of this type of ore appears to be a very localised feature, becoming friable within centimetres into surrounding unfractured ore.

Late stage fracturing, creating pathways along which fluids migrated, is widespread. Some redistribution of sulphides and PGE minerals may be found along these cracks (Hiemstra, 1988a). Schiffries and Skinner (1987) reported extensive alteration of the silicate minerals in the wallrock adjacent to fractures.

2.3.6 UG2 chromitite exposed to surface weathering

Another important alteration process, known to affect recovery processes, is surface weathering. During sample collection, sampling of weathered material was studiously avoided, as the effects of supergene alteration are beyond the scope of this investigation.

3. SAMPLING STRATEGY

3.1 Project outline

To achieve the stated objectives, the mineralogy, chemistry and flotation behaviour of fourteen samples of UG2 ore were compared as outlined in Figure 4. Each sample was crushed to <2 mm to produce a sample with mineralogical and chemical characteristics representative of unbroken ore. This was followed by comminution and rate flotation tests on each sample. Mineralogical and chemical analysis were performed on samples of crushed ore, milled feed and flotation products.

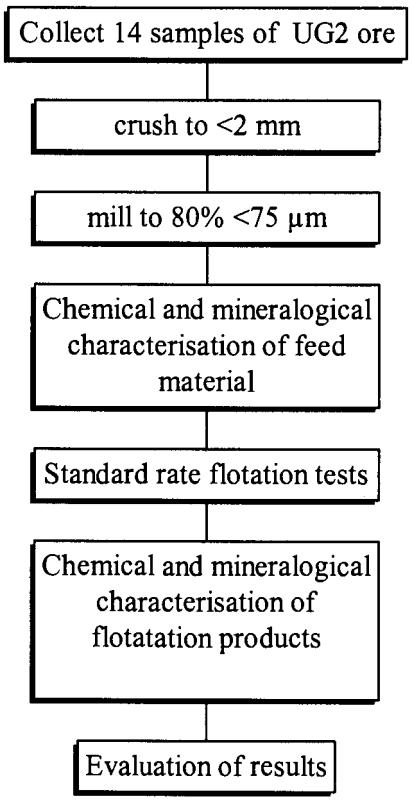

Figure 4 *Outline of experimental treatment of fourteen samples of UG2 ore.*

3.2 Sample collection

Samples were collected underground on the Lonrho mining property in the Marikana-Brits area (Figure 5). Appropriate sampling locations were identified and described by Lonrho geologists to include a variety of different "types" of UG2 chromitite. The rationale behind the sampling scheme was to obtain samples of UG2 ore with as wide a variation in mineralogical characteristics, and consequently flotation behaviour, as possible.

For reasons of confidentiality, exact sample locations cannot be disclosed. Fourteen samples were taken from three different mining areas (denoted A, B and C). A description of the geological context of each sample is given in Table 3.1. Note that Area C is characterised by more disruptions such as faults, potholes and dolerite dykes, compared to Areas A and B.

Sampling was complicated by the fact that the UG2 chromitite at a specific location had frequently been subjected to a combination of different geological disturbances. For example, sample B3, taken at the edge of a pothole, may also have been affected by iron-rich ultrabasic replacement pegmatoid present in the vicinity.

Composite samples were obtained by cutting channels across the UG2 chromitite, including ±1 cm of footwall and hangingwall respectively. In order to make up enough mass for flotation tests on each sample, a number of channels were cut adjacent to one another. The composite samples were despatched to Mintek in sample bags, where further observations on the macroscopic appearance of the samples were made by the investigator. With the exception of sample A5, all of the samples were relatively friable, crumbling upon being handled.

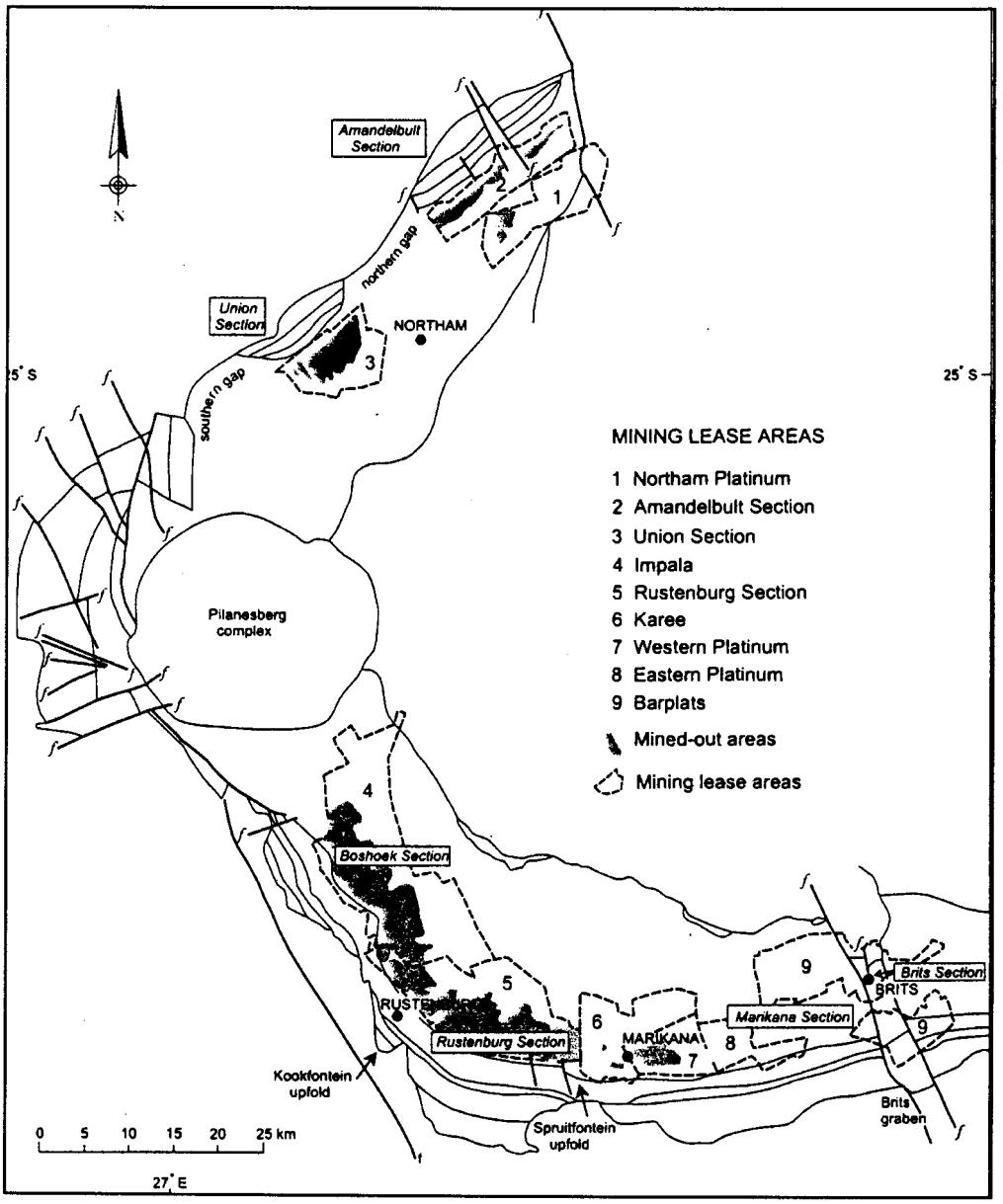

Figure 5 *Lease boundaries of the main platinum-mining operations in the Western Bushveld Complex (after Viljoen & Schürmann, 1998).*

Table 3.1 Sample description

Sample	Origin	Comments
A2	UG2 chromitite with mottled anorthosite footwall.	Lenses of coarse sugary chromite common.
B2	UG2 chromitite with norite footwall.	
A1	UG2 chromitite with pegmatoid footwall.	Anorthositic lenses with phlogopite.
B1	UG2 chromitite with pegmatoid footwall. Iron-rich ultrabasic replacement pegmatoid in the vicinity.	Extremely friable
A3	UG2 chromitite with pegmatoid footwall on the downdip side of a pothole structure.	
B3	UG2 chromitite with pegmatoid footwall taken at the edge of a pothole. Iron-rich ultrabasic replacement pegmatoid in the vicinity.	Sintering of chromite grains visible in places. Friable and coarse-grained.
A4	UG2 chromitite with footwall consisting of iron-rich ultrabasic replacement pegmatoid.	Sintering of chromite grains could be seen at the bottom of the layer. In places quite coarse-grained and crumbly. Lenses and bands of anorthosite (±0.5 cm thick).
B4	UG2 chromitite with pegmatoid footwall taken next to a fault. Iron-rich ultrabasic replacement pegmatoid footwall in the vicinity.	Pitch black and coarse-grained with high degree of sintering of chromite grains. Associated with pegmatitic veins consisting of quartz, hornblende and biotite.
A5	UG2 chromitite in fault zone. Iron-rich ultrabasic replacement pegmatoid in the vicinity.	The general appearance of the sample is extremely fine-grained and massive. Abundant veins of secondary minerals.

Table 3.1 continued *Sample description.*

Sample	Location	Comments
C1	UG2 chromitite at the edge of a pothole structure.	Coarse calcite veins present. Abundant hydrous silicates along shear planes and in veins. Sintering of chromite grains in places. Coarse and crumbly.
C2	UG2 chromitite in an area where the pegmatoid footwall pinches out. The footwall consists of a 2 cm thick anorthosite band followed by norite.	Relatively hard sample, even where coarse-grained. The hardest sample from area C.
C3	UG2 chromitite from a fault zone.	Criss-crossed by veins of hydrous silicates and quartz. Relatively hard and cohesive.
C4	UG2 chromitite with pegmatoid footwall. About 50 m from the pothole in C1.	Relatively hard. Occasional cracks healed by secondary minerals such as hydrous silicates.
C5	This sample was taken from an area where the UG2 chromitite layer is characterised by the presence of an anorthosite band, sharp top and bottom, approximately 6 cm thick. About 20 m from a dolerite dyke.	Relatively hard. Similar to C2 and C4. Very little signs of alteration. No veins visible.

4. METHOD

4.1 Comminution

Liberation of the valuable components of an ore, in this case PGE minerals and base-metal sulphides, from the gangue minerals is accomplished by comminution, i.e. crushing and milling, to such a degree that the product approaches a mixture of liberated particles of valuable minerals and gangue.

For the purpose of this project, each sample was subjected to jaw crushing followed by cone crushing to reduce the particle size to <2mm. A representative sub-sample of each sample at <2mm was taken for mineralogical and chemical analysis. A rotary sample splitter was used to ensure that sub-samples were obtained in a representative manner.

The remainder of the sample was crushed to <1.7 mm before milling to 80% <75 μm in a rod mill, using standard milling procedures for this type of ore.

4.2 Froth flotation

4.2.1 ***General principles*** (Gaudin, 1957; Rogers, 1962; Wills, 1981; Herrera-Urbina *et al.*, 1990)

Froth flotation involves the chemical treatment of a mixture of ground ore and water to create conditions favourable for the attachment of certain mineral particles to air bubbles. The air bubbles carry the selected minerals to the surface of the pulp and form a stabilised froth, which is skimmed off, while the other minerals remain submerged in the pulp.

Whether or not a mineral can be recovered by flotation, is determined by its surface characteristics. A surface formed by rupture of Van der Waals bonds does not readily attach to water dipoles, and will be hydrophobic (water-repellant). Minerals characterised by this type of surface are naturally floatable and include graphite, sulphur, molybdenite and talc.

In contrast to this, a surface formed by the rupture of covalent or ionic bonds can chemically react with the environment and is therefore hydrophylic. The surface

characteristics of minerals can be modified to create hydrophobic surfaces by the interaction with flotation reagents (collectors and activators). The xanthate collector used to promote flotation of the sulphide minerals will generally not attach to oxide and silicate gangue minerals. To further ensure that gangue minerals do not float, depressants, which enhance the hydrophylic nature of the gangue minerals, are added to the system.

4.2.2 Standard rate flotation tests

Since the purpose of the rate flotation tests were to determine the effect of changes in the mineralogy of the ore on the flotation behaviour, all other factors (equipment, operating factors and reagents) affecting flotation response were kept constant for all samples.

Conditions of rate flotation tests

Standardised rate flotation tests were carried out by the Minerals Processing Division at Mintek. A standard 3*l* Denver laboratory flotation cell was used for the flotation testwork. Froth was removed manually by operating two scraper blades simultaneously across the complete cell area every 15 seconds (Figure 6). The scraping depth was controlled at 0.6 cm below the overflow lip. Reagent conditions and contact times are listed in Table 4.1.

The ground ore was floated in one kilogram batches. Rougher concentrates were collected after 1, 3, 8, 15 and 20 minutes of flotation. Six kilograms of each sample had to be floated in this way to generate enough sample mass for chemical and mineralogical analysis.

After weighing of the wet concentrate and tailings fractions, excess water was filtered off, and solids dried in an oven. The dry samples were weighed and representative samples taken for chemical and mineralogical analysis.

Figure 6 *Operator performing rate flotation tests.*

Table 4.1 *Reagent additions and contact times*

Reagent dosage and contact times	*g/t*	*minutes*
*$CuSO_4.5H_2O$ (activator)**	40	5
SIBX (collector)	180	2
Norilose (depressant)	120	2
Dow 200 (frother)	30	1
Flotation	20 minutes	
pH	~9	
Temperature	~20 ° C	

* *The activator forms a precipitate on the surface of the sulphide minerals, thereby improving floatability and contact with the xanthate collector.*

Reproducibility of rate flotation tests

Reproducibility of rate flotation tests was determined from the mass recoveries obtained during flotation tests on eighteen 1 kilogram sub-samples of sample A1. The results reported in Table 4.2 show that the reproducibility of the rate flotation tests is acceptable with a relative error well below 10 per cent at the 95% confidence limit.

Interpretation of flotation test results

It has been demonstrated that plant rougher flotation results correlate better with differences in the rate of recovery in the laboratory, rather than with changes in equilibrium recovery (recovery at long flotation times) (Klimpel, 1980; 1988). Mathematical flotation models that incorporate both a recovery and a rate function can completely describe flotation time-recovery profiles and provide an excellent tool to evaluate flotation tests (Dowling *et al.*, 1985). Surprisingly small differences in rate flotation parameters in laboratory tests are real, and often much bigger, in a plant sense. Marais (1989) identified the modified Kelsall model (Kelsall, 1961) as being appropriate for the evaluation of the time-recovery profiles of PGE+Au from UG2 ore. This model is based on the assumption that PGE mineral-bearing particles have two distinct and different rates of flotation. The model states:

$$R = U\,[1-((1-\phi)\exp(-k_f t) + \phi \exp(-k_s t))]$$

where R = recovery at time t; ϕ = fraction of slow floating mineral; k_s = rate constant for slow floating mineral min^{-1}; k_f = rate constant for fast floating mineral min^{-1}; U = ultimate recovery at infinite time.

Application of this model to the PGE+Au data for sample A1 (Table 4.3 and Figure 7) indicates that the ultimate recovery, U, for PGE+Au in this sample, at a grind of 80%<75µm, and under the given flotation conditions, is 96 per cent. Of the floatable fraction, 18 per cent (∴ 16 per cent of the total PGE+Au) is slow-floating with a flotation rate constant of 0.22 min^{-1}, hence 96-16=80 per cent is fast-floating (flotation rate constant: 2.38 min^{-1}). Goodness of fit of the model was evaluated by a loss function, Loss=(Observed-Predicted)^2, i.e. the sum of the squared deviation about the predicted values. The better the fit, the closer to 0 the Loss value will be.

Table 4.2 *Mass recoveries to rougher concentrate after 1, 3, 8 15 and 20 minutes of flotation for eighteen 1 kilogram sub-samples of sample A1. Upper and lower confidence limits around the average were calculated for sets of six individual tests at the 95% confidence level using resampling statistics (Simon & Bruce, 1991).*

	Mass recovery (%)						**Cumulative mass recovery (%)**					
Flotation product	*RC1*	*RC2*	*RC3*	*RC4*	*RC5*	*RT*	*RC1*	*RC2*	*RC3*	*RC4*	*RC5*	*RT*
Time	*0-1 mins.*	*1- 3 mins.*	*3-8 mins.*	*8-15 mins.*	*15-20 mins.*		*0-1 mins.*	*1-3 mins.*	*3-8 mins.*	*8-15 mins.*	*15-20 mins.*	
Test #1	3.6	2.0	2.6	1.7	0.5	89.6	3.6	5.6	8.2	9.9	10.4	89.6
Test #2	3.8	2.3	2.6	1.5	0.5	89.4	3.8	6.0	8.6	10.1	10.6	89.4
Test #3	3.8	2.5	2.9	1.6	0.6	88.8	3.8	6.3	9.1	10.7	11.2	88.8
Test #4	4.1	2.5	2.7	1.6	0.5	88.6	4.1	6.5	9.3	10.9	11.4	88.6
Test #5	3.4	2.4	2.8	1.6	0.6	89.2	3.4	5.8	8.6	10.2	10.8	89.2
Test #6	3.3	2.5	2.8	1.7	0.5	89.2	3.3	5.8	8.6	10.3	10.8	89.2
Test #7	3.7	2.6	2.9	1.6	0.6	88.6	3.7	6.4	9.2	10.8	11.4	88.6
Test #8	4.0	2.4	2.7	1.5	0.7	88.8	4.0	6.4	9.1	10.6	11.2	88.8
Test #9	4.2	2.5	2.8	1.6	0.6	88.3	4.2	6.7	9.5	11.1	11.7	88.3
Test #10	4.3	2.9	3.0	1.5	0.5	87.8	4.3	7.2	10.2	11.7	12.2	87.8
Test #11	3.7	2.6	2.9	1.7	0.6	88.5	3.7	6.3	9.2	10.9	11.5	88.5
Test #12	3.2	2.4	2.8	1.5	0.6	89.5	3.2	5.6	8.5	9.9	10.5	89.5
Test #13	3.5	2.3	2.4	1.5	0.6	89.7	3.5	5.8	8.2	9.7	10.3	89.7
Test #14	4.1	2.2	2.8	1.6	0.6	88.7	4.1	6.3	9.1	10.8	11.3	88.7
Test #15	3.9	2.5	2.7	1.5	0.6	88.8	3.9	6.4	9.1	10.6	11.2	88.8
Test #16	3.4	2.1	2.5	1.5	0.6	89.9	3.4	5.5	8.0	9.5	10.1	89.9
Test #17	4.0	2.3	2.7	1.5	0.6	88.9	4.0	6.3	9.0	10.6	11.1	88.9
Test#18	3.6	2.2	2.3	1.4	0.6	90.0	3.6	5.8	8.0	9.4	10.0	90.0
Average	3.7	2.4	2.7	1.6	0.6	89.0	3.7	6.1	8.9	10.4	11.0	89.0
Lower limit	3.5	2.2	2.6	1.5	0.5	88.5	3.5	5.8	8.4	10.0	10.6	88.6
Upper limit	4.0	2.6	2.8	1.6	0.6	89.5	4.0	6.5	9.3	10.9	11.5	89.5
Absolute error %	0.3	0.2	0.1	0.1	0.1	0.5	0.3	0.4	0.5	0.5	0.5	0.5
Relative error %	6.7	8.3	3.7	3.2	8.7	0.6	6.7	5.7	5.1	4.3	4.1	0.5

RC = Rougher concentrate RT = Rougher tailings

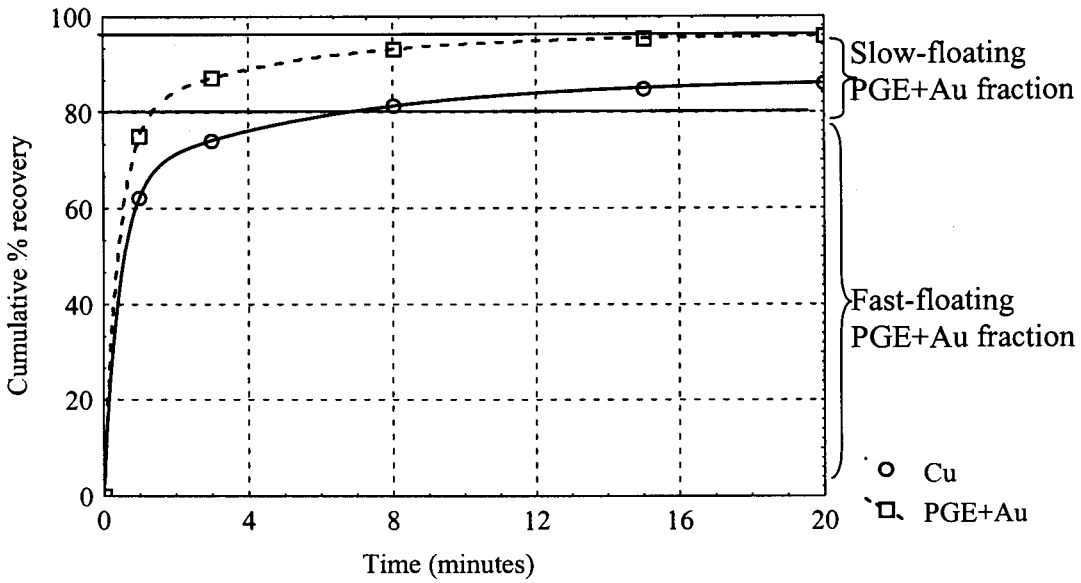

Figure 7 *Time-recovery profile for Cu and PGE+Au from sample A1. The curves were fitted to the data using the modified Kelsall model. The loss function (Loss = (Observed-Predicted)^2) of 0.018 and 0.024 for Cu and PGE+Au, respectively, indicates a good fit.*

Table 4.3 *Model parameters of three replicate tests on sample A1 for PGE+Au and 90% confidence interval using the Student t-distribution.*

PGE+Au	*U (%)*	ϕ	k_f (min^{-1})	k_s (min^{-1})
Test 1	96.1	0.17	2.39	0.22
Test 2	96.6	0.15	2.30	0.20
Test 3	95.7	0.20	2.47	0.23
Average	96.1	0.18	2.38	0.22
90% confidence interval	±0.6	±0.04	±0.12	±0.02

4.3 Chemical analysis procedures

Chemical analysis of feed material and flotation products were performed by the Analytical Services Division (ISO Guide 25 accredited) at Mintek. The techniques used are briefly outlined in Table 4.4. The precision of the analyses for the different

elements, calculated from duplicate analyses (Kaiser & Specker, 1955), is listed in Tables 4.5 and 4.6.

Table 4.4 *Chemical analysis techniques.*

Elements	**Sample preparation**	**Measurement technique**
Cr, Fe, Ca, Mg, Al, Si, Ti and Mn	Fusion with sodium peroxide followed by dissolution in HNO_3.	ICP-OES
K and Na	Dissolution in HF, HCl and $HClO_4$ followed by drying and HCl dissolution.	AA
Acid soluble Cu and Ni	Dissolution in brominated HCl and HNO_3.	ICP-OES (>500 ppm) AA (< 500 ppm)
Total Cu and Ni	Fusion with sodium peroxide followed by dissolution in brominated HCl and HNO_3.	ICP-OES (>500 ppm) AA (< 500 ppm)
Co	Fusion with sodium peroxide followed by dissolution in brominated HCl and HNO_3.	ICP-MS
Sulphur	Oxidation of sulphur to SO_2 by combustion at high temperature.	Infrared absorption
PGE+Au (Pt, Pd, Rh and Au)	Fire assay with Pb collection	ICP-MS

ICP-OES Inductively Coupled Plasma-Optical Emission Spectrometry

AA Atomic Absorption

ICP-MS Inductively Coupled Plasma-Mass Spectrometry

The lead collection technique is routinely used throughout the platinum-mining industry in South Africa to determine the platinum, palladium, rhodium and gold content (PGE+Au) of ores and plant products (Van Wyk, 1980). It is known however, that this method systematically underestimates the PGE+Au content, especially rhodium, compared with the more tedious and expensive nickel-sulphide collection

technique (Robért *et al.*, 1971; Robért *et al.*, 1997). Unfortunately, due to technical problems experienced during nickel-sulphide collection, coupled with the small amount of sample available, the analysts had to revert to the Pb collection technique for analysis of the samples produced during this study.

Table 4.5 *Analytical error calculated at the 95% confidence level for S, acid soluble Cu, total Ni , acid soluble Ni, PGE+Au (Pt+Pd+Rh+Au), Pt, Pd and Rh, over different ranges of concentration levels. N, e and E refer to the number of analyses, absolute error, and relative error respectively.*

Element	N	Range	e	E
S	38	0.01-0.10 %	± 0.01	~ 20 %
	50	0.10-1.00 %	± 0.01	~ 2 %
	6	1-10 %	± 0.11	~ 2 %
Cu a.s.	60	10-100 ppm	± 1	~ 2 %
	174	100-1000 ppm	± 13	~ 2 %
	28	0.1-1 %	± 0.02	~ 4 %
Ni t.	78	0.1-0.5 %	± 0.01	~ 4 %
Ni a.s.	156	100-1000 ppm	± 23	~ 5 %
	140	0.10-1.00 %	± 0.01	~ 2 %
PGE+Au	16	0.2-1.0 ppm	± 0.05	~ 11 %
	70	1-10 ppm	± 0.2	~ 4 %
	38	10-50 ppm	± 1	~ 5 %
Pt	34	0.1-1.0 ppm	± 0.03	~ 15 %
	76	1-10 ppm	± 0.7	~ 14 %
	78	10-100 ppm	± 3	~ 6 %
Pd	50	0.1-10 ppm	± 0.02	~ 9 %
	88	1-10 ppm	± 0.3	~ 8 %
	52	10-50 ppm	± 1.3	~ 5 %
Rh	62	0.1-1.0 ppm	± 0.06	~ 15 %
	106	1-15 ppm	± 0.59	~ 9 %

a.s.= acid soluble *t.=total*

Table 4.6 *Analytical error calculated at the 95% confidence level for Cr, Fe, Mg, Al, Si, Ca and Ti (expressed as oxides) over different ranges of concentration levels. N, e and E refer to the number of analyses, absolute error, and relative error respectively.*

Oxide	N	Range	e	E
Cr_2O_3	82	10-35 %	0.26 %	~ 1 %
Fe_2O_3	70	10-30 %	0.27 %	~ 1 %
MgO	68	10-20 %	0.10 %	~ 1 %
Al_2O_3	68	10-20 %	0.15 %	~ 1%
SiO_2	80	10-35 %	0.16 %	~ 1 %
CaO	64	2-6 %	0.1 %	~ 3 %
TiO_2	58	0.2-1.0 %	0.0 %	< 1 %

4.4 Comparison of calculated and analysed feed grades

A further indication of the quality of the flotation results (mass recoveries and chemical analyses combined) is given by the comparison of analysed and calculated feed grades. The latter value is back-calculated from the mass distributions and chemical analyses of flotation products. In Table 4.7 the analysed and calculated PGE+Au, platinum, palladium and rhodium feed grades of three sub-samples of sample A1 are compared. In the case of PGE+Au, platinum and palladium, the analysed and calculated feed values tally well, with the percentage difference between the two values consistently below 5 per cent. In the case of rhodium the differences are larger (31, 22 and 24 per cent for the three sub-samples), due to the increased error associated with the lower concentration levels of this element.

Table 4.7 *A comparison of calculated and analysed PGE+Au, Pt, Pd and Rh feed grades for three sub-samples of sample A1.* [1] *= feed grades calculated from mass distributions and analysed grades of flotation product samples* [2] *= analysed feed grade* [3] *= % difference*

A1 Test A	*Dry mass (g)*	*Dry mass (g) cum.*	*Mass Distr. %*	*Mass Distr. % cum.*	*PGE+Au g/t*	*PGE+Au g/t cum.*	*Pt cont. g/t*	*Pt cont. g/t cum.*	*Pd cont. g/t*	*Pd cont. g/t cum.*	*Rh cont. g/t*	*Rh cont. g/t cum.*
RC1	218.00	218.00	3.64	3.64	108.84	108.84	66.25	66.25	29.03	29.03	11.63	11.63
RC2	141.20	359.20	2.36	5.99	26.45	76.45	16.00	46.50	7.44	20.54	2.91	8.20
RC3-5	292.90	652.10	4.89	10.88	9.45	46.36	5.66	28.15	2.77	12.56	1.02	4.97
RT	5339.60	5991.70	89.12	100.00	0.24	**5.26**[1]	0.13	**3.18**[1]	0.09	**1.44**[1]	0.02	**0.56**[1]
						5.06[2]		**3.08**[2]		**1.42**[2]		**0.43**[2]
						4[3]		**3**[3]		**1**[3]		**31**[3]
A1 Test B	*Dry mass (g)*	*Dry mass (g) cum.*	*Mass Distr. %*	*Mass Distr. % cum.*	*PGE+Au g/t*	*PGE+Au g/t cum.*	*Pt cont. g/t*	*Pt cont. g/t cum.*	*Pd cont. g/t*	*Pd cont. g/t cum.*	*Rh cont. g/t*	*Rh cont. g/t cum.*
RC1	231.30	231.30	3.86	3.86	101.33	101.33	58.70	58.70	29.40	29.40	10.38	10.38
RC2	154.50	385.80	2.58	6.44	24.03	70.37	14.15	40.86	7.00	20.43	2.55	7.24
RC3-5	298.50	684.30	4.98	11.41	9.00	43.60	5.28	25.34	2.80	12.74	0.85	4.46
RT	5310.70	5995.00	88.59	100.00	0.21	**5.16**[1]	0.13	**3.01**[1]	0.08	**1.53**[1]	0.02	**0.53**[1]
						5.06[2]		**3.08**[2]		**1.42**[2]		**0.43**[2]
						2[3]		**2**[3]		**7**[3]		**22**[3]
A1 Test C	*Dry mass (g)*	*Dry mass (g) cum.*	*Mass Distr. %*	*Mass Distr. % cum.*	*PGE+Au g/t*	*PGE+Au g/t cum.*	*Pt cont. g/t*	*Pt cont. g/t cum.*	*Pd cont. g/t*	*Pd cont. g/t cum.*	*Rh cont. g/t*	*Rh cont. g/t cum.*
RC1	224.40	224.40	3.74	3.74	99.37	99.37	60.53	60.53	29.38	29.38	10.20	10.20
RC2	136.10	360.50	2.27	6.01	26.50	71.86	16.30	43.83	7.20	21.01	2.80	7.41
RC3-5	280.40	640.90	4.68	10.69	10.80	45.15	6.30	27.41	3.10	13.17	1.27	4.72
RT	5354.60	5995.50	89.31	100.00	0.25	**5.04**[1]	0.16	**3.07**[1]	0.09	**1.49**[1]	0.03	**0.53**[1]
						5.06[2]		**3.08**[2]		**1.42**[2]		**0.43**[2]
						0[3]		**0**[3]		**5**[3]		**24**[3]

4.5 Mineralogical techniques

4.5.1 X-ray diffraction (XRD)

Prior to analysis, samples were pulverised in a Siebtechnik vibratory ring mill for 2 minutes. This was followed by a 10 minute grinding session in the McCrone Micronising Mill to minimise particle-size effects during analysis. A Siemens D-500 diffractometer using CuKα radiation was employed. The sample was scanned over the range of 4 to 76° 2θ at a step size of 0.02° 2θ and a counting time of 1 second per step. This configuration gives a lower detection limit of approximately 3 to 4 volume per cent of the crystalline phases present in the sample. In the case of layer silicates such as talc and chlorite, the detection limit can be expected to be lower due to preferred orientation of these phases.

X-ray diffraction was used to investigate major variations in the mineralogy of the ore and product samples, particularly with regard to the layer silicates such as talc, chlorite and amphibole. The low concentrations of these minerals, combined with their tendency for preferred orientation, make quantification of these phases almost impossible task. Consequently, X-ray diffractograms were evaluated in a purely qualitative manner.

4.5.2 Preparation of polished sections

The stereological principles on which the analysis of polished sections are based are valid only if the features to be measured are in random plane sections, and are sampled representatively. Sample preparation frequently represents the main source of error in measurements on polished sections (Petruk, 1976; Rowlands *et al.*,1991). To minimise the error introduced during sampling, a rotary sample splitter was used to ensure that sub-samples were obtained in a representative manner.

One of the problems during preparation of polished sections of powdered samples is the segregation of particles of different shape, size and density. To counteract the effect of segregation, the following procedures were followed: The sample is mixed with Araldite resin in a small pill-vial and then left to cure at 60°C. The result is a small cylindrical piece of araldite (~1cm diameter by 0.5 cm length) containing the

sample particles. This cylinder is then cut parallel to the direction of settling with a diamond saw. The resulting sliver is remounted in Perspex rings and polished according to standard procedures. To obtain data on a representative sample, measurements have to be made on continuous traverses, parallel to the direction of settling (Bushell, 1987; Oosthuyzen, 1987).

It is essential that sample contamination, such as that due to the introduction of brass and lead from sawing and polishing equipment for instance, or cross-contamination between samples during sample handling, is avoided. In addition, artefacts, such as air bubbles, can cause electrostatic charging of the surface, leading to errors during image-analysis measurements.

The conventional approach is to screen each sample into several size fractions, followed by weighing, chemical analysis, and image-analysis measurements on polished sections of each size fraction (Petruk *et al.*, 1986; Van den Heever, 1995). However, in the case of the samples under investigation, it was decided to perform the measurements on unscreened samples. Furthermore, no attempt was made to avoid touching grains by the addition of a filler material, such as graphite (Miller *et al.*, 1982; Jackson *et al.*, 1984). The reasons for this approach are as follows: As a result of the low concentration levels at which the base-metal sulphides and PGE minerals are present in these samples, very little concentrate is generated during flotation. To generate enough flotation concentrate to allow chemical and mineralogical analysis of several size fractions, would necessitate the flotation of several more kilograms of sample. Dilution of samples by addition of a filler material, would mean that a larger number of polished sections have to be scanned. If enough filler is added for effective separation of touching grains in a fine-grained fraction fraction, several times the area has to be scanned to find the same number of PGE mineral grains, increasing analysis time per sample from days to weeks.

4.5.3 Optical microscopy

Polished sections of crushed feed, milled feed, and flotation products were examined under the ore microscope (Zeiss Axioplan) to identify the major ore minerals and their

relationships. A number of thin sections were examined to determine the identity and mode of occurrence of the silicate minerals.

4.5.4 Scanning-electron microscopy (SEM)- Energy-dispersive X-ray spectrometry (EDS)

Scanning electron microscopy (Cambridge S360 and LEO S440) coupled with energy-dispersive X-ray analysis (Link AN 10000 and Oxford Isis) was used as an aid to mineral identification. Full quantitative to semi-quantitative EDS analysis was carried out on a number of silicate minerals. The elements analysed for, and the standards used, are listed in Table 4.8.

Analytical conditions were 20 kV accelerating voltage, a beam current of 3 nA, and a counting time of 50 seconds. A $\phi(\rho Z)$ matrix correction procedure was applied to the raw data. Under these conditions the level of precision for all elements, at concentration levels down to 0.5 mass per cent, was less than ±0.1 mass per cent (99% confidence level). Secondary standards of enstatite, diopside, hypersthene, hornblende and anorthite were analysed to ensure the level of accuracy. Beam stability was monitored by measuring the sample current every 15 minutes.

Table 4.8 *Elements (expressed as oxides) analysed for and standards used during quantitative EDS analysis of silicate minerals.*

Element	**Standard**
Na_2O	Albite
MgO	MgO Periclase
Al_2O_3	Al_2O_3 Corundum
SiO_2	SiO_2 Quartz
K_2O	Microcline
CaO	$CaSiO_3$ Wollastonite
TiO_2	TiO_2 Rutile
Cr_2O_3	Cr_2O_3
MnO	Mn_3O_4 Hausmanite
Fe_2O_3	Fe_2O_3 Hematite
NiO	NiO

4.5.5 Electron-microprobe analysis

Chromite

Quantitative electron-microprobe analysis using WDS (wavelength dispersive X-ray spectrometry) on chromite was carried out on an ARL-SEMQ instrument. The following oxides were analysed for: SiO_2, TiO_2, V_2O_3, Al_2O_3, Cr_2O_3, FeO, MnO, NiO, CoO, Cu_2O, ZnO, MgO and CaO. Standards used were pure oxides except in the case of Ca for which diopside ($CaMgSi_2O_6$) was used.

Duplicate analyses were obtained for each grain. The operating conditions were 15 kV accelerating voltage and 35 nA beam current. Counting times were 50 seconds on background and 100 seconds on the peak. A $\phi(\rho Z)$ matrix correction procedure was applied to the raw counting data. The detection limits under these conditions are listed in Table 4.9.

Table 4.9 *Detection limits (D.L.) (99% confidence level) and precision (95% confidence level) for oxides analysed. Analytical precision was calculated at the 95% confidence level from duplicate analyses of 155 grains (Kaiser & Specker, 1955).*

Oxide	D.L. (ppm)	Range (wt%)	Precision (wt%)	X-ray line
MnO	230	0.23 to 0.32	±0.03	K_α
NiO	300	0.06 to 0.20	±0.03	K_α
ZnO	500	0.00 to 0.19	±0.05	K_α
V_2O_3	1040	0.17 to 0.64	±0.10	K_α
CoO	740	0.00 to 0.12	±0.05	K_α
Cu_2O	1170	0.00 to 0.17	±0.06	K_α
MgO	360	7.67 to 11.03	±0.39	K_α
Al_2O_3	370	13.50 to 18.70	±0.23	K_α
FeO	100	26.41 to 32.06	±0.34	K_α
SiO_2	90	0.00 to 3.89	±0.62	K_α
TiO_2	80	0.49 to 5.75	±0.51	K_α
Cr_2O_3	70	39.86 to 46.26	±0.54	K_α
CaO	70	0.00 to 0.13	±0.00	K_α

Base-metal sulphides and PGE minerals

Quantitative electron-microprobe analyses of PGE minerals and base-metal sulphides were carried out on a JEOL-Superprobe 733 with a Voyager 3 upgrade WDS/EDS.

Base-metal sulphides

Wavelength dispersive X-ray analysis was used for the determination of Pt, Pd, Rh, Cu, Fe, Ni, Cu, Co and S in pentlandite, chalcopyrite, pyrite, pyrrhotite, millerite and siegenite.

The following standards were used:

Pure metal for Rh.
$Pt_{0.7}Pd_{0.3}S_{1.0}$ for Pt.
PdS for Pd.
Co_9S_8 for Co.
NiS for Ni.
FeS for Fe and S in all phases except chalcopyrite.
$CuFeS_2$ for Cu and Fe in chalcopyrite.

The operating conditions were an accelerating voltage of 15 kV and a beam current of 30 nA. Counting times were 200 seconds on the peak and 200 seconds on background for the platinum-group elements and 30 seconds for the major elements. A PROZA matrix correction procedure was applied to the raw counting data. The detection limits and reproducibility under these conditions are reported in Tables 4.10 and 4.11.

The purpose of these analyses was twofold - firstly to chemically characterise the base-metal sulphides in terms of their major components, and secondly to investigate the presence of trace amounts of platinum, palladium, and rhodium in solid solution form in these phases. At least two analyses were performed on each grain - the reported values are the mean values of these two analyses. If only one of the analyses indicated the presence of significant platinum, palladium or rhodium, additional points were analysed. Isolated high values were assumed to be due to the presence of discrete PGE minerals either too small to be recognised on the backscattered-electron image, or below the surface of the polished section.

Table 4.10 *Analytical reproducibility of S, Fe, Cu, Co and Ni in pyrrhotite, pentlandite, chalcopyrite, pyrite, millerite and siegenite calculated at the 95% confidence level from duplicate analyses (Kaiser & Specker, 1955). n = the number of grains on which the calculations were based.*

	Pyrrhotite	**Pentlandite**	**Chalcopyrite**	**Pyrite**	**Millerite**	**Siegenite**
n	42	55	53	52	29	7
S	38.10 ±0.58	33.26 ±0.49	34.91 ±0.67	52.45 ±0.83	35.27 ±0.58	41.70 ±0.84
Fe	61.41 ±0.96	33.81 ±0.53	30.44 ±0.59	44.69 ±0.95	1.27 ±0.16	1.64 ±0.97
Ni	0.10 ±0.39	31.75 ±0.62	0.04 ±0.11	2.57 ±0.41	62.24 ±0.84	32.78 ±1.19
Co	0.07 ±0.05	0.58 ±0.07	0.04 ±0.05	0.68 ±0.62	0.82 ±0.08	21.74 ±0.64
Cu	0.02 ±0.04	0.05 ±0.07	34.04 ±0.79	0.33 ±0.05	0.05 ±0.09	0.03 ±0.04

Table 4.11 *Detection limits of Pt, Rh, Pd and Ru in ppm in pyrrhotite, pyrite, chalcopyrite, pentlandite and millerite calculated at the 99% confidence level.*

	Pyrrhotite	**Pyrite**	**Chalcopyrite**	**Pentlandite**	**Millerite**	**X-ray line**
Pt	295	320	315	300	300	M_α
Rh	225	200	210	225	215	L_α
Pd	285	265	290	295	285	L_β
Ru	210	205	210	205	215	L_α

It should be noted that, in the case of trace element analysis, inaccuracies are introduced when standard correction procedures are applied due to differences in the concentration levels of the relevant elements between calibration standards and the sample being analysed. As no suitable calibration standards of sulphide with trace amounts of PGEs were available, the determination of trace amounts of PGEs in base-metal sulphides should be considered semi-quantitative.

PGE minerals

The major objective of the analysis of the PGE minerals was mineral identification. No attempt was made to investigate differences in PGE mineral composition between samples. Due to the small grain sizes of the PGE minerals, duplicate analyses could not be obtained on all grains.

The following elements were analysed for by wavelength dispersive X-ray analysis: As, S, Ru, Rh, Pd, Te, Pt, Hg, Pb, Bi, Fe, Co, Ni and Cu. The operating conditions were accelerating voltage 20kV, beam current 20 nA, and counting time 20 seconds peak count. A Duncumb-Reed correction procedure was applied to the raw counting data.

4.6 Image-analysis techniques

4.6.1 Introduction

Microscopic investigations play a crucial role in the development and monitoring of metallurgical processes. Traditionally, such investigations were carried out by mineralogists who used their training and experience to make observations regarding aspects such as mineral identification, the modal proportions of minerals, their grain sizes, shapes, associations and degree of liberation of valuable constituents. These observations are generally made on polished sections of ores and mineral processing products. Over the years, researchers (amongst others Chayes, 1956; 1963; Jones & Shaw, 1973; Petruk, 1976; 1986; 1988a; 1993; 1994; Gateau, 1978; Gateau & Prevosteau, 1978; Oosthuyzen, 1983; 1987) have proposed and used various methods and techniques to quantify microscopic observations, eventually leading to the development of automated image-analysis techniques.

4.6.2 Application to UG2 feed and product samples – general principles

The Leica Cambridge morphochemical-analysis system at Mintek consists of a Quantimet 570 image analyser fully integrated with a Stereoscan 360 SEM and a Link AN 10000 EDS system (Figure 8). Using the programming language, QBASIC, this system can be programmed to automatically scan across polished sections, and to perform image-analysis routines tailor-made for different applications. These include quantitative information on the modal composition of the samples, as well as grain-size distributions and mode of occurrence of specific minerals. All the image analysis routines used during this investigation consist of various combinations of a number of basic steps:

Image generation and transfer

Backscattered-electron images generated by the SEM are used as input to the image analyser. Conversion of the analogue image into a digital image results in a grid of 512 x 512 pixels (or picture elements), each with a specific grey level value between 0 (black) and 255 (white). ‡

Figure 9 represents a typical backscattered-electron image of crushed UG2 ore. In this image different mineral phases show up with different shades of grey (or grey levels), such that phases with a high weighted mean atomic number (and consequently high backscattered-electron coefficient, $\bar{\eta}$ (Reed, 1975; Heinrich, 1981)) like the PGE minerals, appear very bright, while phases with a low weighted mean atomic number, such as silicates, are dark.

Figure 8 *The Leica Cambridge morphochemical-analysis system.*

‡ Note that this information is specific to the instrumentation used.

Image segmentation

Before image-analysis measurements can be performed on such a backscattered-electron image, it needs to be converted into a series of binary images in which each pixel can have only one of two states - on or off (background or interest). Such a binary image is produced by segmentation of the grey image into regions that are characterised by a specific property, in this case, grey level (Figure 10) (*Anon*, 1985).

An objective method of grey-level segmentation is provided by the grey-level histogram, produced by plotting the number of pixels with each specific grey level in an image (or series of images) against grey level. Figure 11 represents the grey-level histogram of the image in Figure 9. Apart from a peak representing the mounting resin, two major peaks can be seen, a silicate peak between grey level 28 and 52, and a chromite peak stretching from grey level 88 to 120. The area between grey level 118 and 198 (enlarged in Figure 12) comprises a number of overlapping peaks representing different sulphide minerals. The small peak visible at the far right-hand side of the histogram in Figure 12 (grey level 240 to 255) represents braggite.

Overlapping grey levels is one of the biggest problems faced during segmentation of such images. The calculated weighted mean atomic numbers and backscattered-electron coefficients for most of the phases found in the samples investigated, are listed in Table 4.12. Measured mean grey-level values for some of these phases are also listed. It is clear that many of the phases present in samples derived from UG2 ore have similar backscattered-electron coefficients and grey-level values (pyrite & magnetite and pentlandite & chalcopyrite for instance).

Note that the relationship between mean atomic number and backscattered-electron coefficient (and consequently grey level) is not linear (Figure 13). Consequently, for the heavier phases, a difference in mean atomic number between two phases does not necessarily signify a measurable difference in backscattered-electron intensity (or grey level). Compare for instance the mean atomic numbers and backscattered-electron intensities of brass and laurite.

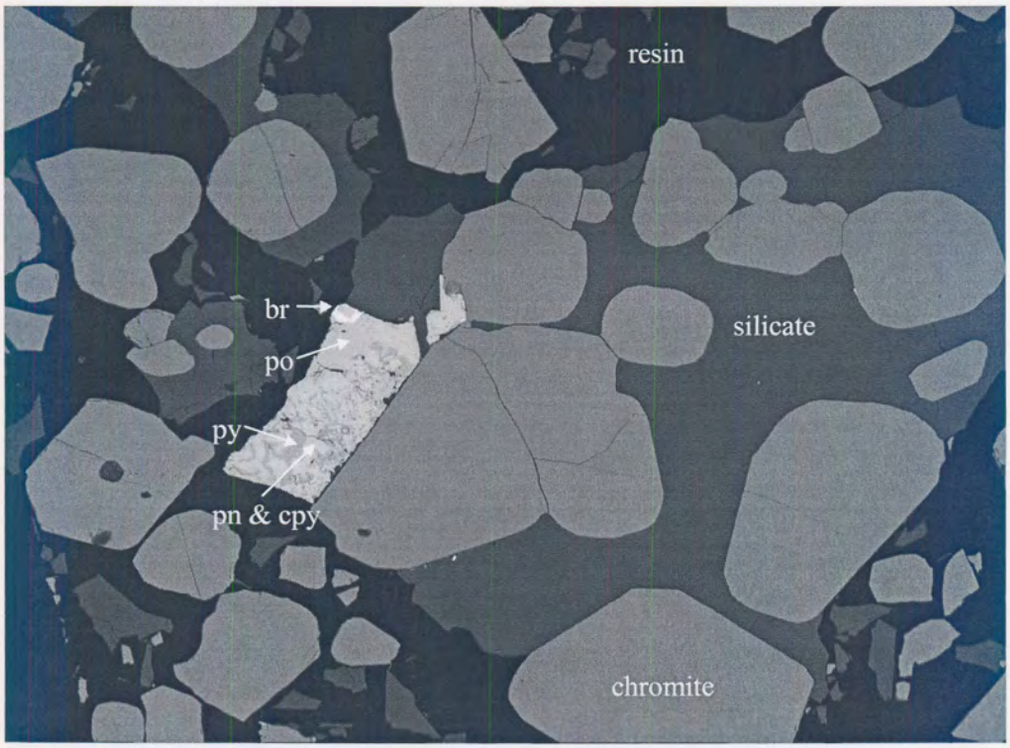

Figure 9 *Backscattered-electron image of UG2 ore containing, in order of increasing grey level: mounting resin → silicates → chromite → pyrite (py) → pyrrhotite (po) → chalcopyrite (cpy) = pentlandite (pn) → braggite (br).*

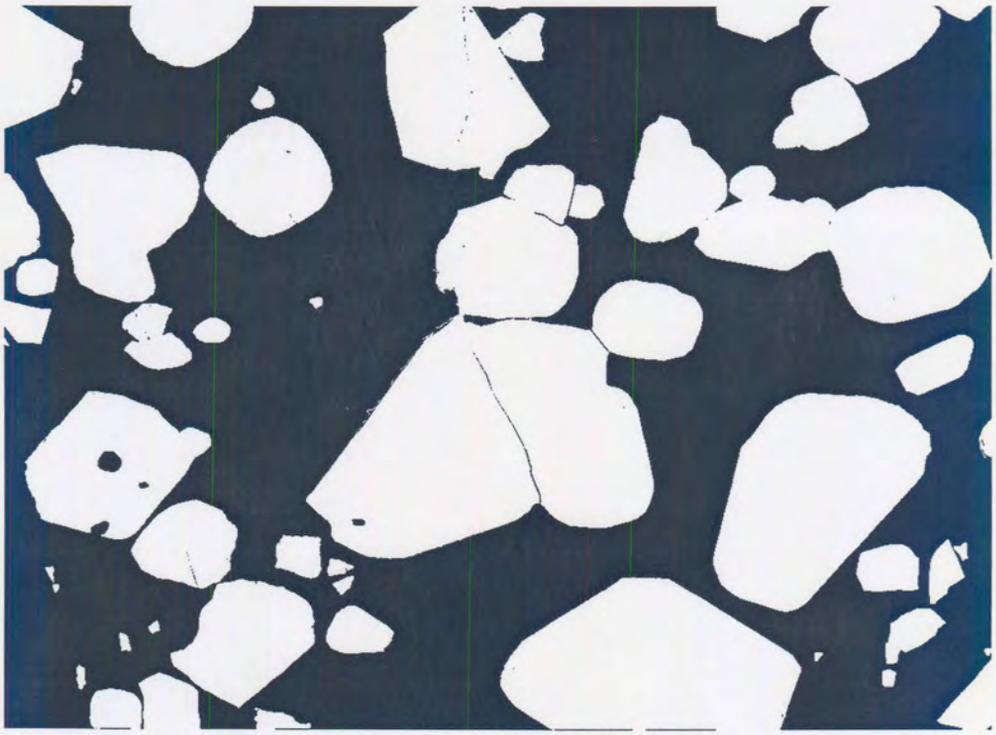

Figure 10 *Binary image of chromite in Figure 9.*

In addition, as can be seen from Figures 11 and 12, the histogram peak for any specific phase is often quite broad, comprising a range of grey-level values. This can be attributed to variations in chemical composition, both between and within grains, as well as artefacts introduced during sample preparation, grain-edge effects (especially in the case of small grains), and the quality and stability of the backscattered-electron signal.

Image processing techniques and the integration of image analysis with EDS analysis make it possible to resolve the problem of overlapping grey levels to a certain extent.

Table 4.12 *Weighted mean atomic number ($\bar{Z}$), backscattered-electron coefficient ($\bar{\eta}$) and measured mean grey level (m.g.l.) of commonly found phases present in UG2 ore and product samples arranged in order of ascending $\bar{Z}$. Where possible, calculations of weighted mean atomic numbers and backscattered-electron coefficients were based on electron-microprobe analyses of the phases.*

Phase	$\bar{Z}$	$\bar{\eta}$	***m.g.l.***
Talc	11.0	0.14	30
Anorthite	11.6	0.12	38
Bronzite	12.5	0.18	52
"Normal" chromite	17.4	0.20	93
"Sintered" chromite	18.4	0.21	106
Pyrite	20.7	0.23	154
Magnetite	21.0	0.23	
Pyrrhotite	22.1	0.24	174
Millerite	22.4	0.25	
Pentlandite	23.3	0.25	186
Chalcopyrite	23.5	0.25	188
Stainless steel	25.7	0.28	
Brass	29.4	0.31	
Laurite	33.1	0.31	
Vysotskite	39.1	0.35	
Malanite	48.3	0.36	
Braggite	54.5	0.39	248
Cooperite	68.0	0.44	
Pt-Fe alloy	72.2	0.46	
Galena	73.2	0.45	

See Appendix A for the method of calculation of mean atomic numbers and backscattered-electron coefficients.

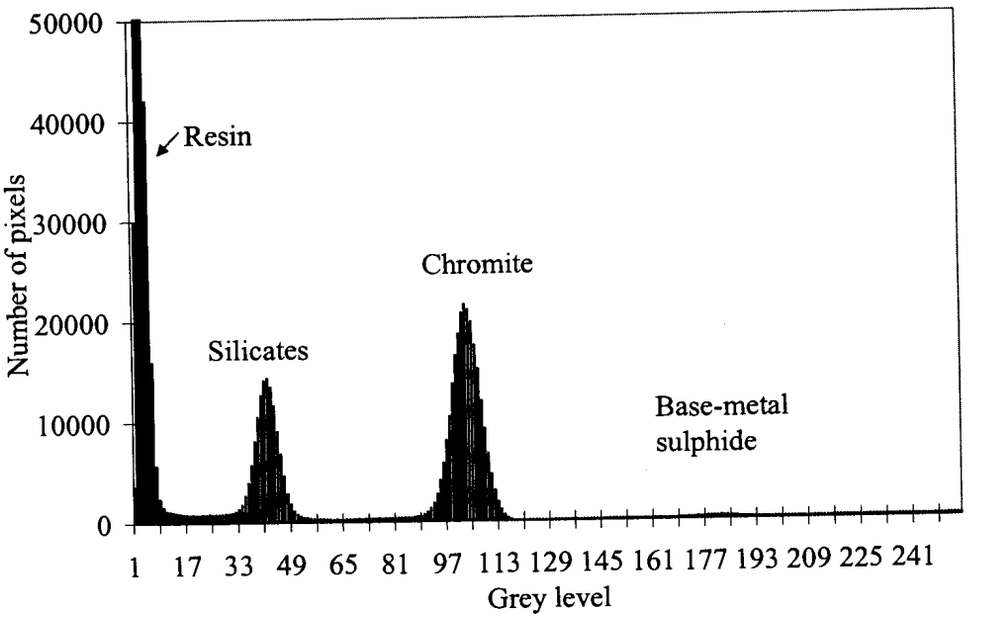

Figure 11 *Grey-level histogram of a backscattered-electron image of UG2 ore.*

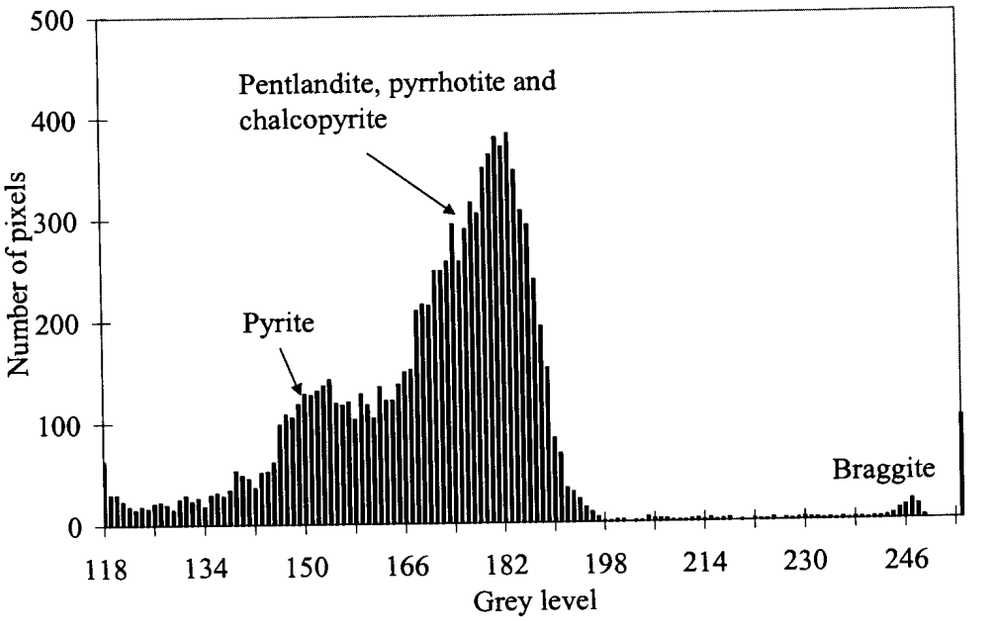

Figure 12 *Grey-level histogram from grey level 116 to 255.*

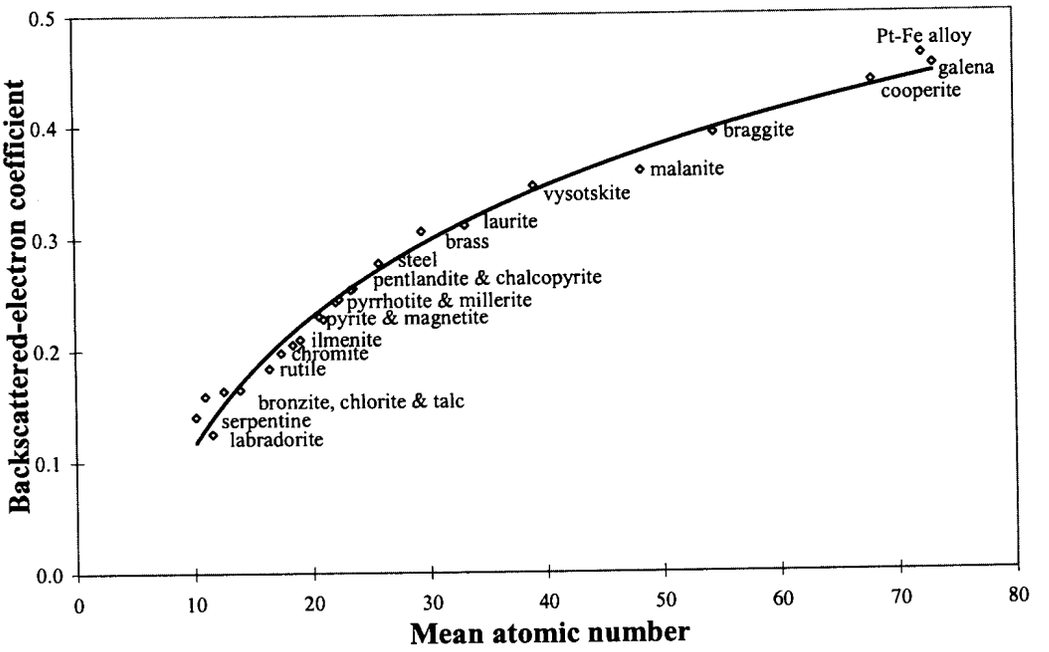

Figure 13 *Graph of weighted mean atomic number ($\bar{z}$) against backscattered-electron coefficient ($\bar{\eta}$) for phases in UG2 flotation feed and products.*

Image processing

Image processing operations can be carried out both on grey and binary images. Grey-level image processing can be used to simplify or improve an image prior to analysis, by eliminating irrelevant data such as that produced by electronic noise, or artefacts introduced during preparation of polished sections.

The effect of grey-level processing on the image in Figure 9 is illustrated in Figure 14. The image was subjected to a series of grey-level processing operations to first produce a less noisy image, followed by a sharpening of the grain-edges. After grey-level processing, the peaks on the histogram are clearly better defined than before processing.

Binary image processing is significantly faster than grey-level processing. However, since a binary image contains less information than a grey image, errors introduced during image segmentation can be compounded during binary image processing. A

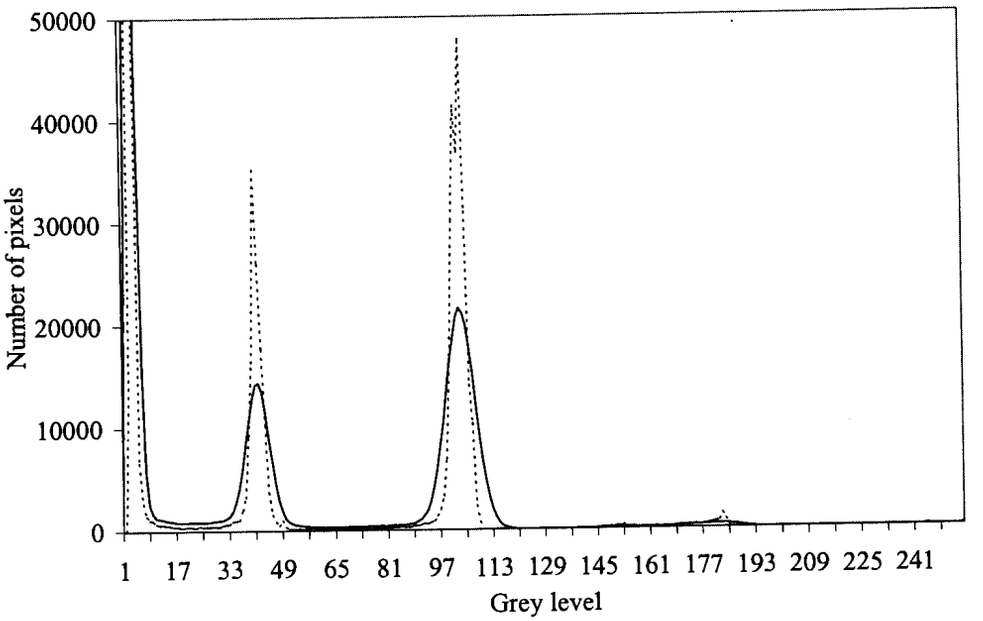

Figure 14 *Grey-level histogram of the image in Figure 9 before (solid line), and after (broken line) grey image processing.*

variety of binary image processing tools are available to perform functions such as separating of touching particles and elimination of polishing imperfections. The use of some binary image processing functions during analysis of UG2 samples is illustrated in Figure 15.

Image analysis combined with EDS analysis

In some cases, no amount of image processing will make it possible to discriminate between two phases based on grey level alone. In such cases the grey-level data can be combined with chemical data obtained by EDS analysis. This does, however, increase the analysis time substantially. The relatively poor spatial resolution of the EDS analysis compared to that of the backscattered-electron signal is a further disadvantage (Jones & Shaw, 1973; Rowlands *et al.*, 1991; Gu, 1998).

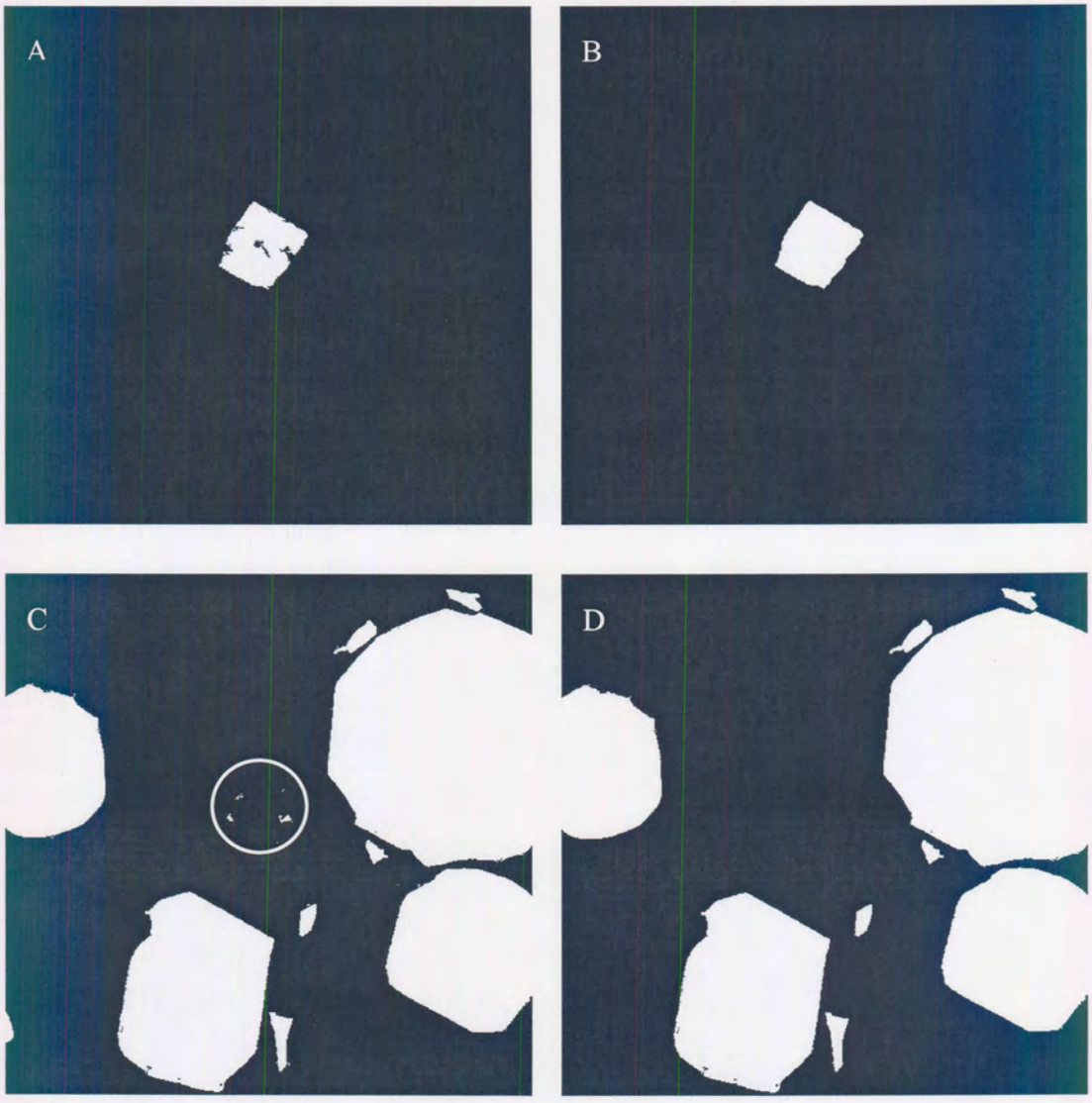

Figure 15 *Examples of binary image processing used on UG2 samples.*

A. Binary image of a sulphide grain. Note the presence of "holes" in the grain caused by polishing imperfections.

B. Binary image of the same sulphide grain after binary image processing to fill the holes.

C. Binary image of chromite - note the presence of artefacts in the circled area.

D. Binary image of chromite after binary image processing to remove artefacts.

Measurement

Once a binary image of each phase of interest in a field has been successfully created, the image is ready for quantification. Provided a statistically valid number of measurements are made, the relative amounts (modal composition), size distribution and mode of occurrence (mineral association and degree of liberation) of specific phases in a sample can be estimated.

Modal analysis

The modal composition of a sample can be estimated from point, line or area measurements on randomly sectioned polished surfaces (Chayes, 1956; DeHoff & Rhines, 1968; Weibel, 1980; Jones, 1987). For example, the number of pixels in the binary image of chromite (see Figure 10), calculated as a percentage of the total number of pixels for all minerals, gives the area proportion (which is equivalent to volume proportion) of chromite in the sample. The volumetric proportion of a phase can be readily converted to mass proportion if the relative densities of the phases are known.

Grain-size distribution

Provided all touching grains have been separated (either physically during sample preparation or by image-processing techniques), grain-size distributions can be derived from line or area measurements on polished sections. Since grains may be cut across their extremities and appear smaller than their true size, these measured size distributions produce biased estimates of the true, three-dimensional sizes of the grains. Obtaining a true grain-size distribution from measurements made on polished sections is one of the most difficult problems of stereology. No attempt was made to apply stereological corrections to the grain-size data collected during the course of this study.

In this report grain size will be expressed as equivalent circle diameter ($ECD = 2 * \sqrt{Area / \pi}$, *i.e.* the diameter of a circle with the same area as that of the measured grain).

For more in-depth information on grain-size measurements and three-dimensional reconstruction the reader is referred to DeHoff (1965), Saltikov (1967), DeHoff & Rhines (1968), Underwood (1970), Petruk (1976), King (1978), Weibel (1980), and Vander Voort (1984).

Degree of liberation

Degree of liberation can be defined as the extent to which valuable phases have been separated from gangue during comminution, and can be measured either by linear intercepts (e.g. King, 1993; 1994b) or area measurements (Petruk, 1993; Petruk & Lastra, 1995). Estimations of degree of liberation based on measurements on polished sections yield apparent values, because only two dimensions of three-dimensional particles are exposed. Consequently, the number of liberated grains will always be overestimated because a number of composite particles will have been sectioned in such a way that they appear free.

Various mathematical models have been proposed for converting apparent liberation to absolute liberation (King, 1979; Lin *et al.*, 1984; Barbery, 1992a; 1992b; King, 1993; Leigh, 1993; King, 1994a; 1994b; King & Stirling, 1994; Woollacott & Valenta, 1996; Gay, 1999). However, the mechanics of ore breakage during milling is still poorly understood. Most models for predicting liberation are based on an assumption of non-preferential or random breakage, i.e. breakage is independent of texture, occurring across grain boundaries and by chipping edges off particles (King, 1979; Leigh, 1993; King, 1994; Gay, 1999, Wei & Gay, 1999). This approach has been questioned by authors such as Petruk (1988b), Ferrara *et al.* (1989), Laslett *et al.* (1990), Woollacott & Valenta (1996) and Thomas & Filipov (1999), as many ores, including the UG2 chromitite, are characterised by preferential breakage along grain boundaries, fractures, or layers and veinlets of softer minerals.

For the purpose of this project, the apparent degree of liberation of PGE minerals and base-metal sulphides from UG2 ore was calculated by measuring the area per cent of

4.6.3 Modal analysis

Major phases (base-metal sulphide, oxide and silicate)

The relative proportions of sulphide, oxide (almost exclusively chromite) and silicate in the samples were estimated by areal analysis with phase discrimination based on backscattered-electron intensity.

Individual base-metal sulphides

Measurement of the relative amounts of individual sulphides was hampered by overlapping grey levels (see Table 4.12 and Figures 12 & 13). Consequently, the modal amounts of the base-metal sulphide minerals were determined by automated EDS point analysis along a grid pattern, superimposed on the binary image of all minerals with grey levels corresponding to that of the base-metal sulphides. The grid pattern was determined by the estimated grain size of the sulphides, ensuring that only one point was measured on each grain, thus improving the statistical reliability of the results. The EDS residence time per point was 1s. EDS analysis was only performed where the grid intersected sulphide. The relative intensities of raw X-ray counting data were used to classify points.

Statistical considerations – modal analysis of major phases based on grey level

Crushed feed samples

Test measurements were done on 25 polished sections of crushed sample A1. Based on the results of these measurements, the percentage relative error in the modal amounts of base-metal sulphide, oxide and silicate at the 95% confidence level was estimated (Simon & Bruce, 1991) for 1 to a 1000 polished sections (Figure 16). The results indicate that measurements on five polished sections are sufficient to ensure a relative error of less than 5 per cent for both chromite (at 55.4 area per cent) and silicate (at 44.5 area per cent). It is estimated that at the low concentration levels at which the sulphide minerals are present (~0.10 area per cent), ~100 polished sections would have to be measured to ensure a relative error of less than 10 per cent. For practical reasons it was decided to carry out these measurements on ~5 polished

sections of each crushed sample, giving a relative error of ~40 per cent for the total base-metal sulphide.

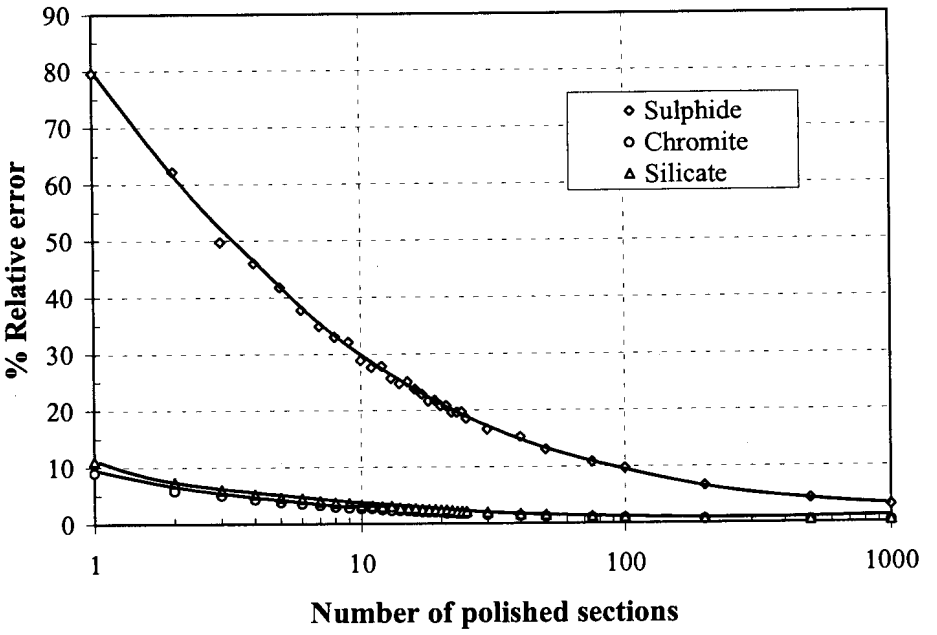

Figure 16 *% Relative error of the modal estimates of base-metal sulphide, chromite and silicate in crushed UG2.*

Milled feed

Figure 17 shows the results of similar tests on UG2 ore milled to 80% <75µm. Comparison of figures 16 and 17 illustrates the homogenising effect of milling, with a higher degree of precision obtained during measurements on the milled samples.

The measured value of base-metal sulphide is 0.16 area per cent in the milled sample compared to 0.10 area per cent in the crushed sample. Careful monitoring of the measurements indicated that the amount of base-metal sulphide in the milled feed is consistently estimated at a higher value, indicating that the difference is not merely a statistical artefact. The discrepancy is mostly caused by the introduction of stainless steel particles during milling. Even though the average backscattered-electron intensity of stainless steel is slightly higher than that of the base-metal sulphides, the small particle sizes of both stainless steel and base-metal sulphide makes it difficult to discriminate between the two types of particle based on backscattered-electron

intensity alone. Image analysis combined with EDS analysis indicate a corrected base-metal sulphide value of 0.08 area per cent.

Statistical considerations – base-metal sulphide modal analysis using EDS analysis

From test measurements on 30 polished sections of crushed sample A1, the percentage relative variation at the 95% confidence level was estimated for 1 to 1000 polished sections (Figure 18). On each polished section approximately 1200 points on sulphide were analysed by EDS. Based on these results it was decided to do measurements on ~10 polished sections (12 000 points on each sample), thereby achieving a relative error of ~20 per cent or less for the relative proportions of the major sulphide phases. Under these conditions the total error (relative) associated with the absolute volume per cent of the individual sulphides is approximately 45 per cent.*

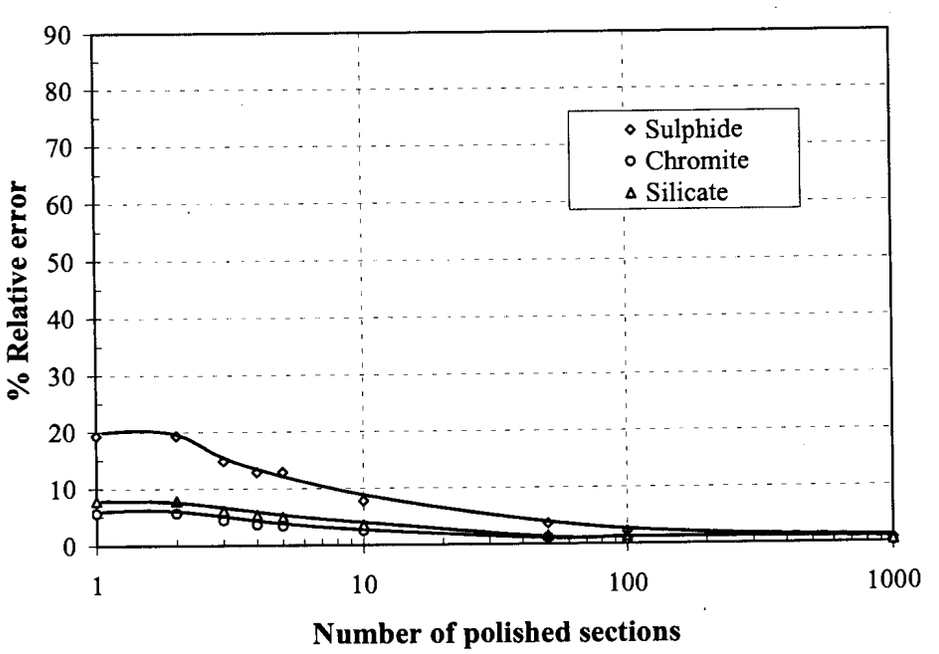

Figure 17 *% Relative error of the modal estimates of base-metal sulphide, chromite and silicate in milled UG2.*

---

* For example: Total BMS = 0.10± 0.04 volume % (~40% relative error) and pentlandite = 49± 10% of total BMS (~20% relative error). Total error^2=Error1^2+Error2^2=45% ∴ Absolute value of pentlandite =0.05±0.02 volume %.

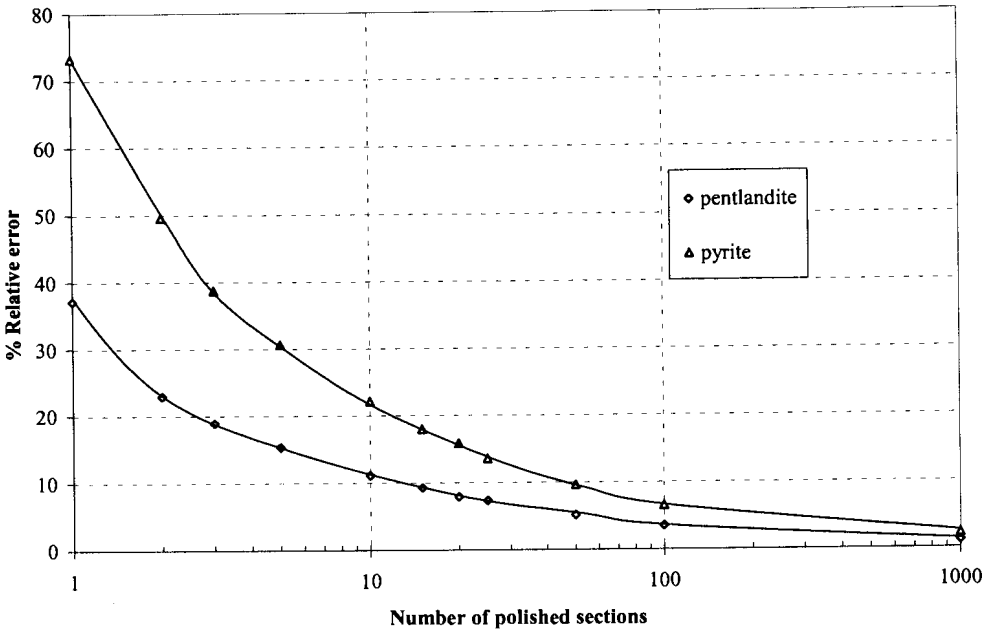

Figure 18 *Effect of the number of polished sections measured on the % relative error in measured pentlandite (at 49 % of total sulphide) and pyrite (at 8% of total sulphide) at the 95% confidence level. Approximately 1200 points were counted on sulphide for each polished section.*

Silicate modal analysis

Image analysis combined with EDS point analysis was also used for silicate modal analysis. Due to the qualitative nature of the EDS analysis and the short analysis time (1s/point) employed, phases with similar chemical compositions, such as talc and bronzite could not be reliably distinguished during the automated analysis. The following 'phases' were recognised: Ca-Al-silicate (predominantly plagioclase, but also includes prehnite, pumpellyite and epidote), Mg-Fe-silicate (predominantly orthopyroxene, minor talc, and rarely serpentine and olivine), phlogopite, clinopyroxene, quartz, chlorite, amphibole, albite, and K-Al-silicate (K-feldspar and sericite).

4.6.4 Chromite and silicate grain-size distributions

Crushed samples

Statistical analysis of measurements on fifteen polished sections of sample A1 indicates that measurements on five polished sections per sample (±15000 chromite

grains) is sufficient to provide a median chromite grain-size value within a 2% error range at the 95% confidence level (Table 1, Appendix C).

Milled feed and flotation products

Due to the homogenising effect of milling, measurements on a much lower number of grains are needed to provide a median chromite grain-size value at the same level of confidence in milled feed and flotation product samples. Data collected along twelve traverses of a polished section of milled feed, showed that measurements on ±5000 chromite grains (two traverses) provide a median chromite grain-size value within a 2% error range at the 95% confidence level (Table 2, Appendix C). The same statistics hold for silicate particle-size measurements.

4.6.5 Base-metal sulphide grain-size distribution and mode of occurrence

Grey level overlaps between different base-metal sulphides and, in the case of milled feed and flotation product samples, between sulphides and stainless steel, coupled with fine grain sizes and low concentration levels, culminated in impractically long analysis times.† For this reason the grain-size distribution and mode of occurrence of individual base-metal sulphide phases were not measured.

Grain-size distribution

Based on statistical analysis of measurements on 30 polished sections of crushed sample A1, it was determined that measurements on more than 100 polished sections are required to provide a median sulphide grain-size value within a <10 per cent error range at the 95% confidence level. For practical reasons, it was decided to perform measurements on between 5 and 10 polished sections per sample.

---

† A relatively coarse grid could be used to determine the relative proportions of the individual base-metal sulphides. To obtain textural information (grain size and mode of occurrence) on individual base-metal sulphides, a very fine grid would have to be used, culminating in long analysis times. Therefore, although the relative amounts of the individual base-metal sulphides could be determined, no textural information could be obtained.

Mode of occurrence and liberation

Base-metal sulphide-bearing particles were classified as liberated if more than 80 per cent of the total area of the particle consisted of sulphide.

4.6.6 PGE mineral characterisation

Problems associated with the characterisation of the UG2 PGE mineral assemblage

Mineral identification

The PGE minerals in the UG2 chromitite generally occur as very small grains (typically <5 μm diameter) making locating and identifying these grains very difficult. Hiemstra (1988a) reported that tests conducted at Mintek showed that many of the smaller PGE mineral grains were not recognised during a manual search using an optical microscope, even by experienced workers.

Although this task becomes easier with the aid of an SEM equipped with EDS, the process mineralogist is often confronted with a finely milled sample, frequently containing significant concentrations of contaminants with high BSE intensities such as brass and stainless steel. A polished section of a flotation tailings sample, for example, may contain several hundred or thousand particles of stainless steel, and less than ten PGE mineral grains. Recognising PGE mineral grains under these conditions is a problem, especially when they have been liberated from the mineral matrix.

Low concentration levels

A number of workers have pointed out the problems in collecting data on a statistically adequate number of grains of trace amounts of minerals in general (Jones & Gavrilovic, 1968; Oosthuyzen, 1985; Cook, 1990), and PGE minerals in particular (Hiemstra, 1988a; Lea, 1996). The low PGE concentration levels in UG2 flotation feed and tailings samples means that a large number of polished sections have to be examined to obtain statistically reliable data.

The question of just how many PGE mineral grains represent a statistically adequate sample will be addressed in a later paragraph. For the moment, suffice it to say that manual collection of data is a tedious, time-consuming and subjective exercise.

Introduction to automated trace-mineral searches

Jones and Gavrolic (1968) made the first documented automated electron microscope-based search for trace amounts of mineral phases. Although it was an excruciatingly slow procedure, it did demonstrate the value of this type of investigation.

Since then, researchers have used integrated systems consisting of various combinations of image analysers and electron microscopes, equipped with energy- or wavelength-dispersive X-ray analysers, to automatically search for trace amounts of Au and/or PGEs:

- Leica Cambridge morphochemical analysis system at Mintek in South Africa (Penberthy & Oosthuyzen, 1992)
- MP-SEM-IPS system at Canmet in Canada (Petruk, 1988a; Walker *et al.*, 1989, Lastra *et al.*, 1999)
- ALF at CSIRO in Australia (Harrowfield *et al.*, 1988; McDonald *et al.*, 1991a; 1991b; McDonald & Sparrow, 1992)
- QEMScan system at CSIRO (Gottlieb *et al.*, 1993)

There are major differences between these systems. The purpose of this investigation is not to discuss the merits of the different systems. Considering the fast pace at which technology is improving, this is in any case a difficult, if not impossible task.

Development of the search routine

During the course of this investigation, it was realised that fully automated characterisation of the PGE minerals of UG2 ore and mineral processing products is an unrealistic goal:

- Firstly, the success of fully automated particle classification depends on particles not touching. This can be achieved by screening each sample into a number of size fractions and adding a filler such as graphite to physically separate sample particles (Miller *et al.*, 1982; Jackson *et al.*, 1984). The reasons for not following this approach, is discussed in section 4.5.2.

  Although image-analysis algorithms to separate touching grains are available, they do not work well on unsized samples or on very fine-grained size fractions. Since

a large proportion of the PGE minerals in the UG2 flotation feed and products are liberated and fine-grained, this is not a viable option for these samples.

One possible approach is to simply assume that all grains in the very fine size fraction (<10 µm) are liberated. Data collected during this investigation however showed that this is not a correct assumption - more than 80 per cent of the PGE mineral-bearing particles in the feed sample at 80% <75µm are finer than 10 µm. Of these fine particles, 27 per cent consists of locked PGE minerals. In addition, information on chemical composition, albeit qualitative, and textural features will be lost by this approach.

- Secondly, the small grain-size and mode of occurrence of PGE minerals in the UG2 ore simply does not lend itself to automated characterisation by X-ray analysis - most of the PGE minerals are smaller than 5µm diameter, and a significant proportion (7 to 8 per cent) occurs as composite PGE mineral grains (e.g. laurite + cooperite). Under these conditions, the short EDS acquisition times typically used during this type of analysis, combined with the poor spatial resolution for X-rays, (2 to 8 µm compared with 0.05 to 0.1 µm for the BSE signal (Gu, 1998)), and the overlap between the X-ray peaks of the different PGEs on an EDS spectrum, do not provide accurate enough data for automated measurement and classification.

For the purpose of this investigation, the samples were therefore analysed unsized and undiluted. A two-stage approach was adopted: The first stage consists of a fully automated, unsupervised routine that simply searches for PGE minerals and records the co-ordinates, without attempting to classify the grains in terms of mode of occurrence or chemical composition (Figure 19). Potential PGE minerals are identified by the high BSE intensity of these phases. A sample containing a 0.5µm grain of laurite, together with cooperite, chalcopyrite and stainless steel is used as a standard to set the grey-level window. If a field contains a potential PGE mineral grain, a digital image transfer is done followed by EDS analysis at the centroid of the grain (1s/grain). The purpose of the EDS analysis is to exclude other particles with high BSE intensity such as galena, brass, and stainless steel. Co-ordinates of PGE mineral grains are stored in a file. During such a run several polished sections are searched, usually overnight. As a control on beam stability, the grey levels and areas

of the phases in the standard field were measured before and after scanning of each polished section. If the measured values were different to those measured during set-up of the run, the results were rejected and the run repeated at a later stage.

The second stage of the analysis consists of a menu-driven interactive routine (Figure 20) during which the stored co-ordinates of each PGE mineral grain is recalled automatically, followed by semi-automated determination of the qualitative chemical composition and area of each PGE mineral grain and associated phases. This information is recorded and stored for off-line statistical evaluation.

Statistical considerations

Apart from any operational errors, the results of such a search may not accurately reflect the true nature of the mineralogy of the PGE minerals for two reasons:

Spatial resolution

If too low a magnification is used, then grains at the lower end of the size range will not be detected during the search. At 200x magnification, 1 pixel is equivalent to 0.79 µm. At this magnification ±1000 fields are scanned on each polished section, covering an area of ~1.8 cm^2. To effect even a small improvement in resolution beyond this value requires that a significantly larger number of fields have to be searched to cover the area of a polished section (Figure 21). The average search time under these conditions are 3 hours per polished section, but varies between 1.5 and 7 hours depending on the nature of the sample.

Nugget effect

Enough polished sections have to be searched to collect data on a statistically representative sample of the PGE minerals in any sample. For example, a search of 146 polished sections of crushed UG2 chromitite yielded data on 4000 PGE mineral grains. Although less than 2 per cent (76 grains) of these grains are coarser than 10 µm, they represent almost 30 per cent of the total area of PGE mineral found (Figure

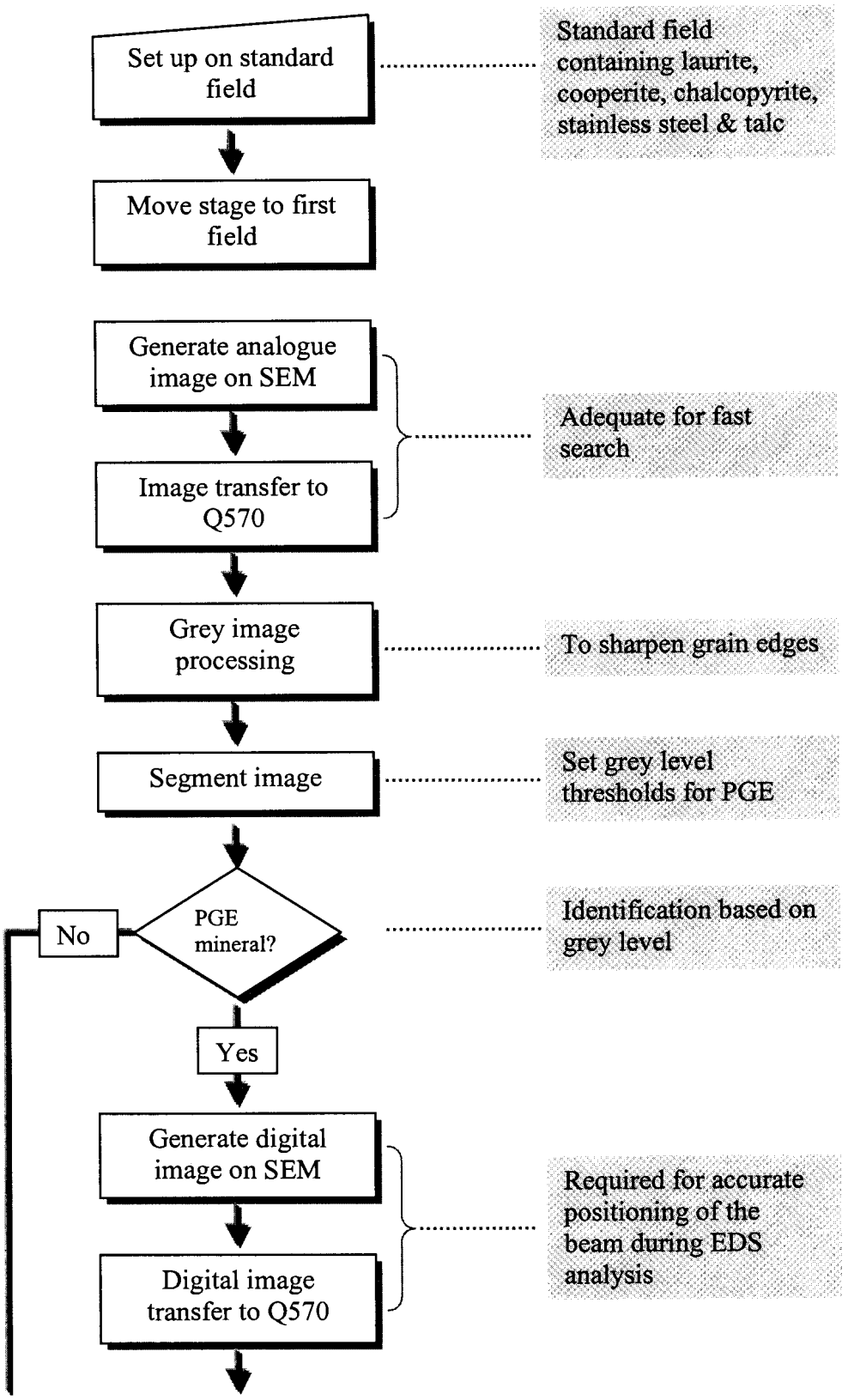

Figure 19 *Flow diagram for automated PGE mineral search.*

p.t.o.

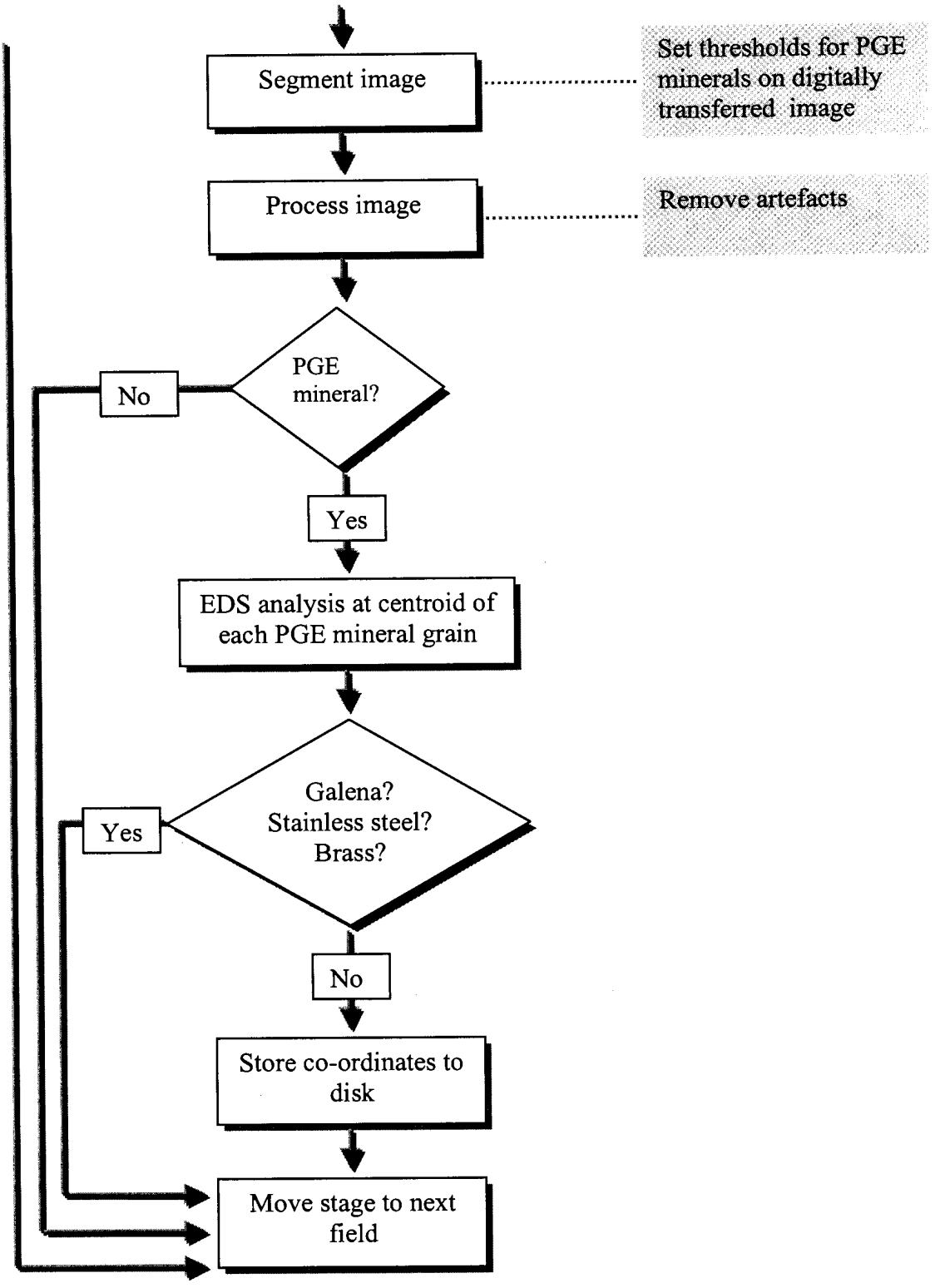

Figure 19 continued *Flow diagram for automated PGE mineral search.*

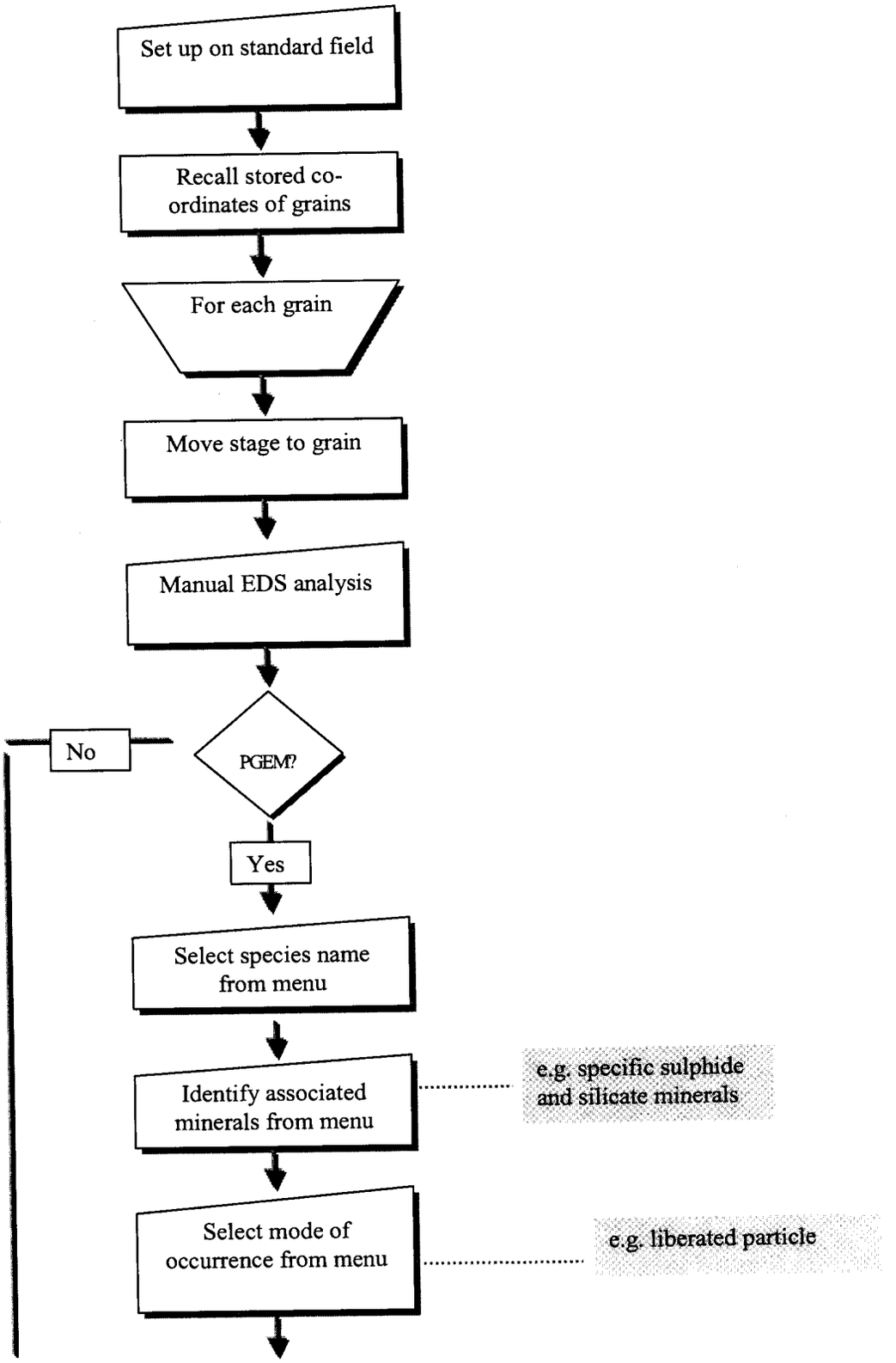

Figure 20 *Flow diagram for semi-automated measurement and classification of PGE minerals.*

p.t.o.

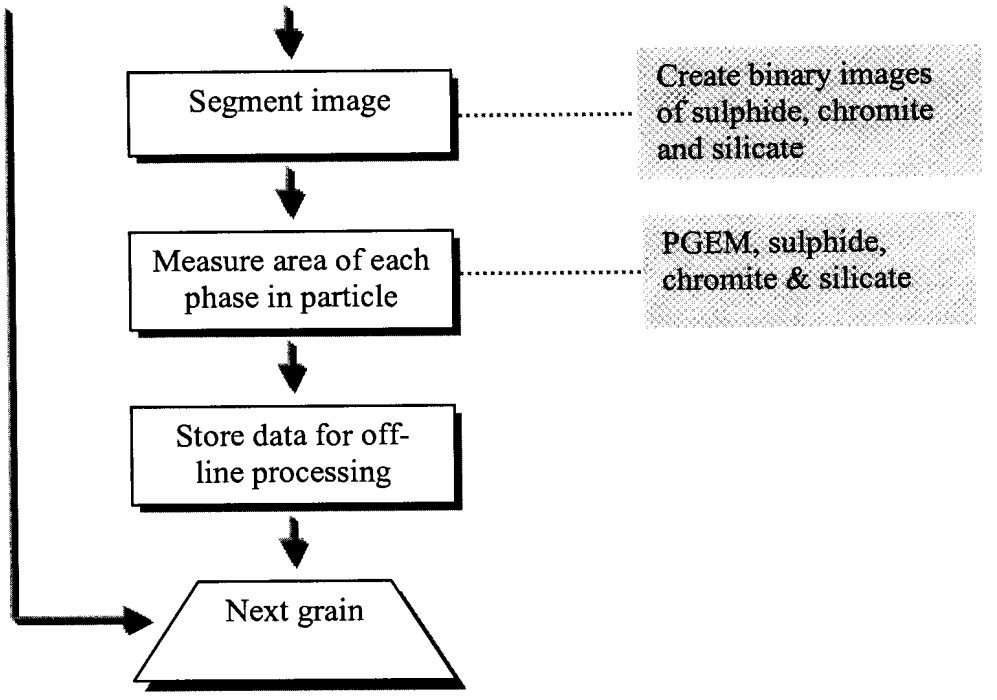

Figure 20 continued *Flow diagram for semi-automated measurement and classification of PGE minerals.*

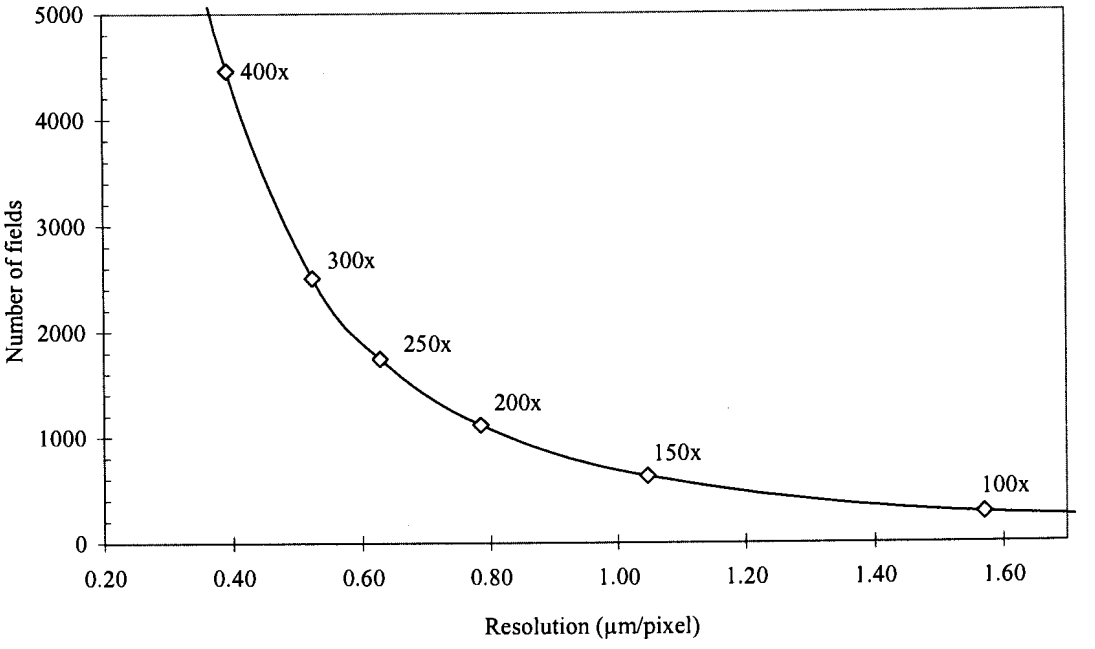

Figure 21 *The relationship between spatial resolution (µm per pixel) on a BSE image at different magnifications, and the number of fields of view required to cover the area of a polished section.*

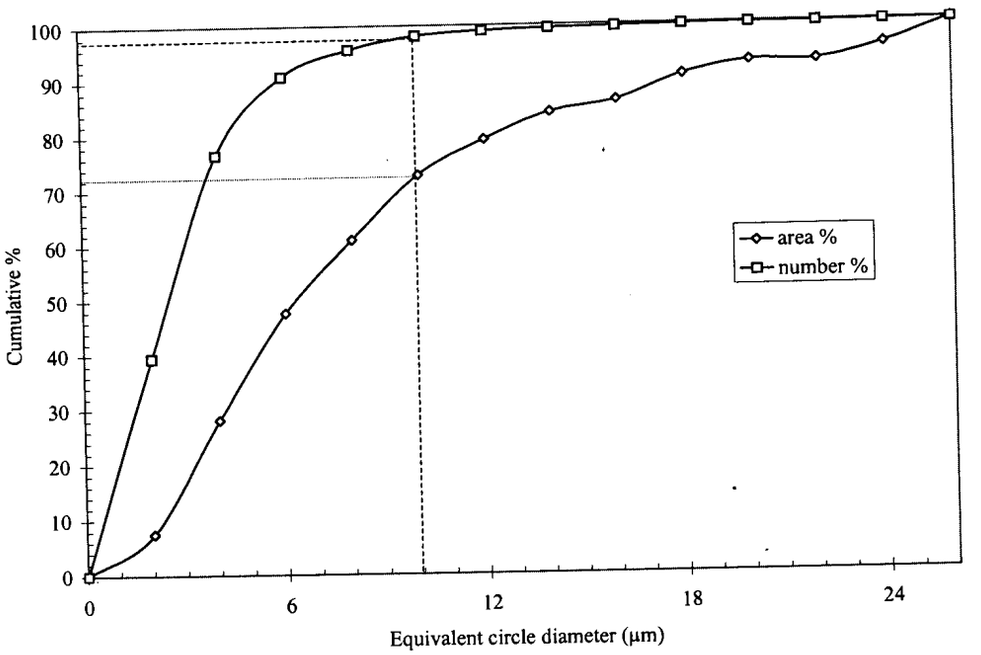

Figure 22 *Grain-size distribution of 4000 PGE mineral grains found in crushed UG2 chromitite.*

22). In addition, although one can expect to find an average of one >10 µm PGE mineral grain in every two polished sections, statistically there is only a 37 per cent probability that such a grain will be found in any specific two polished sections (see also Jones & Gavrolic, 1968).

It should be kept in mind that one grain with a diameter of 10 µm has an area equivalent to that of one hundred 1µm grains. This so-called nugget effect (Oosthuyzen, 1985) can lead to the overestimation or underestimation of the amount of PGE mineral if an insufficient number of polished sections are searched. This effect is demonstrated by data collected during analysis of sample A1 (Figure 23).

A new value for Σ(Pt+Pd+Rh) was calculated from the modal composition following the measurement of each of eighty polished sections.[+] The percentage relative error at

---

[+] Average mineral compositions obtained by electron-microprobe analyses were used as far as possible (Appendix G). For phases for which electron-microprobe analyses

the 90% confidence limit in the calculated value of Σ(Pt+Pd+Rh) associated with different numbers of PGE mineral grains was calculated using resampling statitistics (Figure 24). To obtain an error of less than 10 per cent, data on approximately 3000 grains are required. A practically attainable number of grains is ~200 (except in the flotation tailings), which yields an error of 30 to 40 per cent.

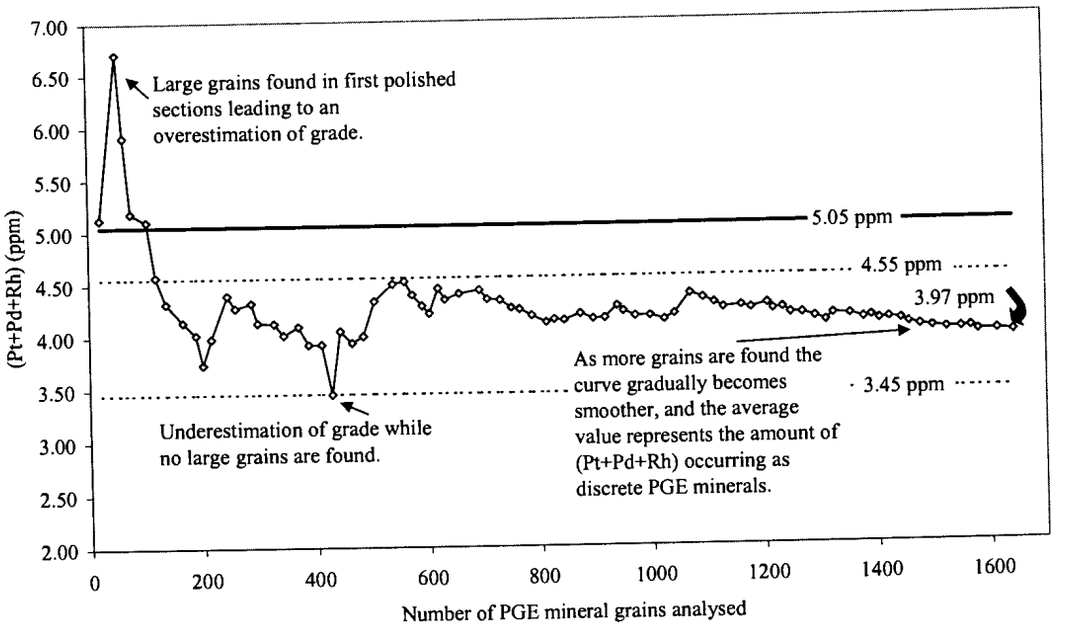

Figure 23 *Variation in Σ(Pt+Pd+Rh) calculated from the mineralogical composition depending on the number of PGE mineral grains recorded. The two dashed horizontals at 3.45 ppm and 4.55 ppm represent the 90% confidence interval for 1642 grains found in 80 polished sections. The chemical assay value of 5.05 ppm is indicated by the solid horizontal.*

PGE mineral modal distribution

During the course of this study more than 25 chemically distinct PGE mineral phases were observed. PGE mineral phases were classified according to the presence of

---

were not available, ideal mineral compositions were assumed (Appendix B). Mineral densities used are listed in Appendix B. Pycnometer measurements indicated a density of 3.87 for sample A1. A density value of 3.85 was calculated from modal analysis data.

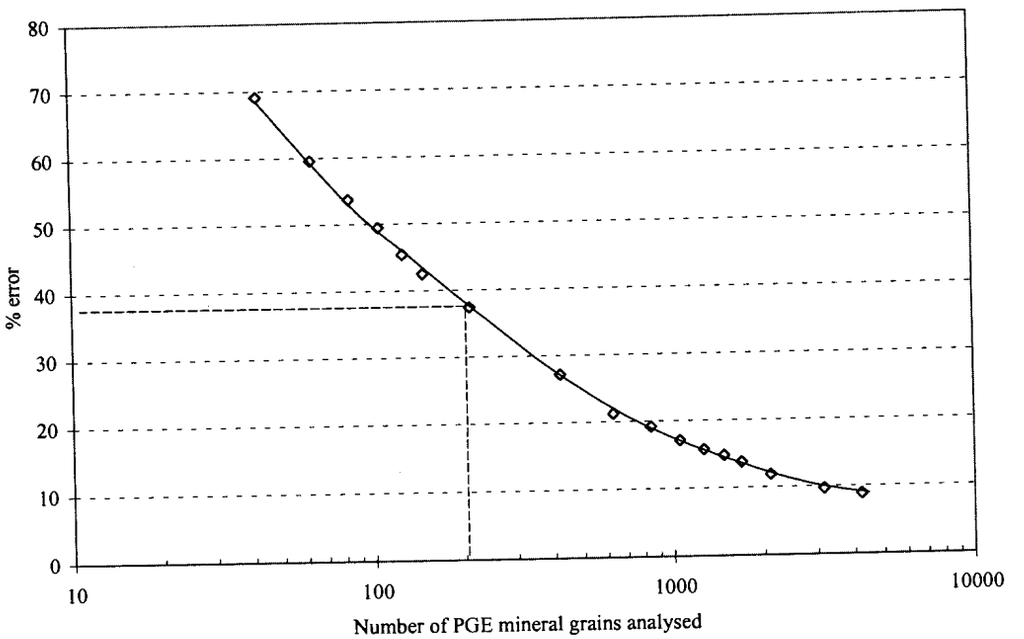

Figure 24 *% Error in the calculated assay value at the 90% confidence limit associated with different numbers of PGE mineral grains.*

major elements identified using qualitative EDS analysis. Due to resolution limitations, the presence of nickel, copper, cobalt and iron can not always be established during analysis of small PGE mineral grains included in base-metal sulphides. For this reason, these elements are not specifically mentioned in the text unless they constitute a substantial component of the PGE mineral concerned e.g. Pt-Fe alloy. Quantitative electron-microprobe analysis of selected grains was used to confirm the identities of the most commonly occurring phases. For practical purposes these phases can be grouped together in the following eight categories:

- Pt-Pd-Ni-sulphide (braggite and less commonly vysotskite)
- Pt-S (probably mostly cooperite)
- Pt-Rh-Cu-Ni-S (probably mostly nickeloan malanite, usually cobalt-bearing)
- Ru-Os-Ir-S (laurite-erlichmanite), as well as rare grains of metallic Ir-Ru-Os.
- PGE-Bi-Te (various tellurides, bismuthinides and bismuthtellurides of platinum and palladium)
- PGE-As±S (includes a variety of sulpharsenides and arsenides such as hollingworthite, irarsite, ruarsite, sperrylite and majakite)

- Pt-Fe (alloys of platinum and iron, often contain palladium and rhodium, sometimes copper)
- Other non-sulphide (a host of minerals, usually palladium-bearing, consisting of various compounds of PGEs with Hg, Pb, Ge, Sb, As, Bi, Te and Sn).

Using the data on 665 and 619 PGE mineral grains for the crushed and milled feed samples of sample A1 respectively, the precision was calculated for a random sample of 200 grains (Table 4.13). The higher degree of precision in the milled sample is a reflection of the homogenising effect of milling.

Table 4.13 *Modal proportions of PGE minerals in sample A1 and the error (absolute) at the 90% confidence limit associated with a sample of 200 grains. Error calculated using resampling statistics (Simon & Bruce, 1991).*

PGE Phase	*Modal %*	*<2 mm ±%*	*80% <75µm ±%*
Pt-Pd-Ni-S	34	17	12
Pt-S	20	15	9
Pt-Rh-Cu-Ni-S	18	12	10
Ru-Os-Ir-S	18	10	7
PGE-Bi-Te	2	3	3
PGE-As±S	3	5	3
Pt-Fe	2	2	1
Other non-sulphide	2	3	3

PGE mineral mode of occurrence

All PGE mineral grains observed in crushed ore were classified according to their textural setting into one of the following categories (Table 4.14):

- Liberated PGE mineral grains, i.e. grains that were freed from the rock matrix during crushing. Most of these grains were probably located at grain boundaries prior to size reduction.
- Locked in base-metal sulphide, refers to PGE mineral grains enclosed in base-metal sulphide composite grains, including PGE mineral grains at sulphide-sulphide grain boundaries.

- Locked in oxide, refers to PGE mineral grains enclosed in oxide minerals, usually chromite, rarely rutile or magnetite.
- Locked in silicate, includes PGE mineral grains occurring both as inclusions in silicate and at silicate-silicate grain boundaries.
- PGE mineral grains occurring at the grain boundaries of base-metal sulphide with silicate and/or chromite.
- PGE mineral grains occurring at the grain edges of chromite and/or silicate, i.e. at the grain boundary of mineral and mounting resin.

Table 4.14 *Mode of occurrence of PGE minerals in sample A1 crushed to <2mm and the precision at the 90% confidence limit associated with a sample of 200 grains. Absolute error calculated using resampling statistics (Simon & Bruce, 1991).*

Mode of occurrence	*Area %*	*±%*
Liberated PGEM	7	9
PGEM locked in BMS	26	14
PGEM locked in oxide	2	1
PGEM locked in silicate	2	2
PGE at GB BMS/Gangue	57	16
PGE at gangue grain edge	6	7

In the case of milled samples an even simpler classification was adopted (Table 4.15).

Table 4.15 *Mode of occurrence of PGE minerals in sample A1 milled to 80% <75µm and the precision at the 90% confidence limit associated with a sample of 200 grains. Absolute error calculated using resampling statistics (Simon & Bruce, 1991).*

Mode of occurrence	*%*	*±%*
Liberated PGEM	57	12
PGEM + liberated BMS	29	11
PGEM ± (BMS)+ Gangue	14	6

In addition, a combined liberation index was calculated for all PGE mineral-bearing grains (Figure 25 and Table 4.16): *Combined liberation index = area of floatable mineral in particle/total area of particle* where *floatable mineral = BMS and PGEM.* This calculation yields a value between 0 and 1, with 1 indicating a particle consisting of a liberated PGE mineral grain, or, a PGE mineral attached to, or locked in a liberated base-metal sulphide grain. A particle consisting of a large silicate grain with a small PGE mineral inclusion will be characterised by a combined liberation index approaching 0. †

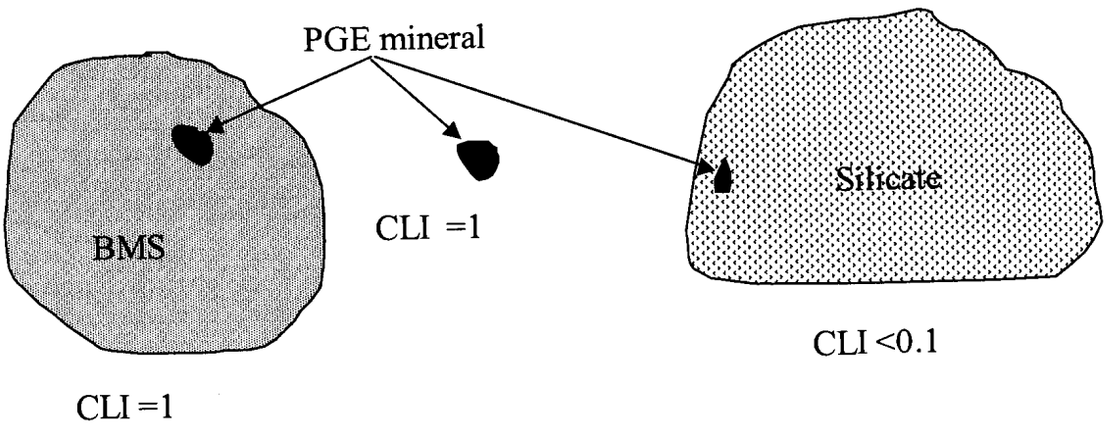

Figure 25 *Graphical representation of three PGE mineral-bearing particles illustrating the combined liberation index (CLI) principle.*

† A liberation index based on area measurements does not always give a true reflection of floatability, which depends on exposed surface area. For instance, a large PGE mineral grain rimmed by silicate may have a high CLI, but will not be recoverable by flotation. However, in the case of small grains, perimeter measurements necessary for the calculation of exposed surface area are inaccurate, hence the decision to base the liberation index on area measurements.

Table 4.16 *Combined liberation index of PGE minerals in sample A1 at 80% <75µm, and precision at the 90% confidence limit associated with a sample of 200 grains. Absolute error calculated using resampling statistics (Simon & Bruce, 1991).*

Combined liberation index	*Area %*	*± %*	*Cumulative area %*
0.0-0.2	16	9	16
0.2-0.4	1	1	17
0.4-0.6	0	1	17
0.6-0.8	0	0	17
0.8-1.0	83	9	100

PGE mineral grain-size distribution

A PGE mineral grain-size distribution was also calculated for each sample. From the grain-size distribution a median value was calculated both in terms of number of grains and area. The errors associated with the median values calculated from a sample of 200 grains for sample A1 at <2mm and at 80%<75µm are given in Table 4.17. These values demonstrate that, for a sample of 200 grains, the median grain size based on per cent number of grains is statistically more reliable, than the median grain size based on area per cent. Thus, although the median grain size based on per cent number of grains is not a very good reflection of the true grain size, it does allow for comparisons between samples.

Table 4.17 *Median grain diameter of PGE minerals in sample A1 at <2mm and 80% <75µm, and precision at the 90% confidence limit associated with a sample of 200 grains. Error calculated using resampling statistics (Simon & Bruce, 1991).*

	Median (µm)	*± (µm)*
<2 mm by area	7.2	3.7
<2 mm by number	2.2	0.1
80%<75 µm by area	3.9	1.5
80%<75 µm by number	2.2	0.2

5. RESULTS

The chemical, mineralogical, milling and flotation characteristics of the fourteen samples are compared in Table 5.1.

5.1 Chemical composition

The chemical compositions of the samples are reported in terms of major element oxide, sulphur, nickel, copper and platinum-group element contents (Table 5.1A to D). Cr_2O_3 contents for the fourteen samples vary between 20.05 and 34.58%. Note the relatively high TiO_2 contents of samples A4, B4 and C1.

Of particular interest are the relatively low sulphur and acid soluble copper and nickel values in samples from area C (C1 to C5) and, in the case of copper and sulphur, in samples B2, A2 and A5. Since copper occurs almost exclusively in sulphide minerals in the UG2 chromitite, total copper values are similar to acid soluble copper values (see analyses for samples A1 and C1). Total nickel values are considerably higher than acid soluble nickel indicating that most of the nickel occurs in phases other than sulphide minerals, probably predominantly in chromite (De Waal, 1975; Von Gruenewaldt, 1979), and to a lesser extent in silicate minerals. Curiously, although acid soluble nickel is low in samples from area C, total nickel values are similar or higher compared to the other samples. The Cu_{as}/Ni_{as}[+] ratio varies between 0.10 to 0.16, except for samples A3, B3, A4, B4 and C1 in which it is 0.20 or higher. As also observed by Smits (1988), very little of the cobalt appears to be present in acid soluble form.

Total PGE+Au[*] values range between 3.17 and 5.87 ppm with platinum the major PGE present at levels ranging between 2.13 and 3.34 ppm, representing between 55 and 67 per cent of the total PGE+Au. Palladium ranges from 0.66 to 2.05 ppm (21 to 36 per cent of the total PGE+Au) and rhodium between 0.33 and 0.61 ppm (9 to 11 per cent of the total PGE+Au).

[+] as = acid soluble
[*] Total PGE+Au refers to Σ(Pt,Pd,Rh,Au)

Table 5.1 *Chemical, mineralogical, milling and flotation characteristics of fourteen samples of UG2 chromitite.*

Sample locality	***An fw***	***Nor fw***	***Peg fw***		***Pothole***		***RPeg fw***	***Faulted***	***Faulted***	***Pothole***	***Nor fw***	***Faulted***	***Peg fw***	***An fw***
	A2	***B2***	***A1***	***B1***	***A3***	***B3***	***A4***	***B4***	***A5***	***C1***	***C2***	***C3***	***C4***	***C5***
A. Major element oxide composition (mass %)														
Cr_2O_3	29.10	20.90	29.33	25.05	33.80	30.70	34.50	32.90	27.70	34.58	31.80	32.40	31.20	33.80
Fe_2O_3	22.30	18.40	22.58	22.97	25.40	23.30	28.00	28.30	22.40	27.48	24.00	24.50	23.00	25.20
CaO	3.27	4.77	2.67	2.71	2.45	3.03	2.33	2.47	3.38	2.14	2.84	2.20	2.95	2.14
MgO	10.20	11.50	10.60	14.55	9.35	10.10	10.40	9.73	11.50	9.46	9.23	9.81	9.83	10.40
Al_2O_3	18.10	16.70	16.78	13.40	16.80	16.90	14.90	15.05	16.40	15.33	17.60	17.10	17.80	16.10
SiO_2	17.10	27.30	16.11	20.20	12.50	15.20	10.40	11.70	16.00	10.40	13.90	12.80	15.05	12.50
TiO_2	0.71	0.55	0.67	0.66	0.73	0.69	0.97	1.02	0.57	0.95	0.74	0.78	0.67	0.76
MnO	0.18	0.17	0.19	0.20	0.19	0.19	n.d.	0.21	0.23	0.21	0.19	0.19	0.19	0.20
Na_2O	n.d.	n.d.	0.64	0.60	n.d.	0.60	0.13	0.35	0.05	0.36	0.61	0.53	0.66	0.43
K_2O	n.d.	n.d.	0.12	0.16	n.d.	0.09	0.01	0.07	0.47	0.05	0.07	0.07	0.07	0.08
B. Cu, Ni, Co and S determined by chemical analysis														
S (%)	0.02	0.01	0.03	0.05	0.04	0.03	0.05	0.08	0.02	0.01	0.01	0.01	0.01	0.01
Ni_{total} *(ppm)* $^{+}$	1000	1000	1070	1450	1300	1150	1148	1335	914	1151	1400	1400	1300	1400
$Ni_{acid\ soluble}$ *(ppm)* $^{+}$	238	126	271	525	151	202	295	316	356	82	114	108	114	88
Co_{total} *(ppm)*	n.d.	n.d.	170	n.d.	n.d.	n.d.	n.d.	n.d.	n.d.	225	n.d.	n.d.	n.d.	n.d.
$Co_{acid\ soluble}$ *(ppm)*	n.d.	n.d.	28	n.d.	n.d.	n.d.	n.d.	n.d.	n.d.	<20	n.d.	n.d.	n.d.	n.d.
Cu_{total} *(ppm)*	n.d.	n.d.	75	n.d.	n.d.	n.d.	n.d.	n.d.	n.d.	60	n.d.	n.d.	n.d.	n.d.
$Cu_{acid\ soluble}$ *(ppm)*	48	42	73	95	107	91	109	170	44	57	45	47	30	35
$Ni_{acid\ soluble}/Ni_{total}$	0.29	0.30	0.39	0.50	0.34	0.35	0.48	0.42	0.38	0.24	0.22	0.21	0.20	0.20
$Cu_{acid\ soluble}/Ni_{acid\ soluble}$	0.20	0.33	0.25	0.18	0.71	0.45	0.37	0.54	0.12	0.70	0.40	0.44	0.26	0.40

An fw = Anorthosite footwall Nor fw = Norite footwall Peg fw = Pegmatoid footwal Pothole = Pothole edge RPeg fw = Replacement pegmatoid footwall Faulted = Faulted UG2

n.d. = not determined $^{+}$ Ni analyses performed on samples crushed to <2mm to avoid contamination by stainless steel

Table 5.1 continued *Chemical, mineralogical, milling and flotation characteristics of fourteen samples of UG2 chromitite*

Sample locality	***An fw***	***Nor fw***	***Peg fw***		***Pothole***		***RPeg fw***	***Faulted***	***Faulted***	***Pothole***	***Nor fw***	***Faulted***	***Peg fw***	***An fw***
	A2	***B2***	***A1***	***B1***	***A3***	***B3***	***A4***	***B4***	***A5***	***C1***	***C2***	***C3***	***C4***	***C5***
C. PGE content														
Pt (ppm)	2.13	2.04	3.08	2.42	3.67	2.81	3.05	3.34	3.13	3.03	2.97	3.25	2.90	3.06
Pd (ppm)	0.66	1.17	1.41	1.30	1.57	1.43	1.48	1.87	2.05	1.04	1.14	1.12	0.94	1.31
Rh (ppm)	0.35	0.33	0.43	0.37	0.61	0.43	0.46	0.53	0.52	0.45	0.47	0.55	0.47	0.50
Ru (ppm)	0.74	0.58	1.08	0.68	0.94	n.d.	n.d.	n.d.	n.d.	n.d.	n.d.	n.d.	n.d.	n.d.
Ir (ppm)	0.19	0.16	0.22	0.19	0.25	n.d.	n.d.	n.d.	n.d.	n.d.	n.d.	n.d.	n.d.	n.d.
Au (ppm)	0.04	0.02	0.07	0.03	0.02	0.05	0.04	0.07	0.05	<0.05	<0.05	<0.05	<0.05	<0.05
PGE+Au (ppm)	3.17	3.55	4.99	4.12	5.87	4.71	5.02	5.81	5.74	4.52	4.58	4.92	4.31	4.87
D. PGE distribution														
Pt (%)	67.14	57.35	61.72	58.74	62.52	59.54	60.75	57.48	54.53	67.04	64.85	66.06	67.29	62.83
Pd (%)	20.70	32.93	28.26	31.55	26.75	30.35	29.38	32.18	35.63	23.01	24.89	22.76	21.81	26.90
Rh (%)	11.06	9.15	8.62	8.98	10.39	9.13	9.06	9.12	9.06	9.96	10.26	11.18	10.90	10.27
E. Bulk modal analysis measured by image analysis. Precision determined at the 95% confidence level. Chromite content measured by image analysis (i.a.) is compared with chromite content calculated from Cr_2O_3 values.														
BMS (mass %)	0.10 ±0.03	0.11 ±0.05	0.13 ±0.02	0.17 ±0.04	0.11 ±0.02	0.15 ±0.08	0.18 ±0.04	0.15 ±0.02	0.09 ±0.08	0.03 ±0.01	0.07 ±0.03	0.04 ±0.01	0.04 ±0.01	0.04 ±0.02
Chromite (mass %)(IA)	64.6 ±1.2	50.1 ±3.8	65.7 ±1.1	58.3 ±1.9	71.9 ±2.7	62.4 ±2.9	70.5 ±6.8	68.8 ±1.5	54.3 ±2.7	75.9 ±1.2	71.4 ±2.1	67.3 ±2.2	67.7 ±2.3	65.3 ±4.2
Chromite (mass %) (calc)	67.9	48.8	68.4	58.4	78.9	71.6	80.5	76.8	64.6	80.7	74.2	75.6	72.8	78.9
Difference	3.3	-1.3	2.7	0.2	6.9	9.2	10.0	8.0	10.3	4.8	2.8	8.3	5.1	13.5
Silicate (mass %)	35.3 ±0.7	49.8 ±2.4	34.1 ±0.7	41.6 ±1.2	28.0 ±1.7	37.4 ±1.9	29.4 ±4.4	31.1 ±1.0	45.6 ±1.9	24.1 ±0.7	28.5 ±1.3	32.7 ±1.4	32.2 ±1.4	34.6 ±2.7

An fw = Anorthosite footwall Nor fw = Norite footwall Peg fw = Pegmatoid footwal Pothole = Pothole edge RPeg fw = Replacement pegmatoid footwall Faulted = Faulted UG2

n.d. = not determined PGE+Au =Σ(Pt,Pd,Rh,Au) BMS=base-metal sulphide

Table 5.1 continued *Chemical, mineralogical, milling and flotation characteristics of fourteen samples of UG2 chromitite*

Sample locality	***An fw***	***Nor fw***	***Peg fw***		***Pothole***		***RPeg fw***	***Faulted***	***Faulted***	***Pothole***	***Nor fw***	***Faulted***	***Peg fw***	***An fw***
	A2	***B2***	***A1***	***B1***	***A3***	***B3***	***A4***	***B4***	***A5***	***C1***	***C2***	***C3***	***C4***	***C5***
F. Relative proportions of sulphide minerals (volume %). Precision determined at the 95% confidence level.														
Chalcopyrite	27 ±4	29±6	24±4	25±5	28±8	19±5	26±10	15±1	23±8	43±9	32±15	54±13	34±10	49±6
Pentlandite	52±3	48±6	49±4	45±4	46±7	55±9	51±8	46±7	71±8	2±1	5±3	5±2	5±5	5±6
Pyrrhotite	13±4	4±2	19±3	29±7	14±4	25±5	22±5	35±7	6±4	-	1±1	2±3	5±5	0±2
Pyrite	8±1	16±5	8±1	1±1	11±6	1±1	1±0	3±2	-	11±8	31±13	15±16	16±4	20±5
Millerite	-	2±1	-	-	-	-	-	-	-	43±6	32±7	24±10	41±9	26±1
G. Sulphide modal composition in mass %, calculated from E and F. Precision determined at the 95% confidence level.														
Chalcopyrite	0.02 ±0.01	0.03 ±0.02	0.03 ±0.01	0.04 ±0.01	0.03 ±0.01	0.02 ±0.02	0.04 ±0.02	0.02 ±0.00	0.01 ±0.01	0.01 ±0.00	0.01 ±0.01	0.02 ±0.01	0.01 ±0.00	0.01 ±0.01
Pentlandite	0.05 ±0.02	0.05 ±0.02	0.07 ±0.02	0.08 ±0.02	0.05 ±0.01	0.07 ±0.05	0.09 ±0.02	0.07 ±0.01	0.07 ±0.03	0.00 ±0.00	0.00 ±0.00	0.00 ±0.00	0.00 ±0.00	0.00 ±0.00
Pyrrhotite	0.01 ±0.01	0.00 ±0.00	0.02 ±0.01	0.04 ±0.02	0.01 ±0.00	0.04 ±0.03	0.04 ±0.01	0.05 ±0.01	0.00 ±0.00	0.00 ±0.00	0.00 ±0.00	0.00 ±0.00	0.00 ±0.00	0.00 ±0.00
Pyrite	0.01 ±0.00	0.02 ±0.01	0.02 ±0.00	0.01 ±0.00	0.01 ±0.01	0.00 ±0.00	0.00 ±0.00	0.01 ±0.00	0.00 ±0.00	0.00 ±0.00	0.03 ±0.02	0.00 ±0.00	0.01 ±0.00	0.02 ±0.02
Millerite	0.00 ±0.00	0.00 ±0.00	0.00 ±0.00	0.00 ±0.00	0.00 ±0.00	0.00 ±0.00	0.00 ±0.00	0.00 ±0.00	0.00 ±0.00	0.01 ±0.01	0.02 ±0.01	0.01 ±0.00	0.02 ±0.01	0.01 ±0.00
H. Pentlandite/millerite ratio expressed as mass % pentlandite/(mass % pentlandite + mass % millerite)														
pn/(pn+mil)	0.998	0.935	0.996	1.000	0.997	0.998	0.999	0.999	1.000	0.045	0.043	0.156	0.038	0.129
I. S and acid soluble Cu, Ni, and Fe calculated from image analysis measurements														
S (%)	0.03	0.04	0.05	0.06	0.04	0.05	0.06	0.05	0.03	0.01	0.03	0.01	0.01	0.02
Cu (ppm)	78	99	93	137	106	77	134	69	47	31	50	69	39	37
Ni (ppm)	160	171	209	246	164	238	287	217	224	86	158	63	120	47
Fe in BMS (ppm)	241	250	306	387	269	324	427	297	280	30	50	67	38	38

An fw = Anorthosite footwall Nor fw = Norite footwall Peg fw = Pegmatoid footwal Pothole = Pothole edge RPeg fw = Replacement pegmatoid footwall Faulted = Faulted UG2

Table 5.1 continued. *Chemical, mineralogical and flotation characteristics of fourteen samples of UG2 chromitite.*

Sample locality	***An fw***	***Nor fw***	***Peg fw***		***Pothole***		***RPeg fw***	***Faulted***	***Faulted***	***Pothole***	***Nor fw***	***Faulted***	***Peg fw***	***An fw***
	A2	***B2***	***A1***	***B1***	***A3***	***B3***	***A4***	***B4***	***A5***	***C1***	***C2***	***C3***	***C4***	***C5***
J. Chromite equivalent circle diameter calculated from area measurements (µm)														
20th percentile	102	98	105	108	117	120	84	143	72	110	103	104	83	113
median	164	164	169	177	191	187	221	221	127	184	173	175	142	177
80th percentile	250	266	252	269	298	273	356	322	194	294	276	267	222	260
K. Relative proportions of silicate minerals (volume %)														
*Ca-Al-silicate**	n.d.	n.d.	66	n.d.	68	56	24	25	50	69	75	n.d.	66	n.d.
Mg-Fe-silicate+	n.d.	n.d.	30	n.d.	28	33	47	49	18	15	17	n.d.	30	n.d.
Phlogopite	n.d.	n.d.	2	n.d.	1	3	<1	<1	1	<1	1	n.d.	1	n.d.
Clinopyroxene	n.d.	n.d.	1	n.d.	<1	6	22	23	8	1	<1	n.d.	<1	n.d.
Quartz	n.d.	n.d.	<1	n.d.	<1	<1	<1	<1	1	3	1	n.d.	<1	n.d.
Chlorite	n.d.	n.d.	<1	n.d.	1	1	1	1	13	4	3	n.d.	1	n.d.
Amphibole	n.d.	n.d.	<1	n.d.	<1	<1	1	1	4	1	2	n.d.	1	n.d.
Albite	n.d.	n.d.	<1	n.d.	<1	<1	<1	<1	4	6	1	n.d.	1	n.d.
K-Al-silicate°	n.d.	n.d.	<1	n.d.	<1	<1	<1	<1	<1	1	<1	n.d.	<1	n.d.

An fw = Anorthosite footwall Nor fw = Norite footwall Peg fw = Pegmatoid footwal Pothole = Pothole edge RPeg fw = Replacement pegmatoid footwall Faulted = Faulted UG2

n.d. = not determined

* *Predominantly plagioclase. Also includes pumpellyite, prehnite and epidote, especially in samples from area C.*

\+ *Predominantly orthopyroxene, minor talc, and rarely serpentine and olivine*

° *K-feldspar and sericite*

Table 5.1 continued. *Chemical, mineralogical and flotation characteristics of fourteen samples of UG2 chromitite.*

Sample locality	***An fw***	***Nor fw***	***Peg fw***		***Pothole***		***RPeg fw***	***Faulted***	***Faulted***	***Pothole***	***Nor fw***	***Faulted***	***Peg fw***	***An fw***
	A2	***B2***	***A1***	***B1***	***A3***	***B3***	***A4***	***B4***	***A5***	***C1***	***C2***	***C3***	***C4***	***C5***
L. BMS mode of occurrence and grain size in feed samples crushed to <2mm (area %)														
BMS median ECD (μm)	32	30	32	30	39	33	45	38	17	19	21	22	22	17
Liberated BMS	24	12	16	13	21	2	2	8	3	8	18	15	18	11
Grain boundary	60	80	73	74	56	72	68	71	37	68	46	49	55	42
*Locked in oxide**	1	4	1	3	3	2	1	1	7	3	3	1	3	6
Locked in silicate•	15	5	11	10	19	24	29	20	53	20	33	36	24	41
Predicted BMS liberation+	84	92	89	87	78	74	70	79	40	76	64	64	73	53
M. Relative proportions of PGE minerals (PGEM) (volume %). Statistical uncertainty determined at the 90% confidence level and reported as absolute variation.														
Number of grains	543	471	1766	426	433	420	420	437	425	441	445	400	425	385
Pt-Pd-Ni-S	21±7	38±10	36±6	20±5	17±9	26±7	2±1	7±6	14±5	39±7	33±12	37±8	36±11	38±11
Pt-S	26±8	8±3	19±5	20±5	26±7	15±4	5±2	6±3	1±1	2±1	4±2	3±2	3±2	7±6
Pt-Rh-Cu- Ni-S	24±5	28±8	18±4	10±3	27±7	13±5	4±3	2±1	11±5	33±7	42±15	35±9	40±9	29±7
Ru-Os-Ir-S	23±6	17±6	19±4	27±7	22±6	29±7	31±8	33±8	30±9	22±7	16±6	20±9	18±5	23±8
PGE-Bi-Te	1±0	0±0	2±1	3±1	1±1	3±2	4±2	3±1	3±1	0±0	1±2	0±0	0±0	1±1
PGE-As-S	2±1	6±7	3±2	5±4	2±1	2±1	1±1	2±3	9±5	2±1	2±1	2±1	1±1	1±1
Pt-Fe alloy	2±1	0±0	2±1	9±4	5±4	10±4	40±8	45±9	17±9	0±0	0±0	0±0	0±0	0±0
Other non-sulphide PGEM	1±1	2±1	2±1	7±2	1±1	3±2	14±5	2±2	17±5	2±1	2±1	3±1	2±1	2±2

An fw = Anorthosite footwall Nor fw = Norite footwall Peg fw = Pegmatoid footwal Pothole = Pothole edge RPeg fw = Replacement pegmatoid footwall Faulted = Faulted UG2

n.d. = not determined

ECD = equivalent circle diameter

* May also be at oxide-oxide grain boundaries

• May also be at silicate-silicate grain boundaries

+ Predicted BMS liberation = area % BMS at grain boundaries+liberated BMS

Table 5.1 continued. *Chemical, mineralogical and flotation characteristics of fourteen samples of UG2 chromitite*

Sample locality	***An fw***	***Nor fw***	***Peg fw***		***Pothole***		***RPeg fw***	***Faulted***	***Faulted***	***Pothole***	***Nor fw***	***Faulted***	***Peg fw***	***An fw***
	A2	***B2***	***A1***	***B1***	***A3***	***B3***	***A4***	***B4***	***A5***	***C1***	***C2***	***C3***	***C4***	***C5***
N. PGE mineral (PGEM) modal composition (volume %).														
Total non-sulphide PGEM	7	11	12	32	11	24	84	77	81	5	6	7	4	5
O. PGE mineral median equivalent circle diameter (ECD) (µm) in feed samples at <2mm														
By number	2.6	2.2	2.5	1.8	2.8	1.9	1.8	2.5	1.8	2.9	2.9	2.8	2.9	2.7
By area	5.6	8.0	7.2	4.2	5.5	3.9	3.9	6.2	3.0	6.3	10.2	9.4	8.1	5.3
P. PGE mineral mode of occurrence in feed samples at <2mm (area %). Statistical uncertainty determined at the 90% confidence level and reported as absolute variation.														
Number of grains	334	257	665	228	184	214	199	199	196	179	205	189	207	192
Liberated PGEM	13±7	11±9	7±6	11±6	10±7	1±1	1±1	-	-	9±10	3±3	14±13	19±16	-
Locked in BMS	23±8	24±8	26±9	32±8	27±14	26±8	27±8	40±19	7±4	7±4	8±5	0±0	12±8	6±4
Locked in chromite	7±4	4±3	2±1	9±10	3±2	12±9	12±10	6±5	8±5	2±2	4±3	6±3	5±3	7±4
Locked in silicate	6±3	10±10	2±1	10±5	12±5	5±2	10±6	12±6	44±9	42±11	40±17	29±11	34±10	44±12
BMS/Gangue GB	44±10	42±14	57±10	30±8	31±10	53±10	40±10	30±12	25±9	20±8	37±21	25±12	16±8	19±7
Chromite/Silicate GB	7±4	10±8	6±5	8±4	17±8	4±2	10±6	11±6	16±5	20±9	8±5	26±10	15±7	23±8
Predicted PGEM liberation[+]	82	83	89	83	71	75	77	74	45	45	46	48	49	55
Q. Volume % PGE mineral associated with different base-metal sulphides in feed samples at <2mm														
Number of grains	241	236	512	174	90	71	157	127	54	54	62	34	49	51
Chalcopyrite	23	15	26	22	11	48	22	17	2	24	21	3	2	8
Pentlandite	60	61	49	74	67	38	72	68	98	2	8	32	2	43
Pyrrhotite	1	0	11	3	2	8	6	13	-	-	-	3	-	-
Pyrite	16	22	14	1	20	6	-	2	-	10	29	6	45	6
Millerite	-	2	-	-	-	-	-	-	-	45	31	35	41	41
Siegenite	-	0	-	-	-	-	-	-	-	20	11	21	10	2

An fw = Anorthosite footwall Nor fw = Norite footwall Peg fw = Pegmatoid footwal Pothole = Pothole edge RPeg fw = Replacement pegmatoid footwall Faulted = Faulted UG2

BMS = base-metal sulphide PGEM=platinum-group element mineral GB=grain boundary

Total Non-sulphide PGEM = (Pt-Fe alloy+PGE-As-S+PGE-Bi-Te+other non-sulphide PGEM)/Total PGEM (excluding laurite)

Predicted PGEM liberation = (liberated PGEM+PGEM at grain boundaries)+(PGEM assoaciated with BMS*predicted BMS liberation)

Table 5.1 continued. *Chemical, mineralogical and flotation characteristics of fourteen samples of UG2 chromitite*

Sample locality	*An fw*	*Nor fw*	*Peg fw*		*Pothole*		*RPeg fw*	*Faulted*	*Faulted*	*Pothole*	*Nor fw*	*Faulted*	*Peg fw*	*An fw*
	A2	*B2*	*A1*	*B1*	*A3*	*B3*	*A4*	*B4*	*A5*	*C1*	*C2*	*C3*	*C4*	*C5*
R. Median chromite grain diameter at 80%<75 µm based on area measurements														
Median ECD (µm)	44	38	40	41	36	38	37	41	32	42	39	41	n.d.	38
S. Median silicate grain diameter at 80%<75 µm based on area measurements														
Median ECD (µm)	39	35	34	35	34	32	31	35	30	36	32	34	n.d.	34
T. Cumulative BMS liberation and grain size at 80%<75 µm based on area measurements														
Median BMS ECD (µm)	13	12	10	12	10	10	11	10	7	7	11	9	9	2
0.8-1.0	95	100	96	99	87	92	70	99	69	48	91	88	84	33
0.6-0.8	95	100	96	99	87	92	70	99	69	48	91	88	84	33
0.4-0.6	95	100	96	99	87	98	92	99	69	58	91	88	84	33
0.2-0.4	95	100	96	99	90	100	95	99	69	78	91	88	84	46
U. PGE mineral mode of occurrence in feed samples at 80%<75µm. 90% confidence limits were calculated using resampling statistics (area %)														
Number of grains	185	193	619	187	217	190	211	217	216	236	185	191	203	183
Liberated PGEM	49±12	48±15	57±6	64±9	61±15	57±11	76±8	67±13	47±16	62±11	61±12	54±10	61±11	76±11
PGEM+Liberated BMS	28±9	38±15	30±6	18±8	9±5	26±9	16±6	25±14	0±0	6±4	7±6	5±3	5±4	0±0
PGM+(BMS)+Gangue	23±10	14±7	13±4	17±6	30±16	17±6	9±4	9±4	52±16	32±10	32±11	41±10	34±11	24±12
PGEM/(PGEM+BMS)	0.6	0.6	0.7	0.7	0.8	0.6	0.7	0.8	0.9	0.9	0.9	0.9	0.9	0.9
V. Combined liberation index of PGE-bearing particles in feed samples at 80%<75µm (area %). 90% confidence limits calculated using resampling statistics.														
0.0-0.2	15±7	11±6	8±3	12±5	8±5	14±6	4±2	8±3	39±11	22±9	15±7	26±9	28±11	14±8
0.2-0.4	5±7	0±0	0±0	0±0	15±15	0±0	1±1	1±1	4±3	1±1	10±9	4±5	4±5	1±8
0.4-0.6	0±0	2±2	0±0	3±2	3±2	2±2	0±0	0±0	5±4	6±6	5±7	8±8	1±0	6±1
0.6-0.8	1±2	1±1	0±0	3±2	5±7	0±0	2±3	0±0	4±4	1±2	1±2	3±4	1±1	2±2
0.8-1.0	79±9	87±7	92±3	83±6	69±16	84±6	93±4	91±3	48±15	70±10	69±11	59±11	66±12	77±11

An fw = Anorthosite footwall Nor fw = Norite footwall Peg fw = Pegmatoid footwal Pothole = Pothole edge RPeg fw = Replacement pegmatoid footwall Faulted = Faulted UG2

BMS = base-metal sulphide PGEM=platinum-group element mineral GB=grain boundary

PGEM/(PGEM+BMS)= %liberated PGEM/(%liberated PGEM+PGEM associated with liberated BMS)

Table 5.1 continued. *Chemical, mineralogical and flotation characteristics of fourteen samples of UG2 chromitite*

Sample locality	***An fw***	***Nor fw***	***Peg fw***		***Pothole***		***RPeg fw***	***Faulted***	***Faulted***	***Pothole***	***Nor fw***	***Faulted***	***Peg fw***	***An fw***
	A2	***B2***	***A1***	***B1***	***A3***	***B3***	***A4***	***B4***	***A5***	***C1***	***C2***	***C3***	***C4***	***C5***
W. Combined liberation index of PGE-bearing particles other than laurite in feed samples at 80%<75µm (area %).														
n	156	163	502	157	191	152	162	168	182	208	160	171	173	162
0.0-0.2	16	9	7	12	8	12	4	6	36	16	8	27	23	12
0.2-0.4	7	0	0	0	15	0	1	1	5	2	12	5	1	1
0.4-0.6	0	2	0	3	3	2	0	0	6	7	6	10	2	1
0.6-0.8	2	1	0	3	5	0	3	0	5	0	2	3	1	2
0.8-1.0	75	88	92	83	69	85	91	93	49	74	72	56	73	83
X. PGE mineral median equivalent circle diameter (µm) in feed samples at 80%<75µm														
By number	1.9	2.1	2.1	2.1	1.8	2.2	1.6	2.2	2.0	2.3	2.4	2.0	2.3	2.2
By area	3.9	5.5	3.8	3.9	5.9	5.0	3.9	4.2	4.8	3.9	5.4	4.1	4.9	6.9
Y. Time to reduce sample to 80%<75µm														
Time (minutes)	95	72	117	72	106	90	80	72	40	60	72	69	96	74
Z. Cu flotation characteristics														
R_f	61.6	57.3	66.2	76.6	60.0	74.5	54.5	70.4	55.4	34.0	37.3	32.2	34.4	39.0
R_s	24.0	25.7	20.6	15.7	25.7	17.0	30.7	22.2	28.5	24.7	28.2	25.3	29.3	34.6
100-U	14.4	16.9	13.2	7.7	14.3	8.5	14.8	7.4	16.0	41.3	34.5	42.5	36.3	26.4
k_f	2.02	2.06	2.24	3.08	2.01	2.07	1.73	2.05	2.04	1.76	1.74	1.57	1.49	1.92
k_s	0.18	0.20	0.16	0.15	0.17	0.16	0.21	0.14	0.14	0.14	0.13	0.12	0.15	0.17

An fw = Anorthosite footwall Nor fw = Norite footwall Peg fw = Pegmatoid footwal Pothole = Pothole edge RPeg fw = Replacement pegmatoid footwall Faulted = Faulted UG2

BMS=base-metal sulphide equivalent circle diameter BMS liberation index= area of BMS/total area of particle

R_f= recovery of fast-floating material R_s= recovery of slow-floating material 100-U=non-floating fraction

k_f= fast-floating rate constant k_s= slow-floating rate constant

Table 5.1 continued *Chemical, mineralogical, milling and flotation characteristics of fourteen samples of UG2 chromitite*

Sample locality	*An fw*	*Nor fw*	*Peg fw*		*Pothole*		*RPeg fw*	*Faulted*	*Faulted*	*Pothole*	*Nor fw*	*Faulted*	*Peg fw*	*An fw*
	A2	*B2*	*A1*	*B1*	*A3*	*B3*	*A4*	*B4*	*A5*	*C1*	*C2*	*C3*	*C4*	*C5*
AA. Ni flotation characteristics														
R_f	32.4	24.3	38.1	22.7	31.8	37.2	28.1	20.6	19.5	17.7	19.8	14.0	17.8	18.4
R_s	28.7	27.4	22.4	19.1	29.3	26.9	35.7	48.0	29.3	31.4	35.2	29.9	31.7	30.0
100-U	38.9	48.2	39.5	58.2	38.9	35.9	36.2	31.5	51.2	50.9	45.0	56.1	50.5	51.6
k_f	1.41	1.72	1.92	1.91	1.64	1.82	1.20	1.36	1.32	1.42	1.50	1.19	0.99	1.28
k_s	0.17	0.18	0.14	0.14	0.17	0.15	0.17	0.16	0.12	0.12	0.12	0.10	0.13	0.11
AB. PGE+Au flotation characteristics														
R_f	75.1	73.8	79.8	80.3	63.4	74.4	59.9	56.5	39.7	66.3	71.5	68.2	74.8	74.8
R_s	18.8	19.6	16.3	15.3	25.9	21.0	33.7	37.7	28.7	24.5	22.6	24.0	19.9	21.1
100-U	6.2	6.6	3.9	4.4	10.7	4.6	6.4	5.8	31.6	9.2	6.0	7.8	5.3	4.1
k_f	2.13	2.90	2.38	2.45	2.05	2.06	1.60	2.17	1.62	1.98	2.10	2.01	2.24	2.16
k_s	0.20	0.24	0.22	0.18	0.21	0.25	0.22	0.24	0.15	0.21	0.19	0.19	0.22	0.21
AC. Pt flotation characteristics														
R_f	77.3	83.1	81.6	72.4	68.5	79.5	71.5	70.4	32.9	69.2	72.3	71.7	76.7	78.6
R_s	17.4	13.4	14.4	19.6	22.9	15.7	22.7	24.3	34.9	22.5	21.8	21.2	18.3	17.6
100-U	5.2	3.4	4.0	8.0	8.6	4.7	5.8	5.3	32.2	8.3	5.9	7.1	4.9	3.8
k_f	1.91	2.44	2.13	2.27	1.74	1.74	1.41	1.68	1.31	1.68	1.81	1.78	1.97	1.88
k_s	0.06	0.07	0.07	0.05	0.05	0.06	0.07	0.08	0.02	0.05	0.07	0.06	0.07	0.08

An fw = Anorthosite footwall Nor fw = Norite footwall Peg fw = Pegmatoid footwal Pothole = Pothole edge RPeg fw = Replacement pegmatoid footwall Faulted = Faulted UG2

R_f= recovery of fast-floating material R_s= recovery of slow-floating material 100-U=non-floating fraction

k_f= fast-floating rate constant k_s= slow-floating rate constant

Table 5.1 continued *Chemical, mineralogical, milling and flotation characteristics of fourteen samples of UG2 chromitite*

Sample locality	***An fw***	***Nor fw***	***Peg fw***		***Pothole***		***RPeg fw***	***Faulted***	***Faulted***	***Pothole***	***Nor fw***	***Faulted***	***Peg fw***	***An fw***
	A2	***B2***	***A1***	***B1***	***A3***	***B3***	***A4***	***B4***	***A5***	***C1***	***C2***	***C3***	***C4***	***C5***
AD. Pd flotation characteristics														
R_f	73.0	79.3	79.1	68.8	61.4	77.2	59.8	56.5	31.9	66.1	73.2	67.1	74.1	76.0
R_s	20.5	15.8	15.9	22.3	27.4	17.6	31.8	36.6	34.6	23.3	19.9	22.7	18.7	18.4
100-U	6.5	4.9	5.1	8.9	11.2	5.2	8.5	6.8	33.6	10.6	6.9	10.2	7.3	5.5
k_f	1.71	2.44	2.11	1.98	1.65	1.80	1.19	1.54	1.38	1.87	2.07	1.78	2.01	2.02
k_s	0.06	0.06	0.06	0.05	0.05	0.06	0.07	0.09	0.02	0.04	0.06	0.05	0.05	0.06
AE. Rh flotation characteristics														
R_f	69.9	84.7	75.4	70.5	65.1	78.0	60.9	54.9	23.7	55.3	61.6	57.7	72.9	70.8
R_s	29.8	15.1	20.5	29.2	26.9	17.1	34.7	39.8	41.5	32.3	30.9	32.3	22.9	24.7
100-U	0.2	0.3	4.1	0.3	8.0	4.9	4.4	5.3	34.8	12.4	7.5	10.0	4.2	4.4
k_f	2.13	2.92	2.24	2.46	1.63	1.70	1.16	1.54	1.15	1.40	1.59	1.45	1.89	1.62
k_s	0.25	0.21	0.25	0.23	0.06	0.06	0.11	0.10	0.03	0.05	0.07	0.06	0.09	0.09

An fw = Anorthosite footwall Nor fw = Norite footwall Peg fw = Pegmatoid footwal Pothole = Pothole edge RPeg fw = Replacement pegmatoid footwall Faulted = Faulted UG2

R_f= recovery of fast-floating material R_s= recovery of slow-floating material 100-U=non-floating fraction

k_f= fast-floating rate constant k_s= slow-floating rate constant

5.2 Mineralogy of crushed feed samples

5.2.1 Bulk modal analysis

Image analysis results

Image analysis measurements indicated that the chromite content of the samples investigated range between 50.1 to 75.9 mass per cent (Table 5.1E). Base-metal sulphide minerals are present at concentration levels between 0.03 and 0.18 mass per cent, with the lowest values recorded in samples from area C, i.e. samples C1 to C5 (Table 5.1E).

Comparison with chemical assay values

Cr_2O_3 assay values were recalculated to mass per cent chromite, assuming an average Cr_2O_3 content in chromite of 42.86%.* Generally, there is good agreement between the chromite content measured by image analysis, and the chromite content calculated from Cr_2O_3 values, with differences smaller than 10 per cent for most samples (Table 5.1E). Most of the differences can be ascribed to plucking out of chromite grains during polishing, especially in samples containing sintered chromite on which it is difficult to obtain a good polish. Deviations of the actual Cr_2O_3 content from the average value would also lead to discrepancies.

5.2.2 Base-metal sulphide modal composition

Image analysis results

The relative amounts of the different base-metal sulphides in the samples examined are reported in Table 5.1F and graphically depicted in Figure 26. With the exception of sample B2, samples from areas A and B are characterised by the presence of pentlandite, chalcopyrite, pyrrhotite and, to a lesser extent, pyrite. Qualitative EDS analysis indicated that Fe>Ni in pentlandite. In sample B2, pyrrhotite has been replaced by pyrite and the pentlandite is nickeliferous (Ni>Fe). Sample B2 also

---

* Based on the average of electron-microprobe analyses of chromite in Appendix D.

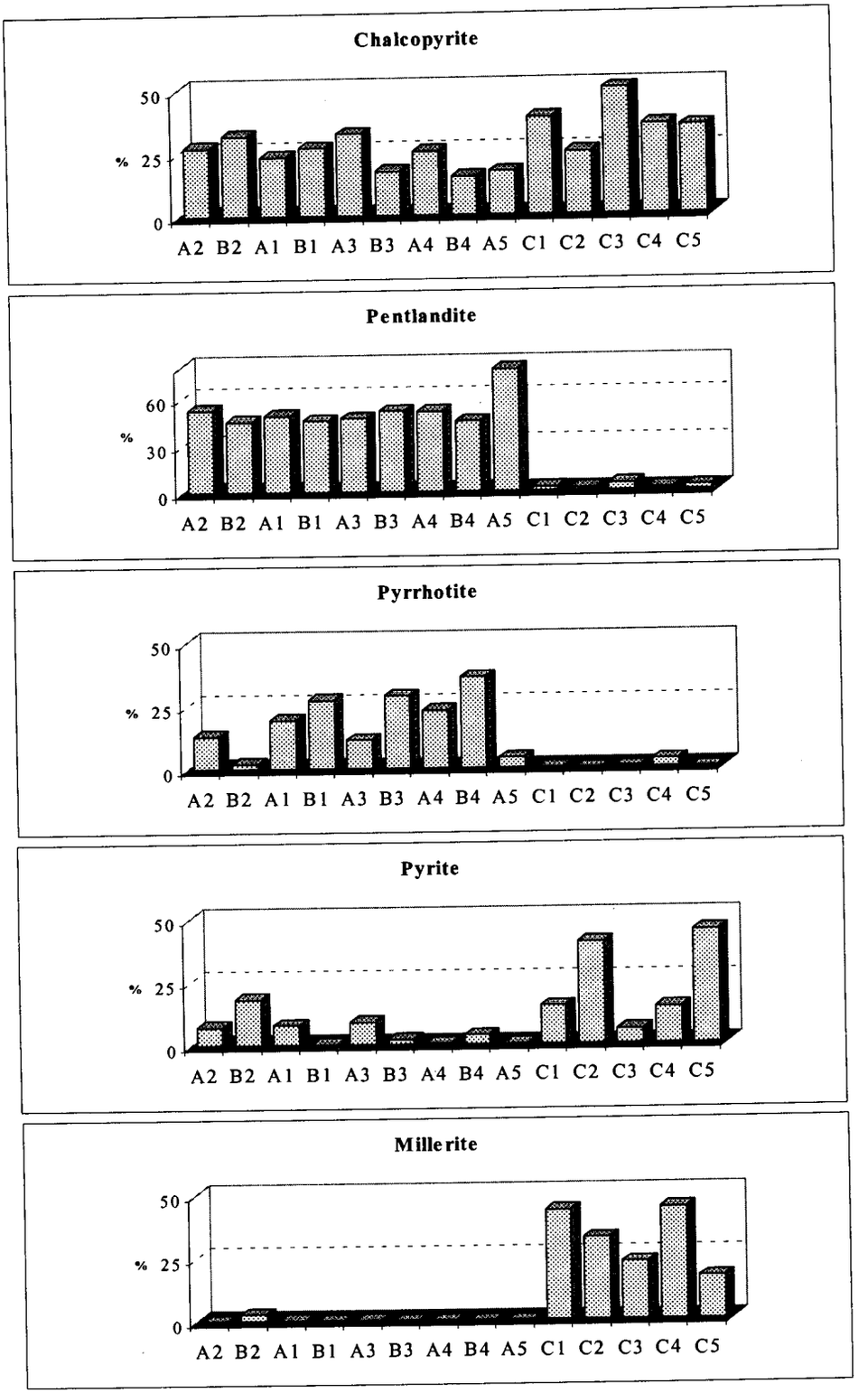

Figure 26 *Volumetric proportions of base-metal sulphide minerals in fourteen samples of UG2 chromitite.*

contains low but significant amounts of millerite, a mineral rarely encountered in samples from areas A and B.

Millerite, pyrite and chalcopyrite are the major base-metal sulphide phases in samples from area C, with pentlandite (Ni>Fe) and pyrrhotite representing minor components. Examination of polished sections of samples from area C by optical and scanning-electron microscopy also indicated the presence of occasional grains of siegenite.

Comparison with chemical assay values

From the modal amounts of pentlandite, chalcopyrite, millerite, pyrite and pyrrhotite (Table 5.1G), copper, nickel and sulphur contents were calculated for each sample. The following assumptions were made: copper content in chalcopyrite of 34.04%; nickel content in pentlandite and millerite of 31.75% and 62.24% respectively; iron content in chalcopyrite, pentlandite, pyrite, pyrrhotite and millerite of 30.44%, 33.81%, 44.69%, 61.41% and 1.27% respectively; and sulphur content in chalcopyrite, pentlandite, pyrite, pyrrhotite and millerite of 34.91%, 33.26%, 38.10%, 52.45% and 35.27% respectively.[+]

As a result of the low concentration levels of these elements, the associated measurement errors are considerable, and the chemical assay values for copper, nickel and sulphur do not always compare well with the calculated values (compare Table 5.1B with I). Nevertheless, the same general trends reported in section 5.1 could be discerned, in particular the low values of copper, nickel and sulphur in samples from area C. Note also the very low amounts of iron contained in sulphide minerals in samples from area C compared to samples from areas A and B – below 70 ppm compared to more than 240 ppm.

5.2.3 Chromite textures and grain-size distributions

Textural features of chromite in the samples investigated are similar to those described by Hiemstra (1985), Hulbert and Von Gruenewaldt (1985), and Eales and

---

[+] Based on the averages of electron-microprobe analyses of the sulphide minerals in Appendix F.

Reynolds (1986), ranging from scattered chromite subhedra in a silicate matrix (Figure 27), to patches where chromite grains appear to have been sintered together, resulting in large polygonal chromite grains with little or no interstitial silicate (Figure 28).

Chromite grain-size measurements (Figure 29 and Table 5.1J) indicate that the median measured chromite grain diameters for most samples (A1, A2, B1, B2, C2, C3, C4, C5) range between 164 and 177 μm. Due to the sintering of chromite grains, median chromite diameters in samples A3, B3, C1, and to a greater extent A4 and B4, are much larger, ranging between 184 and 221μm. All of the samples in the second group were associated with iron-rich replacement pegmatoid and/or potholes.

Minor fracturing of chromite grains was observed in most of the samples. Sample A5, collected from an intensely faulted area, is the only sample displaying extensive cataclasis (Figure 30). This is reflected in the small median measured chromite diameter of this sample (127 μm).

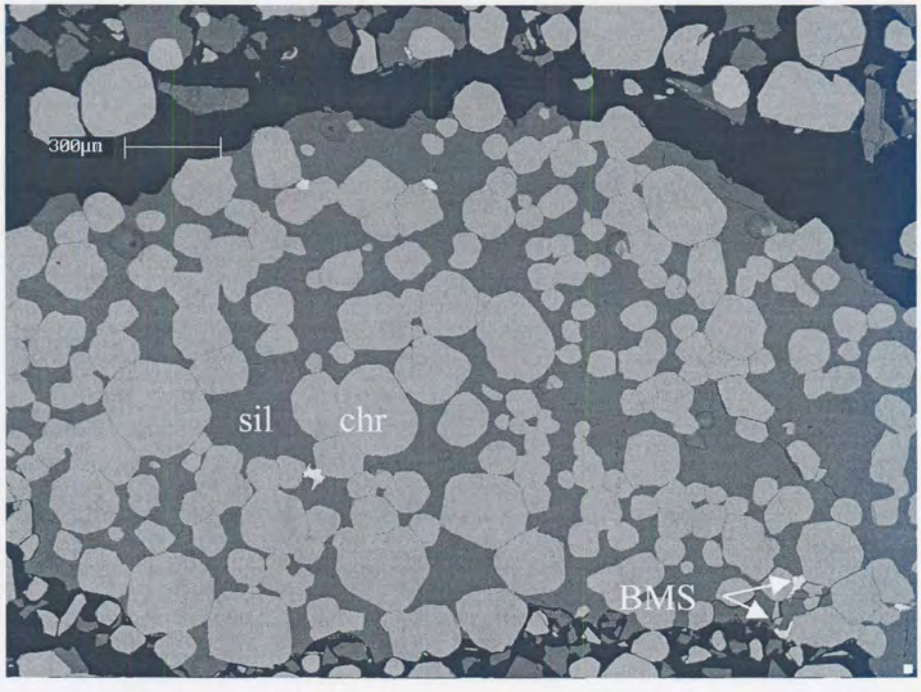

Figure 27 *Chromite textures (chr=chromite, sil=silicate, BMS=base-metal sulphide). Backscattered-electron image.*

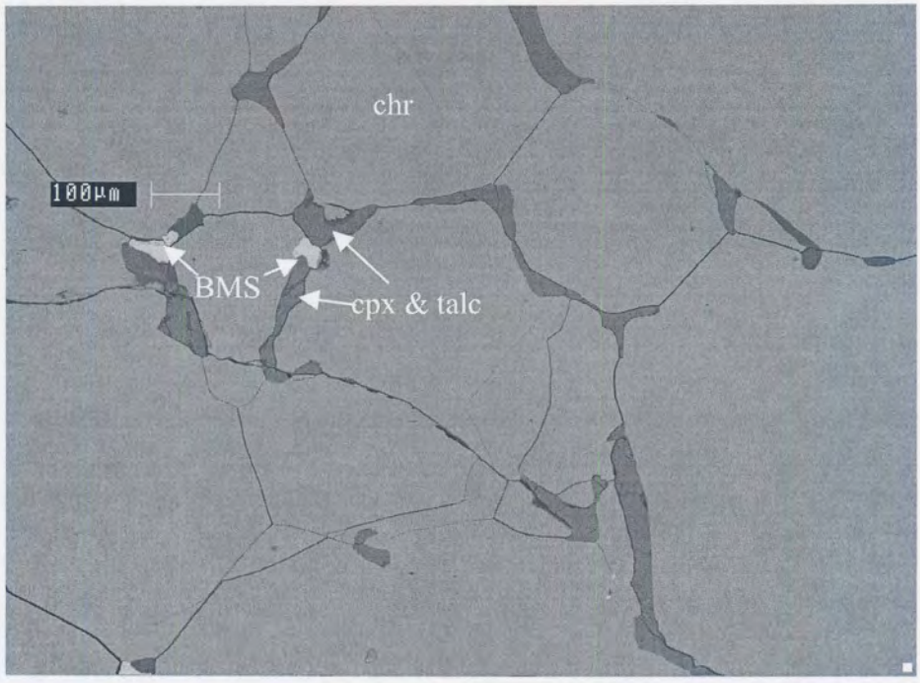

Figure 28 *Sintered chromite (chr) grains with interstitial clinopyroxene (cpx) and talc. Base-metal sulphides (BMS) are pentlandite and chalcopyrite. Backscattered-electron image.*

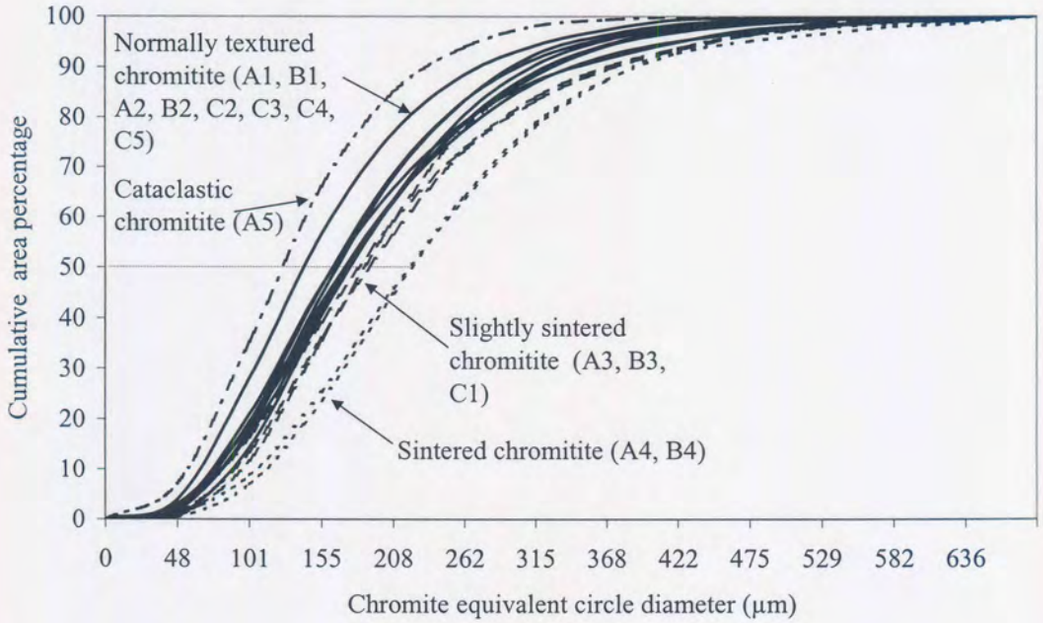

Figure 29 *Cumulative chromite grain-size distributions of 14 samples based on area measurements on polished sections. Median equivalent circle diameter values for each sample can be read off along the X-axis where the 50% line indicated on the graph intersects the size distribution curve for that sample. The slight bin size inequalities is an artefact of the measuring technique.*

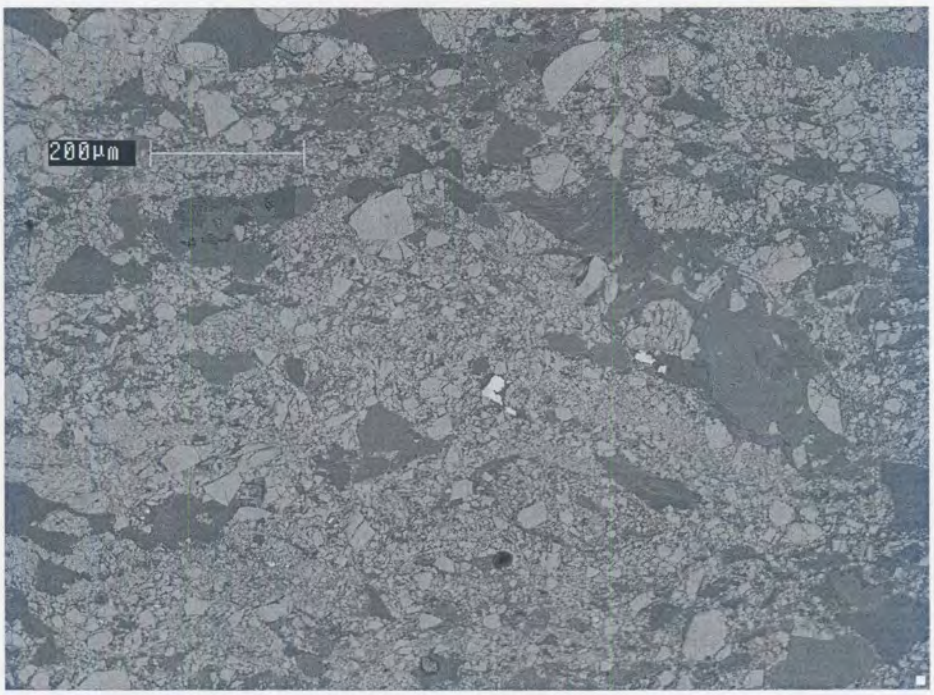

Figure 30 *Cataclastic chromite cemented by prehnite, quartz and chlorite (dark areas in image). Bright grains are pentlandite. Backscattered-electron image.*

5.2.4 Other oxide phases

Other oxide minerals occur in trace amounts. Tiny laths of rutile are often found in chromite grains. An increase in the rutile grain size was frequently observed in sintered chromite grains.

An interesting oxide assemblage, consisting of baddeleyite, an unidentified Zr-Ti oxide phase (possibly srilankite) and rutile, was observed in association with base-metal sulphides and other late- to post-magmatic phases a number of times (Figure 31), especially in samples from area C. Rare-earth element oxides are present but scarce. Magnetite occurs in trace amounts, mostly in hangingwall or footwall material from samples A4 and B1, usually at the centre of serpentine veinlets.

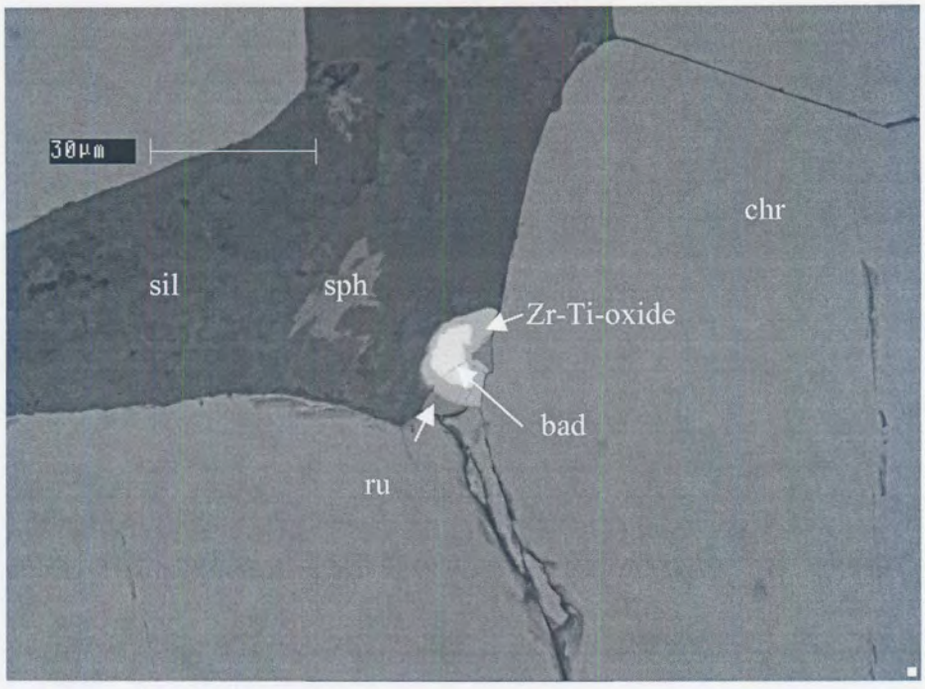

Figure 31 *Complex oxide assemblage consisting of baddeleyite (bad) (brightest grain) in the centre, rimmed by Zr-Ti-oxide (slightly darker), and rutile (ru) at the grain boundary of chromite (chr) and a fine-grained intergrowth of secondary hydrous silicates (sil) and sphene (sph). Backscattered-electron image.*

5.2.5 Silicate mineralogy

Great variabilility is displayed in the silicate mineralogy, both between and within samples. In general, plagioclase is the most commonly found silicate phase, followed by orthopyroxene (Tables 5.1 K and 5.2). Where plagioclase is the dominant silicate, chromite grains may be separated from plagioclase by a thin rind of orthopyroxene. Similarly, orthopyroxene grains are sometimes separated from chromite by a plagioclase rim. Such textures have been interpreted by Eales and Reynolds (1986) as the products of reactions involving oxide, orthopyroxene, feldspar and liquid.

With the possible exception of sample A1, most samples of UG2 chromitite display some degree of alteration of orthopyroxene to talc, usually along grain boundaries and cleavage planes (Figure 32). Chloritization of plagioclase occurs locally.

Minor amounts of diopsidic clinopyroxene are present in most samples. An increase in clinopyroxene was observed in sintered samples, especially A4 and B4 (Tables 5.1K and 5.2), often displaying a similar type of texture as that described for plagioclase and orthopyroxene. In this case though, embayed grains of clinopyroxene and plagioclase are separated from chromite by a thin layer of pargasitic hornblende (edenite) (Figure 33). Tremolite + talc and tremolite + chlorite assemblages, formed from clinopyroxene, were observed in a few areas.

Trace to minor amounts of a variety of phases including phlogopite (invariably chlorine-bearing), talc, chlorite (sometimes chlorine-bearing), rutile, baddeleyite, sphene, chlorapatite, rare-earth element oxides, Zr-Ti oxide, epidote, prehnite, tremolite, quartz, albite, pumpellyite and calcite, as well as base-metal sulphides and PGE minerals, occur interstitially between chromite and orthopyroxene or plagioclase grains. Sphene appears to have a particular affinity for phlogopite, often occurring along phlogopite cleavage planes and grain edges. A similar association of base-metal sulphide and PGE minerals with biotite, phlogopite and other hydrous silicates, quartz, rutile and zircon have been reported in samples from the Merensky Reef (Ballhaus & Stumpfl, 1986).

Olivine, partly serpentinised, occurs in small amounts in most samples. Since the olivine is usually not associated with chromite, it is assumed to have originated from the footwall and/or hangingwall.

Some samples, in particular those from area C (C1 to C5), are characterised by the replacement of the primary silicates by complex assemblages containing albite, quartz, pumpellyite, epidote, chlorite, talc, and less commonly sphene, tremolite, prehnite, K-feldspar, calcite and serpentine and sericite (Figures 34 and 35 and Tables 5.1K and 5.2). The extent of alteration ranges from isolated pockets to almost complete replacement of orthopyroxene and plagioclase in some samples (C1 and C3 in particular).

Table 5.2 *Relative amounts of silicate minerals based on qualitative observations using optical and scanning-electron microscopy, as well as XRD analysis. An=calcic plagioclase, opx=orthopyroxene, cpx=clinopyroxene, ed=edenite, tr=tremolite, phl=phlogopite, chl=chlorite, calc=calcite, qtz=quartz, ab=albite, epd=epidote, pre=prehnite, pu=pumpellyite, sph=sphene, apa=chlorapatite, kfsp=K-feldspar, serp=serpentine, schl=septechlorite, grap=graphite*

	An	**Opx**	**Cpx**	**Ed**	**Tr**	**Phl**	**Talc**	**Chl**	**Calc**	**Qtz**	**Ab**	**Epd**	**Pre**	**Pu**	**Sph**	**Apa**	**Other**
A2	●●●	●●●				●●	•	•			•			•			
B2	●●●	●●●	•			●●	●●	•	•								Kfsp
A1	●●●	●●●	●●			●●	•	•	•		•					•	
B1	●●●	●●●	●●	●●	•	●●	●●	●●	•						●●	•	
A3	●●●	●●●			•	●●	•	•			•		•	•	•		
B3	●●●	●●●	●●	●●		●●	•	•					•	•		•	
A4	●●●	●●●	●●	●●		●●	•	•						•			
B4	●●●	●●●	●●	●●	•	●●	•	•				•				•	Kfsp
A5	●●●	●●●			•	•	●●	●●		●●	●●		●●	•	•		serp schl grap
C1	●●●	●●●	•		•	●●	●●	●●		●●	●●	●●	•	●●	●●	•	
C2	●●●	●●●				●●	•	•		•	•	•		•	•		
C3	●●●	●●●			•	●●	●●	●●	•	●●	●●	●●	•	●●	●●	•	serp
C4	●●●	●●●			•	●●	●●	●●	•	●●	●●	●●		●●	●●		
C5	●●●	●●●			•	●●	•	•		•	•	•		•			

●●● *>~10%* ●● *1-10%* • *trace*

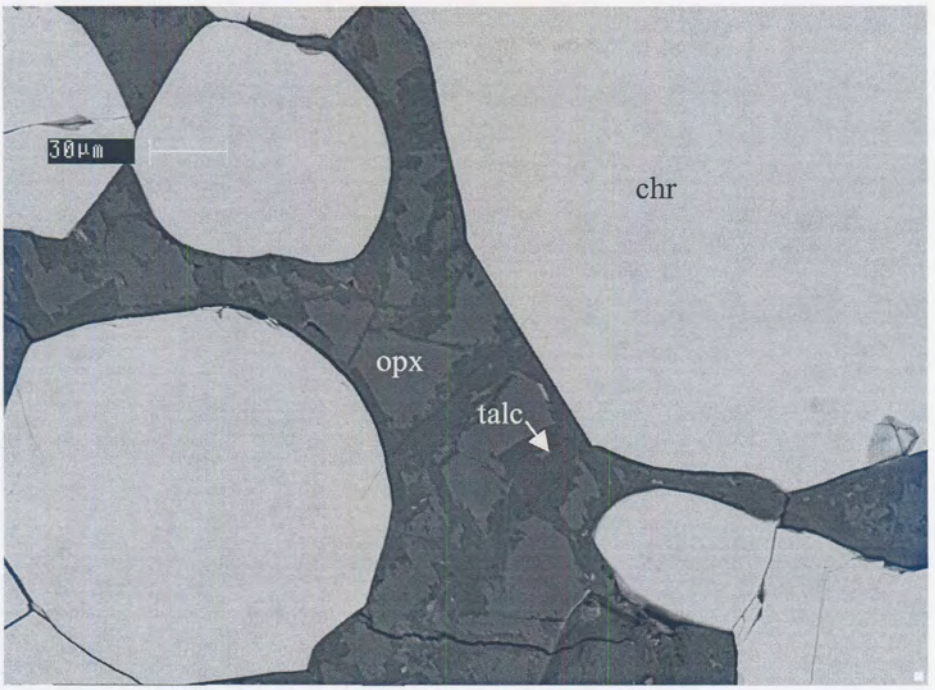

Figure 32 *Alteration of bronzite (opx) to talc along cleavage planes and grain boundaries. Backscattered-electron image*

Figure 33 *Resorbed grains of clinopyroxene (cpx) and plagioclase (an) (with dark chlorite veinlets (chl)) in amphibole (edenite)(ed). Backscattered-electron image.*

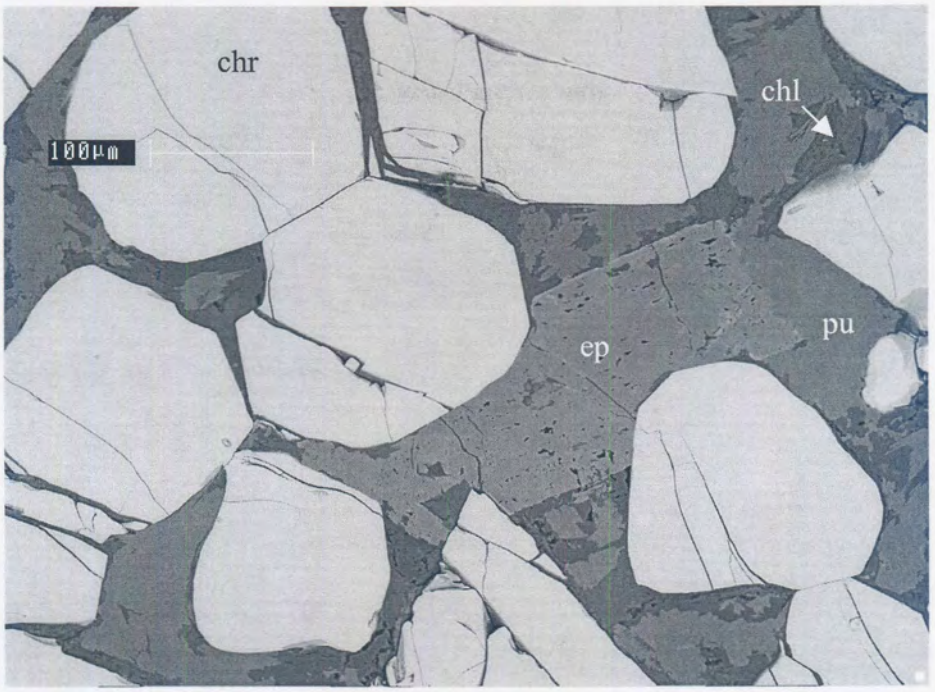

Figure 34 *Zoned epidote (ep) crystal crosscutting pumpellyite (pu) rimmed by chlorite (chl). Backscattered-electron image.*

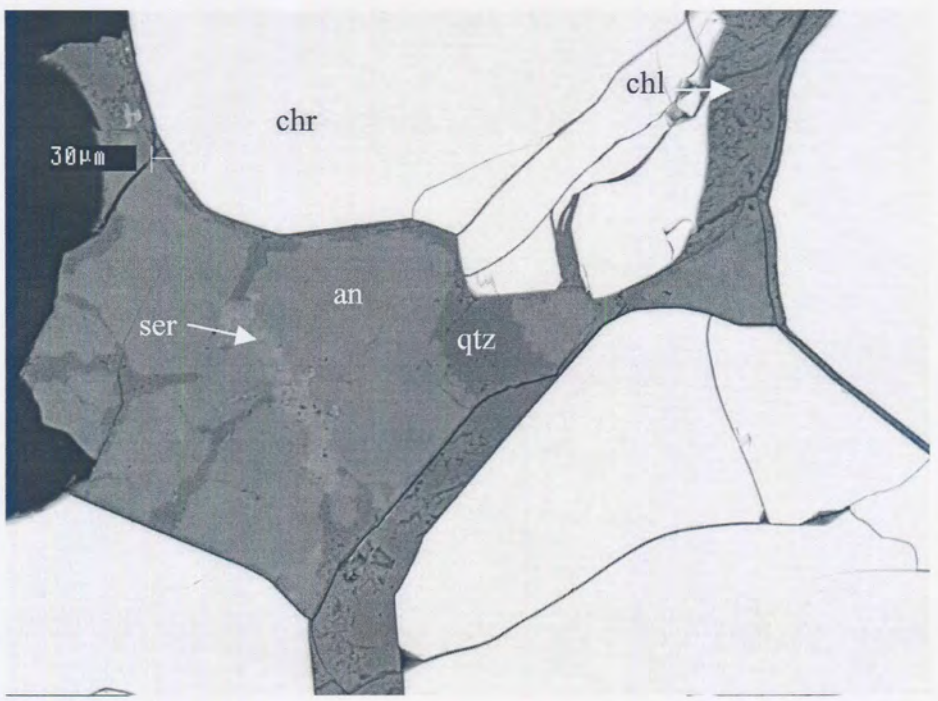

Figure 35 *Alteration of plagioclase (an) to quartz (qtz), chlorite (chl) and sericite (ser). Backscattered-electron image.*

In cataclastic chromitite (sample A5), fractured chromite grains are cemented by a number of secondary phases including septechlorites, serpentine, quartz, pumpellyite, prehnite, chlorite, calcite, tremolite, albite and graphite (Figure 30, Tables 5.1K and 5.2).

5.2.6 Base-metal sulphide mode of occurrence

Pentlandite - chalcopyrite - pyrrhotite ± pyrite assemblages

In the samples from areas A and B, chalcopyrite, pentlandite and pyrrhotite generally form composite grains at chromite-silicate grain boundaries (Table 5.1L and Figure 36), commonly in association with phlogopite and trace amounts of other late- and post-magmatic phases. In intensely sintered areas, sulphide grains may become locked between chromite grains.

Pentlandite rarely occurs as flames in pyrrhotite. Pyrrhotite is sometimes partially rimmed by pentlandite and occasionally also by chalcopyrite (Figure 37). Slight fraying of sulphide grain edges can sometimes be seen where in contact with secondary silicates. Sulphide minerals, especially pentlandite and chalcopyrite, can occasionally be seen together with secondary silicates along microfissures traversing primary silicates and chromite.

Pyrite usually occurs as chains of small grains along pentlandite cleavage planes and grain edges (Figure 38). In rare cases millerite appears to be replacing pentlandite. Trace amounts of galena were observed in most of the samples, usually occurring as small grains associated with secondary silicates, especially in samples B1, B3, C1 and C2. A few isolated grains of copper-rich sulphides (mostly bornite) were observed as inclusions in chromite.

In cataclastic UG2 chromite sulphide minerals generally occur in the silicate matrix that cements the chromite grains (Figure 30). Relatively coarse, euhedral pentlandite grains were observed in places in cataclastic UG2, suggesting recrystallization.

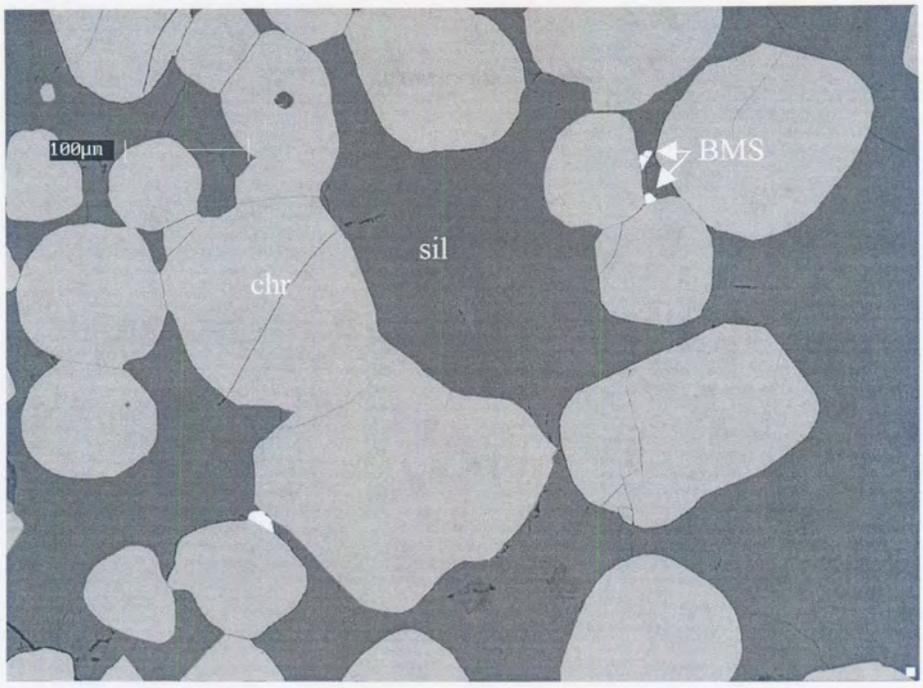

Figure 36 *UG2 chromitite consisting of rounded chromite grains in a matrix of plagioclase. Small base-metal sulphide (BMS) grains occur at chromite (chr) - silicate (sil) grain boundaries. Backscattered-electron image.*

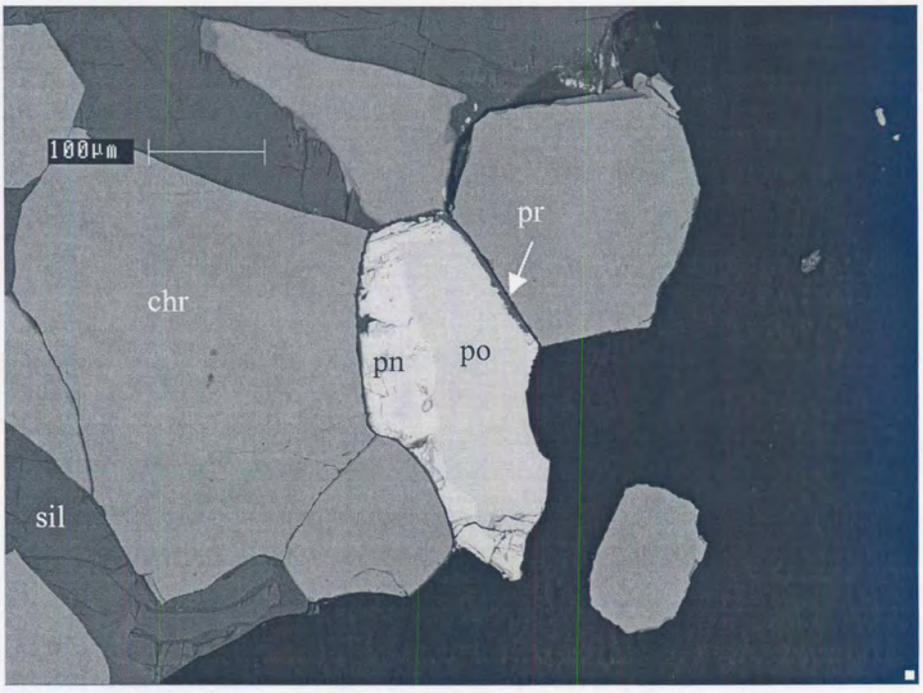

Figure 37 *Pyrhhotite (po) partially rimmed by pentlandite (pn) at a chromite(chr) – silicate (sil) grain boundary. A thin rim of prehnite (pr) separates sulphide from gangue. Backscattered-electron image.*

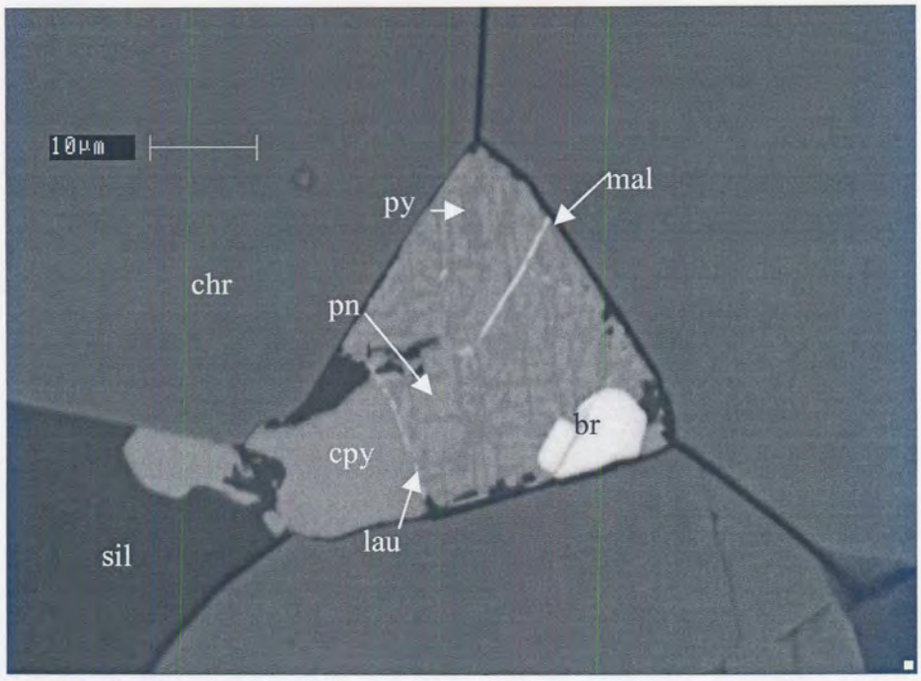

Figure 38 *Pentlandite (pn) being replaced by pyrite (py) along cleavage planes. Note the presence of a thin laurite (lau) parting at the grain boundary between chalcopyrite (cpy) and pentlandite. Other PGE minerals present are braggite (br) and malanite (mal). Silicates (sil) are quartz and plagioclase. Backscattered-electron image.*

Millerite - chalcopyrite - pyrite assemblages (samples C1 to C5)

In patches where primary silicate minerals persist, composite sulphide grains occur at chromite-silicate grain boundaries, usually associated with phlogopite and a host of secondary silicate minerals. Sulphide grains often display corroded outlines, appearing to have been partly replaced by secondary hydrous silicates (Figures 39 to 41). More extensive alteration of primary silicate assemblages leads to local redistribution (probably on a scale of tens or hundreds of microns) and recrystallization of sulphide minerals, resulting in euhedral to subhedral sulphide grains intergrown with secondary silicates (Figure 42, Table 5.1L).

The content of pentlandite in samples C1 to C5 is very low (<0.01%). Thus, pentlandite and millerite are rarely found in direct contact in these samples, making it difficult to establish the genetic relationship between these two phases. Pyrite, the major iron sulphide present, occurs both in composite grains with millerite and chalcopyrite, or, as relatively coarse-grained porous pyrite (especially in samples C1,

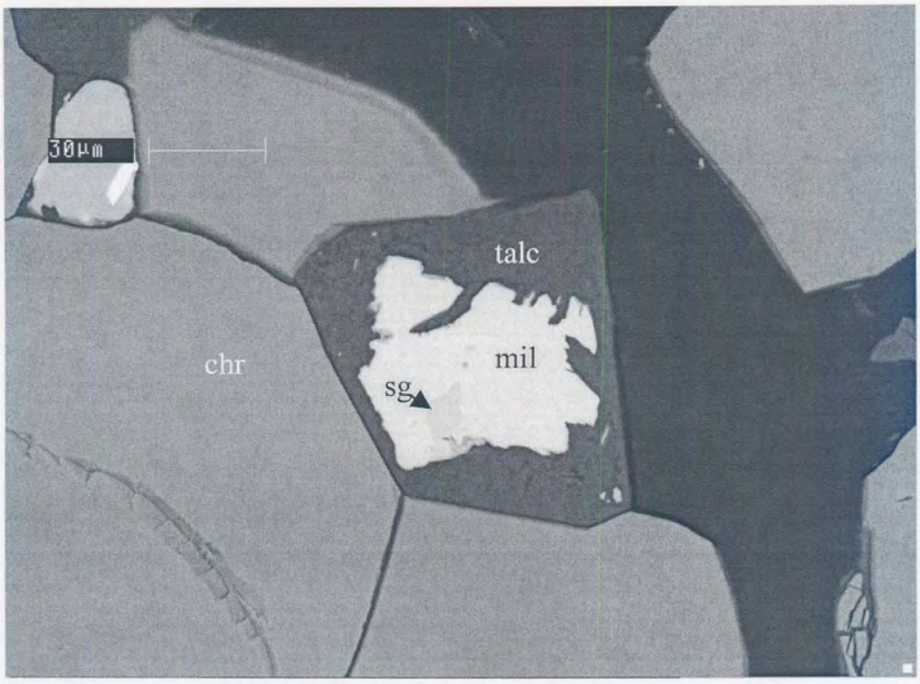

Figure 39 *Corroded base-metal sulphide grain consisting of millerite (mil) and siegenite (sg) in talc. Backscattered-electron image.*

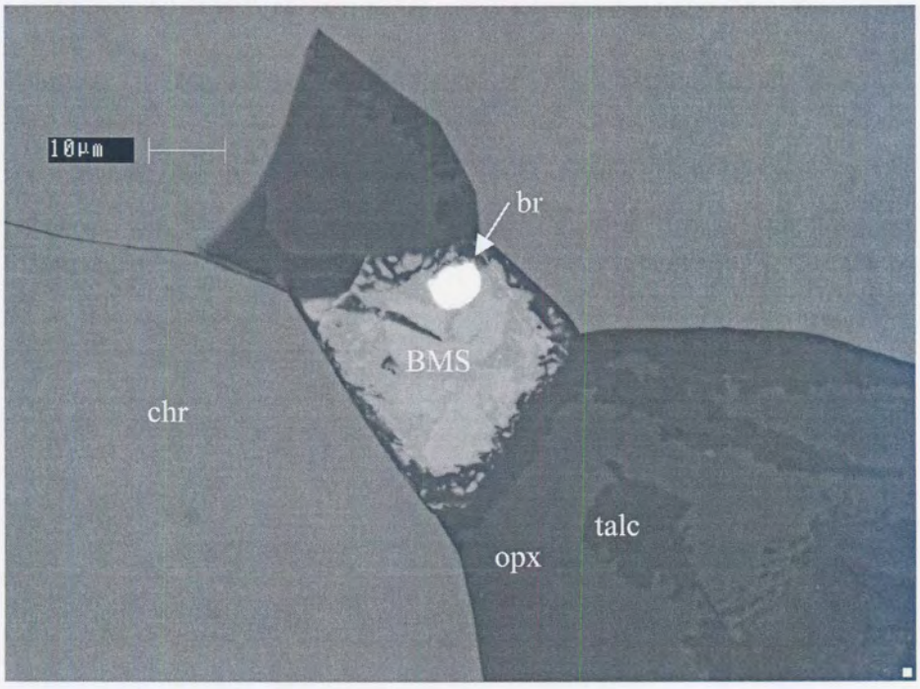

Figure 40 *Corroded base-metal sulphide grain (BMS) (chalcopyrite + millerite + pyrite) with zoned braggite (br). Silicates are orthopyroxene (opx) being altered to talc. Backscattered-electron image.*

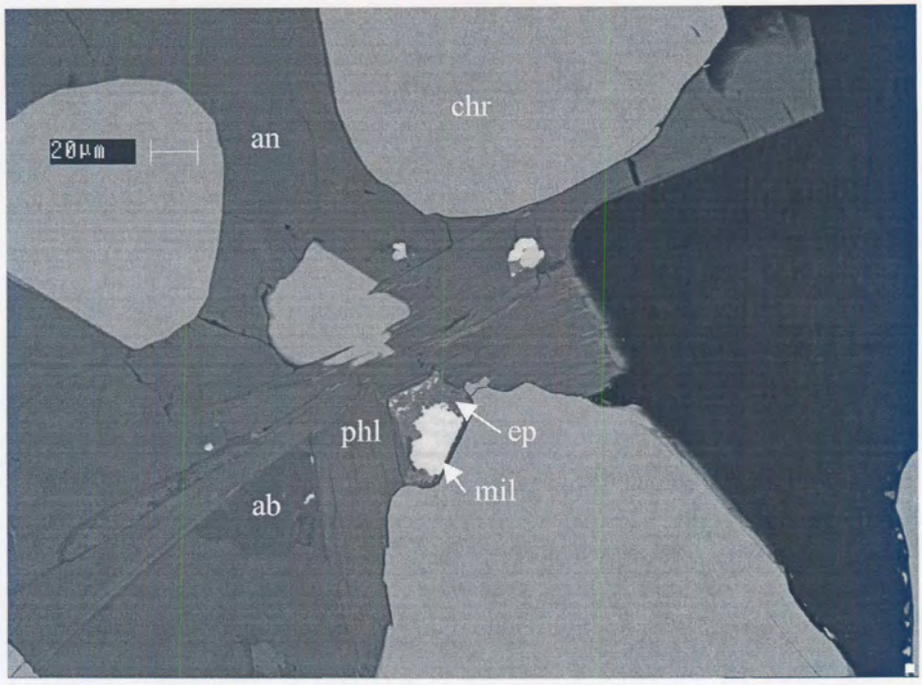

Figure 41 *Corroded millerite (mil) grain associated with epidote (ep). Other phases are phlogopite (phl), albite (ab) and Ca-plagioclase (an). Backscattered-electron image.*

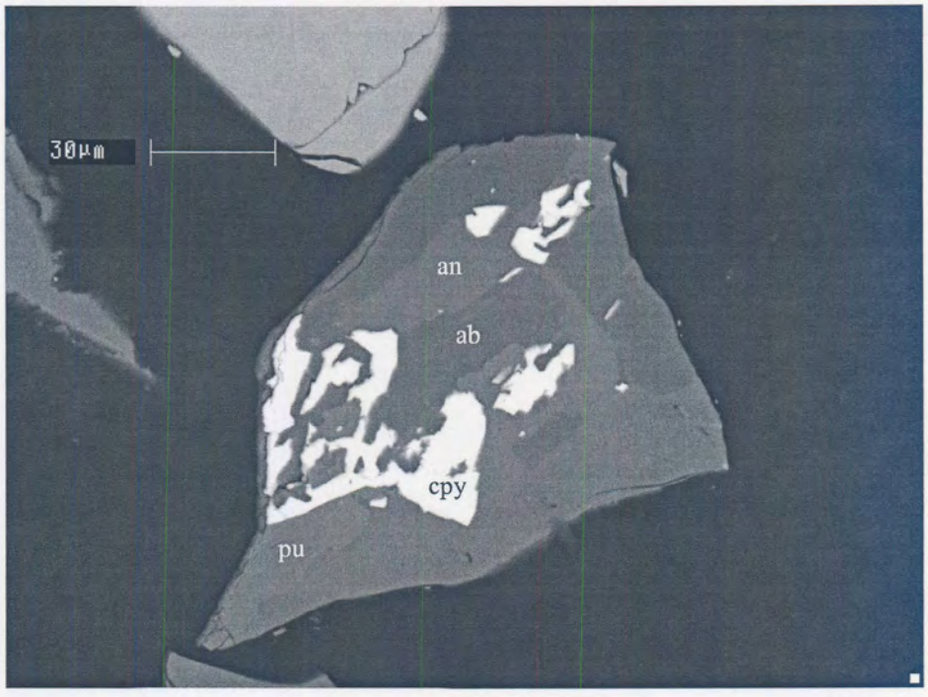

Figure 42 *"Skeletal chalcopyrite" (cpy) associated with Ca-plagioclase (an), albite (ab) and pumpellyite (pu). Backscattered-electron image.*

C3 and C5) at chromite-silicate grain boundaries or filling cracks in chromite. Siegenite is a ubiquitous but minor component, usually associated with millerite.

5.2.7 Base-metal sulphide grain-size distribution

Base-metal sulphide grain-size distributions are graphically illustrated in Figure 43. The median sulphide grain diameters in normally textured chromitite from areas A and B (samples A1, A2, B1 and B2) lies between 30 and 32 µm (Table 5.1L), with maximum diameters coarser than 100 µm. Samples from area C are characterised by much smaller median values - between 17 and 22 µm and grains coarser than 100 µm were rarely observed. The average of the median base-metal sulphide diameters for samples A1, A2, B1 and B2 is 31 µm, and for samples C1 to C6, 20 µm. Statistical analysis (Simon & Bruce, 1991) indicated that the chance of the 11µm difference between these two values being attributable to chance is only 1%. A small chromite diameter of 17 µm was also recorded for cataclastic UG2 (sample A5).

In samples characterised by a coarsening of chromite due to sintering (B3, A3, B4 & A4), the sulphide grains are also bigger with measured median diameters >33 µm (the average value for this group of samples is 39 µm). The exception in the last instance being sample C1, presumably as a result of corrosion of sulphide grains in area C. Statistical analysis (Simon & Bruce, 1991) indicated that the likelihood of the 8µm difference between the average for samples B3, A3, B4 and A4 and that for samples A1, A2, B1 and B2 is attributable to chance, is only 6%.

5.2.8 Modal distribution of PGE minerals

PGE minerals associated with pentlandite-chalcopyrite-pyrrhotite±pyrite assemblages (areas A and B)

The PGE mineral assemblages in samples A1, A2, B2 and A3 consist predominantly (more than 90 volume %) of sulphide minerals, mostly Pt-Pd-Ni sulphide, Pt-sulphide, Pt-Rh-Cu-Ni-sulphide and laurite (Table 5.1M, Figure 44). Samples B1 and B3 contain small amounts of Pt-Fe alloy and other non-sulphide PGE minerals.

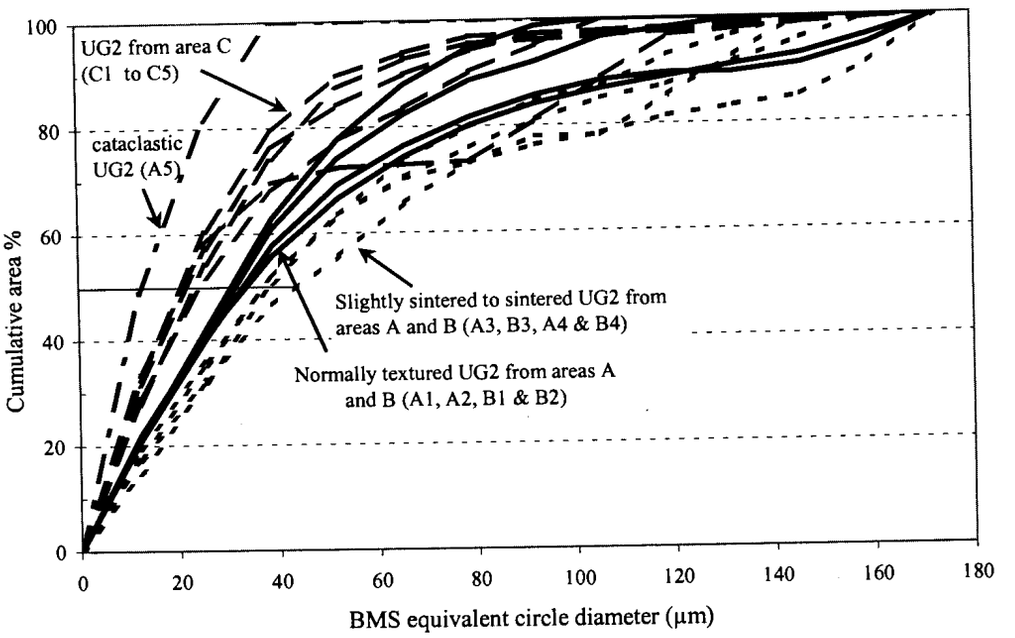

Figure 43 *Measured base-metal sulphide grain-size distributions in fourteen samples of crushed UG2 chromitite. Median equivalent circle diameter values for each sample can be read off along the X-axis where the 50% line indicated on the graph intersects the size distribution curve for that sample.*

Samples A4 and B4 are characterised by PGE mineral assemblages consisting predominantly of Pt-Fe alloys (often rhodium- or palladium-bearing), laurite, and to a lesser extent PGE-Bi-Te compounds, and other non-sulphide PGE minerals (Table 5.1M and Figure 44).

The PGE mineral assemblage of cataclastic UG2 chromitite (sample number A5) is dominated by laurite and non-sulphide PGE minerals such as Pt-Fe alloys (Table 5.1M and Figure 44). Although Pt-Rh-Cu-Ni-sulphide and Pt-Pd-Ni-sulphides represent a significant proportion of the PGE minerals, Pt-sulphide is relatively scarce.

<u>PGE minerals associated with millerite-pyrite-chalcopyrite assemblages (C1 to C5)</u>

One of the most striking aspects of the PGE mineral assemblages from the mining area represented by these samples, is the sharp drop in the modal proportions of Pt-sulphide and a concomitant increase in Pt-Rh-Cu-Ni -sulphide and Pt-Pd-Ni-sulphide compared to that found in most samples from areas A and B (A1, A2, B1, B2, A3 & B3) (Table 5.1M and Figure 44). Qualitative EDS analyses of Pt-Pd-Ni-sulphide also

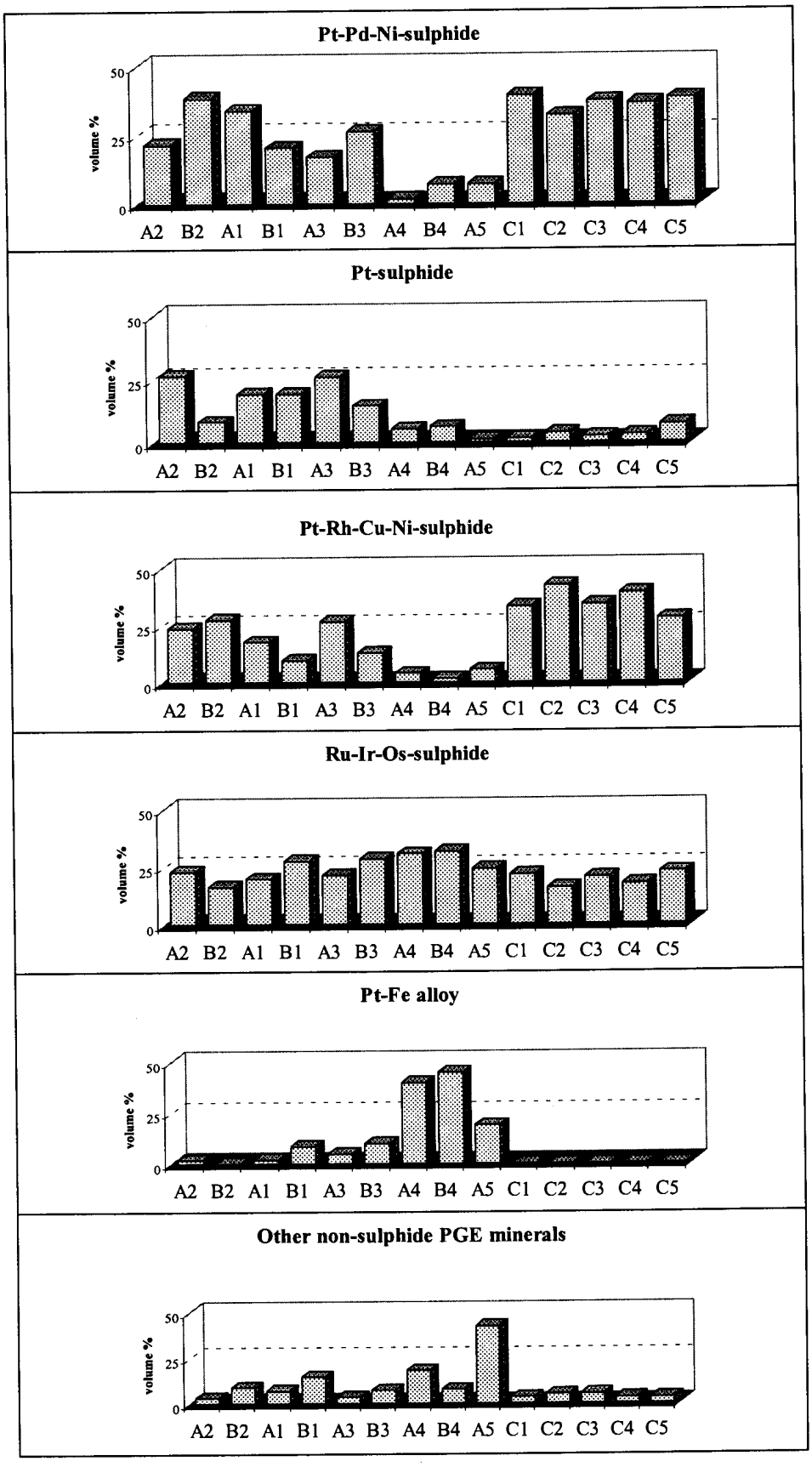

Figure 44 *PGE mineral distribution in fourteen samples of UG2 chromitite.*

suggest a change to more palladian compositions. Note also the evidently complete absence of Pt-Fe alloys from these samples.

5.2.9 PGE mineral grain-size distribution

Based on a composite of all fourteen samples, the median PGE mineral grain diameter in UG2 chromitite from the study area is ~6.5 µm (Figure 45), which agrees well with the average value of 5.1 µm reported by McLaren (1980). PGE mineral grain sizes, expressed as equivalent circle diameter, range from <1 µm to ~ 50 µm.

Median PGE mineral grain-diameter values for the samples examined vary between 3.0 and 10.2 µm, based on area per cent (Table 5.1O). Due to the large error associated with these measurements, the differences between these values are not statistically significant (Table 4.17). That there are significant differences in PGE mineral grain sizes between the samples is indicated by the median PGE mineral diameter calculated from the percentage number of grains, with values ranging from 1.8 to 2.9 (Table 5.1O). Although this value does not reflect the true grain diameter, it is statistically more reliable and does allow for comparisons between samples. Note the generally larger median percentage number of grains for samples from area C with an average value of 2.8 µm (ranging from 2.7 to 2.9 µm), compared to an average of 2.2 µm (between 1.8 and 2.8 µm) for samples from areas A and B.‡

5.2.10 PGE mineral mode of occurrence

The mode of occurrence of PGE minerals in the crushed feed samples have been summarised in Table 5.1P and Figure 46. In all samples, the largest proportion of the PGE minerals (40 to 70%) occurs at grain boundaries of base-metal sulphide and/or oxide and/or silicate, or have been liberated (up to 20%) during crushing of the ore.

With the exception of sample A5, the remainder of the PGE minerals in samples from areas A and B mostly form part of base-metal sulphide composite grains (20 to 40%).

---

‡ This is a small, but statistically significant difference. See Table 4.17.

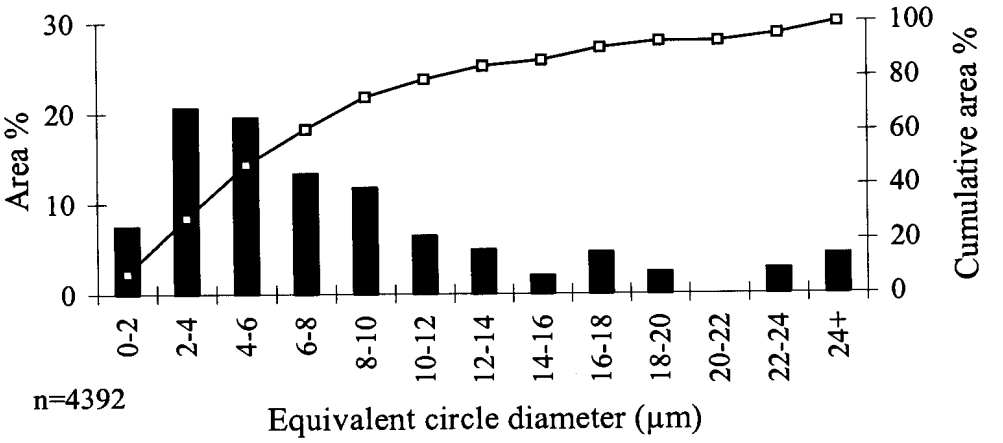

Figure 45 *PGE mineral grain-size distribution in fourteen crushed feed samples.*

The frequency of association of PGE mineral grains with different base metal sulphides is reported in Table 5.1Q. Caution is advised when interpreting these results. For instance, in sample A1, 49 per cent of the PGE minerals in contact with sulphide is associated with pentlandite. This does not necessarily mean that the PGE minerals are preferentially associated with pentlandite, rather, since pentlandite represent 49 per cent of the base-metal sulphide assemblage, it means that there is no preferential PGE mineral-pentlandite association. In addition, in samples where a smaller percentage of the PGE minerals are associated with base-metal sulphides (samples from area C and sample A5), the results are based on a relatively small number of grains and consequently not reliable.

Samples from area C and sample A5 are characterised by a relatively high percentage of PGE mineral grains enclosed in silicate gangue, or at silicate-silicate grain boundaries, generally between 30 and 50% compared to less than 15% in the other samples.

In all samples, less than 10% of PGE mineral grains occur as inclusions in chromite. More than 90% of these inclusions consist of laurite ($(Ru,Os,Ir)S_2$), representing ~25% of the total laurite. Apart from the laurite-chromite association, no evidence could be found that specific PGE minerals occur preferentially in association with either oxide or silicate.

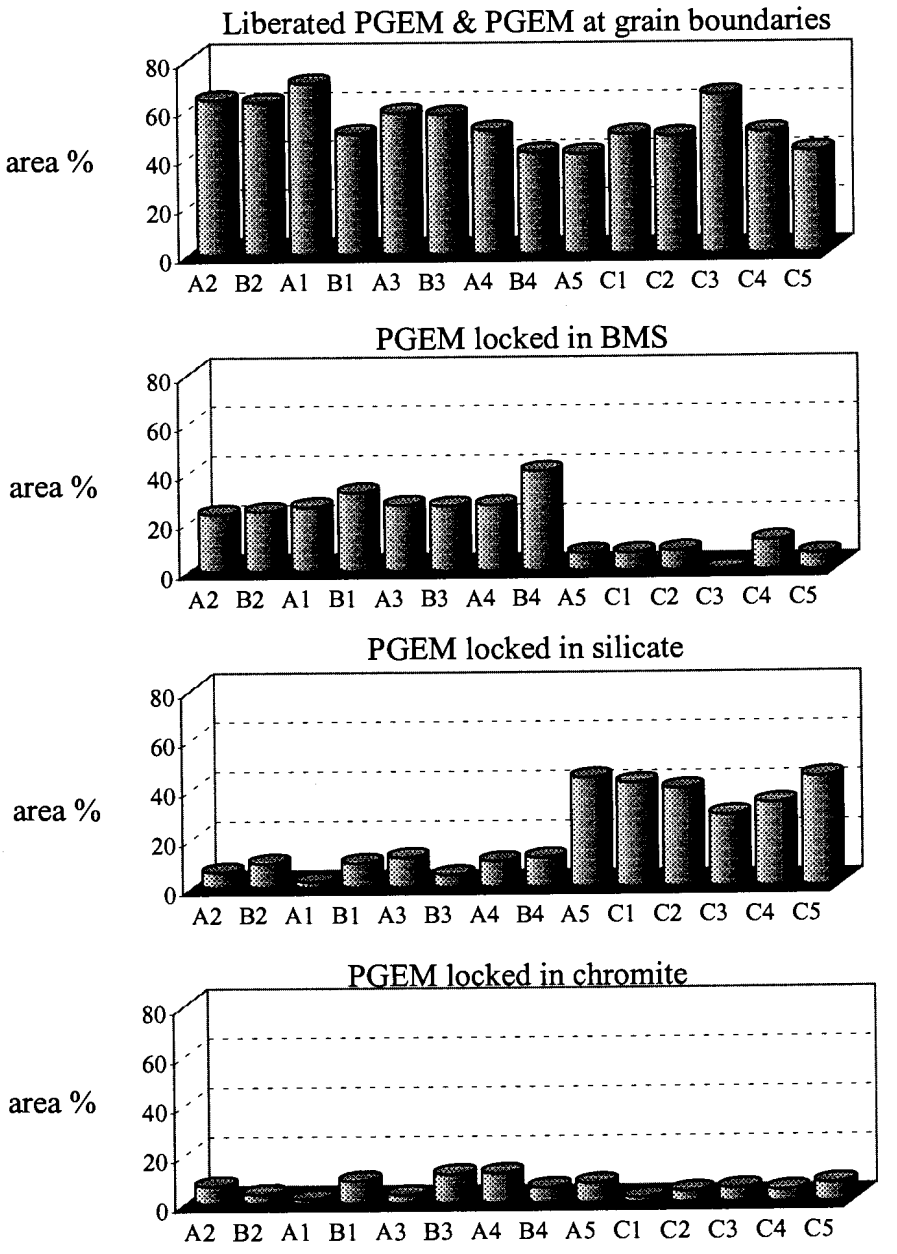

Figure 46 *Mode of occurrence of PGE minerals (PGEM) in fourteen samples of UG2 chromitite at <2mm.*

5.2.11 Chromite composition

Sintered chromite grains display higher optical reflectivity and backscattered-electron intensity compared to normal-textured chromite. Although an in-depth analysis of the variations in chromite compositions is beyond the scope of this investigation, a

number of selected chromite grains from different samples were analysed by electron microprobe to get an indication of the effect sintering of chromite grains has on composition (Table 5.3 and Tables 1 to 8 Appendix D).

Sporadic core-rim analyses indicated no systematic compositional variation within chromite grains. Silicon and calcium are generally not present at levels above the detection limits. Nickel, vanadium, cobalt, copper, manganese and zinc are present in concentrations above the detection limits, but show very little variation. The average chromite nickel content is about 0.15 per cent, which, for UG2 ore containing 50 to 75 per cent chromite is equivalent to 600 to 900 ppm nickel, accounting for most of the nickel not present in acid soluble form (Table 5.1B). Similarly, most of the cobalt that is not present in acid soluble form appears to be accommodated by chromite.

A comparison of the chemical composition of normal and sintered chromite grains in sample A1 shows an increase in titanium, chromium, and iron values, and a decrease in aluminium and possibly magnesium, in the sintered grains. Chromite grains from sample A4 showed an increase in titanium and iron, but a decrease in chromium, aluminium, and magnesium in sintered grains. Compositions of sintered grains in sample B4 are similar to those in sample A4. A comparison of compositions of chromite grains in sample C1 shows an increase in titanium in the sintered grains, no further systematic variations could be discerned from the data.

Some of the compositional variation can probably be ascribed to systematic changes in chromite composition with stratigraphic height (McLaren & De Villiers, 1982), an aspect not considered in this study. In general the sintered chromite grains appear to be significantly more titaniferous.

5.2.12 Silicate compositions

Feldspar

Feldspar EDS analyses are tabulated in Tables 1 to 8, Appendix E. Calcic plagioclase compositions are highly variable corresponding to that of labradorite-bytownite ($An_{55-85}Ab_{15-44}Or_{0-2}$). Zoning is common. Albite-oligoclase ($Ab_{87-95}An_{5-13}$) and K-feldspar ($Or_{74-86}Ab_{14-25}An_{0-1}$) occur less commonly.

Table 5.3 *Average chromite compositions of UG2 chromitite from samples A1, A4, C1 and B4. The 95% confidence interval was calculated using Student's t-distribution.*

Sample	A1 (pegmatoid fw)				C1 (pothole edge)						A4 (replacement pegmatoid fw)				B4 (replacement pegmatoid fw)	
Texture	<300µm normal		>300µm sintered		<200µm normal		>200µm sintered		>300µm sintered		<300µm normal		>500µm sintered		>200µm sintered	
TiO_2	0.85	±0.03	1.07	±0.08	0.91	±0.15	1.19	±0.01	1.29	±0.02	0.99	±0.02	2.31	±0.28	1.30	±0.03
V_2O_3	0.33	±0.02	0.35	±0.07	0.45	±0.05	0.44	±0.04	0.40	±0.03	0.27	±0.01	0.28	±0.02	0.40	±0.01
Al_2O_3	16.85	±0.36	15.05	±0.62	14.96	±0.44	15.16	±0.08	15.19	±0.07	17.44	±0.14	14.46	±0.75	15.01	±0.09
Cr_2O_3	42.79	±0.34	43.96	±0.42	43.92	±0.63	43.49	±0.11	42.94	±0.06	44.18	±0.21	40.72	±0.19	41.81	±0.08
Fe_2O_3	8.95	±0.16	9.42	±0.16	9.44	±0.34	9.87	±0.07	10.16	±0.10	6.08	±0.09	10.05	±0.47	9.88	±0.35
FeO	19.20	±0.17	19.60	±0.43	20.58	±0.55	19.52	±0.06	20.14	±0.06	21.88	±0.09	25.29	±0.45	22.06	±0.28
MnO	0.26	±0.00	0.27	±0.00	0.28	±0.01	0.28	±0.01	0.26	±0.01	0.26	±0.00	0.30	±0.01	0.27	±0.00
NiO	0.14	±0.01	0.13	±0.02	0.13	±0.02	0.16	±0.01	0.16	±0.01	0.17	±0.00	0.15	±0.01	0.17	±0.00
CoO	0.02	±0.01	0.01	±0.01	0.02	±0.01	0.02	±0.01	0.02	±0.01	0.02	±0.01	0.02	±0.01	0.02	±0.00
CuO	0.02	±0.01	0.03	±0.03	0.03	±0.01	0.04	±0.02	0.04	±0.02	0.03	±0.01	0.03	±0.01	0.02	±0.01
ZnO	0.08	±0.01	0.07	±0.03	0.11	±0.01	0.10	±0.02	0.11	±0.02	0.10	±0.01	0.14	±0.01	0.05	±0.01
MgO	9.65	±0.14	9.23	±0.33	8.59	±0.42	9.32	±0.05	8.93	±0.03	8.01	±0.07	5.43	±0.37	8.21	±0.05
Total	99.01		99.02		99.25		99.39		99.45		99.28		98.86		99.12	

For individual analyses and calculated ion proportions, see Appendix D, Tables 1 to 8.

Pyroxene

Pyroxene compositions are relatively constant, corresponding to that of the orthopyroxene bronzite ($En_{83-88}Fs_{11-16}Wo_{1-2}$). The composition of clinopyroxene compositions is that of diopside ($Wo_{44-48}En_{47-48}Fs_{5-8}$). EDS analyses of pyroxene are listed in Tables 9 to 13, Appendix E.

Phlogopite

Selected phlogopite analyses are summarised in Table 14, Appendix E. The chemical composition of phlogopite is variable. Zoning is sometimes visible on backscattered electron images, especially in samples from area C. Of interest is the presence of Cl at concentration levels of up to 0.5 weight %.

Other silicate phases

Analyses of selected grains of edenitic hornblende and tremolite, and the hydrous Ca-Al silicates, pumpellyite, epidote and prehnite have been recorded in Tables 15, 16 and 17, Appendix E. Due to the fine-grained and intergrown nature of talc, chlorite, septechlorite and serpentine, it was difficult to obtain good analyses. Nevertheless, the analyses in Table 18, Appendix E, give some indication of the compositions of these phases.

5.2.13 Base-metal sulphide compositions

Electron-microprobe analysis was performed on selected grains of base-metal sulphide from samples A1, B4, C1 and C2.

Chalcopyrite

The composition of chalcopyrite is essentially stoichiometric $CuFeS_2$ (Table 5.4 and Appendix F, Tables 1 to 3). Platinum, rhodium and ruthenium contents of chalcopyrite are consistently below the detection limits of the analysis technique. Palladium was found to be present at a concentration level above the detection limit in only one grain out of fifty-four analysed.

Table 5.4 *Average compositions of chalcopyrite in samples A1, B1 and C1 determined by electron-microprobe analysis. The 90% confidence interval was calculated using the Student t-distribution.*

Sample no.	**A1** *(n=20)*		**B4** *(n=13)*		**C1** *(n=21)*	
S	34.93	±0.09	35.04	±0.12	34.74	±0.18
Fe	30.44	±0.11	30.54	±0.20	30.13	±0.17
Ni	0.06	±0.05	0.07	±0.04	0.02	±0.01
Co	0.04	±0.01	0.04	±0.01	0.04	±0.01
Cu	34.02	±0.15	33.92	±0.25	33.77	±0.24
Rh	b.d.l.		b.d.l.		b.d.l.	
Pd	b.d.l.		b.d.l.		b.d.l.	
Pt	b.d.l.		b.d.l.		b.d.l.	
Ru	b.d.l.		b.d.l.		b.d.l.	
Atomic proportions						
S	2.01	±0.00	2.01	±0.01	2.01	±0.00
Fe	1.00	±0.00	1.01	±0.00	1.00	±0.00
Ni	0.00	±0.00	0.00	±0.00	0.00	±0.00
Co	0.00	±0.00	0.00	±0.00	0.00	±0.00
Cu	0.99	±0.00	0.98	±0.00	0.99	±0.00
Rh	b.d.l.		b.d.l.		b.d.l.	
Pd	b.d.l.		b.d.l.		b.d.l.	
Pt	b.d.l.		b.d.l.		b.d.l.	
Ru	b.d.l.		b.d.l.		b.d.l.	

b.d.l. = below detection limits n = number of grains analysed

Pyrrhotite

Pyrrhotite analyses were obtained from two samples, A1 and B4 (Table 5.5, and Appendix F, Tables 4 and 5). These analyses indicate that the average composition of pyrrhotite from samples A1 and B4 is $Fe_{0.99}S_{1.00}$ (close to that of troilite) and $Fe_{0.90}S_{1.00}$ respectively. *

---

* These findings appear to be at odds with those of McLaren (1980) and McLaren and de Villiers (1982). These authors reported troilite in a sample of UG2 taken in the vicinity of a discordant ultramafic pegmatoid. This sample was characterised by a PGEM assemblage consisting of laurite and non-sulphide PGE minerals. Pyrrhotite (Fe_{1-x} with $x \geq 0.01$) dominated at other localities investigated by these authors. Clearly pyrrhotite compositions from more samples need to be compared to determine the relationship between pyrrhotite composition, PGE mineral assemblage and effect of postmagmatic alteration.

Platinum, palladium, rhodium and ruthenium contents of pyrrhotite in both samples are generally below the detection limits of the electron microprobe technique. Out of forty-five grains analysed, the presence of palladium at concentration levels above the detection limit was indicated in two grains. Platinum was found to be present in one grain.

Table 5.5 *Average compositions of pyrrhotite from samples A1 and B4 determined by electron-microprobe analysis. The 90% confidence interval was calculated using the Student t-distribution.*

Sample no.	**A1** *(n=18)*		**B4** *(n=27)*	
S	36.53	±0.16	38.80	±0.15
Fe	62.87	±0.17	60.57	±0.16
Ni	0.05	±0.03	0.13	±0.06
Co	0.07	±0.01	0.06	±0.01
Cu	0.02	±0.01	0.03	±0.01
Rh	b.d.l.		b.d.l.	
Pd	b.d.l.		b.d.l.	
Pt	b.d.l.		b.d.l.	
Ru	b.d.l.		b.d.l.	
Atomic proportions				
S	1.00	±0.00	1.00	±0.00
Fe	0.99	±0.00	0.90	±0.00
Ni	0.00	±0.00	0.00	±0.00
Co	0.00	±0.00	0.00	±0.00
Cu	0.00	±0.00	0.00	±0.00
Rh	b.d.l.		b.d.l.	
Pd	b.d.l.		b.d.l.	
Pt	b.d.l.		b.d.l.	
Ru	b.d.l.		b.d.l.	

b.d.l. = below detection limit n = number of grains analysed

Pyrite

Pyrite compositions in the four samples analysed are variable – $Fe_{0.92\text{-}1.04}Ni_{0.00\text{-}0.04}Co_{0.00\text{-}0.04}S_{2.00}$ (Table 5.6, analyses of individual grains in Appendix F, Tables 6 to 9). Platinum, palladium and ruthenium were not detected above the detection limits in any of the grains analysed. Rhodium however was detected in three grains out of a total of forty-six analysed, in one case at a concentration level of ~0.1 mass per cent (see also Figure 47).

Table 5.6 *Average compositions of pyrite in samples A1, B4, C1, C2 determined by electron-microprobe analysis. The 90% confidence interval was calculated using the Student t-distribution.*

Sample no.	A1 (n=10)		B4 (n=6)		C1 (n=18)		C2 (n=12)	
S	53.60	±0.32	53.65	±0.68	53.10	±0.23	53.49	±0.18
Fe	45.70	±0.26	47.17	±0.42	46.28	±0.38	45.68	±0.38
Ni	0.21	±0.14	0.02	±0.01	0.39	±0.19	0.34	±0.14
Co	1.18	±0.28	0.06	±0.02	0.43	±0.19	1.04	±0.24
Cu	0.02	±0.02	0.09	±0.10	0.03	±0.01	0.27	±0.12
Rh	b.d.l.		b.d.l.		b.d.l.		b.d.l.	
Pd	b.d.l.		b.d.l.		b.d.l.		b.d.l.	
Pt	b.d.l.		b.d.l.		b.d.l.		b.d.l.	
Ru	b.d.l.		b.d.l.		b.d.l.		b.d.l.	
Atomic proportions								
S	2.00	±0.00	2.00	±0.00	2.00	±0.00	2.00	±0.00
Fe	0.97	±0.01	1.01	±0.01	1.00	±0.01	0.98	±0.01
Ni	0.00	±0.00	0.00	±0.00	0.01	±0.00	0.01	±0.00
Co	0.03	±0.01	0.00	±0.00	0.01	±0.00	0.02	±0.00
Cu	0.00	±0.00	0.00	±0.00	0.00	±0.00	0.01	±0.00
Rh	b.d.l.		b.d.l.		b.d.l.		b.d.l.	
Pd	b.d.l.		b.d.l.		b.d.l.		b.d.l.	
Pt	b.d.l.		b.d.l.		b.d.l.		b.d.l.	
Ru	b.d.l.		b.d.l.		b.d.l.		b.d.l.	

b.d.l. = below detection limit n = number of grains analysed

Millerite

Electron microprobe analyses from two samples (C1 and C2) indicate millerite compositions of $Ni_{0.93\text{-}0.98}Fe_{0.01\text{-}0.05}Co_{0.00\text{-}0.02}S_{1.00}$ (Table 5.7 and Appendix F, Tables 10 and 11). Platinum, palladium, and ruthenium concentrations in millerite are consistently below the detection limit of the electron microprobe. Out of thirty grains analysed, one grain was found to contain rhodium above the detection limit.

Pentlandite

Pentlandite compositions vary considerably both between and within samples with average compositions of $Fe_{4.58}Ni_{4.32}Co_{0.06}S_{8.00}$, $Fe_{4.67}Ni_{4.15}Co_{0.10}S_{8.00}$, and $Fe_{4.29}Ni_{4.58}Co_{0.06}S_{8.00}$ for samples A1, B4 and C1 respectively (Table 5.8 and Appendix F, Tables 12 to 14). Note the comparatively high nickel content of the

Table 5.7 *Average millerite compositions in samples C1 and C2 determined by electron-microprobe analysis. The 90% confidence interval was calculated using the Student t-distribution.*

Sample no.	**C1** *(n=20)*		**C2** *(n=10)*	
S	35.22	±0.18	35.35	±0.11
Fe	1.25	±0.23	1.33	±0.42
Ni	62.15	±0.34	62.14	±0.41
Co	0.92	±0.09	0.68	±0.28
Cu	0.05	±0.01	0.05	±0.02
Rh	b.d.l.		b.d.l.	
Pd	b.d.l.		b.d.l.	
Pt	b.d.l.		b.d.l.	
Ru	b.d.l.		b.d.l.	
Atomic proportions				
S	1.00	±0.00	1.00	±0.00
Fe	0.02	±0.00	0.02	±0.01
Ni	0.96	±0.01	0.96	±0.01
Co	0.01	±0.00	0.01	±0.00
Cu	0.001	±0.000	0.001	±0.000
Rh	b.d.l.		b.d.l.	
Pd	b.d.l.		b.d.l.	
Pt	b.d.l.		b.d.l.	
Ru	b.d.l.		b.d.l.	

b.d.l. = below detection limit n = number of grains analysed

pentlandite grains from sample C1, a typical feature of pentlandite from millerite-bearing assemblages (Misra & Fleet, 1973). Cobalt-contents of all grains analysed are relatively low, generally <1 mass per cent. Most pentlandite grains contain significant amounts of palladium and rhodium. Of the fifty-six pentlandite grains analysed, fifty grains contain palladium above the detection limit (at concentration levels up to10 914 ppm), and thirty-one grains rhodium (up to 7 879 ppm). The concentration levels of palladium and rhodium in pentlandite are highly variable, and consequently a much larger number of grains will have to be analysed to obtain reliable average values. Platinum and ruthenium contents are generally below the detection limits.

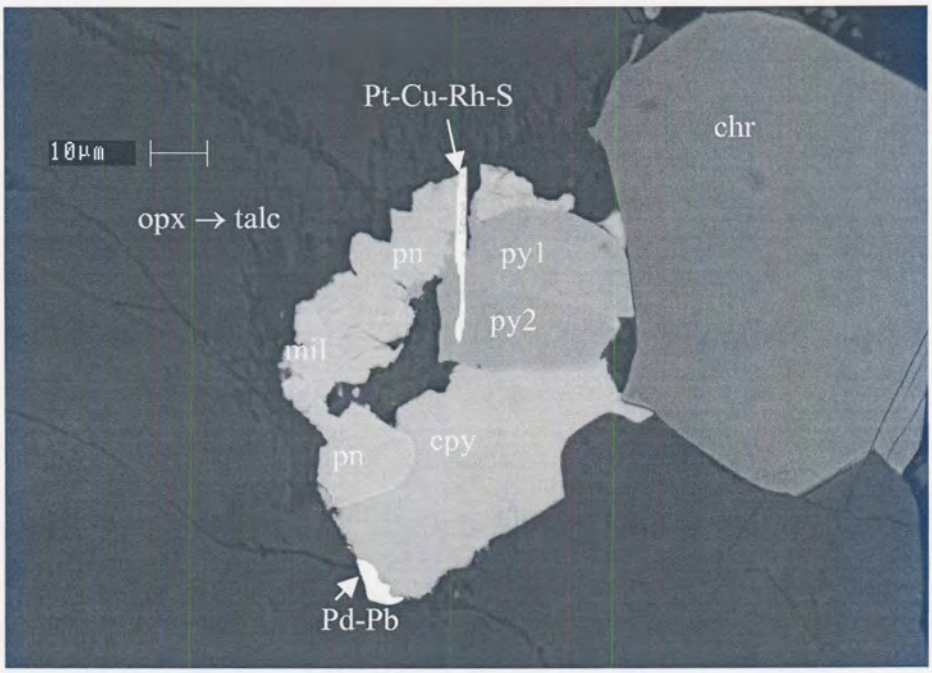

Figure 47 *Composite sulphide grain consisting of pentlandite (pn), chalcopyrite (cpy), millerite (mil) and pyrite (py) with malanite (Pt-Rh-Cu-Ni -S) and Pd-Pb occurring at the grain boundary of chromite (chr) and bronzite being altered to talc (opx → talc). Of special interest is the two grains of pyrite (py1 & py2) with different backscattered electron intensity due to the presence of submicroscopic PGE, probably rhodium or ruthenium.* [§]

Siegenite

A mineral with the average composition $Ni_{1.73}Co_{1.13}Fe_{0.08}S_4$, corresponding to that of siegenite, the intermediate member of the linnaeite-polydymite solid solution series, was commonly observed in trace amounts in the samples from area C. What makes these grains interesting is the fact that of the six grains analysed, three contained platinum (up to ~2 mass per cent) and/or rhodium (up to ~3.5 mass per cent) at concentration levels above the detection limits (Appendix F, Table 15). No palladium was observed in any of these grains.

[§] Concentration levels too low to determine positively whether the PGE is Rh or Ru by EDS analysis using a scanning-electron microscope.

Table 5.8 *Average pentlandite compositions in samples A1, B4 and C1 determined by electron-microprobe analysis. The 90% confidence interval was calculated using the Student t-distribution.*

Sample no.	**A1** *(n=25)*		**B4** *(n=27)*		**C1** *(n=4)*	
S	32.99	±0.08	33.39	±0.09	32.79	±0.25
Fe	32.92	±0.16	33.88	±0.21	30.62	±0.39
Ni	32.63	±0.23	31.80	±0.21	34.34	±0.67
Co	0.45	±0.06	0.73	±0.05	0.46	±0.43
Cu	0.04	±0.01	0.05	±0.01	0.05	±0.03
Rh	b.d.l.-0.7879		b.d.l.-0.5864		b.d.l.-0.0226	
Pd	b.d.l.-1.0914		b.d.l.-0.3499		b.d.l.-0.4059	
Pt	b.d.l.		b.d.l.		b.d.l.	
Ru	b.d.l.		b.d.l.		b.d.l.	
Atomic proportions						
S	8.00	±0.00	8.00	±0.00	8.00	±0.00
Fe	4.58	±0.00	4.67	±0.03	4.29	±0.05
Ni	4.32	±0.03	4.15	±0.03	4.58	±0.08
Co	0.06	±0.01	0.10	±0.01	0.06	±0.06
Cu	0.00	±0.00	0.01	±0.00	0.01	±0.00
Rh	b.d.l.-0.06		b.d.l.-0.04		b.d.l.	
Pd	b.d.l.-0.08		b.d.l.-0.03		b.d.l.-0.03	
Pt	b.d.l.		b.d.l.		b.d.l.	
Ru	b.d.l.-0.01		b.d.l.		b.d.l.	

b.d.l. = below detection limit n = number of grains analysed

5.2.14 PGE mineral characteristics

No attempt was made to determine compositional differences in PGE minerals between samples. Electron microprobe analyses of the major PGE minerals are reported in Appendix G, Tables 1 to 5.

Sulphides of platinum and palladium include cooperite (~average composition $Pt_{0.9}Pd_{0.1}Ni_{0.1}S_{1.0}$) (Appendix G, Table 1), braggite (~average composition $Pt_{0.4}Pd_{0.5}Ni_{0.1}S_{1.0}$) and vysotskite ($Pd_{0.7}Ni_{0.2}S_{1.0}$) (Appendix G, Table 2). These minerals tend to form euhedral to subhedral crystals occurring singly or in composite grains with other PGE minerals as inclusions in, or at grain-boundaries of, base-metal

sulphides and gangue. Complex zoning, which in its simplest form consists of a platinum-rich rim and palladian core, was frequently observed especially in samples from area C and sample B2 (Figures 48 and 49).

*Pt-Rh-Cu-Ni-sulphide (*average composition $Cu_{1.0}Pt_{1.1}Rh_{0.4}Co_{0.3}Ni_{0.2}Fe_{0.1}S_{4.0}$) (Appendix G, Table 3) appears to belong to the malanite-cuprorhodsite-cuproiridsite solid solution series (ideal composition $Cu(Pt,Rh,Ir)_2S_4$). The compositions of the analysed grains are very similar to that of nickeloan malanite reported from the Imandra Layered Complex in northwestern Russia (Barkov *et al.*, 1997). This mineral commonly forms laths (Figure 49), often skeletal (Figures 48 and 50), especially when it occurs in pentlandite with which it seems to have a special affinity. In some grains this mineral (or one similar to it) seems to have exsolved along pentlandite cleavage planes (see Figure 71 for an example).

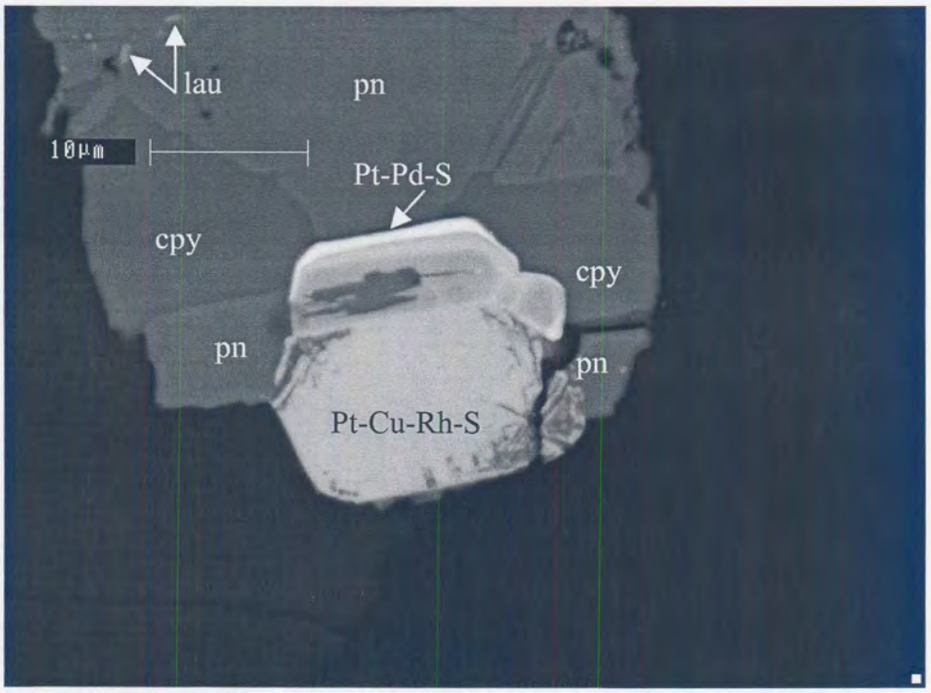

Figure 48 *Zoned Pt-Pd-S (more Pt-rich towards the rim) attached to Pt-Rh-Cu-Ni-S. Note the skeletal appearance of Pt-Rh-Cu-Ni-S at the grain edge. Associated sulphides are pentlandite (pn) and chalcopyrite (cpy). Some laurite (lau) inclusions are also visible. Backscattered-electron image.*

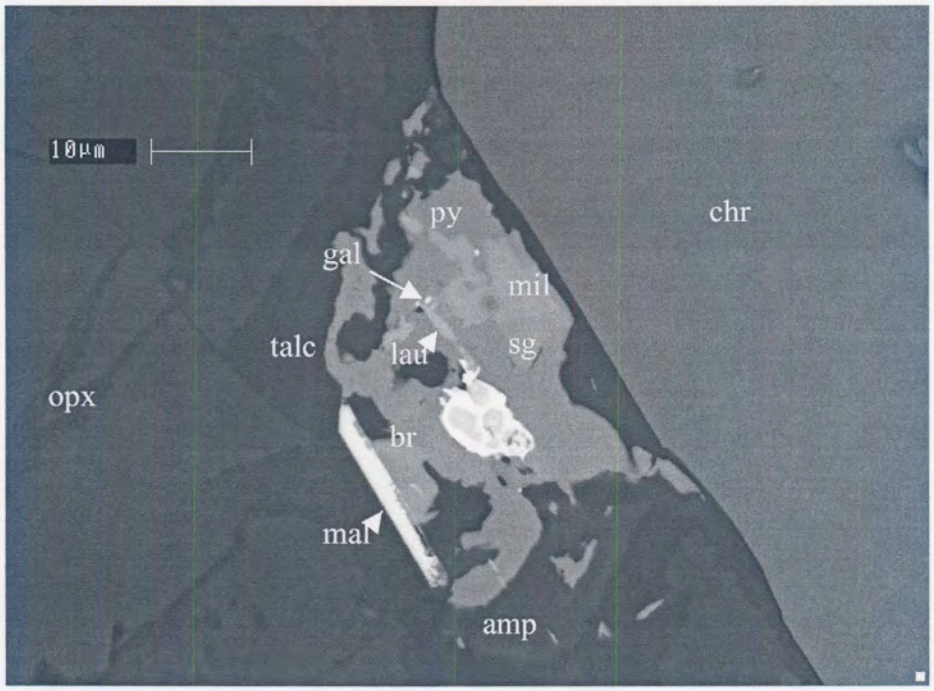

Figure 49 *Zoned Pt-Pd-sulphide (br) (more Pt-rich towards the rim), laurite (lau) and malanite (mal) associated with a composite sulphide grain consisting of siegenite (sg), millerite (mil), pyrite (py) and galena (gal) at the grain boundary of chromite (chr) and orthopyroxene (opx) being altered to talc. Small amounts of amphibole (amp) and pumpellyite (not visible in image) are also present. Backscattered-electron image.*

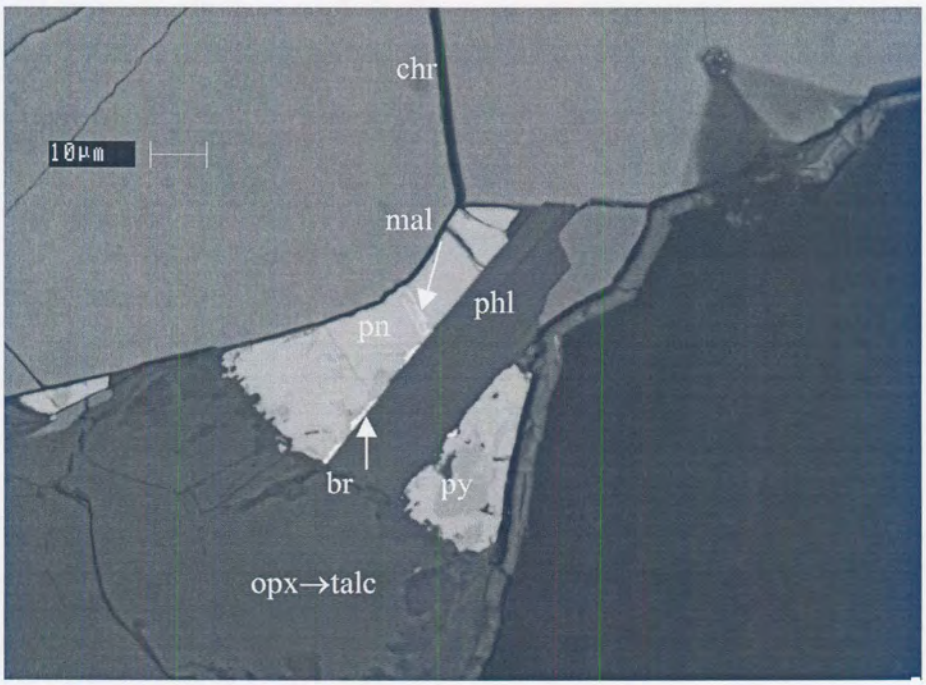

Figure 50 *Skeletal Pt-Rh-Cu-Ni-sulphide (mal) in pentlandite (pn) with pyrite (py) at chromite (chr)-orthopyroxene (opx)→talc. Note the presence of braggite (br) along the grain boundary of sulphide and crosscutting phlogopite (phl). Backscattered-electron image.*

Laurite (ideal composition (Ru,Os,Ir)S_2) commonly occurs as idiomorphic to hypidiomorphic grains in chromite (~20 volume per cent), silicate and base-metal sulphides, or at the grain-boundaries of these minerals. Laurite is sometimes zoned (Figure 51). Less commonly, laurite forms trails of small anhedral inclusions in composite base-metal sulphide grains, often appearing to have exsolved from pentlandite.

Pt-Fe alloys

The average composition of this phase is $Pt_{2.8}Fe_{1.1}$ (Appendix G, Table 4). It occurs as anhedral to euhedral grains in base-metal sulphides and silicate. Note the presence of small amounts of rhodium and palladium. Merkle (1988) also observed the presence of rhodium and palladium in Pt-Fe alloys from the UG1 layer. Pt-Fe alloys often display emulsion intergrowth textures with base-metal sulphides, similar to those described by other researchers (McLaren & de Villiers, 1982; Peyerl, 1982; Kinloch & Peyerl, 1990; Grimbeek, 1995) (Figure 51).

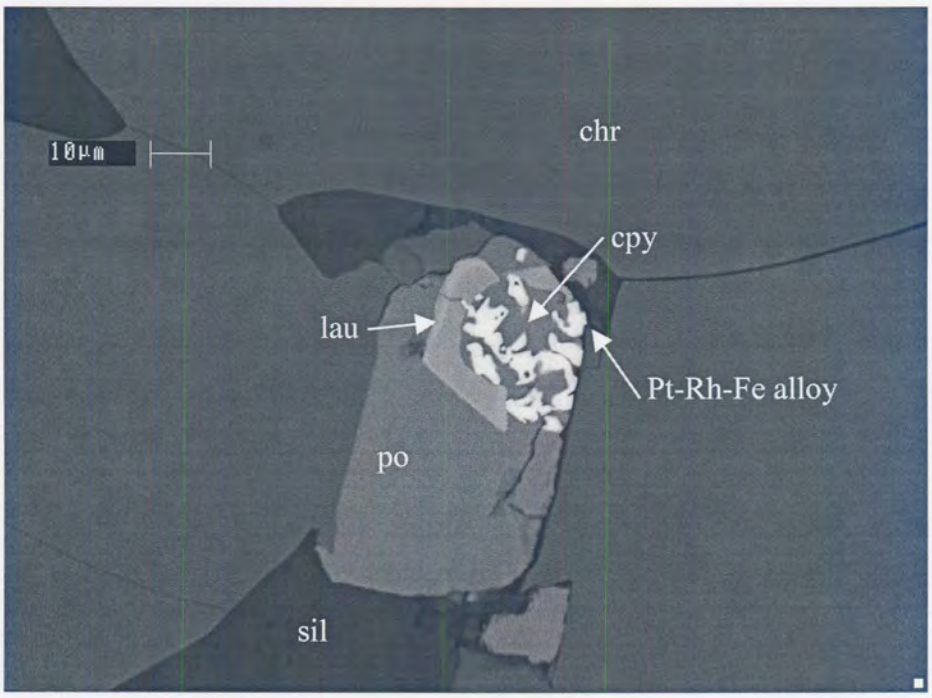

Figure 51 *Pt-Rh-Fe alloy (brightest grains) associated with zoned laurite (lau)(the higher backscattered-electron intensity is the result of a higher Os concentration in the rim) included in a composite chalcopyrite (cpy) and pyrrhotite (po) grain at the grain-boundary of silicate (sil) and chromite (chr). Backscattered-electron image.*

Analyses of *other non-sulphide PGE minerals* such as kotulskite, moncheite, and atheneite can be found in Appendix G, Table 5). Palladium-bearing phases, especially Pd-Pb, are occasionally present as tiny veinlets, of the order of 1 μm across, usually forming part of base-metal sulphide composite grains.

5.3 Characterisation of milled feed samples

5.3.1 General

In all samples except for sample A5, chromite grains were liberated from the silicate matrix during size reduction (Figure 52). Cataclastic textures, as found in sample A5, result in incomplete liberation of chromite, as fractured grains of chromite often remain cemented together by secondary silicates (Figure 53).

Trace amounts of nickel-bearing stainless steel particles were noted in all the samples. These particles originate from the milling rods and cause the introduction of unacceptably high levels of nickel to the samples. The effect can be demonstrated by comparing the nickel contents in two samples before and after rod milling (Table 5.9). The nickel values for both samples were considerably higher after rod milling.

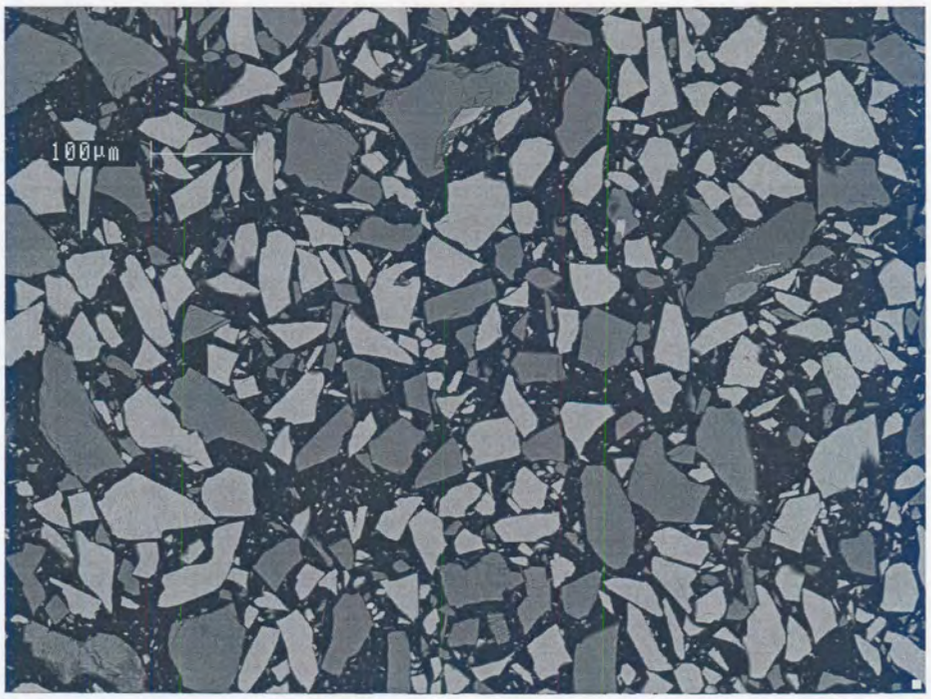

Figure 52 *Milled UG2 chromitite. Silicate = dark grey. Chromite = light grey. Backscattered-electron image.*

Table 5.9 *A comparison of acid soluble and total nickel values in two samples before and after rod milling.*

Sample no.	Total nickel (ppm)		Acid soluble nickel (ppm)	
	Before	After	Before	After
A1	942	1220	271	411
C1	637	993	82	219

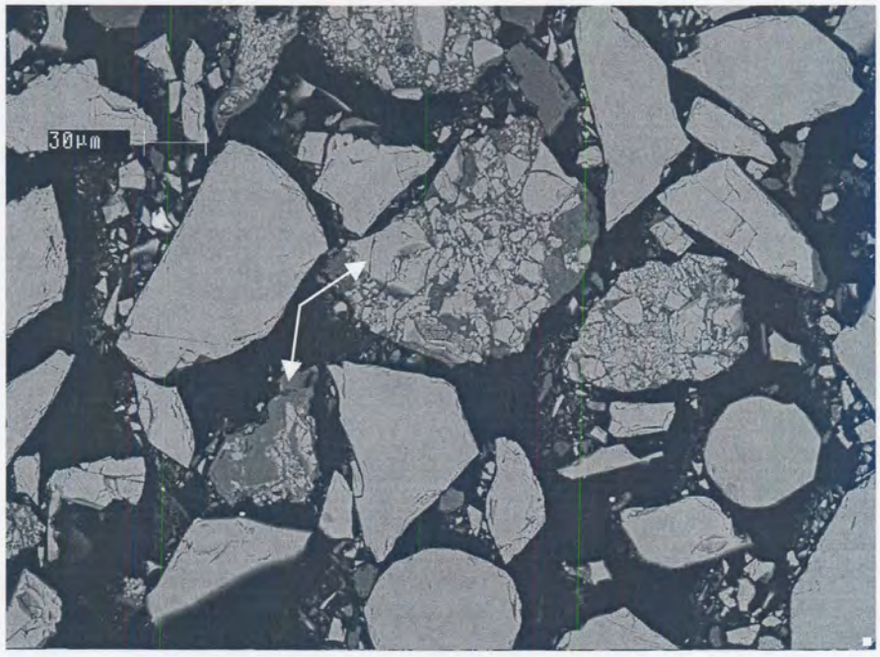

Figure 53 *Cataclastic UG2 milled to 80% <75µm. Arrows indicate fractured chromite grains cemented by hydrous sheet silicates. Backscattered-electron image.*

5.3.2 Chromite and silicate grain-size distributions

At 80% <75µm, chromite grain-sizes in all of the samples range from <10 µm to ~150 µm (Appendix H, Table 1). Differences between samples are small, with measured median equivalent circle diameters ranging from 32 µm to 44 µm (Table 5.1R).

Silicate grain-size distributions in all of the samples are also very similar, ranging from <10 µm to ~130 µm (Appendix H, Table 2), with measured median equivalent circle diameter values varying between 30 and 39 µm (Table 5.1S). More silicate fines are created, with an average of 39 per cent silicate reporting to the <17µm

fraction compared to only 15 per cent of the chromite. This can probably be ascribed to the natural tendency of sheet silicates such as talc, chlorite and phlogopite to form fines during size reduction.

5.3.3 Base-metal sulphide

Base-metal sulphide grain diameters in the milled feed samples range from <5 µm up to ~50 µm with median values between ~2 and 13 µm (Table 5.1T). Base-metal sulphide liberation is generally good (estimated >90 per cent) in most samples from areas A and B. The exceptions being samples A3 at 87%, A4 at 70%, and A5 at 69%. The degree of liberation is generally lower but extremely variable in the samples from area C (33 to 91 per cent).

5.3.4 PGE minerals

PGE mineral mode of occurrence & liberation in fourteen UG2 chromitite samples milled to 80% <75µm

The mode of occurrence of PGE minerals observed in all fourteen milled feed samples is tabulated in Table 3 of Appendix H. A simplified classification scheme is presented in Table 5.1U and Figure 54.

In all of the samples, between 48 and 79 per cent of the PGE minerals were liberated during milling. Except for sample A5, the remainder of the PGE minerals in the milled samples from areas A and B are mostly associated with liberated base-metal sulphide grains (9 to 38 per cent). By contrast, less than 7 per cent of the PGE minerals in the milled feed samples from area C and sample A5 are associated with liberated base-metal sulphides. In these samples, a significant proportion of the PGE minerals (24 to 41 per cent for samples from area C and 52 per cent for sample A5) is associated with gangue, mostly silicate.

The preferred association of PGE minerals with base-metal sulphides, coupled with the higher degree of liberation of these sulphides in samples from area A (except for sample A5) and B, results in a higher proportion of PGE mineral-bearing particles with a high combined liberation index in these samples compared to those from area C

and sample A5 (Table 5.1V). Exclusion of laurite from the combined liberation index calculations does not yield statistically different values (Table 5.1W).

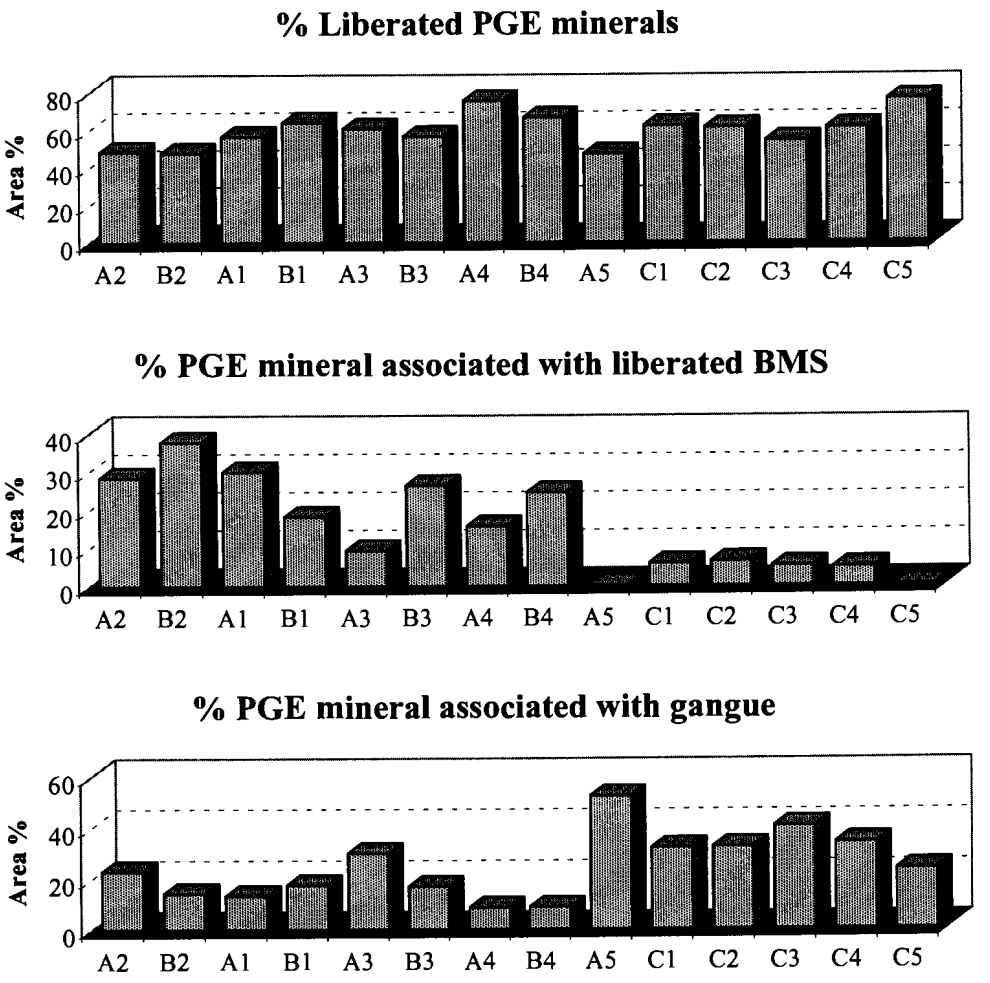

Figure 54 *Mode of occurrence of PGE minerals in fourteen samples of UG2 chromitite milled to 80% <75μm.*

PGE mineral grain-size distribution

Measured median PGE mineral grain diameters range between 3.8 and 6.9 μm based on area per cent, and between 1.6 and 2.4 μm based on number per cent (Table 5.1X).

The measured grain-size distributions of a composite of the PGE minerals found in all fourteen samples, before and after milling to 80% <75μm, are compared in Figure 55

and Table 5.10, and indicates that milling of the ore caused an even further reduction in the grain size of the PGE minerals.

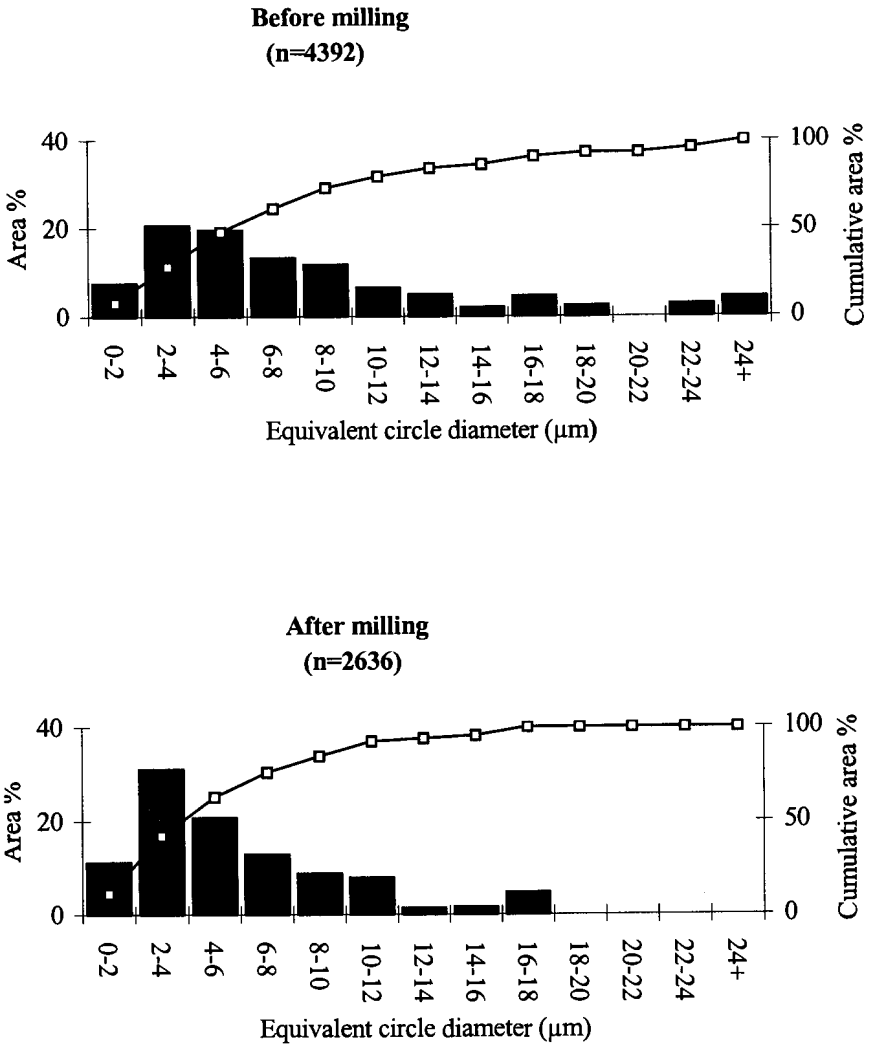

Figure 55 *PGE mineral grain-size distribution of UG2 chromitite at <2mm and at 80% <75µm.*

5.4 Characterisation of flotation product samples

5.4.1 Chromite in flotation products

Comparison of the chromite grain-size distributions in the different flotation products, shows that the chromite in the concentrates is fine-grained compared to that in the tailings (Figure 56 and Table 4, Appendix H). About 90 per cent of the chromite in the fast-floating concentrates occurs as grains smaller than 10 µm. Most of the chromite in the flotation concentrates is present as liberated grains.

Table 5.10 *A comparison of the grain-size distributions of PGE minerals in a composite of fourteen samples of UG2 feed crushed to <2mm and at 80% <75µm. n=number of PGE mineral grains measured.*

Particle size	***< 2mm***		***80% <75µm***	
n	4392		2636	
	area	*number*	*area*	*number*
Median 50th percentile (µm)	6.3	2.6	4.8	2.0
20th percentile (µm)	3.2	1.0	2.6	0.4
80th percentile (µm)	12.4	4.5	9.0	3.7

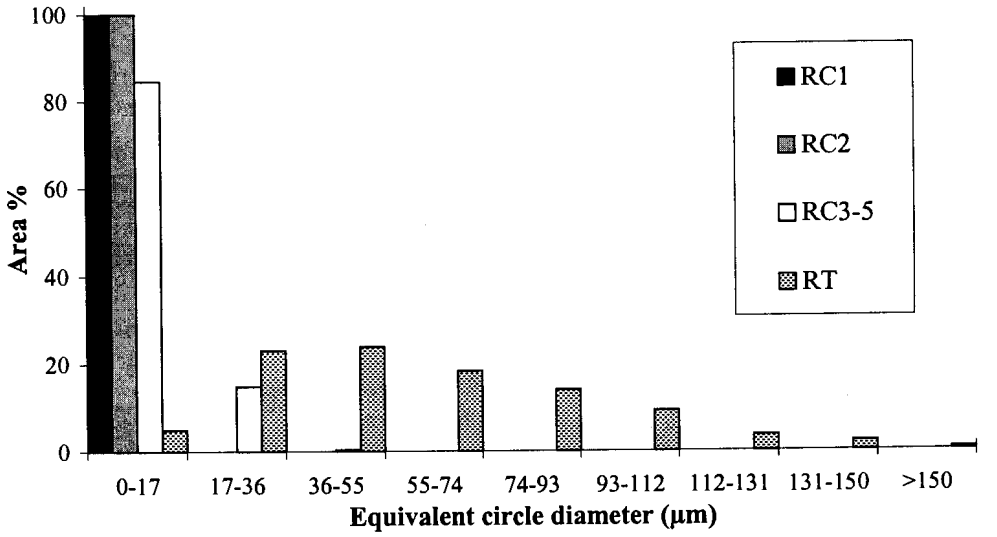

Figure 56 *Chromite grain size-distribution in flotation products of sample C1. RC1 = Rougher concentrate 1 (0-1 minutes), RC2 = Rougher concentrate 2 (1-3 minutes), RC3-5 = Combined rougher concentrates 3, 4 and 5 (3-20 minutes), RT = Rougher Tailings*

5.4.2 Silicate in flotation products

Silicate minerals are present in the flotation concentrates in two forms:

- as part of composite grains together with base-metal sulphide and/or PGE minerals (Figure 57)
- as fine-grained liberated silicates (Figure 57).

The silicate minerals in the flotation concentrates are generally very fine-grained with the coarser-grained silicates reporting to the flotation tailings (Figures 57, 58 and 59, and Table 5, Appendix H).

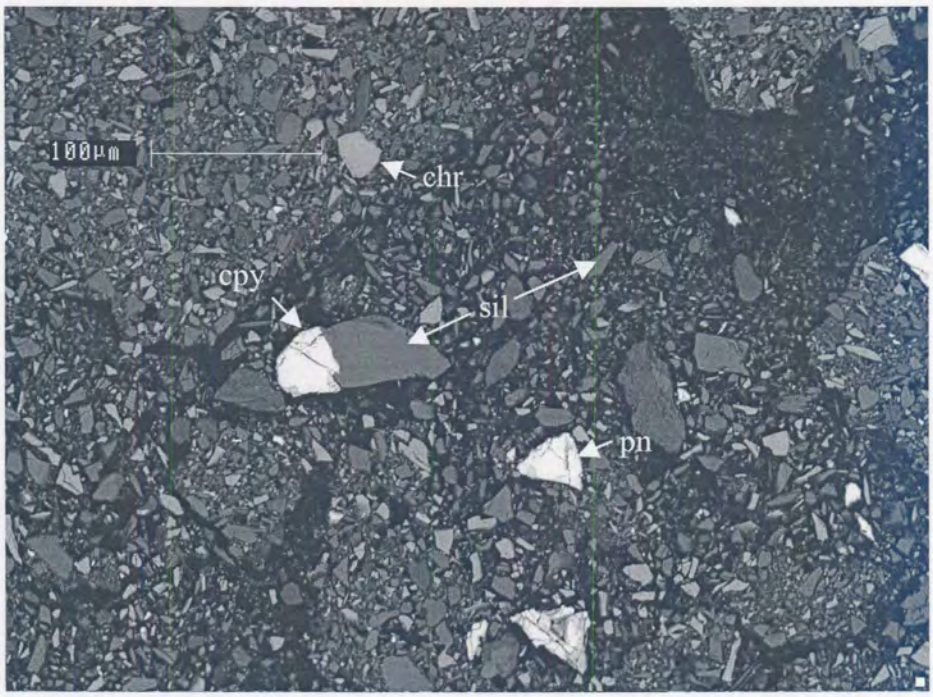

Figure 57 *Backscattered-electron image of a flotation concentrate sample. The sample consists predominantly of fine-grained liberated chromite (chr) and silicate (sil). Note the coarser silicate grain forming part of a composite particle with chalcopyrite (cpy). A liberated pentlandite (pn) grain can also be seen.*

The silicate mineralogy of the flotation products of six samples (A1, A3, B3, B4, C1 and C4) was quantified in terms of the relative proportions of Ca-Al-silicate, Mg-Fe-silicate, phlogopite, clinopyroxene, quartz, albite and K-Al silicate by EDS point counting (Appendix H, Table 6). These results, combined with the silicate gangue

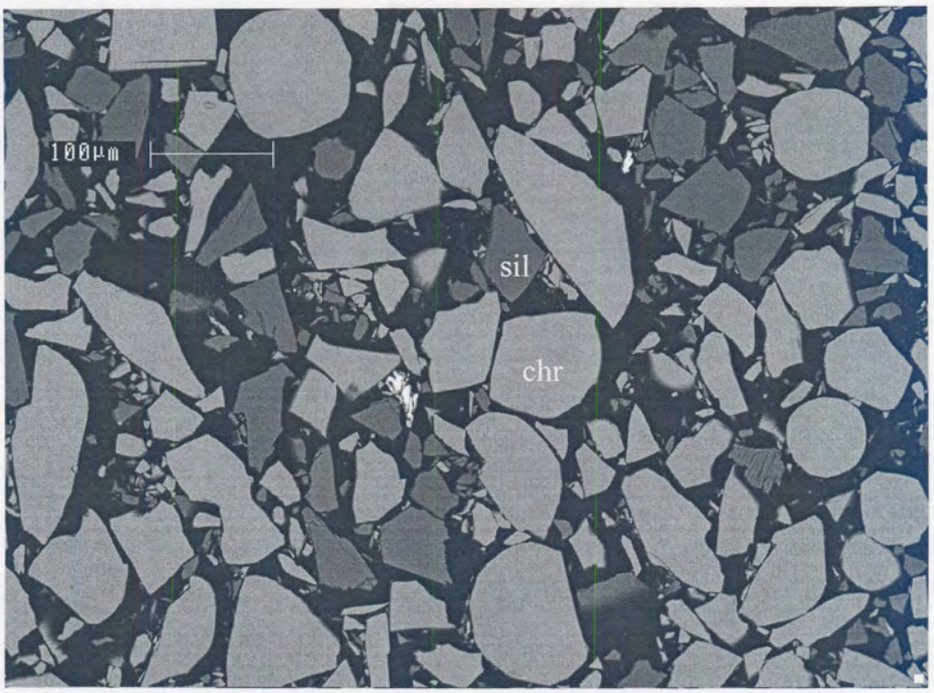

Figure 58 *Coarse liberated chromite (chr) and silicate (sil) grains in flotation tailings. Backscattered-electron image.*

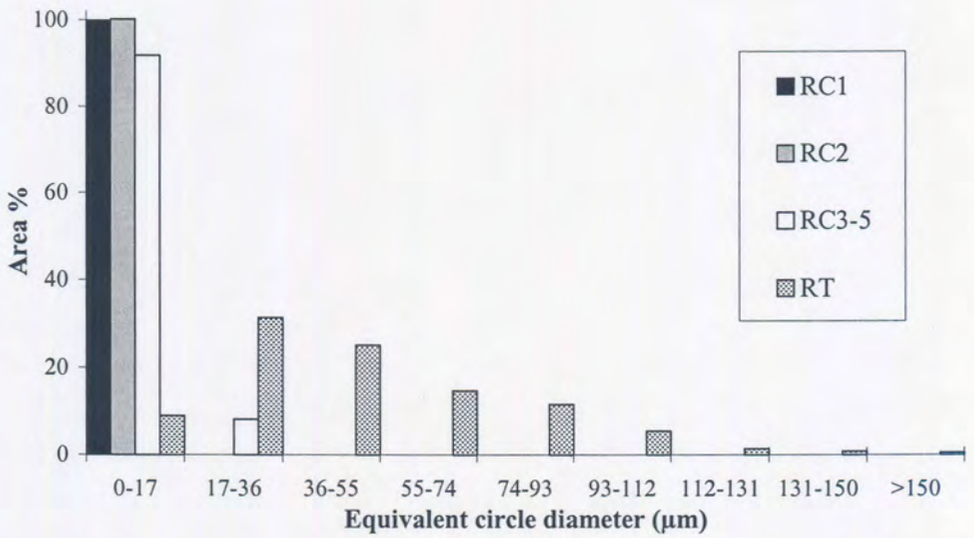

Figure 59 *Silicate grain size-distribution in flotation products of sample C1. RC1 = Rougher concentrate 1 (0-1 minutes), RC2 = Rougher concentrate 2 (1-3 minutes), RC3-5 = Combined rougher concentrates 3, 4 and 5 (3-20 minutes), RT = Rougher Tailings*

flotation results (Appendix J, Table 3), were used to calculate time-recovery profiles for Ca-Al-silicate (predominantly plagioclase) and Mg-Fe silicate (orthopyroxene and talc) (Figure 60).

Recoveries of Ca-Al-silicate after 20 minutes flotation range between seven and eighteen per cent (indicated in red). For sample A1, Fe-Mg-silicate recovery (in blue) after 20 minutes is very similar to that of Ca-Al-silicate, 13 per cent compared to 17 per cent respectively. For the other samples Fe-Mg-silicate recovery is higher than that of Ca-Al-silicate, especially in the samples from area C. In sample C1, Fe-Mg-silicate recovery after 20 minutes is 64 per cent compared to 7 per cent for Ca-Al-silicate.

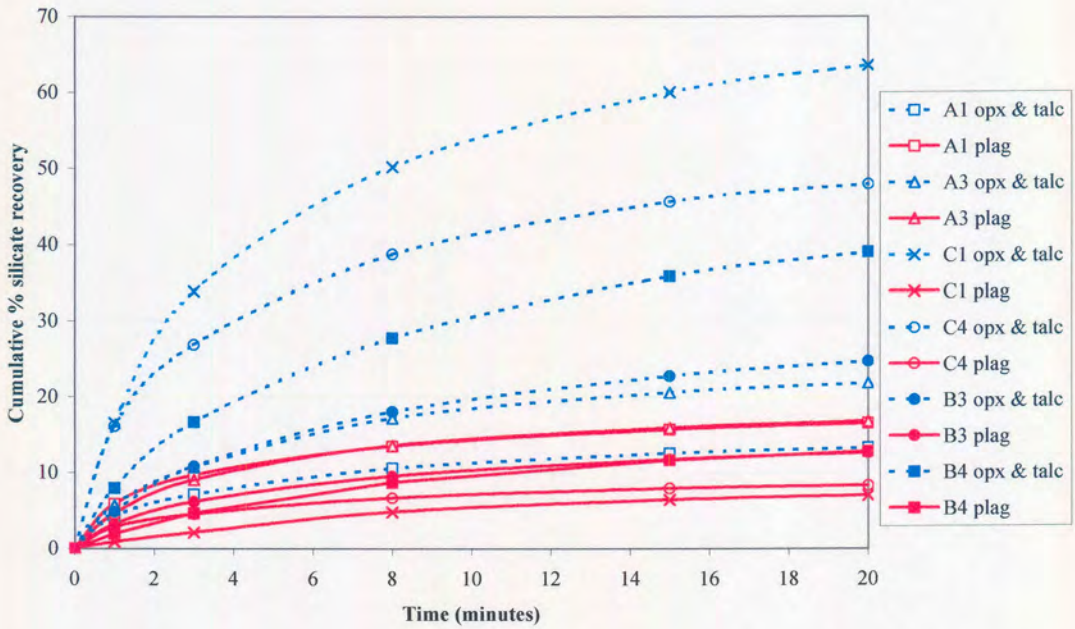

Figure 60 *A comparison of time-recovery profiles for Fe-Mg-silicate, orthopyroxene (opx) and talc, (blue) and Ca-Al-silicate, predominantly plagioclase (plag), (red) in six samples.*

Although the EDS point-counting technique cannot reliably distinguish between minerals with similar compositions, such as talc and orthopyroxene occurring in fine-grained intergrowths (see section 4.6.3), X-ray diffraction indicates that talc is concentrated in the flotation concentrates relative to the other silicate minerals (Figure 61).

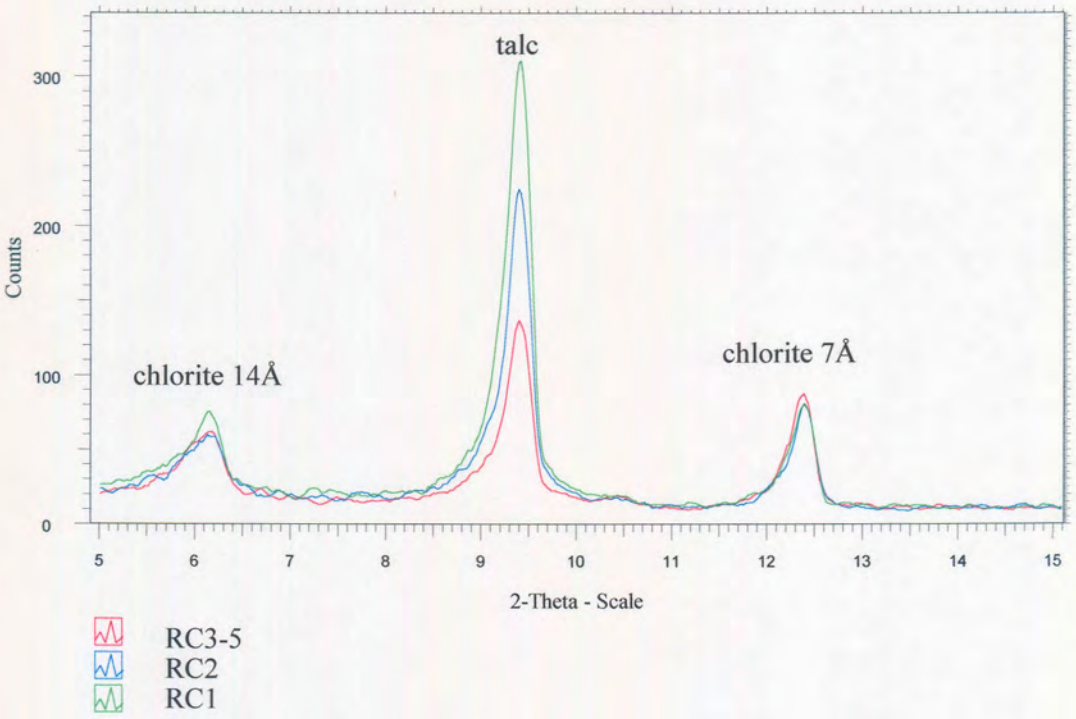

Figure 61 *X-ray diffractogram from 5°2θ to 15°2θ for RC1 (rougher concentrate 1, 0-1 minutes), RC2 (rougher concentrate 2, 1-3 minutes) and RC3-5 (combined rougher concentrate 3, 4 and 5, 3-20 minutes) of sample C1.*

5.4.3 Base-metal sulphides in flotation products

Grain-size distribution

The coarsest base-metal sulphide grains are recovered to the fastest floating concentrates, with progressively finer grains being recovered with time (Figure 62). Equivalent circle diameters of base-metal sulphide grains in the flotation concentrates are generally below 80 µm, with median values between 10 and 15 µm in the fast-floating concentrate (RC1), between 5 and 10 µm in the medium-floating concentrate (RC2), and smaller than 5 µm in the slow-floating (RC3-5) concentrate. Base-metal sulphide grains in flotation tailings samples are generally below 10 µm in size.

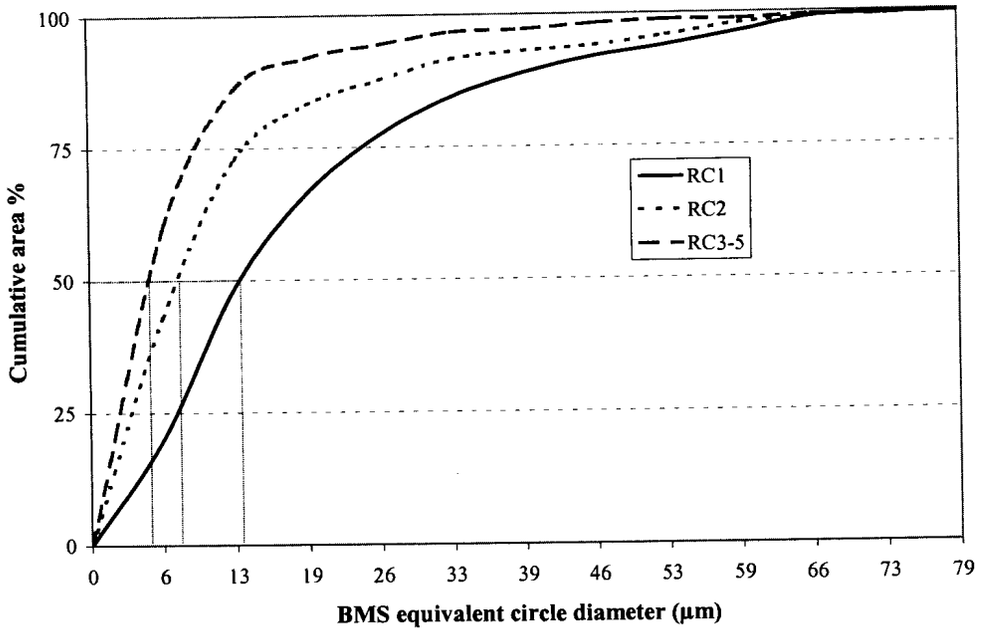

Figure 62 *Base-metal sulphide (BMS) size distributions in composite flotation concentrates of samples A1, A3, A5, and B4. RC1 = (rougher concentrate 1, 0-1 minutes), RC2 = (rougher concentrate 2, 1-3 minutes) and RC3-5 = (combined rougher concentrate 3, 4 and 5, 3-20 minutes).*

Liberation characteristics

In all of the samples, most of the base-metal sulphides in the concentrate samples appear to be liberated from gangue, with a decrease in the degree of liberation of base-metal sulphides from the fast-floating concentrate through to the slower floating concentrates (Table 7, Appendix H and Figure 63). Note the high degree of liberation measured in the concentrates of samples A1, A4 and B5 (more than 90 per cent in all concentrates). The degree of liberation of the base-metal sulphides recovered in the concentrates of samples A3, C1, C2 and A5 is lower (70 to 90 per cent).

Base-metal sulphides in the tailings samples occur almost exclusively as <10 µm grains at silicate-silicate grain boundaries, or as inclusions in silicate grains (Figure 64).

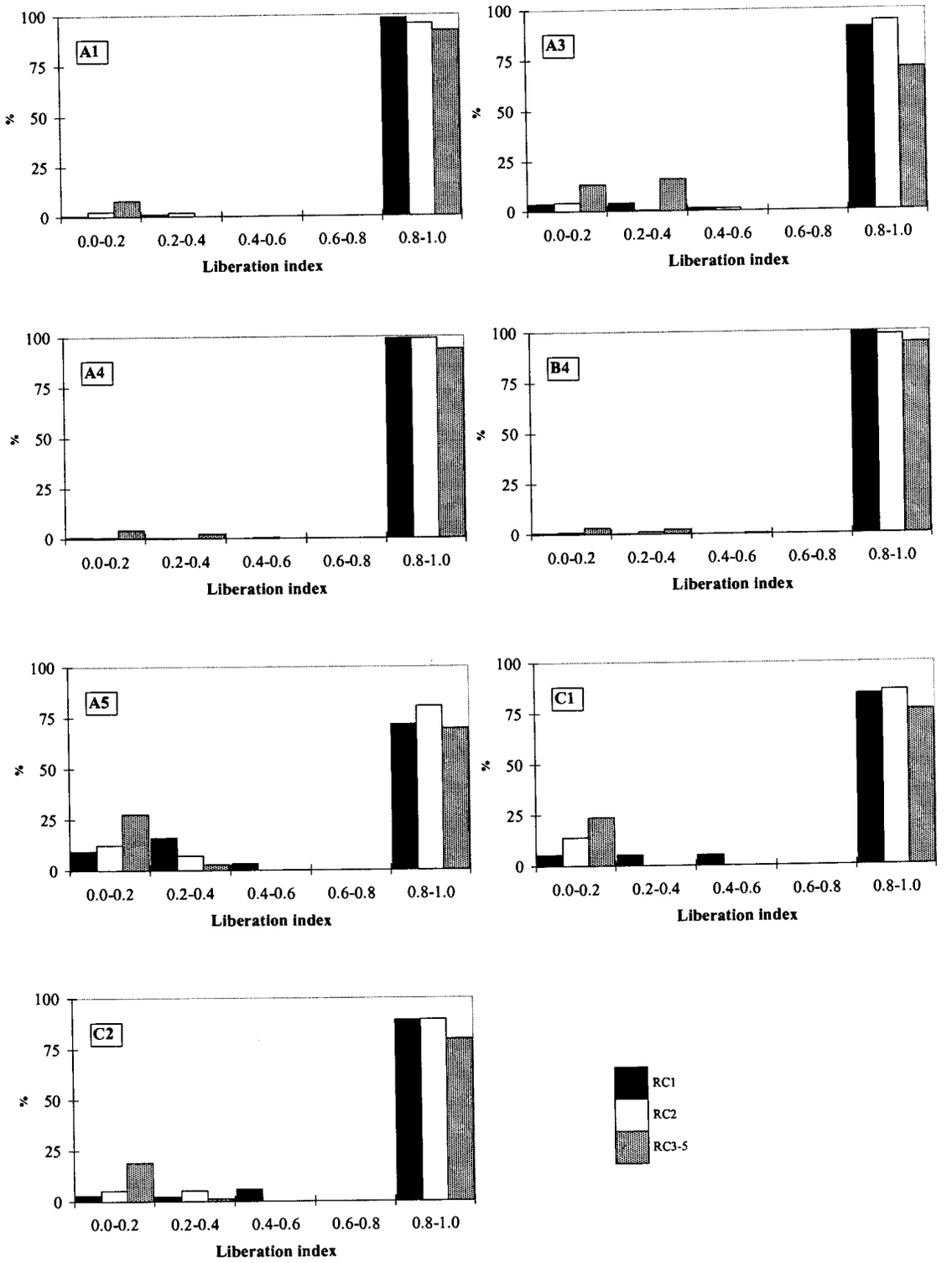

Figure 63 *Base-metal sulphide liberation index in flotation concentrates of samples A1, A3, C1, C2, A4, A5 and B4. RC1 = rougher concentrate 1 (0-1 minutes), RC2 = rougher concentrate 2 (1-3 minutes) and RC3-5 = combined rougher concentrates 3, 4 and 5 (3-20 minutes).*

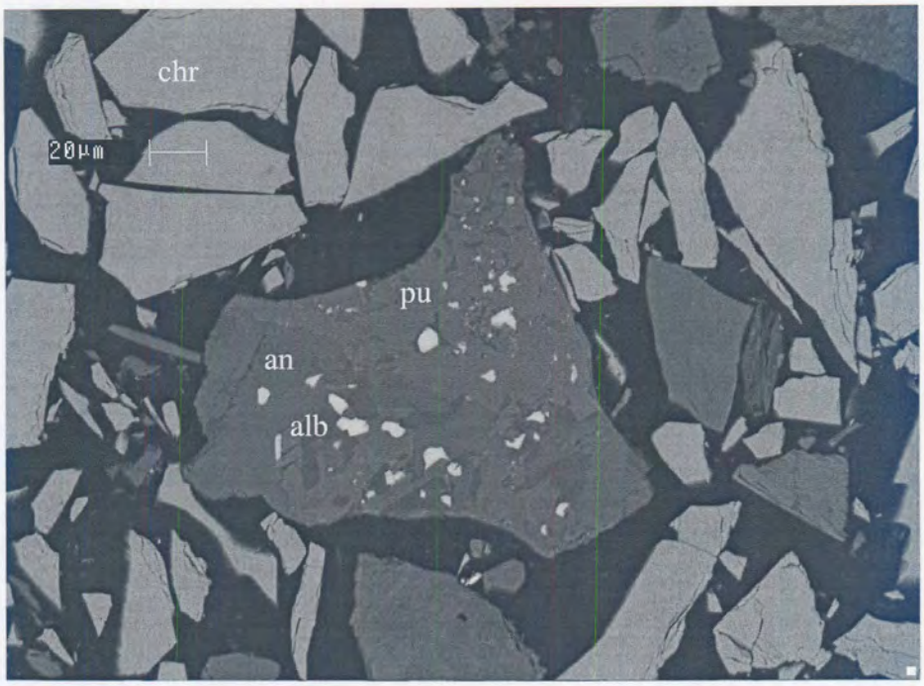

Figure 64 *Millerite and chalcopyrite (bright grains) associated with anorthite (an), pumpellyite (pu) and albite (alb) in flotation tailings. Backscattered-electron image.*

Type of base-metal sulphide

The relative proportions of the base-metal sulphides in the flotation feeds from areas A and B are graphically compared to that in the rougher concentrate 1, rougher concentrate 2, and a combined rougher concentrate 3, 4 and 5 in Figure 65. In most of the samples pyrrhotite appears to be relatively slow-floating compared to chalcopyrite, pentlandite and pyrite. Microscopic investigation of flotation concentrates indicated the presence of relatively coarse (up to 100 µm) liberated pyrrhotite particles reporting to slow-floating concentrates of samples B2 and A4.

The modal proportions of the base-metal sulphides in the flotation feeds and concentrates of samples from area C are compared in Figure 66. Where pyrrhotite is present, it is once again relatively slow-floating. Pyrite generally appears to be recovered at a faster rate than chalcopyrite.

A time-recovery profile was calculated for pentlandite, chalcopyrite, pyrrhotite, pyrite and millerite in each of the samples, and also for a composite of all the samples

(Tables 8 to 12, Appendix H).[§] The results for the composite sample are graphically illustrated by Figure 67. Overall, the rate of recovery for the individual sulphides appears to be pyrite>chalcopyrite≅millerite≅pentlandite>>pyrrhotite.[+]

Electron-microprobe analyses indicated that the compositions of pyrrhotite from different samples differ. This will affect the surface chemistry, and therefore flotation behaviour of pyrrhotite, and could potentially affect the recovery of PGEs. However, as pyrrhotite does not appear to host significant amounts of PGEs in solid solution (Table 5.4) or as discrete grains (Table 5.1Q), this line of investigation was not pursued any further.

5.4.4 Behaviour of PGE minerals during recovery

The flotation products of seven samples, A1, A3, A5, A4, B4, C1 and C2, were selected for the investigation of PGE mineral behaviour during flotation. To be able to reliably detect small differences between particle types reporting to different flotation products, the results for the seven samples were composited to improve the statistics.

PGE mineral mode of occurrence and liberation

The combined liberation index distributions of the PGE mineral-bearing particles in the different flotation products are compared in Figure 68 and Table 5.11. Most of the PGE minerals recovered to the fast-floating concentrate (rougher concentrate 1) occur

---

[§] As sulphide concentration levels in the flotation tailings were too low to obtain meaningful modal analysis results, a total recovery of 100 per cent was assumed. The amount of chalcopyrite in each of the sulphide concentrates was calculated from the copper content. This value, combined with the modal proportions of the other sulphides, was used to calculate the pentlandite, millerite, pyrite and pyrrhotite contents of each concentrate.

[+] Millerite is widely believed to be of a slow-floating nature. No indication could be found that this is true of millerite found in these samples of UG2 chromitite. At the same time the slow-floating nature of pyrrhotite is clearly borne out by the data.

Figure 65 *Relative proportions of chalcopyrite, pentlandite, pyrrhotite, pyrite and millerite in three flotation concentrates of samples from Areas A and B. RC1 = (rougher concentrate 1, 0-1 minutes), RC2 = (rougher concentrate 2, 1-3 minutes) and RC3-5 = (combined rougher concentrate 3, 4 and 5, 3-20 minutes)*

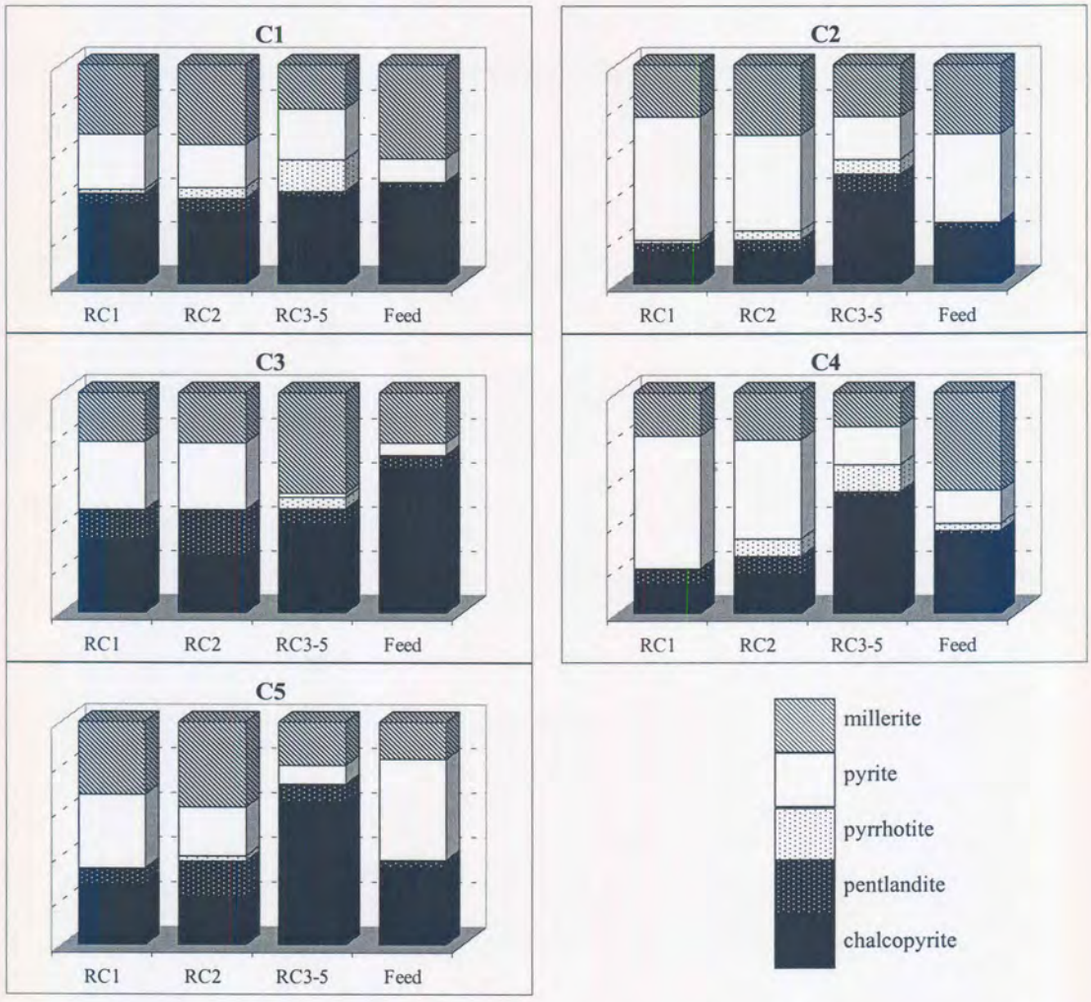

Figure 66 *Relative proportions of chalcopyrite, pentlandite, pyrrhotite, pyrite and millerite in three flotation concentrates of samples from Area C. RC1 = rougher concentrate 1 (0-1 minutes), RC2 = rougher concentrate 2 (1-3 minutes) and RC3-5 = combined rougher concentrates 3, 4 and 5 (3-20 minutes).*

in particles with a high combined liberation index, i.e. >0.8. These PGE minerals are predominantly liberated PGE minerals (Figure 69 and 70, Table 5.12) and PGE minerals associated with liberated base-metal sulphide grains (Figure 69, 71 and 72).

With time, an increased proportion of PGE minerals associated with gangue, mostly silicate, is recovered. During flotation of samples A3, C1, C2 and A5, a significant proportion of PGE minerals associated with gangue was recovered even to the faster-floating concentrates. The rougher tailings contain predominantly PGE mineral grains associated with gangue. This is reflected by the low combined liberation indices of PGE mineral-bearing particles in tailings samples (Table 5.11 and Figure 68).

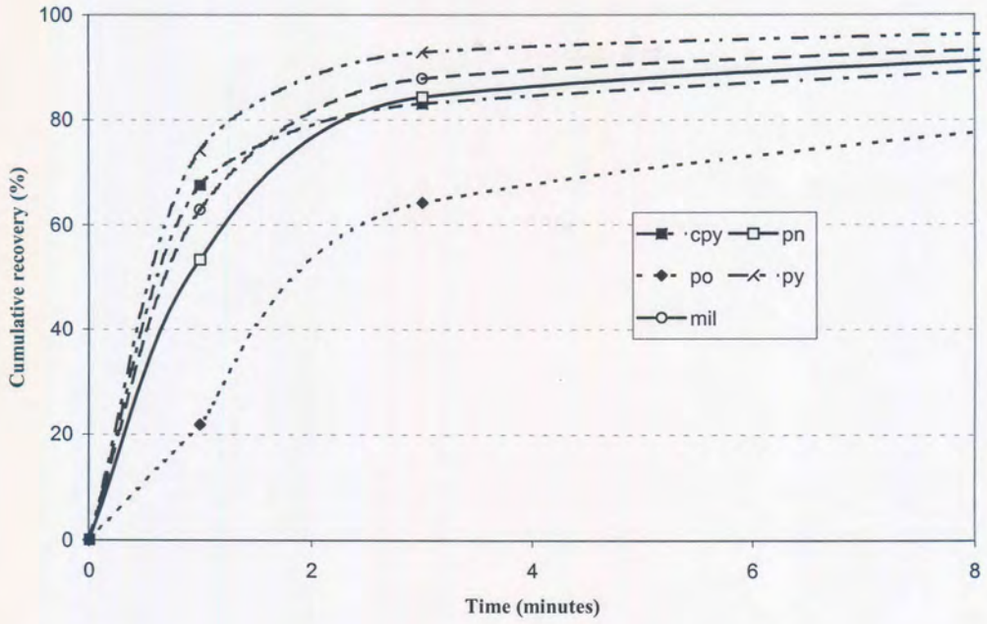

Figure 67 *Time-recovery profile for chalcopyrite (cpy), pyrite (py), pentlandite (pn), pyrrhotite (po) and millerite (mil) calculated from a composite of all the samples and assuming an ultimate sulphide recovery of 100%.*

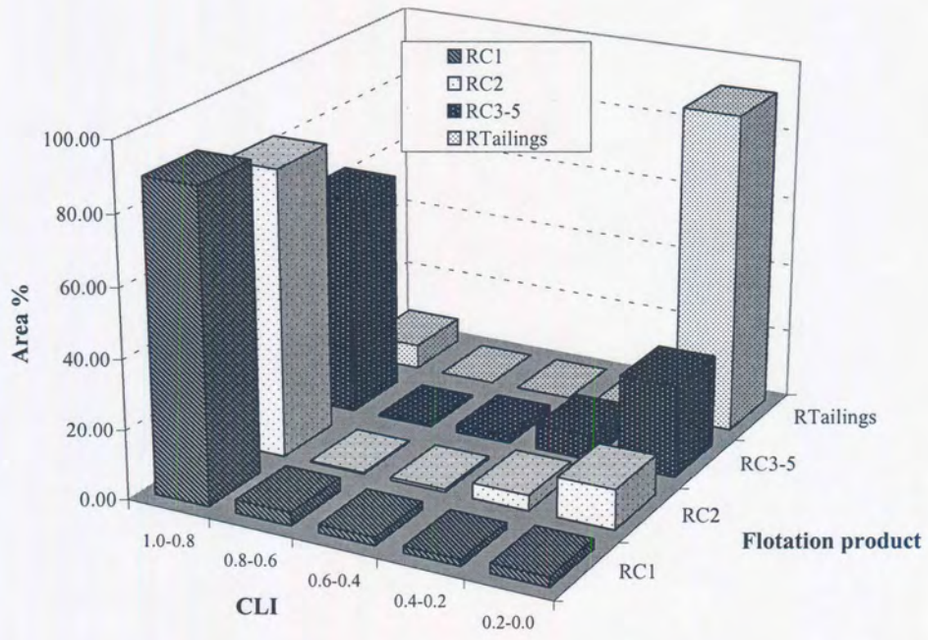

Figure 68 *Combined liberation index (CLI) of PGE minerals (excluding laurite) in the composite flotation products of samples A1, A3, A4, A5, B4, C1 and C2.*

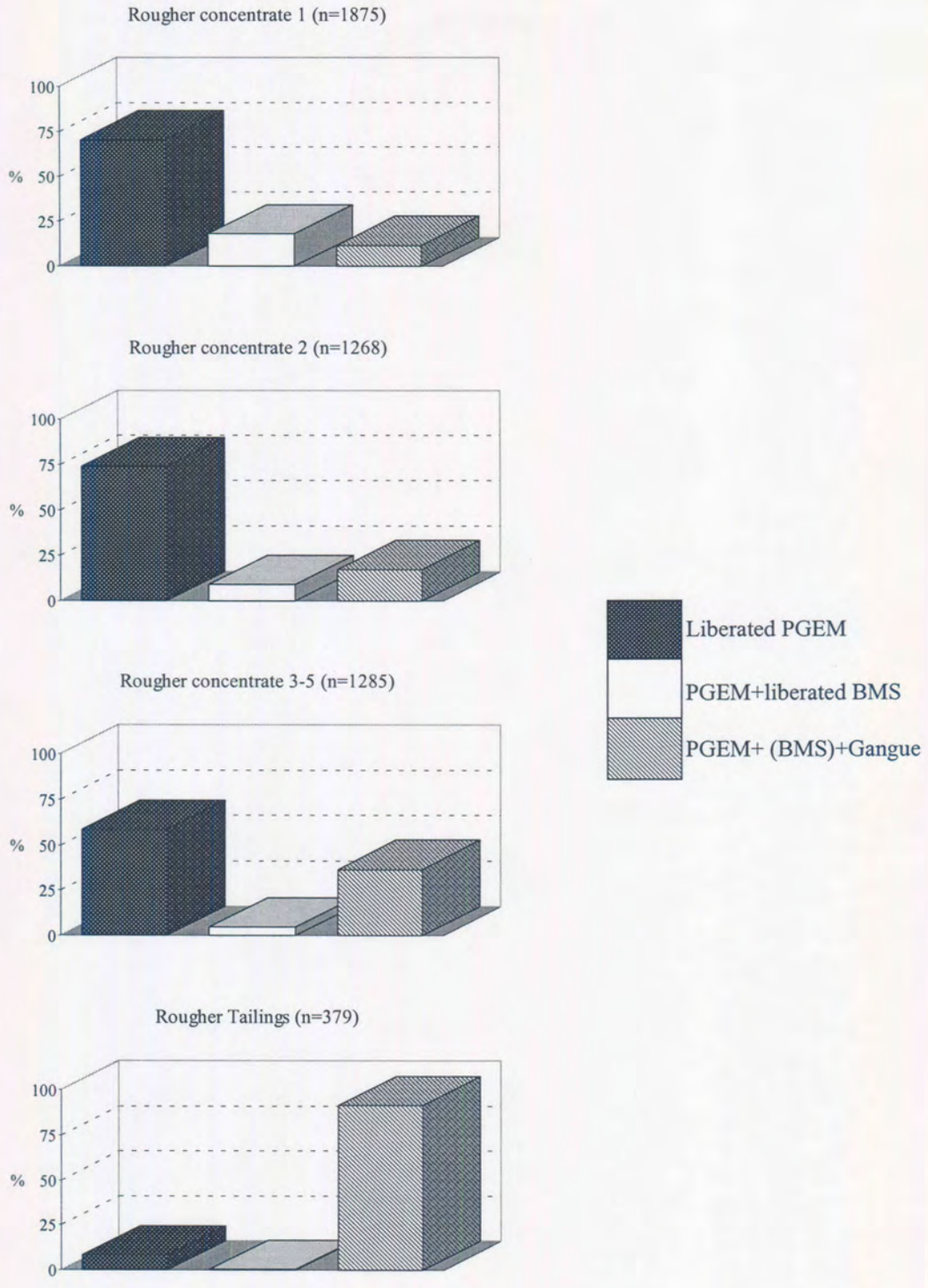

Figure 69 *Mode of occurrence of PGE minerals (PGEM) in different flotation products based on combined data of seven samples. (BMS = base-metal sulphide, n = number of PGE mineral grains measured).*

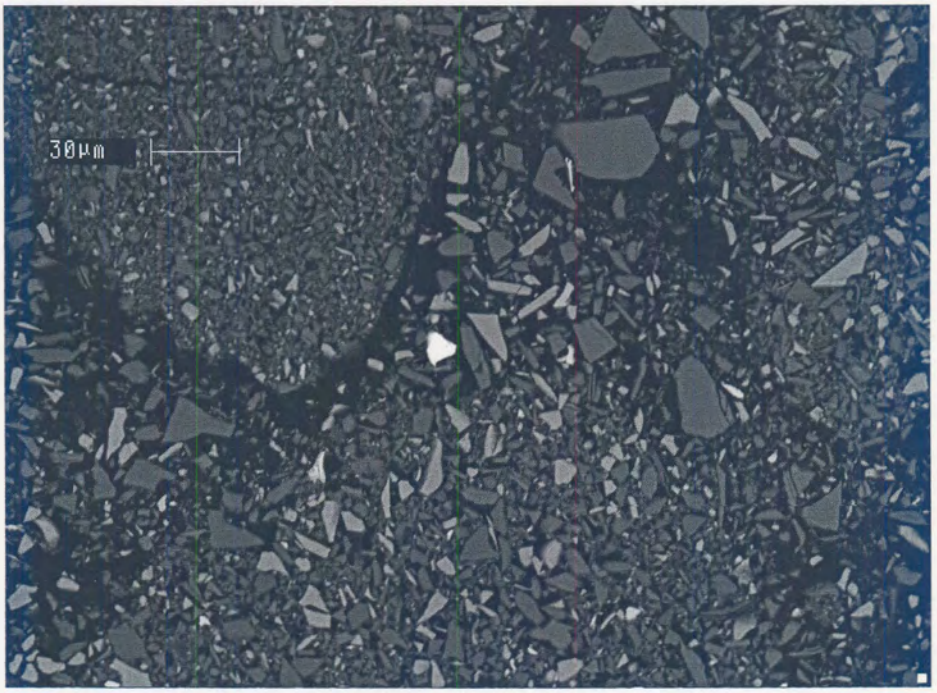

Figure 70 *Liberated PGE mineral (bright grain in the centre of the image) in flotation concentrate. Backscattered-electron image.*

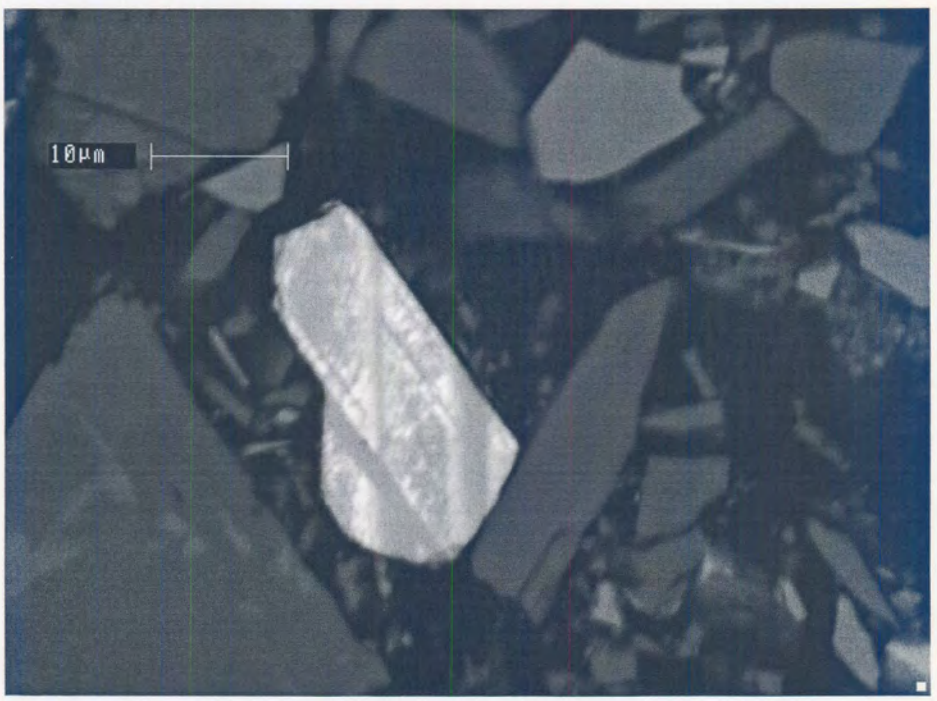

Figure 71 *Liberated pentlandite grain with exsolved Pt-Rh-Cu-Ni-sulphide in flotation concentrate. Backscattered-electron image.*

Figure 72 *Braggite (br) grain attached to pentlandite (pn) with pyrite inclusions (slightly darker). Backscattered-electron image.*

Flotation behaviour of liberated PGE mineral grains

Effect of grain size

In all of the samples, the coarsest PGE mineral grains were recovered in the fastest-floating concentrates, with progressively smaller grains reporting to the slower-floating concentrates and the tailings (Table 5.13 and Figure 73).

Type of PGE mineral

The relative proportions of the different PGE minerals present as liberated grains in the different flotation products of the seven samples are listed in Table 13 of Appendix H. The rates of flotation of the individual PGE mineral species were calculated based on a composite of the data for the seven samples. The results (Table 5.14 and Figure 74) indicate that there are differences in the rate of flotation of the different PGE mineral phases, with the rate of flotation being (Pt,Pd)-sulphide > Pt-sulphide > (Pt,Rh,Cu,Ni)-sulphide ≅ Pt-Fe alloy and the other non-sulphide PGE mineral phases ≅ (Ru,Os,Ir)-sulphide. To determine whether these differences may be

ascribed to differences in grain size, the grain-size distributions of (Pt,Pd)-sulphide (including cooperite), (Pt,Rh,Cu,Ni)-sulphide, (Ru,Os,Ir)-sulphide and non-sulphide PGEM (including Pt-Fe alloy) in the feed material were compared both in terms of area per cent and per cent number of grains (Figure 75A and B). The grain-size distributions for the four mineral groups are very similar, with median diameter values of 4 to 5µm, 5 to 6µm, ~7µm, ~7µm respectively. This does indicate that the slow-floating non-sulphide PGE minerals are also finer grained. On the other hand, the relatively slow-floating malanite appear to be coarser-grained compared to the faster-floating Pt-Pd–sulphide minerals.

Table 5.11 *Combined liberation index distribution in the flotation concentrates (RC1, 0 to 1 minutes, RC2, 1 to 3 minutes and RC3-5, 3 to 20 minutes) and tailings of selected samples.*

RC1	*A1*	*A3*	*A4*	*B4*	*A5*	*C1*	*C2*
0.0-0.2	1	2	0	3	9	2	2
0.2-0.4	0	6	2	0	1	2	1
0.4-0.6	0	1	0	0	5	2	8
0.6-0.8	0	1	0	0	1	1	23
0.8-1.0	98	90	97	96	84	93	66
RC2	*A1*	*A3*	*A4*	*B4*	*A5*	*C1*	*C2*
0.0-0.2	6	18	1	11	15	8	20
0.2-0.4	0	5	0	1	15	1	8
0.4-0.6	0	2	1	0	2	1	0
0.6-0.8	0	0	0	2	1	0	0
0.8-1.0	94	75	98	86	68	90	71
RC3	*A1*	*A3*	*A4*	*B4*	*A5*	*C1*	*C2*
0.0-0.2	13	17	9	12	33	51	52
0.2-0.4	1	22	0	4	18	3	2
0.4-0.6	0	3	0	2	7	2	3
0.6-0.8	1	0	0	1	2	0	0
0.8-1.0	85	58	90	82	40	45	43
RTailings	*A1*	*A3*	*A4*	*B4*	*A5*	*C1*	*C2*
0.0-0.2	97	90	74	94	92	98	98
0.2-0.4	0	0	0	3	3	0	0
0.4-0.6	0	0	0	0	1	0	0
0.6-0.8	0	0	0	0	0	0	0
0.8-1.0	3	10	26	3	4	2	2

Table 5.12 *PGE mineral (excluding laurite) mode of occurrence in flotation products of sample A1, A3, C2, A5, C1, B4 and A4. Bracketed values are the number of PGE mineral grains detected.*

	A1 (372)		***A3*** (276)		***A4*** (201)		***B4*** (253)		***A5*** (182)		***C1*** (306)		***C2*** (284)	
RC1	*No. %*	*Area %*	*No. %*	*Area %*	*No. %*	*Area %*	*No. %*	*Area %*	*No. %*	*Area %*	*No. %*	*Area %*	*No. %*	*Area %*
Liberated PGM	62	68	63	64	59	60	67	67	66	85	77	86	81	64
PGM + Liberated BMS	34	29	22	19	34	38	26	28	10	3	9	4	6	4
PGM+(BMS)+Gangue	3	3	15	17	7	2	8	5	23	12	14	10	13	33
	A1 (335)		***A3*** (163)		***A4*** (106)		***B4*** (202)		***A5*** (164)		***C1*** (145)		***C2*** (154)	
RC2	*No. %*	*Area %*	*No. %*	*Area %*	*No. %*	*Area %*	*No. %*	*Area %*	*No. %*	*Area %*	*No. %*	*Area %*	*No. %*	*Area %*
Liberated PGM	81	77	69	59	66	79	80	82	69	64	82	81	85	73
PGM+BMS	13	15	14	14	30	19	13	8	5	5	4	3	0	0
PGM+(BMS)+Gangue	6	8	17	27	4	2	7	10	26	31	14	16	15	27
	A1 (182)		***A3*** (248)		***A4*** (137)		***B4*** (184)		***A5*** (157)		***C1*** (208)		***C2*** (169)	
RC3-5	*No. %*	*Area %*	*No. %*	*Area %*	*No. %*	*Area %*	*No. %*	*Area %*	*No. %*	*Area %*	*No. %*	*Area %*	*No. %*	*Area %*
Liberated PGM	79	78	67	45	75	80	76	78	47	29	64	49	72	50
PGM+BMS	5	6	8	10	15	11	7	5	6	1	0	0	2	0
PGM+(BMS)+Gangue	16	16	26	46	10	9	18	17	46	69	36	51	26	49
	A1 (16)		***A3*** (25)		***A4*** (60)		***B4*** (26)		***A5*** (171)		***C1*** (52)		***C2*** (25)	
RTailings	*No. %*	*Area %*	*No. %*	*Area %*	*No. %*	*Area %*	*No. %*	*Area %*	*No. %*	*Area %*	*No. %*	*Area %*	*No. %*	*Area %*
Liberated PGM	13	1	20	7	20	22	4	2	5	3	8	3	7	20
PGM+BMS	6	1	0	0	3	2	0	0	1	0	0	0	0	0
PGM+(BMS)+Gangue	81	98	80	93	77	76	96	98	95	97	92	97	93	80

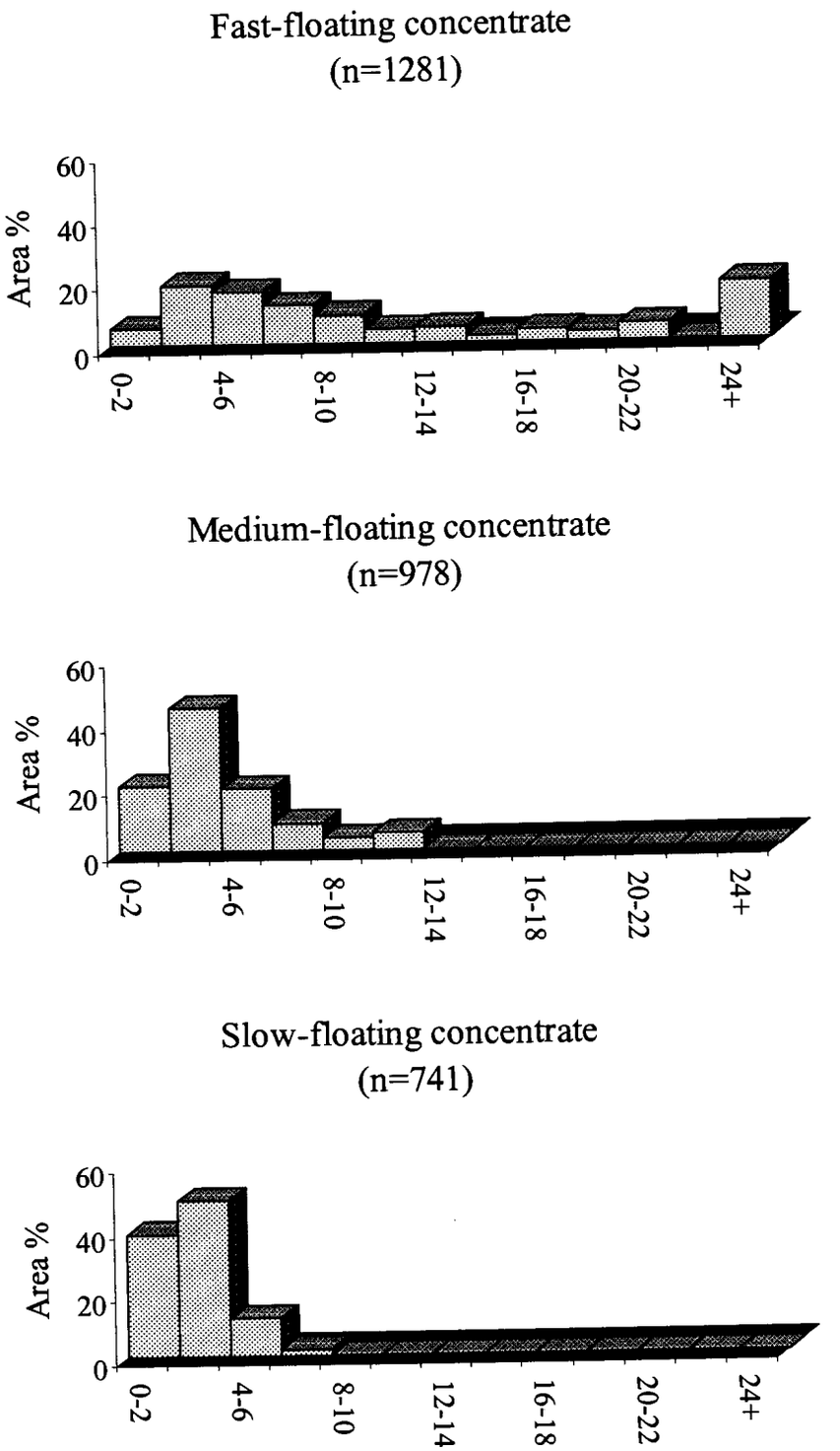

Figure 73 *Grain-size distribution of liberated PGE mineral grains in the combined slow-, medium-, and fast-floating concentrate of samples A1, A3, C1, C2, A5 and B4. (n = number of PGE mineral grains measured)*

Table 5.13 *Median grain diameter based on area percentage results of* ***liberated*** *PGE mineral grains in the flotation products of seven samples. All grain sizes values are reported as equivalent circle diameter in μm. Bracketed value is the number of liberated grains (excluding laurite) analysed in each sample.*

Sample	***RC1***	***RC2***	***RC3-5***	***RT***
A1	7.2 *(168)*	2.9 *(237)*	2.3 *(125)*	1.0 *(2)*
A3	6.6 *(157)*	3.0 *(105)*	1.9 *(146)*	1.9 *(5)*
A4	2.9 *(98)*	2.9 *(58)*	2.1 *(83)*	1.0 *(4)*
B4	4.6 *(131)*	3.0 *(122)*	1.9 *(108)*	1.0 *(1)*
A5	6.0 *(95)*	2.9 *(95)*	3.2 *(29)*	1.8 *(7)*
C1	11.4 *(204)*	3.4 *(112)*	2.5 *(111)*	2.5 *(3)*
C2	5.7 *(214)*	3.6 *(116)*	2.1 *(34)*	1.0 *(1)*

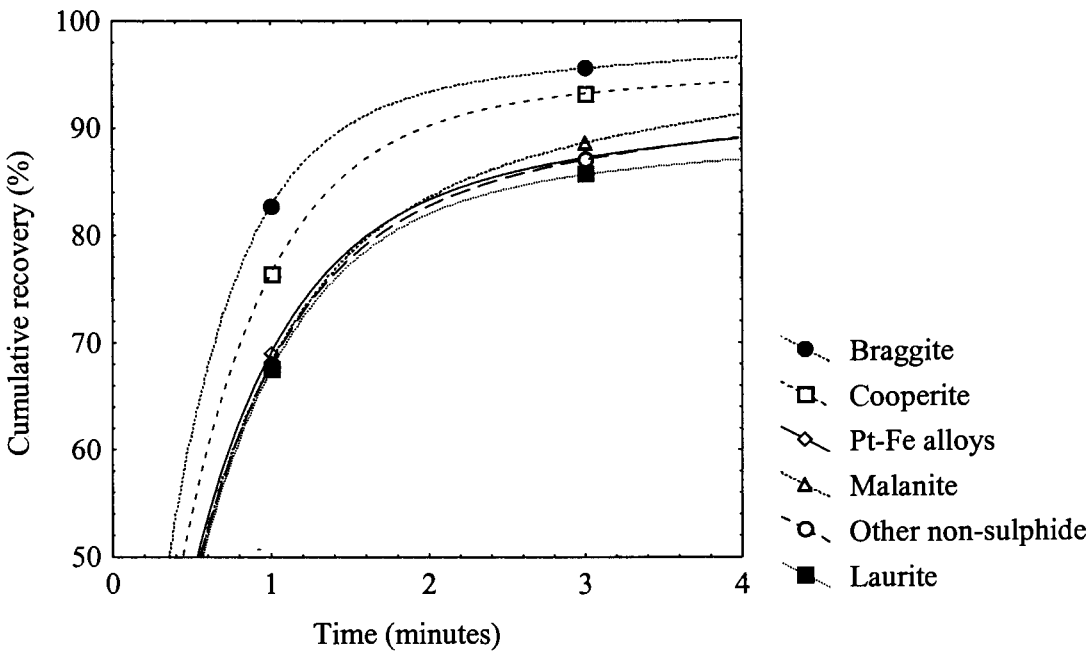

Figure 74 *Time-recovery curves for different PGE mineral phases. 'Other non-sulphide' refers to non-sulphide PGE minerals other than Pt-Fe alloys. A modified Kelsall model (Kelsall, 1961; Marais, 1989) was used to fit the data.*

Table 5.14 *Flotation behaviour of different PGE minerals. An ultimate recovery of 100% was assumed as not enough data points were available for the estimation of four parameters.*

	% Recovery				Cumulative % Recovery			Model parameters			
	RC1	**RC2**	**RC3-5**	**RT**	**RC1**	**RC2**	**RC3-5**	**ϕ**	**k_s**	**k_f**	**Final loss**
Time (mins.)	0-1	1-3	3-20		0-1	1-3	3-20		(min^{-1})	(min^{-1})	
Pt-Pd-S	83	13	4	0	83	96	100	0.09	0.24	2.17	0.00
Pt-S	76	17	6	1	83	93	99	0.09	0.12	1.76	0.00
Pt-Rh-Cu-Ni-S	68	21	11	0	83	89	100	0.22	0.23	1.67	0.00
Ru-S	68	18	10	4	83	86	96	0.17	0.07	1.60	0.00
Pt-Fe alloy	69	18	11	2	83	87	98	0.17	0.12	1.67	0.00
Other non-sulphide	68	19	12	1	83	87	99	0.19	0.14	1.65	0.00

ϕ = *slow-floating fraction*
k_s = *rate of flotation of slow-floating fraction*
k_f = *rate of flotation of fast-floating fraction*
Final loss = Σ*(observed value-predicted value)*^{2}

PGE minerals associated with liberated base-metal sulphide

The ratio $$\frac{\%\ \text{liberated PGEM}}{\%\ (\text{PGEM associated with liberated BMS}) + \%\ (\text{liberated PGEM})}$$

(where PGEM= PGE mineral, BMS=base-metal sulphide) in the slow-, medium- and fast-floating concentrates indicates that liberated PGE minerals are slower to respond to the flotation process than PGE minerals associated with liberated base-metal sulphides (Table 5.15).

Table 5.15 *% liberated PGE minerals as a fraction of (% liberated PGE mineral + PGE mineral associated with liberated base-metal sulphide) in the flotation concentrates of selected samples.*

	A1	*A3*	*A4*	*B4*	*A5*	*C1*	*C2*
RC1	0.70	0.77	0.61	0.71	0.96	0.95	0.94
RC2	0.84	0.81	0.80	0.91	0.93	0.97	1.00
RC3-5	0.93	0.82	0.88	0.93	0.95	1.00	0.99

Flotation behaviour of composite grains

PGE mineral-bearing particles with low combined liberation indices, i.e. those associated with silicate (Figure 76), or rarely chromite, tend to report to the slow-floating concentrates and tailings (Figures 68 and 69) (Tables 5.11 and 5.12).

Degree of exposed surface area

Comparing the amount of PGE mineral that is fully locked, or occur at grain boundaries between two phases, and those located at particle edges, gives a measure of the exposed surface area of PGE mineral in a particle. A composite of the flotation products of the seven samples indicated that of the particles with a combined

liberation index of less than 0.2, 33 per cent in rougher concentrate 1, 35 per cent in rougher concentrate 2, and 35 per cent in combined rougher concentrates 3, 4 and 5 appear to be completely enclosed by gangue, compared to 56 per cent in the tailings (Table 5.16).

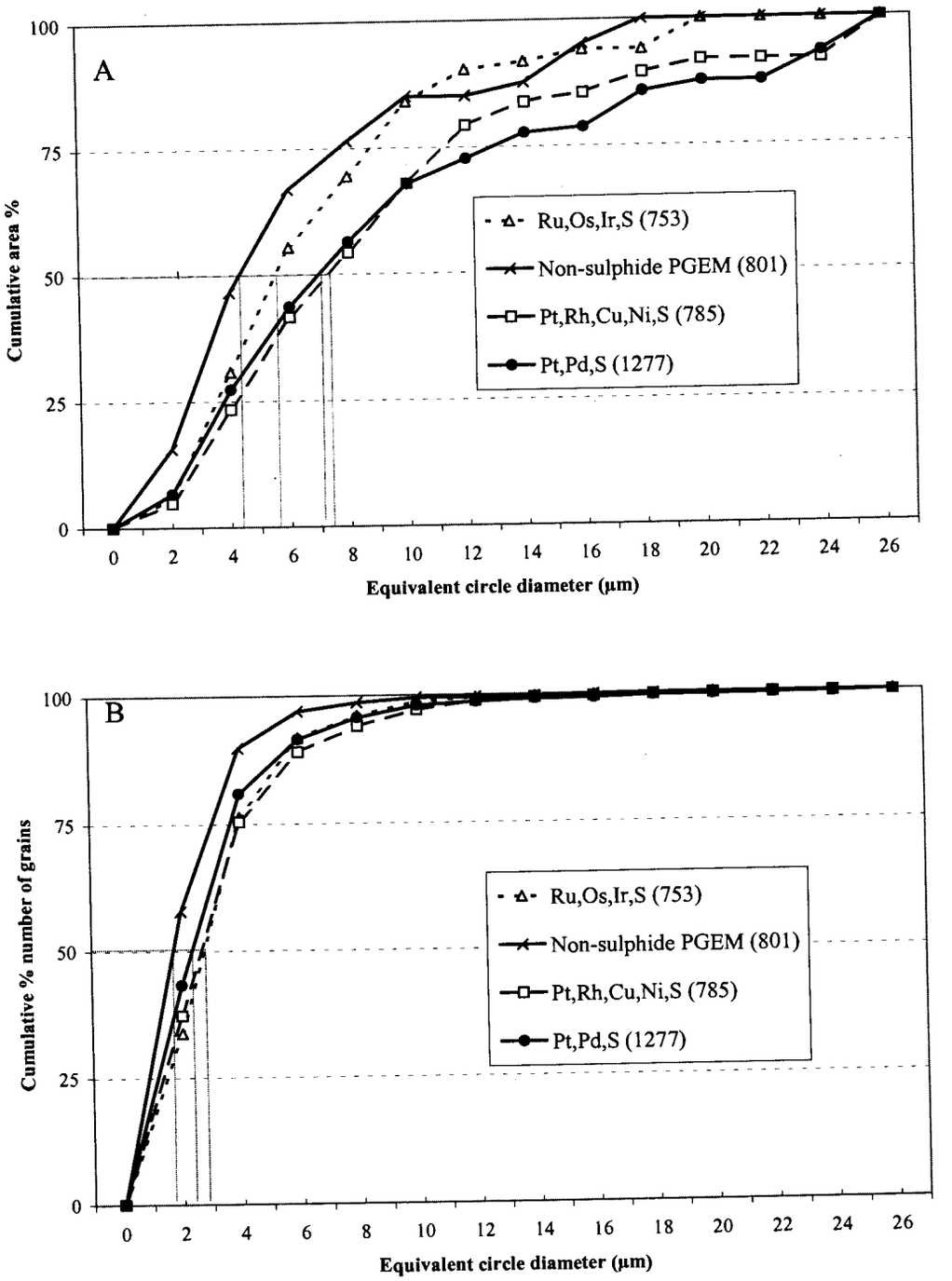

Figure 75 *Grain-size distributions of (Pt,Pd)-sulphide, (Pt,Rh,Cu,Ni)-sulphide, (Ru,Os,Ir)-sulphide and non-sulphide PGE minerals in UG2 chromitite expressed as area % (A) and % number of grains (B). Bracketed values indicate the number of grains on which the distribution is based.*

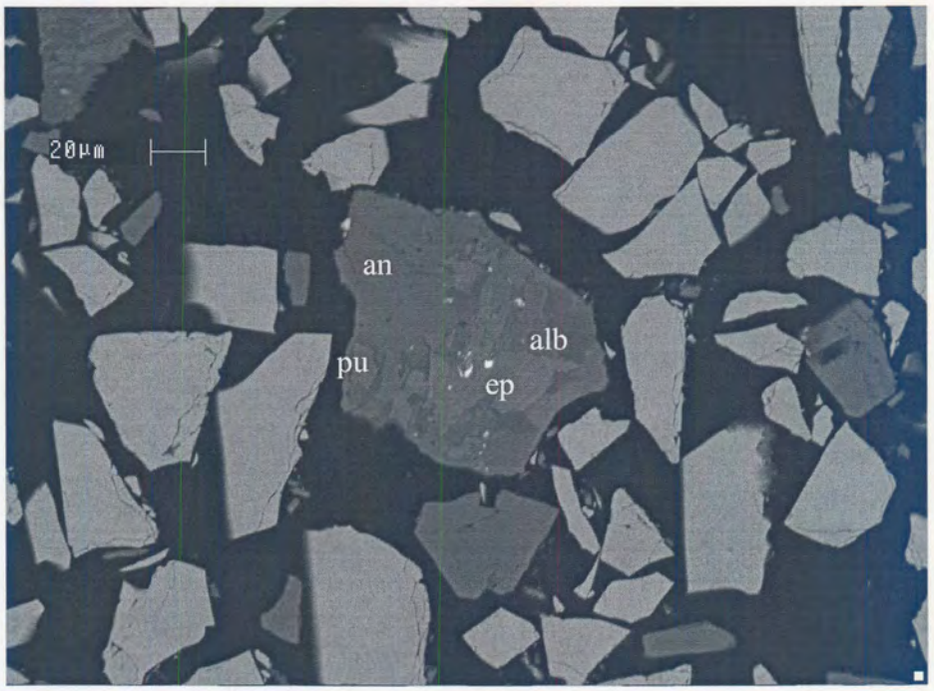

Figure 76 *Pt-Rh-sulpharsenide (bright grains) intergrown with epidote (ep), plagioclase (an) and pumpellyite (pu) in flotation tailings. Backscattered-electron image.*

Table 5.16 *Mode of occurrence of PGE minerals in particles with a combined liberation index of <0.2 in a composite of the flotation products of seven samples.*

PGEM association	*RC1*	*RC2*	*RC3-5*	*RTailings*
Associated with locked BMS	27	26	41	30
At grain edge of gangue	39	39	24	14
Enclosed in gangue	33	35	35	56

Particle size

The effect of particle size on the flotation behaviour of particles with a low combined liberation index (<0.2) is demonstrated by Figure 77. The median equivalent circle diameter of such particles in a composite of the flotation tailings is >40µm, compared to ~30 µm in combined rougher concentrate 3, 4 and 5, and between 10 and 20 µm in rougher concentrates 1 and 2.

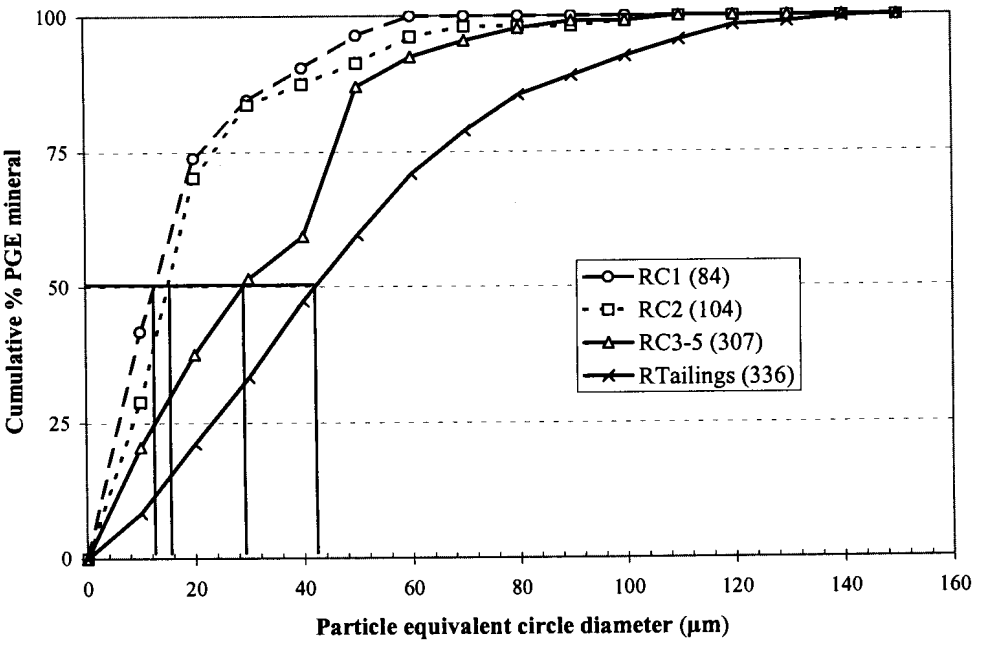

Figure 77 *A comparison of the size distributions of PGE mineral-bearing particles with combined liberation index of <0.2 in the fast-, medium- and slow-floating concentrates and rougher tailings. Bracketed values indicate the number of particles on which the distribution is based.*

5.5 Milling behaviour

5.5.1 Milling curves

The response of the fourteen samples to milling differs considerably, with sample A1 requiring about 120 minutes to achieve 80% <75µm, compared to just 40 minutes for sample A5 (Table 5.1Y and Figure 78, detailed results in Appendix I, Table 1).

5.5.2 Screen analysis

The screen analyses of the fourteen samples under investigation, milled to 80% <75µm, can be seen in Table 2, Appendix I. In all of the samples between 40 and 50 per cent of the sample mass is finer than 38 µm, and less than 2 per cent coarser than 106 µm. Differences between the samples are small.

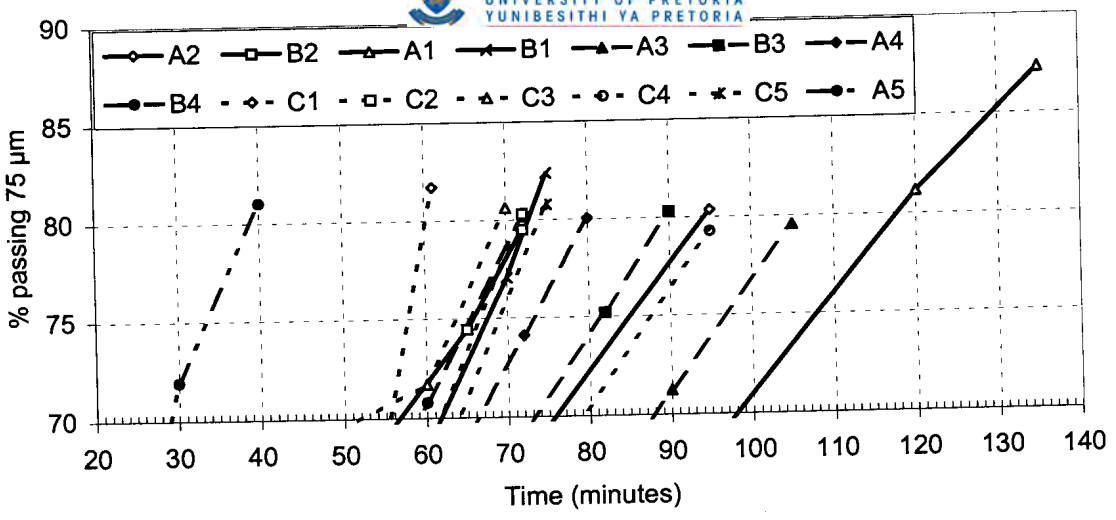

Figure 78 *Milling curves for fourteen samples of UG2 chromitite.*

——— *Normal UG2 (A1, A2, B1, B2)* - - - -*Sintered UG2 (A3, B3, B4, A4)*

..... *UG 2 from area C (C1, C2, C3, C4, C5)* —· · —*Cataclastic UG2 (A5)*

5.6 Flotation behaviour

5.6.1 Mass recoveries

Mass recoveries from the fourteen test samples at 80% <75µm range from 2.3 to 3.7 per cent after 1 minute flotation, and 10.3 to 14.7 per cent after 20 minutes (Table 1, Appendix J).

5.6.2 Cr_2O_3 recoveries

Cr_2O_3 values for the feed material determined from mass balance calculations, compare well with the assay values, with relative differences below 3 per cent in all of the samples, indicating a high level of precision during analytical and flotation procedures (Table 2, Appendix J). Cr_2O_3 recoveries after 1 minute flotation were below 3 per cent for all fourteen samples (Figure 79), with Cr_2O_3 contents of the combined concentrate ranging between 13 and 25 per cent (Table 2, Appendix J). After 20 minutes flotation recoveries had increased to between 6 and 9 per cent, with a Cr_2O_3 grade for the combined concentrate similar to that after 1 minute.

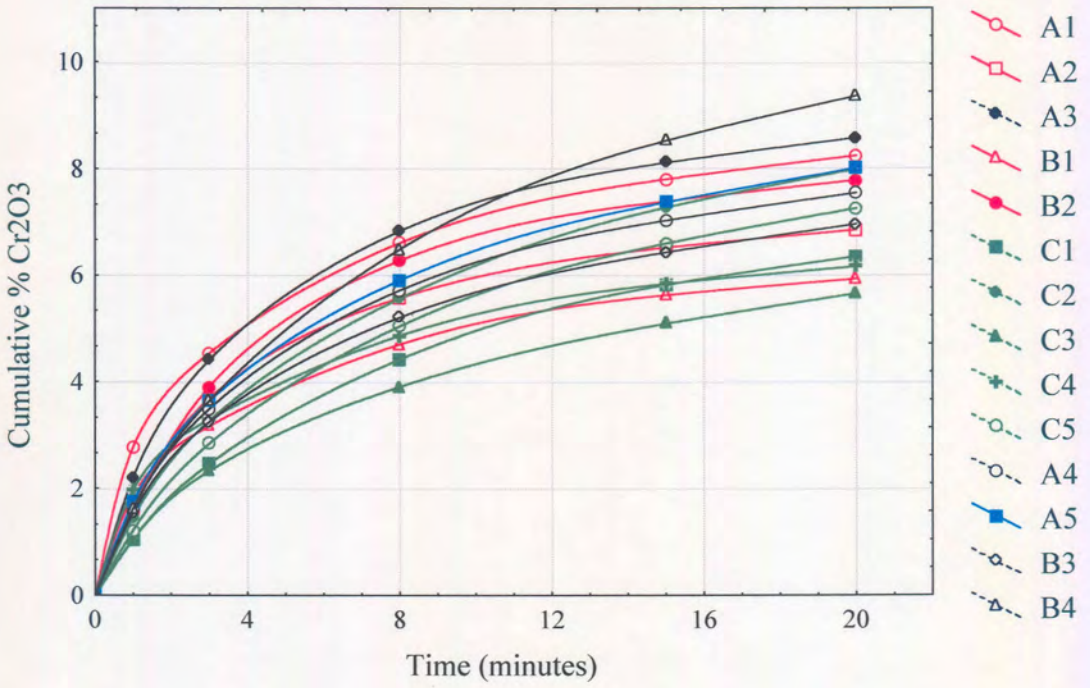

Figure 79 *Cr_2O_3 recoveries from fourteen UG2 chromitite samples milled to 80% <75 μm.*

5.6.3 Silicate gangue recoveries

By subtracting the amount of chromite and sulphide in each flotation product from the total dry mass, the behaviour of the silicate gangue component can be evaluated. Total silicate gangue recoveries after 20 minutes flotation ranged from 15 to 27 per cent (Figure 80 and Table 3, Appendix J). In general, silicate gangue recoveries are the lowest from samples A1, A2, B1 and B2 (indicated in red) with an increase in samples A3, B3, A4 and B4 (indicated in black) and A5 (blue). The highest silicate gangue recoveries were observed in samples from area C (indicated in green).

5.6.4 Copper recoveries

The Kelsall model fits the data well with loss values for all samples of less than 0.2 (Table 5, Appendix J). The differences between the calculated and assayed copper values are unacceptably large in some cases (Table 4, Appendix J). Nevertheless,

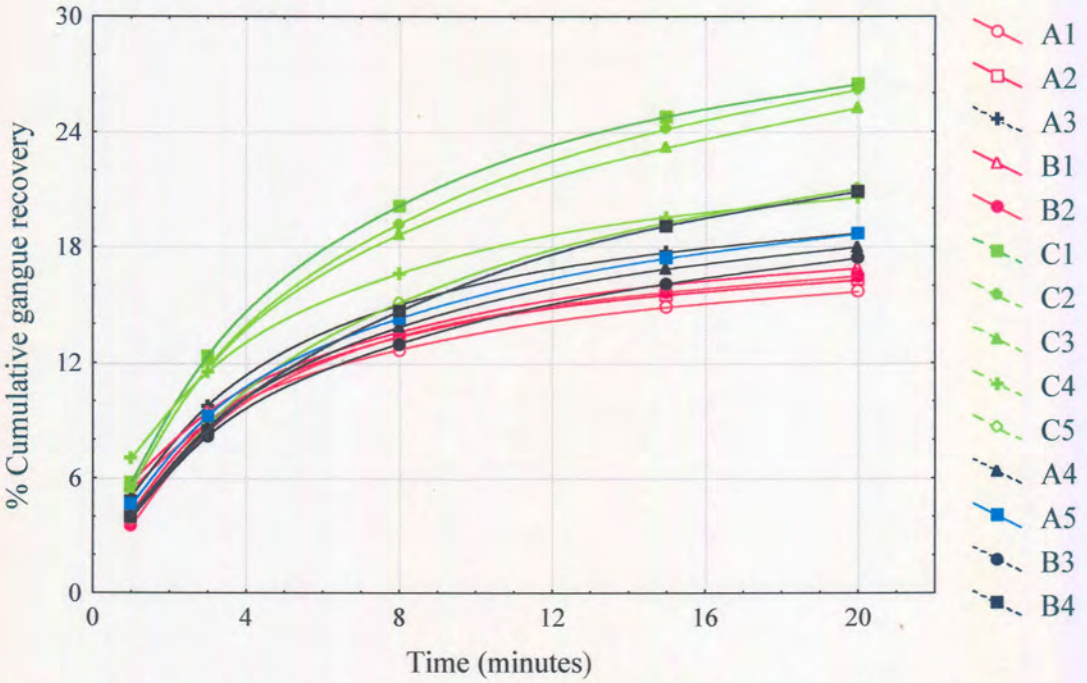

Figure 80 *Silicate recoveries from fourteen UG2 chromitite samples milled to 80% <75 µm.*

significant differences were observed between different groups of samples, with low ultimate recoveries for samples from Area C (Table 5.1Z and Figure 81). These samples are also characterised by relatively low fast-floating rate constants. Note the lower concentrate grades of the samples from Area C at all recoveries (Figure 82 and Table 4, Appendix J).

5.6.5 Nickel recoveries

Acid soluble nickel concentrations for the milled feed material, determined from mass balance calculations, compare well with the assay values, indicating a high level of precision during analytical and flotation procedures (Table 6, Appendix J). Loss values were below 0.3 for all samples (Table 7, Appendix J). However, due to the presence of nickel-bearing stainless steel particles in the flotation products, acid soluble nickel values for these samples are of little use. As the stainless steel particles reported mostly to the flotation tailings, acid soluble nickel recoveries are poor for all samples (Table 5.1AA).

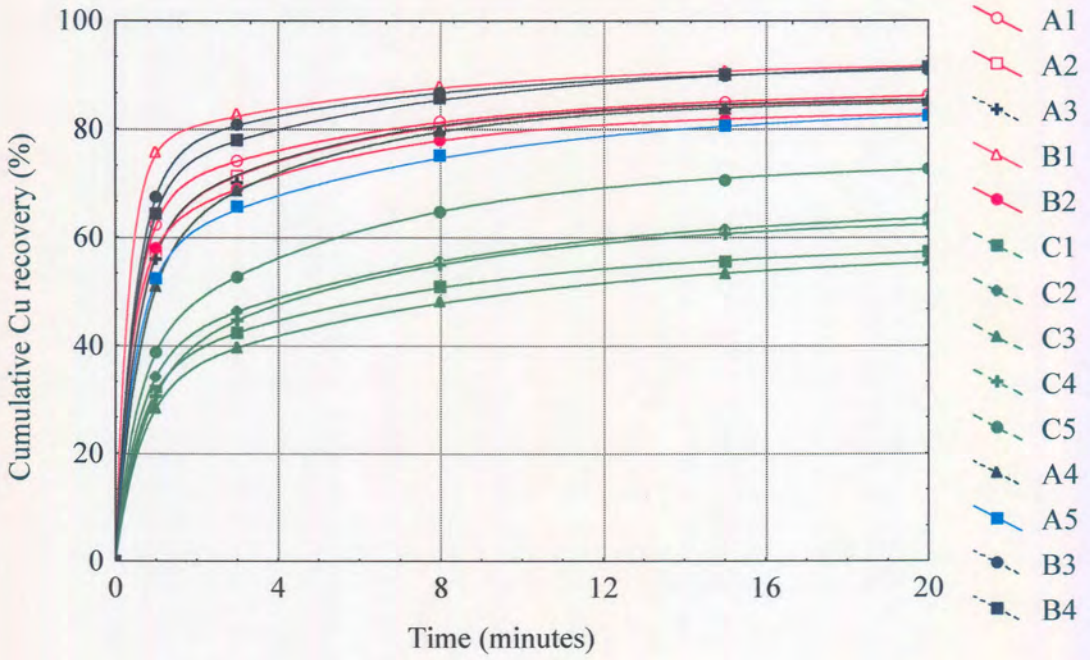

Figure 81 *Time-recovery curves for copper from fourteen samples of UG2 chromitite milled to 80% <75µm. A modified Kelsall model (Kelsall, 1961; Marais, 1989) was used to fit the data.*

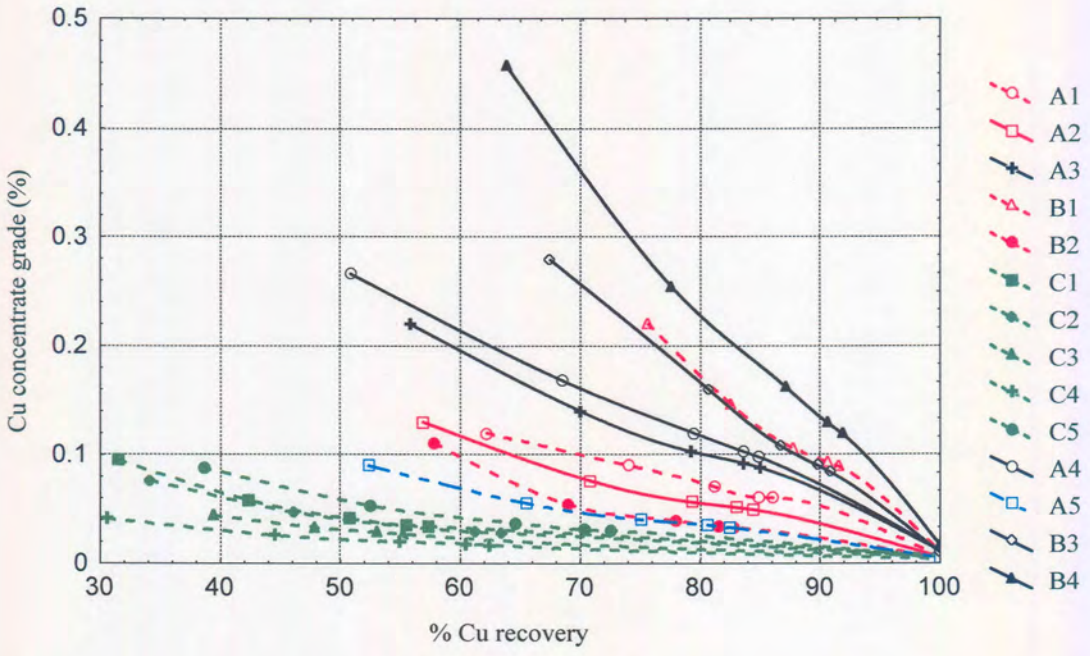

Figure 82 *Grade-recovery curves for copper for fourteen samples of UG2 chromitite milled to 80% <75µm.*

5.6.6 Total PGE+Au recovery

PGE+Au flotation results are given in Tables 8 and 9 of Appendix J and summarised in Table 5.1AB. Calculated and assayed PGE+Au values generally compare well. The Kelsall model fits the data exceptionally well with loss values of less than 0.1 for all samples. With the exception of sample A5, the ultimate PGE+Au recoveries predicted for all the samples are relatively high, ranging between 89 and 96 per cent (Figure 83). The non-floating fraction in sample A5 is 32 per cent with a 40 per cent recovery of fast-floating material. Samples A4 and B4 are characterised by relatively small recoveries of fast-floating material, 60 and 57 per cent respectively, compared to the rest of the samples at 63 to 80 per cent. Concentrate grades for all the samples are less than 80 g/t at 90% recovery (Figure 84).

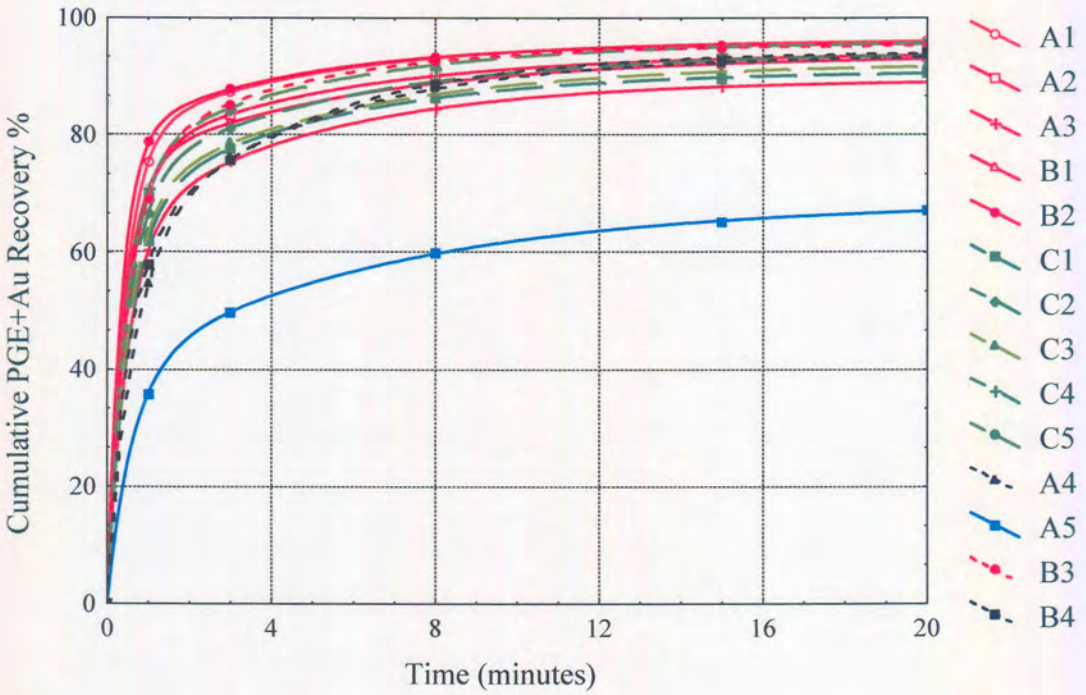

Figure 83 *PGE+Au time-recovery curves for fourteen UG2 chromitite samples milled to 80% <75µm. Data fitted according to a modified Kelsall model (Kelsall, 1961; Marais, 1989).*

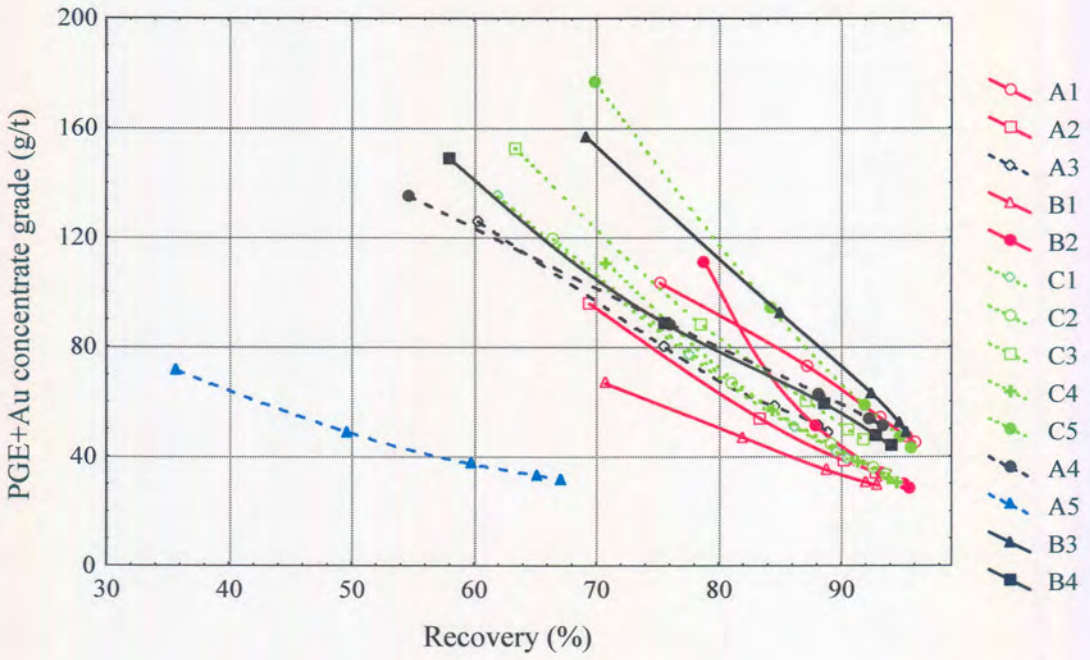

Figure 84 *Grade-recovery curves for PGE+Au for fourteen samples of UG2 chromitite milled to 80% <75μm.*

5.6.7 Platinum, palladium and rhodium

To generate enough material for individual PGE analysis, rougher concentrates 3, 4 and 5 were combined (Tables 10 to 15, Appendix J). Consequently only three data points were available for modelling of the flotation data. Assuming an ultimate recovery of 100 for platinum, palladium and rhodium makes it possible to obtain values for ϕ, k_f and k_s which can be used to compare the flotation behaviour of these elements. As PGE+Au recoveries after 20 minutes were very similar to ultimate recoveries, it was assumed that recoveries of the individual PGEs after 20 minutes approximate ultimate recoveries. These values, together with ϕ, were then used to calculate the values for R_f, R_s and 100-U reported in Table 5.1 AC to AE. The alternative approach of direct substitution of recovery after 20 minutes for U in the model equation, gave poor results.

For most samples, the amount of fast-floating platinum (Figure 85) is very similar to that for palladium (Figure 86). Notable exceptions are samples A4 and B4, which are characterised by very small fast-floating palladium fractions, with relatively large slow-floating palladium fractions. The non-floating fractions of platinum and

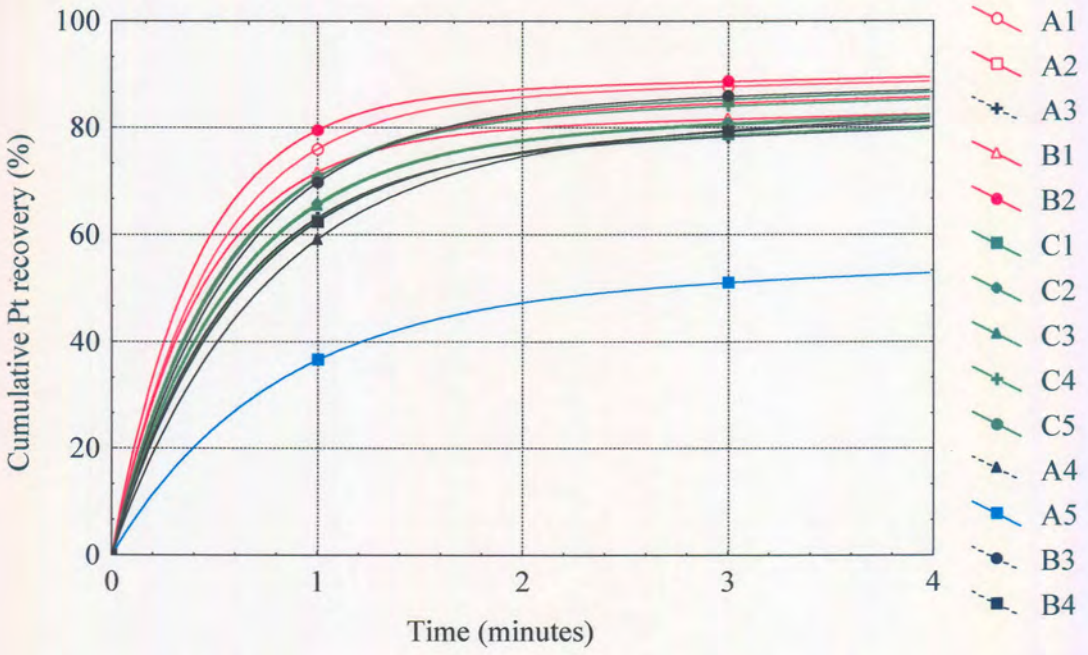

Figure 85 *Platinum time-recovery curves for fourteen UG2 chromitite samples milled to 80% <75µm. Data fitted using a modified Kelsall model (Kelsall, 1961; Marais, 1989) assuming an ultimate recovery of 100 per cent.*

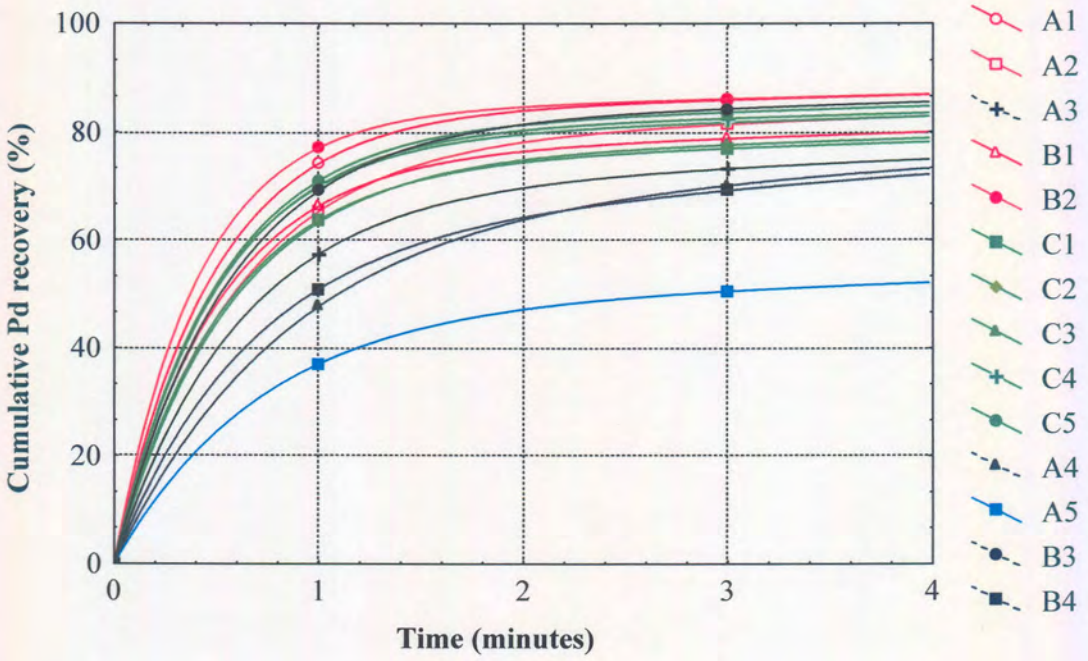

Figure 86 *Palladium time-recovery curves for fourteen UG2 chromitite samples milled to 80% <75µm. Data fitted using a modified Kelsall model (Kelsall, 1961; Marais, 1989) assuming an ultimate recovery of 100 per cent.*

palladium are very similar in all samples. Rhodium recoveries (Figure 87) seem to follow the same trend as palladium, but, as explained in section 4.4 there are large uncertainties associated with estimating rhodium recoveries.

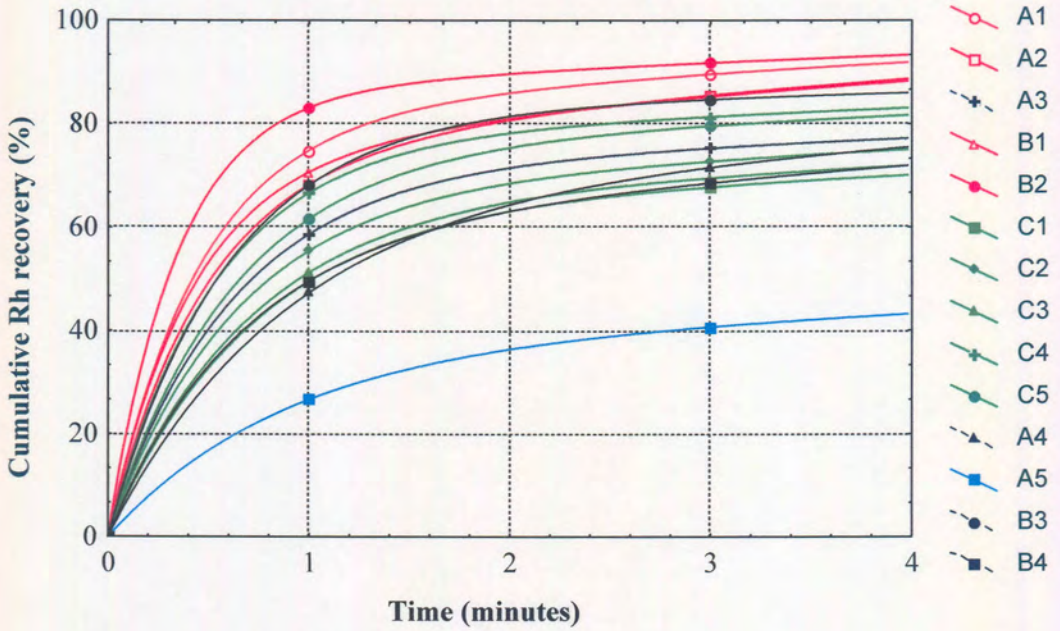

Figure 87 *Rhodium time-recovery curves for fourteen UG2 chromitite samples milled to 80% <75μm. Data fitted using a modified Kelsall model (Kelsall, 1961; Marais, 1989) assuming an ultimate recovery of 100 per cent.*

6. INTERPRETATION OF RESULTS

6.1 Identification of mineralogically and chemically different types of UG2 chromitite

The distribution of selected mineralogical and chemical characteristics of the fourteen feed samples are graphically compared in Figure 88. There are pronounced differences between the fourteen samples in terms of these parameters. The amount of non-sulphide PGE mineral, the median chromite grain diameter, the pentlandite/(pentlandite+millerite) ratio, and the amount of PGE mineral locked in gangue, were selected as being the most diagnostic characteristics of mineralogically different types of UG2 chromitite. Based on these four mineralogical parameters, four groups of samples with different mineralogical characteristics were identified using cluster analysis.[+] The members of the four groups are listed in Table 6.1, together with descriptive statistics for the mineralogical, chemical and flotation characteristics of each group.

- ***Cluster number 1 – Relatively unaltered UG2 chromitite***

  Samples A1, A2, A3, B1, B2 and B3 belong to the first group. The mineralogical characteristics of the members of this group are essentially that of normal UG2 chromitite as summarised in section 2.3.1 – the amount of non-sulphide PGE mineral is low, ranging between 5 and 23 volume per cent, the degree of sintering of chromite grains is low, with median chromite diameters of 164 to 191 µm, the amount of PGE mineral associated with gangue is low, 4 to 20 per cent, and pentlandite is the major nickel-bearing sulphide, with millerite absent or present in very low amounts.

- ***Cluster number 2 – Sintered UG2 chromitite***

  The next group has two members, A4 and B4, which are characterised by a large amount of non-sulphide PGE mineral, 58 and 53 volume per cent respectively,

---

[+] *k-means cluster analysis* using the Statistica package. The program starts with *k* random clusters and then allocates objects between those clusters with the goal to (1) minimize variability within clusters and (2) maximize variability between those clusters.

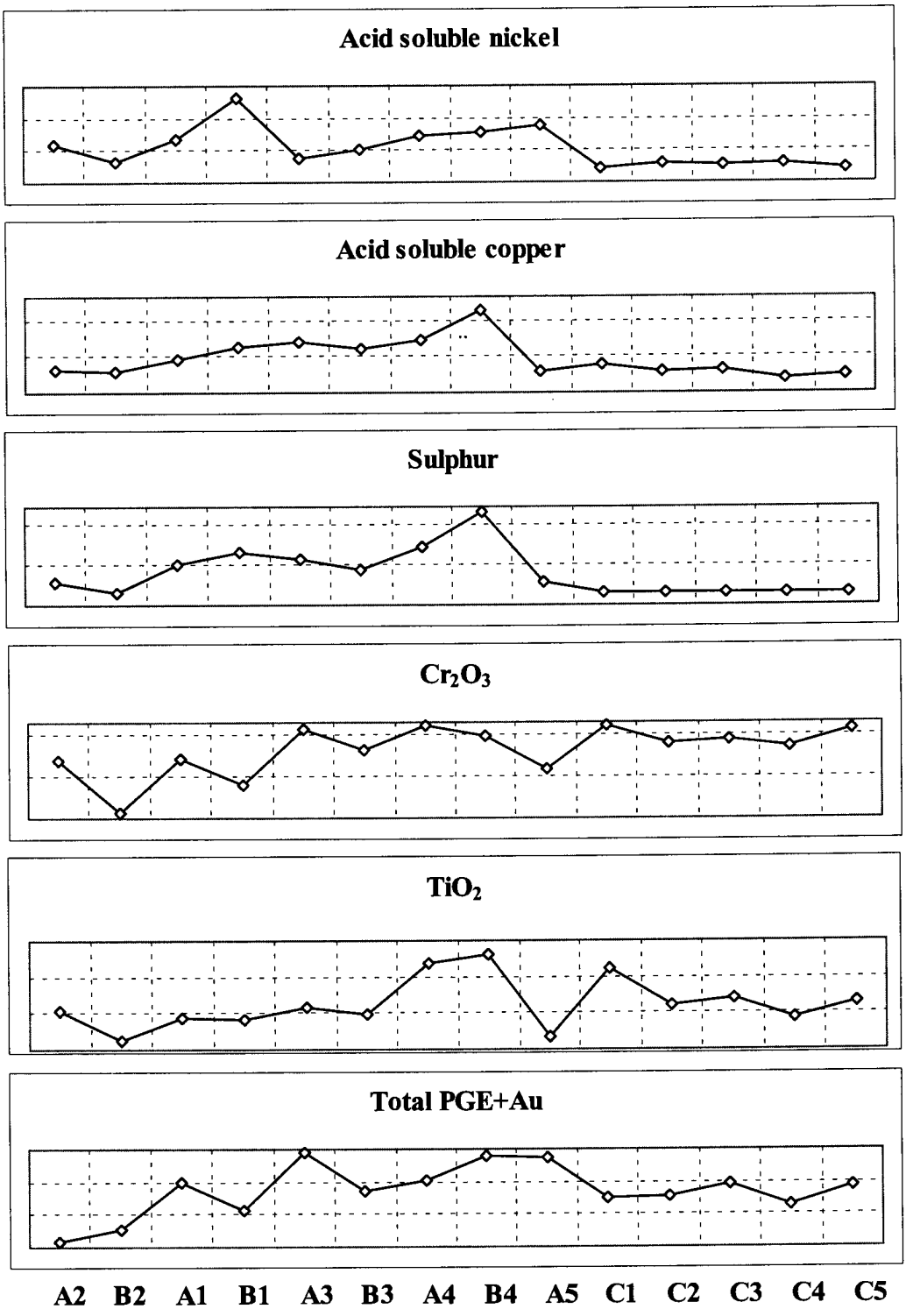

p.t.o.

Figure 88 *The distribution of selected chemical and mineralogical parameters between fourteen samples of UG2 chromitite.*

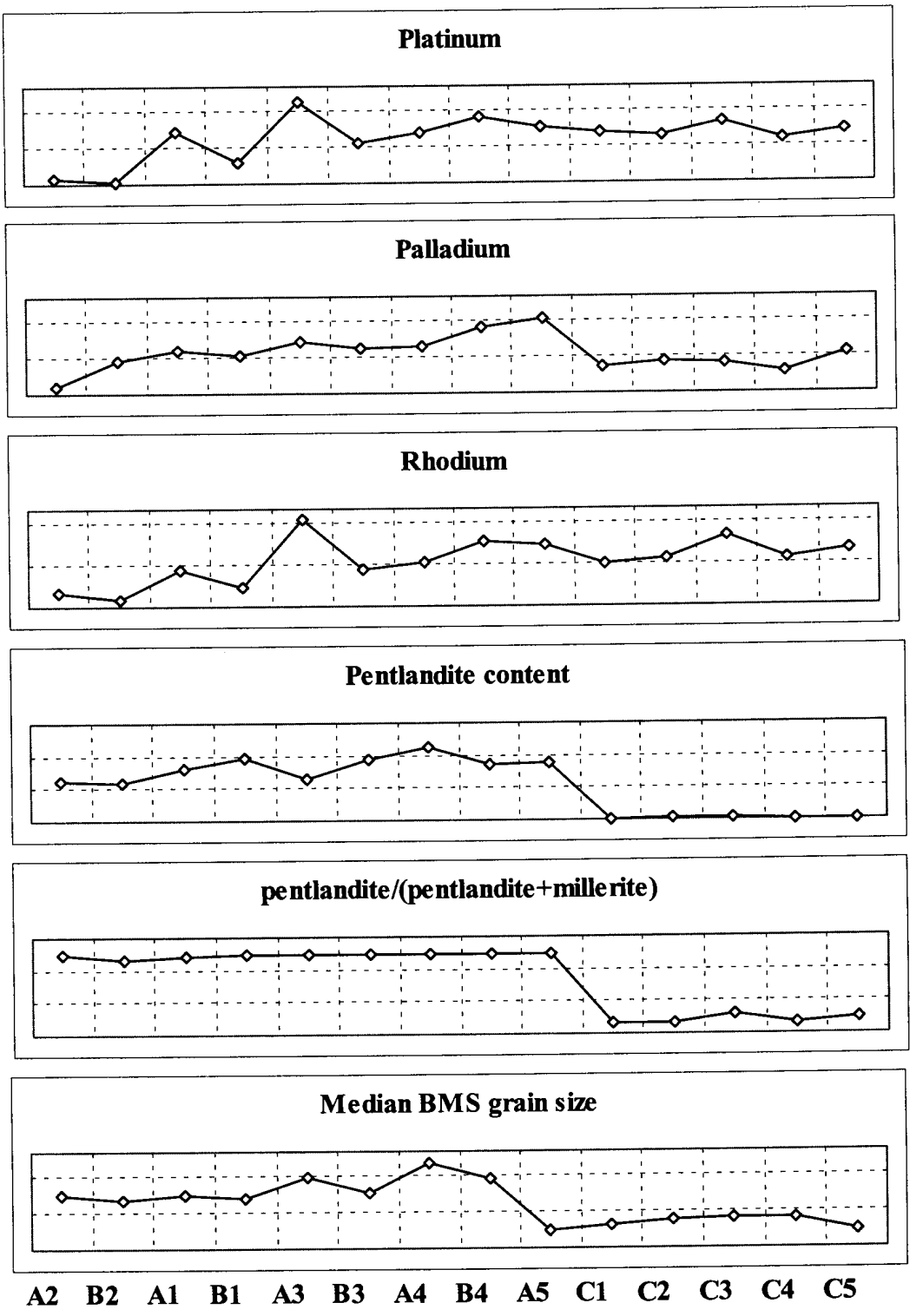

p.t.o.

Figure 88 continued *The distribution of selected chemical and mineralogical parameters between fourteen samples of UG2 chromitite.*

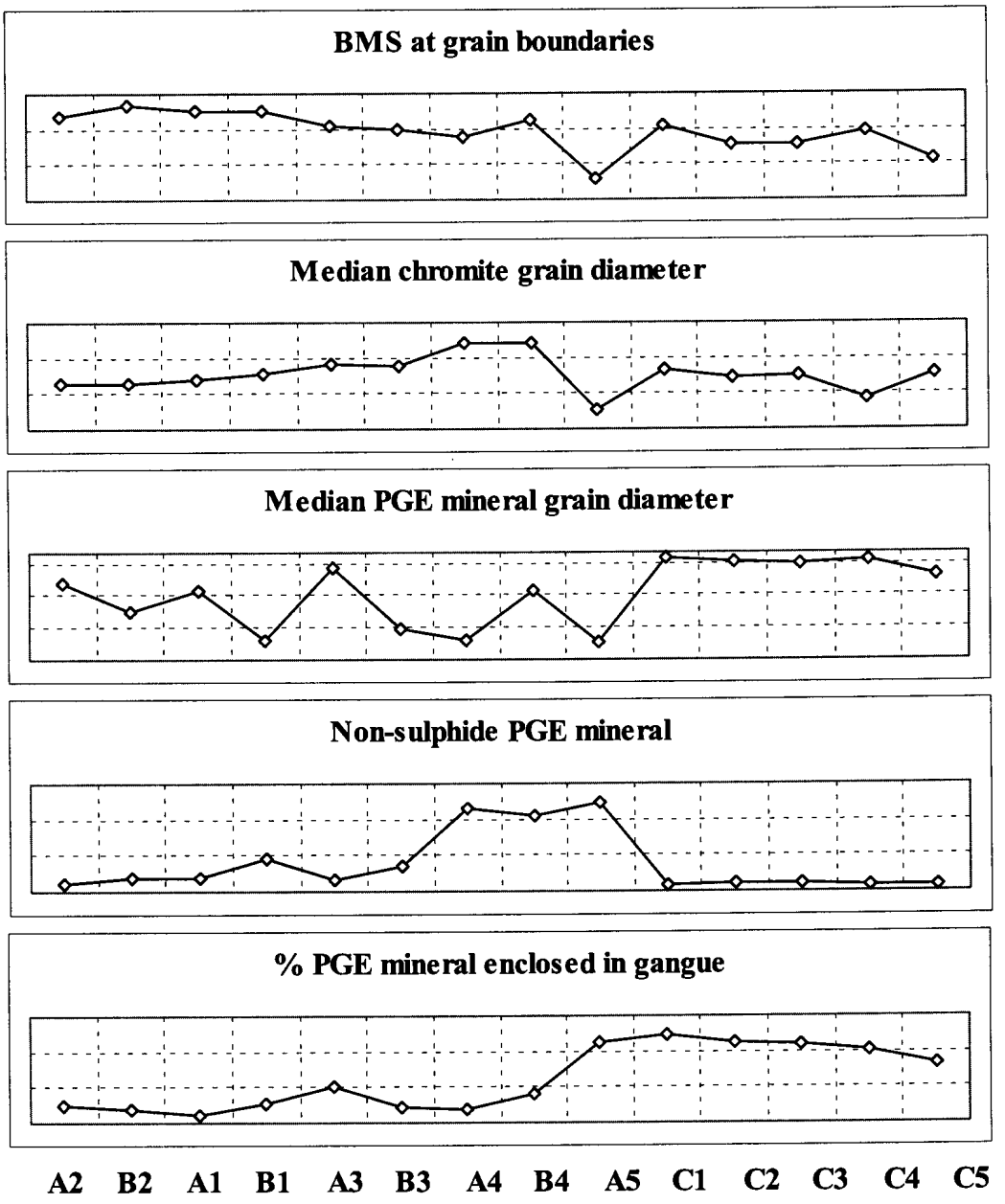

Figure 88 continued *The distribution of selected chemical and mineralogical parameters between fourteen samples of UG2 chromitite.*

Table 6.1 *Members and descriptive statistics for the mineralogical, chemical and flotation characteristics of each cluster.*

Members of Cluster Number 1						
	A1	***A2***	***A3***	***B1***	***B2***	***B3***
Distance from cluster center	4.9	7.4	9.7	8.0	6.5	7.4
Descriptive statistics (n=6)						
Mineralogical and chemical characteristics						
	Mean		*Range*		*Std. Deviation*	
% non-sulphide PGEM	12		5-23		7	
Median chromite grain diameter (µm)	175		164-191		12	
pentlandite/(pentlandite+millerite)	1.0		0.9-1.0		0.0	
% PGEM associated with gangue	10		4-20		5	
Acid soluble nickel (ppm)	252		126-525		144	
Acid soluble copper (ppm)	75		42-107		27	
Sulphur (%)	0.03		0.01-0.05		0.01	
Cr_2O_3 (%)	28.2		20.9-33.8		4.5	
TiO_2 (%)	0.7		0.6-0.7		0.1	
Total PGE+Au (ppm)	4.4		3.2-5.9		1.0	
Platinum (ppm)	2.7		2.0-3.7		0.6	
Palladium (ppm)	1.3		0.7-1.6		0.3	
Rhodium (ppm)	0.4		0.3-0.6		0.1	
Pentlandite content (%)	0.06		0.05-0.08		0.01	
Median BMS grain size (µm)	32		30-39		3	
% BMS at grain boundaries	84		74-92		7	
Median PGEM grain diameter (µm)	2.2		1.8-2.8		0.4	
Flotation characteristics						
	Mean		*Range*		*Std. Deviation*	
R_f (%)	75		63-80		6	
R_s (%)	19		15-26		4	
100-U (%)	6		4-11		3	
k_f (min^{-1})	2.3		2.1-2.9		0.3	
k_s (min^{-1})	0.22		0.18-0.25		0.03	

p.t.o.

Table 6.1 continued *Members and descriptive statistics for the mineralogical, chemical and flotation characteristics of each cluster.*

Members of Cluster Number 2			
	A4	***B4***	
Distance from cluster center	2.5	2.5	
Descriptive statistics (n=2)			
Mineralogical and chemical characteristics			
	Mean	*Range*	*Std. Deviation*
% non-sulphide PGEM	55	53-58	4
Median chromite grain diameter (µm)	221	-	-
pentlandite/(pentlandite+millerite)	1.0	-	-
% PGEM associated with gangue	12	8-16	5
Acid soluble nickel (ppm)	305	295-316	15
Acid soluble copper (ppm)	140	109-170	43
Sulphur (%)	0.07	0.05-0.08	0.02
Cr_2O_3 (%)	33.7	32.9-34.5	1.1
TiO_2 (%)	1.0	-	-
Total PGE+Au (ppm)	5.4	5.0-5.8	0.6
Platinum (ppm)	3.2	3.1-3.3	0.2
Palladium (ppm)	1.7	1.5-1.9	0.3
Rhodium (ppm)	0.5	-	-
Pentlandite content (%)	0.08	0.07-0.09	0.02
Median BMS grain size (µm)	42	38-45	5
% BMS at grain boundaries	76	70-82	8
Median PGEM grain diameter (µm)	2.1	1.8-2.5	0.5
Flotation characteristics			
	Mean	*Range*	*Std. Deviation*
R_f (%)	58	57-60	2
R_s (%)	36	34-38	3
100-U (%)	6	-	0
k_f (min^{-1})	1.9	1.6-2.2	0.4
k_s (min^{-1})	0.23	0.22-0.24	0.01

p.t.o.

Table 6.1 continued *Members and descriptive statistics for the mineralogical, chemical and flotation characteristics of each cluster.*

Members of Cluster Number 3						
	C1	***C2***	***C3***	***C4***	***C5***	
Distance from cluster center	7.8	2.0	2.7	14.0	5.8	
Descriptive statistics (n=5)						
Mineralogical and chemical characteristics						
	Mean		*Range*		*Std. Deviation*	
% non-sulphide PGEM	4		4-6		1	
Median chromite grain diameter (µm)	170		142-184		16	
pentlandite/(pentlandite+millerite)	0.1		0.0-0.2		0.1	
% PGEM associated with gangue	43		33-50		6	
Acid soluble nickel (ppm)	101		82-114		15	
Acid soluble copper (ppm)	43		30-57		11	
Sulphur (%)	<0.01		-		-	
Cr_2O_3 (%)	32.7		31.2-34.6		1.4	
TiO_2 (%)	0.8		0.7-1.0		0.1	
Total PGE+Au (ppm)	4.6		4.3-4.9		0.3	
Platinum (ppm)	3.0		2.9-3.2		0.1	
Palladium (ppm)	1.1		0.9-1.3		0.1	
Rhodium (ppm)	0.5		-		-	
Pentlandite content (%)	0.00		-		-	
Median BMS grain size (µm)	20		17-23		2	
% BMS at grain boundaries	66		53-77		9	
Median PGEM grain diameter (µm)	2.8		2.7-2.9		0.1	
Flotation characteristics						
	Mean		*Range*		*Std. Deviation*	
R_f(%)	71		66-75		4	
R_s (%)	22		20-25		2	
100-U (%)	7		4-9		2	
k_f (min^{-1})	2.1		2.0-2.2		0.1	
k_s (min^{-1})	0.20		0.19-0.22		0.01	

p.t.o.

Table 6.1 continued *Members and descriptive statistics for the mineralogical, chemical and flotation characteristics of each cluster.*

Members of Cluster Number 4			
	A5		
Distance from cluster center	0.0		
Descriptive statistics (n=1)			
Mineralogical and chemical characteristics			
	Mean	*Range*	*Std. Deviation*
% non-sulphide PGEM	81	-	-
Median chromite grain diameter (μm)	127	-	-
pentlandite/(pentlandite+millerite)	1.0	-	-
% PGEM associated with gangue	45	-	-
Acid soluble nickel (ppm)	356	-	-
Acid soluble copper (ppm)	44	-	-
Sulphur (%)	0.02	-	-
Cr_2O_3 (%)	27.70	-	-
TiO_2 (%)	0.57	-	-
Total PGE+Au (ppm)	5.74	-	-
Platinum (ppm)	3.13	-	-
Palladium (ppm)	2.05	-	-
Rhodium (ppm)	0.52	-	-
Pentlandite content (%)	0.07	-	-
Median BMS grain size (μm)	17	-	-
% BMS at grain boundaries	40	-	-
Median PGEM grain diameter (μm)	1.8	-	-
Flotation characteristics			
	Mean	*Range*	*Std. Deviation*
R_f (%)	40	-	-
R_s (%)	29	-	-
100-U (%)	32	-	-
$k_f (min^{-1})$	1.6	-	-
$k_s (min^{-1})$	0.15	-	-

and enlargement of chromite grains (median chromite diameter = 220 µm in both samples). Pentlandite is the dominant nickel-bearing base-metal sulphide, and the amount of PGE mineral associated with gangue (8 to 16 per cent) is similar to that of the relatively unaltered UG2 chromitite. These two samples are characterised by elevated TiO_2 contents (>0.9 per cent). A strong positive linear relationship (Pearson correlation coefficient r=0.80) exists between TiO_2 content and median chromite grain diameter for the fourteen samples (Figure 89, Table 6.2).

- ***Cluster number 3 – Millerite-bearing UG2 chromitite***

Cluster number 3 includes all the samples from area C. Millerite, instead of pentlandite, is the major nickel-bearing sulphide in these samples, and a large proportion of the PGE minerals in these samples is associated with gangue (33 to 50 per cent). Chromite diameters (142 to 184 µm) are similar to that of relatively unaltered UG2, and the amount of non-sulphide PGE mineral is low (<6 volume per cent). These samples are also characterised by smaller base-metal sulphide grain diameters, and a relatively small proportion of the base-metal sulphide grains located at grain boundaries. Note the relatively low sulphur, acid soluble nickel, copper and palladium values. Platinum and rhodium don't seem to follow the same trend. A parameter not quantified, and therefore not taken into account during the statistical analysis, is the degree of silicate alteration, which is relatively high for this group of samples.

- ***Cluster number 4 – Cataclastic UG2 chromitite***

This group, which comprises only sample A5, is characterised by a small chromite grain size (median chromite diameter =127 µm), as a result of fracturing of chromite grains, a large amount of PGE mineral associated with gangue (45 per cent), and a high proportion of non-sulphide PGE mineral (81 per cent). The median grain diameter of base-metal sulphide in this sample is small, and most of the base-metal sulphide grains are enclosed in silicate. The degree of silicate alteration is relatively high in cataclastic UG2 chromitite.

Table 6.2 *Pearson correlation matrix for selected mineralogical and chemical parameters in fourteen samples of UG2 chromitite. Marked correlations (boldface) are significant at p<0.05.*

	Ni_{as}	Cu_{as}	S	Cr_2O_3	TiO_2	PGE	Pt	Pd	Rh	pn	pn:mil	BMSS	BMSM	ChrS	NSul	PSN	PBMS	PSil
Ni_{as}	1.00	0.48	**0.64**	-0.36	-0.07	0.11	-0.16	0.44	-0.22	**0.78**	**0.69**	0.37	0.15	0.08	**0.63**	**-0.75**	0.52	-0.46
Cu_{as}	0.48	1.00	**0.96**	0.24	0.59	0.50	0.36	0.54	0.25	**0.62**	0.56	**0.76**	0.33	**0.79**	0.55	-0.29	0.39	-0.48
S	**0.64**	**0.96**	1.00	0.15	0.49	0.47	0.29	**0.57**	0.18	**0.71**	**0.64**	**0.76**	0.32	**0.68**	**0.64**	-0.39	0.45	-0.55
Cr_2O_3	-0.36	0.24	0.15	1.00	0.74	0.51	**0.75**	0.06	**0.68**	-0.31	-0.41	0.05	-0.35	0.48	0.02	0.46	-0.54	0.37
TiO_2	-0.07	**0.59**	0.49	**0.74**	1.00	0.33	0.45	0.09	0.33	-0.03	-0.16	0.33	0.04	0.80	0.28	0.22	-0.15	0.08
PGE	0.11	0.50	0.47	0.51	0.33	1.00	**0.92**	**0.84**	**0.87**	0.18	0.11	0.12	-0.46	0.28	0.51	-0.04	-0.30	0.21
Pt	-0.16	0.36	0.29	**0.75**	0.45	**0.92**	1.00	0.55	**0.95**	-0.12	-0.18	0.04	-0.43	0.30	0.22	0.30	-0.50	0.38
Pd	0.44	0.54	**0.57**	0.06	0.09	**0.84**	0.55	1.00	0.50	0.54	0.47	0.20	-0.36	0.18	**0.77**	-0.50	0.07	-0.07
Rh	-0.22	0.25	0.18	**0.68**	0.33	**0.87**	**0.95**	0.50	1.00	-0.21	-0.23	-0.06	-0.54	0.18	0.18	0.34	-0.63	0.48
pn	**0.78**	**0.62**	**0.71**	-0.31	-0.03	0.18	-0.12	0.54	-0.21	1.00	**0.95**	**0.72**	0.27	0.29	**0.69**	**-0.84**	**0.78**	**-0.76**
pn:mil	**0.69**	0.56	**0.64**	-0.41	-0.16	0.11	-0.18	0.47	-0.23	**0.95**	1.00	**0.71**	0.36	0.20	0.54	**-0.72**	**0.78**	**-0.80**
BMSS	0.37	**0.76**	**0.76**	0.05	0.33	0.12	0.04	0.20	-0.06	**0.72**	**0.71**	1.00	0.56	**0.70**	0.35	-0.36	**0.72**	**-0.80**
BMSM	0.15	0.33	0.32	-0.35	0.04	-0.46	-0.43	-0.36	-0.54	0.27	0.36	0.56	1.00	0.32	-0.30	0.03	**0.68**	**-0.67**
ChrS	0.08	**0.79**	**0.68**	0.48	0.80	0.28	0.30	0.18	0.18	0.29	0.20	**0.70**	0.32	1.00	0.25	-0.05	0.29	-0.40
NSul	**0.63**	0.55	**0.64**	0.02	0.28	0.51	0.22	**0.77**	0.18	**0.69**	0.54	0.35	-0.30	0.25	1.00	**-0.70**	0.23	-0.16
PSN	**-0.75**	-0.29	-0.39	0.46	0.22	-0.04	0.30	-0.50	0.34	**-0.84**	**-0.72**	-0.36	0.03	-0.05	-0.70	1.00	**-0.65**	0.51
PBMS	0.52	0.39	0.45	-0.54	-0.15	-0.30	-0.50	0.07	**-0.63**	**0.78**	**0.78**	**0.72**	**0.68**	0.29	0.23	**-0.65**	1.00	**-0.91**
PSil	-0.46	-0.48	-0.55	0.37	0.08	0.21	0.38	-0.07	0.48	**-0.76**	**-0.80**	**-0.80**	**-0.67**	-0.40	-0.16	0.51	**-0.91**	1.00

Nias, Cuas = acid soluble nickel and copper contents *S – sulphur content* *CR_2O_3 = Cr_2O_3 content* *TiO_2 = TiO_2 content*

PGE = (Pt,Pd,Rh,Au) *Pt = platinum content* *Pd = palladium content* *Rh= rhodium content*

pn = pentlandite content *pn:mil = pentlandite/(pentlandite+millerite) ratio* *BMSS = base-metal sulphide median grain diameter*

BMSM = % base-metal sulphide located at grain boundaries *ChrS = chromite median grain diameter* *NSul = % non-sulphide PGE mineral*

PSN = PGE mineral median grain diameter i.t.o. number of grains *PBMS = % PGE mineral associated with base-metal sulphide* *PSil = % PGE mineral enclosed in gangue*

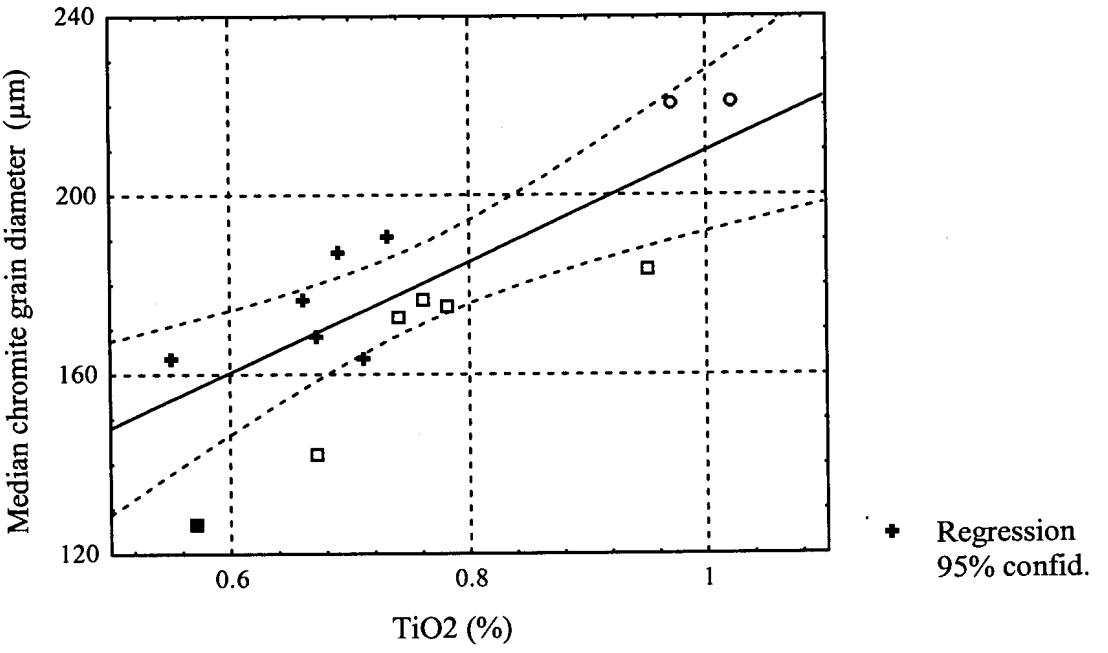

Figure 89 *Relationship between median chromite grain diameter (µm) and TiO_2 content for fourteen samples of UG2 chromitite. Pearson correlation coefficient for all fourteen samples, r=0.80. + = samples A1, A2, A3, B1, B2, and B3. □= samples C1, C2, C3, C4 and C5. o = samples A4 and B4. ■ = sample A5.*

In terms of most of the other mineralogical and chemical parameters compared in Figure 88, the differences between the four groups of samples are less clear, and often overlap. There is a positive linear relationship between median chromite and base-metal sulphide diameter, with a Pearson correlation coefficient r=0.7 (Table 6.2). This relationship does not appear to hold for the samples from area C (Figure 90), presumably because the processes causing corrosion of sulphide grains in these samples did not affect chromite grain size. If sample A5, in which chromite grain size was determined by cataclasis, and the samples from area C are excluded from the calculation, the relationship becomes even stronger (r=0.86). There does not appear to be any systematic relationship between chromite or base-metal sulphide grain size, and that of the PGE minerals (Table 6.2), indicating that an increase in base-metal sulphide grain size is not necessarily associated with an increase in PGE mineral grain size.

Total PGE+Au, platinum, rhodium and Cr_2O_3 do not appear to vary in a systematic manner in terms of the mineralogically different types of UG2 chromitite. Some

interesting trends do, however, emerge from a closer look at the relationships between the different chemical components of the UG2 chromitite (Table 6.2).

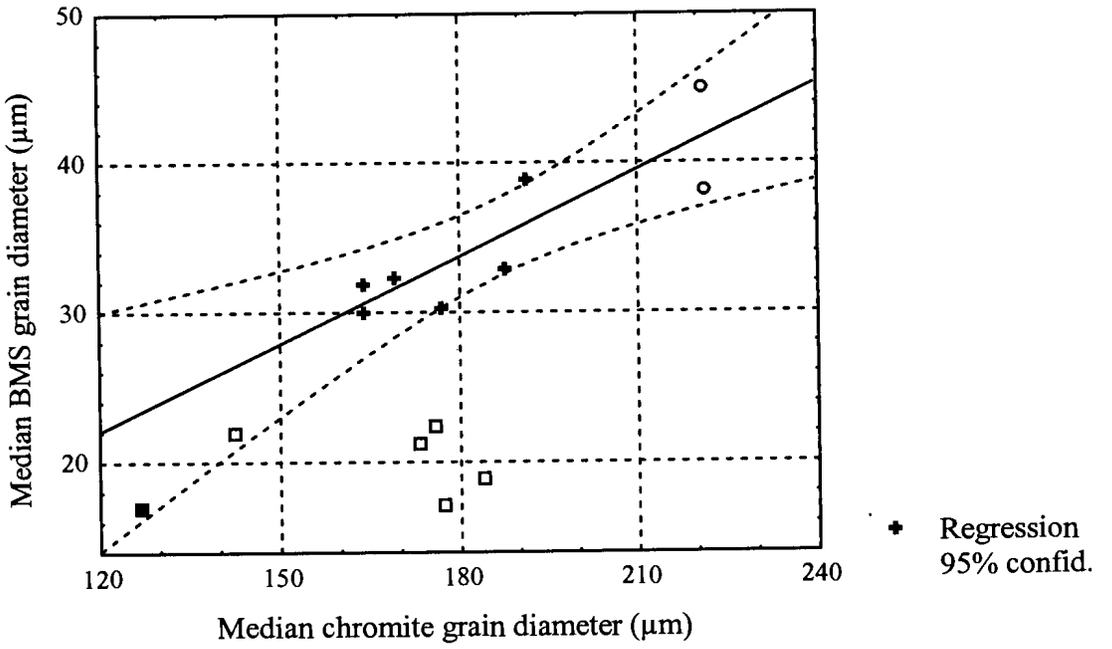

Figure 90 *Relationship between median chromite and base-metal sulphide (BMS) grain diameter. Pearson correlation coefficient r=0.86 for all samples excluding sample A5 and samples from area C. + = samples A1, A2, A3, B1, B2, and B3. □= samples C1, C2, C3, C4 and C5. o = samples A4 and B4. ■ = sample A5.*

A strong linear relationship exists between copper and sulphur (Pearson correlation coefficient r=0.96) (Figure 91). There is also a positive correlation between nickel and sulphur, albeit much weaker (r=0.64) (Figure 92).

A weak positive correlation (r=0.57) (Table 6.2) exists between palladium and sulphur. If two apparent outliers (A2 and A5), are excluded from the analysis, the correlation becomes much stronger (r=0.89) (Figure 93). If the same two outliers are excluded there is also a strong positive correlation between palladium and copper (r=0.90) (Figure 94). It is not clear why samples A2 and A5 do not follow the same trend as the remainder of the samples. After exclusion of two apparent outliers, A2 and B1, there also appear to be a positive correlation between palladium and nickel (r=0.86) (Figure 95). Considering the observation that copper, nickel, sulphur and palladium values for samples from area C are low compared to that in relatively unaltered UG2, these relationships are no surprise.

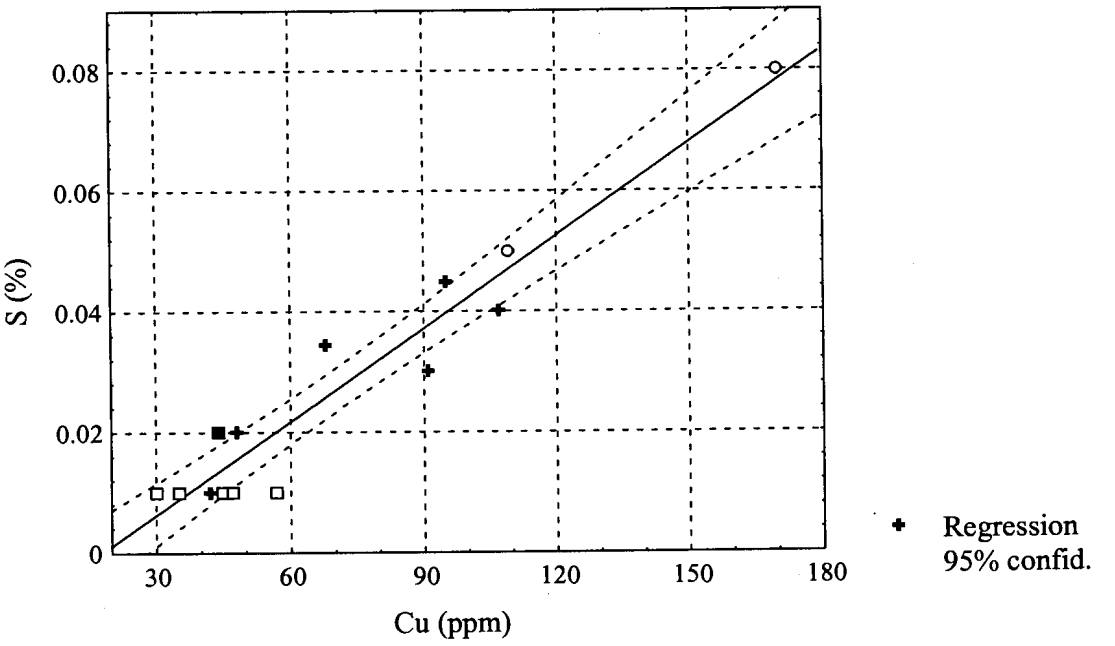

Figure 91 *Relationship between acid soluble copper and sulphur for fourteen samples of UG2 chromitite. Pearson correlation coefficient for all fourteen samples, r=0.96. + = samples A1, A2, A3, B1, B2, and B3. □ = samples C1, C2, C3, C4 and C5. o = samples A4 and B4. ■ = sample A5.*

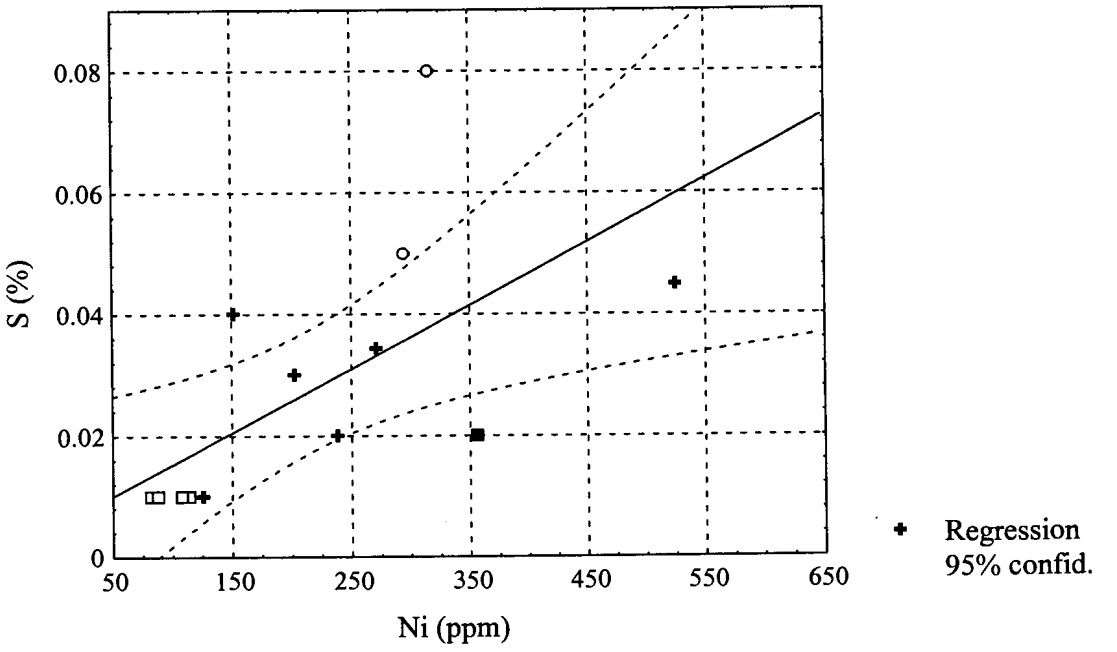

Figure 92 *Relationship between nickel and sulphur for fourteen samples of UG2 chromitite. Pearson correlation coefficient r=0.64. + = samples A1, A2, A3, B1, B2, and B3. □ = samples C1, C2, C3, C4 and C5. o = samples A4 and B4. ■ = sample A5.*

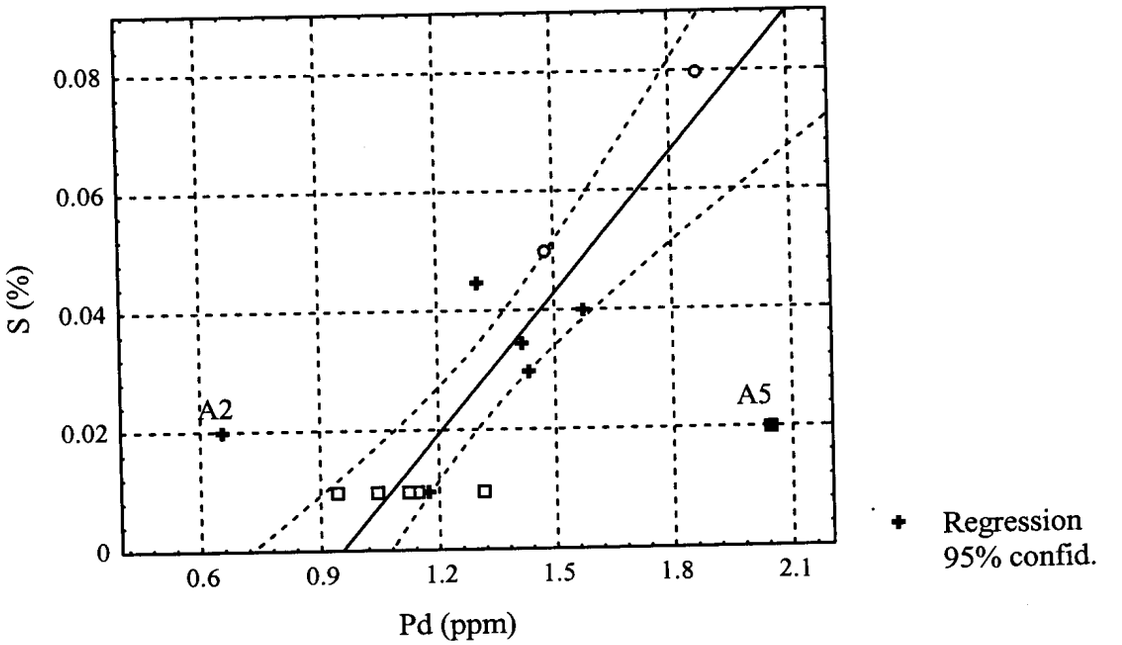

Figure 93 *Relationship between palladium and sulphur for fourteen samples of UG2 chromitite. Pearson correlation coefficient r=0.89 if A2 and A5 are excluded during the calculation of the regression line. + = samples A1, A2, A3, B1, B2, and B3. □ = samples C1, C2, C3, C4 and C5. o = samples A4 and B4. ■ = sample A5.*

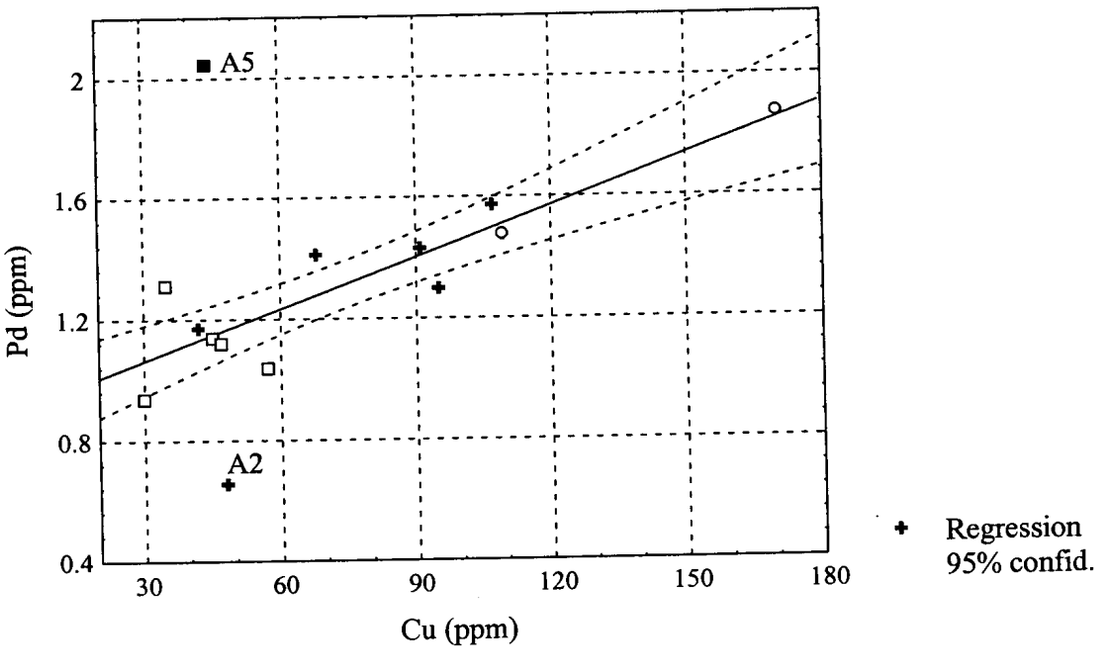

Figure 94 *Relationship between palladium and copper for fourteen samples of UG2 chromitite. Pearson correlation coefficient = 0.90 with outliers A2 and A5 excluded during the calculation of the regression line. + = samples A1, A2, A3, B1, B2, and B3. □ = samples C1, C2, C3, C4 and C5. o = samples A4 and B4. ■ = sample A5.*

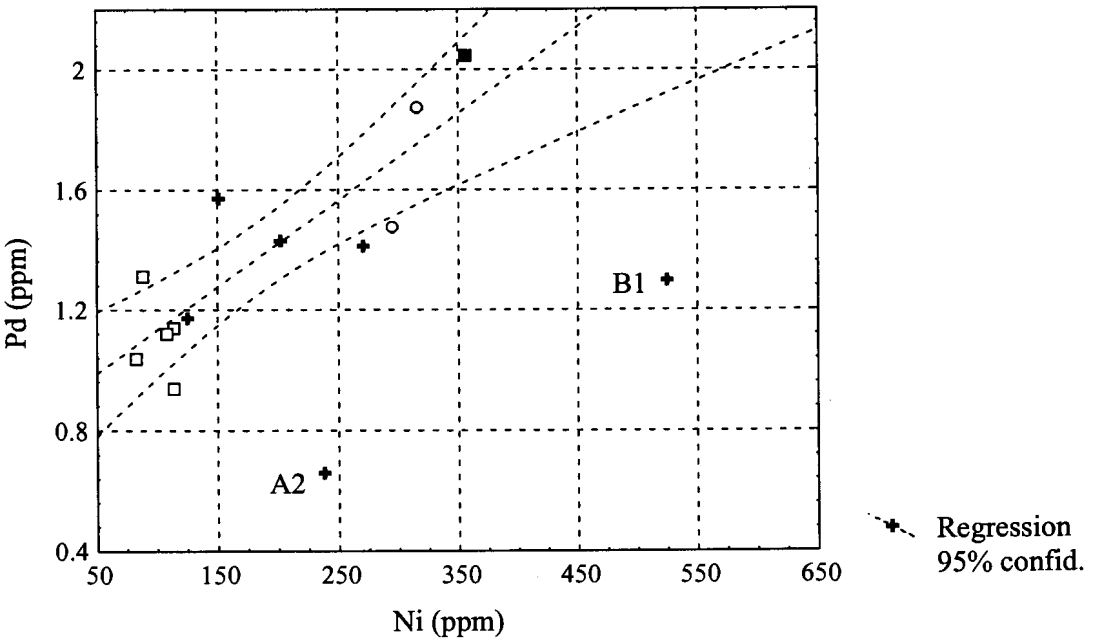

Figure 95 *Relationship between palladium and nickel for fourteen samples of UG2 chromitite. Pearson correlation coefficient = 0.86 with outliers A2 and B1 excluded during calculation of regression line. + = samples A1, A2, A3, B1, B2, and B3. □ = samples C1, C2, C3, C4 and C5. o = samples A4 and B4. ■ = sample A5.*

Platinum and rhodium do not seem to follow the same trend, explaining the weak correlation between platinum and palladium (r=0.55) (Figure 96), and between rhodium and palladium (r=50) (Figure 97). No significant correlation could be found between sulphur and platinum, or sulphur and rhodium. Similarly platinum and rhodium shows no correlation with copper or nickel values.

Platinum and rhodium contents are, however, strongly correlated (r=0.95) (Figure 98). The data also indicate a positive correlation between Cr_2O_3 and platinum (Figure 99) (r=0.75), and between Cr_2O_3 and rhodium (Figure 100) (r=0.68), but no correlation between palladium and Cr_2O_3 (Figure 101) (r=0.06). These relationships could possibly be an indication of the relative immobility of platinum and rhodium, compared to palladium and the base metals, under the conditions prevailing during the formation of the UG2 chromitite.

Note also the positive correlation between TiO_2 and Cr_2O_3 (r=0.74 for all samples). Samples A4, B4 and C1 deviates strongly from the regression line with a much higher TiO_2 content than expected (Figure 102).

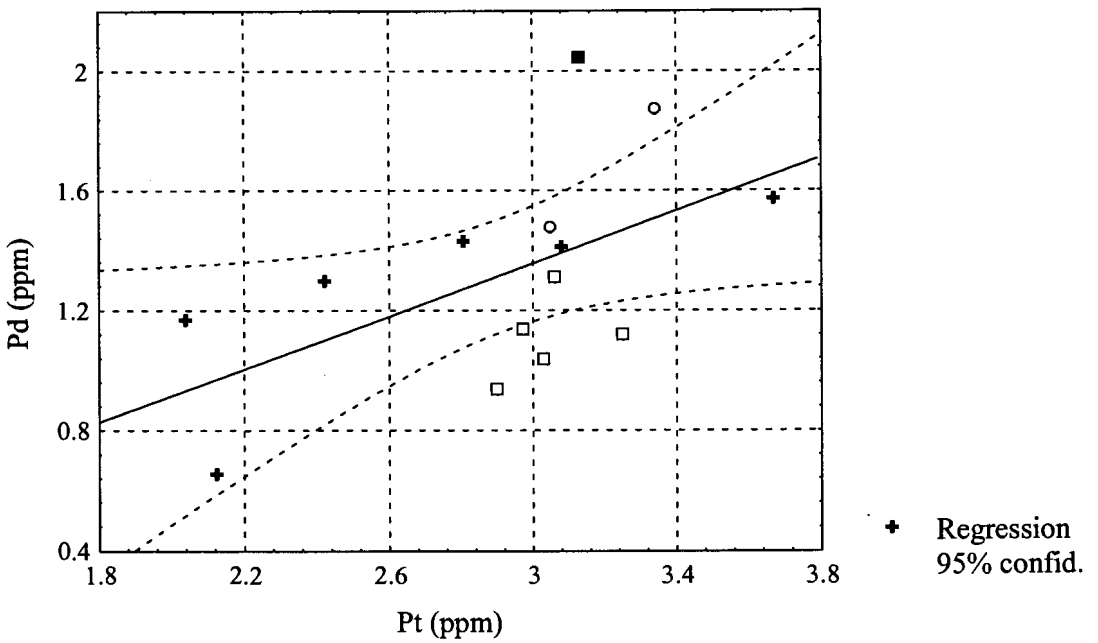

Figure 96 *Relationship between palladium and platinum for fourteen samples of UG2 chromitite. Pearson correlation coefficient r=0.55. + = samples A1, A2, A3, B1, B2, and B3. □ = samples C1, C2, C3, C4 and C5. o = samples A4 and B4. ■ = sample A5.*

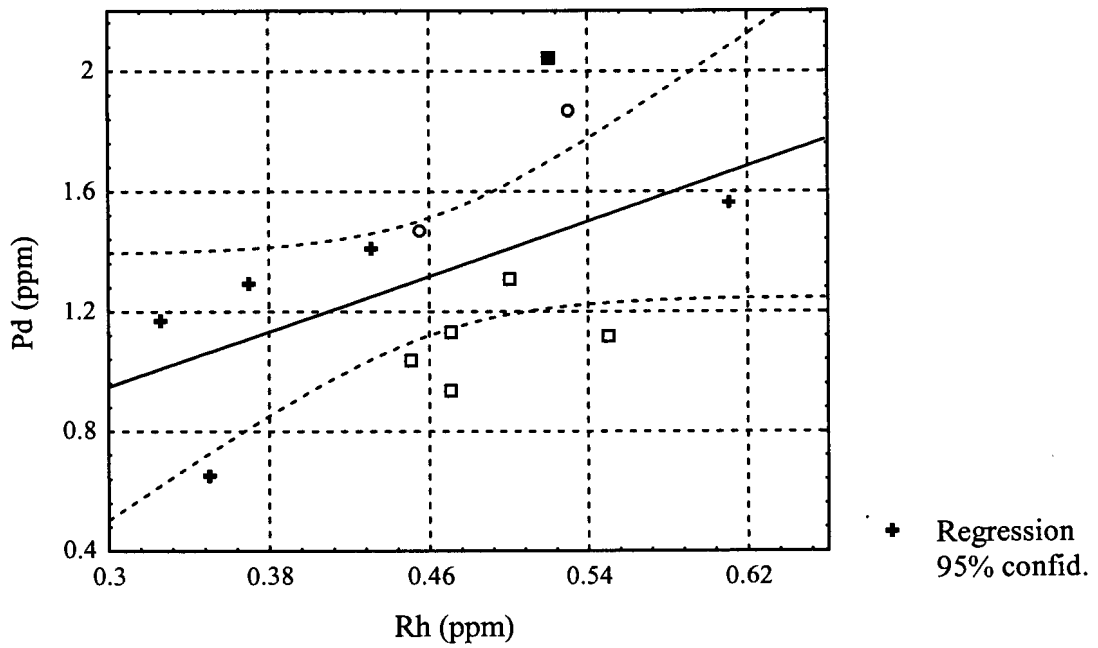

Figure 97 *Relationship between rhodium and palladium for fourteen samples of UG2 chromitite. Pearson correlation coefficient r=0.50. + = samples A1, A2, A3, B1, B2, and B3. □ = samples C1, C2, C3, C4 and C5. o = samples A4 and B4. ■ = sample A5.*

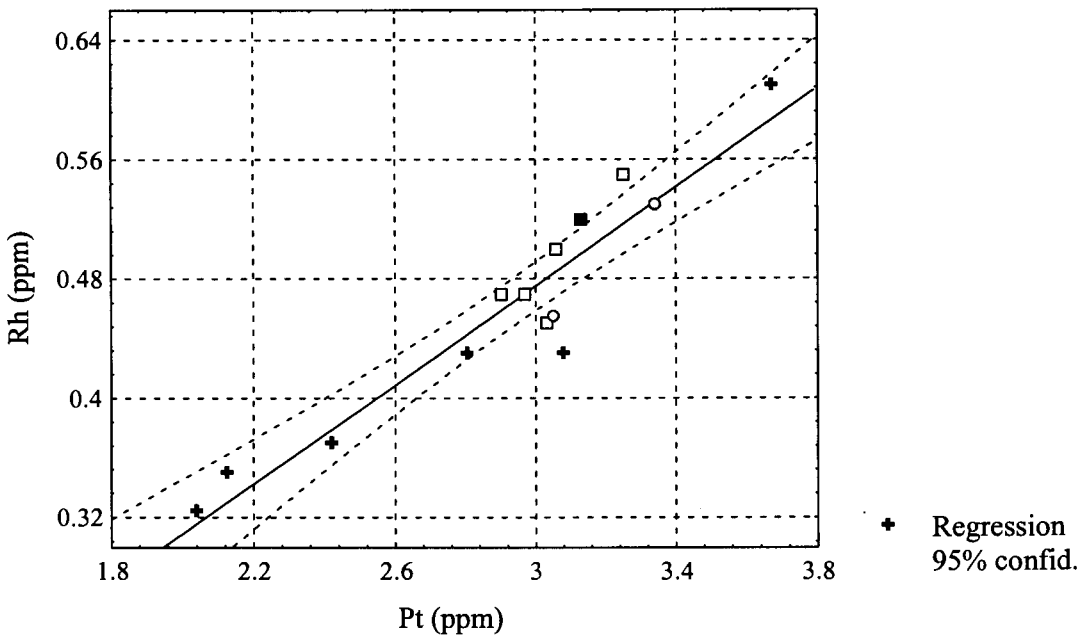

Figure 98 *Relationship between rhodium and platinum for fourteen samples of UG2 chromitite. Pearson correlation coefficient for all fourteen samples, r=0.95. + = samples A1, A2, A3, B1, B2, and B3. □ = samples C1, C2, C3, C4 and C5. o = samples A4 and B4. ■ = sample A5.*

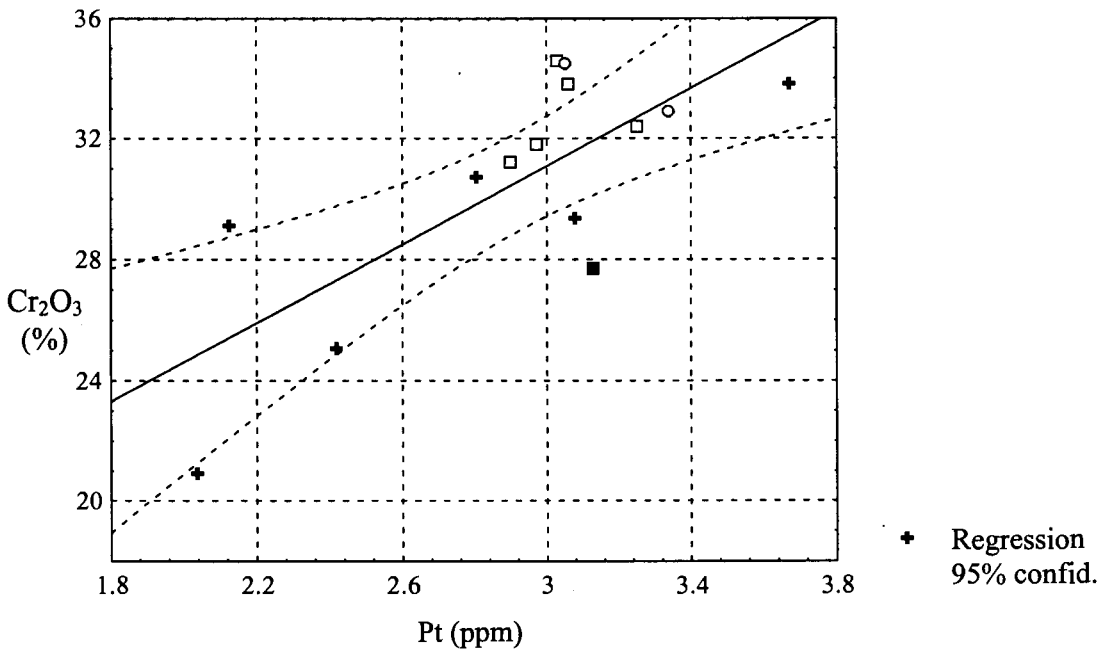

Figure 99 *Relationship between platinum and Cr_2O_3 for fourteen samples of UG2 chromitite. Pearson correlation coefficient r=0.75. + = samples A1, A2, A3, B1, B2, and B3. □ = samples C1, C2, C3, C4 and C5. o = samples A4 and B4. ■ = sample A5.*

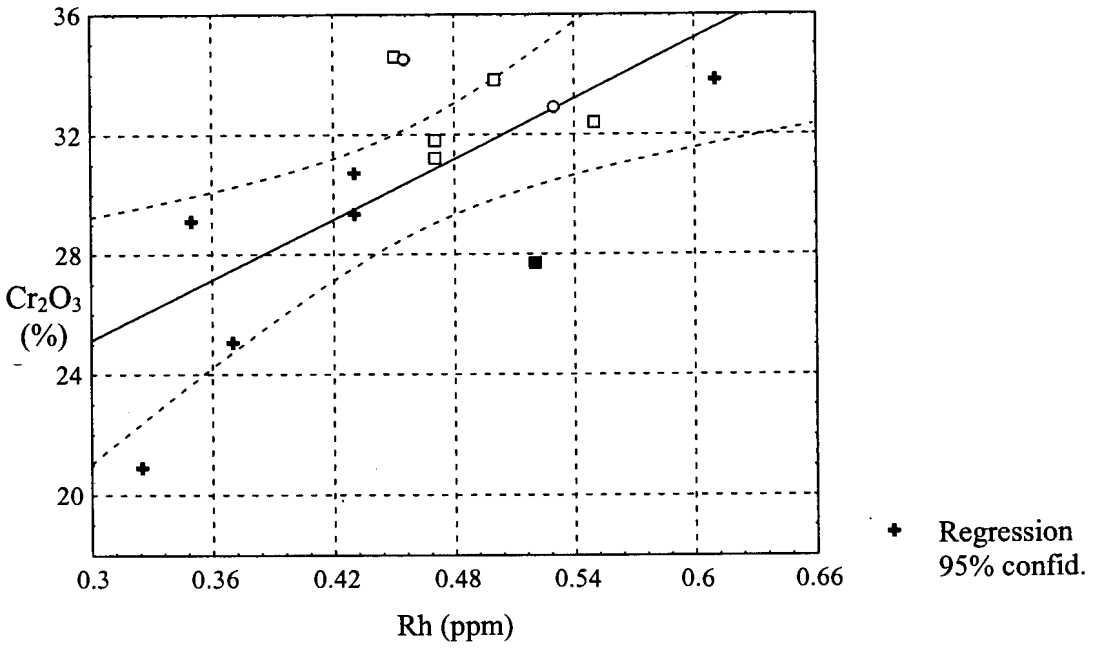

Figure 100 *Relationship between rhodium and Cr_2O_3 for fourteen samples of UG2 chromitite. Pearson correlation coefficient r=0.68. + = samples A1, A2, A3, B1, B2, and B3. □ = samples C1, C2, C3, C4 and C5. o = samples A4 and B4. ■=sample A5.*

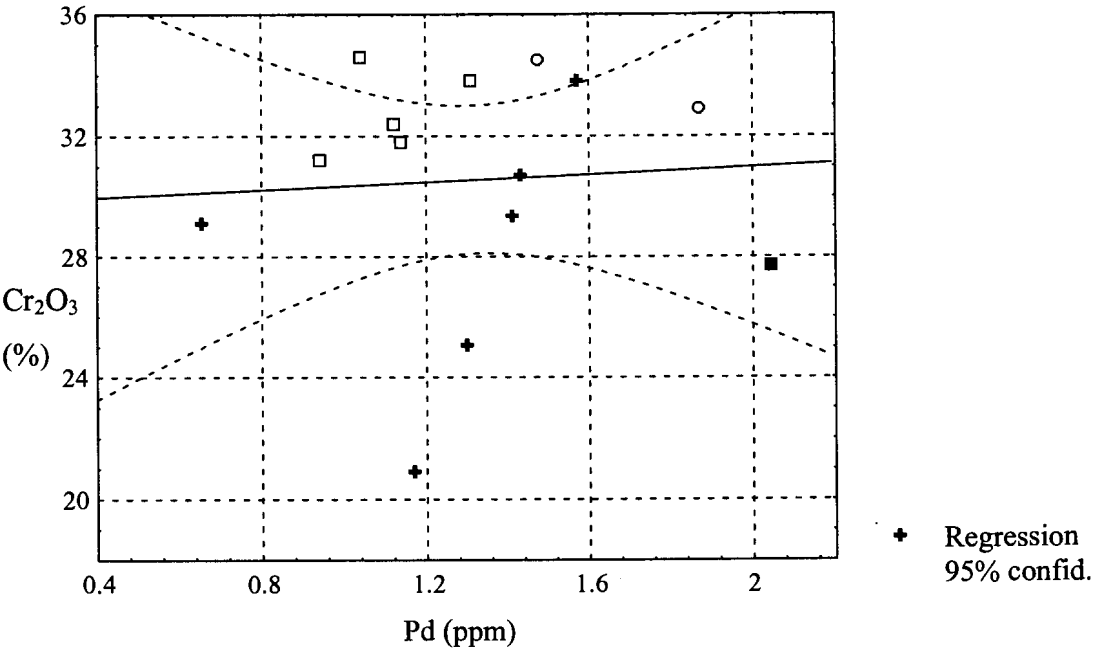

Figure 101 *Relationship between palladium and Cr_2O_3 for fourteen samples of UG2 chromitite. Pearson correlation coefficient r=0.06. + = samples A1, A2, A3, B1, B2, and B3. □ = samples C1, C2, C3, C4 and C5. o = samples A4 and B4. ■=sample A5.*

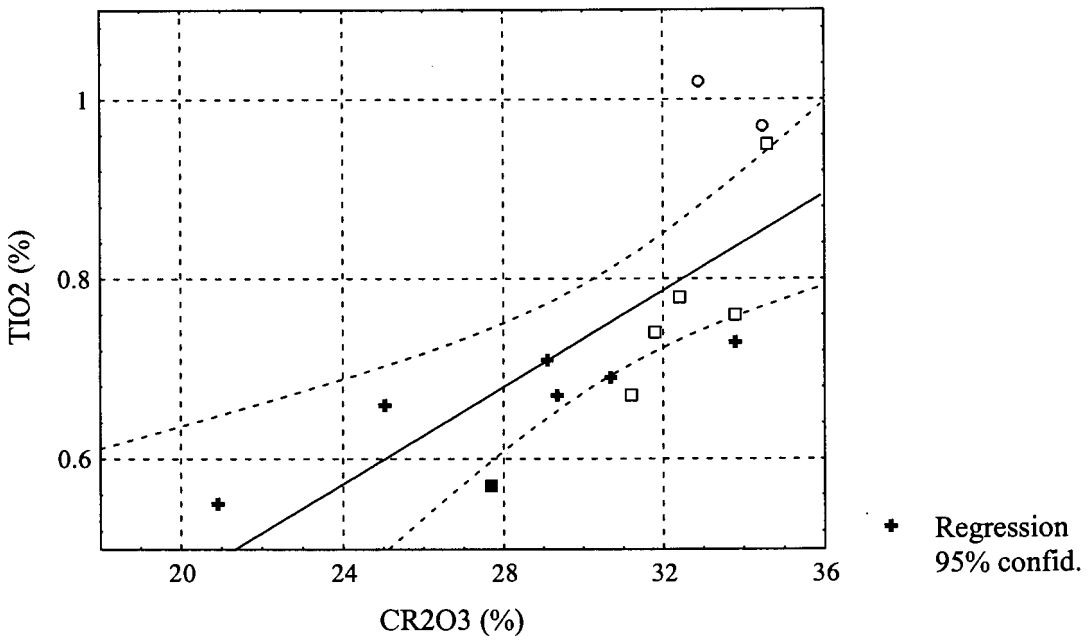

Figure 102 *Relationship between TiO_2 and Cr_2O_3 for fourteen samples of UG2 chromitite. Pearson correlation coefficient r=0.74 for all samples. + = samples A1, A2, A3, B1, B2, and B3. □ = samples C1, C2, C3, C4 and C5. o = samples A4 and B4. ■=sample A5.*

6.2 PGE mass balance calculations

The amounts of platinum, palladium, ruthenium and rhodium represented by the discrete PGE mineral phases found in sample A1 were calculated and are compared with the analytical values in Table 6.3.° Good agreement was found between the calculated and analytical values for platinum. The calculated palladium, rhodium and, to a lesser extent ruthenium values, are significantly lower than the analytical values, implying the presence of these elements in sub-microscopic form in other phases. This is in good agreement with the electron-microprobe analysis results, which indicated that significant amounts of palladium and rhodium are present in base-metal sulphide, particularly pentlandite, while platinum concentration levels are generally below the detection limit of the analysis technique.

° Such a large number of samples need to be searched for an accurate value that this was done only for sample A1.

If it is assumed that all of the acid soluble nickel occurs in pentlandite with the composition $Fe_{4.58}Ni_{4.32}Co_{0.06}S_{8.00}$, a pentlandite content of 0.08 mass per cent is indicated (compared to 0.06 mass per cent indicated by image analysis). If it is further assumed that all of the palladium and rhodium that do not occur in discrete PGE minerals, is present sub-microscopically in pentlandite, then the average palladium and rhodium content of pentlandite would be 755 ±350 ppm and 320 ±150 ppm respectively.* Unfortunately, in the absence of accurate trace element analyses of the base-metal sulphides, there is no way of testing the accuracy of these values.

Paktunc *et al.* (1990) published proton-microprobe and electron-microprobe analyses of pentlandite, chalcopyrite and pyrrhotite from two samples of UG2 chromitite. No PGEs were detected in chalcopyrite or pyrrhotite. In pentlandite, palladium values of 292±8 ppm (proton microprobe) and 342±110 ppm (electron-microprobe) were detected in the one sample, and 56±6 ppm in the other. No rhodium or platinum was recorded. These values are significantly lower than those suggested by the current study, but in the case of palladium at least, do show the same trend.

Electron-, ion- and proton-microprobe analyses of sulphide minerals from many ore deposits indicate that palladium can occur in appreciable amounts (several hundred ppm, and even up to a few per cent) in pentlandite (Genkin *et al.*, 1974; Cabri & LaFlamme, 1979; 1981; Kinloch, 1982; Peyerl, 1983; Cabri *et al.*, 1984; Paktunc *et al.*, 1990; Prendergast, 1990; Cabri, 1992; Czamanske *et al.*, 1992; Ripley & Chryssoulis, 1994; Ballhaus & Ryan, 1995; Weiser *et al.*, 1998). Traces of palladium have also been found in chalcopyrite, pyrrhotite and pyrite (Cabri *et al.*, 1984; Paktunc *et al.*, 1990; Cabri, 1992; Czamanske *et al.*, 1992; Oberthür *et al.*, 1997).

Up to a few hundred ppm rhodium have been measured in pentlandite (Genkin *et al.*, 1974; Peyerl, 1983; Cabri, 1992; Ballhaus & Ryan, 1995; Oberthür *et al.*, 1997; Garuti *et al.*, 1999). All the rhodium in the Merensky Reef is believed to occur as

---

* 90% confidence limits calculated taking into account both the precision associated with the PGE mineral modal analysis and the chemical assay.

solid solution in pentlandite (Kinloch, 1982). Traces of rhodium have been detected in pyrrhotite and pyrite (Oberthür *et al.*, 1997).

Table 6.3 *A comparison of the PGE values in sample A1 calculated from the modal analysis with chemical assay values. These values are based on data collected on 1642 PGE mineral grains found in eighty polished sections.*

Element	***Calculated value (ppm)***	***Absolute error (ppm)***	***Analytical value (ppm)***	***Absolute error (ppm)***
Platinum	3.02	±0.42	3.08	±0.70
Palladium	0.78	±0.19	1.41	±0.30
Rhodium	0.17	±0.06	0.43	±0.06
Ruthenium	0.79	±0.15	1.08	-
Σ(Pt,Pd,Rh)	3.97	±0.55	5.05	±0.23

The only reported occurrence of significant amounts of platinum in sulphides is that by Oberthür and co-workers (1997) who found up to 244 ppm platinum in pyrite. They also found traces of platinum in pyrrhotite and pentlandite.

Experimental work by Makovicky and co-workers (1985) indicated that ruthenium, rhodium and palladium can fully occupy the octahedral position in pentlandites with Fe:Ni ≈ 1:1, with complete solid solution towards PGE-free pentlandite.

In summary, it can be said that results of the current study indicated that rhodium and palladium occur in appreciable amounts in sub-microscopic form in pentlandite. Most of the platinum seems to be present as discrete PGE minerals. Electron-microprobe analysis rarely indicated the presence of sub-microscopic PGEs in chalcopyrite, pyrrhotite, millerite and pyrite. Rare grains of siegenite from area C contain significant amounts of sub-microscopic platinum and rhodium. In general terms, these observations are in agreement with findings by other workers of PGE-bearing ores from the Bushveld Complex and elsewhere.

The likelihood that trace amounts of PGE may also occur sub-microscopically in chromite and silicates was suggested by Peyerl (1983). Experiments by Capobianco and co-workers (1990; 1994) showed large crystal-chemical compatibility for ruthenium and rhodium in spinel. Unfortunately, these experiments were conducted at f_{O_2} levels not applicable to the UG2 chromitite. Hofmeyr (1998), based on SIMS analyses of a sample of UG2 chromitite, subsequently suggested that of the order of 4

per cent of the platinum, 6 per cent of the palladium, 0.4 per cent of the rhodium, and 19 per cent of the iridium, occur in solid solution in chromite.

6.3 The effect of postmagmatic alteration processes on the UG2 chromitite

6.3.1 Relatively unaltered UG2 chromitite

The mineralogical characteristics of samples A1, B1, B2, A2, B3 and A3 is typical of that of normal or undisturbed UG2 chromitite. These samples originated from a variety of environments: samples A2 and B2 represent UG2 chromitite with anorthosite and norite footwall, respectively; samples A1 and B1 were characterised by the presence of pegmatoid footwall, and samples A3 and B3 were collected from the edges of pothole structures. In addition, samples B1 and B3 may also have been exposed to the effects of iron-rich ultrabasic replacement pegmatoid present in the vicinity. Sample A1 appears to be the least altered of the samples. The presence of a notable amount of non-sulphide PGE mineral in sample B1, the increase in chromite grain size in samples B2 and A3, and even in B1, the presence of millerite and pyrite in sample B2, and the presence of varying amounts of secondary silicates in all of these samples, indicate that a variety of postmagmatic processes have left their mark on these samples. However, compared to the samples in the other groups, the degree of alteration is low.

Barnes and Campbell (1988) postulated that during formation of the Merensky Reef, molten sulphide liquid and the fractionated dregs of vapour saturated intercumulus silicate melt were pushed into the residual pore space. This sharing of pore space during the final stages of solidification accounts for the observed association of base-metal sulphide and PGE minerals with phlogopite and other hydrous silicates and an assortment of phases such as quartz, rutile and zircon. Based on the mineralogical evidence presented here, a similar scenario is proposed for the UG2 chromitite.

In the Merensky Reef, rimming of pyrrhotite by pentlandite and chalcopyrite have been interpreted as resulting from fractional crystallisation (Kingston, 1966, Vermaak & Hendriks, 1976; Mostert *et al.*, 1982; Ballhaus & Stumpfl, 1986). Similar textures were observed in the UG2 chromitite. During magmatic fractionation the sulphide liquid solidifies over at temperature interval, starting with monosulphide solid

solution at ~1050°C, and culminating in the solidification of copper-rich residual liquid at ~850°C (Craig & Kullerud, 1969). During cooling, the monosulphide solid solution field narrows to form pentlandite in a pyrrhotite-dominated matrix, which becomes stable at ~610 °C (Kullerud *et al.*, 1969).

The present pentlandite-rich assemblage in the UG2 does not represent the primary magmatic sulphide assemblage. Sulphide assemblages associated with the chromitite layers of the Bushveld Complex are enriched in PGEs, nickel and copper compared to typical magmatic sulphide assemblages (McLaren & de Villiers, 1982; Gain, 1985; Von Gruenewaldt *et al.*, 1986; Naldrett & Lehmann, 1987; Naldrett, 1989). Gain (1985) and Von Gruenewaldt *et al.* (1986) suggested that the original mass of these sulphides has been greatly reduced by the removal of iron and sulphur, with the consequent enrichment of other metals. Naldrett (1989) calculated that, assuming that all the original copper and nickel remain, approximately one half to two thirds of the original sulphide present has been lost.

Naldrett and Lehmann (1987) and Naldrett *et al.* (1989) demonstrated the feasibility of a process whereby iron may be lost from magmatic sulphides to fill vacancies in non-stoichiometric chromite crystallizing from basaltic magma. Release of sulphur resulting from the dissociation of magmatic pyrrhotite may lead to the formation of pyrite from pyrrhotite. Once the most sulphur-rich assemblage possible under the prevailing conditions has formed, further extraction of iron will lead to a bulk loss of sulphur (Merkle, 1992).

Most of the PGEs were probably scavenged by the sulphide melt. Experimental work (Distler *et al.*, 1977; Fleet *et al.*, 1993; Li *et al*, 1996) indicates that during cooling, rhodium and ruthenium will preferentially partition into the monosulphide solid solution, with palladium favouring the copper-rich residual melt. Platinum forms alloy phases at low f_{S2}, and follows palladium into the sulphide liquid at high f_{S2}.

At elevated temperatures the base-metal sulphides, especially pyrrhotite and pentlandite, can accommodate significant amounts of PGEs in solid solution (Distler *et al.*, 1977; Makovicky *et al.*, 1986; Ballhaus & Ulmer, 1995), most of which will be expelled on cooling to form discrete PGE minerals. Chalcopyrite appears to be barren of PGEs, even at elevated temperatures. This explains the observed association of

most of the PGE minerals with base-metal sulphides, occurring either at sulphide grain boundaries with silicates or chromite, at sulphide-sulphide grain boundaries, or as inclusions in sulphide. Ballhaus and Ryan (1995), and Ballhaus and Ulmer (1995) suggested that the association of discrete PGE minerals with base-metal sulphides reflect equilibration to temperatures below 100 °C.

The small proportion (~5 per cent) of PGE minerals that are present as inclusions in chromite, almost exclusively laurite, possibly formed during cooling, as a result of exsolution of PGEs in solid solution in chromite (Capobianco *et al.*, 1994).

6.3.2 Sintered UG2 chromitite - the effect of Fe-rich ultrabasic replacement pegmatoid

Late-stage hydrothermal fluids, rich in iron and titanium, sporadically altered the chemistry and mineral assemblage of the UG2 chromitite (Viljoen & Scoon, 1985; Grimbeek, 1995). The UG2 chromitite layer may have acted as a physical barrier resulting in sintering of chromite at the bottom of the layer, together with changes in the spinel composition, and the formation of ilmenite and magnetite.

The enlargement and change in the composition of chromite grains, the presence of elevated amounts of TiO_2, and the PGE mineral assemblages dominated by Pt-Fe alloys (often rhodium- or palladium-bearing), laurite, and to a lesser extent PGE-Bi-Te compounds, and other non-sulphide PGE minerals in sintered samples A4 and B4 are typical of UG2 chromitite associated with replacement pegmatoid (McLaren & De Villiers, 1982; Peyerl, 1982; Viljoen & Scoon, 1985; Grimbeek, 1995). Samples B1 and B3 also appear to have been affected by replacement pegmatoid, albeit to a lower degree. The formation of such PGE mineral assemblages have been attributed to higher f_{O2}, possibly as a result of increased volatile activity resulting in lower f_{S2} (Peyerl, 1982; Kinloch, 1982; McLaren & de Villiers, 1982; Evstigneeva *et al.*, 1995).

Based on reports in the literature (McLaren & de Villiers, 1982; Peyerl, 1982; Viljoen & Scoon, 1985; Gain, 1985; Viljoen *et al.*, 1986a, b; Leeb-du-Toit, 1986; Farquhar, 1986; Hofmeyr & Adair, 1993; Grimbeek, 1995; Van der Merwe *et al.*, 1998), the base-metal sulphide mineralogy of samples associated with dunite pipes and iron-rich ultrabasic replacement pegmatoid ranges from being similar to that of relatively unaltered UG2 chromitite, to more complex sulphide assemblages containing minerals

such as chalcocite, bornite, violarite, mooihoekite, haycockite, digenite, native copper, cubanite, mackinawite, heazlewoodite and millerite. These variations can be attributed to variable degrees of metasomatic effects from the replacement pegmatoid. In the samples investigated, the base-metal sulphide mineralogy is, aside from a slight increase in grain size, similar to that of relatively unaltered UG2 chromitite.

6.3.3 Millerite-bearing UG2 chromitite – the effect of low-temperature hydrothermal alteration

The UG2 chromitite from area C appears to have been subjected to a regional low-temperature hydrothermal alteration, not directly related to any small-scale geological disturbance. The samples displaying the highest degree of alteration often have abundant hydrothermal veins containing minerals such as calcite, quartz, prehnite, and chlorite.

The replacement of primary silicates by mineral assemblages containing albite, quartz, pumpellyite, epidote, chlorite, prehnite, sphene and talc is similar to that described by Schiffries and Skinner (1987) and Schiffries and Rye (1990) resulting from the interaction of hydrothermal fluids with wallrock at temperatures below about 600°C.

The sulphide assemblage found in these samples, chalcopyrite, millerite, pyrite and subsidiary siegenite, could not have exsolved from a magmatic sulphide melt (Kullerud *et al.*, 1969; Craig & Kullerud, 1969). Merkle (1992) suggested that the corrosion of base-metal sulphides by hydrothermal fluids leads, in places, to iron and sulphur loss, in addition to the losses as a result of sulphide-chromite equilibration. This could lead to the formation of such low temperature, high f_{S2} sulphide assemblages. Based on the lack of mineral textures suggesting replacement of pentlandite by millerite, and phase relations in the Ni-Fe-S and Ni-S systems (Kullerud & Yund, 1962; Vaughan & Craig, 1978), Verryn and Merkle (1994) suggested that millerite in such samples formed directly from hydrothermal fluids at temperatures below 379°C. Reduction of the volume of base-metal sulphides through such losses results in the PGE minerals (previously associated with base-metal sulphides) becoming isolated in hydrous silicates, filling the spaces previously occupied by sulphides.

PGE mineral assemblages in these areas are similar to those occurring in normal UG2, but with noticeably lower concentrations of cooperite, and a concomitant increase in malanite, braggite and vysotskite, possibly indicating lower temperature of formation under conditions of higher f_{S2} (Knacke *et al.,* 1991). The absence of Pt-Fe alloys, especially in sintered sample C1, also points to conditions of increased sulphur fugacity.

It is proposed that the relatively high modal proportions of palladium- and rhodium-bearing sulphides compared to PGE mineral assemblages from normal UG2 is a consequence of the paucity of pentlandite in these samples. Since pentlandite contains small amounts of palladium and rhodium in solid solution, a reduction in the amount of pentlandite may lead to a higher proportion of palladium- and rhodium-bearing PGE minerals.

Many researchers have reported the relative mobility of palladium during surface weathering (Fuchs & Rose, 1974; McCallum *et al.,* 1976; Prichard & Lord, 1994; Hey, 1999). Cousins and Kinloch (1976) speculated that during weathering, nickel and palladium are preferentially leached out of braggite, resulting in a phase with a chemical composition corresponding to that of cooperite, and the structure and optical properties of braggite. A similar process, operating under hydrothermal conditions, may account for zoned Pt-Pd-Ni-sulphide grains in UG2 chromitite (Merkle & Verryn, in preparation). This, together with corroded sulphide textures, may be an indication that the relatively low acid soluble nickel, copper, sulphur and palladium values characterising these samples are the result of secondary processes rather than a primary feature of the UG2 chromitite in this area. Platinum and rhodium values do not seem to have been affected by these processes indicating the relative immobility of these elements.

Further investigation into the significance of baddeleyite — Zr-Ti oxide —rutile assemblages in association with late- to post-magmatic phases, may shed some more light on the conditions prevailing during ore genesis. Similar assemblages have been reported by Merkle (1992) in Middle Group chromitite, and by Cabella and co-workers (1997) in ophiolitic chrome spinel from Italy.

6.3.4 Cataclastic UG2 chromitite – the effect of faulting

Three samples were taken from fault zones, sample A5, B5 and C1. Sample A5 is, however, the only sample displaying extensive cataclasis. The formation of massive chromitite from faulted areas have also been reported by Kupferbürger *et al.* (1937) and Worst (1986), who reported that the formation of this type of ore appears to be a very localised feature, the texture again becoming friable within centimetres.

The presence of fractures in faulted areas makes the UG2 chromitite layer more accessible to circulating fluids. Interaction of these fluids with primary silicate minerals causes the formation of hydrous silicates, quartz and calcite, cementing fractured chromite grains. The PGE mineral assemblage is characterised by the presence of significant amounts of non-sulphide minerals such as Pt-Fe alloy and PGE sulpharsenides which can also be attributed to the effects of fluids at intermediate to high temperatures.

6.3.3 Effect of pothole structures

Samples B3, A3, and C1 were all taken from the edges of pothole structures. The mineralogical properties of C1 were largely determined by the low temperature regional hydrothermal alteration affecting all the samples from area C. It is noteworthy that these three samples are all characterised by an enlargement in chromite grain size, and in the case of C1, elevated TiO_2 contents, but, in the case of sample B3, this can also be attributed to the presence of iron-rich ultrabasic replacement pegmatoid. It is concluded that although all three samples show evidence of secondary alteration, it is unclear whether this is related to their proximity to pothole structures.

6.4 Flotation behaviour of different types of UG2 chromitite

The flotation characteristics of the different samples are graphically compared in Figure 103 (see also Table 6.1) and vary depending on the type of UG2 chromitite. For relatively unaltered UG2 chromitite and samples from area C, the flotation characteristics for the PGEs appear to be very similar, with between 63 and 80 per cent fast-floating PGE, 15 to 26 per cent slow-floating PGE and less than 10 per cent non-floating PGE. Samples of sintered UG2 chromitite are characterised by slightly

less fast-floating PGE (57 to 60 per cent), a higher proportion of slow-floating PGE (34 to 38) and about 6 per cent non-floating PGE. Cataclastic UG2 displayed the poorest flotation characteristics with only 40 per cent fast-floating PGE+Au, 29 per cent slow-floating PGE+Au and 32% non-floating PGE+Au. The rate of flotation for the fast- and slow-floating PGE+Au fractions are more difficult to interpret as these values seem to be more erratic.

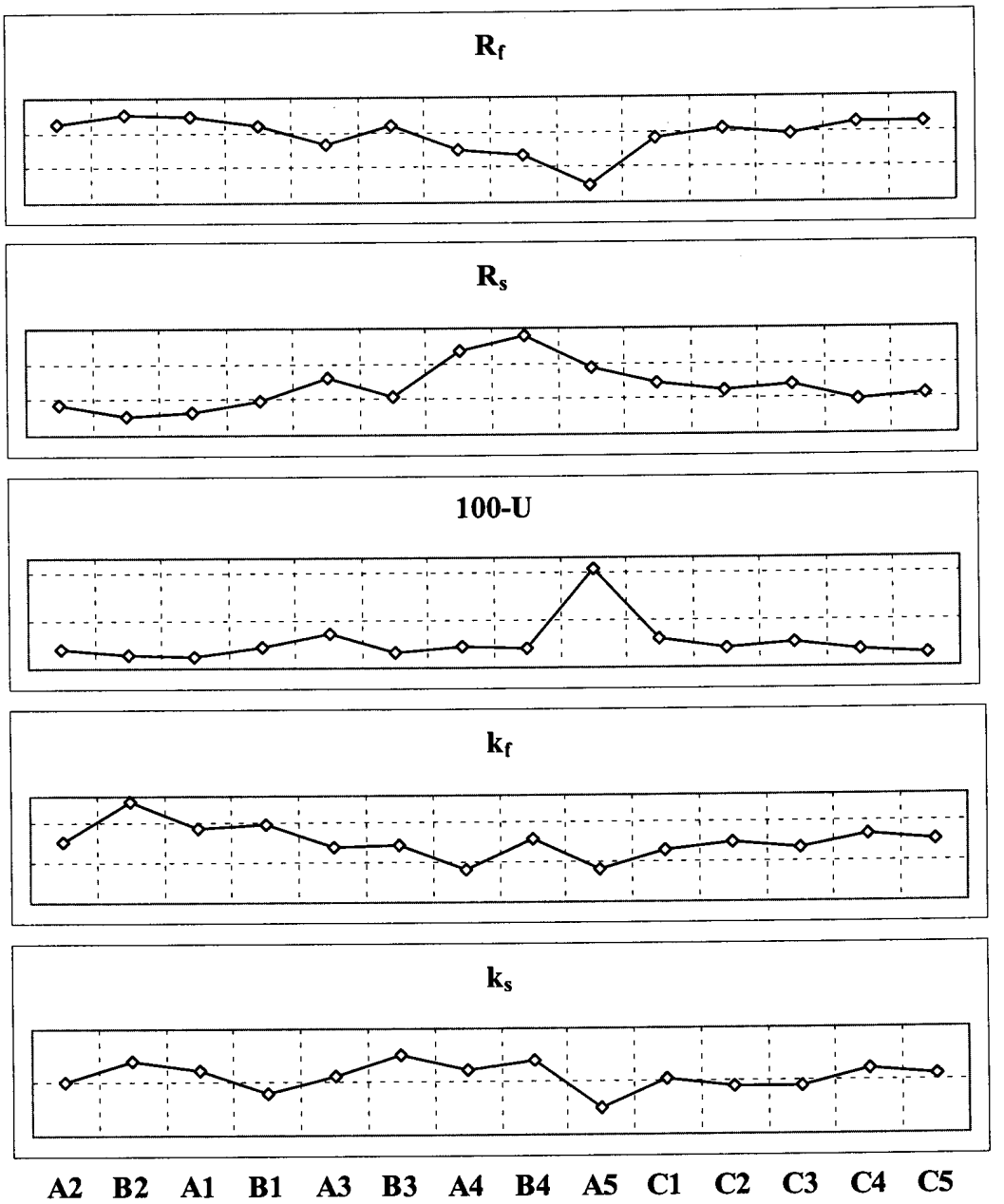

Figure 103 *Comparison of the flotation characteristics of fourteen samples of UG2 chromitite.*

6.5 Interpretation of milling and flotation results

6.5.1 Factors affecting milling time

All of the samples, except for the sample of cataclastic UG2 (A5), were relatively friable, appearing to break along grain boundaries and fractures during the initial stages of size reduction. Further milling resulted in random breakage of mineral grains.

De Waal (1972) concluded that the friability of the chromitites from the Bushveld Complex is controlled by the degree of poikilitic intergrowth of gangue with chromite, or where the gangue fraction is very small, by the degree of annealing of chromite grains. Similar factors probably also determine the response of the sample to comminution, especially during the early stages of size reduction.

Sample A5 was reduced to 80% <75µm in less than forty minutes, with the remainder of the samples requiring between sixty and one hundred and twenty minutes to achieve the same degree of size reduction. The reason for this is probably related to the fact that the chromite and primary silicate grains in this sample had already been broken during cataclasis. Some fracturing of chromite, a difficult parameter to quantify, is present in all the samples, and probably affected milling time to some extent.

Although annealing of chromite grains was observed in some of the samples (especially A4 and B4), it does not appear to have played much of a role during size reduction, possibly because the degree of sintering of chromite grains in these samples is relatively low compared to that of some samples described in the literature (*cf.* Grimbeek, 1995). No correlation was found between the time taken to reduce the samples to 80% <75µm, and chromite grain-size prior to milling, or amount of chromite in the samples (Table 6.4 and Figures 104 and 105).

What is considered more significant, is the fact that the one sample displaying virtually no alteration of plagioclase and orthopyroxene, i.e. A1, required almost twice as much milling time as samples C1 and C3, which, apart from sample A5, were characterised by the highest degree of alteration of the primary silicates. The ease of milling of these samples probably depends largely on the type and degree of silicate

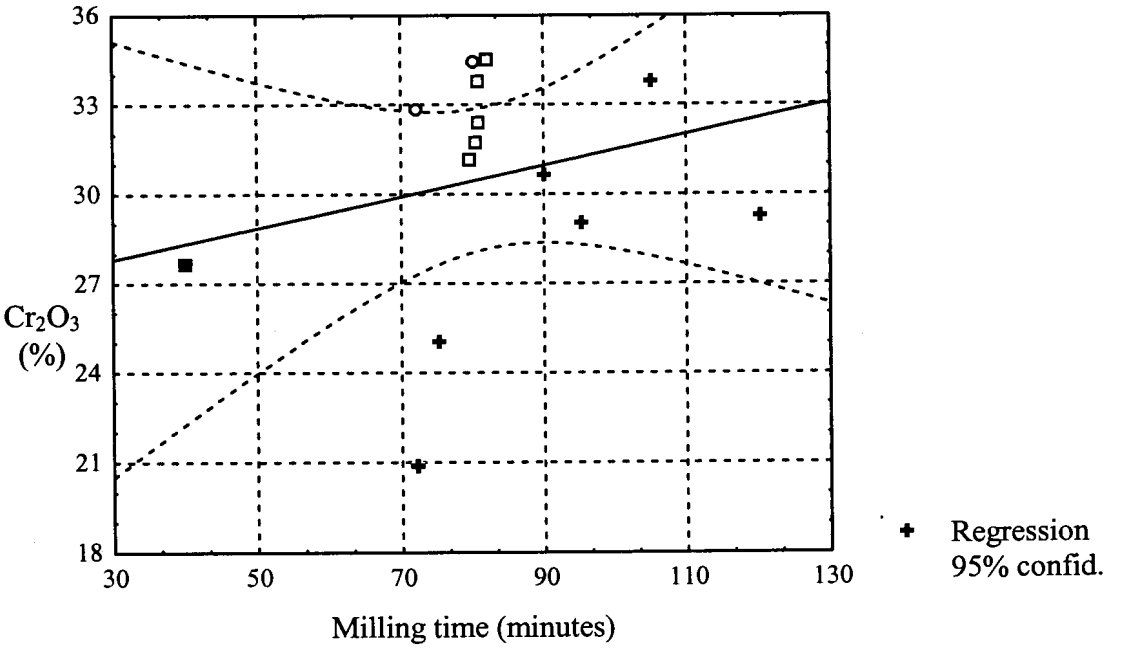

Figure 104 *Relationship between Cr_2O_3 content and time to reduce to 80%<75µm in fourteen UG2 chromitite samples. Pearson correlation coefficient for all fourteen samples, r=0.25. + = samples A1, A2, A3, B1, B2, and B3. □ = samples C1, C2, C3, C4 and C5. o = samples A4 and B4. ■ = sample A5.*

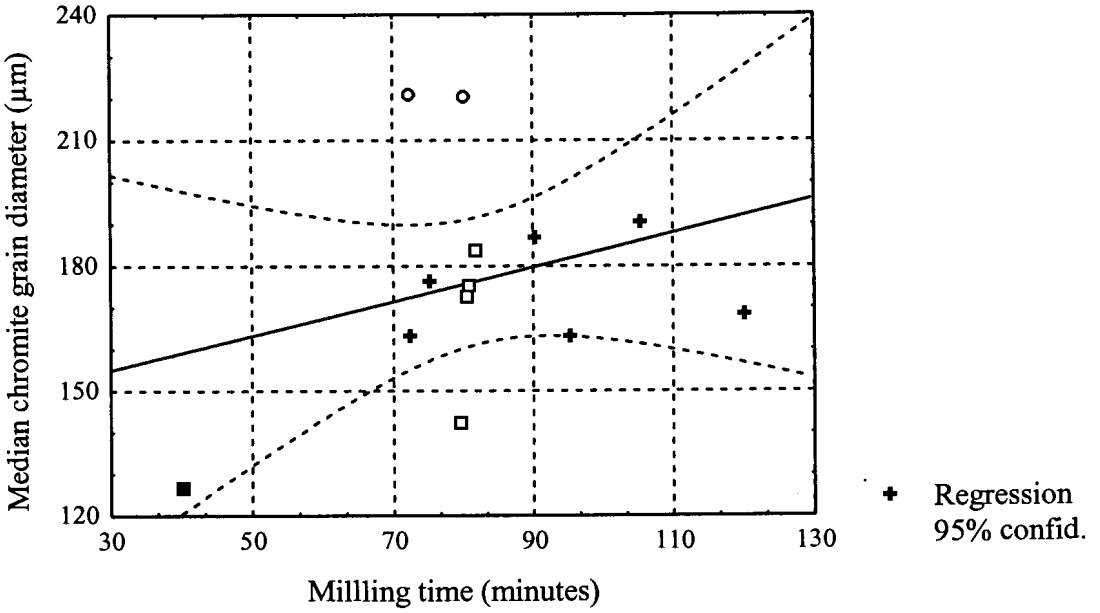

Figure 105 *Relationship between chromite grain size (median equivalent circle diameter) and time to reduce to 80%<75µm in fourteen UG2 chromitite samples. Pearson correlation coefficient, r=-0.26, for all fourteen samples. + = samples A1, A2, A3, B1, B2, and B3. □ = samples C1, C2, C3, C4 and C5. o = samples A4 and B4. ■ = sample A5.*

Table 6.4 *Pearson correlation matrix for time in minutes to mill to 80%<75µm (milltime), Cr_2O_3 content of the feed sample, chromite median grain diameter (in µm) prior to milling (chr1), chromite median grain diameter (in µm) after milling (chr2), silicate median grain diameter (in µm) after milling (sil2), % chromite recovery after 1 minute (chrrec1), % chromite recovery after 20 minutes (chrrec2), % silicate recovery after 1 minute (silrec1), % silicate recovery after 20 minutes (silrec2). Marked correlations (boldface) are significant at p<0.05.*

	Milltime	**Cr_2O_3**	**Chr1**	**Chr2**	**Sil2**	**Chrrec1**	**Chrrec2**	**Silrec1**	**Silrec2**
Milltime	1.00	0.25	-0.26	0.51	0.48	0.50	0.04	0.20	-0.20
Cr_2O_3	0.25	1.00	**0.55**	0.03	-0.18	-0.25	0.08	0.17	0.54
Chr1	-0.26	**0.55**	1.00	-0.48	**-0.60**	-0.06	0.41	-0.25	0.06
Chr2	0.51	0.03	-0.48	1.00	**0.86**	-0.21	**-0.56**	0.20	0.10
Sil2	0.48	-0.18	**-0.60**	**0.86**	1.00	-0.09	-0.48	0.08	-0.13
Chrrec1	0.50	-0.25	-0.06	-0.21	-0.09	1.00	0.49	0.10	**-0.68**
Chrrec2	0.04	0.08	0.41	-0.56	-0.48	0.49	1.00	-0.38	-0.21
Silrec1	0.20	0.17	-0.25	0.20	0.08	0.10	-0.38	1.00	0.46
Silrec1	-0.20	0.54	0.06	0.10	-0.13	**-0.68**	-0.21	0.46	1.00

alteration, with intensely altered samples (e.g. C1 and C3) being fairly friable, and requiring a relative short milling time. In comparison, sample A1 shows hardly any indication of alteration of the silicates, hence the extended milling time required.

6.5.2 Mechanisms affecting gangue recovery

The presence of gangue minerals in flotation concentrates is undesirable, as it affects both concentrate grades and recovery negatively. For the samples under investigation, the flotation concentrates were produced by rougher flotation without any cleaning stages, hence the low grades. However, it is worthwhile examining the flotation behaviour of the gangue minerals, in as far as it does shed some light on the behaviour of composite mineral particles during flotation.

Chromite recovery

Chromite grains in the flotation concentrates are fine-grained and liberated. Statistical analysis indicates a negative correlation between chromite grain size in the milled feed sample and chromite recovery after twenty minutes flotation (Table 6.4 and Figure 106). The recovery of fine-grained, liberated chromite grains, is an indication that these grains reported to the flotation concentrates as a result of entrainment rather than flotation.

True flotation occurs when hydrophobic mineral particles attach to air bubbles in an aerated, agitated pulp. The mineralised bubbles rise till they reach the top of the froth and are scraped off. This is, however, not the only mechanism responsible for the presence of mineral grains in flotation concentrates. Entrainment occurs when fine-grained material suspended in inter-bubble water is recovered with the froth. The rate of gangue mineral recovery by entrainment is dependent on the particle size of the gangue minerals, with finer gangue particles entrained more readily than coarse gangue particles (Trahar, 1981; Subrahmanyam & Forssberg, 1990; Kirjavainen, 1992; 1996).

Warren (1985) suggested that recovery due to entrainment increases linearly with water recovery. By relating water recovery to chromite recovery, Marais (1989) determined that entrainment is responsible for most of the chromite recovered during laboratory rate flotation tests of UG2 ore. It should be noted though, that recent work

by Wesseldijk and co-workers (1999), indicated that under certain conditions chromite may be activated by the reagent suite used for the flotation of UG2 ore, rendering it hydrophobic and amenable to true flotation.

Gottlieb & Adair (1991) sited rimming of chromite grains by talc as one of the reasons for chromite reporting to flotation concentrates. No evidence was found that this mechanism of chromite recovery played a role during flotation of the samples under investigation.

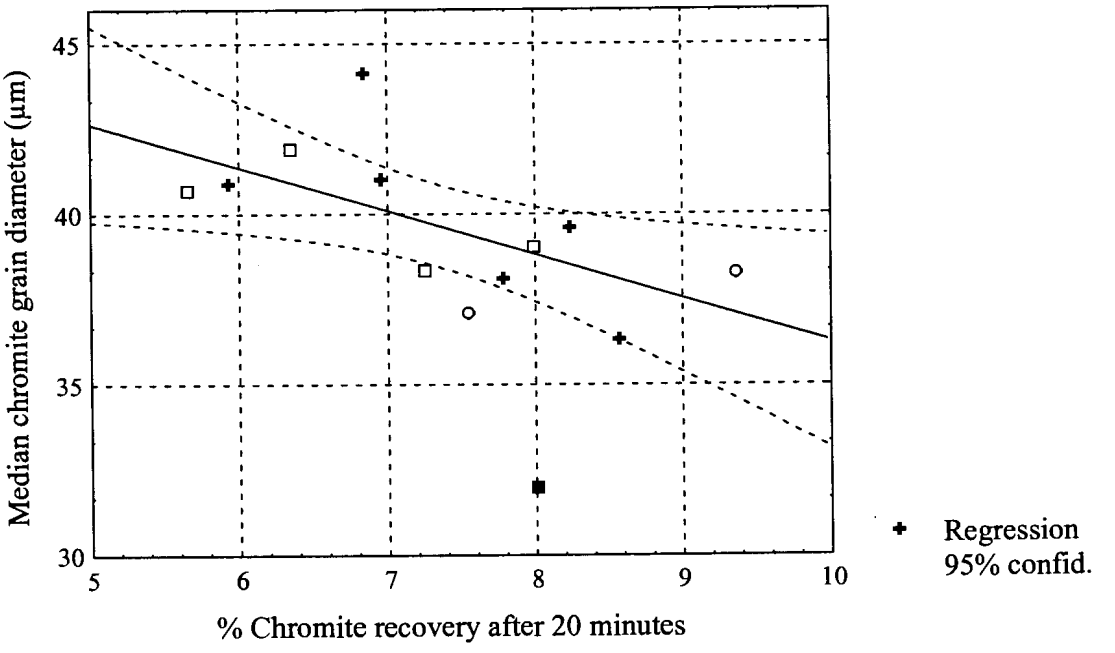

Figure 106 *% chromite recovery after 20 minutes flotation versus median chromite diameter in milled feed samples. Pearson correlation coefficient, r=-0.56 for all samples except A5. + = samples A1, A2, A3, B1, B2, and B3. □ = samples C1, C2, C3, C4 and C5. o = samples A4 and B4. ■ = sample A5.*

Silicate recovery

Entrainment probably also plays a key role in the presence of silicate minerals in flotation concentrates. Although most of the silicates in the flotation concentrates are fine-grained, no correlation was found between silicate particle size and silicate recovery (Table 6.4). This is an indication that factors other than size may affect silicate behaviour during flotation. Because of their soft platy habit, minerals belonging to the phyllosilicate group (chlorite, serpentine, talc, phlogopite, prehnite)

tend to form fines during comminution. Kirjavainen (1992; 1996) found that apart from pulp density and water recovery, which is determined by operational factors, particle mass and shape also affects the probability of entrainment of fine particles. Fine-grained, flaky minerals with low mass have the highest probability of being entrained.

Some of the liberated silicates in the flotation concentrates were, however, probably recovered by true flotation. A mineral surface will be hydrophobic if that surface was created without breakage of interatomic bonds other than residual van der Waals bonds. For that reason, talc is naturally flotable (Gaudin, 1957; Zheng & Lin, 1994). This accounts for the higher observed recovery of Fe-Mg silicates in the more altered samples and the high total silicate recoveries for samples from area C. As a result of the floatability of talc, not only talc was recovered, but also orthopyroxene attached to it. Although the flotation reagent suite included talc depressant, the dose was clearly not sufficient to effect complete depression of talc. Complete depression of talc may not be all that desirable, as it could lead to base-metal and PGE losses, due to suppression of both partly liberated sulphide and PGE mineral grains, and of liberated grains coated with talc slimes.

6.5.3 Base-metal sulphide and PGE mineral liberation

Base-metal sulphide liberation

During milling, base-metal sulphide grains occurring at chromite-silicate grain boundaries can be expected to be liberated more readily compared to those occurring as inclusions in silicate or chromite. Base-metal sulphide liberation may therefore, to a certain extent, be predicted from the amount of base-metal sulphide occurring as liberated grains and at chromite-silicate grain boundaries in the crushed feed (Table 5.1L). A comparison between this predicted liberation, and the measured amount of liberated base-metal sulphide in the milled feeds, indicates that a correlation does indeed exist ($r=0.62$, $p=0.019$) (Figure 107). The measured apparent degree of liberation is higher than predicted liberation in all but two samples, C1 and C5. Exclusion of these two outliers improves the correlation significantly ($r=0.81$, $p=0.001$).

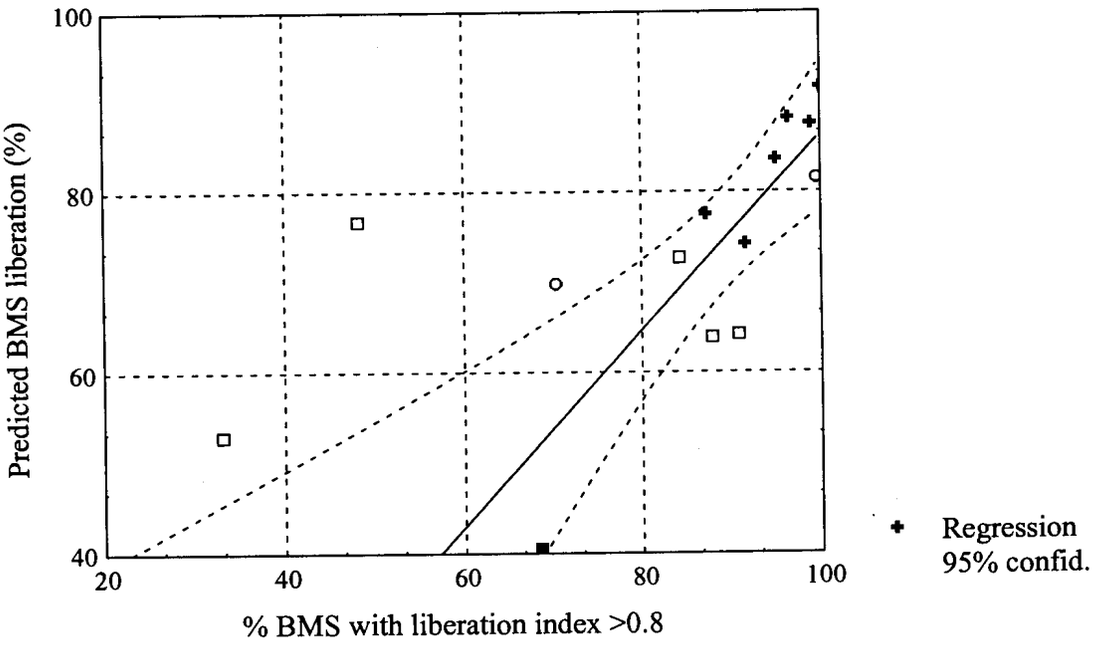

Figure 107 *Relationship between actual and predicted base-metal sulphide liberation. Pearson correlation coefficient r=0.81 for all samples except C1 and C5. + = samples A1, A2, A3, B1, B2, and B3. □ = samples C1, C2, C3, C4 and C5. o = samples A4 and B4. ■ = sample A5.*

Liberation of PGE mineral-bearing particles

Of more relevance is the degree of liberation of PGE mineral-bearing particles. A predicted combined mineral liberation index was calculated by adding together PGE minerals already liberated in the crushed feed, or located at grain boundaries (either of sulphide and gangue, or chromite and silicate), and the amount associated with sulphide multiplied by predicted sulphide liberation (Table 5.1P). There appears to be a linear relationship between this predicted combined liberation index and the percentage PGE mineral in the milled feed occurring in particles with a combined liberation index (CLI) greater than 0.8 (Pearson correlation coefficient r = 0.82) (Figure 108). Exclusion of samples C1 and C5 increases the correlation slightly to r=0.85.

As for the sulphide minerals, the actual measured liberation values are higher than the predicted values. The reason for this is twofold. Firstly, the rather simplified predicted liberation parameters calculated do not take into account base-metal sulphides and PGE minerals located at silicate-silicate grain boundaries (a difficult

parameter to quantify), nor the effect of cleavage and other planes of weakness which may affect milling response. Secondly, as discussed in section 4.6.2, the measured liberation is an overestimation of true liberation. However, these results do indicate that the liberation characteristics of base-metal sulphides and PGE minerals are not random, but depend on the texture of the samples prior to milling.

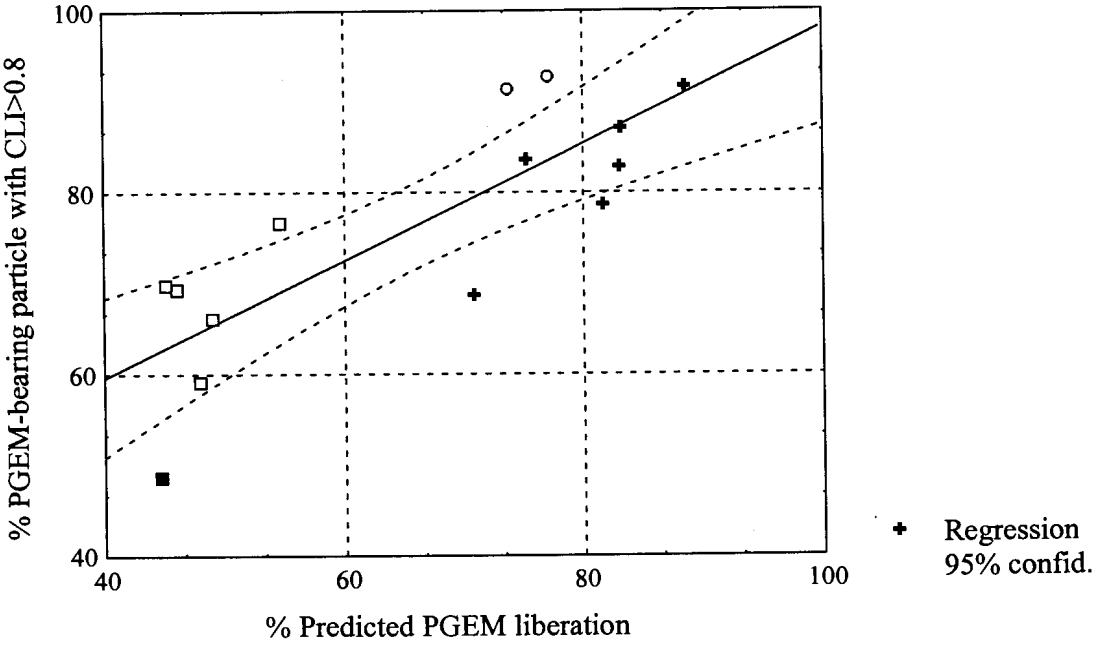

Figure 108 *Relationship between % liberated PGE mineral at 80% <75µm and the predicted PGE mineral liberation. Pearson correlation coefficient r=0.82. + = samples A1, A2, A3, B1, B2, and B3. □ = samples C1, C2, C3, C4 and C5. o = samples A4 and B4. ■ = sample A5.*

Effect of milling on PGE mineral and base-metal sulphide grain size

Both PGE mineral and base-metal sulphide grain sizes were reduced considerably during milling. There appears to be a weak positive correlation between the median equivalent circle diameter of base-metal sulphide grains before and after milling (Pearson correlation coefficient r = 0.61) (Figure 109). No correlation could be found between median equivalent circle diameter of PGE mineral before and after milling (Figure 110).

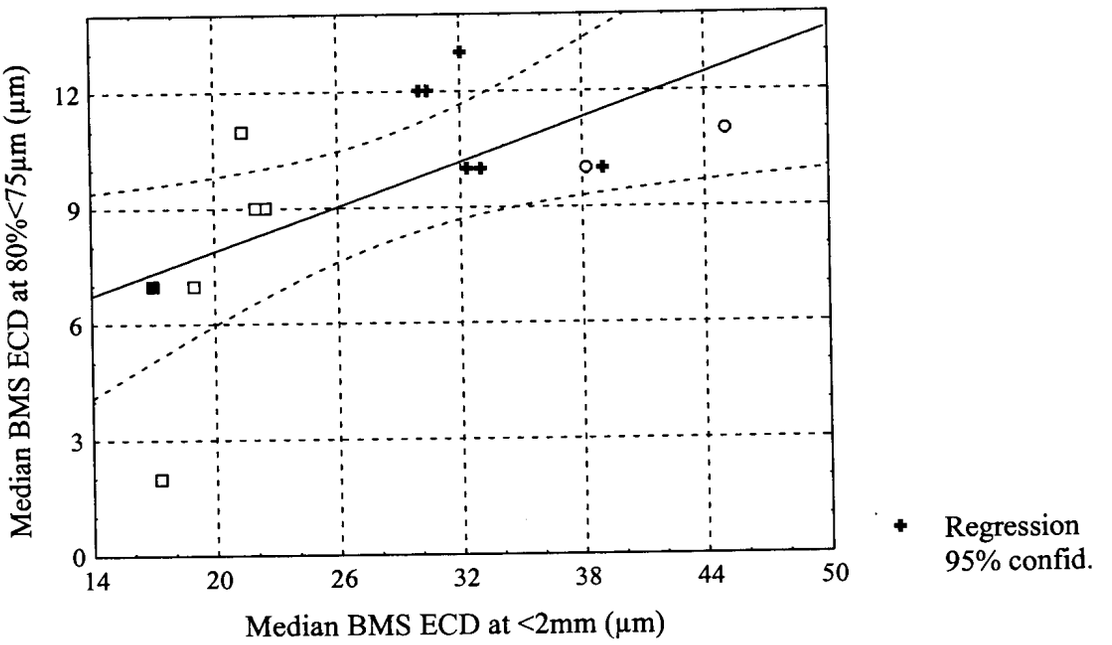

Figure 109 *Effect of milling on base-metal sulphide (BMS) mineral median equivalent circle diameter (ECD). Pearson correlation coefficient r=0.61 + = samples A1, A2, A3, B1, B2, and B3. □ = samples C1, C2, C3, C4 and C5. o = samples A4 and B4. ■ = sample A5.*

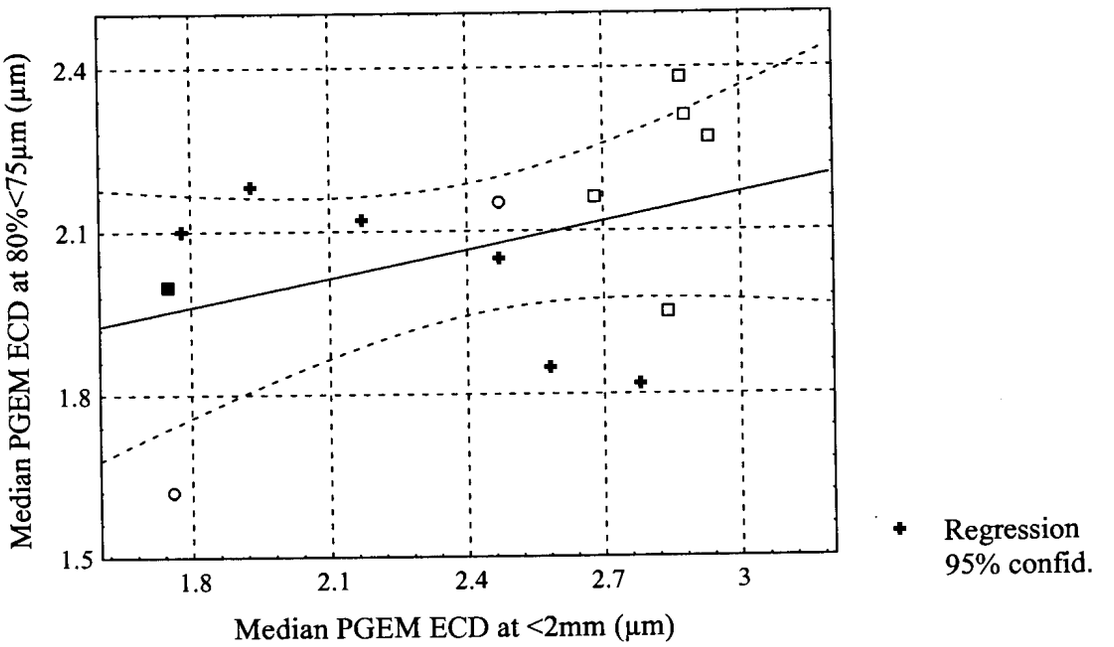

Figure 110 *Effect of milling on PGE mineral (PGEM) median equivalent circle diameter (ECD) based on % number of grains. Pearson correlation coefficient r=0.38. + = samples A1, A2, A3, B1, B2, and B3. □ = samples C1, C2, C3, C4 and C5. o = samples A4 and B4. ■ = sample A5.*

6.5.4 Flotation behaviour of base-metal sulphides

Effective recovery of the base-metal sulphides, especially pentlandite, is of the utmost importance because of their association with PGEs, both as discrete PGE minerals and in solid solution. Mineralogical examination of the flotation products indicates that most of the base-metal sulphide report to the flotation concentrates as liberated grains, with an increase in composite particles in the slower-floating concentrates. The sulphides in the tailings samples are present almost exclusively as fine-grained inclusions in coarse composite silicate particles.

Recovery of liberated base-metal sulphides

Although the flotation tailings do not contain significant concentrations of liberated base-metal sulphides, the slower-floating concentrates do. In a plant situation these slower-floating sulphides will form part of middling streams, such as tailings of cleaning circuits, which may constitute losses if they are not properly treated. In order to maximise sulphide recovery, it is important to understand the mechanisms governing the flotation rates of liberated sulphide grains.

This investigation indicated that coarse liberated base-metal sulphides are recovered at a relatively fast rate, with progressively finer grains recovered with time. Particle size is known to be a major limitation on separation efficiency, with losses in both coarse (> about 70μm) and fine fractions (below approximately 5 to 10 μm) (Trahar, 1981; Senior *et al.*, 1994; Lange *et al.*, 1997). These size ranges vary for different minerals and are also dependent on the scale of operation.

It is believed that a significant proportion of fine-grained sulphides is recovered due to entrainment rather than true flotation (Trahar, 1981). Senior *et al.* (1994) estimated from tests on synthetic mixtures of pentlandite, pyrrhotite, chalcopyrite and quartz, that less than 35 percent of 4 to 10 μm pentlandite genuinely floated, and about 15 percent of –4μm pentlandite.

However, particle size is not the only factor determining the flotation rate of liberated sulphide grains. Different sulphides float at different rates because of differences in their surface characteristics (Herrera-Urbina *et al.*, 1990). Pyrrhotite is known to be

relatively slow-floating, hence the presence of relatively coarse liberated pyrrhotite grains in the slower-floating concentrates of some of the samples.

Sulphide mineral hydrophobicity is affected by a number of variables such as reagent conditions and surface preparation conditions (e.g. pH and Eh), the presence of adsorbed hydrophylic fines e.g. gangue minerals (Edwards *et al.*, 1980; Parsonage, 1985), electrochemical interaction between minerals (Guy & Trahar, 1985; Cheng & Iwasaki, 1992, Bozkurt *et al.*, 1997) and between minerals and the grinding media (amongst others Kocabag & Smith, 1985; Pozzo *et al.*, 1990; Cheng & Iwasaki, 1992, Senior *et al.*, 1994; Yuan *et al.*, 1996). The latter is believed to be partly responsible for the slow-floating nature of pyrrhotite (Pozzo *et al.*, 1990).

The behaviour of composite particles during flotation

The behaviour of composite particles during flotation is not well documented or understood. This is partly because it is not possible to distinguish between the effects of particle composition and the effects of particle size, as composites tend to be in the slower-floating coarse sizes. It is generally assumed that locked particles float in some manner intermediate between fast-floating free particles and non-floating gangue particles. Investigations by Trahar (1991) and Sutherland (1989) indicated that a very small amount of floatable mineral is required to induce flotation of a composite particle.

In the samples under investigation, it was found that where the flotation feed was characterised by a higher proportion of the sulphide minerals occurring as part of composite particles, such as in samples from area C and sample A5, a high proportion of these composite particles reported to the flotation concentrates. The presence of talc in composite particles probably contributed to the floatability of some of these particles. The presence or absence of slow-floating pyrrhotite may also have an effect.

6.5.5 Flotation behaviour of PGE minerals

Most of the PGE minerals were recovered in the form of liberated PGE mineral grains or PGE mineral grains associated with base-metal sulphide. The rate of flotation of liberated base-metal sulphide grains is faster than that of liberated PGE minerals,

partly due to the smaller grain size of PGE mineral grains. Inherent differences in the hydrophobicity of base-metal sulphides and PGE minerals probably also play a role.

Considering the small grain size of the PGE minerals, doubt exist as to whether the liberated grains truly float, or whether their presence in flotation concentrates can be attributed to some other process such as entrainment. It would seem that at least a portion of the liberated PGE minerals were recovered by true flotation rather than entrainment, despite their small grain sizes, hence the observation that progressively finer PGE minerals are being recovered with time, in contrast to chromite and silicate of which the finest grains were recovered to the fastest-floating concentrate. The observed differences in the recoveries of the different type of PGE minerals also indicate that some selectivity is present during flotation process, although the slower rate of flotation of the non-sulphide PGE minerals may partly be related to their smaller sizes. During plant flotation some of the smaller liberated grains, especially of slow-floating types of PGE minerals may report to cleaner tailings streams and, if not properly treated, may eventually be lost. Most of the losses of PGE minerals to the tailings are in the form of incomplete liberation from silicate minerals, mostly in the coarser particle sizes.

6.6 Prediction of PGE recovery characteristics based on mineralogical and chemical parameters

The milled flotation feed samples contain a variety of different types of particles composed of a number of different minerals, occurring in different proportions, and with different grain sizes. During the mineralogical examination of the different flotation products fast-, slow- and non-floating particles were identified. Based on the type of particles present in a milled feed sample, it should therefore be possible to predict the flotation characteristics of an ore. Furthermore, as the types of particles in the milled flotation feed is determined by the mineralogical characteristics of the ore prior to milling, the flotation characteristics may also be predicted from the mineralogical characteristics of the crushed ore.

6.6.1 Relationship between flotation characteristics and selected mineralogical and chemical parameters in UG2 ore prior to milling.

The following mineralogical and chemical parameters can be used to describe the

crushed ore, and will, to a large extent, determine the types of particles generated during milling:

- mode of occurrence of PGE minerals, expressed as predicted liberation of PGE minerals
- amount of non-sulphide PGE mineral
- PGE mineral grain size, expressed as median PGE mineral grain diameter based on per cent number of grains. (As shown in Table 4.17, although the median PGE mineral grain diameter based on area per cent is a closer approximation of the true grain diameter, the median grain diameter based on per cent number of grains is a statistically more reliable parameter, allowing for comparison between samples.)
- base-metal sulphide mode of occurrence expressed as predicted liberation
- base-metal sulphide grain size expressed as median diameter
- amount of pentlandite
- pentlandite/(pentlandite+millerite) ratio
- chromite grain size expressed as median diameter
- acid copper and nickel, and PGE+Au contents.

The relationships between these parameters and the flotation characteristics of the different types of UG2 ore are reported in Table 6.5 and graphically depicted in Figure 111.

Predicted PGE mineral liberation (PGEMLib1)

For the relatively unaltered ores (A1, B1, A2, B2, A3 & B3), a positive relationship exists between the predicted degree of liberation of PGE minerals and R_f (Figure 112), with a Pearson correlation coefficient of 0.85. If extended, the regression line will intercept the y-axis at a relatively low value, suggesting that for this group of samples, the value of R_f is determined almost exclusively by the mode of occurrence of the PGE minerals.

In the case of the millerite-bearing ores (C1 to C5) the relationship is also a positive one (r=0.72), but, even though the slope of the regression line is similar to that of the relatively unaltered samples, the y-intercept value is much higher. One possible explanation for the higher than expected values of R_f for these samples, could be that the predicted degree of liberation is underestimated for these samples, partly due to

Table 6.5 *Correlation matrix of selected mineralogical and chemical parameters against R_f, R_s, 100-U, k_f and ks. Marked correlations (boldface) are significant at $p<0.05$.*

A. Samples A1, B1, A2, B2, A3 and B3 (Relatively unaltered UG2 ore)													
n=6	R_f	R_s	*100-U*	k_f	k_s	*PGEMLib1*	*NSul*	*PGEMS1*	*BMSLib1*	*BMSS1*	*pn*	*pn:mil*	*ChrS*
R_f	1.00	**-0.98**	**-0.96**	0.66	0.30	**0.85**	-0.03	-0.39	0.67	**-0.87**	0.08	-0.47	-0.79
R_s	**-0.98**	1.00	**0.88**	-0.74	-0.19	**-0.89**	0.11	0.31	-0.79	**0.87**	0.05	0.55	**0.87**
100-U	**-0.96**	**0.88**	1.00	-0.48	-0.45	-0.73	-0.09	0.48	-0.43	0.81	-0.27	0.33	0.60
k_f	0.66	-0.74	-0.48	1.00	0.12	0.59	0.04	-0.34	**0.87**	-0.67	-0.20	-0.85	-0.62
k_s	0.30	-0.19	-0.45	0.12	1.00	-0.16	-0.19	-0.07	-0.24	0.00	-0.12	-0.46	0.09
PGEMLib1	**0.85**	**-0.89**	-0.73	0.59	-0.16	1.00	-0.03	-0.22	**0.83**	-0.77	0.12	-0.22	**-0.82**
NSul	-0.03	0.11	-0.09	0.04	-0.19	-0.03	1.00	**-0.87**	-0.10	-0.29	**0.88**	0.25	0.40
PGEMS1	-0.39	0.31	0.48	-0.34	-0.07	-0.22	**-0.87**	1.00	-0.13	0.66	-0.73	0.11	-0.03
BMSLib1	0.67	-0.79	-0.43	**0.87**	-0.24	**0.83**	-0.10	-0.13	1.00	-0.68	-0.22	-0.58	-0.82
BMSS1	**-0.87**	**0.87**	0.81	-0.67	0.00	-0.77	-0.29	0.66	-0.68	1.00	-0.24	0.40	0.73
pn	0.08	0.05	-0.27	-0.20	-0.12	0.12	**0.88**	-0.73	-0.22	-0.24	1.00	0.52	0.37
pn:mil	-0.47	0.55	0.33	**-0.85**	-0.46	-0.22	0.25	0.11	-0.58	0.40	0.52	1.00	0.48
ChrS	-0.79	**0.87**	0.60	-0.62	0.09	**-0.82**	0.40	-0.03	**-0.82**	0.73	0.37	0.48	1.00
Cu_{as}	-0.76	**0.82**	0.61	-0.57	-0.22	-0.62	0.56	-0.10	-0.63	0.62	0.54	0.62	0.93
Ni_{as}	0.07	-0.08	-0.05	0.03	-0.73	0.38	0.72	-0.56	0.25	-0.40	0.71	0.45	-0.03
ΣPGE	-0.62	0.66	0.50	-0.45	0.11	-0.50	0.09	0.31	-0.51	0.80	0.19	0.40	0.79
CLI>0.8	**0.94**	**-0.89**	**-0.95**	0.58	0.31	**0.84**	0.17	-0.48	0.58	-0.78	0.34	-0.32	-0.58
CLI>0.6	**0.90**	**-0.86**	**-0.88**	0.63	0.23	**0.86**	0.21	-0.48	0.64	-0.75	0.35	-0.32	-0.55
CLI>0.4	**0.82**	-0.79	-0.81	0.67	0.22	0.79	0.35	-0.57	0.63	-0.72	0.43	-0.34	-0.43
PGEMS2	0.61	-0.50	-0.73	0.47	0.47	0.34	0.64	**-0.87**	0.19	-0.64	0.61	-0.32	-0.05
BMSLib2	**0.83**	**-0.89**	-0.68	**0.83**	-0.14	**0.85**	0.20	-0.53	**0.88**	**-0.94**	0.10	-0.51	-0.79
BMSS2	0.34	-0.41	-0.20	0.11	-0.65	0.76	-0.12	0.16	0.57	-0.32	0.10	0.31	-0.56
PGEM:BMS	**-0.86**	0.81	**0.88**	-0.47	-0.54	-0.51	0.14	0.36	-0.35	0.76	0.08	0.53	0.67

p.t.o.

Table 6.5 continued *Correlation matrix of selected mineralogical and chemical parameters against R_f, R_s, 100-U, k_f and ks. Marked correlations (boldface) are significant at $p<0.05$.*

A. Samples A1, B1, A2, B2, A3 and B3 (Relatively unaltered UG2 ore)										
n=6	*Cu $_{as}$*	*Ni $_{as}$*	*ΣPGE*	*CLI>0.8*	*CLI>0.6*	*CLI>0.4*	*PGEMS2*	*BMSLib2*	*BMSS2*	*PGEM:BMS*
R_f	-0.76	0.07	-0.62	**0.94**	**0.90**	**0.82**	0.61	**0.83**	0.34	**-0.86**
R_s	**0.82**	-0.08	0.66	**-0.89**	**-0.86**	-0.79	-0.50	**-0.89**	-0.41	0.81
100-U	0.61	-0.05	0.50	**-0.95**	**-0.88**	-0.81	-0.73	-0.68	-0.20	**0.88**
k_f	-0.57	0.03	-0.45	0.58	0.63	0.67	0.47	**0.83**	0.11	-0.47
k_s	-0.22	-0.73	0.11	0.31	0.23	0.22	0.47	-0.14	-0.65	-0.54
PGEMLib1	-0.62	0.38	-0.50	**0.84**	**0.86**	0.79	0.34	**0.85**	0.76	-0.51
NSul	0.56	0.72	0.09	0.17	0.21	0.35	0.64	0.20	-0.12	0.14
PGEMS1	-0.10	-0.56	0.31	-0.48	-0.48	-0.57	**-0.87**	-0.53	0.16	0.36
BMSLib1	-0.63	0.25	-0.51	0.58	0.64	0.63	0.19	**0.88**	0.57	-0.35
BMSS1	0.62	-0.40	0.80	-0.78	-0.75	-0.72	-0.64	**-0.94**	-0.32	0.76
pn	0.54	0.71	0.19	0.34	0.35	0.43	0.61	0.10	0.10	0.08
pn:mil	0.62	0.45	0.40	-0.32	-0.32	-0.34	-0.32	-0.51	0.31	0.53
ChrS	**0.93**	-0.03	0.79	-0.58	-0.55	-0.43	-0.05	-0.79	-0.56	0.67
Cu_{as}	1.00	0.30	0.78	-0.50	-0.43	-0.30	-0.06	-0.63	-0.25	0.80
Ni_{as}	0.30	1.00	-0.15	0.19	0.26	0.32	0.23	0.42	0.56	0.23
ΣPGE	0.78	-0.15	1.00	-0.35	-0.28	-0.19	-0.17	-0.72	-0.21	0.73
CLI>0.8	-0.50	0.19	-0.35	1.00	0.99	**0.95**	0.74	0.75	0.36	-0.70
CLI>0.6	-0.43	0.26	-0.28	**0.99**	1.00	**0.98**	0.73	0.77	0.41	-0.59
CLI>0.4	-0.30	0.32	-0.19	**0.95**	**0.98**	1.00	0.80	0.75	0.33	-0.50
PGEMS2	-0.06	0.23	-0.17	0.74	0.73	0.80	1.00	0.52	-0.22	-0.54
BMSLib2	-0.63	0.42	-0.72	0.75	0.77	0.75	0.52	1.00	0.44	-0.60
BMSS2	-0.25	0.56	-0.21	0.36	0.41	0.33	-0.22	0.44	1.00	0.05
PGEM:BMS	0.80	0.23	0.73	-0.70	-0.59	-0.50	-0.54	-0.60	0.05	1.00

p.t.o.

Table 6.5 continued *Correlation matrix of selected mineralogical and chemical parameters against R_f, R_s, 100-U, k_f and ks. Marked correlations (boldface) are significant at $p<0.05$.*

B. Samples C1, C2, C3, C4 and C5 (Millerite-bearing UG2 ore)													
n=5	R_f	R_s	*100-U*	k_f	k_s	*PGEMLib1*	*NSul*	*PGEMS1*	*BMSLib1*	*BMSS1*	*pn*	*pn:mil*	*ChrS*
R_f	1.00	**-0.97**	**-0.97**	**0.96**	0.56	0.72	-0.42	-0.59	-0.49	-0.14	-0.16	-0.05	-0.64
R_s	**-0.97**	1.00	**0.89**	-1.00	-0.69	-0.61	0.50	0.41	0.27	0.03	0.28	0.18	0.79
100-U	**-0.97**	**0.89**	1.00	-0.88	-0.41	-0.78	0.31	0.72	0.66	0.23	0.03	-0.08	0.46
k_f	**0.96**	-1.00	-0.88	1.00	0.67	0.56	-0.47	-0.36	-0.24	0.02	-0.28	-0.23	-0.81
k_s	0.56	-0.69	-0.41	0.67	1.00	0.43	-0.92	-0.13	0.20	-0.32	-0.71	-0.32	-0.60
PGEMLib1	0.72	-0.61	-0.78	0.56	0.43	1.00	-0.41	**-0.94**	-0.78	-0.53	0.10	0.54	-0.12
NSul	-0.42	0.50	0.31	-0.47	**-0.92**	-0.41	1.00	0.18	-0.16	0.62	0.84	0.36	0.28
PGEMS1	-0.59	0.41	0.72	-0.36	-0.13	**-0.94**	0.18	1.00	**0.93**	0.56	-0.28	-0.65	-0.14
BMSLib1	-0.49	0.27	0.66	-0.24	0.20	-0.78	-0.16	0.93	1.00	0.37	-0.51	-0.68	-0.24
BMSS1	-0.14	0.03	0.23	0.02	-0.32	-0.53	0.62	0.56	0.37	1.00	0.43	-0.10	-0.49
pn	-0.16	0.28	0.03	-0.28	-0.71	0.10	0.84	-0.28	-0.51	0.43	1.00	0.78	0.23
pn:mil	-0.05	0.18	-0.08	-0.23	-0.32	0.54	0.36	-0.65	-0.68	-0.10	0.78	1.00	0.36
ChrS	-0.64	0.79	0.46	-0.81	-0.60	-0.12	0.28	-0.14	-0.24	-0.49	0.23	0.36	1.00
Cu_{as}	**-0.96**	**0.97**	**0.90**	**-0.96**	-0.59	-0.69	0.36	0.52	0.40	-0.05	0.05	-0.05	0.77
Ni_{as}	0.32	-0.36	-0.26	0.41	-0.21	-0.21	0.52	0.23	0.03	0.86	0.39	-0.14	-0.65
ΣPGE	-0.17	0.36	-0.02	-0.40	-0.54	0.44	0.45	-0.65	-0.75	-0.25	0.76	0.93	0.64
CLI>0.8	0.44	-0.33	-0.51	0.31	0.39	0.51	-0.65	-0.52	-0.39	**-0.89**	-0.56	-0.20	0.22
CLI>0.6	0.41	-0.29	-0.51	0.26	0.33	0.56	-0.59	-0.60	-0.47	**-0.91**	-0.47	-0.09	0.30
CLI>0.4	-0.04	0.21	-0.12	-0.23	-0.10	0.29	-0.26	-0.46	-0.44	**-0.89**	-0.24	0.07	0.73
PGEMS2	0.28	-0.34	-0.21	0.38	0.30	-0.29	-0.38	0.35	0.36	-0.10	-0.75	-0.93	-0.29
BMSLib2	-0.06	-0.01	0.12	0.07	-0.41	-0.53	0.68	0.51	0.27	**0.97**	0.43	-0.18	-0.46
BMSS2	-0.76	0.80	0.67	-0.76	-0.87	-0.79	0.75	0.55	0.26	0.34	0.32	-0.11	0.56
PGEM:BMS	**0.92**	-0.83	**-0.95**	0.83	0.44	0.66	-0.44	-0.61	-0.55	-0.38	-0.28	-0.17	-0.37

p.t.o.

Table 6.5 continued *Correlation matrix of selected mineralogical and chemical parameters against R_f, R_s, 100-U, k_f and ks. Marked correlations (boldface) are significant at $p<0.05$.*

F. Samples C1, C2, C3, C4 and C5 (Millerite-bearing UG2 ore)										
n=5	*Cu_{as}*	*Ni_{as}*	*ΣPGE*	*CLI>0.8*	*CLI>0.6*	*CLI>0.4*	*PGEMS2*	*BMSLib2*	*BMSS2*	*PGEM:BMS*
R_f	**-0.96**	0.32	-0.17	0.44	0.41	-0.04	0.28	-0.06	-0.76	**0.92**
R_s	**0.97**	-0.36	0.36	-0.33	-0.29	0.21	-0.34	-0.01	0.80	-0.83
100-U	**0.90**	-0.26	-0.02	-0.51	-0.51	-0.12	-0.21	0.12	0.67	**-0.95**
k_f	**-0.96**	0.41	-0.40	0.31	0.26	-0.23	0.38	0.07	-0.76	0.83
k_s	-0.59	-0.21	-0.54	0.39	0.33	-0.10	0.30	-0.41	-0.87	0.44
PGEMLib1	-0.69	-0.21	0.44	0.51	0.56	0.29	-0.29	-0.53	-0.79	0.66
NSul	0.36	0.52	0.45	-0.65	-0.59	-0.26	-0.38	0.68	0.75	-0.44
PGEMS1	0.52	0.23	-0.65	-0.52	-0.60	-0.46	0.35	0.51	0.55	-0.61
BMSLib1	0.40	0.03	-0.75	-0.39	-0.47	-0.44	0.36	0.27	0.26	-0.55
BMSS1	-0.05	0.86	-0.25	**-0.89**	**-0.91**	**-0.89**	-0.10	0.97	0.34	-0.38
pn	0.05	0.39	0.76	-0.56	-0.47	-0.24	-0.75	0.43	0.32	-0.28
pn:mil	-0.05	-0.14	**0.93**	-0.20	-0.09	0.07	-0.93	-0.18	-0.11	-0.17
ChrS	0.77	-0.65	0.64	0.22	0.30	0.73	-0.29	-0.46	0.56	-0.37
Cu_{as}	1.00	-0.43	0.16	-0.20	-0.18	0.29	-0.11	-0.07	0.81	-0.77
Ni_{as}	-0.43	1.00	-0.25	-0.57	-0.59	-0.73	0.12	**0.93**	0.13	0.13
ΣPGE	0.16	-0.25	1.00	-0.02	0.09	0.36	-0.79	-0.26	0.13	-0.14
CLI>0.8	-0.20	-0.57	-0.02	1.00	**0.99**	0.83	0.47	-0.77	-0.38	0.71
CLI>0.6	-0.18	-0.59	0.09	**0.99**	1.00	0.87	0.38	-0.79	-0.36	0.69
CLI>0.4	0.29	-0.73	0.36	0.83	0.87	1.00	0.17	-0.77	0.07	0.31
PGEMS2	-0.11	0.12	-0.79	0.47	0.38	0.17	1.00	0.05	0.03	0.47
BMSLib2	-0.07	0.93	-0.26	-0.77	-0.79	-0.77	0.05	1.00	0.42	-0.23
BMSS2	0.81	0.13	0.13	-0.38	-0.36	0.07	0.03	0.42	1.00	-0.58
PGEM:BMS	-0.77	0.13	-0.14	0.71	0.69	0.31	0.47	-0.23	-0.58	1.00

p.t.o.

Table 6.5 continued *Correlation matrix of selected mineralogical and chemical parameters against R_f, R_s, 100-U, k_f and ks. Marked correlations (boldface) are significant at $p<0.05$.*

KEY

R_f = fast-floating fraction
R_s= slow-floating fraction
100-U = non-floating fraction
k_f = rate of recovery of fast-floating fraction
k_s = rate of recovery of slow-floating fraction
PGEMLib1 = Predicted PGE mineral liberation
NSul = % non-sulphide PGE mineral
PGEMS1 = PGE mineral median grain diameter prior to milling, i.t.o. number of grains
BMSLib1 = Predicted base-metal sulphide liberation
BMSS1 = base-metal sulphide median grain diameter prior to milling
pn = pentlandite content
pn:mil = pentlandite/(pentlandite+millerite) ratio
ChrS = chromite median grain diameter
Ni_{as}, Cu_{as} = acid soluble nickel and copper contents
ΣPGE = Σ(Pt,Pd,Rh,Au) content
CLI>0.8 = % PGE mineral-bearing particles with cumulative liberation index >0.8
CLI>0.6 = % PGE mineral-bearing particles with cumulative liberation index >0.6
CLI>0.6 = % PGE mineral-bearing particles with cumulative liberation index >0.6
PGEMS2 = PGE mineral median grain diameter after milling, i.t.o. number of grains
BMSLib2 = Base-metal sulphide apparent degree of liberation
BMSS2 = base-metal sulphide median grain diameter after milling
PGEM:BMS = (liberated PGE mineral)/(liberated PGE mineral+BMS) for PGE mineral bearing particles with CLI>0.8

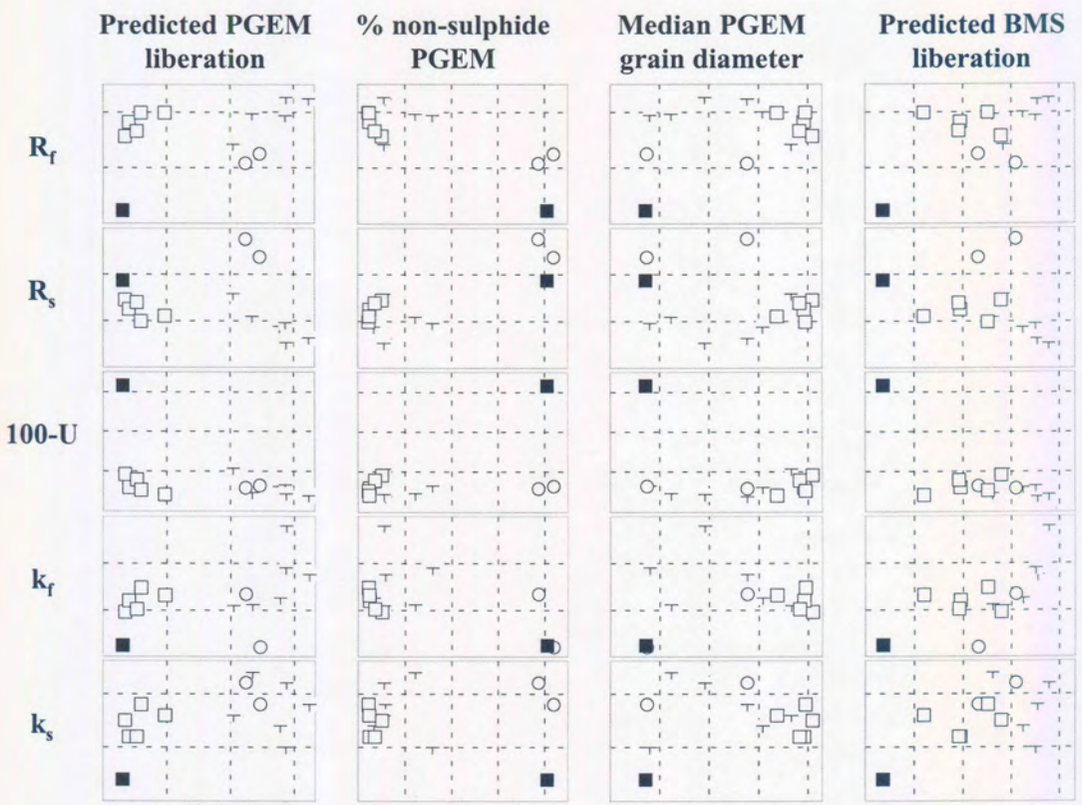

Figure 111 *Relationship between mineralogical, chemical and flotation parameters + = samples A1, A2, A3, B1, B2, and B3. □ = samples C1, C2, C3, C4 and C5. o = samples A4 and B4. ■ = sample A5.*

p.t.o.

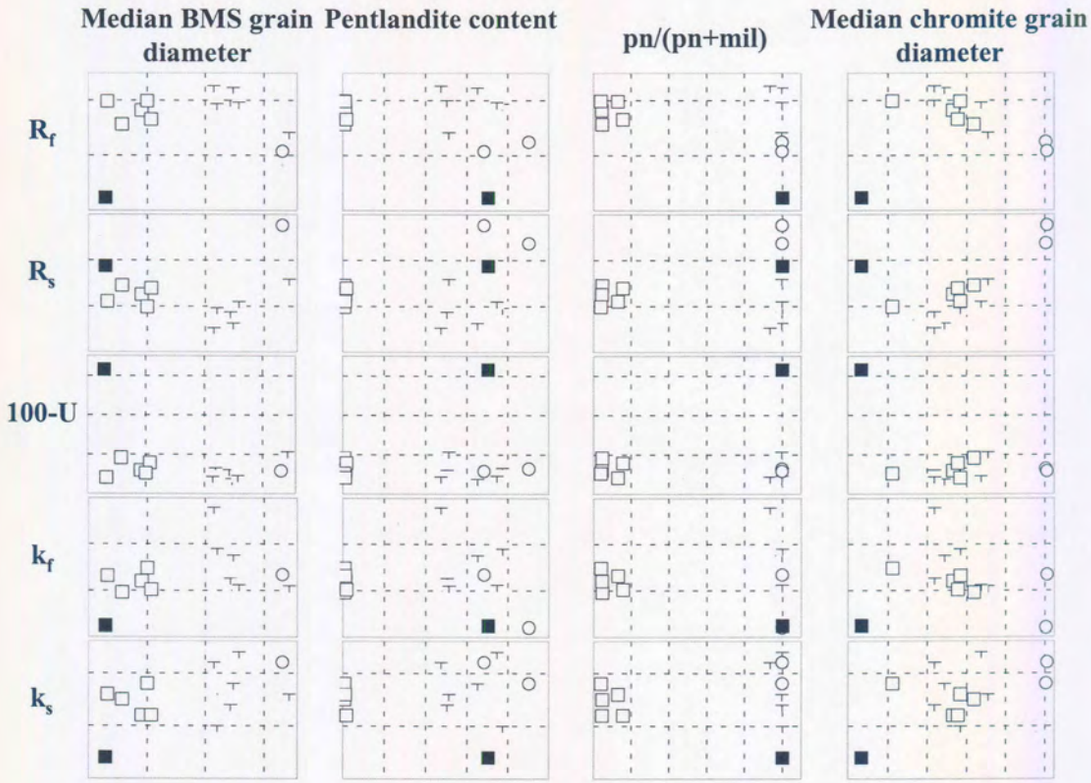

Figure 111 continued *Relationship between mineralogical, chemical and flotation parameters + = samples A1, A2, A3, B1, B2, and B3. □ = samples C1, C2, C3, C4 and C5. o = samples A4 and B4. ■ = sample A5.*

p.t.o.

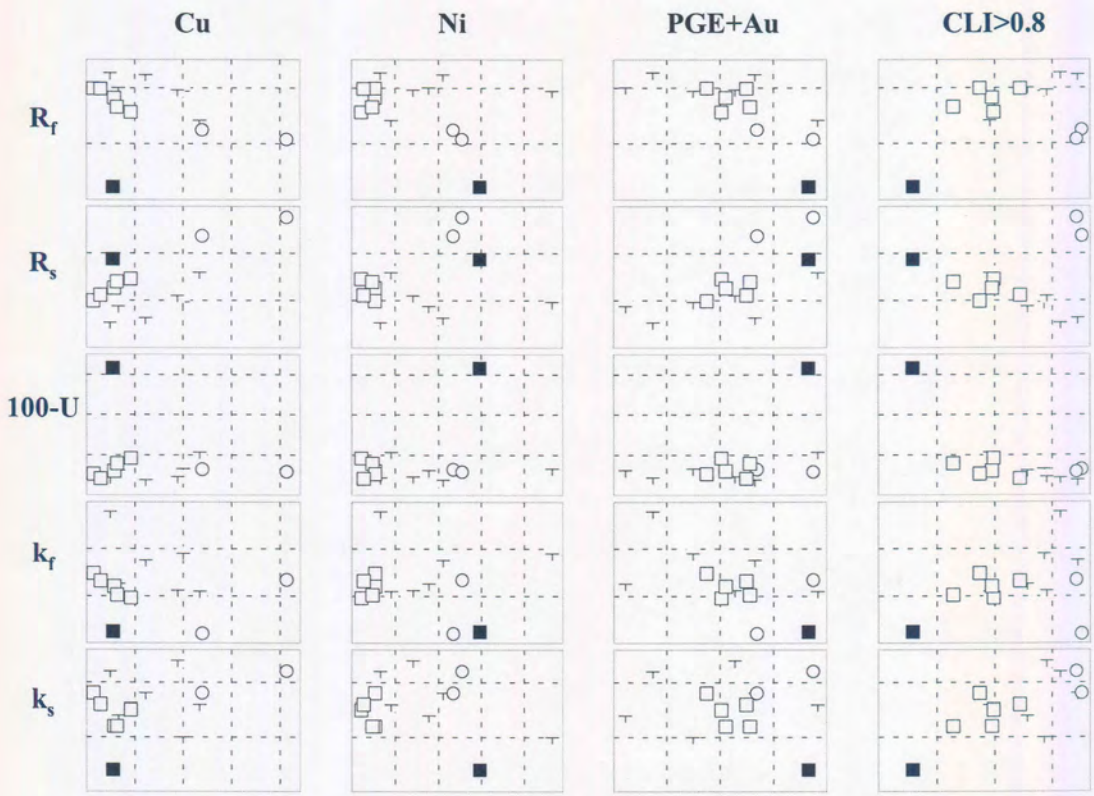

Figure 111 continued *Relationship between mineralogical, chemical and flotation parameters + = samples A1, A2, A3, B1, B2, and B3. □ = samples C1, C2, C3, C4 and C5. o = samples A4 and B4. ■ = sample A5.*

p.t.o.

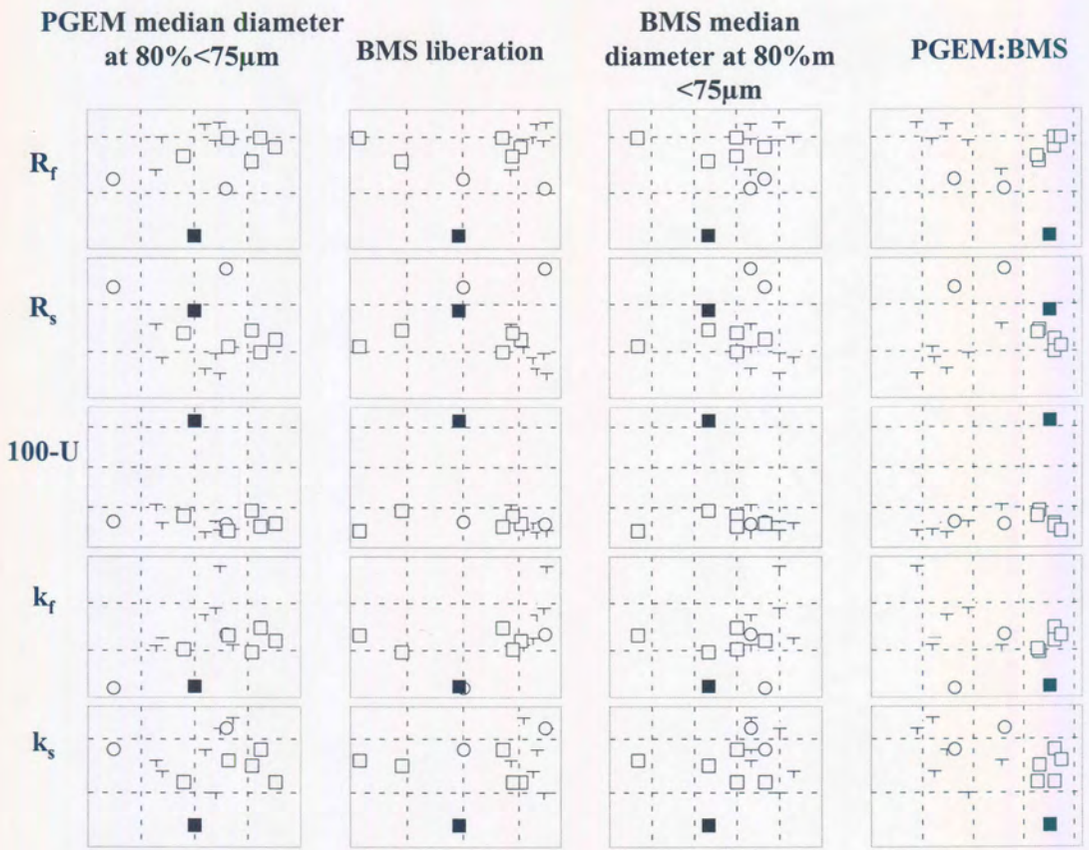

Figure 111 continued *Relationship between mineralogical, chemical and flotation parameters + = samples A1, A2, A3, B1, B2, and B3. □ = samples C1, C2, C3, C4 and C5. o = samples A4 and B4. ■ = sample A5.*

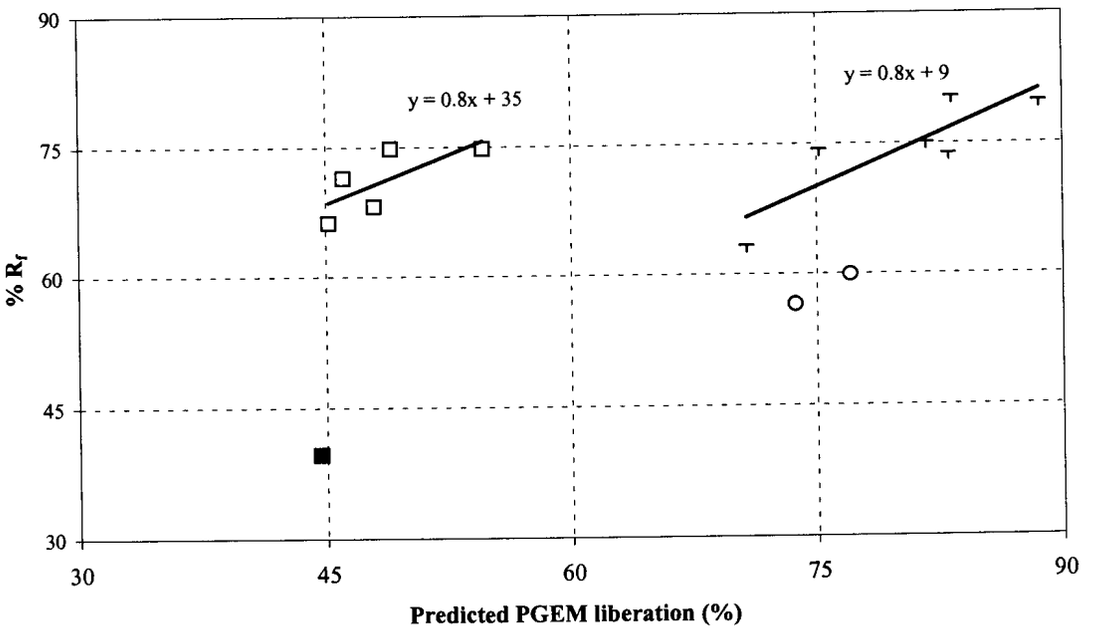

Figure 112 *Relationship between predicted PGE mineral liberation in flotation feed and % R_f. + = samples A1, A2, A3, B1, B2, and B3. □ = samples C1, C2, C3, C4 and C5. o = samples A4 and B4. ■ = sample A5.*

the large amount of PGE minerals at silicate-silicate grain boundaries, a difficult parameter to quantify. Such grains may be liberated quite easily. In addition, the presence of higher concentrations of secondary silicates in these samples, in particular talc, as well as the absence of slow-floating pyrrhotite, may lead to better recovery of composite particles compared to the relatively unaltered samples.

Values of R_f for the sintered samples A4 and B4, are low, presumably because of the large proportion of liberated, but slow-floating, non-sulphide PGE mineral grains in these samples.

For R_s the inverse relationship holds, with a Pearson correlation coefficient of r=-0.89 and –0.61, for the relatively unaltered samples and the millerite-bearing samples, respectively (Figure 113). The amount of slow-floating PGE+Au in sintered samples A4 and B4 is high, due to the contribution of liberated, but slow-floating PGE minerals in these samples.

Similarly, the non-floatable PGE+Au fraction, correlates negatively with predicted PGEM liberation. Sintered samples A4 and B4 falls on the regression line for

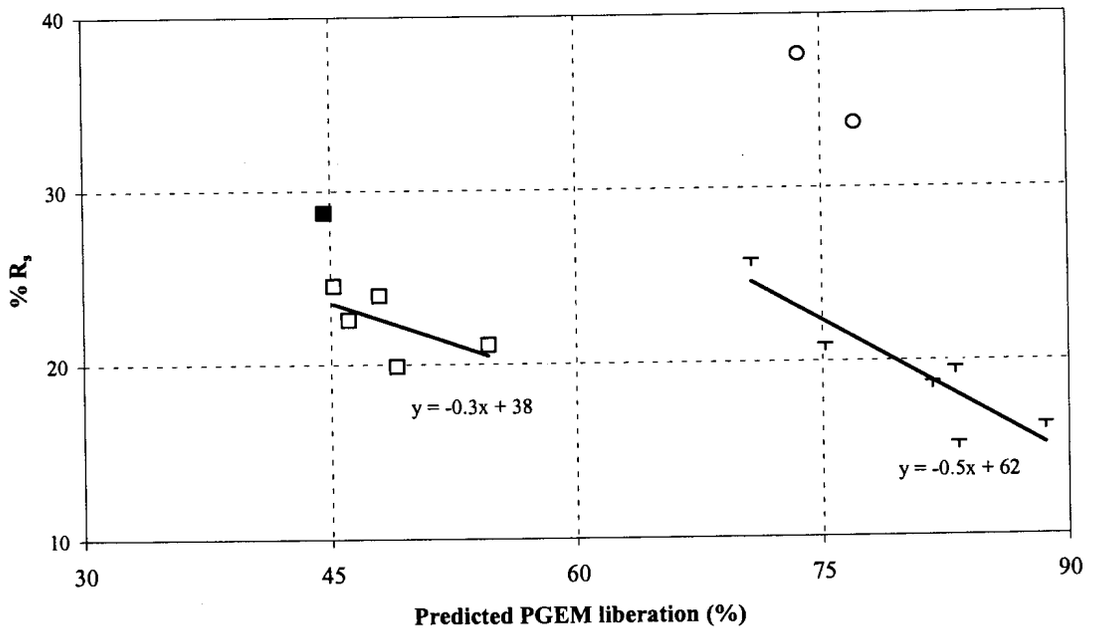

Figure 113 *Relationship between predicted PGE mineral liberation in flotation feed and R_s. + = samples A1, A2, A3, B1, B2, and B3. □ = samples C1, C2, C3, C4 and C5. o = samples A4 and B4. ■ = sample A5.*

relatively unaltered ore (Figure 114). This confirms mineralogical observations that the non-sulphide PGE minerals, given sufficient time, will report to the flotation concentrates.

The relationship between predicted PGE mineral liberation and k_f is similar to that with R_f, but a lot more scattering of the data points is present (Figure 111). No systematic relationship could be discerned between predicted PGE mineral liberation and k_s.

Type of PGE mineral (NSul)

Samples with a high non-sulphide PGE mineral content (A4, B4 and A5) are characterised by relatively low values for R_f, and high values for R_s, due to the slow-floating nature of these minerals. However, due to the big difference in non-sulphide PGE mineral content between these samples and the rest of the samples, the existence of a linear relationship could not be confirmed, and the data essentially falls into two groups (Figure 111). The amount of non-floatable PGE+Au is similar in samples A4 and B4 to the rest of the samples. The reason for the high amount of non-floatable

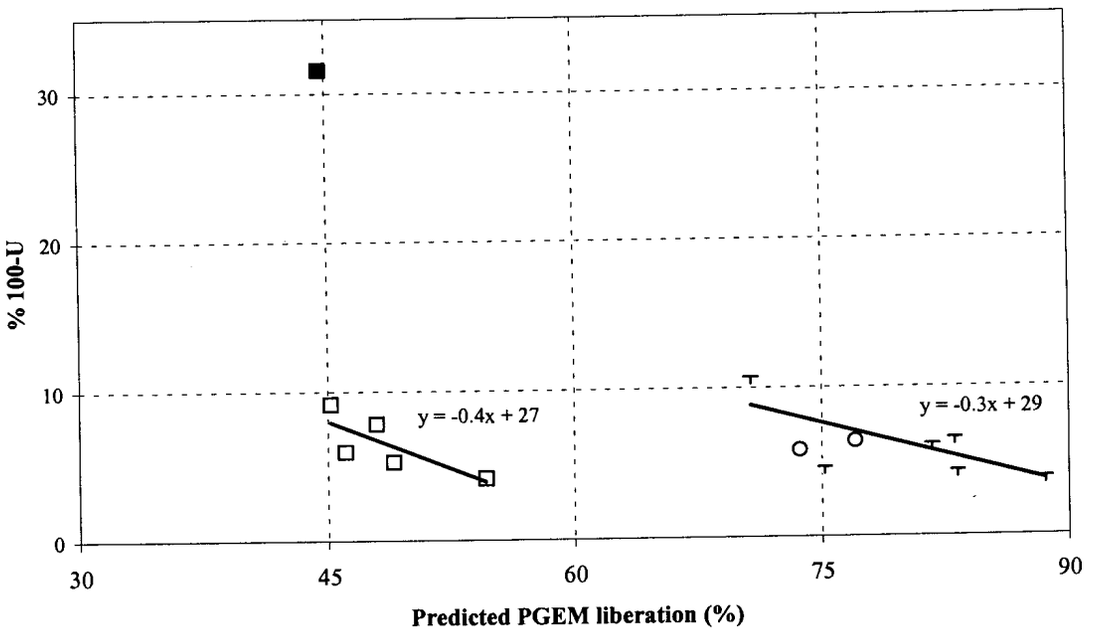

Figure 114 *Relationship between predicted PGE mineral liberation in flotation feed and R_s. + = samples A1, A2, A3, B1, B2, and B3. □ = samples C1, C2, C3, C4 and C5. o = samples A4 and B4. ■ = sample A5.*

PGE+Au in sample A5 is probably related to poor liberation, rather than type of PGE mineral.

PGE mineral grain diameter at <2mm (PGEMS1)

No clear relationship can be seen between any of the flotation parameters and PGE mineral grain diameter prior to milling (Figure 111).

Predicted base-metal sulphide liberation (BMSLib1)

In general, the relationships between the flotation characteristics and predicted base-metal sulphide liberation is similar to that with predicted PGE mineral liberation, but with more scattering of the data points (Figure 111). This is to be expected as the predicted degree of PGE mineral liberation also takes into account the degree of liberation of base-metal sulphide grains associated with PGE minerals.

Base-metal sulphide grain size prior to milling (BMSS1)

No meaningful relationship were found between the base-metal sulphide grain size prior to milling and any of the flotation parameters.

Pentlandite content (pn) and pentlandite/(pentlandite+millerite) ratio (pn:mil)

Pentlandite content and pentlandite/(pentlandite+millerite) ratio essentially divides the data into two groups, those from areas A and B as opposed to the millerite-bearing ores from area C, with no linear relationship discernible (Figure 111).

Chromite grain size (ChrS)

A strong negative linear relationship (Pearson correlation coefficient r = -0.83, for all samples excluding cataclastic UG2 chromitite, sample A5) exists between median chromite grain diameter in the crushed ore and R_f (Table 6.5 and Figure 111). There is a strong positive correlation between median chromite diameter and R_s (r=0.87). Chromite grain size in itself is not a factor affecting recovery, but is, to a certain extent, a reflection of the increase in slow-floating non-sulphide PGE mineral in sintered UG2 chromitite ore. The Pearson correlation coefficient between chromite grain diameter and % non-sulphide PGE mineral in all samples except A5, is 0.84. No correlations were found between median chromite grain diameter and 100-U, k_f or k_s.

Acid soluble copper, nickel and total PGE+Au

In general, there is a negative correlation between copper and total PGE+Au with R_f and k_f, and a positive correlation between copper and total PGE+Au and R_s and U-100. No correlation could be found between copper or total PGE+Au with k_s. There doesn't appear to be a systematic relationship between nickel and any of the flotation parameters.

6.6.2 Predicting flotation parameters from crushed UG2 ore

Fast-floating fraction (R_f)

Using multiple linear regression analysis* it was determined that R_f can be predicted from the mineralogical characteristics of the crushed feed using the non-sulphide PGE

---

* Statistica package.

R – correlation coefficient, the degree to which two or more x variables are related to y

mineral content, predicted PGE mineral liberation, pentlandite/(pentlandite+millerite) ratio and PGE mineral grain size, as independent parameters (R^2=0.98) (Table 6.6 and Figure 115). The relationship appears to be stable, with the relationship not unduly affected by systematic exclusion of any one of the samples from the analysis (Tables 1a and b, Appendix K).

Based on the results already discussed, it was expected that the predicted PGE mineral liberation and the amount of non-sulphide PGE mineral would be significant independent variables. The pentlandite/(pentlandite+millerite) ratio serves to distinguish between the samples from area C and the rest, and compensates for the faster than expected flotation of composite particles in these samples.

The role of the PGE median mineral grain diameter prior to milling, is more difficult to understand. Mineralogical analysis of flotation product samples indicated that coarser PGE mineral grains are faster floating. There is, however, no correlation between PGE mineral grain diameter before and after milling. In addition, it can be seen from Table 6.6 that the median PGE mineral grain diameter correlates negatively with recovery. It is postulated that the median PGE mineral grain diameter serves a function similar to that of the pentlandite/(pentlandite+millerite) ratio, reflecting a difference between groups of samples not satisfactorily explained by any of the other

---

R^2- measures the reduction in the total variation of the dependent variable due to the multiple independent variables

Adjusted R^2 – R^2 is adjusted by dividing the error sums of squares and total sums of squares by their respective degrees of freedom

The F-value and resulting p-value is an overall F-test of the relationship between the dependent variable and the set of independent variables

Standard error of estimate – This statistic measures the dispersion of the observed values about the regression line

B – regression coefficients for a linear model equation

St. Err. of B – standard error of B

t – the t-value associated with the statistics for the respective variable

p – the statistical significance of the t-value

Partial correlation – correlation of x-variable with y, after controlling for all other independent variable

Semipartial correlation – correlation of unadjusted x-variable with y

independent parameters, rather than directly affecting the rate of flotation. The possibility that this is the result of a spurious correlation can also not be excluded.

The median PGE mineral grain diameter is the least significant of the four independent parameters. Exclusion of this parameter still yields a satisfactory model with a R^2 value of 0.95 (Table 6.7 and Figure 116), although exclusion of some of the samples leads to a less reliable result (Tables 2a and b, Appendix K). If samples from area C are excluded from the analysis, the pentlandite/(pentlandite+millerite) ratio becomes superfluous (Table 6.8 and Figure 117).

Slow-floating fraction (R_s)

Table 6.9 summarises the multiple regression results for R_s (Figure 118). In addition to the amount of non-sulphide PGE mineral, predicted degree of PGE mineral liberation, pentlandite/(pentlandite+millerite) ratio, and PGE mineral grain size, chromite grain diameter is also required as a independent variable. Omission of any one of these parameters leads to unsatisfactory results. The regression is not very stable and depends largely on sample A5 (Tables 3a and b, Appendix K).

However, if sample A5 is excluded from the analysis, a more satisfactory result is obtained with the amount of non-sulphide PGE mineral, predicted degree of PGE mineral liberation, pentlandite/(pentlandite+millerite) ratio and PGE mineral grain size as independent parameters (Table 6.10, Figure 119). Omitting PGE mineral grain size as a parameter still gives a reasonably acceptable result (Figure 120 and Table 6.11), although the regression does seem to rely on sample A3 to a large extent (Tables 4a and b, Appendix K).

Non-floating fraction (100-U)

Regression analysis with 100-U as dependent variable yielded unsatisfactory results. Because of the large difference in the amount of non-floating PGE+Au between sample A5 and the remainder of the samples, the regression depended largely on sample A5 (Table 6.12 and Figure 121). If sample A5 is excluded, no statistically significant regression line could be fitted through the points, using the mineralogical parameters examined (Table 5, Appendix K).

Table 6.6 *Regression summary for dependent variable R_f with four independent variables. Fourteen samples.*

$R = .99$ $R^2 = .98$ Adjusted $R^2 = .97$ $F(4,9) = 102.05$ $p < .00000$ Standard Error of estimate: 1.92						
	B	*St. Err. of B*	*t(10)*	*p-level*	*Partial Correlation*	*Semipartial Correlation*
Intercept	61.65	6.69	9.21	0.00		
Predicted PGEM liberation	0.68	0.06	10.64	0.00	0.96	0.52
% non-sulphide PGEM	-0.22	0.03	-7.60	0.00	-0.93	-0.37
pn/(pn+mil)	-22.30	2.89	-7.72	0.00	-0.93	-0.38
PGEM median diameter <2mm	-7.17	1.97	-3.64	0.01	-0.77	-0.18
Independent variables not in equation						
Predicted BMS liberation				0.95	0.02	0.00
BMS median diameter <2mm				0.96	-0.02	0.00
pentlandite content				0.95	0.02	0.00
Median chromite diameter				0.48	-0.25	-0.04
Cu content				0.85	-0.07	-0.01
Ni content				0.34	-0.33	-0.05
PGE+Au content				0.75	-0.12	-0.02

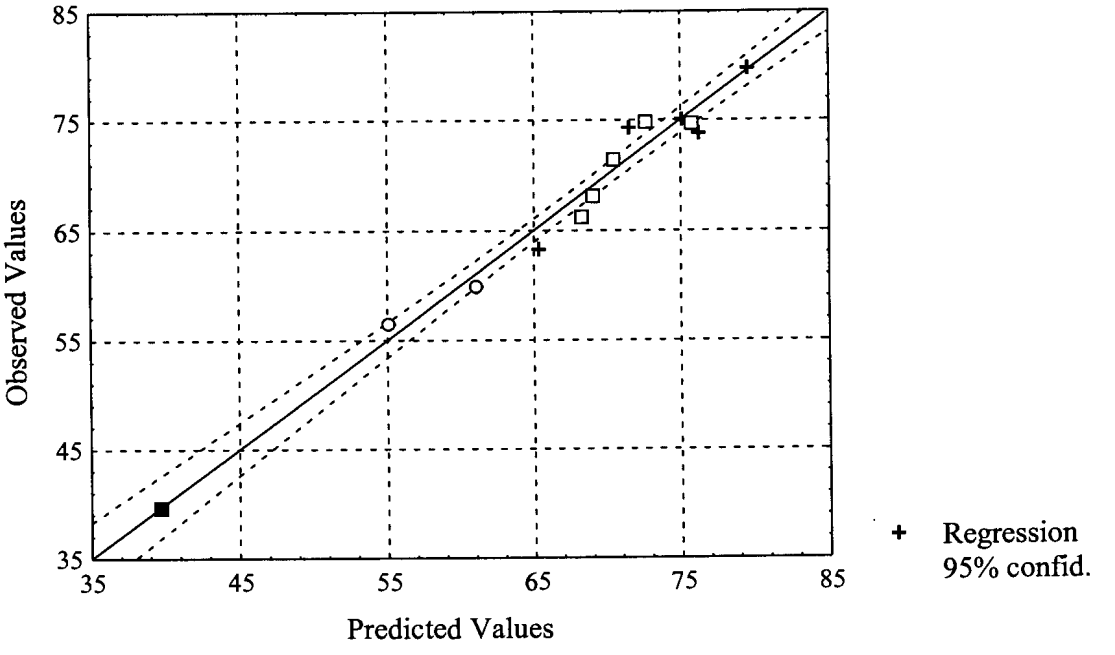

Figure 115 *Comparison of observed and predicted values of R_f based on predicted PGE mineral liberation, pentlandite/(pentlandite+millerite) ratio, amount of non-sulphide PGE mineral and PGE mineral grain diameter prior to milling. + = samples A1, A2, A3, B1, B2, and B3. □ = samples C1, C2, C3, C4 and C5. o = samples A4 and B4. ■ = sample A5.*

Table 6.7 *Regression summary for dependent variable R_f with three independent variables. Fourteen samples.*

$R = .97$ $R^2 = .95$ Adjusted $R^2 = .93$ $F(3,10) = 59.144$ $p < .00000$ Standard Error of estimate: 2.87						
	B	*St. Err. of B*	*t(10)*	*p-level*	*Partial Correlation*	*Semipartial Correlation*
Intercept	40.14	4.69	8.56	0.00		
Predicted PGEM liberation	0.69	0.10	7.27	0.00	0.92	0.53
% non-sulphide PGEM	-0.17	0.04	-4.48	0.00	-0.82	-0.33
pn/(pn+mil)	-19.17	4.12	-4.66	0.00	-0.83	-0.34
Independent variables not in equation						
PGEM median diameter <2mm				0.00	-0.77	-0.18
Predicted BMS liberation				0.42	-0.27	-0.06
BMS median diameter <2mm				0.21	-0.41	-0.09
pentlandite content				0.11	0.51	0.12
Median chromite diameter				0.12	-0.49	-0.11
Cu content				0.13	-0.49	-0.11
Ni content				0.81	0.08	0.02
PGE+Au content				0.19	-0.43	-0.10

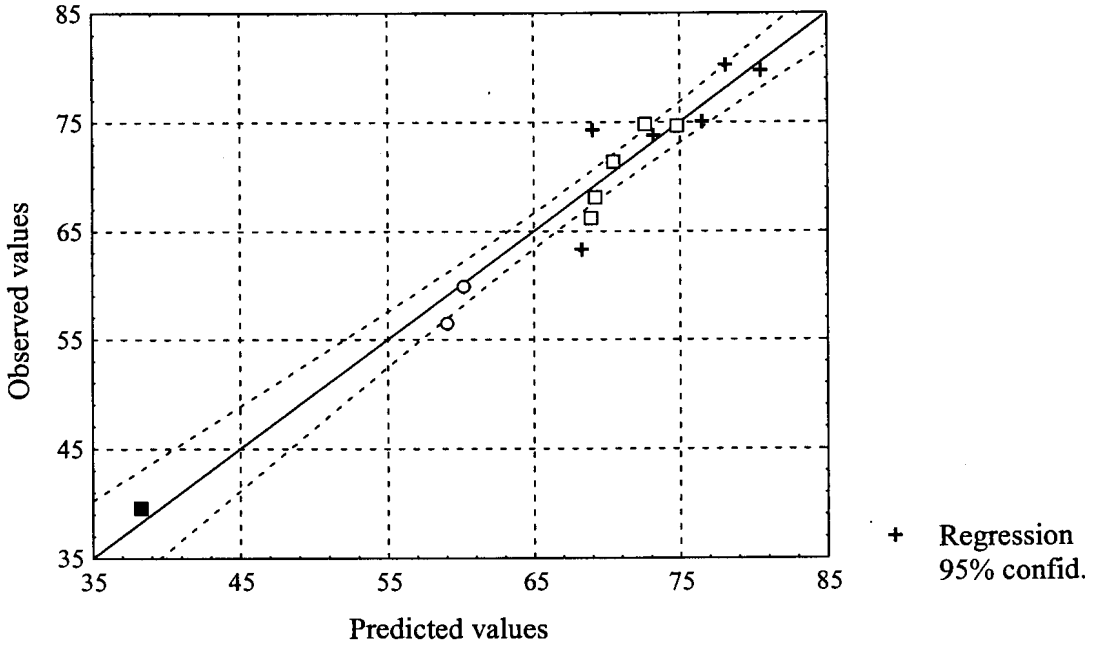

Figure 116 *Comparison of observed and predicted values of R_f based on predicted PGE mineral liberation, pentlandite/(pentlandite+millerite) ratio and amount of non-sulphide PGE mineral. + = samples A1, A2, A3, B1, B2, and B3. □ = samples C1, C2, C3, C4 and C5. o = samples A4 and B4. ■ = sample A5.*

Table 6.8 *Regression summary for dependent variable R_f with two independent variables. Samples from area C excluded.*

$R = .97$ $R^2 = .95$ Adjusted $R^2 = .93$ $F(3,10) = 59.144$ $p < .00000$ Standard Error of estimate: 2.87						
	B	*St. Err. of B*	*t(6)*	*p-level*	*Partial Correlation*	*Semipartial Correlation*
Intercept	22.37	10.26	2.18	0.07		
% non-sulphide PGEM	-0.18	0.05	-3.79	0.01	-0.84	-0.35
Predicted PGEM liberation	0.68	0.12	5.65	0.00	0.92	0.53
Independent variables not in equation						
PGEM median diameter <2mm				0.02	-0.81	-0.19
pn/(pn+mil)				0.35	-0.41	-0.09

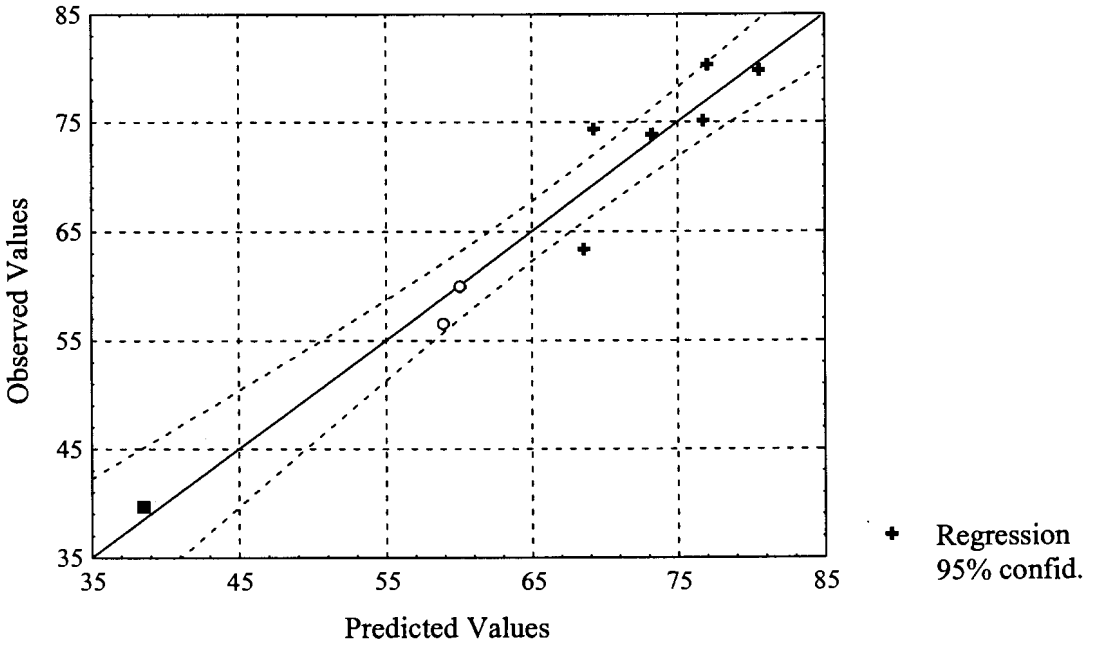

Figure 117 *Comparison of observed and predicted values of R_f for samples from areas A and B based on predicted PGE mineral liberation, and amount of non-sulphide PGE mineral. + = samples A1, A2, A3, B1, B2, and B3. o = samples A4 and B4. ■ = sample A5.*

Table 6.9 *Regression summary for dependent variable R_s*

R= .99 R^2= .99 Adjusted R^2= .98						
F(5,8)=54.12 p<.00000 Standard Error of estimate: 0.83						
	B	*St. Err. of B*	*t(8)*	*p-level*	*Partial Cor.*	*Semipart Cor.*
Intercept	-5.76	2.89	-2.00	0.08		
Predicted PGEM liberation	-0.20	0.04	-5.40	0.00	-0.89	-0.20
% non-sulphide PGEM	0.17	0.02	10.17	0.00	0.96	0.37
pn/(pn+mil)	5.03	1.40	3.59	0.01	0.79	0.13
PGEM median diameter <2mm	6.12	0.95	6.43	0.00	0.92	0.23
Chromite median diameter	0.11	0.01	8.29	0.00	0.95	0.30
Independent variables not in equation						
Predicted BMS liberation				0.82	-0.09	-0.01
BMS median diameter <2mm				0.27	0.41	0.04
pentlandite				0.88	-0.06	-0.01
Cu				0.46	0.28	0.03
Ni				0.39	0.33	0.03
PGE+Au				0.69	-0.16	-0.02

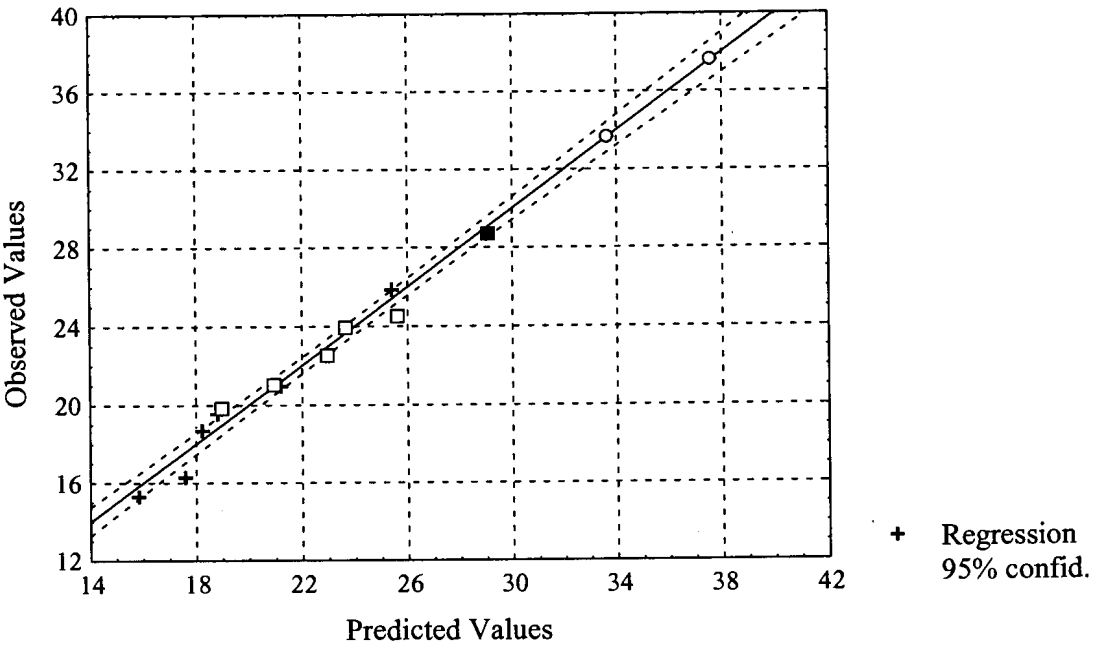

Figure 118 *Comparison of observed and predicted values of R_s based on predicted PGE mineral liberation, pentlandite/(pentlandite+millerite) ratio, amount of non-sulphide PGE mineral, PGEM grain diameter prior to milling, and chromite grain diameter prior to milling. + = samples A1, A2, A3, B1, B2, and B3. □ = samples C1, C2, C3, C4 and C5. o = samples A4 and B4. ■ = sample A5.*

Table 6.10 *Regression summary for dependent variable R_s for four independent variables and excluding sample A5.*

$R= .99$ $R^2= .99$ Adjusted $R^2= .98$ $F(4,8)=130.39$ $p<.00000$ Standard Error of estimate: 0.96						
	B	*St. Err. of B*	*t(9)*	*p-level*	*Partial Correlation*	*Semipartial Correlation*
Intercept	21.94	5.31	4.13	0.00		
Predicted PGEM liberation	-0.40	0.07	-6.07	0.00	-0.91	-0.26
% non-sulphide PGEM	0.23	0.02	15.54	0.00	0.98	0.68
pn/(pn+mil)	12.07	2.29	5.28	0.00	0.88	0.23
PGEM median diameter <2mm	6.10	1.11	5.48	0.00	0.89	0.24

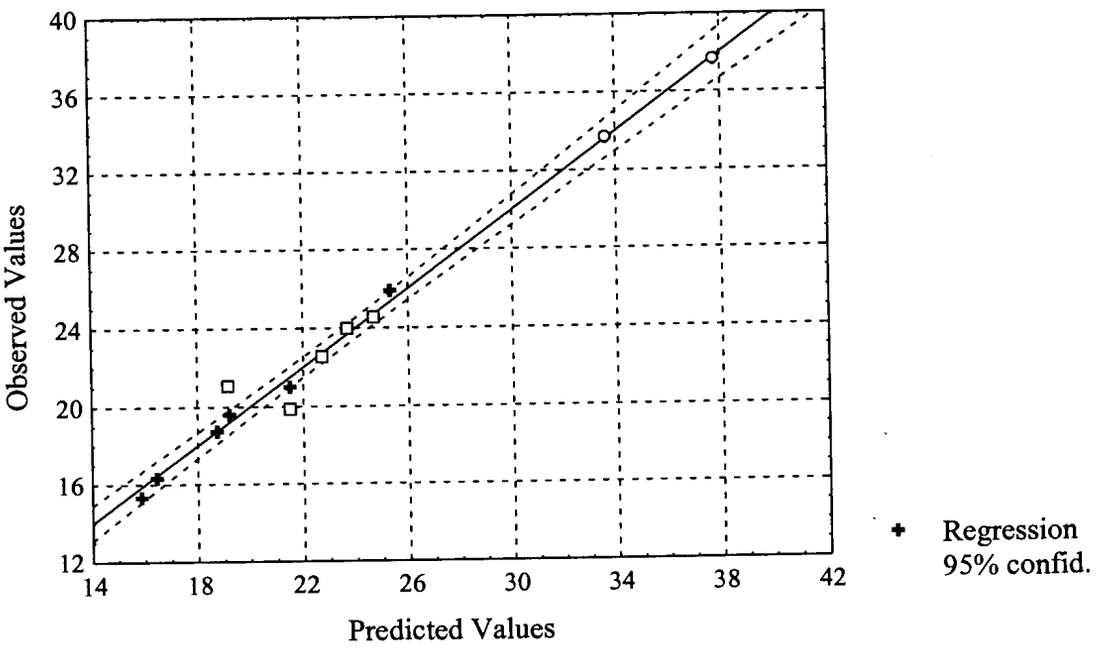

Figure 119 *Comparison of observed and predicted values of R_s based on predicted PGE mineral liberation, pentlandite/(pentlandite+millerite) ratio, amount of non-sulphide PGE mineral and PGEM grain diameter prior to milling. + = samples A1, A2, A3, B1, B2, and B3. □ = samples C1, C2, C3, C4 and C5. o = samples A4 and B4.*

Table 6.11 *Regression summary for dependent variable R_s for three independent variables and excluding sample A5.*

$R = .96$ $R^2 = .93$ Adjusted $R^2 = .90$ $F(3,9) = 38.77$ $p < .00000$ Standard Error of estimate: 1.98						
	B	*St. Err. of B*	*t(9)*	*p-level*	*Partial Correlation*	*Semipartial Correlation*
Intercept	46.74	5.72	8.17	0.00		
Predicted PGEM liberation	-0.55	0.12	-4.51	0.00	-0.83	-0.40
% non-sulphide PGEM	0.19	0.03	7.24	0.00	0.92	0.65
pn/(pn+mil)	14.44	4.62	3.13	0.01	0.72	0.28

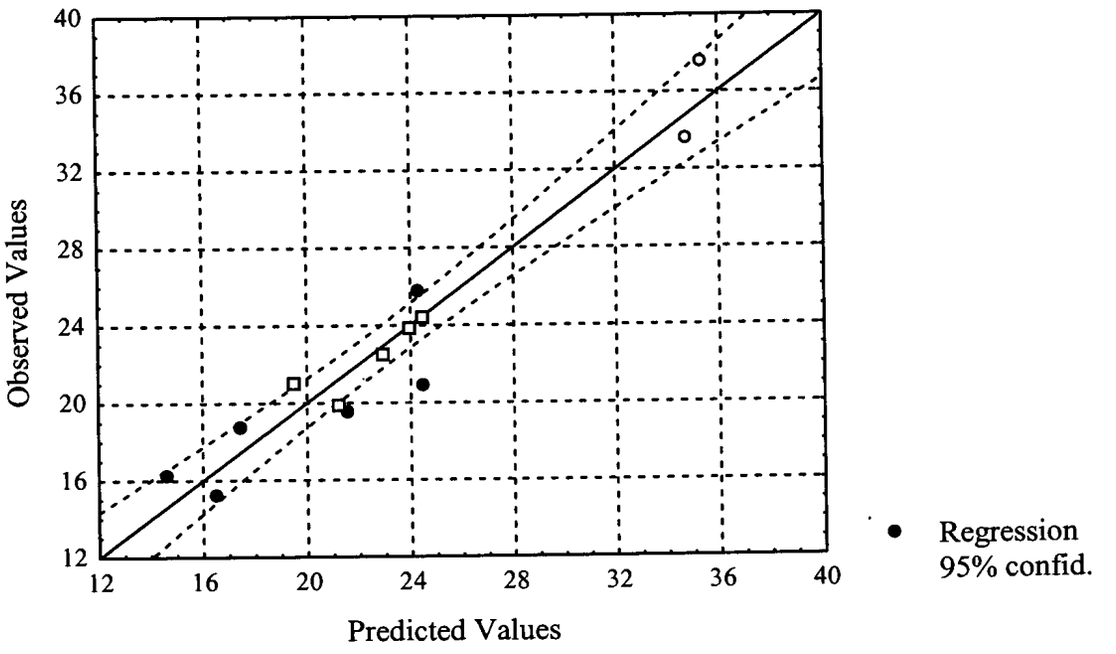

Figure 120 *Comparison of observed and predicted values of R_s based on predicted PGE mineral liberation, pentlandite/(pentlandite+millerite) ratio and amount of non-sulphide PGE mineral. ● = samples A1, A2, A3, B1, B2, and B3. □ = samples C1, C2, C3, C4 and C5. o = samples A4 and B4.*

Table 6.12 *Regression summary for dependent variable 100-U*

R= .97 R^2= .94 Adjusted R^2= .92						
F(3,10)=50.59 p<.00000 Standard Error of estimate: 2.00						
	B	*St. Err. of B*	*t(11)*	*p-level*	*Partial Cor.*	*Semipart Cor.*
Intercept	37.18	2.74	13.58	0.00		
Predicted PGEM liberation	-0.54	0.06	-8.79	0.00	-0.94	-0.69
pn/(pn+mil)	22.80	2.06	11.06	0.00	0.96	0.87
BMS median ECD <2mm	-0.31	0.10	-3.02	0.01	-0.69	-0.24
Independent variables not in equation						
% non-sulphide PGEM				0.94	0.02	0.01
PGEM median ECD <2mm				0.90	0.04	0.01
pentlandite				0.99	0.00	0.00
Predicted BMS liberation				0.76	0.11	0.03
Chromite median ECD <2mm				0.23	-0.39	-0.10
Cu				0.20	0.19	0.05
Ni				0.57	-0.42	-0.10
PGE+Au				0.83	-0.07	-0.02

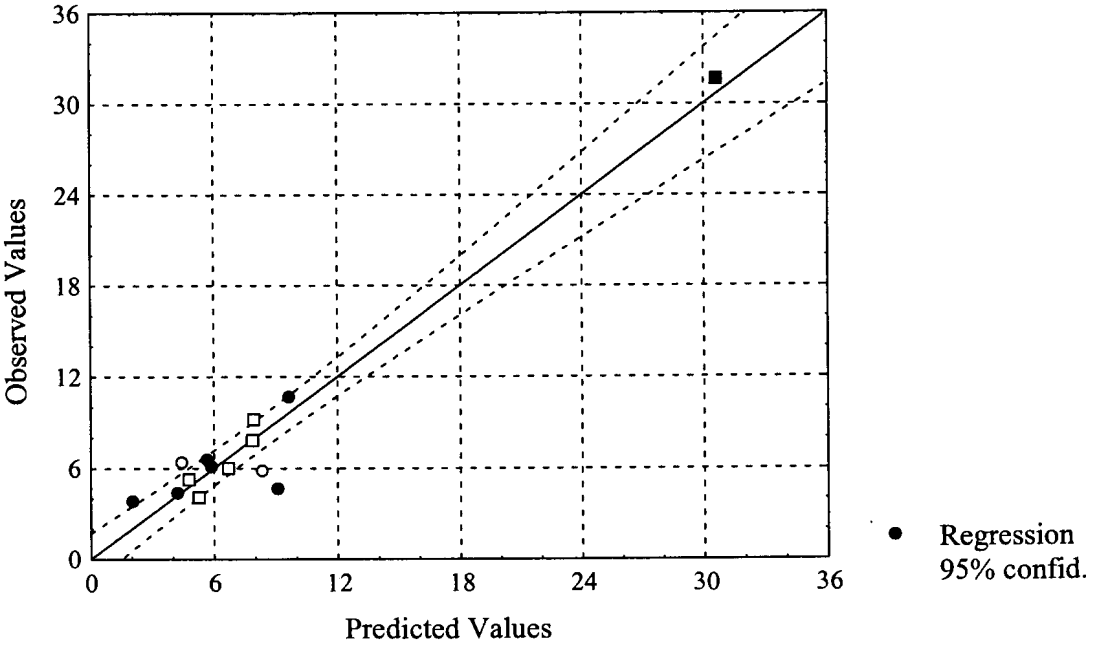

Figure 121 *Comparison of observed and predicted values of 100-U based on predicted PGE mineral liberation, pentlandite/(pentlandite+millerite) ratio, base-metal sulphide grain size prior to milling. ● = samples A1, A2, A3, B1, B2, and B3. □ = samples C1, C2, C3, C4 and C5. o = samples A4 and B4. ■ = sample A5.*

Flotation rate of fast- and slow-floating fractions (k_f and k_s)

No satisfactory model could be found for the prediction of k_f or k_s (Tables 6 and 7, Appendix K).

6.6.3 Relationship between flotation characteristics and selected mineralogical parameters in milled ore.

The mineralogical characteristics of the milled ore can be summarised by the following parameters:

- combined liberation index of PGE mineral-bearing particles
- amount of non-sulphide PGE mineral
- PGE mineral grain diameter expressed as median diameter based on per cent number of grains
- base-metal sulphide degree of liberation
- base-metal sulphide grain size expressed as median diameter
- ratio PGEM/(PGEM+BMS) in particles with a combined liberation index of >0.8
- amount of pentlandite
- pentlandite/(pentlandite+millerite) ratio

PGE mineral liberation (CLI>0.8, CLI>0.6 and CLI>0.4)

The relationships between the degree of PGE mineral liberation and the different flotation parameters are similar to those between the predicted degree of PGE mineral liberation and the flotation parameters. As expected from the examination of mineral particles in the flotation products, the higher the degree of PGE mineral liberation (CLI>0.8), the higher the value for R_f. The regression coefficient for these two parameters for the relatively unaltered UG2 ores (samples A2, B2, A3, B3, A1 and B1) is 0.94 (Table 6.5 and Figure 122). The millerite-bearing samples from area C plot slightly above the regression line for the relatively unaltered ores, due to the better than expected flotation of composite particles from these ores. For the sintered ores (A4 and B4), the actual values for R_f are much lower than expected, as a result of

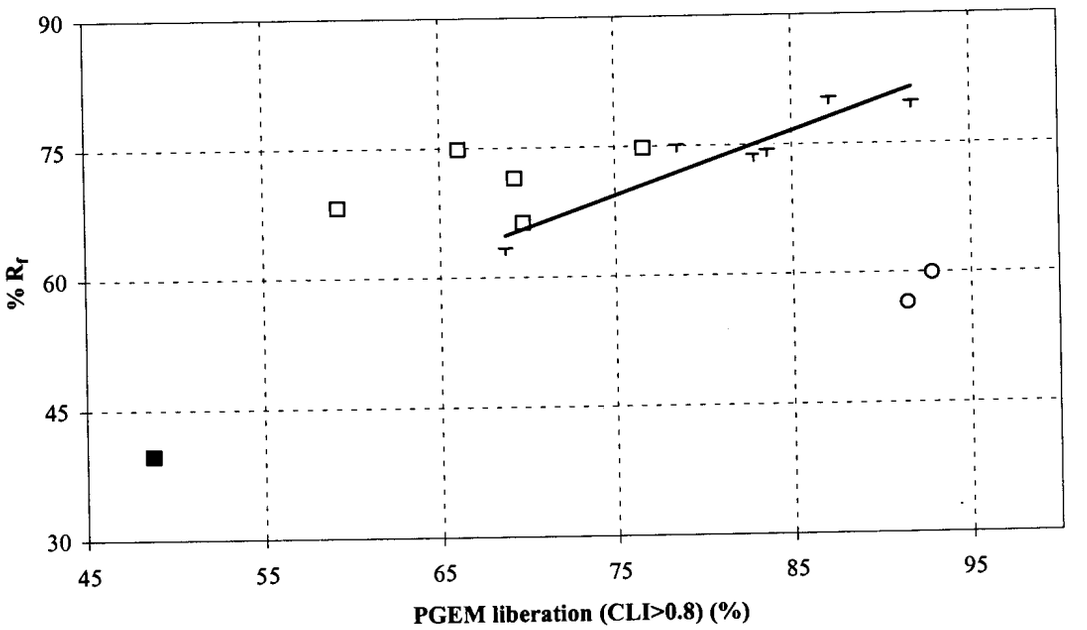

Figure 122 *Relationship between PGE mineral liberation in the milled flotation feed and % R_f. + = samples A1, A2, A3, B1, B2 and B3. □ = samples C1, C2, C3, C4 and C5. o = samples A4 and B4. ■ = sample A5. Regression line calculated for relatively unaltered samples A1, A2, A3, B1, B2 and B3.*

the presence of significant amounts of liberated, but slow-floating, non-sulphide PGE minerals in these two samples.

For R_s the inverse relationship holds – the higher the degree of liberation of PGE minerals and the sulphides associated with them, the lower the proportion of slow-floating PGE minerals (Figure 123) (Pearson correlation coefficient for the relatively unaltered UG2 samples is –0.89 (Table 6.5)). The R_s values for the millerite-bearing samples from area C plot close to, but slightly lower than the regression line. As expected, the R_s values for sintered samples A4 and B4, are relatively high. Cataclastic sample A5 appears to follow the same trend as the millerite-bearing samples. The situation is very similar for the non-floatable PGE+Au (Table 6.5, Figure 124).

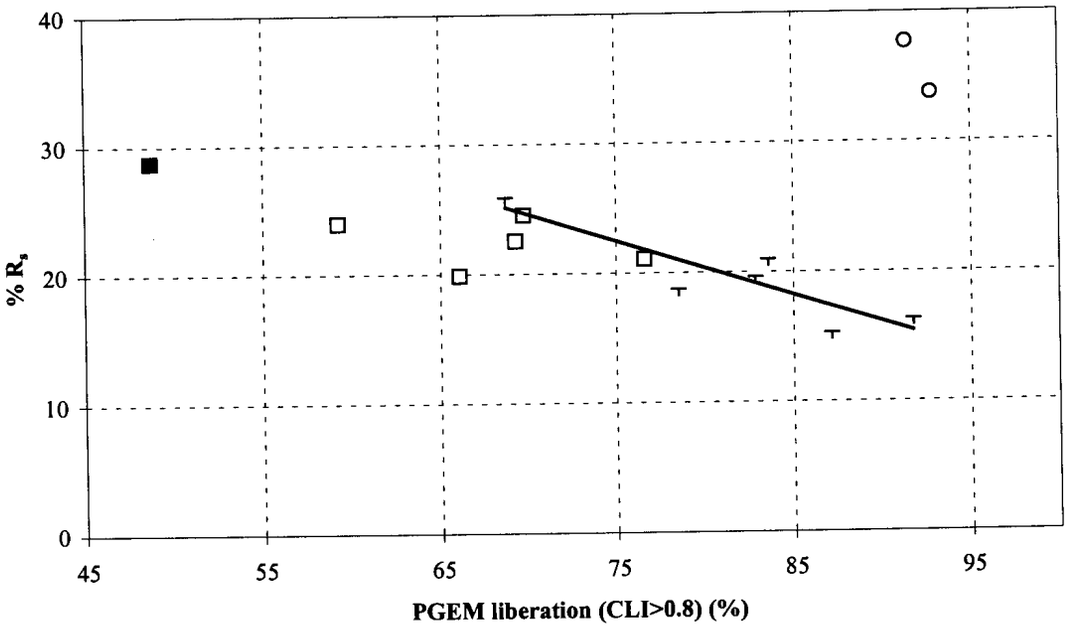

Figure 123 *Relationship between PGE mineral liberation in milled flotation feed and R_s. + = samples A1, A2, A3, B1, B2 and B3. □ = samples C1, C2, C3, C4 and C5. o = samples A4 and B4. ■ = sample A5. Regression line calculated for relatively unaltered samples, A1, A2, A3, B1, B2 and B3.*

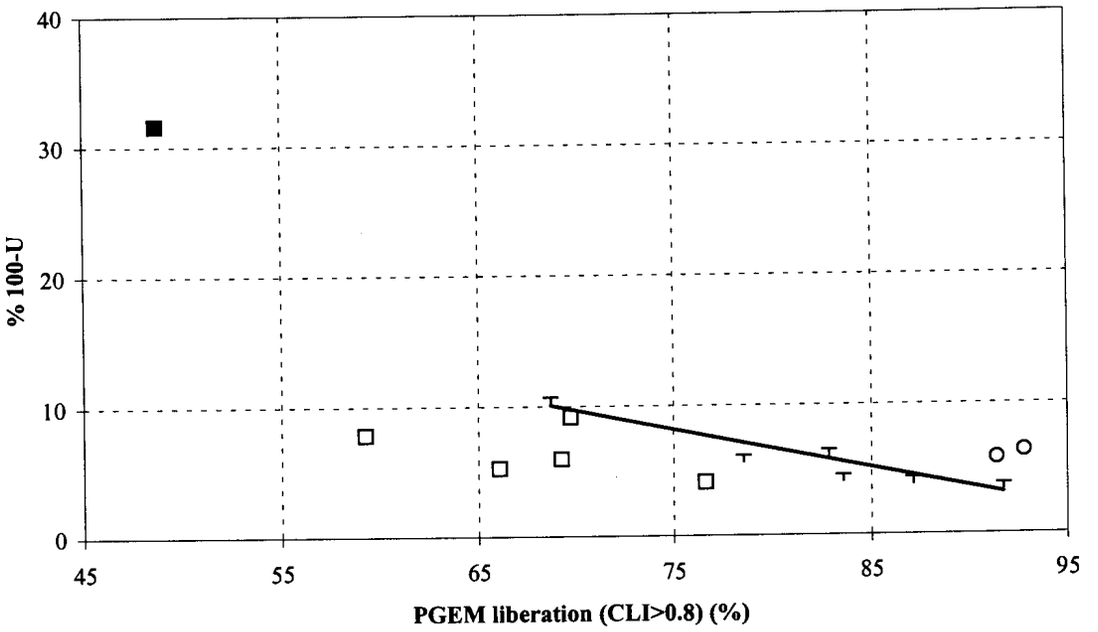

Figure 124 *Relationship between PGE mineral liberation in flotation feed and % non-floatable fraction. + = samples A1, A2, A3, B1, B2 and B3. □ = samples C1, C2, C3, C4 and C5. o = samples A4 and B4. ■ = sample A5. Regression line calculated for relatively unaltered samples, A1, A2, A3, B1, B2 and B3.*

The nature of the relationships between the degree of PGE mineral liberation and k_s and k_f, is unclear (Figure 111).

Since it is known that a very small floatable component can, under the right circumstances, induce flotation of a composite particle (Trahar, 1991; Sutherland, 1989), the relationships between the amount of PGE mineral-bearing particles with CLI>0.6 and CLI>0.4 were also investigated. The general trends were found to be the same as for CLI>0.8, but the regression coefficients are lower (Table 6.5). Consequently, CLI>0.8 was selected as the independent variable during regression analysis.

PGE mineral grain diameter at 80%<75µm (PGEMS2)

The relationship between PGE mineral size after milling, and all five flotation parameters appear to be random (Figure 111). Even though the mineralogical examination of the flotation products have indicated better recovery of coarser PGE mineral grains, the difference in PGE mineral grain size between the different samples may not be large enough to affect flotation results.

Base-metal sulphide degree of liberation (BMSLib2)

For relatively unaltered UG2 samples, a linear relationship exists between base-metal sulphide liberation and R_f (0.83) and R_s (-0.89) (Table 6.5). To a large extent this is a reflection of the correlation between the degree of liberation between PGE minerals and base-metal sulphide. The relationship does not hold for the remainder of the samples.

Base-metal sulphide grain diameter at 80%<75µm (BMSS2)

The relationships between base-metal sulphide grain diameter after milling and all five flotation parameters appear to be random (Figure 111).

Amount of liberated PGE mineral as a ratio of all particles with a combined liberation index of >0.8 (PGEM:BMS)

It has been shown that the higher the base-metal sulphide component in PGE mineral-bearing particles, the faster-floating the particle. In other words, liberated PGE

mineral particles generally float slower than particles consisting of liberated base-metal sulphide grains. For the relatively unaltered samples (A1, A2, A3, B1, B2 and B3) there is a strong negative correlation between R_f and (PGEM:BMS)(r=-0.86 in Table 6.5), with the inverse relationship holding for R_s and 100-U. (Figure 125). For the millerite-bearing samples from area C, the relationships appear to be reversed (Table 6.5). This may be related to differences in the nature of the base-metal sulphide and PGE minerals from the different areas, but more data is required before any conclusions can be drawn.

6.6.4 Predicting flotation parameters from milled UG2 ore

Fast-floating fraction (R_f)

For most samples, R_f largely depends on the degree of liberation of the PGE minerals, with lower than expected values for samples with a significant proportion of slow-floating, non-sulphide PGE mineral contents. Multiple regression analysis confirmed that the amount of fast-floating PGE+Au can be predicted from the PGE mineral liberation and the amount of non-sulphide PGE mineral, but the relationship is not very stable and depends to a large extent on cataclastic sample A5 (Table 6.13 and Figure 125 and Tables 8a and b, Appendix K).

The prediction can be improved by the inclusion of the PGE mineral grain size prior to milling, the degree of base-metal sulphide liberation and the pentlandite/(pentlandite+millerite) ratio (Table 6.14 and Figure 126, Tables 9a and 9b, Appendix K), partly due to the better than expected recovery of composite particles in millerite-bearing samples from area C.

Slow-floating fraction (R_s)

The amount of slow-floating PGE+Au can be predicted using the degree of PGE mineral liberation, the amount of non-sulphide PGE mineral, and the PGE mineral and chromite grain diameters in the crushed ore as independent variables (Table 6.15 and Figure 127 and Tables 10a and b, Appendix K). With increasing retention time, a significant proportion of particles reports to flotation concentrates as a result of other processes, such as entrainment, rather than true flotation. Consequently the recovery process becomes more unpredictable and it is therefore difficult to predict R_s. In

addition, the behaviour of composite grains, many of which report to the slower-floating concentrates, is still poorly understood.

Non-floating fraction (100-U)

No satisfactory model could be generated for the prediction of 100-U (Table 11, Appendix K). Examination of flotation tailings indicated that most of the PGE mineral grains in the flotation tailings are present in composite grains with only a small floatable component. The unpredictable behaviour of such particles has already been discussed. In addition, the presence of occasional liberated PGE mineral grains in some of the tailings samples were difficult to explain. While composition and grain size may have played a role, not enough grains were examined to reach any conclusion in this regard. It is possible that some of these grains may have become trapped between silicate grains and thus prevented from floating, especially where a lot of fine silicates were present.

Table 6.13 *Regression summary for R_f with PGE mineral degree of liberation and amount of non-sulphide PGE mineral as independent parameters.*

R= .96 R^2= .92 Adjusted R^2= .91 F(2,11)=67.23 p<.00000 Standard Error of estimate: 3.26						
	B	*St. Err. of B*	*t(11)*	*p-level*	*Partial Cor.*	*Semipart Cor.*
Intercept	40.80	5.29	7.72	0.00		
PGEM with CLI>0.8	0.47	0.07	6.79	0.00	0.90	0.56
% non-sulphide PGEM	-0.31	0.03	-10.24	0.00	-0.95	-0.85
Independent variables not in equation						
PGEM median diameter <75µm				0.66	0.14	0.04
BMS median diameter <75µm				0.54	0.20	0.05
pentlandite				0.75	0.10	0.03
pn/(pn+mil)				0.82	-0.07	-0.02
Cu				0.05	-0.58	-0.16
Ni				0.29	0.33	0.09
PGE+Au				0.05	-0.58	-0.16
PGEM/PGEM+BMS)				0.51	-0.21	-0.06

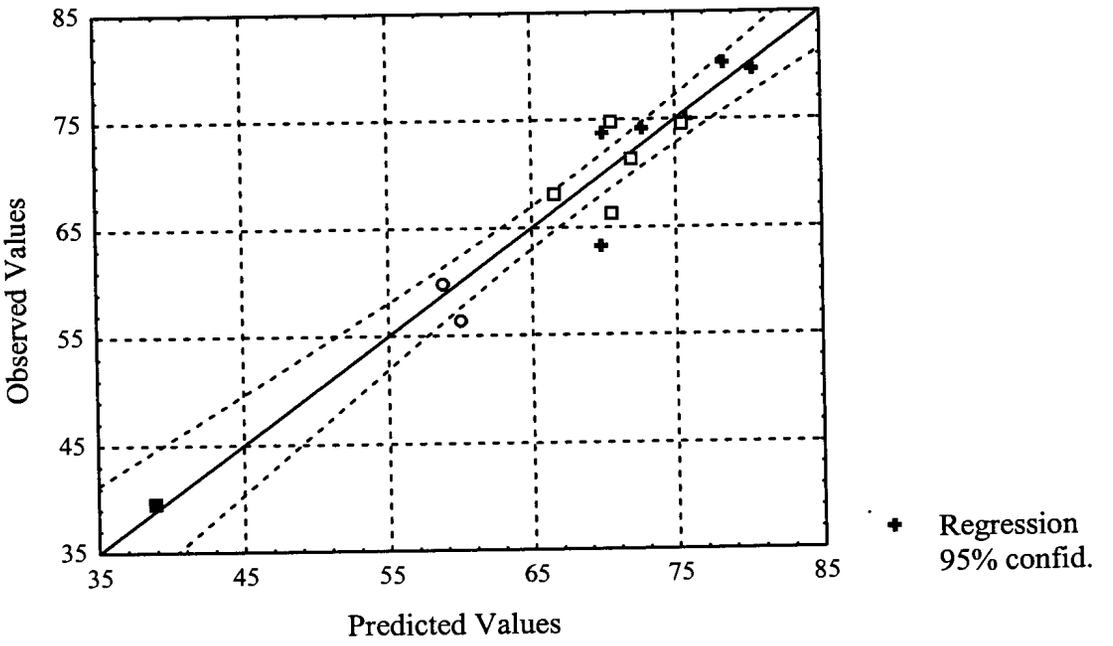

Figure 125 *Comparison of observed and predicted values of R_f based on PGE mineral liberation and amount of non-sulphide PGE mineral. + = samples A1, A2, A3, B1, B2, and B3. □ = samples C1, C2, C3, C4 and C5. o = samples A4 and B4. ■ = sample A5.*

Rate of flotation of fast- and slow-floating fractions (k_f and k_s)

No satisfactory model could be generated to predict the non-floatable fraction, k_f or k_s (Tables 12 and 13, Appendix K). These parameters are probably affected by very small differences between particles. Differences in k_f and k_s may conceivably occur in response to enviromental factors such as humidity or the time lapsed between milling of the ore and flotation, which can affect the surface characteristics of particles.

6.6.5 Factors affecting the recovery of individual PGEs

Although this aspect wasn't investigated in detail, some interesting observations were made. For example, palladium appeared to be slower-floating in samples of sintered UG2 chromitite. The reasons for this could not be established. Palladium levels in

Table 6.14 *Regression summary for R_f with PGE mineral degree of liberation, % non-sulphide PGE mineral, PGE mineral grain diameter before crushing, base-metal sulphide degree of liberation and pentlandite/(pentlandite+millerite) ratio as independent variables.*

$R = .99$ $R^2 = .98$ Adjusted $R^2 = .97$ $F(5,8) = 89.485$ $p < .00000$ Std.Error of estimate: 1.84						
	B	*St. Err. of B*	*t(8)*	*p-level*	*Partial*	*Semipart*
Intercept	62.08	6.39	9.72	0.00		
PGEM with CLI>0.8	0.47	0.04	10.75	0.00	-0.32	-0.04
% non-sulphide PGEM	-0.34	0.02	-14.39	0.00	-0.14	-0.02
PGEM grain diameter <2mm	-9.15	1.91	-4.80	0.00	-0.09	-0.01
BMS degree of liberation	0.08	0.03	2.54	0.03	0.06	0.01
pn/(pn+mil)	-7.56	2.06	-3.67	0.01	-0.33	-0.04
Independent variables not in equation						
PGEM grain diameter <75µm				0.40	-0.53	-0.07
pentlandite content				0.71	-0.55	-0.07
PGEM/PGEM+BMS)				0.82		
Nickel content				0.87		
PGE+Au				0.38		
Cu content				0.13		
Chromite grain diameter				0.12		

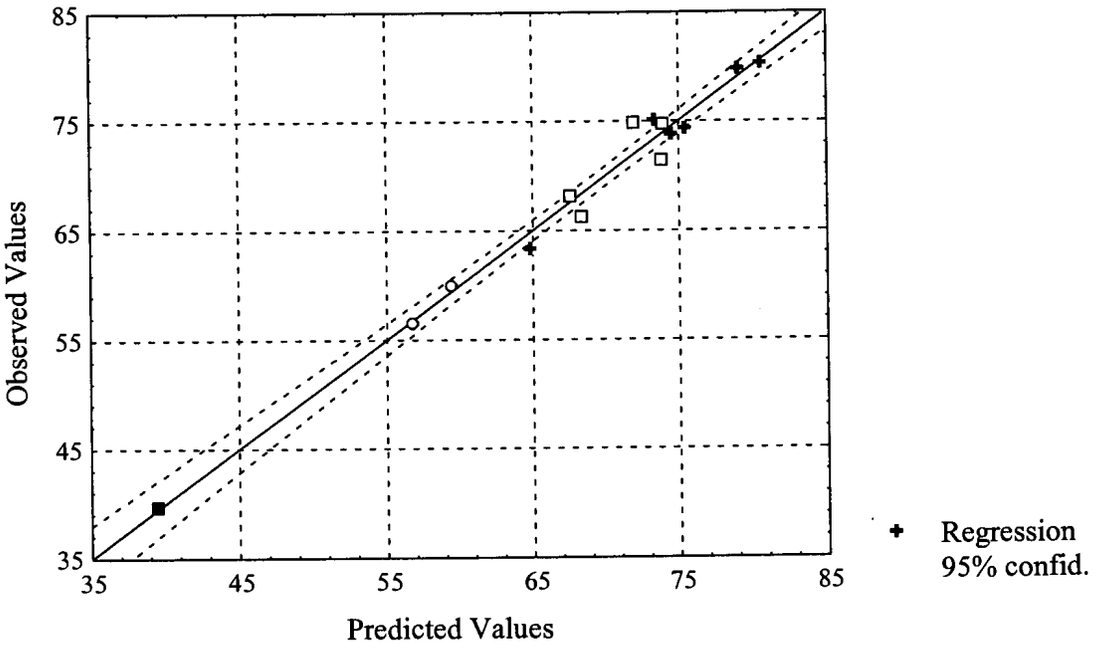

Figure 126 *Comparison of observed and predicted values of R_f based on PGE mineral liberation , amount of non-sulphide PGE mineral, base-metal sulphide liberation, pentlandite/(pentlandite+millerite) ratio, and median PGE mineral grain diameter before crushing. + = samples A1, A2, A3, B1, B2, and B3. □ = samples C1, C2, C3, C4 and C5. o = samples A4 and B4. ■ = sample A5.*

Table 6.15 *Regression summary for R_s based on PGE mineral liberation, amount of non-sulphide PGE mineral and PGE mineral and chromite grain diameter prior to milling.*

$R= .996$ $R^2= .99$ Adjusted $R^2= .99$ $F(4,9)= 317.04$ $p<.00000$ Standard Error of estimate: 0.64						
	B	*St. Err. of B*	*t(10)*	*p-level*	*Partial Cor.*	*Semipart Cor.*
Intercept	-6.04	2.05	-2.94	0.02		
PGEM with CLI>0.8	-0.16	0.02	-7.68	0.00	-0.93	-0.22
% non-sulphide PGEM	0.20	0.01	20.88	0.00	0.99	0.58
PGEM ECD <2mm	6.02	0.66	9.15	0.00	0.95	0.26
Chromite ECD <2mm	0.12	0.01	10.94	0.00	0.96	0.31
Independent variables not in equation						
PGEM ECD 80%<75µm					0.25	0.02
pentlandite					0.02	0.00
PGEM ass. w. BMS					0.15	0.01
BMS liberation					0.02	0.00
BMS ECD 80%<75µm					-0.68	-0.06
pn/(pn+mil)					0.06	0.00

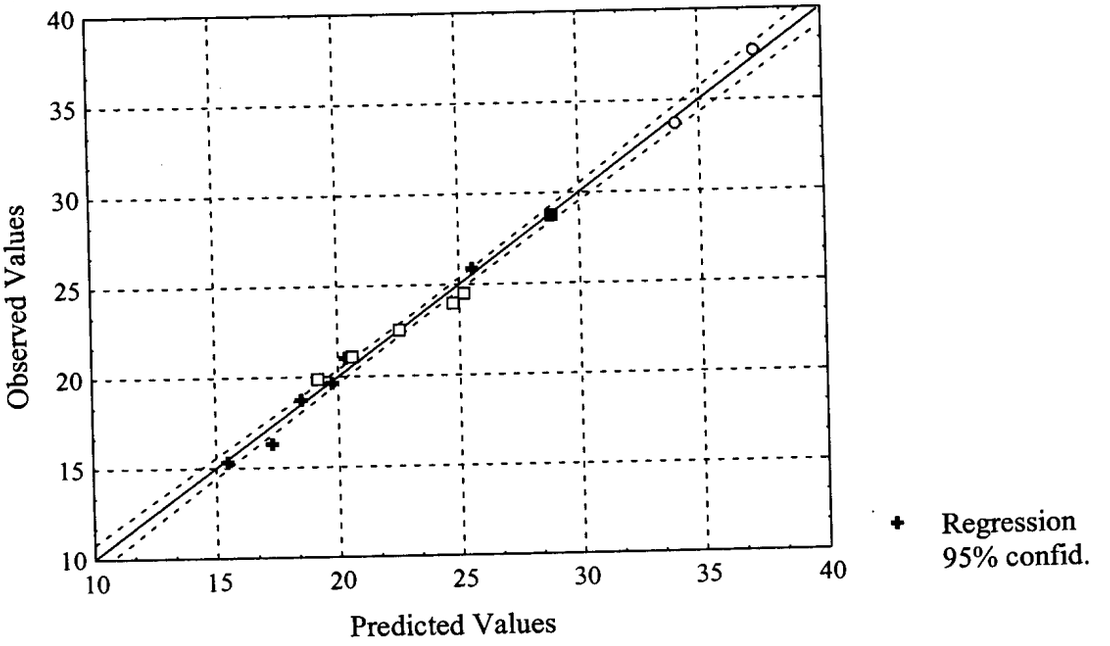

Figure 127 *Comparison of observed and predicted values of R_s based on PGE mineral liberation, amount of non-sulphide PGE mineral and PGE mineral and chromite grain diameter prior to milling. + = samples A1, A2, A3, B1, B2, and B3. □ = samples C1, C2, C3, C4 and C5. o = samples A4 and B4. ■ = sample A5.*

pentlandite appeared to be similar in relatively unaltered and sintered chromitite, and both platinum and palladium tend to occur in non-sulphide PGE minerals.

Another interesting observation relates to the comparison of platinum and palladium rate of flotation in samples of relatively unaltered UG2 with that in millerite-bearing samples from area C. In relatively unaltered UG2 a proportion of the palladium occurs sub-microscopically in pentlandite. Pentlandite is scarce in millerite-bearing samples from area C. The apparent absence of any differences in the flotation behaviour of palladium compared to platinum in the two sets of samples, suggests that the presence of submicroscopic palladium in pentlandite did not have any significant affect on palladium recovery.

7. DISCUSSION

As a result of this study it was possible to identify different types of UG2 chromitite and the major factors affecting the recovery of the PGEs using mineralogical characteristics quantified by image analysis. Although several shortcomings have been identified in this approach, many of these can only be addressed once further technological advances have been made.

7.1 Characterisation of PGE-mineral bearing particles

7.1.1 PGE minerals

Fully automated quantification of grains as small and complex, and present at such low concentration levels as the PGE minerals in the UG2 chromitite, unfortunately remains beyond reach. The semi-automated process proposed here is labour intensive and expensive, but still much faster and more objective than manual searching techniques. For practical reasons, a sample of 200 PGE mineral grains was accepted as being representative of a given sample. This is a relatively small sample, and the errors associated with it are large. In the low-grade tailings samples the problem is even worse, as collection of data on more than approximately fifty PGE mineral grains during routine analysis is impractical. However, in the day-to-day investigations undertaken by most mineral processing laboratories, a limited amount of data on a relatively small number of grains is often all that is required to solve the problem in hand.

7.1.2 Associated minerals

The characterisation of the associated minerals is as important as that of the PGE minerals themselves, as it determines the flotation behaviour of composite particles, as well as the nature of the gangue in flotation concentrates. In the case of the base-metal sulphides, backscattered-electron intensities are sometimes so close together, e.g. for pentlandite and chalcopyrite, that grey level is an unreliable method of discriminating between different phases. Variability in sulphide composition, especially in the case of pentlandite, compounds the problem. The relative proportions of the individual base-metal sulphides was obtained using EDS analysis on a coarse grid pattern. Obtaining textural information on individual sulphides (grain size, mode

of occurrence and liberation) is more problematic as it would require characterisation of each pixel belonging to sulphide by EDS analysis, a process which could take an hour or longer for each particle. As a result, the base-metal sulphide mineralogy was quantified in terms of mode of occurrence and size of total base-metal sulphide, rather than for the individual sulphides. This is a drawback, as the different sulphide minerals do not behave in the same way during processing of the ore. Pyrrhotite for instance, is slow-floating compared to the other base-metal sulphides. In addition, pentlandite appears to be the only sulphide mineral containing appreciable amounts of PGEs in its structure.

For similar reasons, the individual minerals in the silicate component could not be recognised during analysis. Consequently, all silicate minerals were classed together as silicate gangue. As talc is naturally floatable, and most other silicates are not, this is a shortcoming, and certainly one of the reasons for the apparent unpredictability of the flotation behaviour of composite particles.

With newer technology it is already possible to achieve faster analysis and processing times, and the resolution and stability of backscattered-electron detectors are improving. Consequently, accurate characterisation of PGE-bearing particles should become less of a problem in the future.

7.2 In situ trace-element analysis

7.2.1 Base-metal sulphide

Electron-microprobe analysis has indicated that pentlandite hosts significant amounts of submicroscopic palladium and rhodium. In most samples, pentlandite is also the most abundant base-metal sulphide mineral. If the other base-metal sulphide minerals do accommodate submicroscopic PGEs, it is generally at concentration levels below the detection limits of the routine electron-microprobe technique, and probably represents a relatively small proportion of the total PGEs. From a mineral processing point of view, it is more important to obtain a good average value for the PGE concentration in pentlandite. The relatively high detection limits associated with the electron-microprobe technique is therefore not the biggest concern.

Obtaining suitable standards for the in situ trace-element analysis is a bigger problem, and should be addressed before further analyses are attempted. Once this has been achieved, the next challenge is to obtain accurate pentlandite compositions to determine a reliable average for UG2 chromitite, and establishing whether this can be related to different types of UG2 chromitite. Considering the small grain sizes and low, but variable, concentration levels, this is no easy task.

7.2.2 Chromite

Considering the high chromite content of the UG2 ore, any submicroscopic PGEs, even at the ppb level, might represent a significant proportion of the total PGE. For instance, at 67 per cent chromite, an average concentration level of 150 ppb PGE in chromite represents a total of 0.1 ppm. This fraction of PGEs would be impossible to recover using the current technology. The possibility that chromite can accommodate PGEs in its crystal structure deserves to be further investigated.

7.3 Effect of geological environment on mineralogy

As a result of the small number of samples studied, limited information was obtained on the effect of geological environment on the mineralogy of UG2 chromitite. For instance, a much larger number of samples would need to be studied to determine the effect, if any, of pothole structures on the mineralogy. This should ideally involve the collection of samples at different distances from the centre of potholes.

7.4 Relating mineralogical characteristics to recovery

Information obtained from the mineralogical examination of different flotation products indicated that the rate of recovery of PGE+Au depends largely on the degree of liberation of the PGE minerals and base-metal sulphides, and the amount of slow-floating non-sulphide PGE minerals. This premise was confirmed using multiple regression analysis. A number of factors contribute to scattering of data points about the regression line:

- Relatively large statistical errors during data collection is an inevitable consequence of the low concentration levels at which the PGEs are present in the UG2 chromitite.

- Because of the low concentration levels of PGEs, a huge effort is required to collect data on a relatively small number of grains. As a result, only a few samples was analysed, leading to further uncertainties.

- More information on silicate distribution and flotation behaviour is necessary to accurately predict the behaviour of composite particles.

- Although the bulk composition, liberation, and size of a particle are key factors affecting its response to flotation, surface composition and topography control surface reactivity, and therefore also play a major role. Such effects were not taken into account during the current study. Time-of-flight secondary ion mass spectrometry (TOF-SIMS) makes it possible to characterise the surface composition of mineral particles (Stowe *et al.*, 1995). This type of information may further contribute to the understanding of the flotation behaviour of base-metal sulphide and PGE minerals.

7.5 Concentrate grade

Concentrate grade is an important flotation parameter. For the purpose of the current project, the flotation procedure was limited to rougher flotation with no cleaning stages. As a result, the concentrate grades were very low, to a large extent obscuring any trends with regard to grade. Most of the silicate and chromite particles in the flotation concentrates do not have any PGE or base-metal sulphide minerals attached to them. Some of these particles report to the flotation concentrates because of the natural floatability of talc, many more do so as a result of entrainment, which is facilitated by small particle sizes. Understanding all the factors affecting concentrate grade would require a much more detailed study of the behaviour of gangue minerals during flotation.

8. SUMMARY AND CONCLUSIONS

8.1 Characterisation of UG2 ore and mineral processing products

Using the current technology, it is not possible to characterise all aspects of the mineralogy of the UG2 ore and its mineral processing products using fully automated image analysis. However, the data generated using semi-automated image analysis techniques was sufficient to quantify mineralogical differences between the different samples. These mineralogical differences could be related to different geological environments. Characterisation of the mineralogy of different flotation products allowed for the identification of fast-, slow- and non-floating particles, thereby explaining differences in the flotation response of different types of UG2 chromitite.

8.2 Relating variations in mineralogy to geological environment

Large variations in mineralogy, in terms of the modal proportions and compositions of minerals, as well as their textural settings, were observed in the UG2 chromitite layer over a relatively short distance (~50 km). These mineralogical variations can often be related to local geological disturbances such as the presence of iron-rich ultrabasic replacement pegmatoid or faulting, but in some cases appear to result from larger scale hydrothermal activity.

- Relatively unaltered UG2 chromitite (represented by samples A1, A2, A3, B1, B2 and B3) consists of rounded chromite grains in a primary silicate matrix, comprising predominantly plagioclase and orthopyroxene, with minor phlogopite, clinopyroxene, and secondary silicates such as talc and chlorite. Minor sintering of chromite grains may be present. Base-metal sulphides, mostly pentlandite, pyrrhotite, chalcopyrite and minor pyrite, occur at concentration levels of <0.1 volume per cent, frequently as composite grains (median equivalent circle diameter ~30 μm), usually at chromite/silicate grain boundaries.

  PGEs occur both as discrete PGE minerals and sub-microscopically (in solid solution?) in base-metal sulphides. The PGE mineral assemblage consists predominantly of platinum and/or palladium-sulphide (cooperite, braggite and vysotskite), platinum-rhodium-copper-nickel-sulphide (nickeloan malanite) and laurite ($(Ru,Os,Ir)S_2$). The PGE mineral grains are small (median equivalent

circle diameter ~6.5 μm), and are generally associated with base-metal sulphides, predominantly pentlandite, often situated at grain boundaries. Small amounts of palladium and rhodium are hosted submicroscopically in pentlandite.

Although, this group of samples includes UG2 chromitite with anorthosite, norite and pegmatoid footwall, as well as samples collected from the edges of pothole structures, the mineralogical and chemical characteristics are very similar.

- The local interaction of UG2 chromitite with late stage, Fe-and Ti-rich hydrothermal fluids led to the formation of iron-rich ultrabasic replacement pegmatoid footwall, and in the UG2 itself caused the enlargement of chromite grains through sintering. This gave rise to the sintered samples, A4 and B4. The silicate mineralogy is characterised by the formation of minor clinopyroxene and amphibole as a result of the interaction with fluids. PGE mineral assemblages are dominated by laurite, Pt-Rh-Fe and Pt-Pd-Fe alloys, and other non-sulphide PGE minerals. In the samples examined, the base-metal sulphide assemblage does not appear to have been affected, apart from an increase in grain size.

- A more prominent, and regionally important group, is the millerite-bearing UG2 chromitite, represented by samples C1 to C5. Interaction of magmatic base-metal sulphides with low temperature hydrothermal fluids lead to the corrosion of sulphides and the precipitation of sulphide-rich, low temperature chalcopyrite-millerite-pyrite±siegenite assemblages. The size reduction of base-metal sulphide grains resulted in the isolation of PGE minerals from base-metal sulphides, with PGE minerals occurring in the vicinity of, but not necessarily in direct contact with, the base-metal sulphides. PGE mineral assemblages from these areas are characterised by a decrease in the relative amount of cooperite, and an increase in braggite and nickeloan malanite, compared to relatively unaltered UG2. Primary silicate assemblages in UG2 chromitite have to varying extents been replaced by albite, quartz, pumpellyite, epidote, prehnite, chlorite, sphene and talc.

- Faulting can cause local cataclasis of chromitite, and in this study A5 represents such a case. Fractures act as conduits for fluids, leading to the cementation of fractured chromite grains by low-temperature hydrous silicates, quartz and calcite.

These conditions lead to the formation of non-sulphide PGE minerals, often enclosed in silicate.

8.3 Factors affecting the flotation response of PGE mineral-bearing particles

A large proportion of the PGE minerals in the milled feed samples are present as liberated particles (between 48 and 79 per cent). Milling of the ore caused an even further reduction in the grain size of the already small PGE mineral grains, resulting in a median measured PGE mineral diameter of ~5 μm in the milled product. In samples of relatively unaltered (A1, A2, A3, B1, B2 and B3) and sintered UG2 chromitite (A4 and B4), the remainder of the PGE minerals are mostly associated with liberated base-metal sulphide grains. In samples characterised by the association of PGE minerals and base-metal sulphide with secondary silicates, such as the millerite-bearing (C1 to C5) and cataclastic UG2 chromitite (A5), a large proportion of the PGE minerals in the milled product occurs in particles with a significant gangue component. A small proportion of the total PGEs is present submicroscopically in pentlandite, most of which is present as liberated particles, or as part of liberated base-metal sulphide particles. Poor liberation accounts for most of the PGE minerals in the tailings samples.

Examination of the different flotation products indicates that most of the PGE minerals reporting to the flotation concentrates are liberated PGE minerals. The rate of flotation of PGE minerals is determined by grain size and type of mineral, with the coarsest grains recovered to the faster-floating concentrates. Flotation rates for the different PGE minerals, in decreasing order, are braggite > cooperite > malanite ≈ Pt-Fe alloy and other non-sulphide PGE minerals. PGE minerals associated with liberated base-metal sulphides also report to flotation concentrates, and are generally faster-floating than liberated PGE minerals. Some of the PGEs, especially palladium and rhodium, are recovered with the base-metal sulphides, predominantly pentlandite, as a result of their presence in submicroscopic form. The rate of recovery for the individual sulphides appears to be pyrite > chalcopyrite ≥ millerite ≥ pentlandite >> pyrrhotite.

The flotation behaviour of composite particles is largely governed by the amount of exposed surface area of PGE mineral and base-metal sulphide in the particle. PGE

minerals report to the tailings predominantly in the form of inclusions in silicate, predominantly silicate. The recovery of composite particles also depends on particle size, with finer particles reporting to the faster-floating concentrates. Some samples are characterised by a faster than expected rate of recovery of composite particles. This has been attributed, at least partly, to the presence of naturally floatable talc.

8.4 Relating ore type to variations in flotation response

The flotation behaviour of the ores is described in terms of the amount of fast-floating PGE+Au recovered in the first one to two minutes of flotation (R_f), the amount of slow-floating PGE+Au (R_s), and the amount of non-floating PGE+Au (100-U), that fraction which would not be recovered even if flotation continued indefinitely. The rates of recovery for the fast-and slow-floating fractions (k_f and k_s) were also calculated.

Some of these flotation parameters could be related to mineralogical variations in the UG2 chromitite. Samples of sintered UG2 chromitite are characterised by a large amount of slow-floating PGE+Au, compared to relatively unaltered UG2. The non-floatable PGE+Au fraction, however, is similar in relatively unaltered and sintered UG2 chromitite. This is attributed to the presence of slow-floating non-sulphide PGE minerals in the sintered UG2 chromitite. It also seems that palladium, and possibly rhodium, tend to be slow-floating relative to platinum in these samples.

Cataclastic UG2 chromitite contains a large portion of non-floating PGE+Au, as a result of the association of PGE minerals and base-metal sulphides with secondary silicates in this ore. This results in poor liberation characteristics of the PGE minerals and base-metal sulphides, and consequently a large non-floating fraction in this type of ore.

Examination of the relationships between the flotation parameters and various mineralogical parameters indicates that PGE+Au recovery can be correlated with the mode of occurrence of the PGE minerals and base-metal sulphides, the amount of non-sulphide PGE minerals in the samples, the (pentlandite/pentlandite+millerite) ratio and chromite grain size. Using multiple regression analysis with these characteristics as independent parameters, variations in the R_f and R_s can be predicted fairly accurately.

8.5 Relating the characteristics of PGE mineral-bearing particles to flotation parameters

The flotation behaviour of PGE mineral-bearing particles seems to be determined largely by the degree of liberation and type of PGE and base-metal sulphide mineral. Although differences were observed in the median grain diameters of PGE minerals and base-metal sulphides in the different flotation products, differences between the samples are probably too small to have much of an effect. The apparently smaller sizes of the non-sulphide PGE minerals may however contribute to their slower-floating nature.

Multiple linear regression confirmed that R_f can to a large extent be predicted by the type and degree of liberation of the PGE minerals in the milled flotation feed. Much scattering of data-points about the regression line is present. Although this can be explained, at least partly, by the unpredictable behaviour of composite particles, other factors such as the small number of samples analysed and large statistical errors as a result of the low concentration levels of PGEs and base-metal sulphides also contributed. R_s and the non-floating fraction are even more difficult to accurately predict as, with long flotation times, recovery processes become complicated by the contribution of other processes such as entrainment. In the case of k_f and k_s more subtle differences, such as changes in surface composition, probably also affect these values.

8.6 Concluding remarks

While laboratory flotation tests can be performed relatively cheaply, and in a fraction of the time required for mineralogical analysis, these tests can not supply the reasons for variations in recovery. The approach developed and reported here has definite application to the study of PGE+Au recovery from the UG2 chromitite ores.

It has been demonstrated that reasonable estimates of the recovery of PGE+Au from UG2 chromitite can be made from chemical and mineralogical analysis of representative ore samples crushed to <2mm and/or 80%<75μm. When the results of laboratory flotation tests are combined with chemical and mineralogical characterization of samples ore from proposed mining areas, it becomes a powerful tool, making it possible to recognize different types of ore, and, more importantly,

potential problems during processing, allowing for provision for appropriate adjustments to metallurgical flowsheets.

REFERENCES

Anon. (1985). *Image analysis. Principles and Practice.* A Technical Handbook produced by Joyce-Loebl, A Vickers Company. Short Run Press, Exeter, 250 pp.

Anon. (1987). Exploitation of the UG-2 reef. *S.A. Mining, Coal, Gold and Base Minerals*, March 1987, pp.11-13.

Anon. (1988). Breakthrough in UG-2 development. *Hendrik Vorster's Mining Mirror,* **1**:5, pp. 6-10.

Ballhaus, C.G. (1988). Potholes of the Merensky Reef at Brakspruit Shaft, Rustenburg Platinum Mines: Primary disturbances in magmatic stratigraphy. *Economic Geology*, **83**, pp. 1140-1158.

Ballhaus, C. & Ryan, C.G. (1995). Platinum-group elements in the Merensky Reef. I. PGE in solid solution in base-metal sulfides and the down-temperature equilibration history of Merensky ores. *Contributions to Mineralogy and Petrology*, **122**, pp. 241-251.

Ballhaus, C.G. & Stumpfl, E.F. (1986). Sulfide and platinum mineralization in the Merensky Reef: evidence from hydrous silicates and fluid inclusions. *Contributions to Mineralogy and Petrology,* **94**, pp. 193-204.

Ballhaus, C. & Ulmer, P. (1995). Platinum-group elements in the Merensky Reef: II. Experimental solubilities of platinum and palladium in $Fe_{1-x}S$ from 950 to 450°C under controlled f_{S_2} and f_{H_2}. *Geochimica et Cosmochimica Acta*, **59:**23, pp. 4881-4888.

Barbery, G. (1992a). Liberation 1, 2, 3: Theoretical analysis of the effect of space dimension on mineral liberation by size reduction. *Minerals Engineering*, **5**, pp.123-141.

Barbery, G. (1992b). Latest developments in the interpretation of section measurements for liberation – practical aspects. *Canadian Metallurgical Quarterly*, **31**, pp.1-10.

Barkov, A.Y., Halkoaho, T.A.A., Laajoki, K.V.O., Alapieti, T.T., & Peura, R.A. (1997). Ruthenian pyrite and nickeloan malanite from the Imandra Layered Complex, Northwestern Russia. *Canadian Mineralogist*, **35**, pp. 887-897.

Barnes, S.J. & Campbell, I.H. (1988). Role of late magmatic fluids in Merensky type platinum deposits: A discussion. *Geology*, **16**, pp. 488-491.

Boudreau, A.E. (1992). Volatile overpressure in layered intrusion and the formation of potholes. *Australian Journal of Earth Sciences*, **39**, pp. 277-287.

Bozkurt, V., Xu, Z. & Finch, J.A. (1997). Pentlandite/pyrrhotite interaction and xanthate adsorption. *International Journal of Mineral Processing*, **52**, pp. 203-214.

Brugman, C.F. (1985). UG-2 reef of the Bushveld Complex - Executive comment. *Mintek Review,* **1**, Council for Mineral Technology, Randburg, South Africa, p. 2.

Buntin, T.J., Grandstaff, D.E. & Ulmer, G.C. (1985). A pilot study of geochemical and redox relationships between potholes and adjacent normal Merensky Reef of the Bushveld Complex. *Economic Geology*, **80**, pp. 975-987.

Bushell, C.L. (1987). Improved methods for the preparation of polished sections for microscopic analysis. *Mintek Report No. M309,* Council for Mineral Technology, Randburg, South Africa, 6 pp.

Cabella, R., Gazotti, M., & Lucchetti, G. (1997). Loveringite and baddeleyite in layers of chromian spinel from the Bracco ophiolitic unit, Northern Appenines, Italy. *Canadian Mineralogist*, **35**, pp. 899-908.

Cabri, L.J. (1981). The platinum-group minerals. *Platinum-group elements: Mineralogy, geology and recovery*, Cabri, L.J. (ed.). CIM Special Volume 23, The Canadian Institute of Mining and Metallurgy, pp. 83-150.

Cabri, L.J. (1991). Mineralogical balances in platinum-group element-bearing ores. *ICAM '91, International Congress on Applied Mineralogy, Papers,* Haughton, L.F. & Markgraaff, J. (eds.). Mineralogical Association of South Africa, Pretoria, **1,** Paper 9, 16 pp.

Cabri, L.J. (1992). The distribution of trace precious metals in minerals and mineral products. *Mineralogical Magazine*, **56**, pp. 298-308.

Cabri, L. J. (1994). Current status of determination of mineralogical balances for platinum-group element-bearing ores. *Transactions of the Institute of Mining and Metallurgy*, **103**, B3-B9.

Cabri, L.J. & LaFlamme, J.H.G. (1979). Mineralogy of samples from the Lac Des Iles area, Ontario. *Canmet Report 79-27*, Energy, Mines, Resources Canada, 20 pp.

Cabri, L.J. & LaFlamme, J.H.G. (1981). Analyses of minerals containing platinum-group elements. *Platinum-group elements: Mineralogy, geology and recovery*, Cabri, L.J. (ed.). CIM Special Volume 23, The Canadian Institute of Mining and Metallurgy, pp. 151-174.

Cabri, L.J., Blank, H., El Goresy, A., Gilles Laflamme, J.H., Nobiling, R., Sizgoric, M.B., & Traxel, K. (1984). Quantitative trace-element analyses of sulfides from Sudbury and Stillwater by proton microprobe. *The Canadian Mineralogist*, **22**, pp. 521-542.

Cabri, L.J. & McMahon, G. (1995). SIMS analysis of sulfide minerals for Pt and Au: Methodology and relative sensitivity factors (RSF). *The Canadian Mineralogist*, **33**, pp. 349-359.

Cabri, L.J. & McMahon, G. (1996). The quantitative determination of sub-ppm quantities of Au and Pt in sulfide minerals. *EPD Congress 1996*, Warren, G.W. (ed.). The Minerals and Materials Society, pp. 313-322.

Campbell, I.H. (1986). A fluid dynamic model for the potholes of the Merensky Reef. *Economic Geology*, **81**, pp. 1118-1125.

Capobianco, C.J. & Drake, M.J. (1990). Partitioning of ruthenium, rhodium and palladium between spinel and silicate melt and implications for platinum-group element fractionation trends. *Geochimica et Cosmochimica Acta*, **54**, pp. 869-874.

Capobianco, C.J., Hervig, R.L., & Drake, M.J. (1994). Experiments on crystal/liquid partitioning of Ru, Rh and Pd for magnetite and hematite solid solutions crystallized from silicate melt. *Chemical Geology*, **113**, pp. 23-43.

Carr, H.W., Groves, D.I., & Cawthorn, R.G. (1994a). Controls on the distribution of Merensky Reef potholes at the Western Platinum Mine, Bushveld Complex, South Africa: implications for disruptions of the layering and pothole formation in the Complex. *South African Journal of Geology*, **97**(4), pp. 431-441.

Carr, H.W., Groves, D.I., & Cawthorn, R.G. (1994b). The importance of synmagmatic deformation in the formation of Merensky Reef potholes in the Bushveld Complex. *Economic Geology*, **89**, pp. 1398-1410.

Carr, H.W., Kruger, F.J., Groves, D.I., & Cawthorn, R.G. (1999). *Mineralium Deposita*, **34**, pp. 335-347.

Cawthorn, R.G. (1999). The platinum and palladium resources of the Bushveld Complex. *South African Journal of Science*, **95**, 11/12.

Cawthorn, R.G. & Poulton, K.L. (1988). Evidence for fluid in the footwall beneath potholes in the Merensky Reef of the Bushveld Complex. *Geoplatinum '87*, Prichard, H.M., Potts, P.J., Bowles, J.F.W., & Cribb, S.J. (Eds.), Elsevier, pp. 343-356.

Cawthorn, R.G. & Barry, S.D. (1992). The role of intercumulus residua in the formation of pegmatoid associated with the UG-2 chromitite, Bushveld Complex. *Australian Journal of Earth Sciences*, **39**, pp. 263-276.

Chayes, F. (1956). *Petrographic modal analysis - An elementary statistical approach*. John Wiley & Sons Inc., New York, 113 pp.

Chayes, F. (1963). A brief history of petrographic modal analysis. *Proceedings of the 1st International Congress for Stereology,* Austria, pp. 7/1-7/6.

Cheney, E.S. & Twist, D. (1988). The conformable emplacement of the Bushveld mafic rocks along a regional unconformity. *Research Report No. 78,* Institute for Geological Research on the Bushveld Complex, University of Pretoria, 32 pp.

Cheng, X. & Iwasaki, I. (1992). Effect of chalcopyrite and pyrrhotite interaction on flotation separation. Minerals & Metallurgical Processing, **9**, pp. 73-79.

Coetzee, C.B. (ed.) (1976). *Delfstowwe van die Republiek van Suid-Afrika.* Department of Mining and Geological Survey, 477 pp.

Cook, N.J. (1990). Mineralogical examination of gold-bearing samples. *CIM Bulletin*, **83**: 944, pp. 51-55.

Corrans, I.J., Brugman, C.F., Overbeek, P.W. & McRae, L.B. (1982). The recovery of platinum-group metals from ore of the UG2 reef in the Bushveld Complex. *Proceedings of the 12th CMMI Congress,* Glen, H.W. (ed.). South African Institute of Mining and Metallurgy / Geological Society of South Africa, Johannesburg, pp. 629-634.

Cousins, C.A. & Feringa, G. (1964). The chromite deposits of the Western Belt of the Bushveld Complex. *The geology of some ore deposits in Southern Africa,* II, Haughton, S.H. (ed.). Geological Society of South Africa, Johannesburg, pp. 183-202.

Cousins, C.A. & Kinloch, E.D. (1976). Some observations on textures and inclusions in alluvial platinoids. *Economic Geology,* **71**, pp. 1377-1395.

Craig, J.R. & Kullerud, G. (1969). Phase relations in the Cu-Fe-Ni-S system and their application to magmatic ore deposits. *Magmatic ore deposits, Economic Geology, Monograph 4,* Wilson, H.D.B. (Ed.), pp. 344-358.

Czamanske, G.C., Kunilov, V.E., Zientek, M.L., Cabri, L.J., Likhachev, A.P., Calk, L.C. & Oscarson, R.L. (1992). A proton-microprobe study of magmatic sulfide ores from the Noril'sk-Talnakh district, Siberia. *The Canadian Mineralogist*, **30**, pp. 249-287.

Davey, S.R. (1992). Lateral variations within the upper Critical Zone of the Bushveld Complex on the farm Rooikoppies 297Q, Marikana, South Africa. *South African Journal of Geology*, **95**, pp. 141-149.

Deer, W.A., Howie, R.A., & Zussman, J. (1983). *An introduction to the rock-forming minerals.* 14th Impression, Longman Group Limited, 528 pp.

DeHoff, R.T. (1965). The estimation of particle-size distributions from simple counting measurements made on random plane sections. *Transactions of the Metallurgical Society of AIME,* **233**, pp. 25-29.

DeHoff, R.T., & Rhines, F.N. (1968). *Quantitative Microscopy*. McGraw-Hill Series in Materials Science and Engineering, 422 pp.

De Waal, S.A. (1972). The interrelation of the chemical, physical and certain metallurgical properties of chrome spinels from the Bushveld Igneous Complex. NIM Report 1415, National Institute for Metallurgy, Randburg, South Africa. 18 pp.

De Waal, S.A. (1975). The mineralogy, chemistry, and certain aspects of reactivity of chromitite from the Bushveld Igneous Complex. *NIM Report 1709*, National Institute for Metallurgy, Randburg, South Africa. 80 pp.

Dilks, A. & Graham, S.C. (1985). Quantitative mineralogical characterisation of sandstones by back-scattered electron image analysis. *Journal of Sedimentary Petrology*, **55**, pp. 347-355.

Distler, V.V., Malevskiy, A.Y., & Laputina, I.P. (1977). Distribution of platinoids between pyrrhotite and pentlandite in crystallization of a sulphide melt. *Geokhimiya,* **11**, pp. 1646-1657 (in Russian). Translation (1978): *Geochemistry International*, **146**, pp. 30-40.

Dowling, E.C., Klimpel, R.R. & Aplan, F.F. (1985). Model discrimination in the flotation of a porphyry copper ore. *Minerals and Metallurgical Processing*, **2**, pp. 87-101.

Eales, H.V. & Reynolds, I.M. (1986). Cryptic variations within chromitites of the Upper Critical Zone, Northwestern Bushveld Complex. *Economic Geology*, **81**, pp. 1056-1066.

Edwards, D. (1988). The Bushveld – luck of the Irish. *S.A. Mining, Coal, Gold and Base Minerals*, August 1988, p. 5-21.

Edwards, C.R., Kipkie, W.B. & Agar, G.E. (1980). The effect of slime coatings of the serpentine minerals, chrysotile and lizardite, on pentlandite flotation. *International Journal of Mineral Processing*, **7**, pp. 33-42.

Evstigneeva, T., Moh, G.H., & Tarkian, M. (1995). Hydrothermal recrystallization of PGE- and Fe-Ni-sulfide assemblages. *Neues Jahrbuch für Mineralogie Abhandlungen*, **169**, p. 273-277.

Farquhar, J. (1986). The Western Platinum Mine. *Mineral Deposits of Southern Africa,* Anhaeusser, C.R. and Maske, S. (eds.). Geological Society of South Africa, pp.1135-1142.

Ferrara, G., Preti, U., & Meloy, T.P. (1989). Inclusion shape, mineral texture and liberation. *International Journal of Mineral Processing*, **27**, pp. 295-308.

Fleet, M.E., Chryssoulis, S.L., Stone, S.L. & Weisener, C.G. (1993). Partitioning of platinum-group elements and Au in the Fe-Ni-Cu-S system: experiments on the fractional crystallization of sulfide melts. *Contributions to Mineralogy and Petrology*, **115**, pp. 36-44.

Fuchs, W.A. & Rose, A.W. (1974). The geochemical behaviour of platinum and palladium in the weathering cycle in the Stillwater Complex, Montana. *Economic Geology*, **69**, pp. 332-346.

Gain, S.B. (1985). The geologic setting of the platiniferous UG-2 chromitite layer on the farm Maandagshoek, Eastern Bushveld Complex. *Economic Geology*, **80**, pp. 925-943.

Gain, S.B. (1986). The Upper Group Chromitite layers at Maandagshoek, Eastern Bushveld Complex. *Mineral Deposits of Southern Africa,* Anhaeusser, C.R. & Maske, S. (eds.). Geological Society of South Africa, pp.1197-1208.

Garuti, G., Zaccarini, F., Moloshag, V, & Alimov, V. (1999). Platinum-group minerals as indicators of sulfur fugacity in ophiolitic upper mantle : An example from chromitites of the Ray-Iz ultramafic Complex, Polar Urals, Russia. *Canadian Mineralogist*, **37**, pp. 1099-1115.

Gateau, C. (1978). Quantitative image analysis. Applications to mineralogy. *Buletin de Minéralogie.*, **101**, pp. 305-314. (In French) NIM Translation TR 835.

Gateau, C. & Prevosteau, J.M. (1978). Examples of the applications of new possibilities for automatic image analysis. *Special Issues of Metallography,* **8**, pp. 280-287. Riederer-Verlag.

Gaudin, A.M. (1957). *Flotation*. McGraw Hill, New York, 2nd edition, 573 pp.

Gay, S.L. (1999). Numerical verification of a non-preferential-breakage liberation model. *International Journal of Mineral Processing*, **57**, pp. 125-134.

Genkin, A.D., Laputina, I.P. & Muravitskaya, G.N. (1974). Ruthenium- and rhodium containing pentlandite – an indicator of hydrothermal mobilization of platinum metals. *Geol. Rudnykh Mestorozh.*, **6**, pp. 102-106. Translation (1976*): International Geology Review*, **18**, pp. 723-728.

Gottlieb, P. & Adair, I. (1991). Quantification of talc rimming of chromites in Bushveld ores using QEM*SEM. *ICAM '91, International Congress on Applied Mineralogy, Papers,* Haughton, L.F. & Markgraaff, J. (eds.). Mineralogical Association of South Africa, Pretoria, **1,** Paper 18, 6 pp.

Gottlieb, P., Wilkie, G.J. & Adair, I. (1993). Recent developments in the application of QEM*SEM technology. *ICAM'93, International Congress on Applied Mineralogy, Abstracts,* Griffin, B., Graham, J. & Linge, H. (eds.). Held in Fremantle, Western Australia, May 31st – June 2nd, 1993, pp. 222-223.

Grimbeek, J.C. (1995). *The effect of the Vaalkop replacement pegmatoid on the sulphide mineralogy at Western Platinum Mine in the Mooinooi District.* Unpublished MSc. Thesis, University of Pretoria, Pretoria, 110 pp.

Gu, Y. (1998). Rapid mineral liberation analysis using the JKMRC/Philips MLA. *Mineralogy for Mineral Processing Engineers Workshop, SAIMM,* Cape Town, South Africa, 14 pp.

Guy, P.J. & Trahar, W.J. (1985). The effects of oxidation and mineral interaction on sulphide flotation. *Flotation of sulphide minerals*. Forssberg, K.S.E. (ed.). Developments in mineral processing, **6**, pp. 91-110.

Hahn, U.F. & Ovendale, B. (1994). UG2 chromitite potholes at Wildebeestfontein North Mine, Impala Platinum Limited. *XVth CMMI Congress*, Johannesburg, South African Institute for Mining and Metallurgy, **3**, pp. 195-200.

Harrowfield, I.R., MacRae, C.M. & P.F. Simmonds. (1988). The automated scanning electron microscope as a tool for gold microprospecting, *Microbeam Analysis*, Newbury, D.E. (ed.), San Francisco Press Inc, San Francisco, pp. 481-482.

Heinrich, K.F.J. (1981). *Electron beam X-ray microanalysis*. Van Nostrand Reinhold Company, 578 pp.

Herrera-Urbina, R., Hanson, J.S., Harris, G.H., & Furstenau, D.W. (1990). Principles and practice of sulphide mineral flotation. *Sulphide deposits – their origin and processing*, Gray, P.M.J., Bowyer, G.J., Castle, J.F., Vaughan, D.J. & Warner, N.A. (eds.), The Institution of Mining and Metallurgy, Elseviers Science Publishers Ltd., pp. 87-101.

Hey, P.V. (1999). The effects of weathering on the UG2 chromitite reef of the Bushveld Complex, with special reference to the platinum-group minerals. *South African Journal of Geology*, **102**, pp. 251-260.

Hiemstra, S.A. (1985). The distribution of some platinum-group elements in the UG-2 chromitite layer of the Bushveld Complex. *Economic Geology*, **80**, pp. 944-957.

Hiemstra, S.A. (1986). The distribution of chalcophile and platinum-group elements in the UG-2 chromitite layer of the Bushveld Complex. *Economic Geology*, **81**, pp. 1080-1086.

Hiemstra, S.A. (1988a). Platinum group mineralogy of the Bushveld Complex. Concentration and processing of Bushveld ores. *Short Course - Developments in the exploration and production of platinum, Imperial College of Science, Technology and Medicine*, London, 24-25 November 1988, 13 pp.

Hiemstra, S.A. (1988b). Concentration and processing of Bushveld ores. *Short Course - Developments in the exploration and production of platinum, Imperial College of Science, Technology and Medicine*, London, 24-25 November 1988, 13 pp.

Hofmeyr, P.K. & Adair, B.J.I. (1993). The effect on precious metal recovery of an unusual mineralogical regime within the Merensky Reef and UG-2 chromitite layer at Rustenburg, South Africa. *ICAM' 93 Proceedings*, Griffin, B., Graham, J. & Linge, H. (eds.). Held in Fremantle, Western Australia, May 31st – June 2nd, 1993, pp. 209-212.

Hofmeyr, P.K (1998). The role of mineralogy in the effective recovery of platinum-group elements from the UG-2 chromitite layer, Bushveld Complex. *Mineralogy for Mineral Processing Engineers Workshop, South African Institute of Mining and Metallurgy,* Cape Town, South Africa, 9 pp.

Hossy, I.M. (1991). The exploitation of the UG2 ore body. *Proceedings of the International Precious Metals Institute Seminar,* 20-22 January 1991.

Hulbert, L.J. & Von Gruenewaldt, G. (1985). Textural and compositional features of chromite in the Lower and Critical Zones of the Bushveld Complex South of Potgietersrus. *Economic Geology*, **80**, pp. 872-895.

Hurlbut, C.S. Jr., & Klein, C. (1977). *Manual of Mineralogy (after James D. Dana).* 19th edition, John Wiley & Sons, Inc., 532 pp.

Jackson, B.R., Reid, A.F. & Wittenberg, J.C. (1984). Rapid production of high quality polished sections for automated image analysis of minerals. *Proceedings of the Australian Institute of Mining and Metallurgy*, **289**, pp. 93-97.

Johanson, B. & Kojonen, K. (1995). Improved electron probe microanalysis services at the Geological Survey of Finland. *Geological Survey of Finland, Special Paper*, **20**, pp. 181-184.

Jones, M.P. (1987) *Applied Mineralogy: A quantitative approach.* Graham and Trotham Ltd., London. 259 pp.

Jones, M.P. & Gavrilovic, J. (1968). Automatic searching unit for the quantitative location of rare phases by electron-probe X-ray microanalysis. *Transactions of the Institute of Mining and Metallurgy,* **77**, B 137-143.

Jones , M.P. & Shaw, J.L. (1973). Automatic measurement and stereological assessment of mineral data for use in mineral technology. *Proceedings 10th International Mineral Processing Conference,* London, pp. 737-755.

Kallioinen, J. & Heiskanen, K. (1993). Effective flotation of a difficult nickel-ore based on intelligent mineral technology. *Minerals Engineering*, 6:8-10, pp. 917-928.

Kaiser, H. & Specker, H. (1955). Bewertung und Vergleich von Analysenverfahren. *Zeitschrift für Analytische Chemie,* **149**, pp. 46-66.

Kelsall, D.F. (1961). Application of probability in the assessment of flotation systems. *Transactions of the Institute of Mining and Metallugy,* **70**, pp. 191-204.

King, R.P. (1978). Determination of particle size distribution from measurements on sections. *Powder Technology,* **21**, pp. 147-150.

King, R.P. (1979). A model for the quantitative estimation of mineral liberation by grinding. *International Journal of Mineral Processing*, **6**, pp. 207-220.

King, R.P. (1993). Models for mineral liberation and their calibration by image analysis. *ICAM' 93 Proceedings*, Griffin, B., Graham, J. & Linge, H. (eds.). Held in Fremantle, Western Australia, May 31st – June 2nd, 1993, pp. 43-46.

King, R.P. (1994a). Communition and liberation of minerals. *Minerals Engineering*, **7**, pp. 129-140.

King, R.P. (1994b). Quantitative characterisation of mineralogical texture by image analysis. *Process Mineralogy XII – Applications to Environment, Precious Metals, Mineral Beneficiation, Pyrometallurgy, Coal and Refractories*, Petruk, W. & Rule, A.R. (eds.). The Minerals, Metals & Materials Society, pp. 189-200.

King, R.P. & Stirling, P.A. (1994). Linear intercept analysis of mineralogical texture. *Process Mineralogy XII – Application to environment, precious metals, mineral*

beneficiation, pyrometallurgy, coal and refractories, Petruk, W. & Rule, A.R. (eds.). The Minerals and Materials Society, pp. 201-211.

Kingston, G.A. (1966). The occurrence of platinoid bismuthotellurides in the Merensky Reef at Rustenburg platinum mine in the western Bushveld. *Mineralogical Magazine,* **35**, pp. 815-833.

Kinloch, E.D. (1982). Regional trends in the platinum-group mineralogy of the critical zone of the Bushveld Complex, South Africa. *Economic Geology,* **77**, pp. 1328-1347.

Kinloch, E.D. & Peyerl, W. (1990). Platinum-group minerals in various rock types of the Merensky Reef: Genetic implications. *Economic Geology*, **85**, pp. 537-555.

Kirjavainen, V.M. (1992). Mathematical model for the entrainment of hydrophyllic particles in froth flotation. *International Journal of Mineral Processing*, **35**, pp. 1-11.

Kirjavainen, V.M. (1996). Review and analysis of factors controlling the mechanical flotation of gangue minerals. *International Journal of Mineral Processing*, **46**, pp. 21-34.

Klimpel, R. R. (1980). Selection of chemical reagents for flotation. *Mineral processing plant design*, 2nd edition. Mular, A. & Bhappu, R. (eds.), AIME, New York, pp. 907-934.

Klimpel, R. R. (1988). Considerations for improving the performance of froth flotation systems. *Mining Engineering*, December 1988, pp. 1093-1100.

Knacke, O., Kubaschewski, O., & Hesselmann, K. (Eds.) (1991). *Thermochemical properties of inorganic substances.* Springer-Verlag. 2142 pp.

Kocabag, D. & Smith, M.R.. (1985). The effect of grinding media and galvanic interactions upon the flotation of sulphide minerals. *Complex Sulphides: Processing of ores, concentrates and by-products.* Zunkel, A.D., Boorman, R.S., Morris, A.E. & Wesely, R.J. (eds.). Metallurgical Society of AIME, pp. 55-76.

Koniggsmann, K.V. (1985). Flotation techniques for complex ores. *Complex Sulphides: Processing of ores, concentrates and by-products.* Zunkel, A.D.,

Boorman, R.S., Morris, A.E. & Wesely, R.J. (eds.). Metallurgical Society of AIME, pp. 5-20.

Kullerud, G. & Yund, R.A. (1962). The Ni-S system and related minerals. *Journal of Petrology*, **3**, pp. 126-175.

Kullerud, G., Yund, R.A., & Moh, G.H. (1969). Phase relations in the Cu-Fe-S, Cu-Ni-S, and Fe-Ni-S systems. *Magmatic ore deposits, Economic Geology, Monograph 4,* Wilson, H.D.B. (ed.), pp. 323-343.

Kupferbürger, W., Lombaard, B.V., Serstein, B.W. & Schwellnus, C.M. (1937). The chromite deposits of the Bushveld Igneous Complex, Transvaal, South Africa. *Geological Survey Bulletin*, **10**, 48 pp.

Lange, A.G., Skinner, W.M. & Smart, R. St.C. (1997). Fine:coarse particle interactions and aggregation in sphalerite flotation. *Minerals Engineering*, **10**(7), pp. 681-693.

Laslett, G.M., Sutherland, D.N., Gottlieb, P., & Allen, N.R. (1990). Graphical assessment of a random breakage model for mineral liberation. *Powder Technology,* **60**, pp. 83-97.

Lastra, R., Wilson, J.M.D. & Cabri, L.J. (1999). Automated gold search and applications in process mineralogy. *Transactions of the Institution of Mining and Metallurgy*, **108**, C75-84.

Lea, S.D. (1996). The geology of the Upper Critical Zone, northeastern Bushveld Complex. *South African Journal of Geology*, **99**, pp. 263-283.

Leeb-Du Toit, A. (1986). The Impala Platinum Mines. *Mineral Deposits of Southern Africa,* Anhaeusser, C.R. & Maske, S. (eds.). Geological Society of South Africa, pp.1091-1106.

Leigh, G.M. (1993). The reconstruction method of Barbery: estimating particle shape and mineral texture from cross-sectional and line-scan data. *ICAM' 93 Proceedings*, Griffin, B., Graham, J. & Linge, H. (eds.). Held in Fremantle, Western Australia, May 31st – June 2nd, 1993, pp. 50-53.

Li, C., Barnes, S.-J., Makovicky, E., Rose-Hansen, J.R. & Makovicky, M. (1996). Partitioning of nickel, copper, iridium, rhodium, platinum and palladium between monosufide solid solution and sulfide liquid: Effects of composition and temperature. *Geochimica et Cosmochimica Acta,* **60**(7), pp. 1231-1238.

Liddell, K.S., McRae, L.B. & Dunne, R.C. (1986). Process routes for beneficiation of noble metals from Merensky and UG-2 ores. *Mintek Review,* **4**, Council for Mineral Technology, Randburg, South Africa, pp. 33-43.

Lin, C.L., Miller, J.D., Herbst, J.A., Sepulveda, J.E., & Prisbrey, K.A. (1984). Prediction of volumetric abundance from two-dimensional images. *ICAM 84*, 2nd International Congress on Applied Mineralogy, Los Angeles, pp. 158-171.

Lomberg, K.G., Martin, E.S., Patterson, M.A., & Venter, J.E. (1999). The morphology of potholes in the UG2 chromitite Layer and Merensky Reef (pothole reef facies) at Union Section, Rustenburg Platinum Mines. *South African Journal of Geology*, **102**(3), pp. 209-220.

Makovicky, M., Makovicky, E. & Rose-Hansen, J. (1985). Experimental studies on the solubility and distribution of platinum group elements in base-metal sulphides in platinum deposits. *Conference Proceedings: Metallogeny of basic and ultrabasic rocks*, Gallagher, M.J., Ixer, R.A., Neary, C.R., & Prichard, H.M. (eds.), held in Endinburgh, Scotland, 9-12 April, 1985, The Institution of Mining and Metallurgy, pp. 415-425.

Maier, W.D. & Eales, H.V. (1994). Facies model for interval between UG-2 and Merensky Reef, Western Bushveld Complex, South Africa. *Transactions of the Institution of Mining and Metallurgy, Section B: Applied Earth Sciences,* **103**, pp. B22-B30.

Maier, W.D. & Bowen, M.P. (1996). The UG-2-Merensky Reef interval of the Bushveld Complex northwest of Pretoria. *Mineralium Deposita*, **31**, pp. 386-393.

Marais, P. (1989). *Personal Communication,* Mintek, Randburg, South Africa.

McCallum, M.E., Loucks, R.R., Carlson, R.R., Cooley, E.F. & Doerge, T.A. (1976). Platinum metals associated with hydrothermal copper ores of the New Rambler Mine, Medicine Bow Mountains, Wyoming. *Economic Geology*, **71**, pp. 1429-1450.

McDonald, K. J., MacRae, C.M., Rummel, P.H. & Woodcock, J.T. (1991a). Rapid location of gold in polished sections with a scanning electron microscope. *World Gold '91,* The Australasian Institute of Mining and Metallurgy, Melbourne, pp. 323-330.

McDonald, K. J., MacRae, C.M., Rummel, P.H. & Woodcock, J.T. (1991b). Microprospecting for minerals of the platinum group elements. *Fifth AusIMM Extractive Metallurgy Conference*, The Australasian Institute of Mining and Metallurgy, Melbourne, pp. 175-181.

McDonald, K. J. & Sparrow, G. J. (1992). Automated location of gold in samples from Australasian concentrators. *Extractive Metallurgy of gold and base-metals, proceedings of the conference, held 26-28 October 1992 in Kalgoorlie*, Parkville, W. (ed.). pp. 195-201.

McLaren, C.H. (1980) *'n Mineralogiese ondersoek van die platinumgroepminerale in die boonste chromitietlaag (UG2) van die Bosveldkompleks.* Unpublished PhD thesis, Rand Afrikaans University, Johannesburg, South Africa, 360 pp.

McLaren, C.H. & De Villiers, J.P.R. (1982). The platinum-group chemistry and mineralogy of the UG-2 chromitite layer of the Bushveld Complex. *Economic Geology*, **77**, pp.1348-1366.

Merkle, R.K.W. (1988). The effects of metasomatising fluids on the PGE-content of the UG-1 chromitite layer. *Geoplatinum '87,* Prichard, H.M., Potts, P.J., Bowles, J.F.W. & Cribb, S.J. (eds.), Elsevier Sci. Publ. Essex, Milton Keynes, Apr. 22-23, 1987, pp. 359-360.

Merkle, R.K.W. (1992). Platinum-group minerals in the middle group of chromitite layers at Marikana, western Bushveld Complex: indications for collection mechanisms and postmagmatic modification. *Canadian Journal of Earth Sciences,* **29**, pp. 209-221.

Merkle, R.K.W. & Verryn, S.M.C. (in preparation). The cooperite-braggite miscibility gap and problems identifying Pt-Pd-(Ni)-sulphides.

Miller, P.R., Reid, A.F. & Zuiderwyk, M.A. (1982). QEM*SEM image analysis in the determination of modal assays, mineral associations and mineral liberation. *CIM XIV International Mineral Processing Congress, October 17-23 1982, Toronto, Canada*, p. VIII 3.1-3.20.

Misra, K.C. & Fleet, M.E. (1973). The chemical compositions of synthetic and natural pentlandite assemblages. *Economic Geology*, **68**, pp. 618-539.

Mossom, R.J. (1986). The Atok Platinum Mine. *Mineral Deposits of Southern Africa,* Anhaeusser, C.R. & Maske, S (eds.). Geological Society of South Africa, pp.1143-1154.

Mostert, A.B., Hofmeyr, P.K. & Potgieter, G.A. (1982). The platinum-group mineralogy of the Merensky Reef at the Impala Platinum Mines, Bophutatswana. *Economic Geology,* **7**, pp. 1385-1394.

Naldrett, A.J. (1989). *Magmatic Sulfide Deposits*. Clarendon Press, New York. Oxford University Press, Oxford. 186 pp.

Naldrett, A.J. & Lehmann, J. (1987). Spinel non-stoichiometry as the explanation for Ni-, Cu, and PGE-enriched sulphides in chromitites. *Geoplatinum '87,* Prichard, H.M., Potts, P.J., Bowles, J.F.W., and Cribb, S.J. (eds.). Elsevier, Amsterdam, pp. 93-109.

Naldrett, A.J., Lehmann, J., Augé, T. (1989). Spinel non-stoichiometry and reactions between chromite and closely associated sulphides, with examples from ophiolite complexes. *Magmatic sulphides – the Zimbabwe volume,* Prendergast, M.D. & Jones, J. (eds.). The Institution of Mining and Metallurgy, London, pp. 221-227.

Oberthür, T., Cabri, L.J., Weiser, T.W., McMahon, G., & Müller, P. (1997). Pt, Pd and other trace elements in sulfides of the Main Sulfide Zone, Great Dyke, Zimbabwe: A reconnaissance study. *The Canadian Mineralogist*, **35**, 597-609.

Oosthuyzen, E.J. (1983) The application of automatic image analysis to mineralogy and extractive mineralogy. *ICAM '81. Proceedings of the 1st International Congress on Applied Mineralogy,* De Villiers J.P.R. & Cawthorn, P.A. (eds.). The Geological Society of South Africa, Special Publication No. 7, pp. 449-464.

Oosthuyzen, E. J. (1985). Image analysis of gold-bearing ores and products. *Proceedings: International Conference on Mineral Science and Technology*, Haughton, L. (ed.). **2**, Council for Mineral Technology, Johannesburg, South Africa, pp. 965-973.

Oosthuyzen, E.J. (1987). Ore microscopy, image analysis, and the extractive metallurgy of sulphide minerals - an overview. *MINTEK Report no. M338,* Council for Mineral Technology, Randburg, South Africa, 9 pp.

Overbeek, P.W., Loo, J.P. & Dunne, R.C. (1985). The development of a concentrator procedure for the platinum-group metals and chromite from the UG-2 Reef of the Bushveld Complex. *Mintek Review,* **1**, Council for Mineral Technology, Randburg, South Africa, pp. 3-15.

Paktunc, A.D., Hulbert, L.J., & Harris, D.C. (1990). Partitioning of the platinum-group and other trace elements in sulfides from the Bushveld Complex and Canadian occurrences of nickel-copper sulfides. *Canadian Mineralogist*, **28**, pp. 475-488.

Parsonage, P.G. (1985). Effects of slime and colloidal particles on the flotation of galena. *Flotation of sulphide minerals*. Forssberg, K.S.E. (ed.). *Developments in Mineral Processing*, **6**, pp. 111-139.

Penberthy, C.J. & Oosthuyzen, E.J. (1992). The use of an integrated SEM-EDS image-analysis system in an applied mineralogy environment. *Quantimet News Review*, **6**, Leica, pp. 6-7.

Petruk, W. (1976) Application of Quantimet to the analysis of ore minerals for mineral dressing. *Minerals Research Program Processing Contribution No. 13,* **III**, Microscopical Society of Canada, pp. 76-77.

Petruk, W. (1983) The behaviour of minerals during flotation of a base-metal ore from the Brunswick No. 12 deposit in Canada. *ICAM 81. Proceedings of the first international Congress on Applied Mineralogy,* De Villiers, J.P.R.& Cawthorn, G.A. (eds.). Johannesburg, The Geological Society of South Africa, Special Publication No. 7, pp. 201-208.

Petruk, W. (1986). The MP-SEM-IPS- image analysis system. *Canmet Report no. 87-1E,* Mineral Processing Laboratory, Energy, Mines and Resources Canada, 28 pp.

Petruk, W. (1988a) Automatic image analysis for mineral beneficiation. *Journal of metals,* **40**, pp. 29-31.

Petruk, W. (1988b). Ore characteristics that affect breakage and mineral liberation during grinding. *Process Mineralogy VIII*, Carson, D.J.T. & Vassiliou, A.H. (eds.). The Minerals and Materials Society, pp. 181-193.

Petruk, W. (1993) Recent developments in image analysis measurements with respect to extractive metallurgy. *ICAM' 93 Proceedings*, Griffin, B., Graham, J. & Linge, H. (eds.). Held in Fremantle, Western Australia, May 31st – June 2nd, 1993, pp. 42-43.

Petruk,W. (1994). New developments in the applications of SEM/Image analysis in extractive metallurgy. *Process Mineralogy XII – Applications to Environment, Precious Metals, Mineral Beneficiation, Pyrometallurgy, Coal and Refractories,* Petruk, W. & Rule, A.R. (Eds.). The Minerals & Materials Society, pp. 173-187.

Petruk, W. & Lastra, R. (1995). Techniques for measuring mineral liberations by image analysis. *EPD Congress 1996*, Warren, G.W. (ed.), The Minerals, Metals & Materials Society, pp. 559-571.

Petruk, W., Pinard, R.G., & Finch, J. (1986). Relationship between observed mineral liberations in screened fractions and composite samples. *Minerals and Metallurgical Processing*, 3, 60-62.

Petruk, W. & Smith, M.M. (1989). Ore characteristics that affect breakage during grinding. *CANMET Report CM88-5E,* CANMET, Canada Centre for Mineral and Energy Technology, Energy, Mines and Resources, Canada, 20 pp.

Peyerl, W. (1982). The influence of Driekop Dunite Pipe on the platinum-group mineralogy of the UG-2 chromitite in its vicinity. *Economic Geology,* **77**, pp.1432-1438.

Peyerl, W. (1983) The metallurgical implications of the mode of occurrence of platinum-group metals in the Merensky Reef and UG-2 chromitite of the Bushveld Complex. *Special Publication, Geological Society of South Africa*, **7**, pp. 295-300.

Peyerl, W. (1992). Platinum group elements in the Bushveld Complex; their mode of occurrence and some recovery related mineralogical parameters. *School: Mineralogy for minerals processing, South African Institute of Mining and Metallurgy,* 19-20 May 1992, Mintek, Randburg, South Africa. pp. 1-15.

Pozzo, R.L., Malicsi, A.S. & Iwasaki, I. (1990) Pyrite-pyrrhotite-grinding media contact and its effect on flotation. *Minerals and metallurgical processing*, **5**:1 , pp. 16-21.

Prendergast, M.D. (1990). Platinum-group minerals and hydrosilicate 'alteration' in Wedza-Mimosa platinum deposit, Great Dyke, Zimbabwe – genetic and metallurgical implications. *Transactions of the Institute of Mining and Metallurgy*, **99**, B91-B105.

Prichard, H.M. & Lord, R.A. (1994). Evidence for differential mobility of platinum-group elements in the secondary environment in Shetland ophiolite complex. *Transactions of the Institute of Mining and Metallurgy*, **103**, B79-86

Reed, S.J.B. (1975). *Electron microprobe analysis*. Cambridge University Press, 400 pp.

Reid, D.L., Cawthorn, R.G., Kruger, F.J. & Tredoux, M. (1993). Isotope and trace-element patterns below the Merensky Reef, Bushveld Complex, South Africa: evidence for fluids. *Chemical Geology*, **106**, pp. 171-186.

Ripley, E. M. & Chryssoulis, S. L. (1994). Ion microprobe analysis of platinum-group elements in sulfide and arsenide minerals from Babbit Cu-Ni deposit, Duluth Complex, Minnesota. *Economic Geology*, **89**, pp. 201-210.

Robért, R.V.D., Van Wyk, E. & Palmer, R. (1971). Concentration of the noble metals by a fire-assay technique using nickel sulphide as the collector. *NIM Report No. 1371*, National Institute for Metallurgy, Randburg, South Africa, 14 pp.

Robért, R.V.D., Nell, J. & Vine, R.L. (1997) An investigation into some aspects of the fire-assay procedure with lead as the collector for the noble metals. *MINTEK Report No. M 412,* Council for Mineral Technology, Randburg, South Africa, 16 pp.

Rogers, J. (1962). Principles of sulfide mineral flotation. *Froth Flotation, 50th Anniversary Volume,* Fuerstenau, D.W. (ed.), The American Institute of Mining, Metallurgical, and Petroleum Engineers, Inc., New York, pp. 139-169.

Rowlands, N., Finch, J.A., & Hill, G.S. (1991). Factors affecting meaningful presentation of data in two dimensional liberation studies. *EPD Congress 1992,* Hager, J.P. (ed.), The Minerals, Metals & Materials Society, pp. 305-313.

SACS (South African Committee for Stratigraphy). (1980). *Lithostratigraphy of the Republic of South Africa, South West Africa/Namibia, and the Republic of Bophuthatswana, Transkei and Venda.* Handbook **8**, Part 1, Geological Survey of South Africa, 633 pp.

Saltikov, S.A. (1967) The determination of the size distribution of particles in an opaque material from a measurement of the size distribution of their sections. *2nd International Congress for Stereology,* Chicago, pp. 163-173.

Schiffries, C.M. & Skinner, B.J. (1987). The Bushveld Hydrothermal System: Field and petrologic evidence. *American Journal of Science*, **287**, pp. 566-595.

Schiffries, C.M & Rye, D.M. (1990). Stable isotopic systematics of the Bushveld Complex: II. Constraints on hydrothermal processes in layered intrusions. *American Journal of Science,* **290**, pp. 209-245.

Schmidt, E.R. (1952). The structure and composition of the Merensky Reef and associated rocks on the Rustenburg Platinum Mine. *Transactions of the Geological Society of South Africa*, **55**, pp. 233-279.

Schweitzer, J.K., Hatton, C.J. & de Waal, S.A. (1995). Regional lithochemical stratigraphy of the Rooiberg Group, upper Transvaal Supergroup: A proposed new subdivision. *South African Journal of Geology,* **98,** pp. 245-255.

Schweitzer, J.K. & Hatton, C.J. (1995a). Synchronous emplacement of the felsites, granophyres, granites and mafic intrusives of the Bushveld Complex (abstract). *Geocongress '95,* **I**, Geological Society of South Africa, Johannesburg, pp. 532-535.

Schweitzer, J.K. & Hatton, C.J. (1995b). Chemical alteration within the volcanic roof rocks of the Bushveld Complex. *Economic Geology*, **90**, pp. 2218-2231.

Senior, G.D., Shannon, L.K. & Trahar, W.J. (1994). The flotation of pentlandite from pyrrhotite with particular reference to the effects of particle size. *International Journal of Mineral Processing*, **42**, pp. 169-190.

Simon, J.L. & Bruce, P. (1991) Resampling: A tool for everyday statistical work. *Chance: New directions for statistics and computing*, **4**, pp. 22-32.

Smits, G. (1988). The distribution of cobalt in mineral constituents of the Merensky Reef and UG2 chromitite layer of the Bushveld Complex. *Mintek Report No. M356*, Council for Mineral Technology, Randburg, South Africa, 8 pp.

Stowe, K.G., Chryssoulis, S.L. & Kim, J.Y. (1995). *Mapping of composition of mineral surfaces by TOF-SIMS.* Minerals Engineering, **8**, 4/5, pp. 421-430.

Subrahmanyam, T. V. & Forssberg, K. S. (1990). Fine particle processing: shear-flocculation and carrier flotation – a review. *International Journal of Mineral Processing*, **30**, pp. 265-286.

Sutherland, D.N. (1989). Batch flotation behaviour of composite particles. *Minerals Engineering*, **2**:3, pp. 351-367.

Thomas, A. & Filipov, L.O. (1999). Fractures, fractals and breakage energy of mineral particles. *International Journal of Mineral Processing*, **57**, pp. 285-301.

Trahar, W. J. (1981). A rational interpretation of the role of particle size in flotation. *International Journal of Mineral Processing*, **8**, pp. 289-327.

Underwood, E. E. (1970). *Quantitative stereology.* Addison-Wesley Publishing Company, 274 pp.

Van den Heever, P. C. (1995). *A mineralogical approach to the problem of lead loss in the magnetic fraction at the Broken Hill concentrator, Aggeneys, South Africa.* Unpublished MSc Thesis, Potchefstroom University for Christian Higher Education, 114 pp.

Van der Merwe, J.J., Vermaak, A.H., Slabbert, M.J., Mauve, A.C., & Mooney, D.J. (1998). An overview of the geology of the UG-2 chromitite layer and its surrounding lithologies on Lonrho Platinum's lease area. *8th International Platinum Symposium Abstracts*, held June-July 1998, Rustenburg, South Africa. The Geological Society of South Africa and the South African Institute of Mining and Metallurgy, Symposium Series S18, pp. 403-406.

Vander Voort, G.F. (1984). Grain size measurement. *Practical Applications of quantitative metallography, ASTM STP 839,* McCall, J.L. & Steele, J.H., Jr. (Eds.). American Society for Testing and Materials, Philadelphia, pp. 85-131.

Van Wyk, E. (1980). Laboratory method no. 78/29. The determination of platinum, palladium, rhodium, and gold in ores and concentrates by the fusion technique with lead as the collector. *NIM Report No. 2068*, National Institute for Metallurgy, Randburg, South Africa, 5 pp.

Vaughan, D.J., & Craig, J.R. (1978). *Mineral chemistry of metal sulfides.* Cambridge University Press, 493 pp.

Vermaak, C.F. (1995). *The platinum-group metals - A global perspective.* Mintek, Randburg, South Africa, 247 pp.

Vermaak, C.F. & Hendriks, L.P. (1976). A review of the mineralogy of the Merensky Reef, with specific reference to new data on the precious metal mineralogy. *Economic Geology*, **71**, pp. 1244-1269.

Vermaak, C.F. & Von Gruenewaldt, G. (1986). Introduction to the Bushveld Complex. *Mineral Deposits of Southern Africa,* Anhaeusser, C.R. & Maske, S. (eds.). Geological Society of South Africa, pp. 1021-1029.

Verryn, S.M.C. & Merkle, R.K.W. (1994). Compositional variation of cooperite, braggite and vysotskite from the Bushveld Complex. *Mineralogical Magazine,* **58**, pp. 223-234.

Viljoen, M.J. & Scoon, R.N. (1985). The distribution and main geologic features of discordant bodies of iron-rich ultramafic pegmatite in the Bushveld Complex. *Economic Geology*, **80**, pp. 1109-1128.

Viljoen, M.J., De Klerk, W.J., Coetzer, P.M., Hatch, N.P., Kinloch, E. & Peyerl, W. (1986a). The Union section of Rustenburg Platinum Mines Limited with reference to the Merensky Reef. *Mineral Deposits of Southern Africa,* Anhaeusser, C.R. & Maske, S. (eds.). Geological Society of South Africa, pp.1061-1090.

Viljoen, M.J., Theron, J., Underwood, B., Walters, B.M. Weaver, J. and Peyerl, W. (1986b). The Amandelbult section of Rustenburg Platinum Mines Limited with reference to the Merensky Reef. *Mineral Deposits of Southern Africa,* Anhaeusser, C.R. & Maske, S. (eds.). Geological Society of South Africa, pp.1041-1060.

Viljoen, M.J. & Hieber, R. (1986). The Rustenburg section of Rustenburg Platinum Mines Limited with reference to the Merensky Reef. *Mineral Deposits of Southern Africa,* Anhaeusser, C.R. & Maske, S. (eds.). Geological Society of South Africa, pp.1107-1134.

Viljoen, M. J. & Schürmann, L.W. (1998). Platinum-group metals. *The mineral resources of South Africa, 6th Edition,* Wilson, M.G.C. & Annhaeusser, C.R. (eds.). Council for Geoscience, pp. 532-568.

Von Gruenewaldt, G. (1979). A review of some recent concepts of the Bushveld Complex, with particular reference to sulfide mineralization. *Canadian Mineralogist*, **17**, pp. 233-256.

Von Gruenewaldt, G., Sharpe, M. R., & Hatton, C. J. (1985). The Bushveld Complex: Introduction and Review. *Economic Geology*, **80**, pp. 803-812.

Von Gruenewaldt, G., Hatton, C.J., Merkle, R.K.W. & Gain, S.B. (1986). Platinum-group element - chromitite associations in the Bushveld Complex. *Economic Geology*, **81**, pp. 1067-1079.

Von Gruenewaldt, G., Dicks, D., De Wet, J. & Horsch, H. (1990). PGE mineralization in the western sector of the eastern Bushveld Complex. *Mineralogy and Petrology,* **42**, pp. 71-95.

Walker, D.A., Paktunc, A.D. & Villeneuve, M.E. (1989). Automated image analysis applications: Characterisation of (1) platinum-group minerals and (2) heavy mineral separates. *Short Course on image analysis applied to Mineral and Earth Sciences,* Petruk, W. (ed.), Mineralogical Association of Canada, **16**, pp. 94-105.

Walraven, F. (1986). A note on the stratigraphic terminology of the Bushveld Complex. *Mineral Deposits of Southern Africa,* Anhaeusser, C.R. & Maske, S. (eds.). Geological Society of South Africa, pp.1039-1040.

Walraven, F., Armstrong, R.A. & Kruger, F.J. (1990). A chronostratigraphic framework for the north-central Kaapvaal craton, the Bushveld Complex and the Vredefort structure. *Tectonophysics,* **171**, pp. 23-48.

Walraven, F. & Hattingh, E. (1993). Geochronology of the Nebo Granite, Bushveld Complex. *South African Journal of Geology*, **96**, pp. 31-41.

Walraven, F. (1997). Geochronology of the Rooiberg Group, Transvaal Supergroup, South Africa. *Economic Geology Research Unit, Information Circular No. 316*, University of the Witwatersrand, Johannesburg, South Africa. 21 pp.

Warren, L. J. (1985). Determination of the contributions of true flotation and entrainment in batch flotation tests. *International Journal of Mineral Processing*, **14**, pp. 13-44.

Wei, X. & Gay, S. (1999). Liberation modelling using a dispersion function. *Minerals Engineering*, **12**:2, pp. 219-227.

Weibel, E.R. (1980). *Stereological methods. Vol. 2. Theoretical foundations.* Academic Press. 340 pp.

Weiser, T.W., Oberthür, T., and Kojonen, K.K. (1998). Distribution of trace PGE in pentlandite and of PGM in the Main Sulfide Zone (MSZ) at Mimosa Mine, Great Dyke, Zimbabwe. *8th International Platinum Symposium Abstracts*, held June-July 1998, Rustenburg, South Africa. The Geological Society of South Africa and the South African Institute of Mining and Metallurgy, Symposium Series S18, pp. 443-445.

Wesely, R.J. (1985). Complex sulphides: New technology and opprtunities. *Complex Sulphides: Processing of ores, concentrates and by-products.* Zunkel, A.D., Boorman, R.S., Morris, A.E. & Wesely, R.J. (eds.). Metallurgical Society of AIME, pp. 21-34.

Wesseldijk, Q.I., Reuter, M.A., Bradshaw, D.J. & Harris, P.J. (1999). The flotation behaviour of chromite with respect to the beneficiation of UG2 ore. *Minerals Engineering*, **12**:10, pp. 1177-1184.

Willemse, J. (1964). A brief outline of the geology of the Bushveld Igenous Complex. *The geology of some ore deposits in Southern Africa,* **II,** Haughton, S.H. (ed.). Geological Society of South Africa, Johannesburg, pp. 91-128.

Wills, B.A. (1981). *Mineral Processing Technology*, 2nd edition, International Series on Materials Science and Technology Volume 29, Perganon Press, 525 pp.

Winkels-Herding, S., Merkle, R.K.W. & Von Gruenewaldt, G. (1991). Pegmatoidal pockets in the UG-2 chromitite, western Bushveld Complex. *ICAM '91, International Congress on Applied Mineralogy, Papers*, Haughton, L.F. & Markgraaff, J. (eds.). Mineralogical Association of South Africa, Pretoria, **2,** Paper 65, 14 pp.

Woollacott, L.C. & Valenta, M. (1996). Use of synthetic ore particles to test a transformation function in liberation analysis. *Minerals Engineering*, **9**, pp. 1017-1032.

Worst, B.G. (1986). The chromite deposits of the Montrose and Groothoek Mines, Eastern Bushveld Complex. *Mineral Deposits of Southern Africa,* Anhaeusser, C.R. & Maske, S. (eds.). Geological Society of South Africa, pp.1189-1195.

Yuan, X. -M., Palsson, B.I. & Forssberg, K.S.E. (1996). Flotation of a complex sulphide ore II. Influence of grinding environments on Cu/Fe sulphide selectivity and pulp chemistry. *International Journal of Mineral Processing*, **46**, pp. 181-204.

Zheng, X.P. & Lin, H.K. (1994). Effect of mineralogical properties of synthetic mica on its floatability. *Minerals and Metallurgical Processing*, **93-630** , pp. 20-25.

APPENDIX A

Calculation of weighted mean atomic number ($\bar{Z}$) and backscattered-electron coefficient ($\bar{\eta}$)

The backscattered-electron coefficient for pure elements can be approximated by the following empirical formula: $\eta=0.5-0.228*10^{-4}(80-Z)*(|80-Z|)^{1.3}$ where Z is the atomic number of the element (Heinrich, 1981). For a multicomponent target, such as a mineral, the weighted mean backscattered-electron coefficient , $\bar{\eta}$, is used where $\bar{\eta} = \Sigma C_i \eta_I$ and C_i is the weight fraction of element i in the mineral, and η_i is the backscattered-electron coefficient of element i.

Weighted mean atomic number $\bar{Z}=\Sigma C_i Z_i$. For comparison with $\bar{\eta}$ this value can is divided by 100.

By way of illustration $\bar{Z}$ and $\bar{\eta}$ is calculated for pyrite with composition FeS_2 (Table 1).

Table 1 *Calculation of weighted mean atomic number ($\bar{Z}$) and backscattered-electron coefficient ($\bar{\eta}$) for pyrite with composition FeS_2.*

i	***Fe***	***S***
Z	26	16
η	0.28	0.18
C_i	0.47	0.53
$C_i\eta_i$	0.13	0.09
$\bar{\eta}$	0.22	
C_iZ_i	12.10	8.55
$\bar{Z}/100$	0.21	

APPENDIX B

Ideal chemical formulaE and densities of minerals in UG2 chromitite (Hurlbut & Klein,1977; Cabri, 1981; Deer et al.; 1983).

Mineral name	Ideal chemical formula	Density
Pentlandite	$(Fe,Ni)_9S_8$	4.6-5.0
Pyrrhotite	$Fe_{1-x}S$	4.58-4.65
Pyrite	FeS_2	5.02
Millerite	NiS	5.5±0.2
Chalcopyrite	$CuFeS_2$	4.1-4.3
Galena	PbS	7.4-7.6
Braggite	$Pt_{0.64}Pd_{0.27}Ni_{0.14}S_{1.00}$	9.34
Cooperite	PtS	10.12
Vysotskite	PdS	6.71
Laurite	$(Ru,Os,Ir)S_2$	6.22
Malanite	$Cu(Pt,Rh)_2S_4$	7.4
Pt-Fe alloy	Pt_3Fe	18.23
Chromite	$(Fe,Mg)Cr_2O_4$	4.6
Talc	$Mg_3Si_4O_{10}(OH)_2$	2.7-2.8
Bronzite	$(Mg,Fe)SiO_3$	3.3
Anorthite	$CaAl_2Si_2O_8$	2.76
Albite	$NaAlSi_3O_8$	2.62
Quartz	SiO_2	2.65
Calcite	$CaCO_3$	2.71
Pumpellyite	$Ca_4(Mg,Fe)(Al,Fe)_5(OH)_3[Si_2O_7]_2[SiO_4]_2.2H_2O$	3.18-3.23
Chlorite	$(Mg,Fe)_3(Si,Al)_4O_{10}(OH)_2.(Mg,Fe)_3(OH)_6$	3.1-3.2
Prehnite	$Ca_2Al(AlSi_3O_{10})(OH)_2$	2.8-2.95
Epidote	$Ca_2(Al,Fe)Al_2O(SiO_4)Si_2O_7(OH)$	3.35-3.45
Phlogopite	$KMg_3(AlSi_3O_{10})(OH)_2$	2.86

APPENDIX C

Chromite grain-size measurements.

Table 1 *Measured chromite grain-size distributions for 15 polished sections of crushed sample A1, expressed as area percentage in 13 size classes.*

Diameter	*1*	*2*	*3*	*4*	*5*	*6*	*7*	*8*	*9*	*10*	*11*	*12*	*13*	*14*	*15*
0-48 µm	2	2	2	2	2	2	2	2	2	2	2	2	2	2	2
48-101 µm	18	17	15	16	15	17	17	17	17	14	18	17	16	15	18
101-155 µm	27	29	26	26	26	26	27	28	27	27	27	28	26	25	2
155-208 µm	25	23	23	23	22	22	23	22	23	24	21	24	25	22	22
208-262 µm	13	15	16	16	17	16	16	15	15	17	15	16	15	15	16
262-315 µm	11	8	10	10	8	9	9	9	9	9	9	6	9	11	8
315-368 µm	3	3	5	4	5	4	4	5	5	5	4	5	4	4	3
368-422 µm	1	2	3	2	3	2	2	2	2	1	3	1	2	3	1
422-475 µm	0	1	1	0	1	2	1	1	1	1	1	1	1	1	1
475-529 µm	1	0	1	1	1	0	0	1	1	0	0	0	0	0	1
529-582 µm	0	0	0	0	0	0	1	0	1	0	1	0	1	1	0
582-636 µm	0	0	0	0	0	1	0	0	0	0	0	0	0	1	0
>636 µm	0	0	0	0	0	0	0	0	0	0	1	0	0	0	0
Median (µm)	164	160	173	170	171	168	166	165	166	171	165	163	170	174	160

Average measured median chromite size: **167 µm**

Using resampling statistics it was determined that measurements on five polished sections (± 15 000 chromite grains) would provide an average value for the median chromite grain-size between 163 and 170 µm, i.e. a relative error of ~2% (95% confidence level).

Table 2 *Measured chromite grain-size distributions for 12 traverses on a polished section of milled feed of sample A1, expressed as area percentage in 13 size classes.*

Traverse no.	***1***	***2***	***3***	***4***	***5***	***6***	***7***	***8***	***9***	***10***	***11***	***12***
No. grains	***3068***	***2990***	***2985***	***2855***	***2988***	***2998***	***2948***	***2968***	***2980***	***2915***	***2887***	***2843***
0-17 µm	6	6	6	6	6	5	6	6	6	6	6	6
17-36 µm	25	26	25	25	23	25	25	24	25	27	27	26
36-55 µm	26	24	25	27	28	25	29	27	27	27	25	24
55-74 µm	22	20	21	21	22	21	21	23	22	20	20	23
74-94 µm	13	15	15	12	14	14	13	15	15	13	12	16
94-113 µm	6	6	7	6	6	8	6	5	5	6	8	4
113-132 µm	3	3	3	3	1	1	1	1	1	3	1	2
132-151 µm	0	0	0	0	0	1	0	0	0	1	1	0
151-170 µm	0	1	0	0	0	0	0	0	0	0	0	0
170-189 µm	0	0	0	0	0	0	0	0	0	0	0	0
189-208 µm	0	0	0	0	0	0	0	0	0	0	0	0
208-227 µm	0	0	0	0	0	0	0	0	0	0	0	0
>227 µm	1	2	3	4	5	6	7	8	9	10	11	12
Median ECD (µm)	50	51	51	50	51	52	49	51	50	49	49	50

Average measured median chromite size: **50 µm**

Using resampling statistics it was determined that measurements along two traverses of a polished section (± 5 000 chromite grains) would provide an average value for the median chromite grain-size between 49 and 51 µm, i.e. a relative error of <2% (95% confidence level).

APPENDIX D

Electron microprobe analyses of selected chromite grains in samples A1, A4, B4 and C1. All analyses were performed in duplicate and are reported as mass % oxide. The number of cations was calculated on the basis of 32 oxygen anions. Fe^{2+}:Fe^{3+} ratios were calculated on the assumption of stoichiometry. Analytical conditions and minimum detection limits are discussed in Chapter 3.

Table 1 *Electron-microprobe analyses of selected chromite grains in sample A1.*

	1	2	3	4	5	6	7	8	9	10	11	12
TiO_2	0.83	0.84	0.87	0.84	0.86	0.84	0.80	0.84	0.85	0.90	0.89	0.87
V_2O_3	0.25	0.28	0.28	0.33	0.30	0.35	0.30	0.32	0.34	0.31	0.33	0.32
Al_2O_3	16.59	16.61	16.81	16.95	17.00	16.76	16.76	16.60	16.75	17.40	16.63	16.71
Cr_2O_3	42.53	42.47	42.06	42.06	42.13	42.38	42.45	42.68	42.62	41.25	41.94	41.93
Fe_2O_3	9.58	9.56	9.72	9.62	9.47	9.35	9.28	9.25	9.38	9.94	9.94	9.83
FeO	19.29	19.34	19.21	19.16	19.27	19.47	19.56	19.53	19.46	19.40	19.56	19.40
MnO	0.25	0.28	0.26	0.26	0.26	0.26	0.27	0.26	0.26	0.27	0.26	0.25
NiO	0.16	0.16	0.17	0.15	0.15	0.15	0.15	0.15	0.15	0.17	0.16	0.15
CoO	0.00	0.05	0.04	0.01	0.05	0.04	0.01	0.01	0.02	0.00	0.00	0.03
Cu_2O	0.03	0.01	0.02	0.00	0.07	0.01	0.00	0.02	0.01	0.00	0.06	0.03
ZnO	0.10	0.07	0.08	0.11	0.10	0.01	0.07	0.07	0.14	0.11	0.04	0.03
MgO	9.56	9.51	9.62	9.69	9.57	9.49	9.41	9.42	9.50	9.60	9.41	9.51
Total	99.03	99.05	99.00	99.03	99.09	98.96	98.91	99.01	99.32	99.21	99.07	98.93
Number of ions on the basis of 32 O												
Ti	0.16	0.16	0.17	0.16	0.17	0.16	0.16	0.17	0.17	0.18	0.17	0.17
V	0.05	0.06	0.06	0.07	0.06	0.07	0.06	0.07	0.07	0.07	0.07	0.07
Al	5.11	5.12	5.17	5.21	5.22	5.16	5.17	5.12	5.14	5.33	5.13	5.15
Cr	8.79	8.78	8.68	8.67	8.69	8.76	8.78	8.83	8.78	8.48	8.67	8.67
Fe^{3+}	1.89	1.88	1.91	1.89	1.86	1.84	1.83	1.82	1.84	1.94	1.96	1.94
Fe^{2+}	4.22	4.23	4.20	4.18	4.20	4.26	4.28	4.27	4.24	4.22	4.28	4.24
Mn	0.06	0.06	0.06	0.06	0.06	0.06	0.06	0.06	0.06	0.06	0.06	0.06
Ni	0.03	0.03	0.04	0.03	0.03	0.03	0.03	0.03	0.03	0.04	0.03	0.03
Co	0.00	0.01	0.01	0.00	0.01	0.01	0.00	0.00	0.00	0.00	0.00	0.01
Cu	0.01	0.00	0.00	0.00	0.02	0.00	0.00	0.00	0.00	0.00	0.01	0.01
Zn	0.02	0.01	0.01	0.02	0.02	0.00	0.01	0.01	0.03	0.02	0.01	0.01
Mg	3.73	3.71	3.74	3.77	3.72	3.70	3.67	3.68	3.69	3.72	3.67	3.71
$\Sigma(M^{3+},M^{4+})$	16.00	16.00	16.00	16.00	16.00	16.00	16.00	16.00	16.00	16.00	16.00	16.00
ΣM^{2+}	8.06	8.06	8.06	8.06	8.06	8.06	8.06	8.06	8.05	8.06	8.06	8.06

Table 1 continued *Electron-microprobe analyses of selected chromite grains in sample A1.*

	13	14	15	16	17	18	19	20	21	22	23	24
TiO_2	0.87	0.87	0.99	0.98	0.97	0.98	0.97	0.96	0.96	0.97	0.93	0.89
V_2O_3	0.30	0.35	0.38	0.46	0.39	0.41	0.44	0.37	0.45	0.43	0.34	0.42
Al_2O_3	16.65	16.59	15.31	15.45	15.27	15.39	15.44	15.35	15.25	15.33	15.35	15.41
Cr_2O_3	41.81	42.42	44.49	44.18	44.45	44.48	44.53	44.41	44.43	44.45	44.21	44.57
Fe_2O_3	10.01	9.57	8.71	8.73	8.70	8.56	8.54	8.61	8.79	8.74	8.69	8.45
FeO	19.32	19.45	19.74	19.83	19.72	19.87	19.66	19.83	19.78	19.73	19.88	19.87
MnO	0.26	0.26	0.27	0.26	0.28	0.27	0.26	0.28	0.27	0.27	0.26	0.26
NiO	0.15	0.15	0.12	0.10	0.13	0.13	0.10	0.12	0.10	0.12	0.13	0.12
CoO	0.05	0.00	0.03	0.01	0.06	0.01	0.00	0.03	0.00	0.02	0.02	0.02
Cu_2O	0.00	0.00	0.00	0.03	0.03	0.01	0.12	0.00	0.00	0.02	0.02	0.01
ZnO	0.04	0.05	0.03	0.07	0.09	0.07	0.07	0.06	0.11	0.09	0.08	0.12
MgO	9.53	9.52	9.23	9.16	9.14	9.12	9.23	9.11	9.16	9.20	9.04	9.09
Total	98.85	99.09	99.14	99.13	99.07	99.15	99.23	98.99	99.16	99.24	98.79	99.09
Number of ions on the basis of 32 O												
Ti	0.17	0.17	0.20	0.19	0.19	0.19	0.19	0.19	0.19	0.19	0.18	0.18
V	0.06	0.07	0.08	0.10	0.08	0.09	0.09	0.08	0.09	0.09	0.07	0.09
Al	5.14	5.11	4.75	4.79	4.74	4.77	4.78	4.77	4.73	4.75	4.78	4.78
Cr	8.66	8.76	9.25	9.19	9.26	9.25	9.25	9.25	9.24	9.24	9.24	9.28
Fe^{3+}	1.97	1.88	1.72	1.73	1.72	1.69	1.69	1.71	1.74	1.73	1.73	1.67
Fe^{2+}	4.23	4.25	4.34	4.36	4.34	4.37	4.32	4.37	4.35	4.34	4.39	4.37
Mn	0.06	0.06	0.06	0.06	0.06	0.06	0.06	0.06	0.06	0.06	0.06	0.06
Ni	0.03	0.03	0.03	0.02	0.03	0.03	0.02	0.03	0.02	0.03	0.03	0.02
Co	0.01	0.00	0.01	0.00	0.01	0.00	0.00	0.01	0.00	0.00	0.00	0.00
Cu	0.00	0.00	0.00	0.01	0.01	0.00	0.03	0.00	0.00	0.01	0.00	0.00
Zn	0.01	0.01	0.01	0.01	0.02	0.01	0.01	0.01	0.02	0.02	0.02	0.02
Mg	3.72	3.71	3.62	3.59	3.59	3.58	3.61	3.58	3.60	3.60	3.56	3.57
$\Sigma(M^{3+},M^{4+})$	16.00	16.00	16.00	16.00	16.00	16.00	16.00	16.00	16.00	16.00	16.00	16.00
ΣM^{2+}	8.06	8.06	8.06	8.06	8.06	8.06	8.05	8.06	8.06	8.05	8.06	8.05

Table 1 continued *Electron-microprobe analyses of selected chromite grains in sample A1.*

	25	26	27	28	29	30	31	32	33	34	35	36
TiO_2	0.97	0.96	0.73	0.76	0.76	0.77	0.78	0.77	0.75	0.77	0.74	0.73
V_2O_3	0.36	0.44	0.32	0.34	0.28	0.29	0.24	0.22	0.32	0.23	0.26	0.30
Al_2O_3	15.35	15.38	17.64	17.82	18.03	17.98	18.26	18.11	18.41	18.32	17.99	18.35
Cr_2O_3	44.18	44.21	42.54	42.30	42.34	42.24	41.84	41.94	41.75	41.59	42.24	41.99
Fe_2O_3	8.77	8.70	8.56	8.59	8.41	8.52	8.64	8.49	8.56	8.80	8.59	8.54
FeO	19.91	19.76	18.71	18.64	18.65	18.62	18.60	18.69	18.56	18.47	18.55	18.39
MnO	0.27	0.28	0.26	0.26	0.26	0.26	0.25	0.25	0.25	0.25	0.25	0.25
NiO	0.12	0.13	0.16	0.15	0.15	0.14	0.15	0.14	0.14	0.16	0.15	0.14
CoO	0.00	0.04	0.00	0.02	0.02	0.03	0.03	0.01	0.02	0.01	0.02	0.04
Cu_2O	0.01	0.03	0.06	0.01	0.02	0.01	0.00	0.02	0.03	0.01	0.01	0.00
ZnO	0.08	0.11	0.09	0.09	0.03	0.08	0.07	0.06	0.12	0.06	0.11	0.15
MgO	9.06	9.10	10.01	10.10	10.15	10.13	10.17	10.06	10.20	10.26	10.17	10.30
Total	98.92	98.99	98.96	98.93	98.99	98.95	98.92	98.65	98.98	98.80	98.96	99.05
Number of ions on the basis of 32 O												
Ti	0.19	0.19	0.14	0.15	0.15	0.15	0.15	0.15	0.15	0.15	0.14	0.14
V	0.08	0.09	0.07	0.07	0.06	0.06	0.05	0.05	0.07	0.05	0.05	0.06
Al	4.77	4.78	5.39	5.44	5.50	5.49	5.56	5.54	5.60	5.58	5.49	5.58
Cr	9.22	9.21	8.73	8.67	8.66	8.64	8.55	8.61	8.52	8.51	8.64	8.56
Fe^{3+}	1.74	1.73	1.67	1.67	1.64	1.66	1.68	1.66	1.66	1.71	1.67	1.66
Fe^{2+}	4.39	4.36	4.06	4.04	4.03	4.03	4.02	4.06	4.01	3.99	4.02	3.97
Mn	0.06	0.06	0.06	0.06	0.06	0.06	0.06	0.06	0.06	0.05	0.06	0.06
Ni	0.03	0.03	0.03	0.03	0.03	0.03	0.03	0.03	0.03	0.03	0.03	0.03
Co	0.00	0.01	0.00	0.00	0.00	0.01	0.01	0.00	0.00	0.00	0.00	0.01
Cu	0.00	0.01	0.01	0.00	0.01	0.00	0.00	0.01	0.01	0.00	0.00	0.00
Zn	0.02	0.02	0.02	0.02	0.01	0.02	0.01	0.01	0.02	0.01	0.02	0.03
Mg	3.56	3.58	3.87	3.90	3.91	3.91	3.92	3.89	3.93	3.96	3.92	3.96
$\Sigma(M^{3+},M^{4+})$	16.00	16.00	16.00	16.00	16.00	16.00	16.00	16.00	16.00	16.00	16.00	16.00
ΣM^{2+}	8.06	8.06	8.05	8.05	8.05	8.05	8.05	8.06	8.05	8.05	8.05	8.05

Table 1 continued *Electron-microprobe analyses of selected chromite grains in sample A1.*

	37	38	39	40	41	$\bar{x}$	s	CL
TiO_2	0.76	0.78	0.75	0.79	0.74	0.85	0.09	0.03
V_2O_3	0.30	0.25	0.31	0.28	0.27	0.33	0.06	0.02
Al_2O_3	17.95	18.28	18.23	18.23	18.14	16.85	1.14	0.36
Cr_2O_3	42.29	41.97	42.11	42.04	41.85	42.79	1.08	0.34
Fe_2O_3	8.60	8.56	8.49	8.47	8.69	8.95	0.51	0.16
FeO	18.49	18.45	18.57	18.51	18.47	19.20	0.53	0.17
MnO	0.25	0.26	0.23	0.25	0.26	0.26	0.01	0.00
NiO	0.16	0.14	0.14	0.16	0.15	0.14	0.02	0.01
CoO	0.00	0.01	0.06	0.00	0.00	0.02	0.02	0.01
Cu_2O	0.05	0.02	0.00	0.05	0.07	0.02	0.03	0.01
ZnO	0.13	0.14	0.10	0.09	0.11	0.08	0.03	0.01
MgO	10.18	10.25	10.21	10.21	10.17	9.65	0.44	0.14
CaO	0.02	0.00	0.00	0.01	0.00	0.00	0.00	0.00
Total	99.04	99.01	99.09	98.97	98.81	99.01	0.13	0.04
Number of ions on the basis of 32 O								
Ti	0.15	0.15	0.15	0.15	0.14	0.17	0.02	0.01
V	0.06	0.05	0.06	0.06	0.06	0.07	0.01	0.00
Al	5.47	5.56	5.55	5.55	5.54	5.18	0.31	0.10
Cr	8.65	8.57	8.59	8.59	8.57	8.83	0.28	0.09
Fe^{3+}	1.67	1.66	1.65	1.65	1.69	1.76	0.10	0.03
Fe^{2+}	4.00	3.98	4.01	4.00	4.00	4.19	0.15	0.05
Mn	0.05	0.06	0.05	0.06	0.06	0.06	0.00	0.00
Ni	0.03	0.03	0.03	0.03	0.03	0.03	0.00	0.00
Co	0.00	0.00	0.01	0.00	0.00	0.00	0.00	0.00
Cu	0.01	0.01	0.00	0.01	0.02	0.00	0.01	0.00
Zn	0.03	0.03	0.02	0.02	0.02	0.02	0.01	0.00
Mg	3.92	3.95	3.93	3.93	3.93	3.75	0.14	0.04
$\Sigma(M^{3+},M^{4+})$	16.00	16.00	16.00	16.00	16.00	16.00	0.00	0.00
ΣM^{2+}	8.05	8.05	8.05	8.05	8.05	8.05		

x = Average s = standard deviation CL = 95% confidence limit

Table 2 *Electron-microprobe analyses of selected sintered chromite grains in sample A1.*

	1	2	3	4	5	6	7	8	$\bar{x}$	s	CL
TiO_2	0.94	0.99	0.94	1.19	1.13	1.15	1.04	1.15	1.07	0.10	0.08
V_2O_3	0.19	0.29	0.32	0.39	0.36	0.33	0.43	0.46	0.35	0.09	0.07
Al_2O_3	15.69	15.07	16.56	14.77	14.74	14.73	14.60	14.23	15.05	0.74	0.62
Cr_2O_3	43.40	44.26	43.16	44.14	43.82	43.87	44.44	44.58	43.96	0.50	0.42
Fe_2O_3	9.46	9.30	9.17	9.41	9.67	9.69	9.26	9.42	9.42	0.19	0.16
FeO	19.66	19.73	18.41	19.74	19.71	19.60	20.15	19.80	19.60	0.51	0.43
MnO	0.27	0.26	0.26	0.26	0.27	0.27	0.27	0.27	0.27	0.00	0.00
NiO	0.13	0.15	0.16	0.12	0.11	0.13	0.12	0.11	0.13	0.02	0.02
CoO	0.01	0.01	0.04	0.02	0.01	0.00	0.00	0.01	0.01	0.01	0.01
Cu_2O	0.09	0.05	0.02	0.07	0.00	0.03	0.00	0.01	0.03	0.03	0.03
ZnO	0.01	0.09	0.04	0.05	0.05	0.12	0.10	0.10	0.07	0.04	0.03
MgO	9.23	9.14	10.16	9.12	9.14	9.16	8.85	9.02	9.23	0.39	0.33
Total	98.93	99.19	99.08	99.11	98.84	98.89	99.10	99.00	99.02	0.12	0.10
Number of ions on the basis of 32 O											
Ti	0.19	0.20	0.18	0.24	0.22	0.23	0.21	0.23	0.21	0.02	0.02
V	0.04	0.06	0.07	0.08	0.08	0.07	0.09	0.10	0.07	0.02	0.02
Al	4.87	4.68	5.08	4.60	4.60	4.59	4.55	4.45	4.68	0.20	0.17
Cr	9.03	9.22	8.88	9.22	9.17	9.18	9.30	9.35	9.17	0.15	0.13
Fe^{3+}	1.87	1.84	1.80	1.87	1.93	1.93	1.85	1.88	1.87	0.04	0.04
Fe^{2+}	4.33	4.35	4.01	4.36	4.36	4.34	4.46	4.39	4.32	0.14	0.11
Mn	0.06	0.06	0.06	0.06	0.06	0.06	0.06	0.06	0.06	0.00	0.00
Ni	0.03	0.03	0.03	0.03	0.02	0.03	0.03	0.02	0.03	0.00	0.00
Co	0.00	0.00	0.01	0.00	0.00	0.00	0.00	0.00	0.00	0.00	0.00
Cu	0.02	0.01	0.00	0.02	0.00	0.01	0.00	0.00	0.01	0.01	0.01
Zn	0.00	0.02	0.01	0.01	0.01	0.02	0.02	0.02	0.01	0.01	0.01
Mg	3.62	3.59	3.94	3.59	3.61	3.61	3.49	3.56	3.63	0.13	0.11
$\Sigma(M^{3+},M^{4+})$	16.00	16.00	16.00	16.00	16.00	16.00	16.00	16.00	16.00		
ΣM^{2+}	8.06	8.06	8.06	8.06	8.07	8.07	8.06	8.06	8.06		

x = Average s = standard deviation CL = 95% confidence limit

Table 3 *Electron-microprobe analyses of selected chromite grains in sample C1.*

	1	2	3	4	5	6	7	8	9	10	11	12
TiO_2	0.61	0.64	0.49	0.69	0.57	0.58	0.73	1.06	1.05	1.12	1.05	1.04
V_2O_3	0.56	0.52	0.42	0.58	0.51	0.47	0.48	0.53	0.51	0.54	0.38	0.40
Al_2O_3	14.03	14.54	13.54	14.58	14.51	14.13	14.47	14.40	14.87	14.58	15.03	15.48
Cr_2O_3	44.72	44.40	46.19	44.10	44.97	46.03	44.16	43.95	43.47	44.29	43.48	43.39
Fe_2O_3	9.28	9.20	8.47	9.38	8.69	8.12	9.44	9.50	9.99	8.98	9.97	9.66
FeO	21.37	21.49	21.63	21.37	21.43	21.51	21.49	21.49	19.82	21.48	19.81	20.02
MnO	0.29	0.28	0.29	0.29	0.30	0.29	0.29	0.30	0.26	0.27	0.29	0.27
NiO	0.09	0.11	0.07	0.10	0.07	0.07	0.12	0.14	0.15	0.12	0.15	0.16
CoO	0.00	0.01	0.02	0.06	0.02	0.03	0.03	0.02	0.02	0.01	0.01	0.00
Cu_2O	0.05	0.00	0.00	0.04	0.02	0.02	0.00	0.00	0.01	0.03	0.00	0.03
ZnO	0.16	0.13	0.14	0.08	0.09	0.13	0.10	0.13	0.09	0.13	0.08	0.11
MgO	7.89	7.93	7.69	7.99	7.97	7.88	7.92	7.93	9.08	7.99	9.10	9.03
Total	98.95	99.14	98.85	99.14	99.08	99.15	99.09	99.29	99.14	99.37	99.18	99.44
Number of ions on the basis of 32 O												
Ti	0.12	0.13	0.10	0.14	0.11	0.12	0.15	0.21	0.21	0.22	0.21	0.20
V	0.12	0.11	0.09	0.12	0.11	0.10	0.10	0.11	0.11	0.11	0.08	0.08
Al	4.42	4.56	4.29	4.57	4.56	4.44	4.55	4.52	4.63	4.56	4.67	4.79
Cr	9.46	9.35	9.81	9.28	9.47	9.71	9.31	9.25	9.07	9.30	9.07	9.01
Fe^{3+}	1.87	1.84	1.71	1.88	1.74	1.63	1.89	1.90	1.98	1.80	1.98	1.91
Fe^{2+}	4.78	4.79	4.86	4.76	4.77	4.80	4.79	4.79	4.38	4.77	4.37	4.40
Mn	0.06	0.06	0.07	0.07	0.07	0.06	0.06	0.07	0.06	0.06	0.06	0.06
Ni	0.02	0.02	0.02	0.02	0.02	0.02	0.03	0.03	0.03	0.03	0.03	0.03
Co	0.00	0.00	0.00	0.01	0.00	0.01	0.01	0.00	0.00	0.00	0.00	0.00
Cu	0.01	0.00	0.00	0.01	0.01	0.00	0.00	0.00	0.00	0.01	0.00	0.01
Zn	0.03	0.03	0.03	0.02	0.02	0.03	0.02	0.03	0.02	0.02	0.02	0.02
Mg	3.15	3.15	3.08	3.17	3.17	3.13	3.15	3.15	3.57	3.16	3.58	3.54
$\Sigma(M^{3+},M^{4+})$	16.00	16.00	16.00	16.00	16.00	16.00	16.00	16.00	16.00	16.00	16.00	16.00
ΣM^{2+}	8.05	8.05	8.05	8.05	8.05	8.05	8.06	8.06	8.06	8.06	8.06	8.06

Table 3 continued *Electron-microprobe analyses of selected chromite grains in sample C1.*

	13	14	15	16	17	18	19	20	21	22	$\bar{x}$	s	CL
TiO_2	1.04	1.03	1.04	1.04	1.03	1.03	1.05	1.03	1.05	1.05	0.91	0.21	0.15
V_2O_3	0.36	0.38	0.41	0.40	0.46	0.47	0.42	0.47	0.38	0.33	0.45	0.07	0.05
Al_2O_3	15.49	15.43	15.50	15.43	15.44	15.51	15.56	15.42	15.58	15.55	14.96	0.61	0.44
Cr_2O_3	43.30	43.15	43.14	43.44	43.31	43.32	43.33	43.52	43.28	43.27	43.92	0.88	0.63
Fe_2O_3	9.81	9.84	9.77	9.58	9.72	9.67	9.60	9.58	9.66	9.69	9.44	0.48	0.34
FeO	19.88	19.96	19.89	20.04	19.97	20.03	20.00	20.02	20.01	20.03	20.58	0.77	0.55
MnO	0.27	0.27	0.26	0.26	0.28	0.28	0.26	0.27	0.26	0.25	0.28	0.01	0.01
NiO	0.16	0.14	0.15	0.15	0.16	0.15	0.15	0.16	0.15	0.16	0.13	0.03	0.02
CoO	0.01	0.00	0.01	0.00	0.03	0.00	0.04	0.03	0.02	0.02	0.02	0.02	0.01
Cu_2O	0.03	0.00	0.01	0.01	0.02	0.03	0.00	0.00	0.01	0.00	0.01	0.02	0.01
ZnO	0.10	0.08	0.11	0.12	0.08	0.07	0.11	0.13	0.09	0.09	0.11	0.02	0.02
MgO	9.12	9.07	9.11	9.02	9.06	9.06	9.06	9.03	9.08	9.05	8.59	0.59	0.42
Total	99.41	99.20	99.23	99.32	99.40	99.47	99.42	99.51	99.40	99.32	99.25		
Number of ions on the basis of 32 O													
Ti	0.21	0.20	0.21	0.21	0.20	0.20	0.21	0.20	0.21	0.21	0.18	0.04	0.03
V	0.08	0.08	0.09	0.09	0.10	0.10	0.09	0.10	0.08	0.07	0.10	0.02	0.01
Al	4.79	4.79	4.80	4.78	4.78	4.80	4.81	4.77	4.82	4.82	4.66	0.16	0.11
Cr	8.99	8.98	8.97	9.03	9.00	8.99	8.99	9.03	8.98	8.99	9.18	0.25	0.18
Fe^{3+}	1.94	1.95	1.93	1.90	1.92	1.91	1.90	1.89	1.91	1.92	1.88	0.09	0.06
Fe^{2+}	4.36	4.39	4.37	4.41	4.39	4.40	4.39	4.39	4.39	4.40	4.55	0.20	0.15
Mn	0.06	0.06	0.06	0.06	0.06	0.06	0.06	0.06	0.06	0.05	0.06	0.00	0.00
Ni	0.03	0.03	0.03	0.03	0.03	0.03	0.03	0.03	0.03	0.03	0.03	0.01	0.00
Co	0.00	0.00	0.00	0.00	0.01	0.00	0.01	0.01	0.00	0.00	0.00	0.00	0.00
Cu	0.01	0.00	0.00	0.00	0.00	0.01	0.00	0.00	0.00	0.00	0.00	0.00	0.00
Zn	0.02	0.01	0.02	0.02	0.02	0.01	0.02	0.03	0.02	0.02	0.02	0.00	0.00
Mg	3.57	3.56	3.57	3.54	3.55	3.54	3.55	3.54	3.55	3.54	3.39	0.21	0.15
$\Sigma(M^{3+},M^{4+})$	16.00	16.00	16.00	16.00	16.00	16.00	16.00	16.00	16.00	16.00	16.00		
ΣM^{2+}	8.06	8.06	8.06	8.06	8.06	8.06	8.06	8.06	8.05	8.06	8.06		

$\bar{x}$ = Average s = standard deviation CL = 95% confidence limit

Table 4 *Electron-microprobe analyses of selected sintered chromite grains in sample C1.*

	1	2	3	4	5	6	7	8	9	10	11	$\bar{x}$	s	CL
TiO_2	1.19	1.17	1.18	1.19	1.19	3.45	1.19	1.20	1.20	1.18	1.18	1.19	0.01	0.01
V_2O_3	0.43	0.51	0.47	0.40	0.48	0.40	0.42	0.49	0.43	0.36	0.35	0.44	0.05	0.04
Al_2O_3	15.15	15.18	15.20	15.27	15.19	14.54	15.16	15.08	14.89	15.16	15.26	15.16	0.11	0.08
Cr_2O_3	43.32	43.41	43.34	43.42	43.45	42.87	43.38	43.55	43.74	43.78	43.55	43.49	0.16	0.11
Fe_2O_3	9.98	9.89	9.92	9.84	9.91	8.46	9.97	9.79	9.76	9.73	9.96	9.87	0.09	0.07
FeO	19.47	19.48	19.51	19.56	19.48	20.67	19.42	19.62	19.68	19.54	19.42	19.52	0.08	0.06
MnO	0.28	0.28	0.28	0.30	0.29	0.25	0.27	0.28	0.29	0.28	0.27	0.28	0.01	0.01
NiO	0.17	0.15	0.14	0.16	0.17	0.14	0.15	0.14	0.16	0.16	0.17	0.16	0.01	0.01
CoO	0.00	0.04	0.04	0.00	0.04	0.03	0.04	0.02	0.02	0.00	0.03	0.02	0.02	0.01
Cu_2O	0.00	0.00	0.01	0.00	0.03	0.04	0.02	0.03	0.04	0.05	0.00	0.02	0.02	0.01
ZnO	0.05	0.09	0.10	0.10	0.12	0.11	0.10	0.11	0.11	0.10	0.13	0.10	0.02	0.02
MgO	9.38	9.37	9.33	9.32	9.33	8.61	9.38	9.25	9.15	9.31	9.42	9.32	0.08	0.05
Total	99.23	99.38	99.35	99.37	99.49	99.12	99.32	99.38	99.29	99.49	99.56	99.39	0.10	0.07
Number of ions on the basis of 32 O														
Ti	0.23	0.23	0.23	0.23	0.23	0.69	0.24	0.24	0.24	0.23	0.23	0.23	0.00	0.00
V	0.09	0.11	0.10	0.08	0.10	0.09	0.09	0.10	0.09	0.08	0.07	0.09	0.01	0.01
Al	4.69	4.70	4.71	4.73	4.70	4.55	4.69	4.67	4.62	4.69	4.71	4.69	0.03	0.02
Cr	9.00	9.01	9.00	9.01	9.01	8.99	9.01	9.05	9.11	9.08	9.02	9.03	0.04	0.03
Fe^{3+}	1.98	1.95	1.96	1.94	1.96	1.69	1.97	1.94	1.93	1.92	1.96	1.95	0.02	0.01
Fe^{2+}	4.28	4.28	4.29	4.29	4.27	4.59	4.27	4.31	4.34	4.29	4.25	4.29	0.02	0.02
Mn	0.06	0.06	0.06	0.07	0.06	0.06	0.06	0.06	0.06	0.06	0.06	0.06	0.00	0.00
Ni	0.04	0.03	0.03	0.03	0.04	0.03	0.03	0.03	0.03	0.03	0.04	0.03	0.00	0.00
Co	0.00	0.01	0.01	0.00	0.01	0.01	0.01	0.00	0.00	0.00	0.01	0.00	0.00	0.00
Cu	0.00	0.00	0.00	0.00	0.01	0.01	0.00	0.01	0.01	0.01	0.00	0.00	0.00	0.00
Zn	0.01	0.02	0.02	0.02	0.02	0.02	0.02	0.02	0.02	0.02	0.02	0.02	0.00	0.00
Mg	3.68	3.67	3.65	3.65	3.65	3.41	3.67	3.63	3.59	3.64	3.68	3.65	0.03	0.02
$\Sigma(M^{3+},M^{4+})$	16.00	16.00	16.00	16.00	16.00	16.00	16.00	16.00	16.00	16.00	16.00	16.00		
ΣM^{2+}	8.06	8.06	8.06	8.06	8.06	8.11	8.06	8.06	8.06	8.06	8.06	8.06		

$\bar{x}$ = Average s = standard deviation CL = 95% confidence limit

Table 5 *Electron-microprobe analyses of selected sintered chromite grains in sample C1.*

	1	2	3	4	5	6	7	8	9	10	$\bar{x}$	s	CL
TiO_2	1.31	1.22	1.30	1.31	1.30	1.29	1.30	1.30	1.31	1.30	1.29	0.03	0.02
V_2O_3	0.46	0.31	0.39	0.35	0.44	0.36	0.42	0.44	0.43	0.43	0.40	0.05	0.03
Al_2O_3	15.00	15.01	15.19	15.27	15.22	15.23	15.19	15.22	15.31	15.21	15.19	0.10	0.07
Cr_2O_3	42.94	42.95	43.07	43.02	42.94	42.80	42.78	42.97	42.94	42.96	42.94	0.09	0.06
Fe_2O_3	10.24	10.44	10.14	10.08	10.09	10.25	10.25	10.01	10.06	10.02	10.16	0.14	0.10
FeO	20.11	20.04	20.05	20.22	20.25	20.11	20.08	20.22	20.10	20.19	20.14	0.08	0.06
MnO	0.27	0.29	0.25	0.24	0.26	0.27	0.25	0.26	0.27	0.26	0.26	0.01	0.01
NiO	0.16	0.15	0.16	0.16	0.17	0.17	0.16	0.16	0.15	0.18	0.16	0.01	0.01
CoO	0.02	0.02	0.02	0.01	0.00	0.01	0.03	0.00	0.03	0.03	0.02	0.01	0.01
Cu_2O	0.03	0.08	0.08	0.05	0.02	0.00	0.03	0.01	0.04	0.01	0.04	0.03	0.02
ZnO	0.09	0.08	0.11	0.11	0.10	0.11	0.10	0.11	0.15	0.14	0.11	0.02	0.02
MgO	8.93	8.93	8.99	8.91	8.90	8.96	8.97	8.91	8.96	8.88	8.93	0.04	0.03
Total	99.37	99.36	99.57	99.55	99.49	99.37	99.37	99.41	99.55	99.43	99.45	0.08	0.06
Number of ions on the basis of 32 O													
Ti	0.26	0.24	0.26	0.26	0.26	0.26	0.26	0.26	0.26	0.26	0.26	0.00	0.00
V	0.10	0.07	0.08	0.07	0.09	0.08	0.09	0.09	0.09	0.09	0.08	0.01	0.01
Al	4.66	4.66	4.71	4.73	4.72	4.73	4.72	4.72	4.74	4.72	4.71	0.03	0.02
Cr	8.95	8.95	8.95	8.94	8.93	8.91	8.91	8.94	8.92	8.94	8.94	0.02	0.01
Fe^{3+}	2.03	2.07	2.01	1.99	2.00	2.03	2.03	1.98	1.99	1.99	2.01	0.03	0.02
Fe^{2+}	4.43	4.42	4.41	4.45	4.46	4.43	4.42	4.45	4.42	4.45	4.43	0.02	0.01
Mn	0.06	0.06	0.05	0.05	0.06	0.06	0.06	0.06	0.06	0.06	0.06	0.00	0.00
Ni	0.03	0.03	0.03	0.03	0.04	0.04	0.03	0.03	0.03	0.04	0.03	0.00	0.00
Co	0.00	0.01	0.00	0.00	0.00	0.00	0.01	0.00	0.01	0.01	0.00	0.00	0.00
Cu	0.01	0.02	0.02	0.01	0.00	0.00	0.01	0.00	0.01	0.00	0.01	0.01	0.00
Zn	0.02	0.02	0.02	0.02	0.02	0.02	0.02	0.02	0.03	0.03	0.02	0.00	0.00
Mg	3.51	3.51	3.52	3.49	3.49	3.52	3.52	3.50	3.51	3.48	3.50	0.01	0.01
$\Sigma(M^{3+},M^{4+})$	16.00	16.00	16.00	16.00	16.00	16.00	16.00	16.00	16.00	16.00	16.00		
ΣM^{2+}	8.06	8.06	8.06	8.06	8.06	8.06	8.06	8.06	8.06	8.06	8.06		

x = Average s = standard deviation CL = 95% confidence limit

Table 6 *Electron-microprobe analyses of selected chromite grains in sample A5.*

	1	2	3	4	5	6	7	8	9	10	11	12	13
TiO_2	1.04	1.04	1.04	1.04	1.04	1.08	1.06	1.03	1.05	1.01	1.07	0.93	0.96
V_2O_3	0.29	0.23	0.23	0.26	0.32	0.27	0.24	0.27	0.25	0.26	0.23	0.22	0.27
Al_2O_3	17.64	17.51	17.23	17.42	17.31	17.78	17.11	16.99	17.25	16.92	17.15	17.38	17.11
Cr_2O_3	44.45	44.57	44.78	44.32	44.60	44.07	44.65	44.96	44.77	44.72	44.56	44.50	44.18
Fe_2O_3	5.70	5.76	5.86	5.98	5.76	5.93	5.94	5.83	5.90	6.01	6.04	5.99	6.30
FeO	21.96	21.98	21.98	21.88	22.06	21.76	22.01	22.05	21.93	21.74	21.92	22.21	22.28
MnO	0.27	0.26	0.25	0.28	0.25	0.26	0.26	0.27	0.26	0.26	0.25	0.28	0.26
NiO	0.19	0.17	0.15	0.17	0.17	0.17	0.16	0.16	0.17	0.19	0.16	0.17	0.17
CoO	0.01	0.03	0.01	0.02	0.00	0.02	0.01	0.02	0.02	0.02	0.03	0.00	0.02
Cu_2O	0.00	0.04	0.01	0.00	0.03	0.00	0.00	0.04	0.03	0.07	0.07	0.01	0.00
ZnO	0.13	0.10	0.08	0.12	0.11	0.12	0.11	0.09	0.09	0.13	0.09	0.12	0.10
MgO	8.01	7.98	8.00	8.01	7.92	8.16	7.92	7.88	8.01	7.96	7.96	7.82	7.71
Total	99.54	99.52	99.48	99.35	99.43	99.46	99.32	99.44	99.59	99.16	99.37	99.48	99.22
Number of ions on the basis of 32 O													
Ti	0.20	0.20	0.20	0.21	0.21	0.21	0.21	0.20	0.21	0.20	0.21	0.18	0.19
V	0.06	0.05	0.05	0.05	0.07	0.06	0.05	0.06	0.05	0.06	0.05	0.05	0.06
Al	5.43	5.40	5.32	5.38	5.35	5.47	5.30	5.26	5.32	5.25	5.30	5.37	5.31
Cr	9.18	9.22	9.27	9.18	9.24	9.10	9.27	9.33	9.26	9.31	9.24	9.22	9.20
Fe^{3+}	1.12	1.13	1.16	1.18	1.14	1.16	1.17	1.15	1.16	1.19	1.19	1.18	1.25
Fe^{2+}	4.80	4.81	4.81	4.79	4.83	4.75	4.83	4.84	4.80	4.79	4.81	4.87	4.91
Mn	0.06	0.06	0.06	0.06	0.06	0.06	0.06	0.06	0.06	0.06	0.06	0.06	0.06
Ni	0.04	0.04	0.03	0.04	0.04	0.04	0.03	0.03	0.04	0.04	0.03	0.04	0.04
Co	0.00	0.01	0.00	0.00	0.00	0.00	0.00	0.00	0.00	0.00	0.01	0.00	0.01
Cu	0.00	0.01	0.00	0.00	0.01	0.00	0.00	0.01	0.01	0.01	0.02	0.00	0.00
Zn	0.02	0.02	0.02	0.02	0.02	0.02	0.02	0.02	0.02	0.02	0.02	0.02	0.02
Mg	3.12	3.11	3.12	3.13	3.09	3.17	3.10	3.08	3.12	3.12	3.11	3.05	3.03
$\Sigma(M^{3+},M^{4+})$	16.00	16.00	16.00	16.00	16.00	16.00	16.00	16.00	16.00	16.00	16.00	16.00	16.00
ΣM^{2+}	8.05	8.05	8.05	8.05	8.05	8.05	8.05	8.05	8.05	8.05	8.05	8.04	8.05

Table 6 continued *Electron-microprobe analyses of selected chromite grains in sample A5.*

	14	15	16	17	18	19	20	21	22	23	24	25	26
TiO_2	0.96	0.97	0.96	0.96	0.96	0.94	0.98	0.96	1.04	1.07	1.07	1.06	1.04
V_2O_3	0.26	0.26	0.25	0.28	0.26	0.22	0.28	0.29	0.25	0.19	0.22	0.25	0.28
Al_2O_3	17.36	17.33	17.22	17.24	17.14	16.98	17.43	17.20	17.41	17.04	17.14	17.17	17.17
Cr_2O_3	43.62	43.99	44.11	44.03	44.23	44.45	43.84	44.06	44.96	45.20	45.05	44.96	45.14
Fe_2O_3	6.55	6.33	6.35	6.32	6.25	6.36	6.27	6.27	5.52	5.76	5.83	5.71	5.60
FeO	22.07	22.19	22.22	22.20	22.23	22.12	22.24	22.24	21.27	21.37	21.31	21.38	21.50
MnO	0.25	0.25	0.28	0.25	0.26	0.26	0.25	0.26	0.25	0.24	0.24	0.26	0.24
NiO	0.16	0.19	0.18	0.19	0.18	0.18	0.17	0.17	0.17	0.15	0.15	0.17	0.17
CoO	0.03	0.02	0.01	0.00	0.01	0.06	0.01	0.02	0.00	0.06	0.01	0.02	0.02
Cu_2O	0.04	0.03	0.00	0.08	0.04	0.05	0.02	0.03	0.00	0.03	0.00	0.06	0.00
ZnO	0.12	0.09	0.13	0.11	0.10	0.11	0.10	0.13	0.11	0.10	0.10	0.11	0.05
MgO	7.82	7.79	7.76	7.74	7.73	7.76	7.77	7.71	8.44	8.32	8.43	8.28	8.31
Total	99.10	99.29	99.30	99.27	99.26	99.34	99.22	99.20	99.25	99.37	99.38	99.28	99.36
Number of ions on the basis of 32 O													
Ti	0.19	0.19	0.19	0.19	0.19	0.19	0.19	0.19	0.20	0.21	0.21	0.21	0.20
V	0.06	0.05	0.05	0.06	0.06	0.05	0.06	0.06	0.05	0.04	0.05	0.05	0.06
Al	5.38	5.37	5.33	5.34	5.32	5.26	5.40	5.34	5.36	5.26	5.28	5.30	5.29
Cr	9.08	9.14	9.17	9.16	9.20	9.25	9.11	9.17	9.29	9.36	9.31	9.31	9.34
Fe^{3+}	1.30	1.25	1.26	1.25	1.24	1.26	1.24	1.24	1.09	1.13	1.15	1.13	1.10
Fe^{2+}	4.86	4.88	4.89	4.88	4.89	4.87	4.89	4.90	4.65	4.68	4.66	4.68	4.71
Mn	0.05	0.06	0.06	0.06	0.06	0.06	0.06	0.06	0.05	0.05	0.05	0.06	0.05
Ni	0.03	0.04	0.04	0.04	0.04	0.04	0.04	0.04	0.04	0.03	0.03	0.04	0.04
Co	0.01	0.00	0.00	0.00	0.00	0.01	0.00	0.00	0.00	0.01	0.00	0.00	0.00
Cu	0.01	0.01	0.00	0.02	0.01	0.01	0.00	0.01	0.00	0.01	0.00	0.01	0.00
Zn	0.02	0.02	0.02	0.02	0.02	0.02	0.02	0.03	0.02	0.02	0.02	0.02	0.01
Mg	3.07	3.05	3.04	3.03	3.03	3.04	3.05	3.03	3.29	3.25	3.28	3.23	3.24
$\Sigma(M^{3+},M^{4+})$	16.00	16.00	16.00	16.00	16.00	16.00	16.00	16.00	16.00	16.00	16.00	16.00	16.00
ΣM^{2+}	8.05	8.05	8.05	8.05	8.05	8.05	8.05	8.05	8.05	8.05	8.05	8.05	8.05

Table 6 continued *Electron-microprobe analyses of selected chromite grains in sample A5.*

	27	28	29	30	31	32	33	34	35	36	37	$\bar{x}$	s	CL
TiO_2	0.90	0.91	0.92	0.93	0.91	0.94	0.95	0.97	0.95	0.97	0.97	0.99	0.05	0.02
V_2O_3	0.34	0.29	0.27	0.27	0.24	0.28	0.38	0.36	0.33	0.34	0.30	0.27	0.04	0.01
Al_2O_3	18.69	18.31	18.18	17.78	18.11	18.30	17.55	17.56	17.53	17.44	17.38	17.44	0.41	0.14
Cr_2O_3	42.91	43.35	43.35	43.53	43.00	43.03	43.73	43.72	43.73	43.64	43.73	44.18	0.63	0.21
Fe_2O_3	5.97	6.03	6.17	6.28	6.38	6.22	6.28	6.31	6.34	6.48	6.35	6.08	0.27	0.09
FeO	21.58	21.71	21.75	21.75	21.61	21.72	21.86	21.93	21.83	21.95	21.94	21.88	0.28	0.09
MnO	0.25	0.25	0.25	0.27	0.26	0.25	0.26	0.27	0.26	0.25	0.25	0.26	0.01	0.00
NiO	0.16	0.18	0.17	0.17	0.17	0.17	0.16	0.18	0.18	0.18	0.16	0.17	0.01	0.00
CoO	0.01	0.05	0.03	0.00	0.05	0.00	0.04	0.00	0.00	0.02	0.00	0.02	0.02	0.01
Cu_2O	0.06	0.04	0.01	0.02	0.03	0.02	0.01	0.08	0.02	0.00	0.03	0.03	0.02	0.01
ZnO	0.09	0.08	0.09	0.08	0.05	0.09	0.08	0.11	0.11	0.12	0.03	0.10	0.02	0.01
MgO	8.30	8.18	8.16	8.10	8.18	8.20	8.03	7.95	8.03	7.94	7.96	8.01	0.21	0.07
Total	99.12	99.24	99.23	99.03	98.84	99.06	99.17	99.29	99.17	99.19	98.96	99.28	0.16	0.05
Number of ions on the basis of 32 O														
Ti	0.18	0.18	0.18	0.18	0.18	0.19	0.19	0.19	0.19	0.19	0.19	0.20	0.01	0.00
V	0.07	0.06	0.06	0.06	0.05	0.06	0.08	0.08	0.07	0.07	0.06	0.06	0.01	0.00
Al	5.74	5.63	5.60	5.49	5.60	5.64	5.42	5.43	5.42	5.40	5.39	5.39	0.12	0.04
Cr	8.84	8.95	8.95	9.03	8.91	8.89	9.07	9.06	9.07	9.06	9.10	9.16	0.13	0.04
Fe^{3+}	1.17	1.18	1.21	1.24	1.26	1.22	1.24	1.24	1.25	1.28	1.26	1.20	0.06	0.02
Fe^{2+}	4.70	4.74	4.75	4.77	4.74	4.75	4.80	4.81	4.79	4.82	4.83	4.80	0.07	0.02
Mn	0.06	0.06	0.06	0.06	0.06	0.05	0.06	0.06	0.06	0.06	0.06	0.06	0.00	0.00
Ni	0.03	0.04	0.04	0.04	0.04	0.03	0.03	0.04	0.04	0.04	0.03	0.04	0.00	0.00
Co	0.00	0.01	0.01	0.00	0.01	0.00	0.01	0.00	0.00	0.00	0.00	0.00	0.00	0.00
Cu	0.01	0.01	0.00	0.00	0.01	0.00	0.00	0.02	0.00	0.00	0.01	0.01	0.01	0.00
Zn	0.02	0.02	0.02	0.02	0.01	0.02	0.01	0.02	0.02	0.02	0.01	0.02	0.00	0.00
Mg	3.22	3.18	3.18	3.17	3.20	3.19	3.14	3.11	3.14	3.11	3.12	3.13	0.07	0.02
$\Sigma(M^{3+},M^{4+})$	16.00	16.00	16.00	16.00	16.00	16.00	16.00	16.00	16.00	16.00	16.00	16.00		
ΣM^{2+}	8.05	8.05	8.05	8.05	8.05	8.05	8.05	8.05	8.05	8.05	8.05	8.05		

$\bar{x}$ = Average s = standard deviation CL = 95% confidence limit

Table 7 *Electron-microprobe analyses of selected sintered chromite grains in sample A5.*

	1	2	3	4	5	6	7	8	9	10	11
TiO_2	1.99	2.01	1.99	2.01	2.00	1.97	2.00	2.01	1.89	1.94	3.03
V_2O_3	0.26	0.32	0.33	0.26	0.30	0.24	0.29	0.33	0.23	0.25	0.26
Al_2O_3	14.88	15.13	15.07	15.06	15.03	15.46	15.80	15.70	15.43	15.66	12.71
Cr_2O_3	41.15	40.72	40.80	41.08	41.09	40.43	40.05	40.54	41.28	40.74	40.43
Fe_2O_3	9.43	9.50	9.40	9.25	9.36	9.82	9.87	9.59	9.35	9.57	11.23
FeO	25.16	25.16	25.10	25.24	25.19	24.36	24.38	24.48	24.48	24.54	26.21
MnO	0.28	0.30	0.28	0.30	0.28	0.28	0.30	0.29	0.29	0.31	0.31
NiO	0.16	0.16	0.16	0.17	0.17	0.14	0.16	0.13	0.14	0.14	0.14
CoO	0.00	0.02	0.02	0.02	0.01	0.04	0.00	0.01	0.02	0.01	0.03
Cu_2O	0.06	0.03	0.04	0.01	0.07	0.00	0.05	0.01	0.06	0.00	0.06
ZnO	0.14	0.14	0.14	0.15	0.15	0.15	0.13	0.13	0.13	0.12	0.15
MgO	5.52	5.55	5.58	5.49	5.52	6.12	6.15	6.15	6.08	6.10	4.65
Total	98.75	98.74	98.68	98.74	98.89	98.72	98.88	99.07	99.13	99.10	98.80
Number of ions on the basis of 32 O											
Ti	0.41	0.41	0.41	0.41	0.41	0.40	0.41	0.41	0.38	0.39	0.63
V	0.06	0.07	0.07	0.06	0.06	0.05	0.06	0.07	0.05	0.05	0.06
Al	4.77	4.84	4.82	4.82	4.81	4.92	5.01	4.97	4.89	4.96	4.14
Cr	8.84	8.74	8.76	8.82	8.81	8.63	8.52	8.61	8.78	8.66	8.84
Fe^{3+}	1.93	1.94	1.92	1.89	1.91	1.99	2.00	1.94	1.89	1.94	2.34
Fe^{2+}	5.72	5.71	5.70	5.73	5.71	5.50	5.49	5.50	5.51	5.52	6.06
Mn	0.06	0.07	0.06	0.07	0.07	0.06	0.07	0.07	0.07	0.07	0.07
Ni	0.04	0.03	0.03	0.04	0.04	0.03	0.03	0.03	0.03	0.03	0.03
Co	0.00	0.00	0.00	0.00	0.00	0.01	0.00	0.00	0.00	0.00	0.01
Cu	0.01	0.01	0.01	0.00	0.02	0.00	0.01	0.00	0.01	0.00	0.01
Zn	0.03	0.03	0.03	0.03	0.03	0.03	0.02	0.03	0.03	0.02	0.03
Mg	2.24	2.24	2.26	2.22	2.23	2.46	2.47	2.46	2.44	2.44	1.92
$\Sigma(M^{3+},M^{4+})$	16.00	16.00	16.00	16.00	16.00	16.00	16.00	16.00	16.00	16.00	16.00
ΣM^{2+}	8.10	8.10	8.10	8.10	8.09	8.10	8.09	8.09	8.08	8.09	8.13

Table 7 continued *Electron-microprobe analyses of selected sintered chromite grains in sample A5.*

	12	13	14	15	$\bar{x}$	s	CL
TiO_2	3.00	2.93	2.93	2.98	2.31	0.49	0.28
V_2O_3	0.29	0.29	0.27	0.31	0.28	0.03	0.02
Al_2O_3	12.77	12.67	12.81	12.79	14.46	1.28	0.75
Cr_2O_3	40.49	40.75	40.65	40.57	40.72	0.33	0.19
Fe_2O_3	11.16	11.02	11.03	11.10	10.05	0.80	0.47
FeO	26.21	26.23	26.27	26.33	25.29	0.77	0.45
MnO	0.31	0.31	0.31	0.30	0.30	0.01	0.01
NiO	0.13	0.16	0.14	0.15	0.15	0.01	0.01
CoO	0.07	0.00	0.02	0.02	0.02	0.02	0.01
Cu_2O	0.07	0.04	0.00	0.01	0.03	0.03	0.02
ZnO	0.17	0.16	0.17	0.11	0.14	0.02	0.01
MgO	4.64	4.64	4.66	4.66	5.43	0.63	0.37
Total	98.88	98.81	98.84	98.91	98.86	0.14	0.08
Number of ions on the basis of 32 O							
Ti	0.62	0.61	0.61	0.62	0.47	0.11	0.06
V	0.06	0.07	0.06	0.07	0.06	0.01	0.00
Al	4.16	4.13	4.17	4.16	4.64	0.36	0.21
Cr	8.84	8.90	8.87	8.85	8.77	0.11	0.06
Fe^{3+}	2.32	2.29	2.29	2.30	2.06	0.18	0.11
Fe^{2+}	6.05	6.06	6.07	6.08	5.76	0.24	0.14
Mn	0.07	0.07	0.07	0.07	0.07	0.00	0.00
Ni	0.03	0.03	0.03	0.03	0.03	0.00	0.00
Co	0.01	0.00	0.00	0.00	0.00	0.00	0.00
Cu	0.02	0.01	0.00	0.00	0.01	0.01	0.00
Zn	0.03	0.03	0.03	0.02	0.03	0.00	0.00
Mg	1.91	1.91	1.92	1.92	2.20	0.23	0.13
$\Sigma(M^{3+},M^{4+})$	16.00	16.00	16.00	16.00	16.00		
ΣM^{2+}	8.13	8.13	8.12	8.12	8.10		

x = Average s = standard deviation CL = 95% confidence limit

Table 8 *Electron-microprobe analyses of selected sintered chromite grains in sample B4.*

	1	2	3	4	5	6	7	8	9	10	11	12	13	14
TiO_2	1.34	1.35	1.34	1.38	1.39	1.40	1.43	1.41	1.38	1.38	1.38	1.30	1.24	1.17
V_2O_3	0.33	0.37	0.36	0.48	0.39	0.35	0.35	0.38	0.42	0.42	0.44	0.36	0.44	0.34
Al_2O_3	15.15	15.34	15.06	14.94	14.50	14.58	14.62	14.80	14.63	14.82	14.62	15.44	15.07	14.98
Cr_2O_3	42.03	41.81	41.89	41.71	42.30	41.75	41.35	41.44	42.07	41.82	41.90	41.64	41.92	41.41
Fe_2O_3	10.78	10.74	10.76	10.87	10.62	11.20	11.42	11.33	10.99	11.04	11.02	10.88	10.73	11.53
FeO	21.56	21.46	21.50	21.43	21.68	21.41	21.41	21.36	21.49	21.45	21.49	20.86	20.91	21.03
MnO	0.28	0.27	0.28	0.27	0.27	0.28	0.26	0.27	0.26	0.27	0.27	0.27	0.26	0.29
NiO	0.19	0.20	0.18	0.18	0.18	0.16	0.19	0.20	0.16	0.15	0.16	0.18	0.17	0.16
CoO	0.01	0.02	0.01	0.02	0.02	0.01	0.01	0.03	0.01	0.04	0.00	0.00	0.03	0.01
Cu_2O	0.01	0.03	0.00	0.04	0.00	0.03	0.00	0.01	0.01	0.04	0.00	0.02	0.00	0.01
ZnO	0.09	0.07	0.00	0.06	0.02	0.05	0.03	0.00	0.03	0.00	0.01	0.03	0.03	0.04
MgO	8.04	8.11	8.07	8.03	7.84	8.00	8.00	8.09	8.03	8.06	8.03	8.51	8.40	8.30
Total	99.62	99.57	99.24	99.22	99.00	99.00	98.86	99.08	99.28	99.29	99.10	99.29	99.00	99.09
Number of ions on the basis of 32 O														
Ti	0.27	0.27	0.27	0.28	0.28	0.28	0.29	0.28	0.28	0.28	0.28	0.26	0.25	0.23
V	0.07	0.08	0.08	0.10	0.08	0.07	0.07	0.08	0.09	0.09	0.09	0.08	0.09	0.07
Al	4.72	4.78	4.71	4.68	4.57	4.58	4.61	4.64	4.59	4.64	4.59	4.81	4.72	4.69
Cr	8.79	8.74	8.79	8.77	8.94	8.81	8.74	8.72	8.85	8.79	8.83	8.70	8.80	8.70
Fe^{3+}	2.15	2.14	2.15	2.17	2.13	2.25	2.30	2.27	2.20	2.21	2.21	2.16	2.14	2.30
Fe^{2+}	4.77	4.74	4.77	4.76	4.84	4.78	4.78	4.76	4.78	4.77	4.79	4.61	4.64	4.67
Mn	0.06	0.06	0.06	0.06	0.06	0.06	0.06	0.06	0.06	0.06	0.06	0.06	0.06	0.07
Ni	0.04	0.04	0.04	0.04	0.04	0.03	0.04	0.04	0.03	0.03	0.03	0.04	0.04	0.04
Co	0.00	0.01	0.00	0.00	0.00	0.00	0.00	0.01	0.00	0.01	0.00	0.00	0.01	0.00
Cu	0.00	0.01	0.00	0.01	0.00	0.01	0.00	0.00	0.00	0.01	0.00	0.01	0.00	0.00
Zn	0.02	0.01	0.00	0.01	0.00	0.01	0.01	0.00	0.01	0.00	0.00	0.01	0.01	0.01
Mg	3.17	3.19	3.19	3.18	3.12	3.18	3.19	3.21	3.19	3.19	3.19	3.35	3.32	3.29
$\Sigma(M^{3+},M^{4+})$	16.00	16.00	16.00	16.00	16.00	16.00	16.00	16.00	16.00	16.00	16.00	16.00	16.00	16.00
ΣM^{2+}	8.06	8.07	8.07	8.07	8.08	8.08	8.08	8.08	8.07	8.07	8.07	8.07	8.07	8.07

Table 8 continued *Electron-microprobe analyses of selected sintered chromite grains in sample B4.*

	15	16	17	18	19	20	21	22	23	24	25	26	27	28
TiO_2	1.32	1.18	1.17	1.30	1.30	1.34	1.32	1.33	1.32	1.29	1.33	1.31	1.31	1.22
V_2O_3	0.42	0.40	0.37	0.47	0.37	0.46	0.44	0.45	0.41	0.36	0.34	0.43	0.32	0.44
Al_2O_3	15.17	14.98	15.42	15.01	14.91	14.81	14.85	14.98	14.87	15.11	14.99	15.08	15.08	15.21
Cr_2O_3	41.58	41.79	41.65	42.05	42.03	41.98	42.18	41.96	41.93	41.48	41.83	41.76	41.72	41.47
Fe_2O_3	10.93	10.97	10.61	10.73	10.88	8.99	8.77	8.88	8.90	9.19	8.84	8.98	8.95	9.06
FeO	20.78	20.94	20.66	20.92	20.88	22.85	23.03	23.01	22.97	22.87	23.06	22.86	23.06	23.00
MnO	0.28	0.28	0.28	0.28	0.26	0.27	0.28	0.29	0.27	0.27	0.28	0.28	0.27	0.26
NiO	0.16	0.15	0.15	0.18	0.16	0.19	0.16	0.19	0.18	0.15	0.16	0.17	0.17	0.16
CoO	0.01	0.01	0.02	0.03	0.01	0.00	0.02	0.00	0.01	0.00	0.02	0.01	0.01	0.00
Cu_2O	0.03	0.02	0.04	0.00	0.00	0.08	0.00	0.04	0.00	0.03	0.00	0.04	0.00	0.02
ZnO	0.04	0.04	0.03	0.02	0.02	0.05	0.05	0.02	0.02	0.04	0.01	0.05	0.03	0.07
MgO	8.47	8.33	8.59	8.41	8.43	8.22	8.20	8.21	8.25	8.25	8.22	8.27	8.21	8.15
Total	98.98	98.92	99.03	99.18	99.05	99.24	99.31	99.34	99.14	99.09	99.08	99.26	99.12	99.06
Number of ions on the basis of 32 O														
Ti	0.26	0.24	0.23	0.26	0.26	0.27	0.26	0.27	0.26	0.26	0.27	0.26	0.26	0.24
V	0.09	0.09	0.08	0.10	0.08	0.10	0.09	0.09	0.09	0.08	0.07	0.09	0.07	0.09
Al	4.74	4.70	4.80	4.69	4.66	4.64	4.65	4.68	4.66	4.73	4.69	4.71	4.72	4.76
Cr	8.72	8.79	8.71	8.81	8.82	8.82	8.85	8.79	8.81	8.71	8.79	8.75	8.76	8.71
Fe^{3+}	2.18	2.20	2.11	2.14	2.17	1.80	1.75	1.77	1.78	1.84	1.77	1.79	1.79	1.81
Fe^{2+}	4.61	4.66	4.57	4.64	4.64	5.07	5.11	5.10	5.10	5.08	5.12	5.07	5.12	5.11
Mn	0.06	0.06	0.06	0.06	0.06	0.06	0.06	0.07	0.06	0.06	0.06	0.06	0.06	0.06
Ni	0.03	0.03	0.03	0.04	0.03	0.04	0.03	0.04	0.04	0.03	0.03	0.04	0.04	0.03
Co	0.00	0.00	0.00	0.01	0.00	0.00	0.00	0.00	0.00	0.00	0.00	0.00	0.00	0.00
Cu	0.01	0.00	0.01	0.00	0.00	0.02	0.00	0.01	0.00	0.01	0.00	0.01	0.00	0.00
Zn	0.01	0.01	0.01	0.00	0.00	0.01	0.01	0.00	0.00	0.01	0.00	0.01	0.01	0.01
Mg	3.35	3.30	3.39	3.32	3.34	3.26	3.24	3.24	3.27	3.26	3.26	3.27	3.25	3.23
$\Sigma(M^{3+},M^{4+})$	16.00	16.00	16.00	16.00	16.00	15.61	15.60	15.61	15.59	15.61	15.59	15.61	15.60	15.62
ΣM^{2+}	8.07	8.07	8.07	8.07	8.07	8.46	8.47	8.46	8.48	8.47	8.48	8.46	8.47	8.45

Table 8 continued *Electron-microprobe analyses of selected sintered chromite grains in sample B4.*

	29	30	31	32	33	34	35	36	37	38	39	$\bar{x}$	s	CL
TiO_2	1.29	1.32	1.29	1.29	1.11	1.25	1.14	1.28	1.25	1.18	1.30	1.30	0.08	0.03
V_2O_3	0.43	0.48	0.42	0.38	0.45	0.42	0.48	0.45	0.39	0.36	0.45	0.40	0.05	0.01
Al_2O_3	14.93	15.00	15.10	15.14	15.81	15.32	15.26	15.32	14.83	14.67	14.97	15.01	0.27	0.09
Cr_2O_3	41.87	41.71	41.54	41.65	42.00	41.93	41.54	41.69	42.16	42.33	41.78	41.81	0.24	0.08
Fe_2O_3	8.98	8.93	8.96	9.11	8.32	8.45	8.94	8.69	8.60	8.81	8.80	9.88	1.08	0.35
FeO	22.80	22.99	22.81	22.56	22.44	22.81	22.58	22.84	22.93	22.90	22.89	22.06	0.87	0.28
MnO	0.28	0.27	0.28	0.28	0.28	0.27	0.27	0.28	0.28	0.27	0.28	0.27	0.01	0.00
NiO	0.17	0.17	0.17	0.18	0.15	0.16	0.16	0.16	0.16	0.16	0.16	0.17	0.01	0.00
CoO	0.03	0.02	0.00	0.02	0.01	0.02	0.02	0.04	0.02	0.03	0.04	0.02	0.01	0.00
Cu_2O	0.02	0.00	0.00	0.09	0.04	0.01	0.00	0.04	0.05	0.02	0.02	0.02	0.02	0.01
ZnO	0.11	0.11	0.13	0.10	0.08	0.06	0.10	0.04	0.09	0.11	0.11	0.05	0.04	0.01
MgO	8.24	8.20	8.27	8.35	8.41	8.30	8.24	8.25	8.07	8.01	8.20	8.21	0.16	0.05
Total	99.16	99.20	98.97	99.15	99.12	98.99	98.88	99.09	98.85	98.91	98.99	99.12	0.17	0.06
Number of ions on the basis of 32 O														
Ti	0.26	0.26	0.26	0.26	0.22	0.25	0.23	0.25	0.25	0.24	0.26	0.26	0.02	0.01
V	0.09	0.10	0.09	0.08	0.09	0.09	0.10	0.10	0.08	0.08	0.10	0.09	0.01	0.00
Al	4.67	4.69	4.73	4.73	4.92	4.79	4.78	4.79	4.66	4.61	4.69	4.70	0.07	0.02
Cr	8.79	8.75	8.73	8.73	8.77	8.80	8.73	8.74	8.89	8.93	8.79	8.78	0.06	0.02
Fe^{3+}	1.80	1.78	1.79	1.82	1.65	1.69	1.79	1.73	1.73	1.77	1.76	1.97	0.22	0.07
Fe^{2+}	5.06	5.10	5.07	5.00	4.96	5.06	5.02	5.07	5.12	5.11	5.09	4.90	0.19	0.06
Mn	0.06	0.06	0.06	0.06	0.06	0.06	0.06	0.06	0.06	0.06	0.06	0.06	0.00	0.00
Ni	0.04	0.04	0.04	0.04	0.03	0.03	0.03	0.03	0.03	0.03	0.03	0.04	0.00	0.00
Co	0.01	0.00	0.00	0.00	0.00	0.00	0.00	0.01	0.00	0.01	0.01	0.00	0.00	0.00
Cu	0.00	0.00	0.00	0.02	0.01	0.00	0.00	0.01	0.01	0.00	0.00	0.00	0.00	0.00
Zn	0.02	0.02	0.02	0.02	0.02	0.01	0.02	0.01	0.02	0.02	0.02	0.01	0.01	0.00
Mg	3.26	3.25	3.28	3.30	3.31	3.28	3.27	3.26	3.21	3.19	3.25	3.25	0.06	0.02
$\Sigma(M^{3+},M^{4+})$	15.61	15.60	15.60	15.62	15.66	15.61	15.63	15.62	15.62	15.63	15.60	15.80		
ΣM^{2+}	8.46	8.47	8.48	8.45	8.40	8.46	8.44	8.45	8.46	8.44	8.47	8.27		

$\bar{x}$ = Average s = standard deviation CL = 95% confidence limit

APPENDIX E

SEM-EDS analyses of selected silicate grains reported as mass % oxide.

Table 1 *Plagioclase analyses: sample A1.*

	1	2	3	4	5	6	7	8	9	10	11	12	13	14	15	16	17
Na_2O	3.0	3.4	3.0	3.0	3.2	3.2	3.5	3.0	3.1	3.4	3.0	3.3	3.5	4.6	3.1	4.0	4.4
MgO	0.1	0.1	0.1	0.1	0.1	0.1	0.1	0.0	0.1	0.1	0.1	0.1	0.1	0.1	0.1	0.1	0.1
Al_2O_3	32.6	32.2	32.8	32.8	32.4	32.6	31.9	32.9	32.6	32.6	32.5	32.3	31.6	30.4	32.2	31.2	30.8
SiO_2	49.2	50.0	49.1	49.4	49.6	49.7	50.5	49.5	49.4	50.0	49.1	49.7	50.2	52.9	49.2	51.4	52.5
K_2O	0.1	0.1	0.1	0.1	0.1	0.1	0.2	0.1	0.1	0.1	0.1	0.1	0.1	0.1	0.1	0.1	0.1
CaO	15.3	14.7	15.4	15.3	15.1	15.2	14.5	15.4	15.3	14.6	15.2	14.9	14.3	12.4	15.0	13.7	12.9
TiO_2	0.0	0.1	0.0	0.0	0.0	0.0	0.0	0.0	0.0	0.1	0.0	0.0	0.0	0.1	0.0	0.0	0.0
Cr_2O_3	0.2	0.2	0.2	0.3	0.2	0.2	0.1	0.2	0.3	0.1	0.1	0.3	0.2	0.3	0.1	0.2	0.2
MnO	0.0	0.0	0.0	0.0	0.0	0.0	0.0	0.0	0.0	0.0	0.0	0.0	0.0	0.0	0.0	0.0	0.0
FeO	0.2	0.2	0.2	0.2	0.2	0.2	0.2	0.2	0.2	0.1	0.1	0.2	0.2	0.2	0.1	0.2	0.2
Total	100.7	100.8	100.9	101.2	100.8	101.3	101.0	101.4	101.1	101.1	100.2	100.8	100.2	101.2	100.0	100.9	101.2
Number of ions on the basis of 32 O																	
Na	1.2	1.3	1.2	1.2	1.3	1.3	1.4	1.2	1.2	1.3	1.2	1.3	1.3	1.8	1.2	1.6	1.7
Mg	0.0	0.0	0.0	0.0	0.0	0.0	0.0	0.0	0.0	0.0	0.0	0.0	0.0	0.0	0.0	0.0	0.0
Al	7.0	6.9	7.0	7.0	6.9	6.9	6.8	7.0	7.0	6.9	7.0	6.9	6.9	6.4	6.9	6.6	6.5
Si	8.9	9.1	8.9	8.9	9.0	9.0	9.1	8.9	8.9	9.0	9.0	9.0	9.0	9.5	9.0	9.3	9.4
K	0.0	0.0	0.0	0.0	0.0	0.0	0.0	0.0	0.0	0.0	0.0	0.0	0.0	0.0	0.0	0.0	0.0
Ca	3.0	2.9	3.0	3.0	2.9	2.9	2.8	3.0	3.0	2.8	3.0	2.9	2.9	2.4	2.9	2.6	2.5
Ti	0.0	0.0	0.0	0.0	0.0	0.0	0.0	0.0	0.0	0.0	0.0	0.0	0.0	0.0	0.0	0.0	0.0
Cr	0.0	0.0	0.0	0.0	0.0	0.0	0.0	0.0	0.0	0.0	0.0	0.0	0.0	0.0	0.0	0.0	0.0
Mn	0.0	0.0	0.0	0.0	0.0	0.0	0.0	0.0	0.0	0.0	0.0	0.0	0.0	0.0	0.0	0.0	0.0
Fe^{2+}	0.0	0.0	0.0	0.0	0.0	0.0	0.0	0.0	0.0	0.0	0.0	0.0	0.0	0.0	0.0	0.0	0.0
Z	16.0	16.0	16.0	16.0	16.0	16.0	16.0	16.0	16.0	16.0	16.0	16.0	16.0	16.0	16.0	16.0	16.0
X	4.2	4.2	4.2	4.2	4.2	4.2	4.2	4.2	4.2	4.2	4.2	4.2	4.2	4.2	4.2	4.2	4.2
An	71	68	71	71	69	69	66	71	71	68	71	69	69	56	70	62	59
Or	1	0	1	1	1	1	1	1	1	1	0	1	1	0	1	0	1
Ab	29	32	28	29	30	30	33	28	29	32	29	30	30	43	30	37	40

Z=Σ(Si,Al), X=Σ(Na,Ca,K)

Table 2 *Plagioclase analyses: sample B1.*

	1	2	3	4	5	6	7	8	9	10	11	12	13	14	15	16
Na_2O	3.6	3.5	3.6	3.4	3.8	3.6	3.7	4.1	3.7	4.1	3.5	3.6	3.2	3.7	4.2	4.1
MgO	0.1	0.2	0.1	0.1	0.1	0.1	0.1	0.1	0.1	0.1	0.1	0.1	0.1	0.0	0.1	0.1
Al_2O_3	31.8	31.7	31.6	31.9	31.6	31.3	30.9	30.6	30.9	30.6	32.5	31.5	32.6	32.0	30.9	30.8
SiO_2	50.6	50.0	50.2	49.6	50.9	50.0	50.0	50.8	50.0	50.8	50.6	49.9	49.4	51.0	51.2	51.1
K_2O	0.0	0.1	0.1	0.0	0.0	0.0	0.1	0.0	0.1	0.0	0.0	0.1	0.0	0.0	0.0	0.0
CaO	14.3	14.3	14.3	14.7	14.0	14.1	13.7	13.2	13.7	13.2	14.8	14.3	15.2	14.3	13.3	13.2
TiO_2	0.0	0.0	0.0	0.0	0.0	0.0	0.0	0.0	0.0	0.0	0.0	0.0	0.0	0.0	0.1	0.0
Cr_2O_3	0.3	0.2	0.2	0.2	0.2	0.2	0.1	0.2	0.1	0.2	0.3	0.2	0.3	0.3	0.3	0.4
MnO	0.0	0.0	0.0	0.0	0.0	0.0	0.0	0.0	0.0	0.0	0.0	0.0	0.0	0.0	-0.1	0.0
FeO	0.2	0.2	0.2	0.2	0.2	0.2	0.2	0.2	0.2	0.2	0.2	0.2	0.2	0.3	0.3	0.2
Total	100.9	100.2	100.2	100.0	100.8	99.3	98.7	99.2	98.7	99.2	102.1	99.9	101.1	101.6	100.2	99.9
Number of ions on the basis of 32 O																
Na	1.4	1.4	1.4	1.3	1.5	1.4	1.5	1.6	1.5	1.6	1.4	1.4	1.3	1.4	1.6	1.6
Mg	0.0	0.1	0.0	0.0	0.0	0.0	0.0	0.0	0.0	0.0	0.0	0.0	0.0	0.0	0.0	0.0
Al	6.8	6.8	6.8	6.8	6.7	6.7	6.7	6.6	6.7	6.6	6.9	6.8	6.9	6.8	6.6	6.6
Si	9.1	9.1	9.1	9.1	9.2	9.2	9.2	9.3	9.2	9.3	9.0	9.1	8.9	9.1	9.3	9.3
K	0.0	0.0	0.0	0.0	0.0	0.0	0.0	0.0	0.0	0.0	0.0	0.0	0.0	0.0	0.0	0.0
Ca	2.8	2.8	2.8	2.8	2.7	2.8	2.7	2.6	2.7	2.6	2.8	2.8	2.9	2.8	2.6	2.6
Ti	0.0	0.0	0.0	0.0	0.0	0.0	0.0	0.0	0.0	0.0	0.0	0.0	0.0	0.0	0.0	0.0
Cr	0.0	0.0	0.0	0.0	0.0	0.0	0.0	0.0	0.0	0.0	0.0	0.0	0.0	0.0	0.0	0.1
Mn	0.0	0.0	0.0	0.0	0.0	0.0	0.0	0.0	0.0	0.0	0.0	0.0	0.0	0.0	0.0	0.0
Fe^{2+}	0.0	0.0	0.0	0.0	0.0	0.0	0.0	0.0	0.0	0.0	0.0	0.0	0.0	0.0	0.0	0.0
Z	16.0	16.0	16.0	16.0	16.0	16.0	16.0	16.0	16.0	16.0	16.0	16.0	16.0	16.0	16.0	16.0
X	4.2	4.2	4.2	4.1	4.2	4.2	4.2	4.2	4.2	4.2	4.2	4.2	4.2	4.2	4.2	4.2
An	66	66	66	68	64	66	64	61	64	61	67	66	70	65	61	61
Or	0	0	0	0	0	0	0	0	0	0	0	0	0	0	0	0
Ab	34	33	34	32	36	34	35	39	35	39	32	34	30	34	39	39

$Z=\Sigma(Si,Al)$, $X=\Sigma(Na,Ca,K)$

Table 2 *Plagioclase analyses: sample B1continued.*

	17	18	19	20	21	22
Na_2O	3.8	3.6	3.1	3.2	2.9	3.5
MgO	0.1	0.1	0.1	0.1	0.0	0.0
Al_2O_3	31.6	31.5	32.0	32.5	32.1	31.3
SiO_2	50.3	49.6	48.6	49.7	48.0	49.1
K_2O	0.0	0.0	0.1	0.0	0.0	0.0
CaO	14.1	14.1	14.9	15.0	15.3	14.4
TiO_2	0.1	0.0	0.0	0.1	0.0	0.1
Cr_2O_3	0.4	0.5	0.1	0.1	0.3	0.1
MnO	0.0	0.0	-0.1	0.0	0.0	0.0
FeO	0.3	0.3	0.3	0.2	0.3	0.3
Total	100.7	99.8	99.1	100.9	99.0	98.8
Number of ions on the basis of 32 O						
Na	1.5	1.4	1.2	1.3	1.2	1.4
Mg	0.0	0.0	0.0	0.0	0.0	0.0
Al	6.7	6.8	6.9	6.9	7.0	6.8
Si	9.1	9.1	9.0	9.0	8.9	9.1
K	0.0	0.0	0.0	0.0	0.0	0.0
Ca	2.7	2.8	3.0	2.9	3.0	2.8
Ti	0.0	0.0	0.0	0.0	0.0	0.0
Cr	0.1	0.1	0.0	0.0	0.0	0.0
Mn	0.0	0.0	0.0	0.0	0.0	0.0
Fe^{2+}	0.0	0.1	0.0	0.0	0.0	0.0
Z	16.0	16.0	16.0	16.0	16.0	16.0
X	4.3	4.2	4.2	4.2	4.2	4.3
An	64	66	70	69	72	67
Or	0	0	0	0	0	0
Ab	36	34	29	30	28	33

Z=Σ(Si,Al), X=Σ(Na,Ca,K)

1-10 cumulus Feldspar
11-14 resorbed Feldspar associated with clinopyroxene
15-22 Feldspar rim around cpx altered to talc+tremolite

Table 3 *Plagioclase analyses: sample B2.*

	1	**2**	**3**	**4**	**5**	**6**	**7**	**8**	**9**	**10**	**11**	**12**	**13**	**14**	**15**	**16**	**17**	**18**	**19**
Na_2O	3.0	3.3	3.3	4.2	4.7	3.8	1.8	1.4	1.8	2.6	3.2	2.8	3.0	2.2	2.8	4.5	4.4	4.6	4.7
MgO	0.0	0.1	0.1	0.1	0.2	0.1	0.0	0.0	0.0	0.0	0.1	0.1	0.1	0.0	0.1	0.1	0.1	0.1	0.1
Al_2O_3	32.2	31.3	31.3	30.5	29.3	31.1	19.1	19.0	18.7	19.3	32.7	33.1	32.5	33.3	33.1	30.2	30.9	30.6	30.1
SiO_2	49.0	49.6	49.6	52.2	52.5	50.8	63.5	63.7	62.7	64.4	49.9	48.8	48.8	47.1	48.4	52.2	52.6	53.4	53.6
K_2O	0.2	0.3	0.2	0.3	0.2	0.2	14.1	15.0	14.0	13.3	0.1	0.1	0.1	0.0	0.1	0.1	0.1	0.2	0.3
CaO	15.2	14.3	14.3	13.0	11.9	13.7	0.1	0.0	0.1	0.2	15.3	16.0	15.5	16.6	16.0	12.8	13.1	12.8	12.3
TiO_2	0.0	0.1	0.0	0.0	0.1	0.0	0.7	0.6	0.8	0.7	0.0	0.1	0.0	0.0	0.0	0.0	0.1	0.1	0.1
Cr_2O_3	0.1	0.1	0.4	0.2	0.2	0.1	0.0	0.2	0.0	0.0	0.2	0.1	0.1	0.2	0.2	0.2	0.2	0.2	0.2
MnO	0.0	0.0	0.0	0.0	0.0	0.0	0.0	0.0	0.0	0.0	0.0	0.0	0.0	0.0	0.0	0.0	0.0	0.0	0.0
FeO	0.2	0.2	0.3	0.2	0.2	0.2	0.1	0.0	0.0	0.1	0.1	0.2	0.1	0.2	0.1	0.2	0.2	0.2	0.2
Total	99.8	99.3	99.6	100.7	99.2	100.1	99.4	100.1	98.1	100.7	101.7	101.2	100.2	99.8	100.8	100.2	101.6	102.0	101.4
Number of ions on the basis of 32 O																			
Na	1.2	1.3	1.3	1.7	1.9	1.5	0.7	0.6	0.7	1.0	1.3	1.1	1.2	0.9	1.1	1.8	1.7	1.8	1.8
Mg	0.0	0.0	0.0	0.0	0.1	0.0	0.0	0.0	0.0	0.0	0.0	0.0	0.0	0.0	0.0	0.0	0.0	0.0	0.0
Al	6.9	6.8	6.8	6.5	6.3	6.7	4.2	4.1	4.1	4.1	6.9	7.1	7.0	7.2	7.1	6.4	6.5	6.4	6.3
Si	9.0	9.1	9.1	9.4	9.6	9.2	11.7	11.8	11.8	11.7	9.0	8.8	8.9	8.7	8.8	9.4	9.4	9.5	9.6
K	0.0	0.1	0.1	0.1	0.0	0.0	3.3	3.5	3.3	3.1	0.0	0.0	0.0	0.0	0.0	0.0	0.0	0.0	0.1
Ca	3.0	2.8	2.8	2.5	2.3	2.7	0.0	0.0	0.0	0.0	2.9	3.1	3.0	3.3	3.1	2.5	2.5	2.4	2.3
Ti	0.0	0.0	0.0	0.0	0.0	0.0	0.1	0.1	0.1	0.1	0.0	0.0	0.0	0.0	0.0	0.0	0.0	0.0	0.0
Cr	0.0	0.0	0.1	0.0	0.0	0.0	0.0	0.0	0.0	0.0	0.0	0.0	0.0	0.0	0.0	0.0	0.0	0.0	0.0
Mn	0.0	0.0	0.0	0.0	0.0	0.0	0.0	0.0	0.0	0.0	0.0	0.0	0.0	0.0	0.0	0.0	0.0	0.0	0.0
Fe^{2+}	0.1	0.1	0.1	0.0	0.1	0.1	0.0	0.0	0.0	0.0	0.0	0.0	0.0	0.1	0.0	0.0	0.1	0.0	0.1
Z	16.0	16.0	16.0	16.0	16.0	16.0	16.0	16.0	16.0	16.0	16.0	16.0	16.0	16.0	16.0	16.0	16.0	16.0	16.0
X	4.2	4.2	4.2	4.2	4.2	4.2	4.1	4.1	4.1	4.1	4.2	4.2	4.2	4.2	4.2	4.3	4.2	4.2	4.2
An	70	67	67	59	55	63	1	0	1	1	70	73	71	78	74	58	59	57	55
Or	1	1	1	2	1	1	82	86	82	74	0	0	0	0	0	1	1	1	1
Ab	29	32	32	39	44	36	18	14	18	25	30	26	28	21	26	41	40	42	43

Z=Σ(Si,Al), X=Σ(Na,Ca,K)

Table 4 *Plagioclase analyses: sample B3.*

	1	2	3	4	5	6	7	8
Na_2O	4.1	3.4	2.3	4.4	3.5	3.5	2.8	3.8
MgO	0.1	0.0	0.0	0.0	0.1	0.1	0.1	0.0
Al_2O_3	30.7	32.3	33.9	31.0	32.5	32.5	33.5	32.2
SiO_2	51.0	50.5	47.6	52.8	50.1	50.2	49.0	51.2
K_2O	0.0	0.0	0.0	0.0	0.0	0.0	0.0	0.1
CaO	13.3	14.6	16.9	13.3	14.9	14.9	15.7	14.2
TiO_2	0.0	0.1	0.0	0.0	0.1	0.0	0.0	0.1
Cr_2O_3	0.1	0.2	0.1	0.2	0.2	0.2	0.1	0.1
MnO	0.0	0.0	0.0	0.0	0.0	0.0	0.0	-0.1
FeO	0.1	0.1	0.1	0.1	0.2	0.2	0.2	0.1
Total	99.5	101.3	100.9	101.8	101.5	101.6	101.4	101.7
Number of ions on the basis of 32 O								
Na	1.6	1.4	0.9	1.7	1.4	1.4	1.4	1.5
Mg	0.0	0.0	0.0	0.0	0.0	0.0	0.0	0.0
Al	6.6	6.8	7.3	6.5	6.9	6.9	6.8	6.8
Si	9.3	9.1	8.7	9.4	9.0	9.0	9.1	9.2
K	0.0	0.0	0.0	0.0	0.0	0.0	0.0	0.0
Ca	2.6	2.8	3.3	2.5	2.9	2.9	2.8	2.7
Ti	0.0	0.0	0.0	0.0	0.0	0.0	0.0	0.0
Cr	0.0	0.0	0.0	0.0	0.0	0.0	0.0	0.0
Mn	0.0	0.0	0.0	0.0	0.0	0.0	0.0	0.0
Fe^{2+}	0.0	0.0	0.0	0.0	0.0	0.0	0.0	0.0
Z	16.0	16.0	16.0	16.0	16.0	16.0	16.0	16.0
X	4.2	4.2	4.2	4.3	4.2	4.2	4.2	4.2
An	61	67	78	59	68	68	67	65
Or	0	0	0	0	0	0	0	0
Ab	38	32	21	40	32	32	33	35

$Z=\Sigma(Si,Al)$, $X=\Sigma(Na,Ca,K)$

Table 5 *Plagioclase analyses: sample A4.*

	1	2	3	4	5	6	7	8	9	10	11	12	13	14	15	16	17	18
Na_2O	3.6	3.5	3.4	3.5	3.6	3.5	3.6	3.5	3.6	3.6	3.5	3.6	3.6	3.5	1.6	1.6	1.6	1.5
MgO	0.1	0.1	0.0	0.1	0.0	0.0	0.0	0.1	0.1	0.1	0.0	0.2	0.0	0.0	0.1	0.0	0.1	0.0
Al_2O_3	31.8	31.8	31.5	31.4	31.5	31.3	32.1	32.3	32.6	32.7	32.0	32.4	32.3	32.2	34.1	33.8	35.2	35.2
SiO_2	50.0	50.3	49.4	49.5	49.8	49.5	50.5	49.9	50.6	50.8	50.1	50.3	50.8	50.6	45.2	45.1	46.2	46.0
K_2O	0.1	0.0	0.0	0.0	0.0	0.0	0.0	0.0	0.0	0.1	0.1	0.0	0.0	0.0	0.1	0.0	0.1	0.1
CaO	14.2	14.2	14.2	14.2	14.0	14.2	14.4	14.4	14.6	14.6	14.4	14.5	14.5	14.6	17.4	17.4	18.1	18.1
TiO_2	0.1	0.0	0.0	0.0	0.1	0.0	0.0	0.0	0.0	0.1	0.0	0.0	0.1	-0.1	0.1	0.1	0.0	0.0
Cr_2O_3	0.2	0.1	0.2	0.2	0.2	0.2	0.3	0.4	0.3	0.4	0.2	0.2	0.2	0.2	0.2	0.1	0.2	0.2
MnO	0.0	0.0	0.0	0.0	0.0	0.1	0.0	0.0	0.1	-0.1	0.0	0.0	0.0	0.0	0.0	0.1	0.0	0.0
FeO	0.1	0.2	0.1	0.1	0.2	0.1	0.2	0.3	0.1	0.2	0.2	0.2	0.1	0.1	0.1	0.1	0.2	0.1
Total	100.1	100.2	98.8	99.1	99.5	98.9	101.1	100.9	101.9	102.5	100.6	101.4	101.6	101.2	98.9	98.4	101.6	101.1
Number of ions on the basis of 32 O																		
Na	1.4	1.4	1.4	1.4	1.4	1.4	1.4	1.4	1.4	1.4	1.4	1.4	1.4	1.4	0.7	0.7	0.6	0.6
Mg	0.0	0.0	0.0	0.0	0.0	0.0	0.0	0.0	0.0	0.0	0.0	0.0	0.0	0.0	0.0	0.0	0.0	0.0
Al	6.8	6.8	6.8	6.8	6.8	6.8	6.8	6.9	6.9	6.9	6.8	6.9	6.8	6.8	7.5	7.5	7.5	7.6
Si	9.1	9.1	9.1	9.1	9.1	9.1	9.1	9.0	9.0	9.0	9.1	9.0	9.1	9.1	8.4	8.4	8.4	8.4
K	0.0	0.0	0.0	0.0	0.0	0.0	0.0	0.0	0.0	0.0	0.0	0.0	0.0	0.0	0.0	0.0	0.0	0.0
Ca	2.8	2.8	2.8	2.8	2.7	2.8	2.8	2.8	2.8	2.8	2.8	2.8	2.8	2.8	3.5	3.5	3.5	3.5
Ti	0.0	0.0	0.0	0.0	0.0	0.0	0.0	0.0	0.0	0.0	0.0	0.0	0.0	0.0	0.0	0.0	0.0	0.0
Cr	0.0	0.0	0.0	0.0	0.0	0.0	0.0	0.1	0.0	0.0	0.0	0.0	0.0	0.0	0.0	0.0	0.0	0.0
Mn	0.0	0.0	0.0	0.0	0.0	0.0	0.0	0.0	0.0	0.0	0.0	0.0	0.0	0.0	0.0	0.0	0.0	0.0
Fe^{2+}	0.0	0.0	0.0	0.0	0.0	0.0	0.0	0.0	0.0	0.0	0.0	0.0	0.0	0.0	0.0	0.0	0.0	0.0
Z	16.0	16.0	16.0	16.0	16.0	16.0	16.0	16.0	16.0	16.0	16.0	16.0	16.0	16.0	16.0	16.0	16.0	16.0
X	4.2	4.1	4.2	4.2	4.2	4.2	4.2	4.2	4.2	4.2	4.2	4.2	4.2	4.2	4.2	4.2	4.2	4.1
An	65	67	67	67	66	66	66	67	67	66	67	67	67	67	84	84	85	85
Or	0	0	0	0	0	0	0	0	0	0	0	0	0	0	0	0	0	0
Ab	34	34	33	34	34	34	34	33	33	34	33	33	33	33	16	16	15	15

$Z=\Sigma(Si,Al)$, $X=\Sigma(Na,Ca,K)$

Table 6 *Plagioclase analyses: sample A5.*

	1	2	3	4	5	6	7	8	9	10	11	14
Na_2O	3.7	3.6	3.6	3.8	4.2	3.8	3.9	3.7	3.9	4.2	11.1	11.4
MgO	0.1	0.1	0.2	0.1	0.1	0.1	0.1	0.1	0.1	0.1	0.2	0.2
Al_2O_3	31.7	31.5	31.7	31.7	31.4	32.0	31.2	31.6	31.1	30.8	21.1	21.2
SiO_2	50.5	50.5	50.4	51.0	52.3	51.9	51.3	50.8	51.2	51.3	67.5	66.9
K_2O	0.3	0.2	0.2	0.2	0.3	0.2	0.2	0.2	0.2	0.2	-0.1	0.0
CaO	14.2	14.1	14.1	14.1	13.6	14.1	13.6	13.9	13.5	13.0	1.2	1.3
TiO_2	0.0	0.0	0.1	0.1	0.0	0.0	0.1	0.0	0.0	0.0	0.0	0.0
Cr_2O_3	0.2	0.2	0.2	0.2	0.2	0.2	0.2	0.2	0.1	0.1	0.1	0.3
MnO	0.0	-0.1	0.0	0.0	0.0	0.0	0.0	-0.1	0.1	-0.1	0.0	0.1
FeO	0.3	0.2	0.2	0.2	0.2	0.3	0.3	0.2	0.2	0.2	0.2	0.3
Total	100.9	100.4	100.6	101.4	102.3	102.6	100.6	100.6	100.4	99.9	101.3	101.7
Number of ions on the basis of 32 O												
Na	1.4	1.4	1.4	1.5	1.6	1.5	1.5	1.4	1.6	1.7	4.2	4.3
Mg	0.0	0.0	0.0	0.0	0.0	0.0	0.0	0.0	0.0	0.0	0.0	0.1
Al	6.8	6.7	6.8	6.7	6.6	6.7	6.6	6.7	6.6	6.6	4.3	4.3
Si	9.1	9.2	9.1	9.2	9.3	9.2	9.3	9.2	9.3	9.3	11.6	11.5
K	0.1	0.0	0.1	0.1	0.1	0.1	0.0	0.0	0.0	0.0	0.0	0.0
Ca	2.7	2.7	2.7	2.7	2.6	2.7	2.6	2.7	2.6	2.5	0.2	0.2
Ti	0.0	0.0	0.0	0.0	0.0	0.0	0.0	0.0	0.0	0.0	0.0	0.0
Cr	0.0	0.0	0.0	0.0	0.0	0.0	0.0	0.0	0.0	0.0	0.0	0.0
Mn	0.0	0.0	0.0	0.0	0.0	0.0	0.0	0.0	0.0	0.0	0.0	0.0
Fe^{2+}	0.0	0.0	0.0	0.0	0.0	0.0	0.0	0.0	0.0	0.0	0.0	0.0
Z	16.0	16.0	16.0	16.0	16.0	16.0	16.0	16.0	16.0	16.0	16.0	15.9
X	4.2	4.2	4.2	4.2	4.3	4.2	4.2	4.2	4.2	4.2	4.4	4.5
An	65	65	65	64	60	64	63	64	62	60	5	5
Or	1	1	1	1	1	1	1	1	1	1	0	0
Ab	34	34	34	35	38	35	37	35	37	39	95	95

$Z=\Sigma(Si,Al)$, $X=\Sigma(Na,Ca,K)$

***Table** 7 Plagioclase analyses: sample C1.*

	1	2	3	4	5	6	7	8	9	10	11	12	13	14	15	16	17	18	19	20
Na_2O	3.4	3.5	3.1	3.1	3.1	3.2	2.3	4.3	3.5	3.6	3.3	3.3	3.1	3.2	3.3	3.5	3.6	3.3	3.3	3.1
MgO	0.0	0.2	0.0	0.0	0.0	0.1	0.1	0.0	0.1	0.1	0.0	0.1	0.1	0.0	0.1	0.1	0.1	0.0	0.1	0.1
Al_2O_3	31.7	31.6	31.2	31.3	31.3	31.4	31.5	28.7	31.6	31.4	32.1	32.5	32.6	32.3	31.1	31.6	31.4	32.1	32.5	32.6
SiO_2	50.7	50.6	48.8	48.9	49.3	49.3	45.6	48.9	50.5	50.6	50.4	50.5	50.3	50.1	50.8	50.5	50.6	50.4	50.5	50.3
K_2O	0.3	0.4	0.3	0.3	0.3	0.3	0.0	0.0	0.3	0.3	0.2	0.3	0.2	0.2	0.7	0.3	0.3	0.2	0.3	0.2
CaO	14.5	14.5	14.5	14.4	14.6	14.5	20.6	16.3	14.1	14.2	14.9	14.9	15.2	15.1	15.3	14.1	14.2	14.9	14.9	15.2
TiO_2	0.0	0.0	0.0	0.0	0.1	0.1	0.0	0.0	0.1	0.0	0.1	0.0	0.1	0.0	0.1	0.1	0.0	0.1	0.0	0.1
Cr_2O_3	0.1	0.1	0.1	0.2	0.1	0.1	0.4	0.5	0.4	0.3	0.3	0.2	0.2	0.2	0.4	0.4	0.3	0.3	0.2	0.2
MnO	0.0	0.1	0.1	0.0	0.0	0.0	0.0	0.0	-0.1	0.0	0.0	0.0	-0.1	0.0	-0.1	-0.1	0.0	0.0	0.0	-0.1
FeO	0.2	0.2	0.2	0.2	0.1	0.2	0.3	0.2	0.3	0.2	0.3	0.3	0.2	0.3	0.3	0.3	0.2	0.3	0.3	0.2
Total	101.0	101.1	98.2	98.4	99.0	99.2	101.0	98.9	100.6	100.7	101.4	102.0	101.9	101.3	101.9	100.6	100.7	101.4	102.0	101.9
Number of ions on the basis of 32 O																				
Na	1.4	1.4	1.2	1.3	1.3	1.3	0.9	1.8	1.4	1.4	1.3	1.3	1.2	1.2	1.3	1.4	1.4	1.3	1.3	1.2
Mg	0.0	0.1	0.0	0.0	0.0	0.0	0.0	0.0	0.0	0.0	0.0	0.0	0.0	0.0	0.0	0.0	0.0	0.0	0.0	0.0
Al	6.7	6.7	6.8	6.8	6.8	6.8	6.9	6.3	6.7	6.7	6.8	6.9	6.9	6.9	6.6	6.7	6.7	6.8	6.9	6.9
Si	9.1	9.1	9.1	9.1	9.1	9.1	8.5	9.1	9.2	9.2	9.1	9.0	9.0	9.0	9.1	9.2	9.2	9.1	9.0	9.0
K	0.1	0.1	0.1	0.1	0.1	0.1	0.0	0.0	0.1	0.1	0.0	0.1	0.1	0.1	0.2	0.1	0.1	0.0	0.1	0.1
Ca	2.8	2.8	2.9	2.9	2.9	2.9	4.1	3.3	2.7	2.7	2.9	2.9	2.9	2.9	2.9	2.7	2.7	2.9	2.9	2.9
Ti	0.0	0.0	0.0	0.0	0.0	0.0	0.0	0.0	0.0	0.0	0.0	0.0	0.0	0.0	0.0	0.0	0.0	0.0	0.0	0.0
Cr	0.0	0.0	0.0	0.0	0.0	0.0	0.1	0.1	0.1	0.0	0.0	0.0	0.0	0.0	0.1	0.1	0.0	0.0	0.0	0.0
Mn	0.0	0.0	0.0	0.0	0.0	0.0	0.0	0.0	0.0	0.0	0.0	0.0	0.0	0.0	0.0	0.0	0.0	0.0	0.0	0.0
Fe^{2+}	0.0	0.0	0.0	0.0	0.0	0.0	0.1	0.0	0.0	0.0	0.0	0.0	0.0	0.0	0.0	0.0	0.0	0.0	0.0	0.0
Z	16.0	16.0	16.0	16.0	15.9	16.0	15.5	15.5	16.0	16.0	16.0	16.0	16.0	16.0	15.9	16.0	16.0	16.0	16.0	16.0
X	4.2	4.3	4.2	4.2	4.2	4.2	5.0	5.0	4.2	4.2	4.2	4.2	4.2	4.2	4.4	4.2	4.2	4.2	4.2	4.2
An	66	66	69	68	69	68	81	65	65	65	68	68	70	69	67	65	65	68	68	70
Or	2	2	2	2	2	2	0	0	1	1	1	1	1	1	4	1	1	1	1	1
Ab	32	32	30	30	30	31	19	35	33	34	31	31	29	30	29	33	34	31	31	29

Z=Σ(Si,Al), X=Σ(Na,Ca,K)

***Table 7 continued**. Plagioclase analyses: sample C1*

	21	**22**	**23**	**24**	**25**	**26**
Na_2O	3.2	3.3	10.1	10.2	10.4	10.7
MgO	0.0	0.1	0.1	0.0	0.1	0.1
Al_2O_3	32.3	31.1	22.7	22.6	21.6	21.5
SiO_2	50.1	50.8	65.5	65.3	66.0	66.1
K_2O	0.2	0.7	0.0	0.0	0.0	0.0
CaO	15.1	15.3	3.1	3.0	1.9	1.7
TiO_2	0.0	0.1	0.0	0.0	0.1	0.0
Cr_2O_3	0.2	0.4	0.1	0.1	0.4	0.4
MnO	0.0	-0.1	0.0	0.0	0.0	0.0
FeO	0.3	0.3	0.2	0.3	0.2	0.2
Total	101.3	101.9	101.7	101.4	100.6	100.8
Number of ions on the basis of 32 O						
Na	1.2	1.3	3.8	3.8	3.9	4.0
Mg	0.0	0.0	0.0	0.0	0.0	0.0
Al	6.9	6.6	4.6	4.6	4.4	4.4
Si	9.0	9.1	11.3	11.3	11.4	11.5
K	0.1	0.2	0.0	0.0	0.0	0.0
Ca	2.9	2.9	0.6	0.6	0.4	0.3
Ti	0.0	0.0	0.0	0.0	0.0	0.0
Cr	0.0	0.1	0.0	0.0	0.1	0.1
Mn	0.0	0.0	0.0	0.0	0.0	0.0
Fe^{2+}	0.0	0.0	0.0	0.0	0.0	0.0
Z	16.0	15.9	15.9	15.9	16.0	0.0
X	4.2	4.4	4.4	4.4	4.3	16.0
An	69	67	13	13	8	7
Or	1	4	0	0	0	0
Ab	30	29	87	87	92	93

$Z=\Sigma(Si,Al)$, $X=\Sigma(Na,Ca,K)$

Table 8 *Plagioclase analyses: sample C5.*

	1	2	3	4	5	6	7	8	9	10	11	12	13	14	15	16	17	18
Na_2O	3.5	2.9	2.9	3.1	3.1	3.2	3.1	2.2	2.4	1.5	2.3	2.3	3.4	3.6	3.3	3.4	3.4	2.9
MgO	0.1	0.1	0.1	0.1	0.1	0.1	0.1	0.1	0.1	0.1	0.1	0.1	0.0	0.1	0.0	0.1	0.1	0.1
Al_2O_3	31.5	31.6	31.6	31.6	31.8	31.7	31.2	33.1	32.8	34.6	33.1	33.1	31.7	31.5	31.9	31.9	31.9	32.1
SiO_2	50.5	48.3	48.3	49.0	49.3	49.9	48.6	47.3	47.9	46.1	47.9	47.9	50.4	50.6	49.9	50.6	50.8	49.0
K_2O	0.3	0.3	0.3	0.3	0.3	0.3	0.3	0.2	0.3	0.4	0.2	0.2	0.3	0.3	0.3	0.3	0.4	0.3
CaO	14.1	14.9	14.9	14.5	14.6	14.4	14.6	16.2	15.8	17.6	16.1	16.1	14.4	14.1	14.6	14.2	14.2	15.0
TiO_2	0.0	0.0	0.0	0.0	0.0	0.1	0.0	0.0	0.0	0.0	0.0	0.0	0.0	0.1	0.0	0.0	0.0	0.0
Cr_2O_3	0.2	0.1	0.1	0.2	0.3	0.1	0.2	0.3	0.4	0.6	0.4	0.4	0.3	0.3	0.3	0.4	0.3	0.3
MnO	0.0	0.0	0.0	0.0	0.0	-0.1	-0.1	0.1	0.0	0.0	0.0	0.0	0.0	0.0	0.0	0.0	0.0	0.0
FeO	0.2	0.2	0.2	0.2	0.2	0.2	0.1	0.3	0.3	0.4	0.4	0.4	0.2	0.3	0.3	0.3	0.4	0.3
Total	100.4	98.2	98.2	99.0	99.7	100.1	98.1	99.7	100.1	101.3	100.5	100.5	100.6	100.9	100.7	101.2	101.6	100.0
Number of ions on the basis of 32 O																		
Na	1.4	1.2	1.2	1.2	1.2	1.3	1.3	0.9	1.0	0.6	0.9	0.9	1.3	1.4	1.3	1.4	1.3	1.2
Mg	0.0	0.0	0.0	0.0	0.0	0.0	0.0	0.0	0.0	0.0	0.0	0.0	0.0	0.0	0.0	0.0	0.0	0.0
Al	6.7	6.9	6.9	6.9	6.9	6.8	6.8	7.2	7.1	7.4	7.1	7.1	6.8	6.7	6.8	6.8	6.8	6.9
Si	9.2	9.0	9.0	9.0	9.0	9.1	9.0	8.7	8.8	8.4	8.8	8.8	9.1	9.1	9.1	9.1	9.1	9.0
K	0.1	0.1	0.1	0.1	0.1	0.1	0.1	0.0	0.1	0.1	0.1	0.1	0.1	0.1	0.1	0.1	0.1	0.1
Ca	2.7	3.0	3.0	2.9	2.9	2.8	2.9	3.2	3.1	3.4	3.1	3.1	2.8	2.7	2.8	2.7	2.7	2.9
Ti	0.0	0.0	0.0	0.0	0.0	0.0	0.0	0.0	0.0	0.0	0.0	0.0	0.0	0.0	0.0	0.0	0.0	0.0
Cr	0.0	0.0	0.0	0.0	0.0	0.0	0.0	0.0	0.1	0.1	0.1	0.1	0.0	0.0	0.0	0.1	0.0	0.0
Mn	0.0	0.0	0.0	0.0	0.0	0.0	0.0	0.0	0.0	0.0	0.0	0.0	0.0	0.0	0.0	0.0	0.0	0.0
Fe^{2+}	0.0	0.0	0.0	0.0	0.0	0.0	0.0	0.0	0.1	0.1	0.1	0.1	0.0	0.0	0.1	0.0	0.1	0.0
Z	16.0	16.0	16.0	16.0	16.0	16.0	16.0	16.0	16.0	16.0	16.0	16.0	16.0	16.0	16.0	16.0	16.0	16.0
X	4.2	4.2	4.2	4.2	4.2	4.2	4.2	4.1	4.1	4.1	4.1	4.1	4.2	4.2	4.2	4.2	4.2	4.2
An	65	71	71	69	69	67	69	77	75	83	76	76	66	65	68	66	66	70
Or	2	1	1	2	2	2	2	1	1	2	1	1	2	2	2	2	2	2
Ab	33	28	28	30	30	31	30	22	24	15	23	23	32	34	31	32	32	28

Z=Σ(Si,Al), X=Σ(Na,Ca,K)

Table 9 *Pyroxene analyses: Sample A1.*

	1	2	3	4	5	6	7	8	9	10	11	12	13	14	15	16	17	18	19	20	21	22
Na_2O	0.5	0.5	0.4	0.5	0.5	0.5	0.5	0.5	0.5	0.5	0.5	0.5	0.5	0.5	0.5	0.5	0.5	0.5	0.5	0.5	0.5	0.5
MgO	33.7	33.2	33.4	32.8	33.3	32.6	32.4	32.6	32.7	32.7	33.1	32.6	32.8	32.9	33.2	33.2	32.6	32.8	32.7	33.3	33.0	33.4
Al_2O_3	1.1	1.0	1.5	0.8	0.9	1.1	1.2	1.1	1.2	1.3	1.0	1.0	0.8	1.1	1.0	1.0	1.2	1.2	1.0	0.9	1.0	0.9
SiO_2	57.0	56.7	56.9	56.2	56.5	56.2	56.0	56.0	56.1	56.0	56.3	55.9	56.2	56.4	56.8	56.8	56.3	56.4	55.8	56.9	56.3	56.9
K_2O	-0.1	0.0	0.0	0.0	0.0	0.0	0.0	0.0	0.0	-0.1	0.0	0.0	0.0	0.0	0.0	0.0	0.0	-0.1	-0.1	0.0	-0.1	-0.1
CaO	0.7	0.8	0.6	0.7	0.6	0.8	0.8	0.7	0.7	0.7	0.7	0.8	0.7	0.8	0.7	0.7	0.7	0.8	0.8	0.5	0.8	0.5
TiO_2	0.1	0.1	0.1	0.1	0.1	0.2	0.1	0.1	0.2	0.2	0.1	0.1	0.1	0.1	0.1	0.1	0.1	0.1	0.2	0.2	0.2	0.2
Cr_2O_3	0.4	0.4	0.5	0.4	0.5	0.5	0.4	0.4	0.4	0.5	0.5	0.4	0.4	0.5	0.5	0.5	0.4	0.5	0.8	0.4	0.5	0.4
MnO	0.2	0.2	0.2	0.2	0.2	0.2	0.2	0.2	0.2	0.2	0.2	0.2	0.2	0.2	0.3	0.3	0.2	0.2	0.2	0.3	0.2	0.2
FeO	8.2	8.6	8.4	8.8	8.3	8.8	9.0	8.7	8.7	8.8	8.2	8.5	8.8	8.4	8.6	8.6	8.4	8.9	8.4	8.7	8.5	8.6
NiO	0.1	0.0	0.1	0.0	0.1	0.1	0.1	0.1	0.1	0.1	0.1	0.0	0.0	0.1	0.1	0.1	0.1	0.0	0.0	0.1	0.0	0.1
Total	102.0	101.5	102.1	100.4	101.0	101.0	100.7	100.4	100.8	100.9	100.6	100.0	100.4	100.9	101.7	101.7	100.4	101.3	100.3	101.7	100.8	101.6
Number of ions on the basis of 6 O																						
Na	0.0	0.0	0.0	0.0	0.0	0.0	0.0	0.0	0.0	0.0	0.0	0.0	0.0	0.0	0.0	0.0	0.0	0.0	0.0	0.0	0.0	0.0
Mg	1.7	1.7	1.7	1.7	1.7	1.7	1.7	1.7	1.7	1.7	1.7	1.7	1.7	1.7	1.7	1.7	1.7	1.7	1.7	1.7	1.7	1.7
Al	0.0	0.0	0.1	0.0	0.0	0.0	0.0	0.0	0.0	0.1	0.0	0.0	0.0	0.0	0.0	0.0	0.0	0.0	0.0	0.0	0.0	0.0
Si	2.0	2.0	1.9	2.0	2.0	2.0	2.0	2.0	2.0	1.9	2.0	2.0	2.0	2.0	2.0	2.0	2.0	2.0	1.9	2.0	2.0	2.0
K	0.0	0.0	0.0	0.0	0.0	0.0	0.0	0.0	0.0	0.0	0.0	0.0	0.0	0.0	0.0	0.0	0.0	0.0	0.0	0.0	0.0	0.0
Ca	0.0	0.0	0.0	0.0	0.0	0.0	0.0	0.0	0.0	0.0	0.0	0.0	0.0	0.0	0.0	0.0	0.0	0.0	0.0	0.0	0.0	0.0
Ti	0.0	0.0	0.0	0.0	0.0	0.0	0.0	0.0	0.0	0.0	0.0	0.0	0.0	0.0	0.0	0.0	0.0	0.0	0.0	0.0	0.0	0.0
Cr	0.0	0.0	0.0	0.0	0.0	0.0	0.0	0.0	0.0	0.0	0.0	0.0	0.0	0.0	0.0	0.0	0.0	0.0	0.0	0.0	0.0	0.0
Mn	0.0	0.0	0.0	0.0	0.0	0.0	0.0	0.0	0.0	0.0	0.0	0.0	0.0	0.0	0.0	0.0	0.0	0.0	0.0	0.0	0.0	0.0
Fe^{2+}	0.2	0.2	0.2	0.3	0.2	0.3	0.3	0.3	0.3	0.3	0.2	0.3	0.3	0.2	0.2	0.2	0.2	0.3	0.2	0.2	0.2	0.2
Ni	0.0	0.0	0.0	0.0	0.0	0.0	0.0	0.0	0.0	0.0	0.0	0.0	0.0	0.0	0.0	0.0	0.0	0.0	0.0	0.0	0.0	0.0
Z	2.0	2.0	2.0	2.0	2.0	2.0	2.0	2.0	2.0	2.0	2.0	2.0	2.0	2.0	2.0	2.0	2.0	2.0	2.0	2.0	2.0	2.0
X	2.0	2.0	2.0	2.0	2.0	2.0	2.0	2.0	2.0	2.0	2.0	2.0	2.0	2.0	2.0	2.0	2.0	2.0	2.0	2.0	2.0	2.0
Wo	1	1	1	1	1	2	2	1	1	1	1	1	1	2	1	1	1	1	1	1	1	1
En	87	86	87	86	87	85	85	86	86	86	87	86	86	86	86	86	86	86	86	86	86	87
Fs	12	13	12	13	12	13	13	13	13	13	12	13	13	12	13	13	12	13	12	13	12	12

$Z=\Sigma(Al,Si)$, $X=\Sigma(Na, Mg, K, Ca, Ti, Cr, Mn, Fe^{2+}, Ni)$

Table 10 *Pyroxene analyses: Sample B1.*

	1	2	3	4	5	6	7	8	9	10	11	12	13	14	15	16	17	18	19	20	21	22
Na_2O	0.5	0.5	0.6	0.5	0.5	0.5	0.6	0.5	0.5	0.5	0.4	0.6	0.6	0.6	0.6	0.5	0.5	0.5	0.5	0.6	0.5	0.6
MgO	33.1	33.0	33.1	31.8	32.2	31.3	32.4	31.8	33.2	33.2	33.0	16.8	16.6	16.7	17.2	17.1	17.1	16.9	16.8	16.7	17.0	16.7
Al_2O_3	1.1	0.8	1.0	1.3	1.1	1.2	1.1	1.3	1.0	1.0	1.3	1.8	2.1	2.0	1.7	1.4	1.6	1.7	1.5	1.6	1.8	1.8
SiO_2	56.7	55.9	56.1	55.2	55.7	54.8	56.2	55.2	56.2	56.2	56.4	52.6	52.4	52.2	53.2	53.1	53.1	52.5	52.8	52.2	53.3	52.5
K_2O	0.0	0.0	0.0	-0.1	0.0	-0.1	0.0	-0.1	0.0	0.0	0.0	0.0	0.0	0.0	0.0	0.0	0.0	0.0	0.0	0.0	0.0	0.0
CaO	0.7	0.4	0.6	0.6	0.8	0.8	0.7	0.6	0.7	0.6	0.7	23.3	22.8	22.9	23.2	23.5	23.2	24.1	23.4	23.0	23.4	23.1
TiO_2	0.2	0.1	0.1	0.1	0.1	0.1	0.1	0.1	0.1	0.2	0.2	0.4	0.3	0.3	0.3	0.3	0.2	0.4	0.3	0.3	0.3	0.3
Cr_2O_3	0.6	0.4	0.6	0.4	0.4	0.4	0.4	0.4	0.6	0.5	0.5	1.1	1.2	1.2	1.1	1.0	1.1	1.1	1.1	1.1	1.1	1.2
MnO	0.2	0.1	0.3	0.3	0.2	0.2	0.2	0.3	0.3	0.2	0.2	0.1	0.1	0.1	0.1	0.1	0.1	0.0	0.0	0.1	0.1	0.1
FeO	8.7	8.0	8.2	9.6	9.5	9.6	9.3	9.6	8.3	8.0	8.5	3.3	3.6	3.4	3.1	3.1	3.3	2.9	3.2	3.1	3.2	3.2
NiO	0.1	0.0	0.1	0.1	0.1	0.0	0.0	0.1	0.0	0.1	0.1	0.0	0.1	0.1	0.0	0.1	0.1	0.1	0.0	0.1	0.1	0.1
Total	101.9	99.1	100.5	99.8	100.6	98.8	101.1	99.8	100.9	100.4	101.2	99.9	99.6	99.4	100.5	100.2	100.3	100.2	99.6	98.8	100.7	99.5
Number of ions on the basis of 6 O																						
Na	0.0	0.0	0.0	0.0	0.0	0.0	0.0	0.0	0.0	0.0	0.0	0.0	0.0	0.0	0.0	0.0	0.0	0.0	0.0	0.0	0.0	0.0
Mg	1.7	1.7	1.7	1.7	1.7	1.7	1.7	1.7	1.7	1.7	1.7	0.9	0.9	0.9	0.9	0.9	0.9	0.9	0.9	0.9	0.9	0.9
Al	0.0	0.0	0.0	0.1	0.0	0.0	0.0	0.1	0.0	0.0	0.1	0.1	0.1	0.1	0.1	0.1	0.1	0.1	0.1	0.1	0.1	0.1
Si	1.9	2.0	2.0	1.9	1.9	2.0	2.0	1.9	1.9	2.0	1.9	1.9	1.9	1.9	1.9	1.9	1.9	1.9	1.9	1.9	1.9	1.9
K	0.0	0.0	0.0	0.0	0.0	0.0	0.0	0.0	0.0	0.0	0.0	0.0	0.0	0.0	0.0	0.0	0.0	0.0	0.0	0.0	0.0	0.0
Ca	0.0	0.0	0.0	0.0	0.0	0.0	0.0	0.0	0.0	0.0	0.0	0.9	0.9	0.9	0.9	0.9	0.9	0.9	0.9	0.9	0.9	0.9
Ti	0.0	0.0	0.0	0.0	0.0	0.0	0.0	0.0	0.0	0.0	0.0	0.0	0.0	0.0	0.0	0.0	0.0	0.0	0.0	0.0	0.0	0.0
Cr	0.0	0.0	0.0	0.0	0.0	0.0	0.0	0.0	0.0	0.0	0.0	0.0	0.0	0.0	0.0	0.0	0.0	0.0	0.0	0.0	0.0	0.0
Mn	0.0	0.0	0.0	0.0	0.0	0.0	0.0	0.0	0.0	0.0	0.0	0.0	0.0	0.0	0.0	0.0	0.0	0.0	0.0	0.0	0.0	0.0
Fe^{2+}	0.3	0.2	0.2	0.3	0.3	0.3	0.3	0.3	0.2	0.2	0.2	0.1	0.1	0.1	0.1	0.1	0.1	0.1	0.1	0.1	0.1	0.1
Ni	0.0	0.0	0.0	0.0	0.0	0.0	0.0	0.0	0.0	0.0	0.0	0.0	0.0	0.0	0.0	0.0	0.0	0.0	0.0	0.0	0.0	0.0
Z	2.0	2.0	2.0	2.0	2.0	2.0	2.0	2.0	2.0	2.0	2.0	2.0	2.0	2.0	2.0	2.0	2.0	2.0	2.0	2.0	2.0	2.0
X	2.0	2.0	2.0	2.0	2.0	2.0	2.0	2.0	2.0	2.0	2.0	2.0	2.0	2.0	2.0	2.0	2.0	2.0	2.0	2.0	2.0	2.0
Wo	1	1	1	1	1	2	1	1	1	1	1	47	47	47	47	47	47	48	47	47	47	47
En	86	87	87	85	85	84	85	85	87	87	86	47	47	48	48	48	48	47	47	48	48	48
Fs	13	12	12	14	14	14	14	14	12	12	12	5	6	5	5	5	5	5	5	5	5	5

$Z=\Sigma(Al,Si)$, $X=\Sigma(Na, Mg, K, Ca, Ti, Cr, Mn, Fe^{2+}, Ni)$

Table 10 continued. *Pyroxene analyses: Sample B1*

	23	24	25	26	27
Na_2O	0.6	0.6	0.6	0.5	0.5
MgO	16.5	17.3	16.9	16.8	16.7
Al_2O_3	1.8	1.6	1.8	1.5	1.5
SiO_2	51.8	53.7	52.9	52.7	52.2
K_2O	0.0	0.0	0.0	0.0	0.0
CaO	22.5	23.5	23.2	23.5	22.9
TiO_2	0.3	0.3	0.3	0.3	0.3
Cr_2O_3	1.1	1.0	1.2	0.9	0.8
MnO	0.0	0.1	0.0	0.1	0.1
FeO	3.6	3.1	3.3	2.8	3.2
NiO	0.1	0.1	0.1	0.0	0.1
Total	98.2	101.1	100.1	99.0	98.3
Number of ions on the basis of 6 O					
Na	0.0	0.0	0.0	0.0	0.0
Mg	0.9	0.9	0.9	0.9	0.9
Al	0.1	0.1	0.1	0.1	0.1
Si	1.9	1.9	1.9	1.9	1.9
K	0.0	0.0	0.0	0.0	0.0
Ca	0.9	0.9	0.9	0.9	0.9
Ti	0.0	0.0	0.0	0.0	0.0
Cr	0.0	0.0	0.0	0.0	0.0
Mn	0.0	0.0	0.0	0.0	0.0
Fe^{2+}	0.1	0.1	0.1	0.1	0.1
Ni	0.0	0.0	0.0	0.0	0.0
Z	2.0	2.0	2.0	2.0	2.0
X	2.0	2.0	2.0	2.0	2.0
Wo	47	47	47	48	47
En	48	48	48	48	48
Fs	6	5	5	5	5

$Z=\Sigma(Al,Si)$, $X=\Sigma(Na, Mg, K, Ca, Ti, Cr, Mn, Fe^{2+}, Ni)$

Table 11 *Pyroxene analyses: Sample B2 (1-4) and B3 (5-9).*

	1	2	3	4	5	6	7	8	9
Na_2O	0.5	0.5	0.5	0.4	0.5	0.5	0.6	0.4	0.5
MgO	32.5	33.0	33.1	33.3	17.3	16.6	16.9	16.8	33.1
Al_2O_3	1.6	1.7	1.7	1.7	1.6	1.7	1.5	1.5	1.5
SiO_2	54.8	56.0	56.2	56.4	53.6	52.3	52.9	52.7	56.8
K_2O	0.0	0.0	0.0	0.0	0.0	0.0	0.0	0.0	-0.1
CaO	0.2	0.4	0.3	0.4	23.9	23.1	23.7	23.7	0.4
TiO_2	0.2	0.2	0.2	0.2	0.3	0.4	0.3	0.3	0.2
Cr_2O_3	0.5	0.5	0.6	0.6	1.0	1.1	1.0	0.9	0.5
MnO	0.2	0.2	0.2	0.2	0.1	0.1	0.0	0.1	0.2
FeO	8.0	8.3	8.2	8.3	3.2	3.4	3.1	3.0	8.5
NiO	0.0	0.1	0.1	0.1	0.1	0.1	0.1	0.1	0.0
Total	98.5	100.8	101.1	101.5	101.5	99.2	100.0	99.4	101.8
Number of ions on the basis of 6 O									
Na	0.0	0.0	0.0	0.0	0.0	0.0	0.0	0.0	0.0
Mg	1.7	1.7	1.7	1.7	0.9	0.9	0.9	0.9	1.7
Al	0.1	0.1	0.1	0.1	0.1	0.1	0.1	0.1	0.1
Si	1.9	1.9	1.9	1.9	1.9	1.9	1.9	1.9	2.0
K	0.0	0.0	0.0	0.0	0.0	0.0	0.0	0.0	0.0
Ca	0.0	0.0	0.0	0.0	0.9	0.9	0.9	0.9	0.0
Ti	0.0	0.0	0.0	0.0	0.0	0.0	0.0	0.0	0.0
Cr	0.0	0.0	0.0	0.0	0.0	0.0	0.0	0.0	0.0
Mn	0.0	0.0	0.0	0.0	0.0	0.0	0.0	0.0	0.0
Fe^{2+}	0.2	0.2	0.2	0.2	0.1	0.1	0.1	0.1	0.2
Ni	0.0	0.0	0.0	0.0	0.0	0.0	0.0	0.0	0.0
Z	2.0	2.0	2.0	2.0	2.0	2.0	2.0	2.0	2.0
X	2.0	2.0	2.0	2.0	2.0	2.0	2.0	2.0	2.0
Wo	0	1	1	1	47	47	48	48	1
En	88	87	87	87	48	47	47	47	87
Fs	12	12	12	12	5	5	5	5	13

$Z=\Sigma(Al,Si)$, $X=\Sigma(Na, Mg, K, Ca, Ti, Cr, Mn, Fe^{2+}, Ni)$

Table 12 *Pyroxene analyses: Sample A4.*

	1	2	3	4	5	6	7	8	9	10	11	12	13	14	15	16	17	18	19	20	21
Na_2O	0.6	0.6	0.5	0.6	0.7	0.6	0.5	0.5	0.5	0.6	0.6	0.6	0.5	0.7	0.6	0.7	0.5	0.4	0.4	0.6	0.5
MgO	31.6	31.8	31.6	16.7	17.0	16.5	16.7	16.8	16.7	17.2	17.2	16.9	16.8	16.8	16.8	17.0	17.0	17.0	16.8	17.1	16.6
Al_2O_3	1.0	1.0	1.3	2.0	1.9	1.7	1.8	1.8	1.7	1.8	1.8	1.6	1.8	1.7	1.8	1.7	1.6	1.4	1.5	1.5	1.7
SiO_2	56.4	56.2	56.4	52.6	52.6	52.9	52.9	53.4	53.3	54.0	54.1	53.4	53.3	53.1	53.1	53.4	53.6	53.8	53.6	53.7	52.8
K_2O	0.0	0.0	-0.1	0.0	0.0	0.0	0.0	0.0	0.0	0.0	0.0	0.0	0.0	0.0	0.0	-0.1	0.0	0.1	0.0	0.0	0.0
CaO	0.7	0.7	1.0	22.1	21.6	22.6	22.6	22.8	22.7	22.9	22.8	22.9	23.0	22.4	22.6	23.2	23.3	23.1	23.2	23.4	22.8
TiO_2	0.1	0.1	0.1	0.3	0.3	0.3	0.3	0.3	0.2	0.3	0.3	0.3	0.3	0.3	0.2	0.3	0.3	0.2	0.2	0.2	0.3
Cr_2O_3	0.5	0.4	0.5	1.0	1.0	1.1	1.1	1.2	1.1	1.2	1.2	1.1	1.0	0.9	1.0	0.9	0.9	0.8	1.1	1.1	1.0
MnO	0.2	0.3	0.2	0.1	0.1	0.2	0.1	0.1	0.1	0.1	0.1	0.0	0.1	0.1	0.1	0.1	0.2	0.1	0.1	0.0	0.1
FeO	10.6	10.6	10.4	4.6	4.9	4.4	4.4	4.4	4.3	4.6	4.7	4.4	4.1	4.5	4.4	4.1	3.7	4.6	4.0	3.7	4.4
NiO	0.0	0.0	0.1	0.1	0.1	0.0	0.1	0.1	0.0	0.0	0.0	0.2	0.1	0.0	0.1	0.0	0.1	0.1	0.1	0.0	0.1
Total	101.7	101.7	102.0	100.0	100.2	100.2	100.6	101.2	100.7	102.5	102.7	101.4	101.0	100.4	100.6	101.3	101.1	101.4	101.1	101.3	100.1
Number of ions on the basis of 6 O																					
Na	0.0	0.0	0.0	0.0	0.1	0.0	0.0	0.0	0.0	0.0	0.0	0.0	0.0	0.1	0.0	0.1	0.0	0.0	0.0	0.0	0.0
Mg	1.6	1.6	1.6	0.9	0.9	0.9	0.9	0.9	0.9	0.9	0.9	0.9	0.9	0.9	0.9	0.9	0.9	0.9	0.9	0.9	0.9
Al	0.0	0.0	0.1	0.1	0.1	0.1	0.1	0.1	0.1	0.1	0.1	0.1	0.1	0.1	0.1	0.1	0.1	0.1	0.1	0.1	0.1
Si	2.0	2.0	2.0	1.9	1.9	1.9	1.9	1.9	1.9	1.9	1.9	1.9	1.9	1.9	1.9	1.9	1.9	1.9	1.9	1.9	1.9
K	0.0	0.0	0.0	0.0	0.0	0.0	0.0	0.0	0.0	0.0	0.0	0.0	0.0	0.0	0.0	0.0	0.0	0.0	0.0	0.0	0.0
Ca	0.0	0.0	0.0	0.9	0.8	0.9	0.9	0.9	0.9	0.9	0.9	0.9	0.9	0.9	0.9	0.9	0.9	0.9	0.9	0.9	0.9
Ti	0.0	0.0	0.0	0.0	0.0	0.0	0.0	0.0	0.0	0.0	0.0	0.0	0.0	0.0	0.0	0.0	0.0	0.0	0.0	0.0	0.0
Cr	0.0	0.0	0.0	0.0	0.0	0.0	0.0	0.0	0.0	0.0	0.0	0.0	0.0	0.0	0.0	0.0	0.0	0.0	0.0	0.0	0.0
Mn	0.0	0.0	0.0	0.0	0.0	0.0	0.0	0.0	0.0	0.0	0.0	0.0	0.0	0.0	0.0	0.0	0.0	0.0	0.0	0.0	0.0
Fe^{2+}	0.3	0.3	0.3	0.1	0.2	0.1	0.1	0.1	0.1	0.1	0.1	0.1	0.1	0.1	0.1	0.1	0.1	0.1	0.1	0.1	0.1
Ni	0.0	0.0	0.0	0.0	0.0	0.0	0.0	0.0	0.0	0.0	0.0	0.0	0.0	0.0	0.0	0.0	0.0	0.0	0.0	0.0	0.0
Z	2.0	2.0	2.0	2.0	2.0	2.0	2.0	2.0	2.0	2.0	2.0	2.0	2.0	2.0	2.0	2.0	2.0	2.0	2.0	2.0	2.0
X	2.0	2.1	2.0	2.0	2.0	2.0	2.0	2.0	2.0	2.0	2.0	2.0	2.0	2.0	2.0	2.0	2.0	2.0	2.0	2.0	2.0
Wo	1	1	2	45	44	46	46	46	46	45	45	46	46	45	46	46	47	46	47	47	46
En	83	83	83	47	48	47	47	47	47	47	48	47	47	47	47	47	47	47	47	47	47
Fs	16	16	15	7	8	7	7	7	7	7	7	7	7	7	7	6	6	7	6	6	7

$Z=\Sigma(Al,Si)$, $X=\Sigma(Na, Mg, K, Ca, Ti, Cr, Mn, Fe^{2+}, Ni)$

Table 12 continued *Pyroxene analyses: Sample A4*

	22	23	24	25	26
Na_2O	0.4	0.4	0.4	0.5	0.5
MgO	16.6	16.5	16.6	16.6	16.5
Al_2O_3	1.9	1.6	1.7	1.7	1.6
SiO_2	52.9	52.3	52.7	52.2	52.0
K_2O	0.0	0.0	0.0	0.0	0.0
CaO	22.7	23.0	22.9	22.5	22.5
TiO_2	0.2	0.3	0.2	0.2	0.2
Cr_2O_3	0.9	1.1	1.0	1.0	0.9
MnO	0.1	0.1	0.2	0.0	0.1
FeO	4.5	4.0	4.1	4.2	4.4
NiO	0.1	0.1	0.2	0.1	0.1
Total	100.3	99.4	99.8	99.0	98.7
Number of ions on the basis of 6 O					
Na	0.0	0.0	0.0	0.0	0.0
Mg	0.9	0.9	0.9	0.9	0.9
Al	0.1	0.1	0.1	0.1	0.1
Si	1.9	1.9	1.9	1.9	1.9
K	0.0	0.0	0.0	0.0	0.0
Ca	0.9	0.9	0.9	0.9	0.9
Ti	0.0	0.0	0.0	0.0	0.0
Cr	0.0	0.0	0.0	0.0	0.0
Mn	0.0	0.0	0.0	0.0	0.0
Fe^{2+}	0.1	0.1	0.1	0.1	0.1
Ni	0.0	0.0	0.0	0.0	0.0
Z	2.0	2.0	2.0	2.0	2.0
X	2.0	2.0	2.0	2.0	2.0
Wo	46	47	47	46	46
En	47	47	47	47	47
Fs	7	6	6	7	7

Z=Σ(Al,Si), X=Σ(Na, Mg, K, Ca, Ti, Cr, Mn, Fe^{2+}, Ni)

Table 13 *Pyroxene analyses: Sample C1(1-7) and C5 (8-9).*

	1	2	3	4	5	6	7	8	9
Na_2O	0.5	0.5	0.5	0.5	0.5	0.5	0.4	0.5	0.4
MgO	33.9	33.7	33.5	33.7	33.8	34.2	34.2	17.1	17.0
Al_2O_3	1.3	1.4	1.4	1.4	1.2	1.2	1.3	1.7	1.9
SiO_2	56.5	56.4	56.6	56.8	56.6	56.8	56.8	53.1	52.5
K_2O	0.0	-0.1	-0.1	0.0	0.0	-0.1	0.0	0.0	0.0
CaO	0.4	0.5	0.5	0.5	0.5	0.4	0.4	24.1	24.0
TiO_2	0.2	0.2	0.1	0.2	0.2	0.2	0.2	0.3	0.4
Cr_2O_3	0.9	0.8	0.7	0.9	0.9	0.7	0.6	1.2	1.3
MnO	0.2	0.3	0.3	0.2	0.2	0.2	0.2	0.1	0.0
FeO	7.8	8.1	8.3	7.9	7.8	7.6	7.7	2.9	3.0
NiO	0.1	0.1	0.1	0.1	0.1	0.1	0.1	0.0	0.1
Total	101.6	101.8	101.9	101.9	101.8	101.8	101.8	101.0	100.4
Number of ions on the basis of 6 O									
Na	0.0	0.0	0.0	0.0	0.0	0.0	0.0	0.0	0.0
Mg	1.7	1.7	1.7	1.7	1.7	1.7	1.7	0.9	0.9
Al	0.1	0.1	0.1	0.1	0.0	0.0	0.1	0.1	0.1
Si	1.9	1.9	1.9	1.9	1.9	1.9	1.9	1.9	1.9
K	0.0	0.0	0.0	0.0	0.0	0.0	0.0	0.0	0.0
Ca	0.0	0.0	0.0	0.0	0.0	0.0	0.0	0.9	0.9
Ti	0.0	0.0	0.0	0.0	0.0	0.0	0.0	0.0	0.0
Cr	0.0	0.0	0.0	0.0	0.0	0.0	0.0	0.0	0.0
Mn	0.0	0.0	0.0	0.0	0.0	0.0	0.0	0.0	0.0
Fe^{2+}	0.2	0.2	0.2	0.2	0.2	0.2	0.2	0.1	0.1
Ni	0.0	0.0	0.0	0.0	0.0	0.0	0.0	0.0	0.0
Z	2.0	2.0	2.0	2.0	2.0	2.0	2.0	2.0	2.0
X	2.0	2.0	2.0	2.0	2.0	2.0	2.0	2.0	2.0
Wo	1	1	1	1	1	1	1	48	48
En	88	87	87	88	88	88	88	47	47
Fs	11	12	12	11	11	11	11	5	5

Z=Σ(Al,Si), X=Σ(Na, Mg, K, Ca, Ti, Cr, Mn, Fe^{2+}, Ni)

Table 14 *Selected phlogopite analyses.*

	1	2	3	4	5	6	7
Na_2O	0.4	1.0	1.7	1.7	0.3	0.3	0.2
MgO	22.3	20.6	24.3	23.8	21.9	22.0	21.8
Al_2O_3	15.6	15.8	17.9	16.9	14.3	14.2	14.3
SiO_2	38.3	38.0	39.8	40.2	38.5	38.6	38.7
K_2O	10.4	9.3	7.9	7.9	9.8	9.7	9.8
CaO	0.0	0.0	0.0	0.0	0.0	0.1	0.1
TiO_2	4.3	1.6	0.6	1.4	4.5	4.6	5.2
Cr_2O_3	1.8	1.5	1.2	1.4	2.0	2.0	1.9
MnO	0.0	0.0	0.0	0.1	0.0	0.0	0.1
FeO	3.0	7.4	2.6	2.8	4.1	4.0	4.0
NiO	0.2	0.3	0.2	0.2	0.2	0.2	0.2
Cl	0.1	0.4	0.1	0.1	0.5	0.5	0.5
Total	96.5	95.5	96.3	96.2	95.7	95.8	96.2
Number of ions on the basis of 24 O							
Na	0.1	0.3	0.5	0.5	0.1	0.1	0.1
Mg	4.8	4.5	5.1	5.0	4.7	4.7	4.7
Al	2.6	2.7	3.0	2.8	2.4	2.4	2.5
Si	5.5	5.5	5.6	5.7	5.6	5.6	5.6
K	1.9	1.7	1.4	1.4	1.8	1.8	1.8
Ca	0.0	0.0	0.0	0.0	0.0	0.0	0.0
Ti	0.5	0.2	0.1	0.1	0.5	0.5	0.6
Cr	0.2	0.2	0.1	0.2	0.2	0.2	0.2
Mn	0.0	0.0	0.0	0.0	0.0	0.0	0.0
Fe^{2+}	0.4	0.9	0.3	0.3	0.5	0.5	0.5
Ni	0.0	0.0	0.0	0.0	0.0	0.0	0.0
OH	3.3	4.0	3.4	3.5	3.7	3.6	3.2
Cl	0.0	0.1	0.0	0.0	0.1	0.1	0.1
Σ(Al,Si)	8.0	8.0	8.0	8.0	8.0	8.0	8.0
Σ(Ca,Na,K)	2.0	2.0	2.0	1.9	1.9	1.9	1.9
Σ(Fe,Mg,Al,Ti,Cr)	6.0	6.0	6.2	6.1	6.0	6.0	6.1
Σ(OH,Cl)	3.3	4.1	3.4	3.6	3.8	3.7	3.3

Table 15 *Selected amphibole analyses: Edenitic hornblende (1,3,5-9) & tremolite (2,4)*

	1	2	3	4	5	6	7	8	9
Na_2O	2.6	0.6	2.5	0.6	2.6	2.7	2.7	2.8	2.4
MgO	17.8	16.5	17.9	15.9	17.3	17.7	17.7	17.5	18.5
Al_2O_3	11.4	4.5	10.1	3.1	11.0	11.1	11.3	11.6	11.7
SiO_2	44.4	52.2	45.2	53.0	44.5	45.1	44.2	44.3	46.0
K_2O	0.6	0.1	0.4	0.0	0.2	0.2	0.3	0.3	0.2
CaO	12.4	11.2	12.3	12.0	12.2	12.5	12.3	12.3	12.5
TiO_2	2.4	0.1	2.3	0.1	2.3	2.4	2.7	2.6	0.9
Cr_2O_3	2.2	0.7	2.0	0.4	2.1	2.1	2.0	2.0	1.7
MnO	0.0	0.4	0.0	0.5	0.1	0.0	0.0	0.1	0.0
FeO	4.4	11.0	4.2	11.0	5.0	4.6	4.4	4.6	4.0
NiO	0.1	0.0	0.1	0.1	0.2	0.1	0.1	0.1	0.1
Total	98.0	97.3	97.0	96.8	97.4	98.5	97.6	98.1	97.9
Number of cations based on 24 O									
Na	0.8	0.2	0.8	0.2	0.8	0.8	0.8	0.9	0.7
Mg	3.8	3.5	3.8	3.4	3.7	3.8	3.8	3.7	3.9
Al	1.9	0.8	1.7	0.5	1.9	1.9	1.9	2.0	2.0
Si	6.4	7.4	6.4	7.5	6.4	6.5	6.3	6.4	6.5
K	0.1	0.0	0.1	0.0	0.0	0.0	0.0	0.0	0.0
Ca	1.9	1.7	1.9	1.8	1.9	1.9	1.9	1.9	1.9
Ti	0.3	0.0	0.2	0.0	0.3	0.3	0.3	0.3	0.1
Cr	0.2	0.1	0.2	0.0	0.2	0.2	0.2	0.2	0.2
Mn	0.0	0.1	0.0	0.1	0.0	0.0	0.0	0.0	0.0
Fe^{2+}	0.5	1.3	0.5	1.3	0.6	0.5	0.5	0.6	0.5
Ni	0.0	0.0	0.0	0.0	0.0	0.0	0.0	0.0	0.0
OH	1.9	2.5	2.9	3.0	2.5	1.5	2.3	1.8	2.0
Σ(Al,Si)	8.0	8.0	8.0	8.0	8.0	8.0	8.0	8.0	8.0
Σ(Ca,Na,K)	2.8	1.9	2.7	2.0	2.7	2.8	2.8	2.8	2.7
Σ(Fe,Mg,Al,Ti,Cr)	5.2	5.1	4.9	4.8	5.0	5.3	5.0	5.2	5.2

Table 16 *Selected pumpellyite analyses.*

	1	2	3	4	5	6
Na_2O	0.3	0.2	0.1	0.1	0.1	0.3
MgO	1.0	4.3	3.7	3.3	3.6	3.9
Al_2O_3	27.2	24.5	26.1	26.6	26.3	25.8
SiO_2	37.4	37.4	37.6	37.7	37.7	37.6
K_2O	-0.0	0.0	0.0	-0.0	0.0	-0.0
CaO	23.1	23.0	23.5	23.5	23.8	23.5
TiO_2	0.0	0.1	0.0	0.0	0.1	0.0
Cr_2O_3	0.2	1.4	0.4	0.3	0.3	0.4
MnO	0.4	0.2	0.4	0.6	0.2	0.1
FeO	4.3	1.9	1.9	1.9	2.1	1.8
NiO	-0.0	0.1	-0.0	0.0	0.0	0.1
Total	93.9	93.1	93.7	94.1	94.2	93.4
Number of ions based on 14 O						
Na	0.1	0.0	0.0	0.0	0.0	0.0
Mg	0.1	0.5	0.4	0.4	0.4	0.5
Al	2.6	2.3	2.5	2.5	2.5	2.4
Si	3.0	3.0	3.0	3.0	3.0	3.0
K	0.0	0.0	0.0	0.0	0.0	0.0
Ca	2.0	2.0	2.0	2.0	2.1	2.0
Ti	0.0	0.0	0.0	0.0	0.0	0.0
Cr	0.0	0.1	0.0	0.0	0.0	0.0
Mn	0.0	0.0	0.0	0.0	0.0	0.0
Fe^{2+}	0.3	0.1	0.1	0.1	0.1	0.1
Ni	0.0	0.0	0.0	0.0	0.0	0.0
OH	3.3	3.7	3.4	3.2	3.1	3.5
Si	3.0	3.0	3.0	3.0	3.0	3.0
Σ(Ca,Na,K)	2.0	2.0	2.0	2.0	2.1	2.1
Σ(Fe^{2+}Mg,Al)	3.0	3.1	3.1	3.1	3.1	3.0

Table 17 *Selected epidote (1-3) and prehnite (4) analyses.*

	1	2	3	4
Na	0.2	0.4	0.1	0.2
Mg	0.3	4.6	0.8	0.0
Al	29.7	26.8	29.6	24.3
Si	38.5	40.1	38.3	43.9
K	0.0	0.0	0.0	0.0
Ca	23.3	23.9	23.4	27.2
Ti	0.1	0.1	0.0	0.0
Cr	0.5	0.3	0.6	0.0
Mn	0.2	0.1	0.3	0.1
Fe2+	4.8	2.2	4.5	0.2
Ni	0.1	0.0	0.0	0.1
Total	97.5	98.2	97.4	96.2
Number of ions based on 12.5 O for epidote and 24 O for prehnite				
Na	0.0	0.1	0.0	0.1
Mg	0.0	0.5	0.1	0.0
Al	2.6	2.3	2.6	4.0
Si	2.9	3.0	2.8	6.1
K	0.0	0.0	0.0	0.0
Ca	1.9	1.9	1.9	4.0
Ti	0.0	0.0	0.0	0.0
Cr	0.0	0.0	0.0	0.0
Mn	0.0	0.0	0.0	0.0
Fe2+	0.3	0.1	0.3	0.0
Ni	0.0	0.0	0.0	0.0
OH	1.2	0.9	1.3	3.7
Σ(Si,Al)	3.0	3.0	3.0	6.0
Σ(Ca,Na,K)	1.9	2.0	1.9	4.1
Σ(Fe^{2+}Mg,Al)	2.8	3.0	2.8	4.0

Table 18 *Selected chlorite (1-2),septechlorite (3-5), serpentine (6-8) and talc (9-10) analyses.*

	1	**2**	**3**	**4**	**5**	**6**	**7**	**8**	**9**	**10**
Na	0.7	0.7	0.5	0.6	0.6	0.4	0.5	0.3	0.5	0.5
Mg	21.6	21.3	23.7	23.4	23.3	38.6	36.0	41.0	29.6	28.8
Al	12.9	12.2	0.0	0.0	0.1	0.2	0.0	-0.1	6.6	4.7
Si	36.5	37.8	55.2	54.4	55.3	42.6	43.8	43.5	51.1	54.1
K	0.0	0.0	0.0	0.0	0.1	0.0	-0.1	0.0	0.1	0.1
Ca	4.7	5.1	0.6	0.6	0.5	0.2	0.3	0.0	0.1	0.4
Ti	0.1	0.0	0.0	0.0	0.0	-0.1	0.0	0.0	0.0	0.0
Cr	2.3	2.2	0.1	0.0	0.0	0.0	0.0	0.0	0.0	0.0
Mn	0.3	0.4	0.2	0.1	0.1	0.1	0.1	0.0	0.1	0.1
Fe	11.7	11.8	11.1	11.0	11.8	4.6	6.0	1.8	5.8	5.1
Ni	0.1	0.1	0.5	0.5	0.4	0.2	0.1	0.4	0.0	0.0
Total	90.8	91.6	91.8	90.7	92.3	86.9	86.8	86.8	94.8	94.6
Number of ions based on 36 O for chlorite, 18 O for septechlorite, 9 O for serpentine, and 24 O for talc										
Na	0.3	0.3	0.1	0.1	0.1	0.0	0.1	0.0	0.2	0.1
Mg	6.5	6.5	3.5	3.4	3.4	2.7	2.5	2.8	5.8	5.6
Al	3.1	2.9	0.0	0.0	0.0	0.0	0.0	0.0	1.0	0.7
Si	7.4	7.7	5.4	5.3	5.4	2.0	2.1	2.0	6.7	7.0
K	0.0	0.0	0.0	0.0	0.0	0.0	0.0	0.0	0.0	0.0
Ca	1.0	1.1	0.1	0.1	0.1	0.0	0.0	0.0	0.0	0.1
Ti	0.0	0.0	0.0	0.0	0.0	0.0	0.0	0.0	0.0	0.0
Cr	0.4	0.4	0.0	0.0	0.0	0.0	0.0	0.0	0.0	0.0
Mn	0.0	0.1	0.0	0.0	0.0	0.0	0.0	0.0	0.0	0.0
Fe^{2+}	2.0	2.0	0.9	0.9	1.0	0.2	0.2	0.1	0.6	0.6
Ni	0.0	0.0	0.1	0.1	0.1	0.0	0.0	0.0	0.0	0.0
OH	12.4	11.4	5.3	6.0	5.1	4.1	4.1	4.1	5.2	5.3
Σ(Al,Si)	8.0	8.0	4.0	4.0	4.0	2.0	2.0	2.0	7.7	7.7
Σ(Fe,Mg,Al,Na,Ca,K)	12.4	11.4	6.6	6.4	6.0	3.0	2.8	2.9	6.4	6.1

APPENDIX F

Electron-microprobe analyses of selected base-metal sulphide grains. Analytical conditions and minimum detection limits are discussed in Chapter 4.

Table 1 *Chalcopyrite compositions from sample A1.*

	1	2	3	4	5	6	7	8	9	10	11	12	13	14	15	16	17	18	19	20	Avg.	SD
S	34.49	34.61	35.04	35.19	35.00	35.07	34.77	35.25	35.23	35.25	35.03	34.57	35.01	34.80	34.90	34.65	34.92	34.94	34.80	35.18	34.93	0.24
Fe	30.36	30.61	30.49	30.29	30.78	30.22	30.95	30.66	30.60	30.97	30.45	30.71	29.98	29.97	30.34	30.48	30.07	30.40	30.19	30.22	30.44	0.29
Ni	0.04	0.00	0.39	0.02	0.00	0.00	0.03	0.02	0.07	0.01	0.41	0.03	0.01	0.01	0.03	0.00	0.00	0.01	0.03	0.01	0.06	0.12
Co	0.07	0.04	0.00	0.06	0.02	0.03	0.02	0.05	0.04	0.04	0.08	0.03	0.06	0.06	0.04	0.02	0.02	0.04	0.03	0.03	0.04	0.02
Cu	33.90	34.53	34.07	34.16	34.43	34.10	34.32	33.86	33.92	34.46	33.85	34.54	33.74	33.65	34.01	34.18	32.91	34.32	33.85	33.64	34.02	0.39
Rh	b.d.l.	b.d.l.	b.d.l.	b.d.l.	b.d.l.	b.d.l.	b.d.l.	b.d.l.	b.d.l.	b.d.l.	b.d.l.	b.d.l.	b.d.l.	b.d.l.	b.d.l.	b.d.l.	b.d.l.	b.d.l.	b.d.l.	b.d.l.	b.d.l.	
Pd	b.d.l.	0.03	b.d.l.	b.d.l.	b.d.l.	b.d.l.	b.d.l.	b.d.l.	b.d.l.	b.d.l.	b.d.l.	b.d.l.	b.d.l.	b.d.l.	b.d.l.	b.d.l.	b.d.l.	b.d.l.	b.d.l.	b.d.l.	b.d.l.	
Pt	b.d.l.	b.d.l.	b.d.l.	b.d.l.	b.d.l.	b.d.l.	b.d.l.	b.d.l.	b.d.l.	b.d.l.	b.d.l.	b.d.l.	b.d.l.	b.d.l.	b.d.l.	b.d.l.	b.d.l.	b.d.l.	b.d.l.	b.d.l.	b.d.l.	
Ru	b.d.l.	b.d.l.	b.d.l.	b.d.l.	b.d.l.	b.d.l.	b.d.l.	b.d.l.	b.d.l.	b.d.l.	b.d.l.	b.d.l.	b.d.l.	b.d.l.	b.d.l.	b.d.l.	b.d.l.	b.d.l.	b.d.l.	b.d.l.	b.d.l.	
Total	98.86	99.83	99.99	99.71	100.24	99.42	100.09	99.84	99.87	100.73	99.83	99.88	98.80	98.49	99.33	99.33	97.93	99.71	98.90	99.09	99.49	
Atomic proportions																						
S	2.00	1.99	2.00	2.02	2.00	2.01	1.99	2.02	2.01	2.00	2.01	1.98	2.02	2.02	2.01	2.00	2.03	2.00	2.01	2.01	2.01	0.00
Fe	1.01	1.01	1.00	1.00	1.01	1.00	1.02	1.01	1.00	1.01	1.00	1.01	0.99	1.00	1.00	1.01	1.00	1.00	1.00	1.00	1.00	0.00
Ni	0.00	0.00	0.01	0.00	0.00	0.00	0.00	0.00	0.00	0.00	0.01	0.00	0.00	0.00	0.00	0.00	0.00	0.00	0.00	0.00	0.00	0.00
Co	0.00	0.00	0.00	0.00	0.00	0.00	0.00	0.00	0.00	0.00	0.00	0.00	0.00	0.00	0.00	0.00	0.00	0.00	0.00	0.00	0.00	0.00
Cu	0.99	1.00	0.98	0.99	0.99	0.99	0.99	0.98	0.98	0.99	0.98	1.00	0.98	0.98	0.99	0.99	0.97	0.99	0.99	0.99	0.99	0.00
Rh	b.d.l.	b.d.l.	b.d.l.	b.d.l.	b.d.l.	b.d.l.	b.d.l.	b.d.l.	b.d.l.	b.d.l.	b.d.l.	b.d.l.	b.d.l.	b.d.l.	b.d.l.	b.d.l.	b.d.l.	b.d.l.	b.d.l.	b.d.l.	b.d.l.	
Pd	b.d.l.	0.00	b.d.l.	b.d.l.	b.d.l.	b.d.l.	b.d.l.	b.d.l.	b.d.l.	b.d.l.	b.d.l.	b.d.l.	b.d.l.	b.d.l.	b.d.l.	b.d.l.	b.d.l.	b.d.l.	b.d.l.	b.d.l.	b.d.l.	
Pt	b.d.l.	b.d.l.	b.d.l.	b.d.l.	b.d.l.	b.d.l.	b.d.l.	b.d.l.	b.d.l.	b.d.l.	b.d.l.	b.d.l.	b.d.l.	b.d.l.	b.d.l.	b.d.l.	b.d.l.	b.d.l.	b.d.l.	b.d.l.	b.d.l.	
Ru	b.d.l.	b.d.l.	b.d.l.	b.d.l.	b.d.l.	b.d.l.	b.d.l.	b.d.l.	b.d.l.	b.d.l.	b.d.l.	b.d.l.	b.d.l.	b.d.l.	b.d.l.	b.d.l.	b.d.l.	b.d.l.	b.d.l.	b.d.l.	b.d.l.	

Table 2 *Chalcopyrite compositions from sample B4.*

	1	2	3	4	5	6	7	8	9	10	11	12	13	Avg.	s
S	34.80	34.96	35.05	34.80	35.23	35.26	34.98	34.92	35.67	35.04	34.98	35.11	34.74	35.04	0.24
Fe	30.50	31.00	29.93	30.06	30.33	30.68	30.59	31.40	30.95	30.17	30.43	30.31	30.65	30.54	0.41
Ni	0.03	0.01	0.09	0.08	0.26	0.04	0.06	0.06	0.02	0.01	0.23	0.02	0.01	0.07	0.08
Co	0.03	0.05	0.05	0.05	0.04	0.02	0.04	0.03	0.03	0.03	0.04	0.02	0.06	0.04	0.01
Cu	33.54	34.62	33.07	33.39	33.81	34.47	33.99	33.37	34.21	33.56	34.60	34.12	34.24	33.92	0.50
Rh	b.d.l.	b.d.l.	b.d.l.	b.d.l.	b.d.l.	b.d.l.	b.d.l.	b.d.l.	b.d.l.	b.d.l.	b.d.l.	b.d.l.	b.d.l.	b.d.l.	
Pd	b.d.l.	b.d.l.	b.d.l.	b.d.l.	b.d.l.	b.d.l.	b.d.l.	b.d.l.	b.d.l.	b.d.l.	b.d.l.	b.d.l.	b.d.l.	b.d.l.	
Pt	b.d.l.	b.d.l.	b.d.l.	b.d.l.	b.d.l.	b.d.l.	b.d.l.	b.d.l.	b.d.l.	b.d.l.	b.d.l.	b.d.l.	b.d.l.	b.d.l.	
Ru	b.d.l.	b.d.l.	b.d.l.	b.d.l.	b.d.l.	b.d.l.	b.d.l.	b.d.l.	b.d.l.	b.d.l.	b.d.l.	b.d.l.	b.d.l.	b.d.l.	
Total	98.90	100.64	98.19	98.38	99.67	100.47	99.66	99.79	100.88	98.82	100.27	99.59	99.70	99.61	
Atomic proportions															
S	2.01	1.99	2.03	2.02	2.02	2.01	2.01	2.00	2.02	2.02	2.00	2.01	1.99	2.01	0.01
Fe	1.01	1.01	1.00	1.00	1.00	1.00	1.01	1.03	1.01	1.00	1.00	1.00	1.01	1.01	0.01
Ni	0.00	0.00	0.00	0.00	0.01	0.00	0.00	0.00	0.00	0.00	0.01	0.00	0.00	0.00	0.00
Co	0.00	0.00	0.00	0.00	0.00	0.00	0.00	0.00	0.00	0.00	0.00	0.00	0.00	0.00	0.00
Cu	0.98	0.99	0.97	0.98	0.98	0.99	0.98	0.96	0.98	0.98	1.00	0.99	0.99	0.98	0.01
Rh	b.d.l.	b.d.l.	b.d.l.	b.d.l.	b.d.l.	b.d.l.	b.d.l.	b.d.l.	b.d.l.	b.d.l.	b.d.l.	b.d.l.	b.d.l.	b.d.l.	
Pd	b.d.l.	b.d.l.	b.d.l.	b.d.l.	b.d.l.	b.d.l.	b.d.l.	b.d.l.	b.d.l.	b.d.l.	b.d.l.	b.d.l.	b.d.l.	b.d.l.	
Pt	b.d.l.	b.d.l.	b.d.l.	b.d.l.	b.d.l.	b.d.l.	b.d.l.	b.d.l.	b.d.l.	b.d.l.	b.d.l.	b.d.l.	b.d.l.	b.d.l.	
Ru	b.d.l.	b.d.l.	b.d.l.	b.d.l.	b.d.l.	b.d.l.	b.d.l.	b.d.l.	b.d.l.	b.d.l.	b.d.l.	b.d.l.	b.d.l.	b.d.l.	

Table 3 *Chalcopyrite compositions from sample C1.*

	1	2	3	4	5	6	7	8	9	10	11	12	13	14	15	16	17	18	19	20	21	Avg.	s
S	35.46	34.92	34.73	34.78	34.86	34.92	35.24	35.10	35.01	34.54	34.85	34.75	34.76	34.95	34.93	34.28	34.83	34.94	34.28	35.10	33.90	34.81	0.47
Fe	30.73	29.79	30.10	29.68	30.49	30.48	30.40	30.80	30.18	29.84	29.85	30.11	29.82	30.02	30.19	30.03	30.59	30.21	30.22	30.23	30.67	30.21	0.46
Ni	0.02	0.08	0.00	0.00	0.00	0.00	0.01	0.00	0.04	0.08	0.00	0.00	0.04	0.01	0.01	0.00	0.01	0.01	0.05	0.02	0.00	0.02	0.02
Co	0.03	0.03	0.06	0.03	0.04	0.06	0.00	0.05	0.04	0.04	0.05	0.02	0.04	0.03	0.04	0.04	0.05	0.05	0.03	0.05	0.02	0.04	0.02
Cu	34.49	33.81	34.05	33.61	34.34	34.00	34.21	33.89	34.26	33.43	33.74	33.43	33.51	33.70	33.95	34.10	33.88	33.76	33.86	34.34	34.04	33.92	0.64
Rh	b.d.l.	b.d.l.	b.d.l.	b.d.l.	b.d.l.	b.d.l.	b.d.l.	b.d.l.	b.d.l.	b.d.l.	b.d.l.	b.d.l.	b.d.l.	b.d.l.	b.d.l.	b.d.l.	b.d.l.	b.d.l.	b.d.l.	b.d.l.	b.d.l.		
Pd	b.d.l.	b.d.l.	b.d.l.	b.d.l.	b.d.l.	b.d.l.	b.d.l.	b.d.l.	b.d.l.	b.d.l.	b.d.l.	b.d.l.	b.d.l.	b.d.l.	b.d.l.	b.d.l.	b.d.l.	b.d.l.	b.d.l.	b.d.l.	b.d.l.		
Pt	b.d.l.	b.d.l.	b.d.l.	b.d.l.	b.d.l.	b.d.l.	b.d.l.	b.d.l.	b.d.l.	b.d.l.	b.d.l.	b.d.l.	b.d.l.	b.d.l.	b.d.l.	b.d.l.	b.d.l.	b.d.l.	b.d.l.	b.d.l.	b.d.l.		
Ru	b.d.l.	b.d.l.	b.d.l.	b.d.l.	b.d.l.	b.d.l.	b.d.l.	b.d.l.	b.d.l.	b.d.l.	b.d.l.	b.d.l.	b.d.l.	b.d.l.	b.d.l.	b.d.l.	b.d.l.	b.d.l.	b.d.l.	b.d.l.	b.d.l.		
Total	100.72	98.64	98.94	98.10	99.72	99.46	99.86	99.84	99.53	97.92	98.50	98.31	98.16	98.70	99.10	98.45	99.36	98.97	98.43	99.73	98.63	99.00	
Atomic proportions																							
S	2.01	2.02	2.01	2.02	2.00	2.01	2.01	2.01	2.01	2.01	2.02	2.02	2.02	2.02	2.01	1.99	2.00	2.02	1.99	2.01	1.97	2.01	0.00
Fe	1.00	0.99	1.00	0.99	1.00	1.01	1.00	1.01	0.99	1.00	0.99	1.00	0.99	1.00	1.00	1.00	1.01	1.00	1.01	0.99	1.03	1.00	0.00
Ni	0.00	0.00	0.00	0.00	0.00	0.00	0.00	0.00	0.00	0.00	0.00	0.00	0.00	0.00	0.00	0.00	0.00	0.00	0.00	0.00	0.00	0.00	0.00
Co	0.00	0.00	0.00	0.00	0.00	0.00	0.00	0.00	0.00	0.00	0.00	0.00	0.00	0.00	0.00	0.00	0.00	0.00	0.00	0.00	0.00	0.00	0.00
Cu	0.99	0.99	0.99	0.99	0.99	0.99	0.99	0.98	0.99	0.98	0.99	0.98	0.98	0.98	0.99	1.00	0.98	0.98	0.99	0.99	1.00	0.99	0.00
Rh	b.d.l.	b.d.l.	b.d.l.	b.d.l.	b.d.l.	b.d.l.	b.d.l.	b.d.l.	b.d.l.	b.d.l.	b.d.l.	b.d.l.	b.d.l.	b.d.l.	b.d.l.	b.d.l.	b.d.l.	b.d.l.	b.d.l.	b.d.l.	b.d.l.		
Pd	b.d.l.	b.d.l.	b.d.l.	b.d.l.	b.d.l.	b.d.l.	b.d.l.	b.d.l.	b.d.l.	b.d.l.	b.d.l.	b.d.l.	b.d.l.	b.d.l.	b.d.l.	b.d.l.	b.d.l.	b.d.l.	b.d.l.	b.d.l.	b.d.l.		
Pt	b.d.l.	b.d.l.	b.d.l.	b.d.l.	b.d.l.	b.d.l.	b.d.l.	b.d.l.	b.d.l.	b.d.l.	b.d.l.	b.d.l.	b.d.l.	b.d.l.	b.d.l.	b.d.l.	b.d.l.	b.d.l.	b.d.l.	b.d.l.	b.d.l.		
Ru	b.d.l.	b.d.l.	b.d.l.	b.d.l.	b.d.l.	b.d.l.	b.d.l.	b.d.l.	b.d.l.	b.d.l.	b.d.l.	b.d.l.	b.d.l.	b.d.l.	b.d.l.	b.d.l.	b.d.l.	b.d.l.	b.d.l.	b.d.l.	b.d.l.		

Table 4 *Pyrrhotite compositions from sample A1.*

	1	2	3	4	5	6	7	8	9	10	11	12	13	14	15	16	17	18	x	s
S	36.28	36.27	36.40	36.56	36.41	36.34	36.38	36.18	36.86	37.78	36.36	36.32	36.33	36.02	36.84	36.84	36.66	36.73	36.53	0.40
Fe	62.76	62.54	63.14	62.75	62.61	63.14	62.69	63.02	63.54	61.94	62.76	63.39	62.63	62.33	62.83	63.36	62.94	63.38	62.87	0.41
Ni	0.02	0.04	0.09	0.04	0.03	0.01	0.01	0.02	0.03	0.28	0.09	0.06	0.07	0.03	0.00	0.02	0.01	0.04	0.05	0.06
Co	0.06	0.08	0.07	0.13	0.07	0.08	0.08	0.04	0.08	0.08	0.05	0.10	0.07	0.05	0.11	0.08	0.06	0.06	0.07	0.02
Cu	0.02	0.01	0.03	0.01	0.02	0.00	0.00	0.05	0.03	0.00	0.03	0.03	0.01	0.02	0.00	0.00	0.00	0.04	0.02	0.01
Rh	b.d.l.	b.d.l.	b.d.l.	b.d.l.	b.d.l.	b.d.l.	b.d.l.	b.d.l.	b.d.l.	b.d.l.	b.d.l.	b.d.l.	b.d.l.	b.d.l.	b.d.l.	b.d.l.	b.d.l.	b.d.l.	b.d.l.	b.d.l.
Pd	0.02	b.d.l.	b.d.l.	b.d.l.	b.d.l.	b.d.l.	b.d.l.	b.d.l.	b.d.l.	b.d.l.	b.d.l.	b.d.l.	0.04	b.d.l.	b.d.l.	b.d.l.	b.d.l.	b.d.l.	b.d.l.	b.d.l.
Pt	b.d.l.	b.d.l.	b.d.l.	b.d.l.	0.02	b.d.l.	b.d.l.	b.d.l.	b.d.l.	b.d.l.	b.d.l.	b.d.l.	b.d.l.	b.d.l.	b.d.l.	b.d.l.	b.d.l.	b.d.l.	b.d.l.	b.d.l.
Ru	b.d.l.	b.d.l.	b.d.l.	b.d.l.	b.d.l.	b.d.l.	b.d.l.	b.d.l.	b.d.l.	b.d.l.	b.d.l.	b.d.l.	b.d.l.	b.d.l.	b.d.l.	b.d.l.	b.d.l.	b.d.l.	b.d.l.	b.d.l.
Total	99.16	98.93	99.72	99.50	99.16	99.57	99.17	99.31	100.53	100.09	99.30	99.89	99.15	98.46	99.78	100.29	99.67	100.25	99.55	
Atomic proportions																				
S	1.00	1.00	1.00	1.00	1.00	1.00	1.00	1.00	1.00	1.00	1.00	1.00	1.00	1.00	1.00	1.00	1.00	1.00	1.00	0.00
Fe	0.99	0.99	1.00	0.99	0.99	1.00	0.99	1.00	0.99	0.94	0.99	1.00	0.99	0.99	0.98	0.99	0.99	0.99	0.99	0.00
Ni	0.00	0.00	0.00	0.00	0.00	0.00	0.00	0.00	0.00	0.00	0.00	0.00	0.00	0.00	0.00	0.00	0.00	0.00	0.00	0.00
Co	0.00	0.00	0.00	0.00	0.00	0.00	0.00	0.00	0.00	0.00	0.00	0.00	0.00	0.00	0.00	0.00	0.00	0.00	0.00	0.00
Cu	0.00	0.00	0.00	0.00	0.00	0.00	0.00	0.00	0.00	0.00	0.00	0.00	0.00	0.00	0.00	0.00	0.00	0.00	0.00	0.00
Rh	b.d.l.	b.d.l.	b.d.l.	b.d.l.	b.d.l.	b.d.l.	b.d.l.	b.d.l.	b.d.l.	b.d.l.	b.d.l.	b.d.l.	b.d.l.	b.d.l.	b.d.l.	b.d.l.	b.d.l.	b.d.l.	b.d.l.	b.d.l.
Pd	0.00	b.d.l.	b.d.l.	b.d.l.	b.d.l.	b.d.l.	b.d.l.	b.d.l.	b.d.l.	b.d.l.	b.d.l.	b.d.l.	0.00	b.d.l.	b.d.l.	b.d.l.	b.d.l.	b.d.l.	b.d.l.	b.d.l.
Pt	b.d.l.	b.d.l.	b.d.l.	b.d.l.	0.00	b.d.l.	b.d.l.	b.d.l.	b.d.l.	b.d.l.	b.d.l.	b.d.l.	b.d.l.	b.d.l.	b.d.l.	b.d.l.	b.d.l.	b.d.l.	b.d.l.	b.d.l.
Ru	b.d.l.	b.d.l.	b.d.l.	b.d.l.	b.d.l.	b.d.l.	b.d.l.	b.d.l.	b.d.l.	b.d.l.	b.d.l.	b.d.l.	b.d.l.	b.d.l.	b.d.l.	b.d.l.	b.d.l.	b.d.l.	b.d.l.	b.d.l.

Table 5 *Pyrrhotite compositions from sample B4.*

	1	2	3	4	5	6	7	8	9	10	11	12	13	14	15	16	17	18	19
S	39.14	38.89	39.06	39.49	39.31	39.12	38.97	39.08	39.06	38.49	38.84	37.64	38.85	38.81	39.51	38.95	39.14	38.60	37.85
Fe	60.09	61.06	61.12	60.82	61.34	60.79	60.75	60.18	60.80	60.10	60.60	60.82	60.52	60.35	59.52	61.11	60.59	59.54	60.31
Ni	0.02	0.25	0.11	0.04	0.09	0.06	0.04	0.20	0.10	1.05	0.17	0.19	0.12	0.04	0.14	0.05	0.09	0.11	0.13
Co	0.06	0.08	0.04	0.08	0.04	0.03	0.09	0.05	0.04	0.13	0.08	0.08	0.09	0.06	0.03	0.03	0.08	0.05	0.07
Cu	0.01	0.00	0.00	0.03	0.02	0.00	0.01	0.03	0.02	0.14	0.08	0.00	0.06	0.04	0.05	0.01	0.06	0.02	0.03
Rh	b.d.l.	b.d.l.	b.d.l.	b.d.l.	b.d.l.	b.d.l.	b.d.l.	b.d.l.	b.d.l.	b.d.l.	b.d.l.	b.d.l.	b.d.l.	b.d.l.	b.d.l.	b.d.l.	b.d.l.	b.d.l.	b.d.l.
Pd	b.d.l.	b.d.l.	b.d.l.	b.d.l.	b.d.l.	b.d.l.	b.d.l.	b.d.l.	b.d.l.	b.d.l.	b.d.l.	b.d.l.	b.d.l.	b.d.l.	b.d.l.	b.d.l.	b.d.l.	b.d.l.	b.d.l.
Pt	b.d.l.	b.d.l.	b.d.l.	b.d.l.	b.d.l.	b.d.l.	b.d.l.	b.d.l.	b.d.l.	b.d.l.	b.d.l.	b.d.l.	b.d.l.	b.d.l.	b.d.l.	b.d.l.	b.d.l.	b.d.l.	b.d.l.
Ru	b.d.l.	b.d.l.	b.d.l.	b.d.l.	b.d.l.	b.d.l.	b.d.l.	b.d.l.	b.d.l.	b.d.l.	b.d.l.	b.d.l.	b.d.l.	b.d.l.	b.d.l.	b.d.l.	b.d.l.	b.d.l.	b.d.l.
Total	99.32	100.28	100.34	100.46	100.81	100.00	99.85	99.54	100.02	99.91	99.76	98.74	99.63	99.31	99.24	100.15	99.96	98.32	98.40
Atomic proportions																			
S	1.00	1.00	1.00	1.00	1.00	1.00	1.00	1.00	1.00	1.00	1.00	1.00	1.00	1.00	1.00	1.00	1.00	1.00	1.00
Fe	0.88	0.90	0.90	0.88	0.90	0.89	0.90	0.88	0.89	0.90	0.90	0.93	0.89	0.89	0.86	0.90	0.89	0.89	0.91
Ni	0.00	0.00	0.00	0.00	0.00	0.00	0.00	0.00	0.00	0.01	0.00	0.00	0.00	0.00	0.00	0.00	0.00	0.00	0.00
Co	0.00	0.00	0.00	0.00	0.00	0.00	0.00	0.00	0.00	0.00	0.00	0.00	0.00	0.00	0.00	0.00	0.00	0.00	0.00
Cu	0.00	0.00	0.00	0.00	0.00	0.00	0.00	0.00	0.00	0.00	0.00	0.00	0.00	0.00	0.00	0.00	0.00	0.00	0.00
Rh	b.d.l.	b.d.l.	b.d.l.	b.d.l.	b.d.l.	b.d.l.	b.d.l.	b.d.l.	b.d.l.	b.d.l.	b.d.l.	b.d.l.	b.d.l.	b.d.l.	b.d.l.	b.d.l.	b.d.l.	b.d.l.	b.d.l.
Pd	b.d.l.	b.d.l.	b.d.l.	b.d.l.	b.d.l.	b.d.l.	b.d.l.	b.d.l.	b.d.l.	b.d.l.	b.d.l.	b.d.l.	b.d.l.	b.d.l.	b.d.l.	b.d.l.	b.d.l.	b.d.l.	b.d.l.
Pt	b.d.l.	b.d.l.	b.d.l.	b.d.l.	b.d.l.	b.d.l.	b.d.l.	b.d.l.	b.d.l.	b.d.l.	b.d.l.	b.d.l.	b.d.l.	b.d.l.	b.d.l.	b.d.l.	b.d.l.	b.d.l.	b.d.l.
Ru	b.d.l.	b.d.l.	b.d.l.	b.d.l.	b.d.l.	b.d.l.	b.d.l.	b.d.l.	b.d.l.	b.d.l.	b.d.l.	b.d.l.	b.d.l.	b.d.l.	b.d.l.	b.d.l.	b.d.l.	b.d.l.	b.d.l.

Table 5 continued. *Pyrrhotite compositions from sample B4*

	20	21	22	23	24	25	26	27	Avg.	s
S	39.39	37.97	38.55	38.65	38.52	38.76	38.54	38.54	38.80	0.46
Fe	60.91	61.14	60.08	60.11	60.71	60.83	60.98	60.17	60.57	0.48
Ni	0.08	0.14	0.01	0.07	0.06	0.05	0.16	0.07	0.13	0.19
Co	0.07	0.06	0.10	0.03	0.07	0.06	0.06	0.06	0.06	0.02
Cu	0.00	0.03	0.02	0.02	0.03	0.02	0.01	0.00	0.03	0.03
Rh	b.d.l.	b.d.l.	b.d.l.	b.d.l.	b.d.l.	b.d.l.	b.d.l.	b.d.l.	b.d.l.	b.d.l.
Pd	b.d.l.	b.d.l.	b.d.l.	b.d.l.	b.d.l.	b.d.l.	b.d.l.	b.d.l.	b.d.l.	b.d.l.
Pt	b.d.l.	b.d.l.	b.d.l.	b.d.l.	b.d.l.	b.d.l.	b.d.l.	b.d.l.	b.d.l.	b.d.l.
Ru	b.d.l.	b.d.l.	b.d.l.	b.d.l.	b.d.l.	b.d.l.	b.d.l.	b.d.l.	b.d.l.	b.d.l.
Total	100.45	99.33	98.77	98.87	99.39	99.73	99.74	98.84	99.60	
Atomic proportions										
S	1.00	1.00	1.00	1.00	1.00	1.00	1.00	1.00	1.00	0.00
Fe	0.89	0.92	0.89	0.89	0.90	0.90	0.91	0.90	0.90	0.00
Ni	0.00	0.00	0.00	0.00	0.00	0.00	0.00	0.00	0.00	0.00
Co	0.00	0.00	0.00	0.00	0.00	0.00	0.00	0.00	0.00	0.00
Cu	0.00	0.00	0.00	0.00	0.00	0.00	0.00	0.00	0.00	0.00
Rh	b.d.l.	b.d.l.	b.d.l.	b.d.l.	b.d.l.	b.d.l.	b.d.l.	b.d.l.	b.d.l.	b.d.l.
Pd	b.d.l.	b.d.l.	b.d.l.	b.d.l.	b.d.l.	b.d.l.	b.d.l.	b.d.l.	b.d.l.	b.d.l.
Pt	b.d.l.	b.d.l.	b.d.l.	b.d.l.	b.d.l.	b.d.l.	b.d.l.	b.d.l.	b.d.l.	b.d.l.
Ru	b.d.l.	b.d.l.	b.d.l.	b.d.l.	b.d.l.	b.d.l.	b.d.l.	b.d.l.	b.d.l.	b.d.l.

Table 6 *Pyrite compositions from sample A1.*

	1	2	3	4	5	6	7	8	9	10	Agv.	s
S	53.75	53.69	53.49	52.43	53.78	52.96	54.21	53.78	54.35	53.63	53.60	0.56
Fe	45.88	45.00	45.75	46.31	45.93	45.33	45.85	45.67	46.21	45.09	45.70	0.44
Ni	0.42	0.42	0.13	0.72	0.02	0.09	0.01	0.19	0.05	0.02	0.21	0.24
Co	1.00	1.48	0.70	0.70	1.35	2.19	1.21	0.54	1.11	1.48	1.18	0.49
Cu	0.02	0.02	0.04	0.01	0.00	0.00	0.02	0.00	0.08	0.00	0.02	0.03
Rh	b.d.l.	0.06	b.d.l.	b.d.l.	b.d.l.	b.d.l.	b.d.l.	b.d.l.	b.d.l.	b.d.l.		
Pd	b.d.l.	b.d.l.	b.d.l.	b.d.l.	b.d.l.	b.d.l.	b.d.l.	b.d.l.	b.d.l.	b.d.l.		
Pt	b.d.l.	b.d.l.	b.d.l.	b.d.l.	b.d.l.	b.d.l.	b.d.l.	b.d.l.	b.d.l.	b.d.l.		
Ru	b.d.l.	b.d.l.	b.d.l.	b.d.l.	b.d.l.	b.d.l.	b.d.l.	b.d.l.	b.d.l.	b.d.l.		
Total	101.07	100.66	100.11	100.17	101.07	100.56	101.29	100.19	101.80	100.21	100.71	
Atomic proportions												
S	2.00	2.00	2.00	2.00	2.00	2.00	2.00	2.00	2.00	2.00	2.00	0.00
Fe	0.98	0.96	0.98	1.01	0.98	0.98	0.97	0.98	0.98	0.97	0.98	0.01
Ni	0.01	0.01	0.00	0.02	0.00	0.00	0.00	0.00	0.00	0.00	0.00	0.00
Co	0.02	0.03	0.01	0.01	0.03	0.04	0.02	0.01	0.02	0.03	0.02	0.01
Cu	0.00	0.00	0.00	0.00	0.00	0.00	0.00	0.00	0.00	0.00	0.00	0.00
Rh	b.d.l.	0.0216	b.d.l.	b.d.l.	b.d.l.	b.d.l.	b.d.l.	b.d.l.	b.d.l.	b.d.l.		
Pd	b.d.l.	b.d.l.	b.d.l.	b.d.l.	b.d.l.	b.d.l.	b.d.l.	b.d.l.	b.d.l.	b.d.l.		
Pt	b.d.l.	b.d.l.	b.d.l.	b.d.l.	b.d.l.	b.d.l.	b.d.l.	b.d.l.	b.d.l.	b.d.l.		
Ru	b.d.l.	b.d.l.	b.d.l.	b.d.l.	b.d.l.	b.d.l.	b.d.l.	b.d.l.	b.d.l.	b.d.l.		

Table 7 *Pyrite compositions from sample B4.*

	1	2	3	4	5	6	Avg.	s
S	54.11	52.03	54.32	53.71	53.77	53.96	53.65	0.82
Fe	47.84	46.39	47.52	46.90	47.37	46.99	47.17	0.51
Ni	0.00	0.01	0.02	0.05	0.02	0.02	0.02	0.02
Co	0.03	0.04	0.09	0.08	0.04	0.06	0.06	0.02
Cu	0.02	0.03	0.00	0.17	0.30	0.03	0.09	0.12
Rh	b.d.l.	b.d.l.	b.d.l.	b.d.l.	b.d.l.	b.d.l.	b.d.l.	
Pd	b.d.l.	b.d.l.	b.d.l.	b.d.l.	b.d.l.	b.d.l.	b.d.l.	
Pt	b.d.l.	b.d.l.	b.d.l.	b.d.l.	b.d.l.	b.d.l.	b.d.l.	
Ru	b.d.l.	b.d.l.	b.d.l.	b.d.l.	b.d.l.	b.d.l.	b.d.l.	
Total	102.00	98.51	101.94	100.92	101.50	101.06	100.99	
Atomic proportions								
S	2.00	2.00	2.00	2.00	2.00	2.00	2.00	0.00
Fe	1.02	1.02	1.00	1.00	1.01	1.00	1.01	0.01
Ni	0.00	0.00	0.00	0.00	0.00	0.00	0.00	0.00
Co	0.00	0.00	0.00	0.00	0.00	0.00	0.00	0.00
Cu	0.00	0.00	0.00	0.00	0.01	0.00	0.00	0.00
Rh	b.d.l.	b.d.l.	b.d.l.	b.d.l.	b.d.l.	b.d.l.	b.d.l.	
Pd	b.d.l.	b.d.l.	b.d.l.	b.d.l.	b.d.l.	b.d.l.	b.d.l.	
Pt	b.d.l.	b.d.l.	b.d.l.	b.d.l.	b.d.l.	b.d.l.	b.d.l.	
Ru	b.d.l.	b.d.l.	b.d.l.	b.d.l.	b.d.l.	b.d.l.	b.d.l.	

Table 8 *Pyrite compositions from sample C1.*

	1	2	3	4	5	6	7	8	9	10	11	12	13	14	15	16	17	18	Avg.	s
S	53.10	53.55	52.19	53.06	53.26	52.27	52.76	52.67	52.61	53.78	54.08	53.64	53.86	53.25	53.12	53.50	52.31	52.71	53.10	0.57
Fe	46.60	46.97	47.17	46.30	46.27	46.48	46.19	46.80	46.18	46.84	43.51	47.13	46.86	44.43	46.07	46.65	46.23	46.43	46.28	0.92
Ni	0.70	0.01	0.02	0.00	0.05	0.00	0.15	0.91	0.76	0.17	0.62	0.07	0.08	0.14	0.94	0.14	1.71	0.53	0.39	0.47
Co	0.59	0.04	0.11	0.98	1.31	0.10	0.67	0.09	0.17	0.05	1.57	0.15	0.45	0.48	0.12	0.37	0.38	0.04	0.43	0.45
Cu	0.05	0.02	0.00	0.04	0.06	0.02	0.03	0.00	0.02	0.01	0.02	0.04	0.04	0.03	0.05	0.05	0.03	0.00	0.03	0.02
Rh	b.d.l.	b.d.l.	b.d.l.	b.d.l.	b.d.l.	b.d.l.	b.d.l.	b.d.l.	b.d.l.	b.d.l.	b.d.l.	b.d.l.	b.d.l.	b.d.l.	b.d.l.	b.d.l.	b.d.l.	b.d.l.	b.d.l.	
Pd	b.d.l.	b.d.l.	b.d.l.	b.d.l.	b.d.l.	b.d.l.	b.d.l.	b.d.l.	b.d.l.	b.d.l.	b.d.l.	b.d.l.	b.d.l.	b.d.l.	b.d.l.	b.d.l.	b.d.l.	b.d.l.	b.d.l.	
Pt	b.d.l.	b.d.l.	b.d.l.	b.d.l.	b.d.l.	b.d.l.	b.d.l.	b.d.l.	b.d.l.	b.d.l.	b.d.l.	b.d.l.	b.d.l.	b.d.l.	b.d.l.	b.d.l.	b.d.l.	b.d.l.	b.d.l.	
Ru	b.d.l.	b.d.l.	b.d.l.	b.d.l.	b.d.l.	b.d.l.	b.d.l.	b.d.l.	b.d.l.	b.d.l.	b.d.l.	b.d.l.	b.d.l.	b.d.l.	b.d.l.	b.d.l.	b.d.l.	b.d.l.	b.d.l.	
Total	101.04	100.60	99.49	100.38	100.94	98.86	99.80	100.48	99.75	100.85	99.81	101.03	101.29	98.33	100.29	100.70	100.65	99.71	100.22	
Atomic proportions																				
S	2.00	2.00	2.00	2.00	2.00	2.00	2.00	2.00	2.00	2.00	2.00	2.00	2.00	2.00	2.00	2.00	2.00	2.00	2.00	0.00
Fe	1.01	1.01	1.04	1.00	1.00	1.02	1.01	1.02	1.01	1.00	0.92	1.01	1.00	0.96	1.00	1.00	1.01	1.01	1.00	0.02
Ni	0.01	0.00	0.00	0.00	0.00	0.00	0.00	0.02	0.02	0.00	0.01	0.00	0.00	0.00	0.02	0.00	0.04	0.01	0.01	0.01
Co	0.01	0.00	0.00	0.02	0.03	0.00	0.01	0.00	0.00	0.00	0.03	0.00	0.01	0.01	0.00	0.01	0.01	0.00	0.01	0.01
Cu	0.00	0.00	0.00	0.00	0.00	0.00	0.00	0.00	0.00	0.00	0.00	0.00	0.00	0.00	0.00	0.00	0.00	0.00	0.00	0.00
Rh	b.d.l.	b.d.l.	b.d.l.	b.d.l.	b.d.l.	b.d.l.	b.d.l.	b.d.l.	b.d.l.	b.d.l.	b.d.l.	b.d.l.	b.d.l.	b.d.l.	b.d.l.	b.d.l.	b.d.l.	b.d.l.	b.d.l.	
Pd	b.d.l.	b.d.l.	b.d.l.	b.d.l.	b.d.l.	b.d.l.	b.d.l.	b.d.l.	b.d.l.	b.d.l.	b.d.l.	b.d.l.	b.d.l.	b.d.l.	b.d.l.	b.d.l.	b.d.l.	b.d.l.	b.d.l.	
Pt	b.d.l.	b.d.l.	b.d.l.	b.d.l.	b.d.l.	b.d.l.	b.d.l.	b.d.l.	b.d.l.	b.d.l.	b.d.l.	b.d.l.	b.d.l.	b.d.l.	b.d.l.	b.d.l.	b.d.l.	b.d.l.	b.d.l.	
Ru	b.d.l.	b.d.l.	b.d.l.	b.d.l.	b.d.l.	b.d.l.	b.d.l.	b.d.l.	b.d.l.	b.d.l.	b.d.l.	b.d.l.	b.d.l.	b.d.l.	b.d.l.	b.d.l.	b.d.l.	b.d.l.	b.d.l.	

Table 9 *Pyrite compositions from sample C2.*

	1	2	3	4	5	6	7	8	9	10	11	12	Avg.	s
S	53.70	53.90	53.94	53.35	53.33	53.75	53.65	53.73	53.58	53.70	52.64	53.52	53.57	0.35
Fe	46.09	45.69	46.47	46.05	46.99	45.32	45.24	44.32	46.04	45.56	45.00	46.44	45.77	0.73
Ni	0.68	0.08	0.21	0.46	0.07	0.35	0.50	0.98	0.13	0.21	0.28	0.10	0.34	0.28
Co	0.65	1.59	0.74	0.68	0.08	1.57	1.22	1.52	0.99	1.55	1.14	0.95	1.06	0.47
Cu	0.01	0.00	0.03	0.11	0.01	0.03	0.01	0.83	0.00	0.06	0.02	0.06	0.10	0.23
Rh	b.d.l.	0.0216	b.d.l.	b.d.l.	b.d.l.	b.d.l.	b.d.l.	b.d.l.	b.d.l.	b.d.l.	b.d.l.	0.1096		
Pd	b.d.l.	b.d.l.	b.d.l.	b.d.l.	b.d.l.	b.d.l.	b.d.l.	b.d.l.	b.d.l.	b.d.l.	b.d.l.	b.d.l.		
Pt	b.d.l.	b.d.l.	b.d.l.	b.d.l.	b.d.l.	b.d.l.	b.d.l.	b.d.l.	b.d.l.	b.d.l.	b.d.l.	b.d.l.		
Ru	b.d.l.	b.d.l.	b.d.l.	b.d.l.	b.d.l.	b.d.l.	b.d.l.	b.d.l.	b.d.l.	b.d.l.	b.d.l.	b.d.l.		
Total	101.13	101.29	101.38	100.66	100.48	101.02	100.62	101.38	100.73	101.08	99.08	101.20	100.83	
Atomic proportions														
S	2.00	2.00	2.00	2.00	2.00	2.00	2.00	2.00	2.00	2.00	2.00	2.00	2.00	0.00
Fe	0.99	0.97	0.99	0.99	1.01	0.97	0.97	0.95	0.99	0.97	0.98	1.00	0.98	0.02
Ni	0.01	0.00	0.00	0.01	0.00	0.01	0.01	0.02	0.00	0.00	0.01	0.00	0.01	0.01
Co	0.01	0.03	0.01	0.01	0.00	0.03	0.02	0.03	0.02	0.03	0.02	0.02	0.02	0.01
Cu	0.00	0.00	0.00	0.00	0.00	0.00	0.00	0.02	0.00	0.00	0.00	0.00	0.00	0.00
Rh	b.d.l.	0.0001	b.d.l.	b.d.l.	b.d.l.	b.d.l.	b.d.l.	b.d.l.	b.d.l.	b.d.l.	b.d.l.	0.0004		
Pd	b.d.l.	b.d.l.	b.d.l.	b.d.l.	b.d.l.	b.d.l.	b.d.l.	b.d.l.	b.d.l.	b.d.l.	b.d.l.	b.d.l.		
Pt	b.d.l.	b.d.l.	b.d.l.	b.d.l.	b.d.l.	b.d.l.	b.d.l.	b.d.l.	b.d.l.	b.d.l.	b.d.l.	b.d.l.		
Ru	b.d.l.	b.d.l.	b.d.l.	b.d.l.	b.d.l.	b.d.l.	b.d.l.	b.d.l.	b.d.l.	b.d.l.	b.d.l.	b.d.l.		

Table 10 *Millerite compositions from sample C1.*

	1	2	3	4	5	6	7	8	9	10	11	12	13	14	15	16	17	18	19	20	Avg.	s
S	36.11	34.69	34.84	34.67	34.84	34.51	34.44	35.13	35.10	35.61	35.99	35.38	35.34	35.63	35.19	35.44	35.05	35.44	35.35	35.56	35.22	0.46
Fe	1.04	1.27	0.83	1.27	1.02	0.86	0.98	1.14	1.08	3.30	1.24	1.56	0.69	1.24	1.03	2.31	1.26	0.95	0.83	1.10	1.25	0.59
Ni	63.32	61.20	62.75	61.68	62.02	61.94	62.18	62.56	61.34	60.61	61.42	61.73	63.23	62.22	62.77	63.62	61.56	61.84	63.73	61.23	62.15	0.87
Co	0.92	1.02	1.02	1.06	0.89	1.00	1.13	1.01	0.62	0.78	1.00	0.90	0.63	1.16	0.81	0.20	1.20	0.95	1.12	1.00	0.92	0.23
Cu	0.06	0.06	0.07	0.05	0.06	0.05	0.06	0.06	0.05	0.06	0.04	0.08	0.06	0.06	0.00	0.04	0.08	0.06	0.07	0.02	0.05	0.02
Rh	b.d.l.	b.d.l.	b.d.l.	b.d.l.	b.d.l.	0.0274	b.d.l.	b.d.l.	b.d.l.	b.d.l.	b.d.l.	b.d.l.	b.d.l.	b.d.l.	b.d.l.	b.d.l.	b.d.l.	b.d.l.	b.d.l.	b.d.l.	b.d.l.	
Pd	b.d.l.	b.d.l.	b.d.l.	b.d.l.	b.d.l.	b.d.l.	b.d.l.	b.d.l.	b.d.l.	b.d.l.	b.d.l.	b.d.l.	b.d.l.	b.d.l.	b.d.l.	b.d.l.	b.d.l.	b.d.l.	b.d.l.	b.d.l.	b.d.l.	
Pt	b.d.l.	b.d.l.	b.d.l.	b.d.l.	b.d.l.	b.d.l.	b.d.l.	b.d.l.	b.d.l.	b.d.l.	b.d.l.	b.d.l.	b.d.l.	b.d.l.	b.d.l.	b.d.l.	b.d.l.	b.d.l.	b.d.l.	b.d.l.	b.d.l.	
Ru	b.d.l.	b.d.l.	b.d.l.	b.d.l.	b.d.l.	b.d.l.	b.d.l.	b.d.l.	b.d.l.	b.d.l.	b.d.l.	b.d.l.	b.d.l.	b.d.l.	b.d.l.	b.d.l.	b.d.l.	b.d.l.	b.d.l.	b.d.l.	b.d.l.	
Total	101.47	98.25	99.51	98.74	98.82	98.39	98.80	99.91	98.19	100.36	99.70	99.66	99.96	100.32	99.81	101.61	99.14	99.24	101.10	98.91	99.59	
Atomic proportions																						
S	1.00	1.00	1.00	1.00	1.00	1.00	1.00	1.00	1.00	1.00	1.00	1.00	1.00	1.00	1.00	1.00	1.00	1.00	1.00	1.00	1.00	0.00
Fe	0.02	0.02	0.01	0.02	0.02	0.01	0.02	0.02	0.02	0.05	0.02	0.03	0.01	0.02	0.02	0.04	0.02	0.02	0.01	0.02	0.02	0.01
Ni	0.96	0.96	0.98	0.97	0.97	0.98	0.99	0.97	0.95	0.93	0.93	0.95	0.98	0.95	0.97	0.98	0.96	0.95	0.98	0.94	0.96	0.02
Co	0.01	0.02	0.02	0.02	0.01	0.02	0.02	0.02	0.01	0.01	0.02	0.01	0.01	0.02	0.01	0.00	0.02	0.01	0.02	0.02	0.01	0.00
Cu	0.00	0.00	0.00	0.00	0.00	0.00	0.00	0.00	0.00	0.00	0.00	0.00	0.00	0.00	0.00	0.00	0.00	0.00	0.00	0.00	0.00	0.00
Rh	b.d.l.	b.d.l.	b.d.l.	b.d.l.	b.d.l.	0.0001	b.d.l.	b.d.l.	b.d.l.	b.d.l.	b.d.l.	b.d.l.	b.d.l.	b.d.l.	b.d.l.	b.d.l.	b.d.l.	b.d.l.	b.d.l.	b.d.l.	b.d.l.	
Pd	b.d.l.	b.d.l.	b.d.l.	b.d.l.	b.d.l.	b.d.l.	b.d.l.	b.d.l.	b.d.l.	b.d.l.	b.d.l.	b.d.l.	b.d.l.	b.d.l.	b.d.l.	b.d.l.	b.d.l.	b.d.l.	b.d.l.	b.d.l.	b.d.l.	
Pt	b.d.l.	b.d.l.	b.d.l.	b.d.l.	b.d.l.	b.d.l.	b.d.l.	b.d.l.	b.d.l.	b.d.l.	b.d.l.	b.d.l.	b.d.l.	b.d.l.	b.d.l.	b.d.l.	b.d.l.	b.d.l.	b.d.l.	b.d.l.	b.d.l.	
Ru	b.d.l.	b.d.l.	b.d.l.	b.d.l.	b.d.l.	b.d.l.	b.d.l.	b.d.l.	b.d.l.	b.d.l.	b.d.l.	b.d.l.	b.d.l.	b.d.l.	b.d.l.	b.d.l.	b.d.l.	b.d.l.	b.d.l.	b.d.l.	b.d.l.	

Table 11 *Millerite compositions from sample C2.*

	1	2	3	4	5	6	7	8	9	10	Avg.	s
S	35.13	35.38	35.69	35.42	35.46	35.06	35.48	35.45	35.12	35.33	35.35	0.20
Fe	1.69	3.27	0.87	0.88	0.86	1.26	1.00	0.97	1.26	1.24	1.33	0.73
Ni	61.94	61.64	61.88	63.90	62.20	62.20	61.98	62.47	62.01	61.17	62.14	0.71
Co	0.80	0.08	1.20	0.01	1.12	0.03	1.01	1.04	0.60	0.95	0.68	0.48
Cu	0.06	0.03	0.02	0.11	0.05	0.06	0.09	0.00	0.04	0.06	0.05	0.03
Rh	b.d.l.	b.d.l.	b.d.l.	b.d.l.	b.d.l.	b.d.l.	b.d.l.	b.d.l.	b.d.l.	b.d.l.		
Pd	b.d.l.	b.d.l.	b.d.l.	b.d.l.	b.d.l.	b.d.l.	b.d.l.	b.d.l.	b.d.l.	b.d.l.		
Pt	b.d.l.	b.d.l.	b.d.l.	b.d.l.	b.d.l.	b.d.l.	b.d.l.	b.d.l.	b.d.l.	b.d.l.		
Ru	b.d.l.	b.d.l.	b.d.l.	b.d.l.	b.d.l.	b.d.l.	b.d.l.	b.d.l.	b.d.l.	b.d.l.		
Total	99.62	100.40	99.66	100.32	99.69	98.61	99.56	99.92	99.02	98.75	99.56	
Atomic proportions												
S	1.00	1.00	1.00	1.00	1.00	1.00	1.00	1.00	1.00	1.00	1.00	0.00
Fe	0.03	0.05	0.01	0.01	0.01	0.02	0.02	0.02	0.02	0.02	0.02	0.01
Ni	0.96	0.95	0.95	0.99	0.96	0.97	0.95	0.96	0.96	0.95	0.96	0.01
Co	0.01	0.00	0.02	0.00	0.02	0.00	0.02	0.02	0.01	0.01	0.01	0.01
Cu	0.00	0.00	0.00	0.00	0.00	0.00	0.00	0.00	0.00	0.00	0.00	0.00
Rh	b.d.l.	b.d.l.	b.d.l.	b.d.l.	b.d.l.	b.d.l.	b.d.l.	b.d.l.	b.d.l.	b.d.l.		
Pd	b.d.l.	b.d.l.	b.d.l.	b.d.l.	b.d.l.	b.d.l.	b.d.l.	b.d.l.	b.d.l.	b.d.l.		
Pt	b.d.l.	b.d.l.	b.d.l.	b.d.l.	b.d.l.	b.d.l.	b.d.l.	b.d.l.	b.d.l.	b.d.l.		
Ru	b.d.l.	b.d.l.	b.d.l.	b.d.l.	b.d.l.	b.d.l.	b.d.l.	b.d.l.	b.d.l.	b.d.l.		

Table 12 *Pentlandite compositions from sample A1.*

	1	2	3	4	5	6	7	8	9	10	11	12	13	14	15	16	17
S	33.05	33.25	32.95	32.94	32.89	32.90	32.91	33.02	32.88	32.87	32.85	33.00	32.97	32.97	33.03	32.50	33.18
Fe	33.11	33.82	33.20	32.48	33.15	33.14	32.33	32.78	31.70	33.09	33.16	33.00	33.05	32.77	32.82	33.56	32.74
Ni	32.46	32.47	33.46	33.17	32.83	33.98	32.78	32.97	33.00	33.64	32.25	32.24	30.96	32.41	32.06	32.54	32.90
Co	0.70	0.77	0.34	0.34	0.67	0.32	0.51	0.35	0.63	0.31	0.61	0.36	0.33	0.51	0.73	0.29	0.19
Cu	0.03	0.00	0.07	0.00	0.04	0.02	0.03	0.05	0.06	0.06	0.01	0.08	0.08	0.03	0.02	0.01	0.03
Rh	b.d.l.	b.d.l.	b.d.l.	0.7879	b.d.l.	b.d.l.	0.0381	0.0403	0.3194	b.d.l.	0.0614	b.d.l.	0.0611	0.0827	0.0486	b.d.l.	b.d.l.
Pd	b.d.l.	0.0299	0.0565	b.d.l.	0.1554	0.0901	0.2742	0.1289	0.3521	0.1972	0.2814	0.7425	1.0914	0.0472	0.0535	0.1647	0.2470
Pt	b.d.l.	b.d.l.	b.d.l.	b.d.l.	b.d.l.	b.d.l.	b.d.l.	b.d.l.	b.d.l.	b.d.l.	b.d.l.	b.d.l.	b.d.l.	b.d.l.	b.d.l.	b.d.l.	b.d.l.
Ru	b.d.l.	b.d.l.	b.d.l.	b.d.l.	b.d.l.	b.d.l.	0.1016	b.d.l.	b.d.l.	0.0678	b.d.l.	b.d.l.	b.d.l.	b.d.l.	b.d.l.	b.d.l.	b.d.l.
Total	99.34	100.34	100.07	99.73	99.75	100.44	98.98	99.33	98.94	100.23	99.22	99.43	98.55	98.82	98.77	99.05	99.29
Atomic proportions																	
S	8.00	8.00	8.00	8.00	8.00	8.00	8.00	8.00	8.00	8.00	8.00	8.00	8.00	8.00	8.00	8.00	8.00
Fe	4.60	4.67	4.63	4.53	4.63	4.63	4.51	4.56	4.43	4.62	4.64	4.59	4.60	4.57	4.56	4.74	4.53
Ni	4.29	4.27	4.44	4.40	4.36	4.51	4.35	4.36	4.39	4.47	4.29	4.27	4.10	4.30	4.24	4.37	4.33
Co	0.09	0.10	0.05	0.04	0.09	0.04	0.07	0.05	0.08	0.04	0.08	0.05	0.04	0.07	0.10	0.04	0.03
Cu	0.00	0.00	0.01	0.00	0.01	0.00	0.00	0.01	0.01	0.01	0.00	0.01	0.01	0.00	0.00	0.00	0.00
Rh	0.00	0.00	0.00	0.06	0.00	0.00	0.00	0.00	0.00	0.00	0.00	0.00	0.00	0.01	0.00	0.00	0.00
Pd	0.00	0.00	0.00	0.00	0.01	0.01	0.02	0.00	0.00	0.00	0.02	0.05	0.08	0.00	0.00	0.01	0.02
Pt	0.00	0.00	0.00	0.00	0.00	0.00	0.00	0.00	0.00	0.00	0.00	0.00	0.00	0.00	0.00	0.00	0.00
Ru	0.00	0.00	0.00	0.00	0.00	0.00	0.01	0.00	0.00	0.00	0.00	0.00	0.00	0.00	0.00	0.00	0.00

Table 12 continued. *Pentlandite compositions from sample A1*

	18	19	20	21	22	23	24	25	Avg.	s
S	32.96	32.82	33.42	32.67	33.42	33.41	32.69	33.28	32.99	0.23
Fe	32.49	32.67	33.28	33.22	33.12	31.84	33.30	33.16	32.92	0.48
Ni	32.67	33.63	31.92	32.01	32.40	31.78	32.72	32.46	32.63	0.66
Co	0.34	0.45	0.40	0.57	0.36	0.44	0.22	0.58	0.45	0.16
Cu	0.05	0.07	0.11	0.03	0.00	0.05	0.03	0.06	0.04	0.03
Rh	b.d.l.	b.d.l.	b.d.l.	0.4121	0.1934	0.6091	b.d.l.	b.d.l.		
Pd	0.0941	0.1051	0.7187	0.5838	0.1091	0.8845	0.0763	0.0663		
Pt	b.d.l.	b.d.l.	b.d.l.	b.d.l.	b.d.l.	b.d.l.	b.d.l.	b.d.l.		
Ru	b.d.l.	b.d.l.	b.d.l.	b.d.l.	b.d.l.	b.d.l.	b.d.l.	b.d.l.		
Total	98.60	99.75	99.85	99.50	99.59	99.01	99.04	99.61	99.49	
Atomic proportions										
S	8.00	8.00	8.00	8.00	8.00	8.00	8.00	8.00	8.00	0.00
Fe	4.53	4.57	4.57	4.67	4.55	4.38	4.68	4.58	4.58	0.00
Ni	4.33	4.48	4.17	4.28	4.24	4.16	4.37	4.26	4.32	0.10
Co	0.04	0.06	0.05	0.08	0.05	0.06	0.03	0.08	0.06	0.02
Cu	0.01	0.01	0.01	0.00	0.00	0.01	0.00	0.01	0.00	0.00
Rh	0.00	0.00	0.00	0.03	0.01	0.05	0.00	0.00		
Pd	0.01	0.01	0.05	0.04	0.01	0.06	0.01	0.00		
Pt	0.00	0.00	0.00	0.00	0.00	0.00	0.00	0.00		
Ru	0.00	0.00	0.00	0.00	0.00	0.00	0.00	0.00		

Table 13 *Pentlandite compositions from sample B4.*

	1	2	3	4	5	6	7	8	9	10	11	12	13	14	15	16	17
S	33.37	33.66	33.84	33.33	33.32	33.70	33.64	33.62	33.47	33.53	33.52	33.54	32.56	33.34	33.52	33.42	33.13
Fe	34.07	33.83	34.61	33.66	33.86	34.83	34.18	34.24	34.04	32.08	33.53	33.73	32.78	34.46	33.39	34.00	34.09
Ni	32.37	33.34	32.08	32.18	31.59	31.02	32.40	32.02	31.24	33.46	31.64	31.27	32.45	31.44	31.24	31.85	31.39
Co	0.64	0.68	0.71	0.75	0.65	0.90	0.87	0.72	0.67	0.73	0.70	0.77	0.66	0.74	0.68	0.60	0.67
Cu	0.06	0.02	0.02	0.11	0.03	0.07	0.08	0.04	0.07	0.06	0.08	0.03	0.08	0.08	0.02	0.03	0.12
Rh	b.d.l.	b.d.l.	b.d.l.	0.0417	0.0314	0.0676	b.d.l.	0.0201	0.0286	0.0527	0.0937	0.1256	b.d.l.	0.0379	0.0953	0.0511	0.1422
Pd	0.1862	0.0440	0.2304	0.0815	0.3449	0.0289	b.d.l.	0.0583	0.2039	0.1273	0.2284	0.1782	b.d.l.	0.1698	b.d.l.	0.0212	0.1674
Pt	b.d.l.	b.d.l.	b.d.l.	b.d.l.	b.d.l.	b.d.l.	b.d.l.	b.d.l.	b.d.l.	b.d.l.	b.d.l.	b.d.l.	b.d.l.	b.d.l.	b.d.l.	b.d.l.	b.d.l.
Ru	b.d.l.	b.d.l.	b.d.l.	b.d.l.	b.d.l.	b.d.l.	b.d.l.	b.d.l.	b.d.l.	b.d.l.	b.d.l.	b.d.l.	b.d.l.	b.d.l.	b.d.l.	b.d.l.	b.d.l.
Total	100.70	101.57	101.49	100.14	99.82	100.61	101.17	100.71	99.71	100.04	99.79	99.65	98.53	100.27	98.93	99.98	99.71
Atomic proportions																	
S	8.00	8.00	8.00	8.00	8.00	8.00	8.00	8.00	8.00	8.00	8.00	8.00	8.00	8.00	8.00	8.00	8.00
Fe	4.69	4.62	4.70	4.64	4.67	4.75	4.67	4.68	4.67	4.39	4.60	4.62	4.62	4.75	4.58	4.67	4.73
Ni	4.24	4.33	4.14	4.22	4.14	4.02	4.21	4.16	4.08	4.36	4.12	4.07	4.35	4.12	4.07	4.16	4.14
Co	0.08	0.09	0.09	0.10	0.08	0.12	0.11	0.09	0.09	0.10	0.09	0.10	0.09	0.10	0.09	0.08	0.09
Cu	0.01	0.00	0.00	0.01	0.00	0.01	0.01	0.00	0.01	0.01	0.01	0.00	0.01	0.01	0.00	0.00	0.01
Rh	0.00	0.00	0.00	0.00	0.00	0.00	0.00	0.00	0.00	0.00	0.01	0.01	0.00	0.00	0.01	0.00	0.01
Pd	0.01	0.00	0.02	0.01	0.02	0.00	0.00	0.00	0.01	0.01	0.02	0.01	0.00	0.01	0.00	0.00	0.01
Pt	0.00	0.00	0.00	0.00	0.00	0.00	0.00	0.00	0.00	0.00	0.00	0.00	0.00	0.00	0.00	0.00	0.00
Ru	0.00	0.00	0.00	0.00	0.00	0.00	0.00	0.00	0.00	0.00	0.00	0.00	0.00	0.00	0.00	0.00	0.00

Table 13 continued. *Pentlandite compositions from sample B4*

	18	19	20	21	22	23	24	25	26	27	Avg.	s
S	33.41	33.69	33.34	32.87	33.42	33.50	33.04	33.39	33.21	33.04	33.39	0.28
Fe	34.11	33.91	33.88	33.35	35.38	34.04	33.57	34.17	34.03	32.88	33.88	0.65
Ni	31.65	32.48	31.43	31.35	30.68	31.46	31.53	31.84	31.68	31.59	31.80	0.64
Co	0.73	0.61	0.67	0.67	0.68	0.67	0.73	0.69	0.80	1.37	0.73	0.14
Cu	0.03	0.02	0.04	0.05	0.05	0.02	0.06	0.00	0.05	0.06	0.05	0.03
Rh	0.0820	b.d.l.	0.0244	b.d.l.	b.d.l.	0.5864	0.0749	0.0382	0.0744	0.0239		
Pd	0.1675	0.1342	0.1729	0.0746	0.2570	0.0511	0.2352	0.3564	0.2590	0.1329		
Pt	0.0325	b.d.l.	b.d.l.	b.d.l.	b.d.l.	b.d.l.	b.d.l.	b.d.l.	b.d.l.	b.d.l.		
Ru	b.d.l.	b.d.l.	b.d.l.	b.d.l.	b.d.l.	b.d.l.	b.d.l.	b.d.l.	b.d.l.	b.d.l.		
Total	100.21	100.84	99.55	98.36	100.48	100.33	99.24	100.48	100.10	99.10	100.05	
Atomic proportions												
S	8.00	8.00	8.00	8.00	8.00	8.00	8.00	8.00	8.00	8.00	8.00	0.00
Fe	4.69	4.62	4.67	4.66	4.86	4.67	4.67	4.70	4.71	4.57	4.67	0.08
Ni	4.14	4.21	4.12	4.17	4.01	4.10	4.17	4.17	4.17	4.18	4.15	0.08
Co	0.09	0.08	0.09	0.09	0.09	0.09	0.10	0.09	0.10	0.18	0.10	0.02
Cu	0.00	0.00	0.01	0.01	0.01	0.00	0.01	0.00	0.01	0.01	0.01	0.00
Rh	0.01	0.00	0.00	0.00	0.00	0.04	0.01	0.00	0.01	0.00	0.01	0.01
Pd	0.01	0.00	0.01	0.00	0.00	0.00	0.02	0.03	0.02	0.01	0.01	0.01
Pt	0.00	0.00	0.00	0.00	0.00	0.00	0.00	0.00	0.00	0.00	0.00	0.00
Ru	0.00	0.00	0.00	0.00	0.00	0.00	0.00	0.00	0.00	0.00	0.00	0.00

Table 14 *Pentlandite compositions from sample C1.*

	1	2	3	4	Avg.	s
S	32.71	33.08	32.58	32.81	32.79	0.21
Fe	30.19	30.73	30.60	30.98	30.62	0.33
Ni	34.86	34.77	34.04	33.69	34.34	0.57
Co	0.38	1.00	0.24	0.23	0.46	0.36
Cu	0.07	0.06	0.07	0.01	0.05	0.03
Rh	b.d.l.	0.0226	b.d.l.	b.d.l.		
Pd	b.d.l.	0.1111	0.3583	0.4059		
Pt	b.d.l.	b.d.l.	b.d.l.	b.d.l.		
Ru	b.d.l.	b.d.l.	b.d.l.	b.d.l.		
Total	98.21	99.77	97.88	98.14	98.28	
Atomic proportions						
S	8.00	8.00	8.00	8.00	8.00	0.00
Fe	4.24	4.27	4.31	4.34	4.29	0.04
Ni	4.66	4.59	4.57	4.49	4.58	0.07
Co	0.05	0.13	0.03	0.03	0.06	0.05
Cu	0.01	0.01	0.01	0.00	0.01	0.00
Rh	0.00	0.00	0.00	0.00	0.00	0.00
Pd	0.00	0.01	0.03	0.03	0.02	0.01
Pt	0.00	0.00	0.00	0.00	0.00	0.00
Ru	0.00	0.00	0.00	0.00	0.00	0.00

Table 15 *Siegenite compositions from samples C1 and C2.*

	1	2	3	4	5	6	Avg.	s
S	42.12	41.43	41.22	41.55	41.78	41.80	41.65	0.32
Fe	3.71	1.57	1.12	1.15	0.76	0.87	1.53	1.10
Ni	32.84	32.40	33.97	33.06	32.56	32.60	32.90	0.57
Co	19.48	19.76	21.40	21.48	23.51	24.13	21.63	1.90
Cu	0.05	0.06	0.03	0.03	0.00	0.01	0.03	0.02
Rh	b.d.l.	3.5389	1.0506	0.1311	b.d.l.	b.d.l.		
Pd	b.d.l.	b.d.l.	b.d.l.	b.d.l.	b.d.l.	b.d.l.		
Pt	b.d.l.	b.d.l.	0.7394	2.0687	b.d.l.	b.d.l.		
Ru	b.d.l.	b.d.l.	b.d.l.	b.d.l.	b.d.l.	b.d.l.		
Total	98.21	98.75	99.53	99.47	98.62	99.42		
Atomic proportions								
S	4.00	4.00	4.00	4.00	4.00	4.00	4.00	0.00
Fe	0.20	0.09	0.06	0.06	0.04	0.05	0.08	0.06
Ni	1.70	1.71	1.80	1.74	1.70	1.70	1.73	0.04
Co	1.01	1.04	1.13	1.13	1.22	1.26	1.13	0.10
Cu	0.00	0.00	0.00	0.00	0.00	0.00	0.00	0.00
Rh	0.00	0.11	0.03	0.00	0.00	0.00		
Pd	0.00	0.00	0.00	0.00	0.00	0.00		
Pt	0.00	0.00	0.01	0.03	0.00	0.00		
Ru	0.00	0.00	0.00	0.00	0.00	0.00		

APPENDIX G

Electron-microprobe analyses of selected PGE mineral grains.

Table 1 Selected electron-microprobe analyses of cooperite.

Table 2 Selected electron-microprobe analyses of braggite and vysotskite.

Table 3 Selected electron-microprobe analyses of malanite.

Table 4 Selected electron-microprobe analyses of Pt-Fe alloy

Table 5 Electron-microprobe analyses of atheneite (1), kotulskite (2,4), and moncheite (3).

Table 1 *Selected electron-microprobe analyses of cooperite.*

	1	2	3	4	5	6	7	Avg.
S	14.4	12.6	15.0	18.9	13.7	12.8	12.9	14.3
Ru	0.0	0.1	0.5	0.0	0.0	0.0	0.0	0.1
Rh	0.2	0.2	0.4	0.2	0.3	0.2	0.2	0.2
Pd	8.3	0.4	0.1	7.7	3.3	0.0	0.1	2.9
Pt	76.8	81.7	79.1	64.0	79.6	85.9	85.3	78.9
Fe	0.6	0.5	0.7	0.8	0.6	0.9	0.5	0.6
Co	0.0	0.0	0.0	0.0	0.0	0.0	0.0	0.0
Ni	0.3	5.0	2.7	8.0	0.9	0.8	1.7	2.8
Cu	0.0	0.0	0.0	0.0	0.1	0.1	0.0	0.0
Total	101.0	100.8	98.9	99.9	98.8	101.0	101.1	100.2
Atomic proportions								
S	1.0	1.0	1.0	1.0	1.0	1.0	1.0	1.0
Ru	0.0	0.0	0.0	0.0	0.0	0.0	0.0	0.0
Rh	0.0	0.0	0.0	0.0	0.0	0.0	0.0	0.0
Pd	0.2	0.0	0.0	0.1	0.1	0.0	0.0	0.1
Pt	0.9	1.1	0.9	0.6	1.0	1.1	1.1	0.9
Fe	0.0	0.0	0.0	0.0	0.0	0.0	0.0	0.0
Co	0.0	0.0	0.0	0.0	0.0	0.0	0.0	0.0
Ni	0.0	0.2	0.1	0.2	0.0	0.0	0.1	0.1
Cu	0.0	0.0	0.0	0.0	0.0	0.0	0.0	0.0

Table 2 *Selected electron-microprobe analyses of braggite and vysotskite.*

	1	2	3	4	5	6	7	8	9	10	11	12	13	14	15	16	17	18
S	19.1	19.3	20.6	19.8	18.9	18.6	15.2	18.0	15.7	21.3	21.0	21.7	14.9	18.3	25.5	23.9	19.9	23.1
Ru	0.2	0.0	0.0	0.0	0.0	0.0	0.0	0.0	0.0	0.0	0.0	0.0	0.0	0.0	0.0	0.0	0.0	0.0
Rh	0.3	0.1	0.1	0.1	0.0	0.0	0.2	0.2	0.2	0.2	0.1	0.0	0.3	0.2	0.0	0.0	0.1	0.1
Pd	22.6	28.2	44.4	27.3	28.6	31.8	15.7	19.6	13.5	20.9	35.9	32.6	11.5	32.1	54.8	55.3	48.8	53.0
Pt	53.1	43.1	26.7	45.2	45.7	44.0	64.6	53.5	68.5	47.4	36.5	35.3	72.0	44.7	7.0	15.2	24.6	15.6
Fe	0.8	0.5	0.7	0.6	0.5	0.5	0.6	0.5	0.5	0.8	0.4	0.5	0.5	0.2	1.9	0.4	0.4	0.9
Co	0.0	0.0	0.0	0.0	0.0	0.0	0.0	0.0	0.0	0.0	0.0	0.0	0.0	0.0	0.0	0.0	0.0	0.0
Ni	5.0	6.6	6.5	6.9	6.8	4.5	1.6	7.8	2.3	9.8	4.4	8.5	1.1	4.2	9.9	6.4	4.7	7.0
Cu	0.0	0.0	0.0	0.1	0.0	0.0	0.0	0.0	0.0	0.0	0.0	0.1	0.0	0.0	0.6	0.0	0.0	0.2
Total	101.4	98.1	99.0	100.0	100.6	99.6	98.1	100.0	100.8	100.7	98.4	99.1	100.7	99.7	99.7	101.4	98.6	99.9
Atomic proportions																		
S	1.0	1.0	1.0	1.0	1.0	1.0	1.0	1.0	1.0	1.0	1.0	1.0	1.0	1.0	1.0	1.0	1.0	1.0
Ru	0.0	0.0	0.0	0.0	0.0	0.0	0.0	0.0	0.0	0.0	0.0	0.0	0.0	0.0	0.0	0.0	0.0	0.0
Rh	0.0	0.0	0.0	0.0	0.0	0.0	0.0	0.0	0.0	0.0	0.0	0.0	0.0	0.0	0.0	0.0	0.0	0.0
Pd	0.4	0.4	0.7	0.4	0.5	0.5	0.3	0.3	0.3	0.3	0.5	0.5	0.2	0.5	0.7	0.7	0.7	0.7
Pt	0.5	0.4	0.2	0.4	0.4	0.2	0.7	0.5	0.7	0.4	0.3	0.3	0.8	0.4	0.0	0.1	0.2	0.1
Fe	0.0	0.0	0.0	0.0	0.0	0.0	0.0	0.0	0.0	0.0	0.0	0.0	0.0	0.0	0.0	0.0	0.0	0.0
Co	0.0	0.0	0.0	0.0	0.0	0.0	0.0	0.0	0.0	0.0	0.0	0.0	0.0	0.0	0.0	0.0	0.0	0.0
Ni	0.1	0.2	0.2	0.2	0.2	0.1	0.1	0.2	0.1	0.3	0.1	0.2	0.0	0.1	0.2	0.2	0.1	0.2
Cu	0.0	0.0	0.0	0.0	0.0	0.0	0.0	0.0	0.0	0.0	0.0	0.0	0.0	0.0	0.0	0.0	0.0	0.0

Table 3 *Selected electron-microprobe analyses of malanite.*

	1	**2**	**3**	**4**	**5**	**6**	**7**	**8**	**9**	**10**
As	0.1	0.0	0.0	0.0	0.0	0.0	0.0	0.0	0.0	0.0
S	26.7	26.0	27.4	26.9	27.0	26.4	26.5	26.4	26.5	26.7
Ru	0.0	0.0	0.0	0.0	0.0	0.0	0.1	0.0	0.0	0.0
Rh	13.3	6.9	7.1	8.6	14.0	9.4	4.6	6.5	10.7	9.0
Pd	0.0	0.0	0.1	0.0	0.1	0.1	0.1	0.1	0.0	0.1
Pt	41.6	47.1	38.6	46.1	40.6	42.0	42.8	47.8	42.2	43.2
Fe	1.0	0.8	3.9	1.6	0.8	0.9	2.1	0.9	1.6	1.5
Co	2.6	3.8	3.0	2.7	3.1	3.3	6.3	3.1	3.7	3.5
Ni	0.5	1.8	7.0	2.8	0.8	6.4	3.4	2.3	0.5	2.8
Cu	12.4	12.6	11.3	12.8	12.9	11.8	12.4	12.5	12.9	12.4
Total	98.3	99.2	98.4	101.7	99.5	100.3	98.3	99.8	98.6	99.3
Atomic proportions										
As	0.0	0.0	0.0	0.0	0.0	0.0	0.0	0.0	0.0	0.0
S	4.0	4.0	4.0	4.0	4.0	4.0	4.0	4.0	4.0	4.0
Ru	0.0	0.0	0.0	0.0	0.0	0.0	0.0	0.0	0.0	0.0
Rh	0.6	0.3	0.3	0.4	0.7	0.4	0.2	0.3	0.5	0.4
Pd	0.0	0.0	0.0	0.0	0.0	0.0	0.0	0.0	0.0	0.0
Pt	1.0	1.2	0.9	1.1	1.0	1.1	1.1	1.2	1.1	1.1
Fe	0.1	0.1	0.3	0.1	0.1	0.1	0.2	0.1	0.1	0.1
Co	0.2	0.3	0.2	0.2	0.3	0.3	0.5	0.3	0.3	0.3
Ni	0.0	0.2	0.6	0.2	0.1	0.5	0.3	0.2	0.0	0.2
Cu	1.0	1.1	0.9	1.0	1.1	1.0	1.0	1.0	1.1	1.0

Table 4 *Selected electron-microprobe analyses of Pt-Fe alloy.*

	1	2	3
S	0.1	0.1	0.3
Ru	0.0	0.0	0.0
Rh	0.2	0.3	0.5
Pd	0.1	0.2	0.2
Pt	89.0	86.7	86.4
Pb	0.4	0.4	0.5
Bi	0.0	0.2	0.1
Fe	9.4	9.3	9.7
Co	0.0	0.0	0.0
Ni	0.1	0.1	0.6
Cu	0.2	0.8	0.3
Total	99.5	98.2	98.7
Atomic proportions			
S	0.0	0.0	0.0
Ru	0.0	0.0	0.0
Rh	0.0	0.0	0.0
Pd	0.0	0.0	0.0
Pt	2.6	2.9	2.8
Pb	0.0	0.0	0.0
Bi	0.0	0.0	0.0
Fe	1.2	1.1	1.0
Co	0.0	0.0	0.0
Ni	0.0	0.0	0.0
Cu	0.1	0.0	0.1
ΣPGE	2.7	2.9	2.8
Σ(Fe,Cu, Ni,Co)	1.3	1.1	1.1
Ni	0.0	0.0	0.0
Cu	0.0	0.0	0.0
ΣPGE	2.8	0.9	1.0
Σ(Te,Bi,Hg,As)	1.2	2.0	3.0

* high total + low total

Table 5 *Electron-microprobe analyses of atheneite (1), kotulskite (2,4), and moncheite (3).*

	1*	2	3+	4
As	22.0	0.0	0.1	0.0
S	0.0	0.0	0.1	0.1
Ru	0.0	0.0	0.0	0.0
Rh	0.0	0.0	0.6	0.0
Pd	64.0	38.9	8.4	35.7
Te	0.1	43.8	53.4	47.4
Pt	0.1	0.0	26.2	5.8
Hg	15.9	0.0	0.0	0.0
Pb	0.0	0.0	0.1	0.2
Bi	0.0	15.1	7.6	10.0
Fe	0.4	0.5	0.5	1.0
Ni	0.0	0.0	0.1	0.0
Cu	0.0	0.0	0.1	0.1
Total	102.4	98.5	97.2	100.2
Atomic proportions				
As	1.2	0.0	0.0	0.0
S	0.0	0.0	0.0	0.0
Ru	0.0	0.0	0.0	0.0
Rh	0.0	0.0	0.0	0.0
Pd	2.4	0.9	0.3	0.8
Te	0.0	0.9	1.8	0.9
Pt	0.0	0.0	0.6	0.1
Hg	0.3	0.0	0.0	0.0
Pb	0.0	0.0	0.0	0.0
Bi	0.0	0.2	0.2	0.1
Fe	0.0	0.0	0.0	0.0
Ni	0.0	0.0	0.0	0.0
Cu	0.0	0.0	0.0	0.0
ΣPGE	2.8	0.9	1.0	0.9
Σ(Te,Bi,Hg,As)	1.2	2.0	3.0	2.0

* high total + low total

APPENDIX H

Mineralogical data for milled feed and flotation products

Table 1 *Chromite grain-size distributions in fourteen UG2 chromitite samples milled to 80% <75µm (reported in area per cent).*

Size class (µm)	A2	B2	A1	B1	A3	B3	A4	B4	A5	C1	C2	C3	C5
0.0-17.0	12	16	15	14	16	14	15	13	21	14	14	13	16
17.0-36.0	29	32	31	31	34	33	34	31	33	29	33	32	31
36.0-55.0	21	18	19	21	20	20	22	20	17	20	22	21	20
55.0-74.1	17	16	14	15	16	14	15	15	12	15	14	15	15
74.1-93.1	12	11	11	11	9	10	9	12	9	11	11	11	10
93.1-112.1	7	5	6	6	3	6	5	6	5	6	5	6	5
112.1-131.1	1	2	2	2	1	2	1	2	2	3	2	2	2
131.1-150.1	0	0	1	0	0	1	0	0	1	1	0	0	0
150.1-169.1	0	0	0	0	0	0	0	0	0	0	0	0	0
169.1-188.1	0	0	0	0	0	0	0	0	0	0	0	0	0
188.1-207.2	0	0	0	0	0	0	0	0	0	0	0	0	0
107.2-226.2	0	0	0	0	0	0	0	0	0	0	0	0	0
>226.2	0	0	0	0	0	0	0	0	0	0	0	0	0
Median	44	38	40	41	36	38	37	41	32	42	39	41	38

Table 2 *Silicate grain-size distributions in fourteen UG2 chromitite samples milled to 80% <75µm (reported in area per cent).*

Size class (µm)	A2	B2	A1	B1	A3	B3	A4	B4	A5	C1	C2	C3	C5
0.0-17.0	23	28	28	27	29	30	32	29	36	30	30	31	27
17.0-36.0	23	23	24	24	24	25	24	22	22	20	25	22	26
36.0-55.0	22	20	21	19	22	19	21	19	16	20	21	20	23
55.0-74.1	19	16	16	15	15	15	13	16	13	15	15	16	14
74.1-93.1	9	10	8	9	7	8	7	9	8	9	7	9	7
93.1-112.1	3	3	2	4	2	3	2	3	4	5	2	2	2
112.1-131.1	0	1	0	1	0	1	1	1	1	2	0	1	1
131.1-150.1	0	0	0	0	0	0	0	0	1	0	0	0	0
150.1-169.1	0	0	0	0	0	0	0	0	0	0	0	0	0
169.1-188.1	0	0	0	0	0	0	0	0	0	0	0	0	0
188.1-207.2	0	0	0	0	0	0	0	0	0	0	0	0	0
107.2-226.2	0	0	0	0	0	0	0	0	0	0	0	0	0
>226.2	0	0	0	0	0	0	0	0	0	0	0	0	0
Median	39	35	34	35	34	32	31	35	30	36	32	34	34

Table 3 *Mode of occurrence of PGE minerals in fourteen samples of UG2 chromitite milled to 80% <75 µm.*

	A2	**B2**	**A1**	**B1**	**A3**	**B3**	**A4**	**B4**	**A5**	**C1**	**C2**	**C3**	**C4**	**C5**
number of PGEMs	185	193	619	187	217	190	211	217	216	236	185	191	203	183
	% Number of grains													
Liberated PGEM	51	46	57	59	62	48	59	67	33	59	68	57	65	71
PGEM locked in BMS	15	16	14	11	8	14	11	9	4	8	1	3	5	3
PGEM locked in oxide	2	4	3	2	3	4	0	2	4	5	5	3	5	4
PGEM locked in silicate	3	4	1	2	5	6	4	4	20	12	4	18	10	5
Grain boundary BMS/Gangue	3	6	4	5	5	3	3	2	16	6	9	7	6	4
Grain edge of BMS	18	20	16	18	10	17	17	7	1	3	5	4	3	4
Grain edge of gangue	8	5	5	4	6	7	5	10	22	7	8	8	6	8
	Volume %													
Liberated PGEM	49	48	57	64	60	57	76	66	48	62	61	54	61	76
PGEM locked in BMS	15	14	13	6	6	10	5	11	1	4	0	2	3	1
PGEM locked in oxide	1	2	3	3	1	3	0	2	3	8	8	2	5	2
PGEM locked in silicate	4	1	1	1	15	5	2	1	22	9	1	17	6	3
Grain boundary BMS/Gangue	3	2	3	3	9	2	2	1	9	8	12	9	14	9
Grain edge of BMS	17	31	18	18	5	18	12	15	0	4	8	3	4	1
Grain edge of gangue	11	3	5	4	5	4	3	5	17	4	10	12	7	8

Table 4 *Chromite grain-size distribution in flotation products of sample C1 (reported in area per cent).*

Size class (µm)	*RC1*	*RC2*	*RC3-5*	*RT*
0.0-17.0	99.2	96.7	98.8	4.9
17.0-36.0	0.8	1.2	1.2	23.2
36.0-55.0	0.0	2.1	0.0	24
55.0-74.1	0	0	0	18.4
74.1-93.1	0	0	0	14.1
93.1-112.1	0	0	0	9.2
112.1-131.1	0	0	0	3.6
131.1-150.1	0	0	0	2.1
150.1-169.1	0	0	0	0.1
169.1-188.1	0	0	0	0
188.1-207.2	0	0	0	0
207.2-226.2	0	0	0	0
>225	0	0	0	0.4
	100	100	100	100

RC1= rougher concentrate 1, RC2=rougher concentrate 2, RC3-5=combined rougher concentrate 3 to 5, RT=rougher tailings

Table 5 *Silicate grain-size distributions in flotation products of sample C1 (reported in area per cent).*

Size class (µm)	*RC1*	*RC2*	*RC3-5*	*RT*
0.0-17.0	85	81.9	88	9
17.0-36.0	12.3	13.6	6.4	31.4
36.0-55.0	2.7	4.4	5.8	25.1
55.0-74.1	0	0	0	14.8
74.1-93.1	0	0	0	11.6
93.1-112.1	0	0	0	5.5
112.1-131.1	0	0	0	1.4
131.1-150.1	0	0	0	0.8
150.1-169.1	0	0	0	0.5
169.1-188.1	0	0	0	0
188.1-207.2	0	0	0	0
207.2-226.2	0	0	0	0
>225	0	0	0	0

RC1= rougher concentrate 1, RC2=rougher concentrate 2, RC3-5=combined rougher concentrate 3 to 5, RT=rougher tailings

Table 6 *Relative proportions of silicate minerals in flotation products of selected samples determined by image analysis. Reported in volume %.*

A1	RC1	RC2	RC3-5	RT
*Ca-Al-silicate**	63	62	58	57
Mg-Fe-silicate+	31	32	35	40
Phlogopite	2	2	2	1
Clinopyroxene	1	1	1	1
Quartz	0	0	0	0
Chlorite	0	1	1	1
Amphibole	2	2	2	0
Albite	0	0	0	0
K-Al-silicate°	0	0	0	0
A3	**RC1**	**RC2**	**RC3-5**	**RT**
*Ca-Al-silicate**	62	63	58	69
Mg-Fe-silicate+	33	31	36	28
Phlogopite	1	2	1	1
Clinopyroxene	1	1	1	0
Quartz	0	0	0	0
Chlorite	1	1	1	0
Amphibole	0	1	2	0
Albite	1	1	1	0
K-Al-silicate°	0	1	1	1
B3	**RC1**	**RC2**	**RC3-5**	**RT**
*Ca-Al-silicate**	50	43	43	65
Mg-Fe-silicate+	42	48	51	31
Phlogopite	1	1	0	2
Clinopyroxene	3	3	4	1
Quartz	0	0	0	0
Chlorite	1	1	1	0
Amphibole	5	3	2	1
Albite	0	0	0	0
K-Al-silicate°	0	0	0	0
A4	**RC1**	**RC2**	**RC3-5**	**RT**
*Ca-Al-silicate**	21	22	21	24
Mg-Fe-silicate+	48	50	47	39
Phlogopite	0	0	0	0
Clinopyroxene	19	19	20	29
Quartz	1	1	1	0
Chlorite	2	2	2	0
Amphibole	6	6	9	1
Albite	0	0	0	0
K-Al-silicate°	0	0	0	0

Table 6 continued *Relative proportions of silicate minerals in flotation products of selected samples determined by image analysis. Reported in volume %.*

B4	RC1	RC2	RC3-5	RT
*Ca-Al-silicate**	33	38	41	68
Mg-Fe-silicate+	54	49	45	19
Phlogopite	0	0	1	1
Clinopyroxene	8	6	7	8
Quartz	0	0	0	0
Chlorite	1	3	2	1
Amphibole	3	4	4	1
Albite	0	0	0	0
K-Al-silicate°	0	0	0	0
A5	**RC1**	**RC2**	**RC3-5**	**RT**
*Ca-Al-silicate**	16	16	23	50
Mg-Fe-silicate+	68	53	44	16
Phlogopite	0	0	0	1
Clinopyroxene	8	8	11	7
Quartz	2	1	0	1
Chlorite	3	15	14	16
Amphibole	2	6	6	6
Albite	2	1	1	4
K-Al-silicate°	0	0	0	0
C1	**RC1**	**RC2**	**RC3-5**	**RT**
*Ca-Al-silicate**	8	10	18	66
Mg-Fe-silicate+	70	64	51	12
Phlogopite	0	0	0	0
Clinopyroxene	4	5	5	4
Quartz	2	2	2	4
Chlorite	12	14	17	6
Amphibole	3	3	3	2
Albite	1	1	2	4
K-Al-silicate°	0	0	1	1
C4	**RC1**	**RC2**	**RC3-5**	**RT**
*Ca-Al-silicate**	27	25	28	77
Mg-Fe-silicate+	63	66	64	18
Phlogopite	0	0	1	1
Clinopyroxene	1	1	1	0
Quartz	1	0	1	1
Chlorite	5	5	4	1
Amphibole	3	3	3	0
Albite	1	0	1	1
K-Al-silicate°	0	0	0	0

RC1= rougher concentrate 1, RC2=rougher concentrate 2, RC3-5=combined rougher concentrate 3 to 5, RT=rougher tailings

* *Predominantly plagioclase. Also includes pumpellyite, prehnite and epidote, especially in samples from area C.*

+ *Predominantly orthopyroxene, minor talc, and rarely serpentine and olivine*

° *K-feldspar and sericite*

***Table** 7 Liberation characteristics of base-metal sulphide grains in flotation products of selected samples (reported in area %).*

RC1	*A1*	*A3*	*A4*	*B4*	*A5*	*C1*	*C2*
0.0-0.2	0	4	1	1	9	5	3
0.2-0.4	1	4	0	0	16	5	2
0.4-0.6	0	1	0	0	3	5	6
0.6-0.8	0	0	0	0	0	0	0
0.8-1.0	98	91	99	99	72	84	89
RC2	*A1*	*A3*	*A4*	*B4*	*A5*	*C1*	*C2*
0.0-0.2	2	4	0	1	12	14	5
0.2-0.4	2	0	0	1	7	0	5
0.4-0.6	0	1	0	0	0	0	0
0.6-0.8	0	0	0	0	0	0	0
0.8-1.0	96	94	99	98	80	86	89
RC3-5	*A1*	*A3*	*A4*	*B4*	*A5*	*C1*	*C2*
0.0-0.2	8	13	4	3	28	24	19
0.2-0.4	0	16	2	2	3	0	1
0.4-0.6	0	0	0	0	0	0	0
0.6-0.8	0	0	0	0	0	0	0
0.8-1.0	92	71	94	94	69	76	80

RC1= rougher concentrate 1, RC2=rougher concentrate 2, RC3-5=combined rougher concentrates 3 to 5

Table 8 *Chalcopyrite recovery to three flotation concentrates, assuming a 100% total recovery.*

A2	*cpy content g/t*	*cpy content g/t cum.*	*cpy distribution. %*	*cpy distribution % cum.*
RC-1	0.38	0.38	67.87	67.87
RC-2	0.08	0.22	16.85	84.71
RC-3-5	0.05	0.14	15.29	100.00
B2	*cpy content g/t*	*cpy content g/t cum.*	*cpy distribution. %*	*cpy distribution % cum.*
RC-1	0.32	0.32	69.54	69.54
RC-2	0.05	0.16	13.69	83.23
RC-3-5	0.03	0.10	16.77	100.00
A1	*cpy content g/t*	*cpy content g/t cum.*	*cpy distribution. %*	*cpy distribution % cum.*
RC-1	0.35	0.35	72.47	72.47
RC-2	0.10	0.25	13.66	86.13
RC-3-5	0.05	0.17	13.87	100.00
B1	*cpy content g/t*	*cpy content g/t cum.*	*cpy distribution. %*	*cpy distribution % cum.*
RC-1	0.65	0.65	82.57	82.57
RC-2	0.09	0.43	7.52	90.09
RC-3-5	0.06	0.26	9.91	100.00
A3	*cpy content g/t*	*cpy content g/t cum.*	*cpy distribution. %*	*cpy distribution % cum.*
RC-1	0.6463	0.65	65.56	65.56
RC-2	0.1699	0.41	16.69	82.25
RC-3-5	0.10	0.26	17.75	100.00
B3	*cpy content g/t*	*cpy content g/t cum.*	*cpy distribution. %*	*cpy distribution % cum.*
RC-1	0.82	0.82	72.34	72.34
RC-2	0.16	0.47	15.04	87.38
RC-3-5	0.06	0.25	12.62	100.00
A4	*cpy content g/t*	*cpy content g/t cum.*	*cpy distribution. %*	*cpy distribution % cum.*
RC-1	0.78	0.78	59.43	59.43
RC-2	0.24	0.50	20.74	80.17
RC-3-5	0.11	0.29	19.83	100.00
B4	*cpy content g/t*	*cpy content g/t cum.*	*cpy distribution. %*	*cpy distribution % cum.*
RC-1	1.34	1.34	69.30	69.30
RC-2	0.24	0.75	14.98	84.28
RC-3-5	0.09	0.35	15.72	100.00
A5	*cpy content g/t*	*cpy content g/t cum.*	*cpy distribution. %*	*cpy distribution % cum.*
RC-1	0.26	0.26	63.65	63.65
RC-2	0.06	0.16	16.04	79.69
RC-3-5	0.04	0.10	20.31	100.00
C1	*cpy content g/t*	*cpy content g/t cum.*	*cpy distribution. %*	*cpy distribution % cum.*
RC-1	0.28	0.28	54.79	54.79
RC-2	0.08	0.17	18.89	73.68
RC-3-5	0.05	0.10	26.32	100.00

Table 8 continued *Chalcopyrite recovery to three flotation concentrates, assuming a 100% total recovery.*

C2	*cpy content g/t*	*cpy content g/t cum.*	*cpy distribution. %*	*cpy distribution % cum.*
RC-1	0.22	0.22	53.39	53.39
RC-2	0.07	0.14	18.67	72.06
RC-3-5	0.04	0.08	27.94	100.00
C3	*cpy content g/t*	*cpy content g/t cum.*	*cpy distribution. %*	*cpy distribution % cum.*
RC-1	0.20	0.20	50.59	50.59
RC-2	0.07	0.13	19.94	70.53
RC-3-5	0.04	0.08	29.47	100.00
C4	*cpy content g/t*	*cpy content g/t cum.*	*cpy distribution. %*	*cpy distribution % cum.*
RC-1	0.12	0.12	48.37	48.37
RC-2	0.04	0.08	22.00	70.37
RC-3-5	0.03	0.05	29.63	100.00
C5	*cpy content g/t*	*cpy content g/t cum.*	*cpy distribution. %*	*cpy distribution % cum.*
RC-1	0.26	0.26	53.67	53.67
RC-2	0.07	0.15	19.15	72.82
RC-3-5	0.04	0.09	27.18	100.00
Comp.	*cpy content g/t*	*cpy content g/t cum.*	*cpy distribution. %*	*cpy distribution % cum.*
RC-1	0.47	0.47	67.56	67.56
RC-2	0.11	0.29	15.52	83.08
RC-3-5	0.06	0.17	16.92	100.00

Table 9 *Pentlandite recovery to three flotation concentrates, assuming a 100% total recovery.*

A2	*pn content g/t*	*pn content g/t cum.*	*pn distribution. %*	*pn distribution % cum.*
RC-1	1.11	1.11	63.60	63.60
RC-2	0.45	0.76	29.19	92.79
RC-3-5	0.07	0.44	7.21	100.00
B2	*pn content g/t*	*pn content g/t cum.*	*pn distribution. %*	*pn distribution % cum.*
RC-1	0.63	0.63	51.33	51.33
RC-2	0.28	0.43	32.56	83.89
RC-3-5	0.08	0.26	16.11	100.00
A1	*pn content g/t*	*pn content g/t cum.*	*pn distribution. %*	*pn distribution % cum.*
RC-1	1.17	1.17	66.02	66.02
RC-2	0.54	0.93	19.43	85.44
RC-3-5	0.20	0.61	14.56	100.00

Table 9 continued *Pentlandite recovery to three flotation concentrates, assuming a 100% total recovery.*

B1	*pn content g/t*	*pn content g/t cum.*	*pn distribution. %*	*pn distribution % cum.*
RC-1	1.23	1.23	58.72	58.72
RC-2	0.97	1.13	29.83	88.55
RC-3-5	0.18	0.70	11.45	100.00
A3	*pn content g/t*	*pn content g/t cum.*	*pn distribution. %*	*pn distribution % cum.*
RC-1	1.32	1.32	52.23	52.23
RC-2	0.83	1.08	31.72	83.95
RC-3-5	0.22	0.67	16.05	100.00
B3	*pn content g/t*	*pn content g/t cum.*	*pn distribution. %*	*pn distribution % cum.*
RC-1	2.12	2.12	67.11	67.11
RC-2	0.74	1.40	25.64	92.75
RC-3-5	0.10	0.71	7.25	100.00
A4	*pn content g/t*	*pn content g/t cum.*	*pn distribution. %*	*pn distribution % cum.*
RC-1	1.79	1.79	40.50	40.50
RC-2	1.52	1.65	38.85	79.35
RC-3-5	0.38	0.98	20.65	100.00
B4	*pn content g/t*	*pn content g/t cum.*	*pn distribution. %*	*pn distribution % cum.*
RC-1	0.63	0.63	53.88	53.88
RC-2	0.31	0.46	31.33	85.21
RC-3-5	0.05	0.21	14.79	100.00
A5	*pn content g/t*	*pn content g/t cum.*	*pn distribution. %*	*pn distribution % cum.*
RC-1	0.42	0.42	32.70	32.70
RC-2	0.45	0.44	35.85	68.55
RC-3-5	0.18	0.30	31.45	100.00
C1	*pn content g/t*	*pn content g/t cum.*	*pn distribution. %*	*pn distribution % cum.*
RC-1	0.04	0.04	57.92	57.92
RC-2	0.02	0.03	30.80	88.72
RC-3-5	0.00	0.01	11.28	100.00
C2	*pn content g/t*	*pn content g/t cum.*	*pn distribution. %*	*pn distribution % cum.*
RC-1	0.07	0.07	53.88	53.88
RC-2	0.03	0.05	25.85	79.72
RC-3-5	0.01	0.03	20.28	100.00
C3	*pn content g/t*	*pn content g/t cum.*	*pn distribution. %*	*pn distribution % cum.*
RC-1	0.09	0.09	48.53	48.53
RC-2	0.06	0.07	39.04	87.57
RC-3-5	0.01	0.04	12.43	100.00

Table 9 continued *Pentlandite recovery to three flotation concentrates, assuming a 100% total recovery.*

C4	*pn content g/t*	*pn content g/t cum.*	*pn distribution. %*	*pn distribution % cum.*
RC-1	0.07	0.07	67.38	67.38
RC-2	0.02	0.04	29.76	97.14
RC-3-5	0.00	0.02	2.86	100.00
C5	*pn content g/t*	*pn content g/t cum.*	*pn distribution. %*	*pn distribution % cum.*
RC-1	0.07	0.07	43.14	43.14
RC-2	0.06	0.07	45.59	88.73
RC-3-5	0.01	0.03	11.27	100.00
Comp.	*pn content g/t*	*pn content g/t cum.*	*pn distribution. %*	*pn distribution % cum.*
RC-1	0.77	0.77	53.31	53.31
RC-2	0.45	0.61	31.01	84.33
RC-3-5	0.11	0.35	15.67	100.00

Table 10 *Pyrrhotite recovery to three flotation concentrates, assuming a 100% total recovery.*

A2	*po content g/t*	*po content g/t cum.*	*po distribution. %*	*po distribution % cum.*
RC-1	0.24	0.24	41.80	41.80
RC-2	0.23	0.23	45.77	87.57
RC-3-5	0.04	0.14	12.43	100.00
B2	*po content g/t*	*po content g/t cum.*	*po distribution. %*	*po distribution % cum.*
RC-1	0.07	0.07	31.03	31.03
RC-2	0.10	0.09	60.71	91.74
RC-3-5	0.01	0.05	8.26	100.00
A1	*po content g/t*	*po content g/t cum.*	*po distribution. %*	*po distribution % cum.*
RC-1	0.48	0.48	28.97	28.97
RC-2	0.84	0.62	32.38	61.36
RC-3-5	0.50	0.57	38.64	100.00
B1	*po content g/t*	*po content g/t cum.*	*po distribution. %*	*po distribution % cum.*
RC-1	0.67	0.67	24.36	24.36
RC-2	1.71	1.08	40.20	64.56
RC-3-5	0.72	0.92	35.44	100.00
A3	*po content g/t*	*po content g/t cum.*	*po distribution. %*	*po distribution % cum.*
RC-1	0.36	0.36	14.27	14.27
RC-2	1.26	0.80	48.67	62.93
RC-3-5	0.51	0.66	37.07	100.00
B3	*po content g/t*	*po content g/t cum.*	*po distribution. %*	*po distribution % cum.*
RC-1	0.69	0.69	21.54	21.54
RC-2	1.49	1.11	51.05	72.58
RC-3-5	0.37	0.71	27.42	100.00

Table 10 continued *Pyrrhotite recovery to three flotation concentrates, assuming a 100% total recovery.*

A4	*po content g/t*	*po content g/t cum.*	*po distribution. %*	*po distribution % cum.*
RC-1	0.36	0.36	17.39	17.39
RC-2	0.66	0.52	35.37	52.76
RC-3-5	0.41	0.46	47.24	100.00
B4	*po content g/t*	*po content g/t cum.*	*po distribution. %*	*po distribution % cum.*
RC-1	0.50	0.50	47.12	47.12
RC-2	0.30	0.39	33.10	80.22
RC-3-5	0.06	0.19	19.78	100.00
A5	*po content g/t*	*po content g/t cum.*	*po distribution. %*	*po distribution % cum.*
RC-1	0.02	0.02	23.16	23.16
RC-2	0.03	0.02	45.02	68.18
RC-3-5	0.01	0.02	31.82	100.00
C1	*po content g/t*	*po content g/t cum.*	*po distribution. %*	*po distribution % cum.*
RC-1	0.01	0.01	17.41	17.41
RC-2	0.01	0.01	18.87	36.28
RC-3-5	0.02	0.02	63.72	100.00
C2	*po content g/t*	*po content g/t cum.*	*po distribution. %*	*po distribution % cum.*
RC-1	0.02	0.02	29.91	29.91
RC-2	0.02	0.02	36.55	66.46
RC-3-5	0.01	0.01	33.54	100.00
C3	*po content g/t*	*po content g/t cum.*	*po distribution. %*	*po distribution % cum.*
RC-1	0.01	0.01	11.95	11.95
RC-2	0.02	0.02	53.86	65.81
RC-3-5	0.01	0.01	34.19	100.00
C5	*po content g/t*	*po content g/t cum.*	*po distribution. %*	*po distribution % cum.*
RC-1	0.01	0.01	33.52	33.52
RC-2	0.01	0.01	66.48	100.00
RC-3-5	0.00	0.00	0.00	100.00
Comp.	*po content g/t*	*po content g/t cum.*	*po distribution. %*	*po distribution % cum.*
RC-1	0.26	0.26	21.80	21.80
RC-2	0.51	0.39	42.33	64.14
RC-3-5	0.20	0.29	35.86	100.00

Table 11 *Pyrite recovery to three flotation concentrates, assuming a 100% total recovery.*

A2	*py content g/t*	*py content g/t cum.*	*py distribution. %*	*py distribution % cum.*
RC-1	0.21	0.21	79.14	79.14
RC-2	0.04	0.12	16.87	96.01
RC-3-5	0.01	0.07	3.99	100.00

Table 11 continued *Pyrite recovery to three flotation concentrates, assuming a 100% total recovery.*

B2	*py content g/t*	*py content g/t cum.*	*py distribution. %*	*py distribution % cum.*
RC-1	0.51	0.51	66.72	66.72
RC-2	0.18	0.32	33.28	100.00
RC-3-5	0.00	0.16	0.00	100.00
A1	*py content g/t*	*py content g/t cum.*	*py distribution. %*	*py distribution % cum.*
RC-1	0.22	0.22	72.87	72.87
RC-2	0.05	0.15	10.38	83.25
RC-3-5	0.04	0.10	16.75	100.00
B1	*py content g/t*	*py content g/t cum.*	*py distribution. %*	*py distribution % cum.*
RC-1	0.00	0.00	7.71	7.71
RC-2	0.00	0.00	9.20	16.91
RC-3-5	0.01	0.01	83.09	100.00
A3	*py content g/t*	*py content g/t cum.*	*py distribution. %*	*py distribution % cum.*
RC-1	0.54	0.54	78.71	78.71
RC-2	0.10	0.32	14.92	93.63
RC-3-5	0.02	0.18	6.37	100.00
B3	*py content g/t*	*py content g/t cum.*	*py distribution. %*	*py distribution % cum.*
RC-1	0.05	0.05	51.28	51.28
RC-2	0.03	0.04	31.84	83.12
RC-3-5	0.01	0.02	16.88	100.00
A4	*py content g/t*	*py content g/t cum.*	*py distribution. %*	*py distribution % cum.*
RC-1	0.06	0.06	40.74	40.74
RC-2	0.02	0.04	13.56	54.30
RC-3-5	0.03	0.03	45.70	100.00
B4	*py content g/t*	*py content g/t cum.*	*py distribution. %*	*py distribution % cum.*
RC-1	0.04	0.04	89.52	89.52
RC-2	0.00	0.02	8.18	97.70
RC-3-5	0.00	0.01	2.30	100.00
A5	*py content g/t*	*py content g/t cum.*	*py distribution. %*	*py distribution % cum.*
RC-1	0.01	0.01	26.88	26.88
RC-2	0.02	0.01	71.34	98.22
RC-3-5	0.00	0.01	1.78	100.00
C1	*py content g/t*	*py content g/t cum.*	*py distribution. %*	*py distribution % cum.*
RC-1	0.23	0.23	58.45	58.45
RC-2	0.06	0.14	17.78	76.23
RC-3-5	0.03	0.08	23.77	100.00

Table 11 continued *Pyrite recovery to three flotation concentrates, assuming a 100% total recovery*

C2	*py content g/t*	*py content g/t cum.*	*py distribution. %*	*py distribution % cum.*
RC-1	1.04	1.04	74.84	74.84
RC-2	0.24	0.61	20.50	95.34
RC-3-5	0.02	0.28	4.66	100.00
C3	*py content g/t*	*py content g/t cum.*	*py distribution. %*	*py distribution % cum.*
RC-1	0.22	0.22	65.81	65.81
RC-2	0.09	0.15	32.29	98.10
RC-3-5	0.00	0.07	1.90	100.00
C4	*py content g/t*	*py content g/t cum.*	*py distribution. %*	*py distribution % cum.*
RC-1	0.67	0.67	76.95	76.95
RC-2	0.13	0.36	19.70	96.64
RC-3-5	0.01	0.18	3.36	100.00
C5	*py content g/t*	*py content g/t cum.*	*py distribution. %*	*py distribution % cum.*
RC-1	0.38	0.38	74.18	74.18
RC-2	0.09	0.21	21.80	95.97
RC-3-5	0.01	0.09	4.03	100.00
Comp	*py content g/t*	*py content g/t cum.*	*py distribution. %*	*py distribution % cum.*
RC-1	0.30	0.30	74.18	74.18
RC-2	0.08	0.19	18.68	92.86
RC-3-5	0.01	0.10	7.14	100.00

Table 12 *Millerite recovery to three flotation concentrates, assuming a 100% total recovery*

B2	*mil content g/t*	*mil content g/t cum.*	*mil distribution. %*	*mil distribution % cum.*
RC-1	0.05	0.05	48.59	48.59
RC-2	0.04	0.04	51.41	100.00
RC-3-5	0.00	0.02	0.00	100.00
C1	*mil content g/t*	*mil content g/t cum.*	*mil distribution. %*	*mil distribution % cum.*
RC-1	0.32	0.32	58.02	58.02
RC-2	0.12	0.21	25.84	83.86
RC-3-5	0.03	0.11	16.14	100.00
C2	*mil content g/t*	*mil content g/t cum.*	*mil distribution. %*	*mil distribution % cum.*
RC-1	0.48	0.48	60.21	60.21
RC-2	0.20	0.33	28.76	88.97
RC-3-5	0.03	0.16	11.03	100.00
C3	*mil content g/t*	*mil content g/t cum.*	*mil distribution. %*	*mil distribution % cum.*
RC-1	0.17	0.17	40.03	40.03
RC-2	0.08	0.12	20.72	60.75
RC-3-5	0.06	0.09	39.25	100.00

Table 12 continued *Millerite recovery to three flotation concentrates, assuming a 100% total recovery*

C4	*mil content g/t*	*mil content g/t cum.*	*mil distribution. %*	*mil distribution % cum.*
RC-1	0.24	0.24	66.92	66.92
RC-2	0.07	0.14	25.16	92.08
RC-3-5	0.01	0.07	7.92	100.00
C5	*mil content g/t*	*mil content g/t cum.*	*mil distribution. %*	*mil distribution % cum.*
RC-1	0.41	0.41	60.53	60.53
RC-2	0.17	0.28	31.63	92.16
RC-3-5	0.02	0.12	7.84	100.00
Comp.	*mil content g/t*	*mil content g/t cum.*	*mil distribution. %*	*mil distribution % cum.*
RC-1	0.28	0.28	62.83	62.83
RC-2	0.11	0.20	25.01	87.84
RC-3-5	0.03	0.11	12.16	100.00

Table 13 *Relative proportions of* ***liberated*** *grains of different PGE minerals in flotation concentrates of samples A1, A3, A4, B4, A5, C1 and C2.*

A1	*RC1 (235)*		*RC2 (271)*		*RC3-5 (143)*	
	% no.	*area %*	*% no.*	*area %*	*% no.*	*area %*
Pt,Pd,S	40	37	27	30	22	20
Pt,S	27	18	29	17	32	23
Pt,Rh,Cu,Ni,S	15	28	16	19	7	9
Ru,Os, Ir,S	9	7	13	22	13	21
PGE,Bi,Te	1	0	4	3	3	2
PGE,As,S	0	0	3	2	2	1
Pt,Pd,Rh,Fe	4	3	6	5	14	19
Pd,Pb,Sb,Hg	3	6	2	3	7	3
A3	*RC1 (175)*		*RC2 (113)*		*RC3-5 (165)*	
	% no.	*area %*	*% no.*	*area %*	*% no.*	*area %*
Pt,Pd,S	17	18	12	16	9	9
Pt,S	33	14	44	38	36	24
Pt,Rh,Cu,Ni,S	29	39	23	22	23	24
Ru,Os, Ir,S	10	15	7	16	12	18
PGE,Bi,Te	3	12	3	2	4	4
PGE,As,S	3	1	2	1	8	8
Pt,Pd,Rh,Fe	1	0	4	1	2	3
Pd,Pb,Sb,Hg	3	1	4	3	7	10
A4	*RC1 (118)*		*RC2 (70)*		*RC3-5 (102)*	
	% no.	*area %*	*% no.*	*area %*	*% no.*	*area %*
Pt,Pd,S	3	1	7	5	3	5
Pt,S	14	6	11	8	9	8
Pt,Rh,Cu,Ni,S	0	0	6	4	3	1
Ru,Os, Ir,S	16	42	17	29	17	30
PGE,Bi,Te	7	6	4	1	13	11
PGE,As,S	2	1	0	0	0	0
Pt,Pd,Rh,Fe	46	36	49	49	43	35
Pd,Pb,Sb,Hg	13	8	6	3	12	9
B4	*RC1 (167)*		*RC2 (161)*		*RC3-5 (185)*	
	% no.	*area %*	*% no.*	*area %*	*% no.*	*area %*
Pt,Pd,S	4	3	10	6	8	4
Pt,S	4	3	6	6	8	4
Pt,Rh,Cu,Ni,S	2	1	3	2	2	1
Ru,Os, Ir,S	25	36	25	40	22	41
PGE,Bi,Te	7	3	6	3	8	5
PGE,As,S	2	0	0	0	2	2
Pt,Pd,Rh,Fe	51	50	47	41	45	40
Pd,Pb,Sb,Hg	4	3	4	2	4	3
A5	*RC1 (121)*		*RC2 (114)*		*RC3-5 (38)*	
	% no.	*area %*	*% no.*	*area %*	*% no.*	*area %*
Pt,Pd,S	8	5	4	3	8	17
Pt,S	6	3	5	4	3	14
Pt,Rh,Cu,Ni,S	9	5	9	8	5	5
Ru,Os, Ir,S	20	39	16	34	24	29
PGE,Bi,Te	1	0	1	0	3	2
PGE,As,S	10	3	17	15	13	4
Pt,Pd,Rh,Fe	11	7	13	10	21	13
Pd,Pb,Sb,Hg	36	38	35	25	24	17

Table 13 continued *Relative proportions of* ***liberated*** *grains of different PGE minerals in flotation concentrates of samples A1, A3, A4, B4, A5, C1 and C2.*

C1	*RC1 (235)*		*RC2 (118)*		*RC3-5 (134)*	
	% no.	*area %*	*% no.*	*area %*	*% no.*	*area %*
Pt,Pd,S	47	63	38	37	33	26
Pt,S	5	6	9	4	7	4
Pt,Rh,Cu,Ni,S	28	17	36	38	31	35
Ru,Os, Ir,S	14	13	6	14	17	28
PGE,Bi,Te	1	0	3	1	2	1
PGE,As,S	1	0	5	3	6	3
Pt,Pd,Rh,Fe	0	0	1	1	0	0
Pd,Pb,Sb,Hg	3	1	3	1	4	3
C2	*RC1 (229)*		*RC2 (230)*		*RC3-5 (169)*	
	% no.	*area %*	*% no.*	*area %*	*% no.*	*area %*
Pt,Pd,S	41	48	36	31	30	23
Pt,S	7	5	5	1	5	5
Pt,Rh,Cu,Ni,S	39	38	44	45	35	26
Ru,Os, Ir,S	7	7	11	20	18	36
PGE,Bi,Te	1	1	1	0	0	0
PGE,As,S	2	0	4	2	10	9
Pt,Pd,Rh,Fe	0	0	0	0	0	0
Pd,Pb,Sb,Hg	4	1	0	0	3	0

APPENDIX I

Milling data

Table 1 *Milling data for fourteen samples of UG2 chromitite.*

Table 2 *Screen analysis of fourteen samples of UG2 chromitite milled to 80% <75μm.*

Table 1 *Milling data, % Cr2O3 and median measured chromite equivalent circle diameter (ECD) of chromite for fourteen samples of UG2 chromitite.*

Sample	***A1***		***A2***		***A3***		***B1***		***B2***		***C1***		***C2***	
	Time	*% <75*	*Time*	*% <75*	*Time*	*% <75*	*Time*	*% <75*	*Time*	*% <75*	*Time*	*% <75*	*Time*	*% <75*
Milling data	0	12.4	0	23.15	0	10.25	0	11.03	0	13.76	0	6.77	0	5.18
	36	36.41	30	42.61	30	34.92	35	47.35	30	55.94	30	35.41	30	50.65
	75	58.37	60	61.52	90	71.22	70	77.06	65	74.45	45	47.68	60	68.45
	120	81.14	95	80.35	105	79.55	75	82.34	72	79.5	61	81.7	72	80.29
	135	87.3												

Sample	***C3***		***C4***		***C5***		***A4***		***A5***		***B3***		***B4***	
	Time	*% <75*	*Time*	*% <75*	*Time*	*% <75*	*Time*	*% <75*	*Time*	*% <75*	*Time*	*% <75*	*Time*	*% <75*
Milling data	0	11.51	0	9.9	0	10.27	0	4.84	0	15.19	0	7.81	0	5.14
	30	65.59	30	35.11	30	44.96	60	65.48	30	71.91	40	50.05	60	70.77
	60	71.7	60	58.69	60	66.26	72	74.11	40	81	72	69.37	72	80.14
	70	80.61	95	79.25	75	80.76	80	80.02			82	75.22		
											90	80.29		

Table 2 *Screen analysis of fourteen samples of UG2 chromitite milled to 80% <75μm.*

mass %														
Screen fraction	**A2**	**B2**	**A1**	**B1**	**B3**	**A3**	**B4**	**A4**	**A5**	**C1**	**C2**	**C3**	**C4**	**C5**
-38μm	41.59	46.87	47.91	44.66	49.22	42.21	46.06	48.65	48.62	44.01	46.41	46.48	49.50	45.97
+38μm	12.09	11.88	12.05	11.38	11.62	18.48	11.17	11.57	9.65	11.02	11.47	11.17	13.10	10.94
+53μm	23.58	21.45	21.98	20.27	19.11	18.32	21.63	17.23	16.61	19.13	20.83	19.86	20.77	20.18
+75μm	21.08	18.03	16.92	19.95	17.16	19.23	18.26	19.23	17.71	19.70	18.30	18.77	14.11	19.80
+106μm	1.65	1.77	1.13	3.60	2.78	1.33	2.84	3.31	6.04	5.46	2.72	3.71	2.22	3.09
+150μm	0.00	0.00	0.02	0.14	0.11	0.17	0.05	0.01	1.29	0.68	0.12	0.02	0.20	0.03
+212μm	0.00	0.00	0.00	0.00	0.00	0.08	0.00	0.00	0.09	0.00	0.08	0.00	0.00	0.00
+300μm	0.00	0.00	0.00	0.00	0.00	0.17	0.00	0.00	0.00	0.00	0.07	0.00	0.10	0.00
cumulative mass %														
Screen fraction	**A2**	**B2**	**A1**	**B1**	**B3**	**A3**	**B4**	**A4**	**A5**	**C1**	**C2**	**C3**	**C4**	**C5**
-38μm	41.59	46.87	47.91	44.66	49.22	42.21	46.06	48.65	48.62	44.01	46.41	46.48	49.50	45.97
+38μm	53.68	58.75	59.96	56.04	60.84	60.70	57.22	60.22	58.27	55.03	57.89	57.65	62.60	56.91
+53μm	77.27	80.20	81.93	76.31	79.95	79.02	78.85	77.45	74.88	74.16	78.72	77.51	83.37	77.09
+75μm	98.35	98.23	98.86	96.26	97.10	98.25	97.11	96.68	92.59	93.86	97.01	96.27	97.48	96.88
+106μm	100.00	100.00	99.98	99.86	99.89	99.58	99.95	99.99	98.62	99.32	99.73	99.98	99.70	99.97
+150μm	100.00	100.00	100.00	100.00	100.00	99.75	100.00	100.00	99.91	100.00	99.85	100.00	99.90	100.00
+212μm	100.00	100.00	100.00	100.00	100.00	99.83	100.00	100.00	100.00	100.00	99.93	100.00	99.90	100.00
+300μm	100.00	100.00	100.00	100.00	100.00	100.00	100.00	100.00	100.00	100.00	100.00	100.00	100.00	100.00

APPENDIX J

Flotation data

The following notation was used in all of the tables:

RC1=Rougher concentrate 1 (1 minute flotation)

RC2=Rougher concentrate 2 (3 minutes flotation)

RC3=Rougher concentrate 3 (8 minutes flotation)

RC4=Rougher concentrate 4 (15 minutes flotation)

RC5=Rougher concentrate 5 (20 minutes flotation)

RC3-5=combined rougher concentrates 3, 4 and 5 (8 to 20 minutes flotation)

RT=Rougher tailings

Table 1 *Mass recoveries for fourteen UG2 chromitite samples milled to 80% <75μm.*

Table 2 *Cr_2O_3 recoveries from fourteen UG2 chromitite samples milled to 80%<75μm.*

Table 3 *Silicate gangue recoveries from fourteen UG2 chromitite samples milled to 80%<75μm.*

Table 4 *Cu recoveries from fourteen test samples milled to 80%<75μm.*

Table 5 *Kelsall flotation constants for Cu recoveries from fourteen samples of UG2 chromitite milled to 80% <75μm.*

Table 6 *Acid soluble Ni recoveries from fourteen test samples milled to 80%<75μm.*

Table 7 *Kelsall flotation constants for acid soluble Ni recoveries from fourteen samples of UG2 chromitite milled to 80% <75μm.*

Table 8 *PGE+Au recoveries from fourteen samples of UG2 chromitite milled to 80% <75μm.*

Table 9 *Kelsall flotation constants for PGE+Au recoveries from fourteen samples of UG2 chromitite milled to 80% <75μm.*

Table 10 *Platinum recoveries from fourteen samples of UG2 chromitite milled to 80% <75μm.*

Table 11 *Kelsall flotation constants for platinum recoveries from fourteen samples of UG2 chromitite milled to 80% <75μm.*

Table 1 *Mass recoveries for fourteen UG2 chromitite samples milled to 80% <75μm. Confidence limits for cumulative recoveries were calculated at the 95% confidence level.*

A2	**0-1 min. RC1**	**1-3 min. RC2**	**3-8 min. RC3**	**8-15 min. RC4**	**15-20 min. RC5**	**RT**
Dry (g)	158.5	180.1	171.1	84.9	29.6	5367.6
Cum. Dry (g)	158.5	338.6	509.7	594.6	624.2	5991.8
Dry (%)	2.6	3.0	2.9	1.4	0.5	89.6
Cum. Dry (%)	2.6± 0.3	5.7± 0.4	8.5± 0.5	9.9± 0.5	10.4± 0.5	100.0
B2	**0-1 min. RC1**	**1-3 min. RC2**	**3-8 min. RC3**	**8-15 min. RC4**	**15-20 min. RC5**	**RT**
Dry (g)	160.1	225.9	229.1	106.7	38.4	5241.3
Cum. Dry (g)	160.1	386.0	615.1	721.8	760.2	6001.5
Dry (%)	2.7	3.8	3.8	1.8	0.6	87.3
Cum. Dry (%)	2.7± 0.3	6.4± 0.6	10.2± 0.7	12.0± 0.7	12.7± 0.8	100.0
A1	**0-1 min. RC1**	**1-3 min. RC2**	**3-8 min. RC3**	**8-15 min. RC4**	**15-20 min. RC5**	**RT**
Dry (g)	673.4	431.8	487.2	281.1	103.5	16004.9
Cum. Dry (g)	673.4	1105.2	1592.4	1873.5	1977.0	17981.9
Dry (%)	3.7	2.4	2.7	1.6	0.6	89.0
Cum. Dry (%)	3.7±0.3	6.1± 0.4	8.9± 0.5	10.4± 0.5	11.0± 0.5	100.0
B1	**0-1 min. RC1**	**1-3 min. RC2**	**3-8 min. RC3**	**8-15 min. RC4**	**15-20 min. RC5**	**RT**
Dry (g)	218.0	141.2	163.1	97.3	32.5	5339.6
Cum. Dry (g)	218.0	359.2	522.3	619.6	652.1	5991.7
Dry (%)	3.6	2.4	2.7	1.6	0.5	89.1
Cum. Dry (%)	3.6± 0.4	6.0± 0.6	8.7± 0.7	10.3± 0.8	10.9± 0.8	100.0
A3	**0-1 min. RC1**	**1-3 min. RC2**	**3-8 min. RC3**	**8-15 min. RC4**	**15-20 min. RC5**	**RT**
Dry (g)	179.7	174.0	192.1	100.8	37.0	5309.6
Cum. Dry (g)	179.7	353.7	545.8	646.6	683.6	5993.2
Dry (%)	3.0	2.9	3.2	1.7	0.6	88.6
Cum. Dry (%)	3.0± 0.6	5.9± 0.8	9.1± 0.9	10.8± 1.0	11.4± 1.0	100.0
B3	**0-1 min. RC1**	**1-3 min. RC2**	**3-8 min. RC3**	**8-15 min. RC4**	**15-20 min. RC5**	**RT**
Dry (g)	139.0	165.2	229.7	164.9	66.5	5215.2
Cum. Dry (g)	139.0	304.2	533.9	698.8	765.3	5980.5
Dry (%)	2.3	2.8	3.8	2.8	1.1	87.2
Cum. Dry (%)	2.3± 0.1	5.1± 0.2	8.9± 0.2	11.7± 0.2	12.8± 0.2	100.0

Table 1 cont. *Mass recoveries for fourteen UG2 chromitite samples milled to 80% <75μm. . Confidence limits for cumulative recoveries were calculated at the 95% confidence level.*

A4	0-1 min. RC1	1-3 min. RC2	3-8 min. RC3	8-15 min. RC4	15-20 min. RC5	RT
Dry (g)	135.3	152.7	179.2	105.0	40.4	5362.1
Cum. Dry (g)	135.3	288.0	467.2	572.2	612.6	5974.7
Dry (%)	2.3	2.6	3.0	1.8	0.7	89.7
Cum. Dry (%)	2.3± 0.1	4.8± 0.2	7.8± 0.2	9.6± 0.4	10.3± 0.4	100.0
B4	**0-1 min. RC1**	**1-3 min. RC2**	**3-8 min. RC3**	**8-15 min. RC4**	**15-20 min. RC5**	**RT**
Dry (g)	141.7	154.4	175.7	112.6	47.5	5356.1
Cum. Dry (g)	141.7	296.1	471.8	584.4	631.9	5988.0
Dry (%)	2.4	2.6	2.9	1.9	0.8	89.4
Cum. Dry (%)	2.4± 0.3	4.9± 0.6	7.9± 0.8	9.8± 0.8	10.6± 0.7	100.0
A5	**0-1 min. RC1**	**1-3 min. RC2**	**3-8 min. RC3**	**8-15 min. RC4**	**15-20 min. RC5**	**RT**
Dry (g)	173.5	179.0	202.9	127.2	53.3	5242.0
Cum. Dry (g)	173.5	352.5	555.4	682.6	735.9	5977.9
Dry (%)	2.9	3.0	3.4	2.1	0.9	87.7
Cum. Dry (%)	2.9± 0.2	5.9± 0.2	9.3± 0.2	11.4± 0.3	12.3± 0.3	100.0
C1	**0-1 min. RC1**	**1-3 min. RC2**	**3-8 min. RC3**	**8-15 min. RC4**	**15-20 min. RC5**	**RT**
Dry (g)	137.9	166.0	209.0	135.1	50.0	5281.8
Cum. Dry (g)	137.9	303.9	512.9	648.0	698.0	5979.8
Dry (%)	2.3	2.8	3.5	2.3	0.8	88.3
Cum. Dry (%)	2.3± 0.2	5.1± 0.3	8.6± 0.3	10.8± 0.4	11.7± 0.3	100.0± 0.2
C2	**0-1 min. RC1**	**1-3 min. RC2**	**3-8 min. RC3**	**8-15 min. RC4**	**15-20 min. RC5**	**RT**
Dry (g)	170.7	200.6	243.8	169.7	70.6	5215.9
Cum. Dry (g)	170.7	371.3	615.1	784.8	855.4	6071.3
Dry (%)	2.8	3.3	4.0	2.8	1.2	85.9
Cum. Dry (%)	2.8± 0.1	6.1± 0.3	10.1± 0.3	12.9± 0.3	14.1± 0.3	100.0
C3	**0-1 min. RC1**	**1-3 min. RC2**	**3-8 min. RC3**	**8-15 min. RC4**	**15-20 min. RC5**	**RT**
Dry (g)	146.8	168.5	195.4	133.9	61.9	5319.8
Cum. Dry (g)	146.8	315.3	510.7	644.6	706.5	6026.3
Dry (%)	2.4	2.8	3.2	2.2	1.0	88.3
Cum. Dry (%)	2.4± 0.2	5.2± 0.3	8.5± 0.5	10.7± 0.5	11.7± 0.6	100.0

Table 1 cont. *Mass recoveries for fourteen UG2 chromitite samples milled to 80% <75µm. Confidence limits for cumulative recoveries were calculated at the 95% confidence level.*

C4	0-1 min. RC1	1-3 min. RC2	3-8 min. RC3	8-15 min. RC4	15-20 min. RC5	RT
Dry (g)	180.4	237.0	259.3	148.1	57.6	5108.5
Cum. Dry (g)	180.4	417.4	676.7	824.8	882.4	5990.9
Dry (%)	3.0	4.0	4.3	2.5	1.0	85.3
Cum. Dry (%)	3.0± 0.1	7.0± 0.1	11.3± 0.3	13.8± 0.4	14.7± 0.5	100.0
C5	**0-1 min. RC1**	**1-3 min. RC2**	**3-8 min. RC3**	**8-15 min. RC4**	**15-20 min. RC5**	**RT**
Dry (g)	119.1	151.5	201.8	137.4	58.1	5318.3
Cum. Dry (g)	119.1	270.6	472.4	609.8	667.9	5986.2
Dry (%)	2.0	2.5	3.4	2.3	1.0	88.8
Cum. Dry (%)	2.0± 0.1	4.5± 0.2	7.9± 0.2	10.2± 0.2	11.2± 0.3	100.0

Table 2 *Cr_2O_3 recovery from fourteen UG2 chromitite samples milled to 80% <75µm.*

A2	Cr_2O_3 content %	Cr_2O_3 content cum. %	Cr_2O_3 distr. %	Cr_2O_3 distr. cum. %	Chromite mass %
RC1	18.7	18.7	1.7	1.7	40
RC2	19.4	19.1	2.0	3.7	41
RC3	19.3	19.2	1.9	5.6	41
RC4	19.5	19.2	1.0	6.5	41
RC5	19.3	19.2	0.3	6.8	41
RT	30.4	29.2	93.2	100.0	65

Cr_2O_3 calculated = 29.2% Cr_2O_3 assay = 29.1% Difference = 0.1% (%Difference = 0%)

B2	Cr_2O_3 content %	Cr_2O_3 content cum. %	Cr_2O_3 distr. %	Cr_2O_3 distr. cum. %	Chromite mass %
RC1	12.2	12.2	1.6	1.6	26
RC2	12.8	12.6	2.3	3.9	27
RC3	12.8	12.6	2.4	6.3	27
RC4	12.9	12.7	1.1	7.4	27
RC5	12.6	12.7	0.4	7.8	27
RT	21.8	20.6	92.2	100.0	46

Cr_2O_3 calculated = 20.6% Cr_2O_3 assay = 20.9% Difference = 0.3% (%Difference = 1%)

A1	Cr_2O_3 content %	Cr_2O_3 content cum. %	Cr_2O_3 distr. %	Cr_2O_3 distr. cum. %	Chromite mass %
RC1	21.9	21.9	2.8	2.8	47
RC2	21.8	21.9	1.8	4.5	46
RC3	22.6	22.1	2.1	6.6	48
RC4	22.6	22.2	1.2	7.8	48
RC5	22.4	22.2	0.4	8.2	48
RT	30.5	29.6	91.8	100.0	65

Cr_2O_3 calculated = 29.6% Cr_2O_3 assay = 29.3% Difference = 0.6% (%Difference = 1%)

B1	Cr_2O_3 content %	Cr_2O_3 content cum. %	Cr_2O_3 distr. %	Cr_2O_3 distr. cum. %	Chromite mass %
RC1	13.2	13.2	1.9	1.9	28
RC2	14.3	13.6	1.3	3.2	30
RC3	14.5	13.9	1.5	4.7	31
RC4	14.6	14.0	0.9	5.6	31
RC5	14.5	14.0	0.3	5.9	31
RT	27.2	25.8	94.1	100.0	58

Cr_2O_3 calculated = 25.8% Cr_2O_3 assay = 25.1% Difference = 0.7% (%Difference = 3%)

Table 2 cont. *Cr_2O_3 recovery from fourteen UG2 chromitite samples milled to 80% <75µm.*

A3	Cr_2O_3 content %	Cr_2O_3 content cum. %	Cr_2O_3 distr. %	Cr_2O_3 distr. cum. %	Chromite mass %
RC1	24.9	24.9	2.2	2.2	53
RC2	25.8	25.3	2.2	4.4	55
RC3	25.6	25.4	2.4	6.8	54
RC4	25.8	25.5	1.3	8.1	55
RC5	25.5	25.5	0.5	8.6	54
RT	35.0	33.9	91.4	100.0	74

Cr_2O_3 calculated = 33.9% Cr_2O_3 assay = 33.8% Difference = 0.1% (%Difference = 0%)

B3	Cr_2O_3 content %	Cr_2O_3 content cum. %	Cr_2O_3 distr. %	Cr_2O_3 distr. cum. %	Chromite mass %
RC-1	20.1	20.1	1.5	1.5	43
RC-2	20.4	20.3	1.7	3.3	43
RC-3	20.6	20.4	2.0	5.2	44
RC-4	20.1	20.3	1.2	6.4	43
RC-5	20.4	20.3	0.5	7.0	43
RT	32.1	30.9	93.1	100.0	68

Cr_2O_3 calculated = 30.9% Cr_2O_3 assay = 30.7% Difference = 0.2% (%Difference = 1%)

A4	Cr_2O_3 content %	Cr_2O_3 content cum. %	Cr_2O_3 distr. %	Cr_2O_3 distr. cum. %	Chromite mass %
RC1	25.1	25.1	1.6	1.6	53
RC2	25.4	25.3	1.9	3.5	54
RC3	25.8	25.5	2.2	5.7	55
RC4	26.0	25.6	1.3	7.0	55
RC5	26.7	25.6	0.5	7.5	57
RT	35.9	34.9	92.5	100.0	76

Cr_2O_3 calculated = 34.9% Cr_2O_3 assay = 34.5% Difference = 0.4% (%Difference = 1%)

B4	Cr_2O_3 content %	Cr_2O_3 content cum. %	Cr_2O_3 distr. %	Cr_2O_3 distr. cum. %	Chromite mass %
RC1	23.0	23.0	1.6	1.6	49
RC2	24.2	23.7	2.0	3.7	51
RC3	24.4	24.0	2.8	6.5	52
RC4	24.4	24.1	2.0	8.5	52
RC5	24.8	24.1	0.8	9.4	53
RT	34.3	33.0	90.6	100.0	73

Cr_2O_3 calculated = 33.0% Cr_2O_3 assay = 32.9% Difference = 0.1% (%Difference = 0%)

A5	Cr_2O_3 content %	Cr_2O_3 content cum. %	Cr_2O_3 distr. %	Cr_2O_3 distr. cum. %	Chromite mass %
RC1	16.9	16.9	1.8	1.8	36
RC2	17.8	17.4	1.9	3.7	38
RC3	18.7	17.9	2.3	5.9	40
RC4	19.3	18.1	1.5	7.4	41
RC5	20.0	18.3	0.6	8.0	43
RT	29.5	28.1	92.0	100.0	63

Cr_2O_3 calculated = 28.1% Cr_2O_3 assay = 27.7% Difference = 0.4% (%Difference = 1%)

Table 2 cont. *Cr_2O_3 recovery from fourteen UG2 chromitite samples milled to 80% <75µm.*

C1	Cr_2O_3 content %	Cr_2O_3 content cum. %	Cr_2O_3 distr. %	Cr_2O_3 distr. cum. %	Chromite mass %
RC1	15.8	15.8	1.1	1.1	34
RC2	17.6	16.8	1.4	2.5	37
RC3	19.4	17.9	2.0	4.4	41
RC4	21.4	18.6	1.4	5.8	45
RC5	22.0	18.8	0.5	6.4	47
RT	36.7	34.6	93.7	100.0	78

Cr_2O_3 calculated = 34.6% Cr_2O_3 assay = 34.6% Difference = 0.0% (%Difference = 0%)

C2	Cr_2O_3 content %	Cr_2O_3 content cum. %	Cr_2O_3 distr. %	Cr_2O_3 distr. cum. %	Chromite mass %
RC1	16.3	16.3	1.5	1.5	35
RC2	17.1	16.7	1.8	3.3	36
RC3	17.9	17.2	2.3	5.6	38
RC4	19.1	17.6	1.7	7.3	41
RC5	19.3	17.7	0.7	8.0	41
RT	33.5	31.3	92.0	100.0	71

Cr_2O_3 calculated = 31.3% Cr_2O_3 assay = 31.8% Difference = 0.5% (%Difference = 2%)

C3	Cr_2O_3 content %	Cr_2O_3 content cum. %	Cr_2O_3 distr. %	Cr_2O_3 distr. cum. %	Chromite mass %
RC1	14.1	14.1	1.1	1.1	30
RC2	14.8	14.5	1.2	2.3	31
RC3	15.8	15.0	1.6	3.9	34
RC4	17.3	15.5	1.2	5.1	37
RC5	17.8	15.7	0.6	5.7	38
RT	34.7	32.5	94.4	100.0	74

Cr_2O_3 calculated = 32.5% Cr_2O_3 assay = 32.4% Difference = 0.1% (%Difference = 0%)

C4	Cr_2O_3 content %	Cr_2O_3 content cum. %	Cr_2O_3 distr. %	Cr_2O_3 distr. cum. %	Chromite mass %
RC1	17.2	17.2	2.0	2.0	37
RC2	17.7	17.4	1.3	3.3	38
RC3	18.2	17.7	1.6	4.9	39
RC4	19.0	17.9	1.0	5.8	40
RC5	18.8	17.9	0.3	6.2	40
RT	33.3	31.6	93.8	100.0	71

Cr_2O_3 calculated = 31.6% Cr_2O_3 assay = 31.2% Difference = 0.4% (%Difference = 1%)

C5	Cr_2O_3 content %	Cr_2O_3 content cum. %	Cr_2O_3 distr. %	Cr_2O_3 distr. cum. %	Chromite mass %
RC1	20.7	20.7	1.2	1.2	44
RC2	21.6	21.2	1.6	2.8	46
RC3	22.0	21.5	2.2	5.0	47
RC4	22.8	21.8	1.6	6.6	48
RC5	22.8	21.9	0.7	7.3	48
RT	35.2	33.7	92.8	100.0	75

Cr_2O_3 calculated = 33.7% Cr_2O_3 assay = 33.8% Difference = 0.1% (%Difference = 0%)

Table 3 *Silicate gangue recoveries from fourteen UG2 chromitite samples at a grind of 80% <75μm.*

A1	*Silicate content g*	*Silicate content cum. g*	*Silicate distr. %*	*Silicate distr. cum. %*
RC1	119.9	119.9	5.4	5.4
RC2	77.3	197.2	3.5	8.9
RC3	84.4	281.6	3.8	12.7
RC4	48.7	330.3	2.2	14.9
RC5	18.1	348.4	0.8	15.7
RT	1873.0	2221.4	84.3	100.0

A2	*Silicate content g*	*Silicate content cum. g*	*Silicate distr. %*	*Silicate distr. cum. %*
RC1	95.5	95.5	4.2	4.2
RC2	105.8	201.3	4.7	8.9
RC3	100.9	302.2	4.4	13.3
RC4	49.7	352.0	2.2	15.5
RC5	17.5	369.4	0.8	16.3
RT	1899.3	2268.7	83.7	100.0

B1	*Silicate content g*	*Silicate content cum. g*	*Silicate distr. %*	*Silicate distr. cum. %*
RC1	156.8	156.8	5.8	5.8
RC2	98.3	255.1	3.6	9.4
RC3	112.8	368.0	4.2	13.6
RC4	67.1	435.1	2.5	16.1
RC5	22.5	457.5	0.8	16.9
RT	2252.6	2710.1	83.1	100.0

B2	*Silicate content g*	*Silicate content cum. g*	*Silicate distr. %*	*Silicate distr. cum. %*
RC1	118.6	118.6	3.5	3.5
RC2	164.4	283.0	4.9	8.4
RC3	166.8	449.8	5.0	13.4
RC4	77.4	527.2	2.3	15.7
RC5	28.1	555.4	0.8	16.5
RT	2812.7	3368.0	83.5	100.0

A3	*Silicate content g*	*Silicate content cum. g*	*Silicate distr. %*	*Silicate distr. cum. %*
RC1	84.6	84.6	5.1	5.1
RC2	78.6	163.2	4.7	9.8
RC3	87.6	250.7	5.2	15.0
RC4	45.5	296.3	2.7	17.7
RC5	16.9	313.2	1.0	18.7
RT	1359.6	1672.9	81.3	100.0

Table 3 cont. *Silicate gangue recoveries from fourteen UG2 chromitite samples at a grind of 80% <75µm.*

A4	*Silicate content g*	*Silicate content cum. g*	*Silicate distr. %*	*Silicate distr. cum. %*
RC1	63.1	63.1	4.1	4.1
RC2	70.3	133.4	4.5	8.6
RC3	80.9	214.3	5.2	13.8
RC4	47.0	261.3	3.0	16.9
RC5	17.5	278.8	1.1	18.0
RT	1270.5	1549.3	82.0	100.0

B3	*Silicate content g*	*Silicate content cum. g*	*Silicate distr. %*	*Silicate distr. cum. %*
RC1	81.2	81.2	3.9	3.9
RC2	87.5	168.6	4.2	8.2
RC3	98.8	267.4	4.8	13.0
RC4	64.5	331.9	3.1	16.1
RC5	26.9	358.8	1.3	17.4
RT	1701.7	2060.5	82.6	100.0

B4	*Silicate content g*	*Silicate content cum. g*	*Silicate distr. %*	*Silicate distr. cum. %*
RC1	71.0	71.0	4.0	4.0
RC2	80.2	151.3	4.5	8.5
RC3	110.6	261.8	6.2	14.7
RC4	79.6	341.4	4.5	19.1
RC5	31.4	372.8	1.8	20.9
RT	1413.1	1785.9	79.1	100.0

A5	*Silicate content g*	*Silicate content cum. g*	*Silicate distr. %*	*Silicate distr. cum. %*
RC1	111.2	111.2	4.6	4.6
RC2	111.3	222.5	4.6	9.2
RC3	122.3	344.7	5.1	14.3
RC4	75.0	419.7	3.1	17.4
RC5	30.6	450.4	1.3	18.7
RT	1960.7	2411.1	81.3	100.0

C1	*Silicate content g*	*Silicate content cum. g*	*Silicate distr. %*	*Silicate distr. cum. %*
RC1	91.6	91.6	5.8	5.8
RC2	103.9	195.5	6.6	12.4
RC3	122.8	318.3	7.8	20.1
RC4	73.6	392.0	4.7	24.8
RC5	26.6	418.6	1.7	26.5
RT	1161.7	1580.3	73.5	100.0

Table 3 cont. *Silicate gangue recoveries from fourteen UG2 chromitite samples at a grind of 80% <75µm.*

C2	*Silicate content g*	*Silicate content cum. g*	*Silicate distr. %*	*Silicate distr. cum. %*
RC1	111.6	111.6	5.5	5.5
RC2	127.7	239.2	6.3	11.8
RC3	151.3	390.6	7.4	19.2
RC4	100.8	491.4	5.0	24.1
RC5	41.6	533.0	2.0	26.2
RT	1501.9	2034.9	73.8	100.0

C3	*Silicate content g*	*Silicate content cum. g*	*Silicate distr. %*	*Silicate distr. cum. %*
RC1	102.8	102.8	5.5	5.5
RC2	115.5	218.3	6.2	11.7
RC3	129.8	348.1	6.9	18.6
RC4	84.8	432.9	4.5	23.2
RC5	38.5	471.4	2.1	25.2
RT	1396.2	1867.5	74.8	100.0

C4	*Silicate content g*	*Silicate content cum. g*	*Silicate distr. %*	*Silicate distr. cum. %*
RC1	138.3	138.3	7.0	7.0
RC2	88.1	226.4	4.5	11.5
RC3	100.0	326.4	5.1	16.6
RC4	58.0	384.4	3.0	19.6
RC5	19.5	403.9	1.0	20.6
RT	1560.3	1964.2	79.4	100.0

C5	*Silicate content g*	*Silicate content cum. g*	*Silicate distr. %*	*Silicate distr. cum. %*
RC1	66.7	66.7	3.9	3.9
RC2	81.9	148.6	4.8	8.8
RC3	107.4	256.1	6.3	15.1
RC4	70.8	326.9	4.2	19.3
RC5	29.9	356.8	1.8	21.0
RT	1339.3	1696.1	79.0	100.0

Table 4 *Cu recoveries from fourteen test samples. Differences between calculated and assayed Cu values for feed material are expressed as relative %.*

A2	*Cu content %*	*Cu content cum. %*	*Cu distribution %*	*Cu distribution cum. %*
RC1	0.130	0.130	56.88	56.88
RC2	0.028	0.076	13.92	70.80
RC3	0.018	0.056	8.50	79.30
RC4	0.016	0.051	3.75	83.05
RC5	0.017	0.049	1.39	84.44
RT	0.001	0.006	15.56	100.00

Cu calculated = 0.006% Cu assay = 0.005% %Difference = 21%

B2	*Cu content %*	*Cu content cum. %*	*Cu distribution %*	*Cu distribution cum. %*
RC1	0.110	0.110	57.85	57.85
RC2	0.015	0.054	11.13	68.98
RC3	0.012	0.039	9.03	78.02
RC4	0.010	0.034	3.51	81.52
RC5	0.010	0.033	1.26	82.78
RT	0.001	0.005	17.22	100.00

Cu calculated = 0.001% Cu assay = 0.004% %Difference = 27%

A1	*Cu content %*	*Cu content cum. %*	*Cu distribution %*	*Cu distribution cum. %*
RC1	0.120	0.12	62.21	62.21
RC2	0.036	0.09	11.88	74.09
RC3	0.020	0.07	7.17	81.26
RC4	0.018	0.06	3.65	84.91
RC5	0.014	0.06	1.16	86.08
RT	0.001	0.007	13.92	100.00

Cu calculated = 0.007% Cu assay = 0.007% %Difference = 5%

B1	*Cu content %*	*Cu content cum. %*	*Cu distribution %*	*Cu distribution cum. %*
RC1	0.220	0.220	75.68	75.68
RC2	0.031	0.146	6.91	82.59
RC3	0.020	0.106	5.15	87.73
RC4	0.019	0.093	2.92	90.65
RC5	0.018	0.089	0.92	91.57
RT	0.001	0.011	8.43	100.00

Cu calculated = 0.011% Cu assay = 0.010% %Difference = 6%

A3	*Cu content %*	*Cu content cum. %*	*Cu distribution %*	*Cu distribution cum. %*
RC1	0.220	0.220	55.79	55.79
RC2	0.058	0.140	14.24	70.03
RC3	0.034	0.103	9.22	79.25
RC4	0.031	0.092	4.41	83.66
RC5	0.026	0.088	1.36	85.01
RT	0.002	0.012	14.99	100.00

Cu calculated = 0.012% Cu assay = 0.011% %Difference = 7%

Table 4 cont. *Cu recoveries from fourteen test samples. Differences between calculated and assayed Cu values for feed material are expressed as relative %.*

B3	*Cu content %*	*Cu content cum. %*	*Cu distribution %*	*Cu distribution cum. %*
RC1	0.279	0.279	67.53	67.53
RC2	0.050	0.160	13.19	80.72
RC3	0.020	0.108	6.00	86.72
RC4	0.016	0.090	3.08	89.80
RC5	0.013	0.084	1.05	90.85
RT	0.001	0.010	9.15	100.00

Cu calculated = 0.010% Cu assay = 0.009% %Difference = 9%

A4	*Cu content %*	*Cu content cum. %*	*Cu distribution %*	*Cu distribution cum. %*
RC1	0.266	0.266	50.85	50.85
RC2	0.082	0.168	17.69	68.55
RC3	0.043	0.120	10.89	79.44
RC4	0.028	0.103	4.15	83.59
RC5	0.022	0.098	1.26	84.85
RT	0.002	0.012	15.15	100.00

Cu calculated = 0.012% Cu assay = 0.011% %Difference = 8%

B4	*Cu content %*	*Cu content cum. %*	*Cu distribution %*	*Cu distribution cum. %*
RC1	0.457	0.457	63.86	63.86
RC2	0.083	0.254	13.80	77.66
RC3	0.041	0.162	9.51	87.17
RC4	0.021	0.129	3.47	90.64
RC5	0.018	0.119	1.23	91.87
RT	0.002	0.017	8.13	100.00

Cu calculated = 0.017% Cu assay = 0.017% %Difference = 2%

A5	*Cu content %*	*Cu content cum. %*	*Cu distribution %*	*Cu distribution cum. %*
RC1	0.090	0.090	52.36	52.36
RC2	0.022	0.055	13.20	65.57
RC3	0.014	0.040	9.53	75.09
RC4	0.013	0.035	5.54	80.64
RC5	0.010	0.033	1.79	82.42
RT	0.001	0.005	17.58	100.00

Cu calculated = 0.005% Cu assay = 0.004% %Difference = 25%

C1	*Cu content %*	*Cu content cum. %*	*Cu distribution %*	*Cu distribution cum. %*
RC1	0.095	0.095	31.48	31.48
RC2	0.027	0.058	10.86	42.34
RC3	0.017	0.041	8.40	50.74
RC4	0.015	0.035	4.74	55.49
RC5	0.015	0.034	1.81	57.30
RT	0.003	0.007	42.70	100.00

Cu calculated = 0.007% Cu assay = 0.006% %Difference = 19%

Table 4 cont. *Cu recoveries from fourteen test samples. Differences between calculated and assayed Cu values for feed material are expressed as relative %.*

C2	*Cu content %*	*Cu content cum. %*	*Cu distribution %*	*Cu distribution cum. %*
RC1	0.076	0.076	34.16	34.16
RC2	0.023	0.047	11.95	46.11
RC3	0.015	0.034	9.36	55.47
RC4	0.013	0.029	5.80	61.26
RC5	0.011	0.028	2.15	63.41
RT	0.003	0.006	36.59	100.00

Cu calculated = 0.006% Cu assay = 0.004% %Difference = 40%

C3	*Cu content %*	*Cu content cum. %*	*Cu distribution %*	*Cu distribution cum. %*
RC1	0.068	0.068	28.30	28.30
RC2	0.023	0.044	11.16	39.46
RC3	0.015	0.033	8.46	47.91
RC4	0.013	0.029	5.11	53.02
RC5	0.013	0.027	2.29	55.31
RT	0.003	0.006	44.69	100.00

Cu calculated = 0.006% Cu assay = 0.005% %Difference = 17%

C4	*Cu content %*	*Cu content cum. %*	*Cu distribution %*	*Cu distribution cum. %*
RC1	0.041	0.041	30.59	30.59
RC2	0.014	0.026	13.91	44.51
RC3	0.010	0.020	10.45	54.96
RC4	0.009	0.018	5.51	60.47
RC5	0.008	0.017	1.91	62.38
RT	0.002	0.004	37.62	100.00

Cu calculated = 0.004% Cu assay = 0.003% %Difference = 38%

C5	*Cu content %*	*Cu content cum. %*	*Cu distribution %*	*Cu distribution cum. %*
RC1	0.088	0.088	38.68	38.68
RC2	0.025	0.053	13.80	52.48
RC3	0.016	0.037	12.14	64.63
RC4	0.011	0.031	5.79	70.42
RC5	0.010	0.030	2.18	72.60
RT	0.001	0.005	27.40	100.00

Cu calculated = 0.005% Cu assay = 0.003% % Difference = 32%

Table 5 ***Kelsall flotation constants for Cu recoveries from fourteen samples of UG2 chromitite milled to 80% <75μm.***

Cu	*U*	ϕ	K_f	K_s	*Loss*
A2	85.6	0.28	2.02	0.18	0.10
B2	83.1	0.31	2.06	0.2	0.12
A1	86.8	0.24	2.24	0.16	0.02
B1	92.3	0.17	3.08	0.15	0.00
A3	85.8	0.30	2.01	0.17	0.03
B3	91.5	0.19	2.07	0.16	0.02
A4	85.2	0.36	1.73	0.21	0.08
B4	92.6	0.24	2.05	0.14	0.01
A5	84.0	0.34	2.04	0.14	0.01
C1	58.7	0.42	1.76	0.14	0.05
C2	65.5	0.43	1.74	0.13	0.03
C3	57.5	0.44	1.57	0.12	0.11
C4	63.7	0.46	1.49	0.15	0.05
C5	73.6	0.47	1.92	0.17	0.19
Avg.	79.0	0.33	1.98	0.16	0.06

Loss = (Observed – Predicted) ^{2}

Table 6 *Acid soluble Ni recoveries from fourteen test samples. Differences between calculated and assayed Ni values for feed material are expressed as relative %.*

A2	*Ni content %*	*Ni content cum. %*	*Ni distribution %*	*Ni distribution cum. %*
RC1	0.320	0.320	28.86	28.86
RC2	0.140	0.224	14.35	43.21
RC3	0.108	0.185	10.52	53.73
RC4	0.101	0.173	4.88	58.61
RC5	0.100	0.170	1.68	60.29
RT	0.013	0.029	39.71	100.00

Ni calculated = 0.029% Ni assay = 0.029% %Difference = 1%

B2	*Ni content %*	*Ni content cum. %*	*Ni distribution %*	*Ni distribution cum. %*
RC1	0.280	0.280	24.56	24.56
RC2	0.089	0.168	11.03	35.60
RC3	0.077	0.134	9.72	45.31
RC4	0.073	0.125	4.29	49.61
RC5	0.075	0.123	1.57	51.18
RT	0.017	0.030	48.82	100.00

Ni calculated = 0.030% Ni assay = 0.030% %Difference = 1%

A1	*Ni content %*	*Ni content cum. %*	*Ni distribution %*	*Ni distribution cum. %*
RC1	0.392	0.392	35.66	35.66
RC2	0.175	0.307	10.16	45.82
RC3	0.120	0.251	7.77	53.59
RC4	0.105	0.229	3.84	57.43
RC5	0.146	0.225	2.07	59.50
RT	0.019	0.042	40.50	100.00

Ni calculated = 0.042% Ni assay = 0.041% %Difference = 2%

B1	*Ni content %*	*Ni content cum. %*	*Ni distribution %*	*Ni distribution cum. %*
RC1	0.405	0.405	21.82	21.82
RC2	0.209	0.328	7.29	29.11
RC3	0.159	0.275	6.39	35.50
RC4	0.160	0.257	3.84	39.33
RC5	0.161	0.252	1.29	40.62
RT	0.045	0.068	59.38	100.00

Ni calculated = 0.068% Ni assay = 0.072% %Difference = 6%

A3	*Ni content %*	*Ni content cum. %*	*Ni distribution %*	*Ni distribution cum. %*
RC1	0.450	0.450	30.24	30.24
RC2	0.200	0.327	12.98	43.23
RC3	0.145	0.263	10.42	53.65
RC4	0.130	0.242	4.90	58.55
RC5	0.126	0.236	1.74	60.28
RT	0.020	0.045	39.72	100.00

Ni calculated = 0.045% Ni assay = 0.044% %Difference = 1%

Table 6 cont. *Acid soluble Ni recoveries from fourteen test samples. Differences between calculated and assayed Ni values for feed material are expressed as relative %.*

A4	*Ni content %*	*Ni content cum. %*	*Ni distribution %*	*Ni distribution cum. %*
RC1	0.648	0.648	25.36	25.36
RC2	0.370	0.501	16.34	41.71
RC3	0.253	0.406	13.12	54.82
RC4	0.199	0.368	6.04	60.87
RC5	0.163	0.354	1.90	62.77
RT	0.024	0.058	37.23	100.00

Ni calculated = 0.058% Ni assay = 0.055% %Difference = 5%

A5	*Ni content %*	*Ni content cum. %*	*Ni distribution %*	*Ni distribution cum. %*
RC1	0.232	0.232	17.85	17.85
RC2	0.133	0.182	10.56	28.40
RC3	0.109	0.155	9.81	38.21
RC4	0.107	0.146	6.04	44.25
RC5	0.097	0.143	2.29	46.54
RT	0.023	0.038	53.46	100.00

Ni calculated = 0.038% Ni assay = 0.035% %Difference = 8%

B3	*Ni content %*	*Ni content cum. %*	*Ni distribution %*	*Ni distribution cum. %*
RC1	0.612	0.612	35.25	35.25
RC2	0.190	0.392	11.92	47.17
RC3	0.130	0.294	9.28	56.45
RC4	0.105	0.258	4.81	61.26
RC5	0.090	0.245	1.74	62.99
RT	0.017	0.041	37.01	100.00

Ni calculated = 0.041% Ni assay = 0.041% %Difference = 0%

B4	*Ni content %*	*Ni content cum. %*	*Ni distribution %*	*Ni distribution cum. %*
RC1	0.738	0.738	31.58	31.58
RC2	0.279	0.489	14.20	45.78
RC3	0.211	0.369	14.89	60.67
RC4	0.145	0.316	7.34	68.01
RC5	0.119	0.299	2.43	70.44
RT	0.018	0.054	29.56	100.00

Ni calculated = 0.054% Ni assay = 0.056% %Difference = 3%

Table 6 cont. *Acid soluble Ni recoveries from fourteen test samples. Differences between calculated and assayed Ni values for feed material are expressed as relative %.*

C1	*Ni content %*	*Ni content cum. %*	*Ni distribution %*	*Ni distribution cum. %*
RC1	0.201	0.201	17.11	17.11
RC2	0.099	0.145	10.12	27.23
RC3	0.080	0.118	10.34	37.58
RC4	0.078	0.110	6.53	44.10
RC5	0.079	0.108	2.45	46.55
RT	0.016	0.027	53.45	100.00

Ni calculated = 0.027% Ni assay = 0.028% %Difference = 4%

C2	*Ni content %*	*Ni content cum. %*	*Ni distribution %*	*Ni distribution cum. %*
RC1	0.228	0.228	19.35	19.35
RC2	0.107	0.163	10.67	30.02
RC3	0.093	0.135	11.21	41.23
RC4	0.089	0.125	7.51	48.73
RC5	0.083	0.121	2.91	51.65
RT	0.019	0.033	48.35	100.00

Ni calculated = 0.033% Ni assay = 0.030% %Difference = 10%

C3	*Ni content %*	*Ni content cum. %*	*Ni distribution %*	*Ni distribution cum. %*
RC1	0.150	0.150	12.62	12.62
RC2	0.090	0.118	8.69	21.31
RC3	0.083	0.105	9.29	30.60
RC4	0.083	0.100	6.37	36.97
RC5	0.084	0.099	2.98	39.95
RT	0.020	0.029	60.05	100.00

Ni calculated = 0.029% Ni assay = 0.029% %Difference = 0%

C4	*Ni content %*	*Ni content cum. %*	*Ni distribution %*	*Ni distribution cum. %*
RC1	0.138	0.138	15.14	15.14
RC2	0.083	0.107	11.97	27.11
RC3	0.071	0.093	11.22	38.34
RC4	0.070	0.089	6.35	44.68
RC5	0.071	0.088	2.49	47.17
RT	0.017	0.027	52.83	100.00

Ni calculated = 0.027% Ni assay = 0.026% %Difference = 6%

C5	*Ni content %*	*Ni content cum. %*	*Ni distribution %*	*Ni distribution cum. %*
RC1	0.231	0.231	16.32	16.32
RC2	0.111	0.164	9.93	26.25
RC3	0.081	0.128	9.66	35.92
RC4	0.080	0.117	6.49	42.40
RC5	0.078	0.114	2.69	45.10
RT	0.017	0.028	54.90	100.00

Ni calculated = 0.028% Ni assay = 0.028% %Difference = 1%

***Table** 7 Kelsall flotation constants for acid soluble Ni recoveries from fourteen samples of UG2 chromitite milled to 80% <75μm.*

Ni (a.s.)	U	ϕ	K_f	K_s	Loss
A1	60.6	0.4	1.9	0.1	0.3
A2	61.2	0.5	1.4	0.2	0.1
A3	61.1	0.5	1.6	0.2	0.1
B1	41.8	0.5	1.9	0.1	0.0
B2	51.8	0.5	1.7	0.2	0.1
C1	49.1	0.6	1.4	0.1	0.0
C2	55.0	0.6	1.5	0.1	0.0
C3	43.9	0.7	1.2	0.1	0.1
C4	49.5	0.6	1.0	0.1	0.1
C5	48.4	0.6	1.3	0.1	0.0
A4	63.8	0.6	1.2	0.2	0.1
A5	48.8	0.6	1.3	0.1	0.0
B3	64.1	0.4	1.8	0.2	0.1
B4	68.5	0.7	1.4	0.2	0.2
Avg.	54.8	0.6	1.5	0.1	0.1

Table 8 *PGE+Au recoveries from fourteen samples of UG2 chromitite milled to 80% <75µm.*

A2	*PGE+Au content ppm*	*PGE+Au content cumulative ppm*	*PGE+Au dist. %*	*PGE+Au dist. cumulative %*
RC1	95.60	95.60	69.47	69.47
RC2	16.87	53.72	13.93	83.39
RC3	8.62	38.58	6.76	90.16
RC4	6.87	34.05	2.67	92.83
RC5	5.70	32.71	0.77	93.60
RT	0.26	3.64	6.40	100.00

PGE+Au calculated = 3.64 ppm PGE+Au assay = 3.08 ppm Difference = 0.56 ppm (%Difference = 18%)

B2	*PGE+Au content ppm*	*PGE+Au content cumulative ppm*	*PGE+Au dist. %*	*PGE+Au dist. cumulative %*
RC1	110.90	110.90	78.82	78.82
RC2	9.02	51.28	9.05	87.87
RC3	5.33	34.16	5.42	93.29
RC4	3.74	29.66	1.77	95.06
RC5	3.06	28.32	0.52	95.58
RT	0.19	3.75	4.42	100.00

PGE+Au calculated = 3.75 ppm PGE+Au assay = 3.55 ppm Difference = 0.20 ppm (%Difference = 6%)

A1	*PGE+Au content ppm*	*PGE+Au content cumulative ppm*	*PGE+Au dist. %*	*PGE+Au dist. cumulative %*
RC1	103.18	103.18	75.22	75.22
RC2	25.66	72.90	11.99	87.21
RC3	11.26	54.05	5.94	93.15
RC4	7.20	47.02	2.19	95.34
RC5	5.79	44.86	0.65	95.99
RT	0.23	5.14	4.01	100.00

PGE+Au calculated = 5.14 ppm PGE+Au assay = 5.15 ppm Difference = 0.01 ppm (%Difference = 0%)

B1	*PGE+Au content ppm*	*PGE+Au content cumulative ppm*	*PGE+Au dist. %*	*PGE+Au dist. cumulative %*
RC1	66.61	66.61	70.75	70.75
RC2	16.33	46.84	11.23	81.98
RC3	8.64	34.91	6.86	88.84
RC4	6.65	30.47	3.15	91.99
RC5	6.23	29.26	0.99	92.98
RT	0.27	3.43	7.02	100.00

PGE+Au calculated = 3.43 ppm PGE+Au assay = 4.10 ppm Difference = 0.67 ppm (%Difference = 16%)

Table 8 cont. *PGE+Au recoveries from fourteen samples of UG2 chromitite milled to 80% <75μm.*

A3	*PGE+Au content ppm*	*PGE+Au content cumulative ppm*	*PGE+Au dist. %*	*PGE+Au dist. cumulative %*
RC1	125.70	125.70	60.34	60.34
RC2	32.74	79.97	15.22	75.56
RC3	17.60	58.02	9.03	84.59
RC4	13.35	51.05	3.59	88.19
RC5	7.61	48.70	0.75	88.94
RT	0.78	6.25	11.06	100.00

PGE+Au calculated = 6.25 ppm PGE+Au assay = 5.85 ppm Difference = 0.40 ppm (%Difference = 7%)

A4	*PGE+Au content ppm*	*PGE+Au content cumulative ppm*	*PGE+Au dist. %*	*PGE+Au dist. cumulative %*
RC1	135.05	135.05	54.72	54.72
RC2	46.63	88.16	21.32	76.05
RC3	22.55	63.00	12.10	88.15
RC4	13.05	53.83	4.10	92.25
RC5	9.58	50.91	1.16	93.41
RT	0.410	5.59	6.59	100.00

PGE+Au calculated = 5.59 ppm PGE+Au assay = 5.02 ppm Difference = 0.57 ppm (%Difference = 11%)

B3	*PGE+Au content ppm*	*PGE+Au content cumulative ppm*	*PGE+Au dist. %*	*PGE+Au dist. cumulative %*
RC1	156.71	156.71	69.17	69.17
RC2	33.00	92.20	15.87	85.04
RC3	13.60	62.93	7.44	92.49
RC4	6.40	52.04	2.24	94.73
RC5	3.93	48.42	0.58	95.31
RT	0.28	5.36	4.69	100.00

PGE+Au calculated = 5.36 ppm PGE+Au assay = 4.70 ppm Difference = 0.66 ppm (%Difference = 14%)

B4	*PGE+Au content ppm*	*PGE+Au content cumulative ppm*	*PGE+Au dist. %*	*PGE+Au dist. cumulative %*
RC1	148.77	148.77	57.98	57.98
RC2	38.02	88.62	17.61	75.58
RC3	20.25	59.21	13.04	88.62
RC4	9.205	47.41	4.26	92.88
RC5	6.27	43.83	1.17	94.05
RT	0.41	5.96	5.95	100.00

PGE+Au calculated = 5.96 ppm PGE+Au assay = 5.81 ppm Difference = 0.15 ppm (%Difference = 3%)

Table 8 cont. *PGE+Au recovery from fourteen samples of UG2 chromitite milled to 80% <75μm.*

A5	*PGE+Au content ppm*	*PGE+Au content cumulative ppm*	*PGE+Au dist. %*	*PGE+Au dist. cumulative %*
RC1	71.27	71.27	35.72	35.72
RC2	26.99	48.78	13.95	49.67
RC3	17.30	37.28	10.14	59.81
RC4	14.55	33.05	5.35	65.16
RC5	12.55	31.56	1.93	67.09
RT	2.17	5.79	32.91	100.00

PGE+Au calculated = 5.79 ppm PGE+Au assay = 5.74 ppm Difference = 0.05 ppm (%Difference = 1%)

C1	*PGE+Au content ppm*	*PGE+Au content cumulative ppm*	*PGE+Au dist. %*	*PGE+Au dist. cumulative %*
RC1	135.01	135.01	61.95	61.95
RC2	28.35	76.75	15.66	77.61
RC3	12.35	50.51	8.59	86.19
RC4	7.56	41.55	3.40	89.59
RC5	5.52	38.97	0.92	90.51
RT	0.54	5.03	9.49	100.00

PGE+Au calculated = 5.03 ppm PGE+Au assay = 4.39 ppm Difference = 0.64 ppm (%Difference = 14%)

C2	*PGE+Au content ppm*	*PGE+Au content cumulative ppm*	*PGE+Au dist. %*	*PGE+Au dist. cumulative %*
RC1	119.30	119.30	66.49	66.49
RC2	22.25	66.87	14.57	81.07
RC3	10.15	44.39	8.08	89.15
RC4	6.24	36.14	3.46	92.60
RC5	4.39	33.52	1.01	93.61
RT	0.375	5.04	6.39	100.00

PGE+Au calculated = 5.04 ppm PGE+Au assay = 4.58 ppm Difference = 0.46 ppm (%Difference = 10%)

C3	*PGE+Au content ppm*	*PGE+Au content cumulative ppm*	*PGE+Au dist. %*	*PGE+Au dist. cumulative %*
RC1	152.66	152.66	63.34	63.34
RC2	32.05	88.20	15.26	78.60
RC3	15.45	60.37	8.53	87.14
RC4	9.09	49.72	3.44	90.58
RC5	7.03	45.98	1.23	91.81
RT	0.545	5.87	8.19	100.00

PGE+Au calculated = 5.87 ppm PGE+Au assay = 4.92 ppm Difference = 0.95 ppm (%Difference = 19%)

Table 8 cont. *PGE+Au recoveries from fourteen samples of UG2 chromitite milled to 80% <75µm.*

C4	*PGE+Au content ppm*	*PGE+Au content cumulative ppm*	*PGE+Au dist. %*	*PGE+Au dist. cumulative %*
RC1	110.59	110.59	70.83	70.83
RC2	16.08	56.93	13.53	84.36
RC3	7.60	38.03	7.00	91.36
RC4	4.84	32.07	2.54	93.90
RC5	3.20	30.18	0.65	94.56
RT	0.300	4.70	5.44	100.00

PGE+Au calculated = 4.70 ppm PGE+Au assay = 4.31 ppm Difference = 0.39 ppm (%Difference = 9%)

C5	*PGE+Au content ppm*	*PGE+Au content cumulative ppm*	*PGE+Au dist. %*	*PGE+Au dist. cumulative %*
RC1	176.89	176.89	69.83	69.83
RC2	28.80	93.98	14.46	84.29
RC3	11.35	58.68	7.59	91.88
RC4	6.44	46.91	2.93	94.81
RC5	4.26	43.20	0.82	95.63
RT	0.248	5.04	4.37	100.00

PGE+Au calculated = 5.04 ppm PGE+Au assay = 4.86 ppm Difference = 0.18 ppm (%Difference = 4%)

Table 9 *Kelsall flotation constants for PGE+Au recoveries from fourteen samples of UG2 chromitite milled to 80% <75µm.*

PGE+Au	*U*	ϕ	K_f	K_s	*Loss*
A2	93.85	0.20	2.13	0.20	0.02
B2	95.63	0.16	2.90	0.24	0.02
A1	96.13	0.17	2.38	0.22	0.02
B1	93.44	0.21	2.45	0.18	0.02
A3	89.29	0.29	2.05	0.21	0.00
B3	95.36	0.22	2.06	0.25	0.03
A4	93.63	0.36	1.60	0.22	0.08
B4	94.19	0.40	2.17	0.24	0.10
A5	68.40	0.42	1.62	0.15	0.07
C1	90.83	0.27	1.98	0.21	0.02
C2	94.02	0.24	2.10	0.19	0.03
C3	92.15	0.26	2.01	0.19	0.10
C4	94.73	0.21	2.24	0.22	0.02
C5	95.87	0.22	2.16	0.21	0.03
Avg.	91.97	0.26	2.13	0.21	0.04

Loss = (Observed – Predicted) ^{2}

Table 10 *Platinum recovery from fourteen samples of UG2 chromitite milled to 80% <75µm.*

A2	*Pt content ppm*	*Pt content cumulative ppm*	*Pt distribution %*	*Pt distribution cumulative %*
RC1	64.13	64.13	70.87	70.87
RC2	10.90	35.82	13.69	84.56
RC3-5	5.13	21.77	10.21	94.76
RT	0.14	2.39	5.24	100.00

Pt calculated = 2.39 ppm Pt assay = 2.13 ppm Difference = 0.26 ppm
Difference = 11%

B2	*Pt content ppm*	*Pt content cumulative ppm*	*Pt distribution %*	*Pt distribution cumulative %*
RC1	65.87	65.87	79.49	79.49
RC2	5.39	30.48	9.18	88.67
RC3-5	2.81	16.85	7.91	96.58
RT	0.09	2.21	3.42	100.00

Pt calculated = 2.21 ppm Pt assay = 2.04 ppm Difference = 0.17 ppm
Difference = 8%

A1	*Pt content ppm*	*Pt content cumulative ppm*	*Pt distribution %*	*Pt distribution cumulative %*
RC1	61.83	61.83	74.97	74.97
RC2	15.48	43.73	12.03	87.00
RC3-5	5.75	26.98	9.01	96.02
RT	0.14	3.09	3.98	100.00

Pt calculated = 3.09 ppm Pt assay = 3.08 ppm Difference = 0.18 ppm
Difference = 0%

B1	*Pt content ppm*	*Pt content cumulative ppm*	*Pt distribution %*	*Pt distribution cumulative %*
RC1	39.63	39.63	71.63	71.63
RC2	8.47	27.38	9.92	81.54
RC3-5	4.32	17.02	10.49	92.03
RT	0.18	2.01	7.97	100.00

Pt calculated = 2.01 ppm Pt assay = 2.41 ppm Difference = 0.40 ppm
Difference = 20%

A3	*Pt content ppm*	*Pt content cumulative ppm*	*Pt distribution %*	*Pt distribution cumulative %*
RC1	80.85	80.85	63.31	63.31
RC2	19.8	50.82	15.01	78.32
RC3-5	9.13	30.70	13.12	91.44
RT	0.37	3.83	8.56	100.00

Pt calculated = 3.83 ppm Pt assay = 3.67 ppm Difference = 0.16 ppm
Difference = 4%

Table 10 cont. *Platinum recoveries from fourteen samples of UG2 chromitite milled to 80% <75μm.*

B3	*Pt content ppm*	*Pt content cumulative ppm*	*Pt distribution %*	*Pt distribution cumulative %*
RC1	94.50	94.50	69.75	69.75
RC2	20.00	55.65	16.08	85.83
RC3-5	5.39	28.94	9.43	95.26
RT	0.17	3.21	4.74	100.00

Pt calculated = 3.21 ppm Pt assay = 2.81 ppm Difference = 0.40 ppm
Difference = 13%

A4	*Pt content ppm*	*Pt content cumulative ppm*	*Pt distribution %*	*Pt distribution cumulative %*
RC1	88.50	88.50	59.09	59.09
RC2	27.00	55.89	20.35	79.44
RC3-5	9.20	31.15	14.74	94.18
RT	0.22	3.39	5.82	100.00

Pt calculated = 3.39 ppm Pt assay = 3.05 ppm Difference = 0.34 ppm
% Difference = 10%

B4	*Pt content ppm*	*Pt content cumulative ppm*	*Pt distribution %*	*Pt distribution cumulative %*
RC1	92.50	92.50	62.39	62.39
RC2	21.00	53.67	16.83	79.22
RC3-5	6.91	25.50	15.46	94.69
RT	0.21	3.45	5.31	100.00

Pt calculated = 3.45 ppm Pt assay = 3.34 ppm Difference = 0.11 ppm
Difference = 3%

A5	*Pt content ppm*	*Pt content cumulative ppm*	*Pt distribution %*	*Pt distribution cumulative %*
RC1	39.50	39.50	36.63	36.63
RC2	15.10	27.11	14.45	51.08
RC3-5	8.15	17.23	16.70	67.78
RT	1.15	3.13	32.22	100.00

Pt calculated = 3.13 ppm Pt assay = 3.13 ppm Difference = 0 ppm
Difference = 0 %

C1	*Pt content ppm*	*Pt content cumulative ppm*	*Pt distribution %*	*Pt distribution cumulative %*
RC1	92.00	92.00	62.67	62.67
RC2	19.50	52.40	15.99	78.66
RC3-5	6.68	26.58	12.99	91.65
RT	0.32	3.39	8.35	100.00

Pt calculated = 3.39 ppm Pt assay = 3.03 ppm Difference = 0.36 ppm
Difference = 11%

Table 10 cont. *Platinum recovery from fourteen samples of UG2 chromitite milled to 80% <75µm.*

C2	*Pt content ppm*	*Pt content cumulative ppm*	*Pt distribution %*	*Pt distribution cumulative %*
RC1	75.50	75.50	65.76	65.76
RC2	14.70	42.65	15.05	80.81
RC3-5	5.40	21.57	13.34	94.14
RT	0.22	3.23	5.86	100.00

Pt calculated = 3.23 ppm *Pt assay = 2.97 ppm* *Difference = 0.26 ppm*
Difference = 8%

C3	*Pt content ppm*	*Pt content cumulative ppm*	*Pt distribution %*	*Pt distribution cumulative %*
RC1	102.25	102.25	65.42	65.42
RC2	20.50	58.56	15.06	80.48
RC3-5	7.30	30.18	12.45	92.93
RT	0.31	3.81	7.07	100.00

Pt calculated = 3.81 ppm *Pt assay = 3.25 ppm* *Difference = 0.56 ppm*
Difference = 15%

C4	*Pt content ppm*	*Pt content cumulative ppm*	*Pt distribution %*	*Pt distribution cumulative %*
RC1	75.25	75.25	70.68	70.68
RC2	10.85	38.68	13.39	84.06
RC3-5	4.55	20.70	11.02	95.08
RT	0.19	3.21	4.92	100.00

Pt calculated = 3.21 ppm *Pt assay = 2.90 ppm* *Difference = 0.31 ppm*
Difference = 10%

C5	*Pt content ppm*	*Pt content cumulative ppm*	*Pt distribution %*	*Pt distribution cumulative %*
RC1	113.50	113.50	70.55	70.55
RC2	18.60	60.37	14.71	85.26
RC3-5	5.30	27.61	10.99	96.25
RT	0.14	3.20	3.75	100.00

Pt calculated = 3.20 ppm *Pt assay = 3.06 ppm* *Difference = 0.14 ppm*
Difference = 4%

Table 11 *Kelsall flotation constants for platinum recoveries from fourteen samples of UG2 chromitite milled to 80% <75μm assuming an ultimate recovery of 100 per cent.*

Pt	ϕ	K_f	K_s	*Loss*
A2	0.18	1.91	0.06	0.00
B2	0.14	2.44	0.07	0.00
A1	0.15	2.13	0.07	0.00
B1	0.21	2.27	0.05	0.00
A3	0.25	1.74	0.05	0.00
B3	0.17	1.74	0.06	0.00
A4	0.24	1.41	0.07	0.00
B4	0.26	1.68	0.08	0.00
A5	0.52	1.31	0.02	0.00
C1	0.25	1.68	0.05	0.00
C2	0.23	1.81	0.07	0.00
C3	0.23	1.78	0.06	0.00
C4	0.19	1.97	0.07	0.00
C5	0.18	1.88	0.08	0.00
Avg.	0.23	1.84	0.06	0.00

Loss = (Observed – Predicted) ^{2}

Table 12 *Palladium recoveries from fourteen samples of UG2 chromitite milled to 80% <75µm.*

A2	*Pd content ppm*	*Pd content cumulative ppm*	*Pd distribution %*	*Pd distribution cumulative %*
RC1	17.03	17.03	65.07	65.07
RC2	3.70	9.94	16.06	81.14
RC3-5	1.80	6.22	12.39	93.53
RT	0.05	0.69	6.47	100.00

Pd calculated = 0.69 ppm Pd assay = 0.66 ppm Difference = 0.03 ppm
Difference = 6%

B2	*Pd content ppm*	*Pd content cumulative ppm*	*Pd distribution %*	*Pd distribution cumulative %*
RC1	33.67	33.67	77.12	77.12
RC2	2.79	15.60	9.02	86.13
RC3-5	1.68	8.75	8.99	95.13
RT	0.07	1.16	4.87	100.00

Pd calculated = 1.16 ppm Pd assay = 1.17 ppm Difference = 0.01 ppm
Difference = 0%

A1	*Pd content ppm*	*Pd content cumulative ppm*	*Pd distribution %*	*Pd distribution cumulative %*
RC1	29.27	29.27	73.82	73.82
RC2	7.21	20.65	11.66	85.48
RC3-5	2.89	12.82	9.43	94.91
RT	0.09	1.49	5.09	100.00

Pd calculated = 1.49 ppm Pd assay = 1.42 ppm Difference = 0.07 ppm
Difference = 5%

B1	*Pd content ppm*	*Pd content cumulative ppm*	*Pd distribution %*	*Pd distribution cumulative %*
RC1	20.03	20.03	66.33	66.33
RC2	5.79	14.43	12.42	78.75
RC3-5	2.77	9.19	12.33	91.08
RT	0.11	1.10	8.92	100.00

Pd calculated = 1.10 ppm Pd assay = 1.30 ppm Difference = 0.20 ppm
Difference = 15%

A3	*Pd content ppm*	*Pd content cumulative ppm*	*Pd distribution %*	*Pd distribution cumulative %*
RC1	30.95	30.95	56.45	56.45
RC2	9.05	20.18	15.98	72.44
RC3-5	4.90	12.80	16.41	88.84
RT	0.21	1.64	11.16	100.00

Pd calculated = 1.64 ppm Pd assay = 1.57 ppm Difference = 0.07 ppm
Difference = 5%

Table 12 cont. *Palladium recoveries from fourteen samples of UG2 chromitite milled to 80% <75µm.*

B3	*Pd content ppm*	*Pd content cumulative ppm*	*Pd distribution %*	*Pd distribution cumulative %*
RC1	45.50	45.50	69.16	69.16
RC2	9.15	26.55	15.15	84.31
RC3-5	2.92	13.99	10.52	94.83
RT	0.09	1.56	5.17	100.00

Pd calculated = 1.56 ppm Pd assay = 1.43 ppm Difference = 0.13 ppm
Difference = 8%

A4	*Pd content ppm*	*Pd content cumulative ppm*	*Pd distribution %*	*Pd distribution cumulative %*
RC1	33.50	33.50	47.71	47.71
RC2	13.90	23.11	22.34	70.06
RC3-5	6.29	14.19	21.48	91.53
RT	0.15	1.59	8.47	100.00

Pd calculated = 1.59 ppm Pd assay = 1.48 ppm Difference = 0.11 ppm
Difference = 7%

B4	*Pd content ppm*	*Pd content cumulative ppm*	*Pd distribution %*	*Pd distribution cumulative %*
RC1	42.00	42.00	50.93	50.93
RC2	12.65	26.06	18.23	69.16
RC3-5	5.97	13.96	24.01	93.18
RT	0.15	1.92	6.82	100.00

Pd calculated = 1. 92 ppm Pd assay = 1.87 ppm Difference = 0.05 ppm
Difference = 2%

A5	*Pd content ppm*	*Pd content cumulative ppm*	*Pd distribution %*	*Pd distribution cumulative %*
RC1	26.00	26.00	37.06	37.06
RC2	9.15	17.44	13.46	50.52
RC3-5	5.05	10.98	15.89	66.41
RT	0.78	2.04	33.59	100.00

Pd calculated = 2.04 ppm Pd assay = 2.05 ppm Difference = 0.01 ppm
Difference = 0%

C1	*Pd content ppm*	*Pd content cumulative ppm*	*Pd distribution %*	*Pd distribution cumulative %*
RC1	31.00	31.00	63.71	63.71
RC2	5.35	16.99	13.24	76.95
RC3-5	2.12	8.59	12.42	89.37
RT	0.135	1.12	10.63	100.00

Pd calculated = 1.12 ppm Pd assay = 1.04 ppm Difference = 0.08 ppm
Difference = 7%

C2	*Pd content ppm*	*Pd content cumulative ppm*	*Pd distribution %*	*Pd distribution cumulative %*
RC1	32.50	32.50	69.90	69.90
RC2	4.70	17.48	11.88	81.78
RC3-5	1.86	8.64	11.32	93.10
RT	0.105	1.31	6.90	100.00

Pd calculated = 1.31 ppm Pd assay = 1.14 ppm Difference = 0.17 ppm

Difference = 13%

C3	*Pd content ppm*	*Pd content cumulative ppm*	*Pd distribution %*	*Pd distribution cumulative %*
RC1	36.00	36.00	63.33	63.33
RC2	7.08	20.54	14.29	77.61
RC3-5	2.60	10.61	12.19	89.80
RT	0.16	1.38	10.20	100.00

Pd calculated = 1.38 ppm *Pd assay = 1.12 ppm* *Difference = 0.26 ppm*
Difference = 19%

Table 12 cont. *Palladium recoveries from fourteen samples of UG2 chromitite milled to 80% <75μm.*

C4	*Pd content ppm*	*Pd content cumulative ppm*	*Pd distribution %*	*Pd distribution cumulative %*
RC1	23.75	23.75	70.12	70.12
RC2	3.20	12.08	12.41	82.53
RC3-5	1.34	6.42	10.20	92.73
RT	0.09	1.02	7.27	100.00

Pd calculated = 1.02 ppm Pd assay = 0.94 ppm Difference = 0.08 ppm
Difference = 8%

C5	*Pd content ppm*	*Pd content cumulative ppm*	*Pd distribution %*	*Pd distribution cumulative %*
RC1	47.50	47.50	71.01	71.01
RC2	6.65	24.63	12.65	83.66
RC3-5	2.17	11.27	10.80	94.46
RT	0.08	1.33	5.54	100.00

Pd calculated = 1.33 ppm Pd assay = 1.31ppm Difference = 0.02 ppm
Difference = 2%

Table 13 *Kelsall flotation constants for Pd recoveries from fourteen samples of UG2 chromitite milled to 80% <75μm assuming an ultimate recovery of 100%.*

Pd	ϕ	K_f	K_s	*Loss*
A2	0.22	1.71	0.06	0.00
B2	0.17	2.44	0.06	0.00
A1	0.17	2.11	0.06	0.00
B1	0.24	1.98	0.05	0.00
A3	0.31	1.65	0.05	0.00
B3	0.19	1.80	0.06	0.00
A4	0.35	1.19	0.07	0.00
B4	0.39	1.54	0.09	0.00
A5	0.52	1.38	0.02	0.00
C1	0.26	1.87	0.04	0.00
C2	0.21	2.07	0.06	0.00
C3	0.25	1.78	0.05	0.00
C4	0.20	2.01	0.05	0.00
C5	0.20	2.02	0.06	0.00
Avg.	0.26	1.84	0.06	0.00

Loss = (Observed – Predicted) ^{2}

Table 14 *Rhodium recovery from fourteen samples of UG2 chromitite milled to 80% <75µm.*

A2	*Rh content ppm*	*Rh content cumulative ppm*	*Rh distribution %*	*Rh distribution cumulative %*
RC1	10.78	10.78	71.89	71.89
RC2	2.03	6.13	15.38	87.28
RC3-5	1.04	3.80	12.50	99.77
RT	0.00	0.40	0.23	100.00

Rh calculated = 0.40 ppm Rh assay = 0.35ppm Difference = 0.05 ppm
Difference = 13%

B1	*Rh content ppm*	*Rh content cumulative ppm*	*Rh distribution %*	*Rh distribution cumulative %*
RC1	6.06	6.06	70.69	70.69
RC2	1.93	4.43	14.59	85.28
RC3-5	0.92	2.86	14.43	99.71
RT	0.00	0.31	0.29	100.00

Rh calculated = 0.31 ppm Rh assay = 0.37 ppm Difference = 0.06 ppm
Difference = 16%

A1	*Rh content ppm*	*Rh content cumulative ppm*	*Rh distribution %*	*Rh distribution cumulative %*
RC1	10.74	10.74	74.35	74.35
RC2	2.75	7.62	12.21	86.56
RC3-5	1.05	4.72	9.38	95.94
RT	0.02	0.54	4.06	100.00

Rh calculated = 0.54 ppm Rh assay = 0.43 ppm Difference = 0.11 ppm
Difference = 26%

B2	*Rh content ppm*	*Rh content cumulative ppm*	*Rh distribution %*	*Rh distribution cumulative %*
RC1	10.78	10.78	83.12	83.12
RC2	0.80	4.94	8.70	91.82
RC3-5	0.44	2.72	7.93	99.75
RT	0.00	0.35	0.25	100.00

Rh calculated = 0.35 ppm Rh assay = 0.33 ppm Difference = 0.02 ppm
Difference = 5%

A3	*Rh content ppm*	*Rh content cumulative ppm*	*Rh distribution %*	*Rh distribution cumulative %*
RC1	13.28	13.28	60.15	60.15
RC2	3.73	8.58	16.36	76.51
RC3-5	1.86	5.34	15.47	91.97
RT	0.06	0.66	8.03	100.00

Rh calculated = 0.66 ppm Rh assay = 0.60 ppm Difference = 0.06 ppm
Difference = 11%

Table 14 cont. *Rhodium recovery from fourteen samples of UG2 chromitite milled to 80% <75µm.*

B3	*Rh content ppm*	*Rh content cumulative ppm*	*Rh distribution %*	*Rh distribution cumulative %*
RC1	15.70	15.70	68.14	68.14
RC2	3.50	9.34	16.55	84.69
RC3-5	1.01	4.91	10.39	95.08
RT	0.03	0.55	4.92	100.00

Rh calculated = 0.55 ppm Rh assay = 0.43 ppm Difference = 0.12 ppm
Difference = 21%

A4	*Rh content ppm*	*Rh content cumulative ppm*	*Rh distribution %*	*Rh distribution cumulative %*
RC1	11.90	11.90	47.34	47.34
RC2	5.40	8.45	24.24	71.58
RC3-5	2.52	5.31	24.00	95.59
RT	0.03	0.57	4.41	100.00

Rh calculated = 0.57 ppm Rh assay = 0.46 ppm Difference = 0.11 ppm
Difference = 20%

B4	*Rh content ppm*	*Rh content cumulative ppm*	*Rh distribution %*	*Rh distribution cumulative %*
RC1	12.25	12.25	49.54	49.54
RC2	3.95	7.74	18.99	68.53
RC3-5	1.95	4.25	26.16	94.69
RT	0.04	0.57	5.31	100.00

Rh calculated = 0.57 ppm Rh assay = 0.53 ppm Difference = 0.04 ppm
Difference = 8%

A5	*Rh content ppm*	*Rh content cumulative ppm*	*Rh distribution %*	*Rh distribution cumulative %*
RC1	5.10	5.10	26.67	26.67
RC2	2.60	3.83	14.03	40.69
RC3-5	2.13	2.94	24.55	65.25
RT	0.22	0.56	34.75	100.00

Rh calculated = 0.56 ppm Rh assay = 0.52 ppm Difference = 0.04 ppm
Difference = 6%

C1	*Rh content ppm*	*Rh content cumulative ppm*	*Rh distribution %*	*Rh distribution cumulative %*
RC1	11.45	11.45	49.52	49.52
RC2	3.50	7.11	18.22	67.74
RC3-5	1.61	4.00	19.84	87.58
RT	0.08	0.53	12.42	100.00

Rh calculated = 0.53 ppm Rh assay = 0.45 ppm Difference = 0.08 ppm
Difference = 17%

Table 14 cont. *Rhodium recovery from fourteen samples of UG2 chromitite milled to 80% <75μm.*

C2	*Rh content ppm*	*Rh content cumulative ppm*	*Rh distribution %*	*Rh distribution cumulative %*
RC1	10.15	10.15	55.42	55.42
RC2	2.70	6.13	17.33	72.75
RC3-5	1.28	3.38	19.74	92.49
RT	0.05	0.51	7.51	100.00

Rh calculated = 0.51 ppm Rh assay = 0.47 ppm Difference = 0.04 ppm
Difference = 9%

C3	*Rh content ppm*	*Rh content cumulative ppm*	*Rh distribution %*	*Rh distribution cumulative %*
RC1	13.90	13.90	51.22	51.22
RC2	4.33	8.78	18.29	69.51
RC3-5	2.09	5.07	20.47	89.99
RT	0.08	0.66	10.01	100.00

Rh calculated = 0.66 ppm Rh assay = 0.55 ppm Difference = 0.11 ppm
Difference = 17%

C4	*Rh content ppm*	*Rh content cumulative ppm*	*Rh distribution %*	*Rh distribution cumulative %*
RC1	11.30	11.30	66.61	66.61
RC2	1.90	5.96	14.71	81.32
RC3-5	0.96	3.32	14.51	95.83
RT	0.03	0.51	4.17	100.00

Rh calculated = 0.51 ppm Rh assay = 0.47 ppm Difference = 0.04 ppm
Difference = 8%

C5	*Rh content ppm*	*Rh content cumulative ppm*	*Rh distribution %*	*Rh distribution cumulative %*
RC1	15.55	15.55	61.66	61.66
RC2	3.55	8.83	17.91	79.57
RC3-5	1.21	4.30	16.01	95.57
RT	0.03	0.50	4.43	100.00

Rh calculated = 0.50 ppm Rh assay = 0.50 ppm Difference = 0.00 ppm
Difference = 1%

Table 15 *Kelsall flotation constants for rhodium recovery from fourteen samples of UG2 chromitite milled to 80% <75μm assuming an ultimate recovery of 100%.*

Rh	ϕ	K_f	K_s	*Loss*
A2	0.30	2.13	0.25	0.00
B2	0.15	2.92	0.21	0.00
A1	0.21	2.24	0.25	0.00
B1	0.29	2.46	0.23	0.00
A3	0.29	1.63	0.06	0.00
B3	0.18	1.70	0.06	0.00
A4	0.36	1.16	0.11	0.00
B4	0.42	1.54	0.10	0.00
A5	0.64	1.15	0.03	0.00
C1	0.37	1.40	0.05	0.00
C2	0.33	1.59	0.07	0.00
C3	0.36	1.45	0.06	0.00
C4	0.24	1.89	0.09	0.00
C5	0.26	1.62	0.09	0.00
Avg.	0.31	1.78	0.12	0.00

Loss = (Observed – Predicted) ^{2}

APPENDIX K

Multiple regression analysis results

Table 1a Observed and predicted values for R_f with % non-sulphide PGE mineral, PGE mineral grain diameter prior to milling, pn/(pn+mil) ratio and the predicted PGE mineral degree of liberation as independent variables, in turn excluding one of the samples.

Table 1b Regression summary for dependent variable R_f with % non-sulphide PGE mineral, PGE mineral grain diameter prior to milling, pn/(pn+mil) ratio and the predicted PGE mineral degree of liberation as independent variables, in turn excluding one of the samples.

Table 2a Observed and predicted values for R_f with % non-sulphide PGE mineral, pn/(pn+mil) ratio and the predicted PGE mineral degree of liberation as independent variables, in turn excluding one of the samples.

Table 2b Regression summary for dependent variable R_f with % non-sulphide PGE mineral, pn/(pn+mil) ratio, and the predicted PGE mineral degree of liberation as independent variables, in turn excluding one of the samples.

Table 3a Observed and predicted values for R_s with % non-sulphide PGE mineral, PGE mineral grain diameter prior to milling, pn/(pn+mil) ratio, median chromite grain diameter and the predicted PGE mineral degree of liberation as independent variables, in turn excluding one of the samples.

Table 3b Regression summary for dependent variable R_s with % non-sulphide PGE mineral, PGE mineral grain diameter prior to milling, pn/(pn+mil) ratio, median chromite grain diameter and the predicted PGE mineral degree of liberation as independent variables, in turn excluding one of the samples.

Table 4a Observed and predicted values for R_s with % non-sulphide PGE mineral, PGE mineral grain diameter prior to milling, pn/(pn+mil) ratio, median chromite grain diameter and the predicted PGE mineral degree of liberation as independent variables, in turn excluding one of the samples.

Table 4b Regression summary for dependent variable R_s with % non-sulphide PGE mineral, pn/(pn+mil) ratio and the predicted PGE mineral degree of

liberation as independent variables, in turn excluding sample A5 and one other sample.

Table 5 Regression summary for dependent variable 100-U with sample A5 excluded.

Table 6 Regression summary for dependent variable k_f. All fourteen samples included.

Table 7 Regression summary for dependent variable k_s. All fourteen samples included.

Table 8a Observed and predicted values for R_s with % non-sulphide PGE mineral and the PGE mineral degree of liberation as independent variables as independent variables, in turn excluding one of the samples.

Table 8b Regression summary for dependent variable R_f with % non-sulphide PGE mineral and the PGE mineral degree of liberation as independent variables, in turn excluding one sample.

Table 9a Observed and predicted values for R_f with % non-sulphide PGE mineral PGE mineral degree of liberation, base-metal sulphide degree of liberation, PGE mineral grain size prior, pentlandite/(pentlandite+millerite), and the PGE mineral degree of liberation as independent variables, in turn excluding one of the samples.

Table 9b Regression summary for dependent variable R_f with % non-sulphide PGE mineral, PGE mineral degree of liberation, base-metal sulphide degree of liberation, PGE mineral grain size prior, pentlandite/(pentlandite+millerite) to milling as independent variables, in turn excluding one sample.

Table 10a Observed and predicted values for variable R_s with % non-sulphide PGE mineral, PGE mineral degree of liberation, chromite grain diameter and PGE mineral diameter prior to milling, as independent variables, in turn excluding one of the samples.

Table 10b Regression summary for dependent variable R_s with % non-sulphide PGE mineral, PGE mineral degree of liberation, chromite grain diameter and PGE mineral diameter prior to milling as independent variables, in turn excluding one sample.

Table 11 Regression summary for dependent variable 100-U excluding sample A5.

Table 12 Regression summary for dependent variable k_f. All fourteen samples included.

Table 13 Regression summary for dependent variable k_s. All fourteen samples included.

Table 1a *Observed and predicted values for R_f with % non-sulphide PGE mineral, PGE mineral grain diameter prior to milling, pn/(pn+mil) ratio and the predicted PGE mineral degree of liberation as independent variables, in turn excluding one of the samples.*

Sample number	R_f Observed	R_f Predicted (n=14)	*R_f Predicted (n=13)	R_f Observed – *R_f predicted
A2	75.1	75.1	75.1	0.0
B2	80.3	79.3	79.0	1.4
A1	79.8	79.1	78.8	1.0
B1	73.8	76.3	77.7	-3.8
A3	63.4	65.3	67.3	-3.9
B3	74.4	71.9	70.9	3.5
A4	59.9	61.2	62.6	-2.7
B4	56.5	55.3	53.0	3.5
A5	39.7	39.3	37.2	2.5
C1	66.3	69.3	70.1	-3.8
C2	71.5	69.8	69.4	2.1
C3	68.2	68.8	68.4	-0.2
C4	74.8	72.3	71.6	3.2
C5	74.8	75.6	75.8	-1.0

**R_f predicted :* *Value of R_f determined from the regression equation calculated from the other 13 samples.*

Table 1b *Regression summary for dependent variable R_f with % non-sulphide PGE mineral, PGE mineral grain diameter prior to milling, pn/(pn+mil) ratio and the predicted PGE mineral degree of liberation as independent variables, in turn excluding one of the samples.*

Regression Summary for Dependent Variable: R_f				**A2 excluded**
R= .98881140 R^2= .97774799 Adjusted R^2= .96662199				
F(4,8)=87.880 p<.00000 Std.Error of estimate: 2.0388				
	B	*St. Err. of B*	*t(8)*	*p-level*
Intercept	61.67	7.23	8.53	0.00
% non sulphide PGEM	-0.22	0.03	-7.04	0.00
PGEM grain diameter at <2mm	-7.18	2.15	-3.34	0.01
pn/(pn+mil)	-22.32	3.20	-6.97	0.00
PGEM pred. degree of liberation	0.68	0.07	10.03	0.00
Regression Summary for Dependent Variable: R_f				**B2 excluded**
R= .98827751 R^2= .97669244 Adjusted R^2= .96503866				
F(4,8)=83.809 p<.00000 Std.Error of estimate: 2.0123				
	B	*St. Err. of B*	*t(8)*	*p-level*
Intercept	61.16	7.08	8.63	0.00
% non sulphide PGEM	-0.21	0.03	-6.93	0.00
PGEM grain diameter at <2mm	-6.95	2.12	-3.27	0.01
pn/(pn+mil)	-22.25	3.03	-7.35	0.00
PGEM pred. degree of liberation	0.68	0.07	10.01	0.00

Table 1b continued *Regression summary for dependent variable R_f with % non-sulphide PGE mineral, PGE mineral grain diameter prior to milling, pn/(pn+mil) ratio, and the predicted PGE mineral degree of liberation as independent variables, in turn excluding one of the samples.*

Regression Summary for Dependent Variable: R_f				**A1 excluded**
R= .98811817 R^2= .97637751 Adjusted R^2= .96456626				
F(4,8)=82.665 p<.00000 Std.Error of estimate: 2.0356				
	B	*St. Err. of B*	*t(8)*	*p-level*
Intercept	61.94	7.33	8.45	0.00
% non sulphide PGEM	-0.22	0.03	-7.18	0.00
PGEM grain diameter at <2mm	-7.23	2.11	-3.42	0.01
pn/(pn+mil)	-22.30	3.06	-7.29	0.00
PGEM pred. degree of liberation	0.68	0.07	9.63	0.00
Regression Summary for Dependent Variable: R_f				**B1 excluded**
R= .99190668 R^2= .98387886 Adjusted R^2= .97581830				
F(4,8)=122.06 p<.00000 Std.Error of estimate: 1.7447				
	B	*St. Err. of B*	*t(8)*	*p-level*
Intercept	65.46	6.47	10.12	0.00
% non sulphide PGEM	-0.22	0.03	-8.55	0.00
PGEM grain diameter at <2mm	-8.85	2.04	-4.34	0.00
pn/(pn+mil)	-23.42	2.70	-8.66	0.00
PGEM pred. degree of liberation	0.70	0.06	11.81	0.00
Regression Summary for Dependent Variable: R_f				**A3 excluded**
R= .99126096 R^2= .98259828 Adjusted R^2= .97389742				
F(4,8)=112.93 p<.00000 Std.Error of estimate: 1.8146				
	B	*St. Err. of B*	*t(8)*	*p-level*
Intercept	58.94	6.59	8.95	0.00
% non sulphide PGEM	-0.23	0.03	-8.14	0.00
PGEM grain diameter at <2mm	-5.56	2.17	-2.57	0.03
pn/(pn+mil)	-19.04	3.54	-5.38	0.00
PGEM pred. degree of liberation	0.64	0.07	9.50	0.00
Regression Summary for Dependent Variable: R_f				**B3 excluded**
R= .99284297 R^2= .98573717 Adjusted R^2= .97860575				
F(4,8)=138.22 p<.00000 Std.Error of estimate: 1.6374				
	B	*St. Err. of B*	*t(8)*	*p-level*
Intercept	56.61	6.19	9.15	0.00
% non sulphide PGEM	-0.20	0.03	-7.59	0.00
PGEM grain diameter at <2mm	-5.72	1.82	-3.15	0.01
pn/(pn+mil)	-22.96	2.48	-9.25	0.00
PGEM pred. degree of liberation	0.70	0.06	12.66	0.00

Table 1b continued *Regression summary for dependent variable R_f with % non-sulphide PGE mineral, PGE mineral grain diameter prior to milling, pn/(pn+mil) ratio and the predicted PGE mineral degree of liberation as independent variables, in turn excluding one of the samples.*

Regression Summary for Dependent Variable: R_f **A4 excluded** R= .98942983 R^2= .97897140 Adjusted R^2= .96845709 F(4,8)=93.109 p<.00000 Std.Error of estimate: 1.9610				
	B	*St. Err. of B*	*t(8)*	*p-level*
Intercept	60.96	6.88	8.86	0.00
% non sulphide PGEM	-0.20	0.04	-5.49	0.00
PGEM grain diameter at <2mm	-7.46	2.04	-3.65	0.01
pn/(pn+mil)	-23.73	3.44	-6.90	0.00
PGEM pred. degree of liberation	0.71	0.08	9.41	0.00
Regression Summary for Dependent Variable: R_f **B4 excluded** R= .99023976 R^2= .98057479 Adjusted R^2= .97086218 F(4,8)=100.96 p<.00000 Std.Error of estimate: 1.8356				
	B	*St. Err. of B*	*t(8)*	*p-level*
Intercept	70.81	9.26	7.65	0.00
% non sulphide PGEM	-0.26	0.04	-6.20	0.00
PGEM grain diameter at <2mm	-9.64	2.61	-3.70	0.01
pn/(pn+mil)	-21.92	2.77	-7.90	0.00
PGEM pred. degree of liberation	0.64	0.07	9.50	0.00
Regression Summary for Dependent Variable: R_f **A5 excluded** R= .97404853 R^2= .94877054 Adjusted R^2= .92315580 F(4,8)=37.040 p<.00003 Std.Error of estimate: 2.0382				
	B	*St. Err. of B*	*t(8)*	*p-level*
Intercept	61.07	11.24	5.44	0.00
% non sulphide PGEM	-0.22	0.03	-6.81	0.00
PGEM grain diameter at <2mm	-7.10	2.35	-3.02	0.02
pn/(pn+mil)	-22.55	4.84	-4.66	0.00
PGEM pred. degree of liberation	0.69	0.14	4.96	0.00
Regression Summary for Dependent Variable: R_f **C1 excluded** R= .99065733 R^2= .98140195 Adjusted R^2= .97210293 F(4,8)=105.54 p<.00000 Std.Error of estimate: 1.8900				
	B	*St. Err. of B*	*t(8)*	*p-level*
Intercept	61.61	6.58	9.37	0.00
% non sulphide PGEM	-0.21	0.03	-7.62	0.00
PGEM grain diameter at <2mm	-6.93	1.95	-3.56	0.01
pn/(pn+mil)	-22.71	2.86	-7.93	0.00
PGEM pred. degree of liberation	0.68	0.06	10.77	0.00

Table 1b continued *Regression summary for dependent variable R_f with % non-sulphide PGE mineral, PGE mineral grain diameter prior to milling, pn/(pn+mil) ratio and the predicted PGE mineral degree of liberation as independent variables, in turn excluding one of the samples.*

Regression Summary for Dependent Variable: R_f **C2 excluded**
R= .98953456 R^2= .97917865 Adjusted R^2= .96876798
F(4,8)=94.055 p<.00000 Std.Error of estimate: 1.9967

	B	*St. Err. of B*	*t(8)*	*p-level*
Intercept	61.25	6.98	8.77	0.00
% non sulphide PGEM	-0.22	0.03	-7.30	0.00
PGEM grain diameter at <2mm	-7.17	2.05	-3.51	0.01
pn/(pn+mil)	-22.07	3.03	-7.29	0.00
PGEM pred. degree of liberation	0.68	0.07	10.26	0.00

Regression Summary for Dependent Variable: R_f **C3 excluded**
R= .98937372 R^2= .97886036 Adjusted R^2= .96829054
F(4,8)=92.609 p<.00000 Std.Error of estimate: 2.0182

	B	*St. Err. of B*	*t(8)*	*p-level*
Intercept	61.87	7.05	8.78	0.00
% non sulphide PGEM	-0.22	0.03	-7.25	0.00
PGEM grain diameter at <2mm	-7.14	2.07	-3.45	0.01
pn/(pn+mil)	-22.33	3.04	-7.36	0.00
PGEM pred. degree of liberation	0.68	0.07	10.02	0.00

Regression Summary for Dependent Variable: R_f **C4 excluded**
R= .99114362 R^2= .98236568 Adjusted R^2= .97354851
F(4,8)=111.42 p<.00000 Std.Error of estimate: 1.8170

	B	St. Err. of B	t(8)	p-level
Intercept	61.31	6.33	9.69	0.00
% non sulphide PGEM	-0.22	0.03	-8.09	0.00
PGEM grain diameter at <2mm	-7.21	1.86	-3.87	0.00
pn/(pn+mil)	-21.43	2.80	-7.66	0.00
PGEM pred. degree of liberation	0.68	0.06	11.15	0.00

Regression Summary for Dependent Variable: R_f **C5 excluded**
R= .98922510 R^2= .97856629 Adjusted R^2= .96784943
F(4,8)=91.311 p<.00000 Std.Error of estimate: 2.0037

	B	*St. Err. of B*	*t(8)*	*p-level*
Intercept	62.18	7.05	8.83	0.00
% non sulphide PGEM	-0.22	0.03	-7.30	0.00
PGEM grain diameter at <2mm	-7.35	2.08	-3.53	0.01
pn/(pn+mil)	-22.80	3.16	-7.23	0.00
PGEM pred. degree of liberation	0.69	0.07	10.18	0.00

Table 2a *Observed and predicted values for R_f with % non-sulphide PGE mineral, pn/(pn+mil) ratio and the predicted PGE mineral degree of liberation as independent variables, in turn excluding one of the samples.*

Sample number	R_f Observed	R_f Predicted (n=14)	*R_f Predicted (n=13)	R_f Observed – *R_f predicted
A2	75.1	76.5	76.9	-1.8
B2	80.3	77.7	77.0	3.3
A1	79.8	80.2	80.3	-0.5
B1	73.8	73.0	72.9	0.9
A3	63.4	68.3	70.9	-7.5
B3	74.4	69.1	68.2	6.2
A4	59.9	60.5	61.1	-1.2
B4	56.5	59.6	41.7	14.8
A5	39.7	37.8	30.4	9.3
C1	66.3	69.7	70.7	-4.4
C2	71.5	70.0	69.6	1.9
C3	68.2	69.1	69.3	-1.1
C4	74.8	72.5	71.8	3.1
C5	74.8	74.6	68.5	6.3

R_f* predicted : *Value of R_f determined from the regression equation calculated from the other 13 samples.*

Table 2b *Regression summary for dependent variable R_f with % non-sulphide PGE mineral, pn/(pn+mil) ratio, and the predicted PGE mineral degree of liberation as independent variables, in turn excluding one of the samples.*

Regression Summary for Dependent Variable: R_f				**A2 excluded**
R= .97297118 R^2= .94667292 Adjusted R^2= .92889723				
F(3,9)=53.257 p<.00000 Std.Error of estimate: 2.9756				
	B	*St. Err. of B*	*t(9)*	*p-level*
Intercept	40.24	4.87	8.26	0.00
% non sulphide PGEM	-0.18	0.04	-4.26	0.00
pn/(pn+mil)	-18.63	4.38	-4.25	0.00
PGEM pred. degree of liberation	0.69	0.10	6.98	0.00
Regression Summary for Dependent Variable: R_f				**B2 excluded**
R= .97234955 R^2= .94546365 Adjusted R^2= .92728486				
F(3,9)=52.009 p<.00001 Std.Error of estimate: 2.9020				
	B	*St. Err. of B*	*t(9)*	*p-level*
Intercept	40.67	4.78	8.50	0.00
% non sulphide PGEM	-0.16	0.04	-4.24	0.00
pn/(pn+mil)	-19.28	4.17	-4.63	0.00
PGEM pred. degree of liberation	0.68	0.10	6.99	0.00

Table 2b continued *Regression summary for dependent variable R_f with % non-sulphide PGE mineral, pn/(pn+mil) ratio, and the predicted PGE mineral degree of liberation as independent variables, in turn excluding one of the samples.*

Regression Summary for Dependent Variable: R_f				**A1 excluded**
R= .97048122 R^2= .94183380 Adjusted R^2= .92244507				
F(3,9)=48.576 p<.00001 Std.Error of estimate: 3.0116				
	B	*St. Err. of B*	*t(9)*	*p-level*
Intercept	39.81	5.09	7.82	0.00
% non sulphide PGEM	-0.17	0.04	-4.27	0.00
pn/(pn+mil)	-19.22	4.33	-4.44	0.00
PGEM pred. degree of liberation	0.70	0.10	6.75	0.00
Regression Summary for Dependent Variable: R_f				**B1 excluded**
R= .97258564 R^2= .94592283 Adjusted R^2= .92789710				
F(3,9)=52.476 p<.00001 Std.Error of estimate: 3.0127				
	B	*St. Err. of B*	*t(9)*	*p-level*
Intercept	40.41	5.04	8.01	0.00
% non sulphide PGEM	-0.17	0.04	-4.27	0.00
pn/(pn+mil)	-19.08	4.34	-4.40	0.00
PGEM pred. degree of liberation	0.69	0.10	6.70	0.00
Regression Summary for Dependent Variable: R_f				**A3 excluded**
R= .98400607 R^2= .96826795 Adjusted R^2= .95769060				
F(3,9)=91.542 p<.00000 Std.Error of estimate: 2.3103				
	B	*St. Err. of B*	*t(9)*	*p-level*
Intercept	44.19	4.10	10.77	0.00
% non sulphide PGEM	-0.21	0.03	-6.09	0.00
pn/(pn+mil)	-14.28	3.84	-3.72	0.00
PGEM pred. degree of liberation	0.61	0.08	7.22	0.00
Regression Summary for Dependent Variable: R_f				**B3 excluded**
R= .97337194 R^2= .94745294 Adjusted R^2= .92993725				
F(3,9)=54.092 p<.00000 Std.Error of estimate: 3.0000				
	B	*St. Err. of B*	*t(9)*	*p-level*
Intercept	40.59	5.05	8.03	0.00
% non sulphide PGEM	-0.17	0.04	-4.30	0.00
pn/(pn+mil)	-19.23	4.31	-4.46	0.00
PGEM pred. degree of liberation	0.69	0.10	6.86	0.00
Regression Summary for Dependent Variable: R_f				**A4 excluded**
R= .97571419 R^2= .95201819 Adjusted R^2= .93602425				
F(3,9)=59.524 p<.00000 Std.Error of estimate: 2.8621				
	B	*St. Err. of B*	*t(9)*	*p-level*
Intercept	41.08	4.77	8.61	0.00
% non sulphide PGEM	-0.17	0.04	-4.45	0.00
pn/(pn+mil)	-19.85	4.16	-4.77	0.00
PGEM pred. degree of liberation	0.69	0.10	7.23	0.00

Table 2b continued *Regression summary for dependent variable R_f with % non-sulphide PGE mineral, pn/(pn+mil) ratio, and the predicted PGE mineral degree of liberation as independent variables, in turn excluding one of the samples.*

Regression Summary for Dependent Variable: R_f				**B4 excluded**
R= .97435099 R^2= .94935986 Adjusted R^2= .93247981				
F(3,9)=56.242 p<.00000 Std.Error of estimate: 2.9029				
	B	*St. Err. of B*	*t(9)*	*p-level*
Intercept	39.72	4.77	8.32	0.00
% non sulphide PGEM	-0.17	0.04	-4.45	0.00
pn/(pn+mil)	-18.31	4.28	-4.28	0.00
PGEM pred. degree of liberation	0.69	0.10	7.12	0.00
Regression Summary for Dependent Variable: R_f				**A5 excluded**
R= .97323841 R^2= .94719300 Adjusted R^2= .92959067				
F(3,9)=53.811 p<.00000 Std.Error of estimate: 2.9980				
	B	*St. Err. of B*	*t(9)*	*p-level*
Intercept	39.75	5.01	7.94	0.00
% non sulphide PGEM	-0.17	0.04	-4.27	0.00
pn/(pn+mil)	-18.94	4.34	-4.36	0.00
PGEM pred. degree of liberation	0.70	0.10	6.96	0.00
Regression Summary for Dependent Variable: R_f				**C1 excluded**
R= .97217230 R^2= .94511898 Adjusted R^2= .92682530				
F(3,9)=51.664 p<.00001 Std.Error of estimate: 3.0229				
	B	*St. Err. of B*	*t(9)*	*p-level*
Intercept	40.14	4.94	8.12	0.00
% non sulphide PGEM	-0.17	0.04	-4.24	0.00
pn/(pn+mil)	-19.14	4.50	-4.26	0.00
PGEM pred. degree of liberation	0.69	0.10	6.82	0.00
Regression Summary for Dependent Variable: R_f				**C2 excluded**
R= .97152886 R^2= .94386833 Adjusted R^2= .92515777				
F(3,9)=50.446 p<.00001 Std.Error of estimate: 3.0206				
	B	*St. Err. of B*	*t(9)*	*p-level*
Intercept	39.80	5.72	6.96	0.00
% non sulphide PGEM	-0.17	0.05	-3.06	0.01
pn/(pn+mil)	-19.46	4.98	-3.90	0.00
PGEM pred. degree of liberation	0.70	0.12	6.01	0.00
Regression Summary for Dependent Variable: R_f				**C3 excluded**
R= .97337194 R^2= .94745294 Adjusted R^2= .92993725				
F(3,9)=54.092 p<.00000 Std.Error of estimate: 3.0000				
	B	*St. Err. of B*	*t(9)*	*p-level*
Intercept	40.59	5.05	8.03	0.00
% non sulphide PGEM	-0.17	0.04	-4.30	0.00
pn/(pn+mil)	-19.23	4.31	-4.46	0.00
PGEM pred. degree of liberation	0.69	0.10	6.86	0.00

Table 2b continued *Regression summary for dependent variable R_f with % non-sulphide PGE mineral, pn/(pn+mil) ratio, and the predicted PGE mineral degree of liberation as independent variables, in turn excluding one of the samples.*

Regression Summary for Dependent Variable: R_f **C4 excluded** R= .98387705 R^2= .96801404 Adjusted R^2= .95735206 F(3,9)=90.791 p<.00000 Std.Error of estimate: 2.3118				
	B	*St. Err. of B*	*t(9)*	*p-level*
Intercept	39.06	3.81	10.26	0.00
% non sulphide PGEM	-0.15	0.03	-4.95	0.00
pn/(pn+mil)	-21.20	3.41	-6.21	0.00
PGEM pred. degree of liberation	0.72	0.08	9.26	0.00
Regression Summary for Dependent Variable: R_f **C5 excluded** R= .97333239 R^2= .94737593 Adjusted R^2= .92983458 F(3,9)=54.008 p<.00000 Std.Error of estimate: 2.8485				
	B	*St. Err. of B*	*t(9)*	*p-level*
Intercept	38.61	4.88	7.92	0.00
% non sulphide PGEM	-0.15	0.04	-3.32	0.01
pn/(pn+mil)	-20.44	4.26	-4.80	0.00
PGEM pred. degree of liberation	0.72	0.10	7.31	0.00

Table 3a *Observed and predicted values for R_s with % non-sulphide PGE mineral, PGE mineral grain diameter prior to milling, pn/(pn+mil) ratio, median chromite grain diameter and the predicted PGE mineral degree of liberation as independent variables, in turn excluding one of the samples.*

Sample number	**R_s Observed**	**R_s Predicted (n=14)**	***R_s Predicted (n=13)**	**R_s Observed – *$R_s$predicted**
A2	18.8	18.0	17.7	1.1
B2	15.3	15.9	16.1	-0.8
A1	16.3	17.7	18.5	-2.2
B1	19.6	18.7	18.3	1.4
A3	25.9	25.5	24.9	1.0
B3	21.0	21.1	21.1	-0.1
A4	33.7	33.7	33.7	0.0
B4	37.7	37.5	37.2	0.5
A5	28.7	29.0	37.1	-8.4
C1	24.5	24.9	25.1	-0.6
C2	22.6	23.4	19.5	3.0
C3	24.0	23.8	23.7	0.3
C4	19.9	18.8	17.8	2.1
C5	21.1	21.1	21.1	0.0

**R_s predicted : Value of R_s determined from the regression equation calculated for the other 13 samples.*

Table 3b *Regression summary for dependent variable R_s with % non-sulphide PGE mineral, PGE mineral grain diameter prior to milling, pn/(pn+mil) ratio, median chromite grain diameter and the predicted PGE mineral degree of liberation as independent variables, in turn excluding one of the samples.*

Regression Summary for Dependent Variable: R_s **A2 excluded** R= .99492020 R^2= .98986621 Adjusted R^2= .98262778 F(5,7)=136.75 p<.00000 Std.Error of estimate: .84867				
	B	*St. Err. of B*	*t(7)*	*p-level*
Intercept	-5.26	3.02	-1.74	0.13
% non sulphide PGEM	0.17	0.02	9.90	0.00
PGEM grain diameter at <2mm	5.85	1.03	5.68	0.00
Chromite grain diameter	0.11	0.01	8.02	0.00
pn/(pn+mil)	4.86	1.45	3.35	0.01
PGEM pred. degree of liberation	-0.20	0.04	-5.34	0.00
Regression Summary for Dependent Variable: R_s **B2 excluded** R= .99425144 R^2= .98853592 Adjusted R^2= .98034730 F(5,7)=120.72 p<.00000 Std.Error of estimate: .85769				
	B	*St. Err. of B*	*t(7)*	*p-level*
Intercept	-5.46	3.02	-1.81	0.11
% non sulphide PGEM	0.17	0.02	9.77	0.00
PGEM grain diameter at <2mm	6.03	0.99	6.07	0.00
Chromite grain diameter	0.11	0.01	7.74	0.00
pn/(pn+mil)	4.91	1.46	3.36	0.01
PGEM pred. degree of liberation	-0.19	0.04	-4.94	0.00
Regression Summary for Dependent Variable: R_s **A1 excluded** R= .99669983 R^2= .99341055 Adjusted R^2= .98870380 F(5,7)=211.06 p<.00000 Std.Error of estimate: .66260				
	B	St. Err. of B	t(7)	p-level
Intercept	-7.44	2.42	-3.08	0.02
% non sulphide PGEM	0.18	0.01	12.87	0.00
PGEM grain diameter at <2mm	6.76	0.81	8.36	0.00
Chromite grain diameter	0.10	0.01	8.48	0.00
pn/(pn+mil)	4.49	1.14	3.92	0.01
PGEM pred. degree of liberation	-0.16	0.03	-4.88	0.00
Regression Summary for Dependent Variable: R_s **B1 excluded** R= .99556347 R^2= .99114663 Adjusted R^2= .98482279 F(5,7)=156.73 p<.00000 Std.Error of estimate: .79951				
	B	*St. Err. of B*	*t(7)*	*p-level*
Intercept	-7.06	2.97	-2.38	0.05
% non sulphide PGEM	0.17	0.02	10.62	0.00
PGEM grain diameter at <2mm	6.70	1.03	6.53	0.00
Chromite grain diameter	0.11	0.01	8.56	0.00
pn/(pn+mil)	5.40	1.38	3.91	0.01
PGEM pred. degree of liberation	-0.20	0.04	-5.73	0.00

Table 3b continued *Regression summary for dependent variable R_s with % non-sulphide PGE mineral, PGE mineral grain diameter prior to milling, pn/(pn+mil) ratio, median chromite grain diameter and the predicted PGE mineral degree of liberation as independent variables, in turn excluding one of the samples.*

Regression Summary for Dependent Variable: R_s				**A3 excluded**
R= .99542266 R^2= .99086628 Adjusted R^2= .98434219				
F(5,7)=151.88 p<.00000 Std.Error of estimate: .82015				
	B	*St. Err. of B*	*t(7)*	*p-level*
Intercept	-4.77	3.00	-1.59	0.16
% non sulphide PGEM	0.18	0.02	9.14	0.00
PGEM grain diameter at <2mm	5.76	1.00	5.78	0.00
Chromite grain diameter	0.10	0.02	6.56	0.00
pn/(pn+mil)	3.32	2.11	1.57	0.16
PGEM pred. degree of liberation	-0.16	0.05	-3.50	0.01
Regression Summary for Dependent Variable: R_s				**B3 excluded**
R= .99470937 R^2= .98944674 Adjusted R^2= .98190870				
F(5,7)=131.26 p<.00000 Std.Error of estimate: .88096				
	B	*St. Err. of B*	*t(7)*	*p-level*
Intercept	-5.31	3.46	-1.53	0.17
% non sulphide PGEM	0.17	0.02	7.54	0.00
PGEM grain diameter at <2mm	5.91	1.24	4.79	0.00
Chromite grain diameter	0.11	0.02	6.83	0.00
pn/(pn+mil)	5.21	1.61	3.24	0.01
PGEM pred. degree of liberation	-0.20	0.04	-4.62	0.00
Regression Summary for Dependent Variable: R_s				**A4 excluded**
R= .99329542 R^2= .98663580 Adjusted R^2= .97708994				
F(5,7)=103.36 p<.00000 Std.Error of estimate: .88413				
	B	*St. Err. of B*	*t(7)*	*p-level*
Intercept	-5.70	3.10	-1.84	0.11
% non sulphide PGEM	0.17	0.02	8.88	0.00
PGEM grain diameter at <2mm	6.17	1.06	5.83	0.00
Chromite grain diameter	0.11	0.01	7.40	0.00
pn/(pn+mil)	5.15	1.62	3.17	0.02
PGEM pred. degree of liberation	-0.20	0.04	-4.94	0.00
Regression Summary for Dependent Variable: R_s				**B4 excluded**
R= .99102283 R^2= .98212625 Adjusted R^2= .96935928				
F(5,7)=76.927 p<.00001 Std.Error of estimate: .88276				
	B	*St. Err. of B*	*t(7)*	*p-level*
Intercept	-5.01	4.45	-1.13	0.30
% non sulphide PGEM	0.17	0.02	7.17	0.00
PGEM grain diameter at <2mm	5.92	1.32	4.47	0.00
Chromite grain diameter	0.11	0.01	7.77	0.00
pn/(pn+mil)	5.06	1.50	3.38	0.01
PGEM pred. degree of liberation	-0.20	0.04	-4.89	0.00

Table 3b continued *Regression summary for dependent variable R_s with % non-sulphide PGE mineral, PGE mineral grain diameter prior to milling, pn/(pn+mil) ratio, median chromite grain diameter and the predicted PGE mineral degree of liberation as independent variables, in turn excluding one of the samples.*

Regression Summary for Dependent Variable: R_s				**A5 excluded**
R= .99684844 R^2= .99370681 Adjusted R^2= .98921168				
F(5,7)=221.06 p<.00000 Std.Error of estimate: .66522				
	B	*St. Err. of B*	*t(7)*	*p-level*
Intercept	7.10	5.99	1.19	0.27
% non sulphide PGEM	0.19	0.02	11.67	0.00
PGEM grain diameter at <2mm	5.86	0.77	7.59	0.00
Chromite grain diameter	0.07	0.02	3.13	0.02
pn/(pn+mil)	8.66	1.92	4.51	0.00
PGEM pred. degree of liberation	-0.30	0.05	-5.60	0.00
Regression Summary for Dependent Variable: R_s				**C1 excluded**
R= .99615900 R^2= .99233275 Adjusted R^2= .98685614				
F(5,7)=181.19 p<.00000 Std.Error of estimate: .75508				
	B	*St. Err. of B*	*t(7)*	*p-level*
Intercept	-5.74	2.63	-2.18	0.07
% non sulphide PGEM	0.17	0.02	10.96	0.00
PGEM grain diameter at <2mm	6.12	0.87	7.05	0.00
Chromite grain diameter	0.12	0.01	9.23	0.00
pn/(pn+mil)	5.01	1.28	3.93	0.01
PGEM pred. degree of liberation	-0.21	0.03	-6.13	0.00
Regression Summary for Dependent Variable: R_s				**C2 excluded**
R= .99488254 R^2= .98979127 Adjusted R^2= .98249931				
F(5,7)=135.74 p<.00000 Std.Error of estimate: .87141				
	B	*St. Err. of B*	*t(7)*	*p-level*
Intercept	-5.61	3.05	-1.84	0.11
% non sulphide PGEM	0.17	0.02	9.58	0.00
PGEM grain diameter at <2mm	6.09	1.00	6.08	0.00
Chromite grain diameter	0.11	0.01	7.89	0.00
pn/(pn+mil)	4.99	1.48	3.38	0.01
PGEM pred. degree of liberation	-0.20	0.04	-5.16	0.00
Regression Summary for Dependent Variable: R_s				**C3 excluded**
R= .99487254 R^2= .98977136 Adjusted R^2= .98246520				
F(5,7)=135.47 p<.00000 Std.Error of estimate: .87287				
	B	*St. Err. of B*	*t(7)*	*p-level*
Intercept	-5.89	3.05	-1.93	0.10
% non sulphide PGEM	0.17	0.02	9.61	0.00
PGEM grain diameter at <2mm	6.14	1.00	6.12	0.00
Chromite grain diameter	0.11	0.01	7.68	0.00
pn/(pn+mil)	5.00	1.48	3.38	0.01
PGEM pred. degree of liberation	-0.19	0.04	-4.94	0.00

Table 3b continued *Regression summary for dependent variable R_s with % non-sulphide PGE mineral, PGE mineral grain diameter prior to milling, pn/(pn+mil) ratio, median chromite grain diameter and the predicted PGE mineral degree of liberation as independent variables, in turn excluding one of the samples.*

Regression Summary for Dependent Variable: R_s				**C4 excluded**
R= .99630132 R^2=.99261631 Adjusted R^2= .98734225				
F(5,7)=188.21 p<.00000 Std.Error of estimate: .73171				
	B	*St. Err. of B*	*t(7)*	*p-level*
Intercept	-5.83	2.55	-2.29	0.06
% non sulphide PGEM	0.16	0.02	9.60	0.00
PGEM grain diameter at <2mm	5.65	0.88	6.42	0.00
Chromite grain diameter	0.13	0.01	8.83	0.00
pn/(pn+mil)	6.24	1.41	4.44	0.00
PGEM pred. degree of liberation	-0.23	0.04	-6.30	0.00
Regression Summary for Dependent Variable: R_s				**C5 excluded**
R= .99469230 R^2= .98941278 Adjusted R^2= .98185048				
F(5,7)=130.83 p<.00000 Std.Error of estimate: .88288				
	B	*St. Err. of B*	*t(7)*	*p-level*
Intercept	-5.87	3.11	-1.89	0.10
% non sulphide PGEM	0.17	0.02	9.54	0.00
PGEM grain diameter at <2mm	6.16	1.03	5.98	0.00
Chromite grain diameter	0.11	0.01	7.73	0.00
pn/(pn+mil)	5.12	1.53	3.34	0.01
PGEM pred. degree of liberation	-0.20	0.04	-5.08	0.00

Table 4a *Observed and predicted values for R_s with % non-sulphide PGE mineral, PGE mineral grain diameter prior to milling, pn/(pn+mil) ratio, median chromite grain diameter and the predicted PGE mineral degree of liberation as independent variables, in turn excluding one of the samples.*

Sample number	**R_s Observed**	**R_s Predicted (n=14)**	***R_s Predicted (n=13)**	**R_s Observed – *R_s predicted**
A2	18.8	17.3	16.8	2.0
B2	19.6	21.5	21.9	-2.3
A1	16.3	14.5	13.2	3.1
B1	15.3	16.6	17.0	-1.7
A3	25.9	24.4	24.0	1.9
B3	21.0	24.4	25.4	-4.4
A4	33.7	34.7	35.9	-2.2
B4	37.7	35.1	33.1	4.6
C1	24.5	23.6	23.3	1.3
C2	22.6	23.5	23.7	-1.1
C3	24.0	24.1	24.2	-0.2
C4	19.9	21.3	21.7	-1.8
C5	21.1	19.4	18.8	2.3

**R_s predicted : Value of R_s determined from the regression equation calculated for the other 13 samples.*

Table 4b *Regression summary for dependent variable R_s with % non-sulphide PGE mineral, pn/(pn+mil) ratio and the predicted PGE mineral degree of liberation as independent variables, in turn excluding sample A5 and one other sample.*

Regression Summary for Dependent Variable: R_s				**A2 excluded**
R= .96436815 R^2= .93000593 Adjusted R^2= .90375816				
F(3,8)=35.432 p<.00006 Std.Error of estimate: 2.0319				
	B	*St. Err. of B*	*t(8)*	*p-level*
Intercept	46.80	5.87	7.98	0.00
% non sulphide PGEM	0.20	0.03	6.95	0.00
pn/(pn+mil)	14.04	4.76	2.95	0.02
PGEM pred. degree of liberation	-0.55	0.13	-4.41	0.00
Regression Summary for Dependent Variable: R_s				**B2 excluded**
R= .95989945 R^2= .92140695 Adjusted R^2= .89193455				
F(3,8)=31.263 p<.00009 Std.Error of estimate: 2.0464				
	B	*St. Err. of B*	*t(8)*	*p-level*
Intercept	45.58	6.17	7.39	0.00
% non sulphide PGEM	0.19	0.03	6.86	0.00
pn/(pn+mil)	13.82	4.86	2.85	0.02
PGEM pred. degree of liberation	-0.53	0.13	-3.98	0.00
Regression Summary for Dependent Variable: R_s				**A1 excluded**
R= .96571593 R^2= .93260726 Adjusted R^2= .90733498				
F(3,8)=36.902 p<.00005 Std.Error of estimate: 1.9311				
	B	*St. Err. of B*	*t(8)*	*p-level*
Intercept	50.79	6.49	7.82	0.00
% non sulphide PGEM	0.19	0.03	7.50	0.00
pn/(pn+mil)	16.89	4.93	3.43	0.01
PGEM pred. degree of liberation	-0.64	0.14	-4.59	0.00
Regression Summary for Dependent Variable: R_s				**B1 excluded**
R= .96697151 R^2= .93503391 Adjusted R^2= .91067162				
F(3,8)=38.380 p<.00004 Std.Error of estimate: 1.9725				
	B	*St. Err. of B*	*t(8)*	*p-level*
Intercept	45.29	5.86	7.73	0.00
% non sulphide PGEM	0.19	0.03	7.34	0.00
pn/(pn+mil)	13.66	4.66	2.93	0.02
PGEM pred. degree of liberation	-0.52	0.13	-4.16	0.00
Regression Summary for Dependent Variable: R_s				**A3 excluded**
R= .96985665 R^2= .94062193 Adjusted R^2= .91835515				
F(3,8)=42.243 p<.00003 Std.Error of estimate: 1.8949				
	B	*St. Err. of B*	*t(8)*	*p-level*
Intercept	39.31	7.74	5.08	0.00
% non sulphide PGEM	0.22	0.03	6.81	0.00
pn/(pn+mil)	7.69	6.64	1.16	0.28
PGEM pred. degree of liberation	-0.39	0.17	-2.34	0.05

Table 4b continued *Regression summary for dependent variable R_s with % non-sulphide PGE mineral, pn/(pn+mil) ratio and the predicted PGE mineral degree of liberation as independent variables, in turn excluding sample A5 and one other sample.*

Regression Summary for Dependent Variable: R_s **B3 excluded**
R= .97878183 R^2= .95801388 Adjusted R^2= .94226909
F(3,8)=60.846 p<.00001 Std.Error of estimate: 1.5993

	B	*St. Err. of B*	*t(8)*	*p-level*
Intercept	50.45	4.87	10.37	0.00
% non sulphide PGEM	0.18	0.02	8.18	0.00
pn/(pn+mil)	18.12	4.03	4.50	0.00
PGEM pred. degree of liberation	-0.63	0.10	-6.07	0.00

Regression Summary for Dependent Variable: R_s **A4 excluded**
R= .95388385 R^2= .90989441 Adjusted R^2= .87610481
F(3,8)=26.928 p<.00016 Std.Error of estimate: 2.0422

	B	*St. Err. of B*	*t(8)*	*p-level*
Intercept	45.98	6.00	7.67	0.00
% non sulphide PGEM	0.21	0.04	5.66	0.00
pn/(pn+mil)	13.74	4.86	2.82	0.02
PGEM pred. degree of liberation	-0.54	0.13	-4.20	0.00

Regression Summary for Dependent Variable: R_s **B4 excluded**
R= .95113706 R^2= .90466172 Adjusted R^2= .86890986
F(3,8)=25.304 p<.00020 Std.Error of estimate: 1.7668

	B	*St. Err. of B*	*t(8)*	*p-level*
Intercept	45.39	5.16	8.80	0.00
% non sulphide PGEM	0.16	0.03	5.98	0.00
pn/(pn+mil)	13.49	4.15	3.25	0.01
PGEM pred. degree of liberation	-0.52	0.11	-4.69	0.00

Regression Summary for Dependent Variable: R_s **C1 excluded**
R= .96326816 R^2= .92788555 Adjusted R^2= .90084263
F(3,8)=34.312 p<.00006 Std.Error of estimate: 2.1017

	B	*St. Err. of B*	*t(8)*	*p-level*
Intercept	46.67	6.20	7.52	0.00
% non sulphide PGEM	0.19	0.03	6.83	0.00
pn/(pn+mil)	14.44	4.90	2.95	0.02
PGEM pred. degree of liberation	-0.55	0.13	-4.21	0.00

Regression Summary for Dependent Variable: R_s **C2 excluded**
R= .96354958 R^2= .92842780 Adjusted R^2= .90158823
F(3,8)=34.592 p<.00006 Std.Error of estimate: 2.0978

	B	*St. Err. of B*	*t(8)*	*p-level*
Intercept	46.94	6.15	7.63	0.00
% non sulphide PGEM	0.19	0.03	6.83	0.00
pn/(pn+mil)	14.41	4.89	2.95	0.02
PGEM pred. degree of liberation	-0.55	0.13	-4.26	0.00

Table 4b continued *Regression summary for dependent variable R_s with % non-sulphide PGE mineral, pn/(pn+mil) ratio and the predicted PGE mineral degree of liberation as independent variables, in turn excluding sample A5 and one other sample.*

Regression Summary for Dependent Variable: R_s				**C3 excluded**
R= .96336193 R^2= .92806621 Adjusted R^2= .90109103				
F(3,8)=34.404 p<.00006 Std.Error of estimate: 2.1021				
	B	*St. Err. of B*	*t(8)*	*p-level*
Intercept	46.70	6.33	7.37	0.00
% non sulphide PGEM	0.19	0.03	6.80	0.00
pn/(pn+mil)	14.42	4.93	2.92	0.02
PGEM pred. degree of liberation	-0.55	0.13	-4.14	0.00
Regression Summary for Dependent Variable: R_s				**C4 excluded**
R= .96478014 R^2=.93080071 Adjusted R^2= .90485098				
F(3,8)=35.869 p<.00005 Std.Error of estimate: 2.0399				
	B	*St. Err. of B*	*t(8)*	*p-level*
Intercept	46.61	5.89	7.91	0.00
% non sulphide PGEM	0.19	0.03	7.06	0.00
pn/(pn+mil)	13.65	4.88	2.80	0.02
PGEM pred. degree of liberation	-0.54	0.13	-4.26	0.00
Regression Summary for Dependent Variable: R_s				**C5 excluded**
R= .96707458 R^2= .93523324 Adjusted R^2= .91094570				
F(3,8)=38.507 p<.00004 Std.Error of estimate: 1.9873				
	B	*St. Err. of B*	*t(8)*	*p-level*
Intercept	47.92	5.86	8.17	0.00
% non sulphide PGEM	0.19	0.03	7.12	0.00
pn/(pn+mil)	16.14	4.95	3.26	0.01
PGEM pred. degree of liberation	-0.59	0.13	-4.59	0.00

Table 5 *Regression summary for dependent variable 100-U with sample A5 excluded.*

R= .80333529 R^2= .64534759 Adjusted R^2= .14883422 F(7,5)=1.2998 p<.39968 Std.Error of estimate: 1.8567				
	B	*St. Err. of B*	*t(5)*	*p-level*
Intercept	12.99	12.38	1.05	0.34
% non-sulphide PGE mineral	-0.03	0.04	-0.71	0.51
PGEM grain diameter at <2mm	0.12	3.43	0.04	0.97
pentlandite content	0.82	108.18	0.01	0.99
BMS grain diameter 1	0.12	0.23	0.54	0.61
pn/(pn+mil)	7.46	7.85	0.95	0.39
Predicted BMS liberation	0.08	0.08	0.99	0.37
Predicted PGEM liberation	-0.31	0.15	-2.11	0.09

Table 6 *Regression summary for dependent variable k_f. All fourteen samples included.*

R= .95863501 R^2= .91898107 Adjusted R^2= .64891799 F(10,3)=3.4028 p<.17100 Std.Error of estimate: .19175				
	B	*St. Err. of B*	*t(3)*	*p-level*
Intercept	1.76	1.23	1.44	0.25
% non-sulphide PGE mineral	0.00	0.00	0.33	0.76
PGEM grain diameter at <2mm	-0.90	0.44	-2.02	0.14
pentlandite content	-30.08	14.27	-2.11	0.13
Nickel content	0.00	0.00	0.22	0.84
PGE+Au content	0.19	0.15	1.28	0.29
Copper content	0.00	0.00	-0.02	0.98
BMS grain diameter at <2mm	-0.01	0.02	-0.62	0.58
pn/(pn+mil)	0.86	0.57	1.51	0.23
Predicted BMS liberation	0.02	0.01	2.13	0.12
Predicted PGEM liberation	0.02	0.01	1.48	0.23

Table 7 *Regression summary for dependent variable k_s. All fourteen samples included.*

R= .94431250 R^2= .89172610 Adjusted R^2= .53081309 F(10,3)=2.4708 p<.24710 Std.Error of estimate: .01813				
	B	*St. Err. of B*	*t(3)*	*p-level*
Intercept	0.19	0.12	1.63	0.20
% non-sulphide PGE mineral	0.00	0.00	0.33	0.76
PGEM grain diameter at <2mm	-0.01	0.04	-0.12	0.91
pentlandite content	1.01	1.35	0.75	0.51
Nickel content	0.00	0.00	-3.16	0.05
PGE+Au content	0.00	0.01	-0.27	0.81
Copper content	0.00	0.00	1.36	0.27
BMS grain diameter at <2mm	0.00	0.00	-1.04	0.37
pn/(pn+mil)	-0.06	0.05	-1.14	0.34
Predicted BMS liberation	0.00	0.00	0.40	0.72
Predicted PGEM liberation	0.00	0.00	1.38	0.26

Table 8a *Observed and predicted values for R_f with % non-sulphide PGE mineral and the PGE mineral degree of liberation as independent variables as independent variables, in turn excluding one of the samples.*

Sample number	**R_f Observed**	**R_f Predicted (n=14)**	***R_f Predicted (n=13)**	**R_f Observed – *R_f predicted**
A2	75.1	75.4	75.5	-0.4
B2	80.3	77.5	77.0	3.3
A1	79.8	79.5	79.4	0.4
B1	73.8	69.7	69.3	4.5
A3	63.4	69.6	70.4	-7.0
B3	74.4	72.4	72.2	2.2
A4	59.9	59.2	59.0	1.0
B4	56.5	60.9	63.1	-6.6
A5	39.7	38.3	33.8	5.9
C1	66.3	72.1	73.0	-6.6
C2	71.5	71.3	71.3	0.2
C3	68.2	66.7	66.3	1.9
C4	74.8	70.6	69.9	5.0
C5	74.8	75.3	75.3	-0.5

**R_f predicted : Value of R_f determined from the regression equation calculated from the other 13 samples.*

Table 8b *Regression summary for dependent variable R_f with % non-sulphide PGE mineral and the PGE mineral degree of liberation as independent variables, in turn excluding one sample.*

Regression Summary for Dependent Variable: R_f **A2 excluded**
R= .96031566 R^2= .92220617 Adjusted R^2= .90664740
F(2,10)=59.272 p<.00000 Std.Error of estimate: 3.4096

	B	*St. Err. of B*	*t(10)*	*p-level*
Intercept	40.80	5.54	7.37	0.00
PGEM degree of liberation	0.47	0.07	6.48	0.00
% non sulphide PGEM	-0.31	0.03	-9.62	0.00

Regression Summary for Dependent Variable: R_f **B2 excluded**
R= .95891845 R^2= .91952459 Adjusted R^2= .90342951
F(2,10)=57.131 p<.00000 Std.Error of estimate: 3.3444

	B	*St. Err. of B*	*t(10)*	*p-level*
Intercept	41.49	5.53	7.50	0.00
PGEM degree of liberation	0.46	0.07	6.20	0.00
% non sulphide PGEM	-0.30	0.03	-9.67	0.00

Regression Summary for Dependent Variable: R_f **A1 excluded**
R= .95769222 R^2= .91717438 Adjusted R^2= .90060926
F(2,10)=55.368 p<.00000 Std.Error of estimate: 3.4093

	B	*St. Err. of B*	*t(10)*	*p-level*
Intercept	40.50	5.80	6.99	0.00
PGEM degree of liberation	0.47	0.08	6.10	0.00
% non sulphide PGEM	-0.31	0.03	-9.61	0.00

Regression Summary for Dependent Variable: R_f **B1 excluded**
R= .96636749 R^2= .93386613 Adjusted R^2= .92063935
F(2,10)=70.604 p<.00000 Std.Error of estimate: 3.1607

	B	St. Err. of B	t(10)	p-level
Intercept	41.46	5.16	8.04	0.00
PGEM degree of liberation	0.46	0.07	6.74	0.00
% non sulphide PGEM	-0.31	0.03	-10.58	0.00

Regression Summary for Dependent Variable: R_f **A3 excluded**
R= .97587086 R^2= .95232394 Adjusted R^2= .94278873
F(2,10)=99.874 p<.00000 Std.Error of estimate: 2.6865

	B	*St. Err. of B*	*t(10)*	*p-level*
Intercept	43.09	4.46	9.66	0.00
PGEM degree of liberation	0.45	0.06	7.78	0.00
% non sulphide PGEM	-0.31	0.02	-12.62	0.00

Regression Summary for Dependent Variable: R_f **B3 excluded**
R= .96172249 R^2= .92491014 Adjusted R^2= .90989217
F(2,10)=61.587 p<.00000 Std.Error of estimate: 3.3604

	B	*St. Err. of B*	*t(10)*	*p-level*
Intercept	41.16	5.49	7.49	0.00
PGEM degree of liberation	0.46	0.07	6.39	0.00
% non sulphide PGEM	-0.31	0.03	-9.89	0.00

Table 8b continued *Regression summary for dependent variable R_f with % non-sulphide PGE mineral and the PGE mineral degree of liberation as independent variables, in turn excluding one sample.*

Regression Summary for Dependent Variable: R_f				**A4 excluded**
R= .96033113 R^2= .92223588 Adjusted R^2= .90668306				
F(2,10)=59.297 p<.00000 Std.Error of estimate: 3.3729				
	B	*St. Err. of B*	*t(10)*	*p-level*
Intercept	41.90	5.91	7.09	0.00
PGEM degree of liberation	0.46	0.08	5.98	0.00
% non sulphide PGEM	-0.32	0.04	-8.62	0.00
Regression Summary for Dependent Variable: R_f				**B4 excluded**
R= .96412672 R^2= .92954033 Adjusted R^2= .91544840				
F(2,10)=65.963 p<.00000 Std.Error of estimate: 3.1269				
	B	*St. Err. of B*	*t(10)*	*p-level*
Intercept	38.37	5.37	7.15	0.00
PGEM degree of liberation	0.50	0.07	7.15	0.00
% non sulphide PGEM	-0.29	0.03	-8.78	0.00
Regression Summary for Dependent Variable: R_f				**A5 excluded**
R= .90792959 R^2= .82433615 Adjusted R^2= .78920337				
F(2,10)=23.463 p<.00017 Std.Error of estimate: 3.3758				
	B	*St. Err. of B*	*t(10)*	*p-level*
Intercept	37.67	8.54	4.41	0.00
PGEM degree of liberation	0.51	0.12	4.40	0.00
% non sulphide PGEM	-0.32	0.05	-6.85	0.00
Regression Summary for Dependent Variable: R_f				**C1 excluded**
R= .96778781 R^2= .93661324 Adjusted R^2= .92393589				
F(2,10)=73.881 p<.00000 Std.Error of estimate: 3.1208				
	B	*St. Err. of B*	*t(10)*	*p-level*
Intercept	42.15	5.16	8.17	0.00
PGEM degree of liberation	0.46	0.07	6.86	0.00
% non sulphide PGEM	-0.31	0.03	-10.77	0.00
Regression Summary for Dependent Variable: R_f				**C2 excluded**
R= .96125836 R^2= .92401764 Adjusted R^2= .90882117				
F(2,10)=60.805 p<.00000 Std.Error of estimate: 3.4116				
	B	*St. Err. of B*	*t(10)*	*p-level*
Intercept	40.94	5.65	7.24	0.00
PGEM degree of liberation	0.47	0.07	6.41	0.00
% non sulphide PGEM	-0.31	0.03	-9.62	0.00
Regression Summary for Dependent Variable: R_f				**C3 excluded**
R= .96276503 R^2= .92691650 Adjusted R^2= .91229981				
F(2,10)=63.415 p<.00000 Std.Error of estimate: 3.3564				
	B	*St. Err. of B*	*t(10)*	*p-level*
Intercept	39.36	5.97	6.59	0.00
PGEM degree of liberation	0.49	0.08	6.37	0.00
% non sulphide PGEM	-0.30	0.03	-9.74	0.00

Table 8b continued *Regression summary for dependent variable R_f with % non-sulphide PGE mineral and the PGE mineral degree of liberation as independent variables, in turn excluding one sample.*

Regression Summary for Dependent Variable: R_f **C4 excluded** R= .96800335 R^2= .93703048 Adjusted R^2= .92443658 F(2,10)=74.403 p<.00000 Std.Error of estimate: 3.0710				
	B	*St. Err. of B*	*t(10)*	*p-level*
Intercept	38.68	5.17	7.48	0.00
PGEM degree of liberation	0.49	0.07	7.36	0.00
% non sulphide PGEM	-0.30	0.03	-10.39	0.00
Regression Summary for Dependent Variable: R_f **C5 excluded** R= .96043776 R^2= .92244070 Adjusted R^2= .90692884 F(2,10)=59.467 p<.00000 Std.Error of estimate: 3.4092				
	B	*St. Err. of B*	*t(10)*	*p-level*
Intercept	40.84	5.54	7.37	0.00
PGEM degree of liberation	0.47	0.07	6.49	0.00
% non sulphide PGEM	-0.31	0.03	-9.60	0.00

Table 9a *Observed and predicted values for R_f with % non-sulphide PGE mineral PGE mineral degree of liberation, base-metal sulphide degree of liberation, PGE mineral grain size prior, pentlandite/(pentlandite+millerite), and the PGE mineral degree of liberation as independent variables, in turn excluding one of the samples.*

Sample number	**R_f Observed**	**R_f Predicted (n=14)**	***R_f Predicted (n=13)**	**R_f Observed – *R_f predicted**
A2	79.8	78.3	77.8	2.0
B2	75.1	73.5	72.9	2.2
A1	63.4	64.8	66.5	-3.1
B1	73.8	74.9	75.6	-1.8
A3	80.3	80.2	76.3	4.0
B3	66.3	69.5	69.3	-3.0
A4	71.5	73.1	74.0	-2.6
B4	68.2	67.8	67.7	0.5
A5	74.8	71.9	70.7	4.2
C1	74.8	73.1	70.3	4.5
C2	59.9	59.4	58.7	1.2
C3	39.7	39.0	35.0	4.6
C4	74.4	75.8	76.4	-2.0
C5	56.5	57.0	58.6	-2.0

**R_f predicted : Value of R_f determined from the regression equation calculated from the other 13 samples.*

Table 9b *Regression summary for dependent variable R_f with % non-sulphide PGE mineral, PGE mineral degree of liberation, base-metal sulphide degree of liberation, PGE mineral grain size prior, pentlandite/(pentlandite+millerite) to milling as independent variables, in turn excluding one sample.*

Regression Summary for Dependent Variable: R_f				**A2 excluded**
R= .99231764 R^2= .98469429 Adjusted R^2= .97376164				
F(5,7)=90.069 p<.00000 Std.Error of estimate: 1.8076				
	B	*St. Err. of B*	*t(7)*	*p-level*
Intercept	63.12	6.34	9.96	0.00
PGEM degree of liberation	0.48	0.04	11.00	0.00
% non-sulphide PGEM	-0.33	0.02	-13.99	0.00
PGEM grain diameter <2mm	-9.69	1.93	-5.01	0.00
BMS degree of liberation	0.08	0.03	2.67	0.03
pn/(pn+millerite)	-8.60	2.22	-3.87	0.01
Regression Summary for Dependent Variable: R_f				**B2 excluded**
R= .99023825 R^2= .98057179 Adjusted R^2= .96669449				
F(5,7)=70.660 p<.00001 Std.Error of estimate: 1.9640				
	B	*St. Err. of B*	*t(7)*	*p-level*
Intercept	62.20	6.87	9.06	0.00
PGEM degree of liberation	0.47	0.05	9.97	0.00
% non-sulphide PGEM	-0.34	0.03	-12.85	0.00
PGEM grain diameter <2mm	-9.23	2.11	-4.37	0.00
BMS degree of liberation	0.08	0.03	2.38	0.05
pn/(pn+millerite)	-7.58	2.20	-3.44	0.01
Regression Summary for Dependent Variable: R_f				**A1 excluded**
R= .99057140 R^2= .98123170 Adjusted R^2= .96782577				
F(5,7)=73.194 p<.00001 Std.Error of estimate: 1.9397				
	B	*St. Err. of B*	*t(7)*	*p-level*
Intercept	62.80	6.93	9.07	0.00
PGEM degree of liberation	0.47	0.05	9.74	0.00
% non-sulphide PGEM	-0.34	0.03	-13.36	0.00
PGEM grain diameter <2mm	-9.28	2.03	-4.57	0.00
BMS degree of liberation	0.08	0.03	2.42	0.05
pn/(pn+millerite)	-7.79	2.23	-3.49	0.01
Regression Summary for Dependent Variable: R_f				**B1 excluded**
R= .99120020 R^2= .98247784 Adjusted R^2= .96996200				
F(5,7)=78.499 p<.00001 Std.Error of estimate: 1.9445				
	B	*St. Err. of B*	*t(7)*	*p-level*
Intercept	63.20	7.30	8.66	0.00
PGEM degree of liberation	0.47	0.05	10.18	0.00
% non-sulphide PGEM	-0.34	0.03	-13.21	0.00
PGEM grain diameter <2mm	-9.64	2.35	-4.10	0.00
BMS degree of liberation	0.08	0.03	2.43	0.05
pn/(pn+millerite)	-7.78	2.24	-3.47	0.01

Table 9b continued *Regression summary for dependent variable R_f with % non-sulphide PGE mineral, PGE mineral degree of liberation, base-metal sulphide degree of liberation, PGE mineral grain size prior, pentlandite/(pentlandite+millerite) to milling as independent variables, in turn excluding one sample.*

Regression Summary for Dependent Variable: R_f				**A3 excluded**
R= .99237798 R^2= .98481405 Adjusted R^2= .97396694				
F(5,7)=90.790 p<.00000 Std.Error of estimate: 1.8122				
	B	*St. Err. of B*	*t(7)*	*p-level*
Intercept	60.07	6.54	9.18	0.00
PGEM degree of liberation	0.45	0.05	9.45	0.00
% non-sulphide PGEM	-0.34	0.02	-14.61	0.00
PGEM grain diameter <2mm	-7.71	2.28	-3.38	0.01
BMS degree of liberation	0.07	0.03	2.15	0.07
pn/(pn+millerite)	-5.50	2.74	-2.00	0.09
Regression Summary for Dependent Variable: R_f				**B3 excluded**
R= .99141211 R^2= .98289798 Adjusted R^2= .97068224				
F(5,7)=80.462 p<.00000 Std.Error of estimate: 1.9168				
	B	*St. Err. of B*	*t(7)*	*p-level*
Intercept	63.33	6.96	9.10	0.00
PGEM degree of liberation	0.47	0.05	10.33	0.00
% non-sulphide PGEM	-0.35	0.03	-13.33	0.00
PGEM grain diameter <2mm	-9.64	2.14	-4.50	0.00
BMS degree of liberation	0.08	0.03	2.46	0.04
pn/(pn+millerite)	-7.61	2.15	-3.55	0.01
Regression Summary for Dependent Variable: R_f				**A4 excluded**
R= .99094658 R^2= .98197513 Adjusted R^2= .96910022				
F(5,7)=76.270 p<.00001 Std.Error of estimate: 1.9409				
	B	*St. Err. of B*	*t(7)*	*p-level*
Intercept	62.20	6.74	9.23	0.00
PGEM degree of liberation	0.46	0.05	8.81	0.00
% non-sulphide PGEM	-0.35	0.03	-12.41	0.00
PGEM grain diameter <2mm	-9.00	2.04	-4.41	0.00
BMS degree of liberation	0.08	0.03	2.45	0.04
pn/(pn+millerite)	-7.34	2.23	-3.29	0.01
Regression Summary for Dependent Variable: R_f				**B4 excluded**
R= .99025840 R^2= .98061170 Adjusted R^2= .96676291				
F(5,7)=70.808 p<.00001 Std.Error of estimate: 1.9605				
	B	*St. Err. of B*	*t(7)*	*p-level*
Intercept	60.25	10.99	5.48	0.00
PGEM degree of liberation	0.48	0.05	8.84	0.00
% non-sulphide PGEM	-0.33	0.04	-7.84	0.00
PGEM grain diameter <2mm	-8.73	2.83	-3.09	0.02
BMS degree of liberation	0.08	0.04	2.28	0.06
pn/(pn+millerite)	-7.56	2.19	-3.45	0.01

Table 9b continued *Regression summary for dependent variable R_f with % non-sulphide PGE mineral, PGE mineral degree of liberation, base-metal sulphide degree of liberation, PGE mineral grain size prior, pentlandite/(pentlandite+millerite) to milling as independent variables, in turn excluding one sample.*

Regression Summary for Dependent Variable: R_f				**A5 excluded**
R= .97920845 R^2= .95884918 Adjusted R^2= .92945574				
F(5,7)=32.621 p<.00010 Std.Error of estimate: 1.9529				
	B	*St. Err. of B*	*t(7)*	*p-level*
Intercept	59.42	10.81	5.50	0.00
PGEM degree of liberation	0.50	0.10	5.21	0.00
% non-sulphide PGEM	-0.34	0.03	-12.26	0.00
PGEM grain diameter <2mm	-8.91	2.16	-4.13	0.00
BMS degree of liberation	0.08	0.03	2.38	0.05
pn/(pn+millerite)	-7.88	2.40	-3.28	0.01
Regression Summary for Dependent Variable: R_f				**C1 excluded**
R= .99316814 R^2= .98638296 Adjusted R^2= .97665651				
F(5,7)=101.41 p<.00000 Std.Error of estimate: 1.7289				
	B	*St. Err. of B*	*t(7)*	*p-level*
Intercept	62.23	6.00	10.37	0.00
PGEM degree of liberation	0.48	0.04	11.52	0.00
% non-sulphide PGEM	-0.34	0.02	-15.26	0.00
PGEM grain diameter <2mm	-8.67	1.82	-4.75	0.00
BMS degree of liberation	0.06	0.03	1.94	0.09
pn/(pn+millerite)	-7.64	1.94	-3.95	0.01
Regression Summary for Dependent Variable: R_f				**C2 excluded**
R= .99406352 R^2= .98816227 Adjusted R^2= .97970675				
F(5,7)=116.87 p<.00000 Std.Error of estimate: 1.6095				
	B	*St. Err. of B*	*t(7)*	*p-level*
Intercept	61.87	5.59	11.07	0.00
PGEM degree of liberation	0.47	0.04	12.31	0.00
% non-sulphide PGEM	-0.34	0.02	-16.12	0.00
PGEM grain diameter <2mm	-9.38	1.67	-5.60	0.00
BMS degree of liberation	0.10	0.03	3.42	0.01
pn/(pn+millerite)	-9.31	2.03	-4.58	0.00
Regression Summary for Dependent Variable: R_f				**C3 excluded**
R= .99140382 R^2= .98288153 Adjusted R^2= .97065406				
F(5,7)=80.383 p<.00000 Std.Error of estimate: 1.9415				
	B	*St. Err. of B*	*t(7)*	*p-level*
Intercept	61.79	6.77	9.12	0.00
PGEM degree of liberation	0.48	0.05	9.85	0.00
% non-sulphide PGEM	-0.34	0.02	-13.64	0.00
PGEM grain diameter <2mm	-9.15	2.01	-4.55	0.00
BMS degree of liberation	0.07	0.03	2.14	0.07
pn/(pn+millerite)	-7.32	2.24	-3.26	0.01

Table 9b continued *Regression summary for dependent variable R_f with % non-sulphide PGE mineral, PGE mineral degree of liberation, base-metal sulphide degree of liberation, PGE mineral grain size prior, pentlandite/(pentlandite+millerite) to milling as independent variables, in turn excluding one sample.*

Regression Summary for Dependent Variable: R_f **C4 excluded** R= .99504397 R R^2= .99011250 Adjusted R^2= .98305001 F(5,7)=140.19 p<.00000 Std.Error of estimate: 1.4545				
	B	*St. Err. of B*	*t(7)*	*p-level*
Intercept	61.62	5.05	12.20	0.00
PGEM degree of liberation	0.48	0.03	13.72	0.00
% non-sulphide PGEM	-0.34	0.02	-18.33	0.00
PGEM grain diameter <2mm	-9.00	1.51	-5.96	0.00
BMS degree of liberation	0.06	0.03	2.32	0.05
pn/(pn+millerite)	-6.01	1.75	-3.43	0.01
Regression Summary for Dependent Variable: R_f **C5 excluded** R= .99169877 R^2= .98346645 Adjusted R^2= .97165678 F(5,7)=83.276 p<.00000 Std.Error of estimate: 1.8813				
	B	*St. Err. of B*	*t(7)*	*p-level*
Intercept	60.24	6.92	8.71	0.00
PGEM degree of liberation	0.46	0.05	9.66	0.00
% non-sulphide PGEM	-0.33	0.03	-12.93	0.00
PGEM grain diameter <2mm	-9.03	1.96	-4.62	0.00
BMS degree of liberation	0.11	0.05	2.31	0.05
pn/(pn+millerite)	-7.65	2.11	-3.63	0.01

Table 10a *Observed and predicted values for variable R_s with % non-sulphide PGE mineral, PGE mineral degree of liberation, chromite grain diameter and PGE mineral diameter prior to milling, as independent variables, in turn excluding one of the samples.*

Sample number	R_s Observed	R_s Predicted (n=14)	*R_s Predicted (n=13)	R_s Observed – *R_s predicted
A2	16.3	17.5	18.3	-1.2
B2	18.8	18.4	18.4	0.4
A1	25.9	25.9	26.0	-0.1
B1	19.6	19.5	19.5	0.1
A3	15.3	15.6	15.7	-0.3
B3	24.5	24.4	24.4	0.2
A4	22.6	23.0	23.1	-0.5
B4	24.0	24.8	24.9	-0.9
A5	19.9	18.9	18.3	1.0
C1	21.1	20.7	20.6	0.4
C2	33.7	34.0	34.0	-0.3
C3	28.7	28.9	30.8	-0.2
C4	21.0	20.2	19.8	0.8
C5	37.7	37.3	36.4	0.4

*R_s predicted : *Value of R_s determined from the regression equation calculated for the other 13 samples.*

Table 10b *Regression summary for dependent variable R_s with % non-sulphide PGE mineral, PGE mineral degree of liberation, chromite grain diameter and PGE mineral diameter prior to milling as independent variables, in turn excluding one sample.*

Regression Summary for Dependent Variable: R_s				**A2 excluded**
R= .99640518 R^2= .99282328 Adjusted R^2= .98923491				
$F(4,8)$=276.68 p<.00000 Std.Error of estimate: .66807				
	B	*St. Err. of B*	*t(8)*	*p-level*
Intercept	-6.02	2.14	-2.81	0.02
PGEM degree of liberation	-0.16	0.02	-7.29	0.00
% non-sulphide PGEM	0.20	0.01	19.97	0.00
PGEM ECD <2mm	5.98	0.69	8.65	0.00
Chromite ECD <2mm	0.13	0.01	10.32	0.00
Regression Summary for Dependent Variable: R_s				**B2 excluded**
R= .99594658 R^2= .99190959 Adjusted R^2= .98786439				
$F(4,8)$=245.21 p<.00000 Std.Error of estimate: .67398				
	B	*St. Err. of B*	*t(8)*	*p-level*
Intercept	-5.94	2.19	-2.71	0.03
PGEM degree of liberation	-0.16	0.02	-6.82	0.00
% non-sulphide PGEM	0.20	0.01	19.52	0.00
PGEM ECD <2mm	5.99	0.70	8.55	0.00
Chromite ECD <2mm	0.12	0.01	9.95	0.00

Table 10b continued *Regression summary for dependent variable R_s with % non-sulphide PGE mineral, PGE mineral degree of liberation, chromite grain diameter and PGE mineral diameter prior to milling as independent variables, in turn excluding one sample.*

Regression Summary for Dependent Variable: R_s **A1 excluded** *R= .99638789 R^2= .99278883 Adjusted R^2= .98918324* *$F(4,8)$=275.35 p<.00000 Std.Error of estimate: .66609*				
	B	*St. Err. of B*	*t(8)*	*p-level*
Intercept	-3.96	4.43	-0.90	0.40
PGEM degree of liberation	-0.17	0.03	-6.06	0.00
% non-sulphide PGEM	0.21	0.02	12.39	0.00
PGEM ECD <2mm	5.94	0.70	8.46	0.00
Chromite ECD <2mm	0.12	0.02	6.61	0.00
Regression Summary for Dependent Variable: R_s **B1 excluded** *R= .99636838 R^2= .99274995 Adjusted R^2= .98912492* *$F(4,8)$=273.86 p<.00000 Std.Error of estimate: .67678*				
	B	*St. Err. of B*	*t(8)*	*p-level*
Intercept	-5.88	2.38	-2.47	0.04
PGEM degree of liberation	-0.16	0.02	-7.22	0.00
% non-sulphide PGEM	0.20	0.01	18.25	0.00
PGEM ECD <2mm	5.95	0.81	7.38	0.00
Chromite ECD <2mm	0.13	0.01	10.19	0.00
Regression Summary for Dependent Variable: R_s **A3 excluded** *R= .99640518 R^2= .99282328 Adjusted R^2= .98923491* *$F(4,8)$=276.68 p<.00000 Std.Error of estimate: .66807*				
	B	St. Err. of B	t(8)	p-level
Intercept	-6.02	2.14	-2.81	0.02
PGEM degree of liberation	-0.16	0.02	-7.29	0.00
% non-sulphide PGEM	0.20	0.01	19.97	0.00
PGEM ECD <2mm	5.98	0.69	8.65	0.00
Chromite ECD <2mm	0.13	0.01	10.32	0.00
Regression Summary for Dependent Variable: R_s **A4 excluded** *R= .99571841 R^2= .99145516 Adjusted R^2= .98718274* *$F(4,8)$=232.06 p<.00000 Std.Error of estimate: .66131*				
	B	St. Err. of B	t(8)	p-level
Intercept	-6.29	2.16	-2.91	0.02
PGEM degree of liberation	-0.16	0.02	-7.42	0.00
% non-sulphide PGEM	0.20	0.01	19.86	0.00
PGEM ECD <2mm	5.94	0.69	8.61	0.00
Chromite ECD <2mm	0.13	0.01	10.24	0.00

Table 10 continued *Regression summary for dependent variable R_s with % non-sulphide PGE mineral, PGE mineral degree of liberation, chromite grain diameter and PGE mineral diameter prior to milling as independent variables, in turn excluding one sample.*

Regression Summary for Dependent Variable: R_s				**B3 excluded**
R= .99714580 R^2= .99429975 Adjusted R^2= .99144963				
$F(4,8)$=348.86 p<.00000 Std.Error of estimate: .60564				
	B	*St. Err. of B*	*t(8)*	*p-level*
Intercept	-7.12	2.09	-3.41	0.01
PGEM degree of liberation	-0.16	0.02	-7.56	0.00
% non-sulphide PGEM	0.21	0.01	20.22	0.00
PGEM ECD <2mm	6.56	0.73	8.96	0.00
Chromite ECD <2mm	0.12	0.01	10.31	0.00
Regression Summary for Dependent Variable: R_s				**B4 excluded**
R= .99485165 R^2= .98972981 Adjusted R^2= .98459472				
$F(4,8)$=192.74 p<.00000 Std.Error of estimate: .62593				
	B	*St. Err. of B*	*t(8)*	*p-level*
Intercept	-3.48	2.96	-1.18	0.27
PGEM degree of liberation	-0.18	0.02	-7.48	0.00
% non-sulphide PGEM	0.19	0.01	13.98	0.00
PGEM ECD <2mm	5.36	0.85	6.29	0.00
Chromite ECD <2mm	0.13	0.01	11.23	0.00
Regression Summary for Dependent Variable: R_s				**A5 excluded**
R= .99638789 R^2= .99278883 Adjusted R^2= .98918324				
$F(4,8)$=275.35 p<.00000 Std.Error of estimate: .66609				
	B	St. Err. of B	t(8)	p-level
Intercept	-3.96	4.43	-0.90	0.40
PGEM degree of liberation	-0.17	0.03	-6.06	0.00
% non-sulphide PGEM	0.21	0.02	12.39	0.00
PGEM ECD <2mm	5.94	0.70	8.46	0.00
Chromite ECD <2mm	0.12	0.02	6.61	0.00
Regression Summary for Dependent Variable: R_s				**C1 excluded**
R= .99699872 R^2= .99400644 Adjusted R^2= .99100967				
$F(4,8)$=331.69 p<.00000 Std.Error of estimate: .62448				
	B	St. Err. of B	t(8)	p-level
Intercept	-6.36	2.02	-3.14	0.01
PGEM degree of liberation	-0.17	0.02	-7.95	0.00
% non-sulphide PGEM	0.20	0.01	21.34	0.00
PGEM ECD <2mm	6.14	0.65	9.43	0.00
Chromite ECD <2mm	0.13	0.01	11.24	0.00

Table 10 continued *Regression summary for dependent variable R_s with % non-sulphide PGE mineral, PGE mineral degree of liberation, chromite grain diameter and PGE mineral diameter prior to milling as independent variables, in turn excluding one sample.*

Regression Summary for Dependent Variable: R_s **C2 excluded** *R= .99646806 R^2= .99294860 Adjusted R^2= .98942290* *$F(4,8)$=281.63 p<.00000 Std.Error of estimate: .67745*				
	B	St. Err. of B	t(8)	p-level
Intercept	-6.03	2.18	-2.77	0.02
PGEM degree of liberation	-0.16	0.02	-7.21	0.00
% non-sulphide PGEM	0.20	0.01	19.68	0.00
PGEM ECD <2mm	6.01	0.70	8.55	0.00
Chromite ECD <2mm	0.12	0.01	10.30	0.00
Regression Summary for Dependent Variable: R_s **C3 excluded** *R= .99730367 R^2= .99461461 Adjusted R^2= .99192191* *$F(4,8)$=369.38 p<.00000 Std.Error of estimate: .59246*				
	B	*St. Err. of B*	*t(8)*	*p-level*
Intercept	-5.49	1.93	-2.84	0.02
PGEM degree of liberation	-0.18	0.02	-8.02	0.00
% non-sulphide PGEM	0.20	0.01	21.36	0.00
PGEM ECD <2mm	5.90	0.61	9.61	0.00
Chromite ECD <2mm	0.13	0.01	11.50	0.00
Regression Summary for Dependent Variable: R_s **C4 excluded** *R= .99716555 R^2= .99433913 Adjusted R^2= .99150870* *$F(4,8)$=351.30 p<.00000 Std.Error of estimate: .59931*				
	B	St. Err. of B	t(8)	p-level
Intercept	-5.87	1.93	-3.05	0.02
PGEM degree of liberation	-0.17	0.02	-8.30	0.00
% non-sulphide PGEM	0.20	0.01	21.05	0.00
PGEM ECD <2mm	5.61	0.68	8.31	0.00
Chromite ECD <2mm	0.13	0.01	11.03	0.00
Regression Summary for Dependent Variable: R_s **C5 excluded** *R= .99668489 R^2= .99338078 Adjusted R^2= .99007116* *$F(4,8)$=300.15 p<.00000 Std.Error of estimate: .65301*				
	B	*St. Err. of B*	*t(8)*	*p-level*
Intercept	-6.01	2.10	-2.87	0.02
PGEM degree of liberation	-0.16	0.02	-7.52	0.00
% non-sulphide PGEM	0.20	0.01	20.37	0.00
PGEM ECD <2mm	6.01	0.67	8.94	0.00
Chromite ECD <2mm	0.12	0.01	10.66	0.00

Table 11 *Regression summary for dependent variable 100-U excluding sample A5.*

$R= .88368204\ R^2= .78089395$ Adjusted $R^2= .56178790$ $F(6,6)=3.5640\ p<.07365$ Std.Error of estimate: 1.3322				
	B	*St. Err. of B*	*t(6)*	*p-level*
Intercept	21.42	6.50	3.29	0.02
PGEM degree of liberation	-0.33	0.08	-3.98	0.01
% non-sulphide PGEM	0.06	0.03	2.35	0.06
PGEM ECD 80%<75µm	3.63	3.51	1.03	0.34
BMS degree of liberation	-0.05	0.03	-1.75	0.13
BMS ECD 80%<75µm	0.25	0.19	1.30	0.24
pn/(pn+mil)	5.61	2.38	2.36	0.06

Table 12 *Regression summary for dependent variable k_f. All fourteen samples included.*

$R= .92487051\ R^2= .85538547$ Adjusted $R^2=$ ----- $F(12,1)=.49291\ p<.82017$ Std.Error of estimate: .44372				
	B	St. Err. of B	t(1)	p-level
Intercept	1.39	8.83	0.16	0.90
PGEM degree of liberation	0.01	0.03	0.48	0.72
% non-sulphide PGEM	0.00	0.01	-0.09	0.95
PGEM ECD 80%<75µm	0.51	1.20	0.42	0.74
pentlandite content	-20.52	31.24	-0.66	0.63
PGEM/(PGEM+BMS)	-2.28	6.69	-0.34	0.79
Chromite ECD <2mm	0.00	0.03	0.02	0.98
BMS degree of liberation	0.00	0.01	0.24	0.85
BMS ECD 80%<75µm	-0.03	0.10	-0.29	0.82
pn/(pn+mil)	0.81	1.67	0.48	0.71

Table 13 *Regression summary for dependent variable k_s. All fourteen samples included.*

$R= .93283790\ R^2= .87018655$ Adjusted $R^2= .57810628$ $F(9,4)=2.9793\ p<.15267$ Std.Error of estimate: .01719				
	B	St. Err. of B	t(4)	p-level
Intercept	0.44	0.19	2.38	0.08
PGEM degree of liberation	0.00	0.00	0.27	0.80
% non-sulphide PGEM	0.00	0.00	-1.04	0.36
PGEM ECD 80%<75µm	-0.01	0.04	-0.20	0.85
pentlandite content	0.58	0.88	0.66	0.55
PGEM/(PGEM+BMS)	-0.20	0.11	-1.75	0.16
Chromite ECD <2mm	0.00	0.00	0.44	0.68
BMS degree of liberation	0.00	0.00	-0.25	0.81
BMS ECD 80%<75µm	-0.01	0.00	-2.44	0.07
pn/(pn+mil)	-0.06	0.06	-0.99	0.38